University of Southampton

Faculty of Engineering and Physical Sciences

Chemistry

The Influence of Aliphatic Fluorination on Lipophilicity

by

Benjamin Francis Joseph Jeffries

Thesis for the degree of Doctor of Philosophy

February 2019

University of Southampton

Abstract

Faculty of Engineering and Physical Sciences

Chemistry

Thesis for the degree of Doctor of Philosophy

The Influence of Aliphatic Fluorination on Lipophilicity

by

Benjamin Francis Joseph Jeffries

Lipophilicity is known to influence a wide range of ADMET (absorption, distribution, metabolism, excretion and toxicity) properties and is widely regarded as one of the most important parameters within drug discovery programs. Unfortunately, in recent years lipophilicity modulation has often been abused to increase the potency of drug molecules. This has caused in an overall increase in lipophilicity for orally available drugs, typically resulting in undesirable effects on the aforementioned ADMET properties. Hence, as late-stage drug attrition is very costly, in order to improve the druggability of a compound there has been an increased awareness of the importance of lipophilicity modulation within drug discovery programs.

Fluorination is a tool commonly used within drug development to modulate a wide range of pharmacokinetic properties, in particular lipophilicity. While the effects of aromatic fluorination on lipophilicity have been well studied, due to constraints of commonly utilized analytical techniques used to measure lipophilicity (requirement of a UV chromophore), aliphatic fluorination has not. Fortunately, through the use of a ^{19}F NMR based method, the effects of aliphatic fluorination can now be reliably measured. Therefore, within this thesis the synthesis and lipophilicity measurement of a wide range of fluorinated alkanols, containing both known and novel motifs, will be covered. This allowed for an in-depth discussion into the effects of aliphatic fluorination on lipophilicity. It is also of interest for medicinal chemists whether these lipophilicity modulations persist on more complex drug scaffolds. Hence, the incorporation of a series of interesting aliphatic fluorinated motifs into a drug molecule was performed and their influence on lipophilicity was reproduced.

Table of Contents

Table of Contents ..... **i**

Table of Tables ..... **ix**

Table of Figures ..... **xi**

Research Thesis: Declaration of Authorship ..... **xvii**

Acknowledgements ..... **xix**

Definitions and Abbreviations ..... **xxi**

Chapter 1 Introduction **1**

1.1 Lipophilicity 1

1.2 Lipophilicity effects on ADMET properties 2

1.2.1 Absorption 2

1.2.1.1 Solubility 2

1.2.1.2 Permeability 3

1.2.1.3 Bioavailability 3

1.2.2 Distribution 4

1.2.3 Metabolism and Excretion 5

1.2.4 Toxicity 6

1.3 Guidelines for lipophilicity in drug design 7

1.4 The measurement and calculation of lipophilicity 9

1.4.1 Shake-flask methods 9

1.4.2 Chromatographic methods 10

1.4.3 Calculated log*P* 11

1.4.4 NMR-based methods 11

1.5 Overview of Fluorine Chemistry 14

1.6 The effects of fluorination on lipophilicity 15

1.7 Aims of the project 22

1.7.1 The investigation of aliphatic fluorination on lipophilicity 22

1.7.2 Investigation of the effects of aliphatic fluorination on a drug scaffold 23

1.7.3 Measurement of the lipophilicity of amide rotamers 23

Chapter 2 Influence of Aliphatic Fluorination on Lipophilicity 25

2.1 Introduction 25

2.2 The influence of simple fluorinated motifs on lipophilicity 26

2.2.1 Monofluorination 26

2.2.2 Difluorination 27

2.2.3 Mono- and difluorination "Matched Pairs" 28

2.2.4 Trifluorination 28

2.2.5 CF_3 "Matched Pairs" 31

2.3 The influence of polyfluorinated motifs on lipophilicity 33

2.3.1 CF_3CF_2 at varying distances 33

2.3.2 CF_3CH_2 vs CF_3CF_2 vs HCF_2CF_2 34

2.3.3 $CF_3 \rightarrow CH_3$ within different motifs 35

2.3.4 Chain elongation reduction in log*P* 39

2.4 Comparison of partially fluorinated motifs 39

2.4.1 Comparison of selected partially fluorinated motifs 39

2.4.2 CF_3CF_2 vs $CF_xH_xCF_2$ 41

2.4.3 The effect of the CFH-CF_2 and CF_2-CFH_2 motifs on lipophilicity 42

2.4.4 The effect of the *vic*-difluoro motif on lipophilicity 43

2.5 The effect of fluorination on the lipophilicity of diols 43

2.5.1 1,4-Butandiol Family 43

2.5.2 1,5-Pentandiol Family 44

2.6 The effects of fluoroalkenes on lipophilicity 45

2.6.1 4-Pentenol family 45

2.7 The effects of other motifs on lipophilicity 47

2.7.1 Fluorinated cyclopropanemethanol and its comparisons 47

2.7.2 The effect of the aliphatic -SCF_3 group on lipophilicity 47

2.8 Methodology development 49

2.8.1 Effects of impurities on lipophilicity 49

2.8.2 Log*P* measurements in D_2O 50

2.9 Conclusion 52

Chapter 3 Synthesis of Fluorinated Alkanols by Mono- and Difluorination 55

3.1 Introduction.....55

3.1.1 Retrosynthetic analysis and synthetic plan.....55

3.2 Electrophilic fluorination.....57

3.2.1 Introduction.....57

3.2.2 Synthesis of 2,2-difluorobutan-1-ol and 2,2-difluoropentan-1-ol.....59

3.2.3 Synthesis of 2-fluorobutan-1,4-diol and 2,2-difluorobutan-1,4-diol.....59

3.2.4 Synthesis of advanced fluorinated pentan-1-ol intermediates *via* electrophilic fluorination.....62

3.3 Nucleophilic fluorination.....63

3.3.1 Introduction.....63

3.3.2 Synthesis of 3,4-difluorobutan-1-ol and 4,5-difluoropentan-1-ol.....64

3.3.3 Synthesis of 3,4,4-trifluorobutan-1-ol and 4,5,5-trifluoropentan-1-ol.....65

3.3.4 Synthesis of 3,3,4-trifluorobutan-1-ol and 4,4,5-trifluoropentanol.....66

3.3.5 Synthesis of 2-fluorobutanol.....68

3.3.6 Synthesis towards 3,3-difluorobutan-2-ol.....69

3.3.7 Synthesis of 3,3-difluorobutan-1-ol and 4,4-difluoropentan-1-ol.....69

3.3.8 Synthesis of 4,4-difluorobutan-1-ol and 5,5-difluoropentanol.....70

3.3.9 Synthesis of 3-fluoropentan-1-ol.....70

3.3.10 Synthesis of 3,3-difluoropentan-1-ol.....71

3.3.11 Synthesis of 5-fluoropentan-2-ol.....72

3.3.12 Synthesis of 5,5-difluoropentan-2-ol.....74

3.3.13 Synthesis of 3,3-difluoropentan-2-ol.....74

3.4 Vicinal difluorination.....76

3.4.1 Introduction.....76

3.4.2 Attempted vicinal difluorination.....77

3.5 Conclusion.....80

Chapter 4 Synthesis of Targets Using Fluorinated Building Blocks 83

4.1 Introduction.....83

4.1.1 Retrosynthetic analysis.....83

4.2 Radical trifluoromethylation 86
4.2.1 Synthesis of 6,6,6-trifluorohexan-2-ol, 6,6,6-trifluorohexan-3-ol and 5,5,5-trifluoropentan-2-ol 86
4.2.2 Synthesis of 3,5,5,5-tetrafluoropentan-1-ol 88
4.2.3 Synthesis of 1,1,1-trifluorohexan-3-ol 89
4.3 Homologation 90
4.3.1 Synthesis of 2,2,4,4,4-pentafluorobutan-1-ol and 2,4,4,4-tetrafluorobutan-1-ol 90
4.4 Nucleophilic trifluoromethylation 94
4.4.1 Introduction 94
4.4.2 Synthesis of 1,1,1-trifluorohexan-2-ol 95
4.4.3 Synthesis of 1,1,1,6,6,6-hexafluorohexan-2-ol 95
4.5 Grignard Reactions 96
4.5.1 Synthesis of 1,1,1-trifluorooctan-4-ol 96
4.5.2 Synthesis of 8,8,8-trifluorooctan-4-ol 97
4.5.3 Synthesis of 7,7,7-trifluoroheptan-3-ol 97
4.5.4 Synthesis of 1,1,1-trifluoroheptan-3-ol 98
4.6 Synthesis of -SCF_3 analogues 98
4.6.1 Introduction 98
4.6.2 Synthesis of 4-(trifluoromethylthio)-butanol 99
4.6.3 Synthesis of 3-(trifluoromethylthio)-propanol 101
4.7 Fluorinated cyclopropylmethanol derivatives 102
4.7.1 Introduction 102
4.7.2 Reduction of fluorinated cyclopropanecarboxylic acid analogues 103
4.8 Polyfluorinated substrates 103
4.8.1 Attempted synthesis of 3,3,4,4-tetrafluoropentan-1-ol 103
4.8.2 Synthesis of 3,3,4,4-tetrafluorobutan-1-ol 106
4.8.3 Synthesis of 2,2,3,3-tetrafluorobutan-1-ol 106
4.8.4 Synthesis of 2,2,3,3,4,4-hexafluoropentan-1-ol 109
4.9 Conclusion 110

Chapter 5 Reducing the Lipophilicity of Perfluoroalkyl Groups by CF_2–F/CF_2-Me or CF_3/CH_3 Exchange....113

5.1 Introduction....113

5.1.1 Previous results and Aims....113

5.1.2 Evenamide....114

5.1.3 Synthetic plan....115

5.2 Synthesis of evenamide and its analogues....116

5.2.1 Synthesis of scaffold....116

5.2.2 *O*-Alkylations *via* a tosylate leaving group....117

5.2.3 *O*-Alkylations *via* a triflate leaving group....118

5.2.4 Deprotection....120

5.3 Results and discussion....120

5.3.1 Results Table....120

5.3.2 Log*D*....122

5.3.3 Solubility....123

5.3.4 Metabolic stability....123

5.3.5 Plasma protein binding (PPB)....124

5.3.6 Human *Ether à-go-go*-Related Gene (hERG)....124

5.4 Conclusion....125

Chapter 6 Conformer Specific Lipophilicity....127

6.1 Introduction....127

6.2 Aims....128

6.3 Synthesis of amide rotamers....128

6.3.1 Attempted synthesis of *N*-acetyl 3-fluoropiperidine....128

6.3.2 Synthesis of *N*-acetylated fluoropiperidines and fluoropyrroldines....129

6.4 Assignment of amide rotamers....130

6.4.1 Establishment of amide rotamers....130

6.4.2 Conformer assignment....131

6.4.3 Rotamer assignment in water (D_2O)....131

6.4.4 Consideration of ^{19}F NMR chemical shifts in different solvents....133

6.4.5 Rotamer assignments in octanol 134

6.4.5.1 Solvent considerations: the use of [1,1-D_2]-octan-1-ol: assignment of *N*-acetyl-3-fluoropyrrolidine in octanol 134

6.4.5.2 Synthesis and evaluation of [1,1-D_2]-octan-1-ol as solvent 134

6.4.5.3 Rotamer assignments in [1,1-D_2]-octan-1-ol 135

6.5 Log*P* results and discussion 137

6.6 Conclusion 142

Chapter 7 Experimental for Lipophilicity 143

7.1 Detailed logP determination protocols 143

7.2 Detailed experimental data for the log*P* determinations 144

7.2.1 Propan-1-ol series 144

7.2.2 Butan-2-ol series 144

7.2.3 Isobutanol series 145

7.2.4 Butan-1-ol series 145

7.2.5 Pentan-2-ol series 147

7.2.6 Pentan-1-ol series 148

7.2.7 Hexan-3-ol series 150

7.2.8 Hexan-2-ol series 151

7.2.9 Hexan-1-ol series 151

7.2.10 Septan-3-ol series 151

7.2.11 Octan-4-ol series 152

7.2.12 4-Penten-1-ol series 152

7.2.13 1,4-Butanediol series 153

7.2.14 1,5-Pentanediol series 153

7.2.15 Cyclopropylmethanol series 154

7.2.16 –SCF_3 motif 155

7.2.17 Oxetan-3-ylmethanol series 155

7.3 Methodology Development 156

7.3.1 Impurity screening 156

7.3.2 Use of D_2O in place of H_2O for log*P* determination procedure 157

Chapter 8 Experimental for Synthesis 159

8.1 General methods 159
8.2 Synthesis of fluorinated alkanols by mono- and difluorination 160
8.3 Synthesis of targets using fluorinated building blocks 197
8.4 Synthesis of evenamide analogues 232
8.4.1 General procedure A for tosylate formation 234
8.4.2 General procedure B for aryl ether formation *via* the tosylate 236
8.4.3 General procedure C for Boc-deprotection 237
8.4.4 General procedure D for aryl ether formation *via* the triflate 240

Chapter 9 Conformer Specific Lipophilicity Experimental 245

9.1 Synthesis of amide rotamers 245
9.2 Synthesis of [1,1-D_2]-octan-1-ol 248
9.3 Detailed experimental data for the log*P* determination 249
9.4 Assignment of amide rotamers in [1,1-D_2]-octan-1-ol 252
9.5 Calculations 258

Bibliography 261

Appendix A Crystal Structures 273

A.1 X- Ray structure analysis data for compound Q4 273
A.2 X- Ray structure analysis data for compound 3.46 274
A.3 X- Ray structure analysis data for compound 4.77 275
A.4 X- Ray structure analysis data for compound 4.36 276
A.5 X- Ray structure analysis data for compound Exp3 277

Table of Tables

Table 2.1 - Calculated dipole moments 37

Table 2.2 - Chemical shift values and weighted partial atomic charges per hydrogen atom of the methyl group[ix] 38

Table 2.3 - Effects of impurities on log*P* 50

Table 2.4 - Comparison of log*P* values recorded in both D_2O and H_2O 51

Table 3.1 - Optimization of electrophilic fluorination. Reaction conditions: rt, 16 h, THF/*i*-PrOH (9:1). NFSI and L-Proline equivs, scale and yields can be found in the table. 61

Table 3.2 - Deoxyfluorination optimization 67

Table 3.3 - Conditions for synthesis of 3.13 71

Table 4.1 - Oxidation of 4.35 92

Table 4.2 - Hydrogenation conditions 94

Table 4.3 - Hydrogenation conditions 101

Table 4.4 - Attempted synthesis of 4.75. [A] Additive added after 45 minutes, [B] Additive added after 5 minutes. 105

Table 5.1 - One-pot *O*-alkylation optimization 119

Table 5.2 - Analysis of evenamide 5.1a and analogues 5.1b–h 121

Table 6.1 - Amide rotamer-specific lipophilicities. *Defined as logP_{cis} – logP_{trans} 138

Table 6.2 - Experimental amide rotamer ratio taken from the log*P* determination experiments 138

Table 6.3 - Calculated dipole moments for 1.1, 1.2 and 1.4 140

Table of Figures

Figure 1.1 - Lead-to-drug optimisation. Adapted from *Ref*[65] 8

Figure 1.2 - Principle of the log*P* determination method. Adapted from *Ref*[94] 13

Figure 1.3 - Fludrocortisone, Prozac® and efavirenz. 14

Figure 1.4 - The effect of fluorination on pK_a and pK_{aH} values, adapted from *Ref*[103] 15

Figure 1.5 - Effect on lipophilicity on the substitution of a hydrogen atom with a fluorine atom, adapted from *Ref*[105] and log*P* values of selected fluorinated compounds[108] 16

Figure 1.6 - Log*P* of fluorinated *N*-propyl indole analogues[110, 112] 17

Figure 1.7 - Effects CH_3/CF_3 exchange at varying distances from an alcohol moiety[86] 17

Figure 1.8 - Effects of fluorination on polar molecules 18

Figure 1.9 - Log*P* values of selected fluorinated alkanols, adapted from Linclau *et al*.[94] 19

Figure 1.10 - The most polar conformation adoptable by the syn- and anti-isomer 19

Figure 1.11 - Monofluorination of conformationally restricted cyclohexanol systems. Adapted from *Ref*[94] 20

Figure 1.12 - Ropivacaine and levobupivacaine 21

Figure 1.13 - Log*P* of selected aryl derivatives similar to the α,β,β-trifluorocyclopropane motif 21

Figure 1.14 - *Gem*-difluorinated butan-1-ol family 22

Figure 1.15 - Selected CF_3 matched pairs 22

Figure 1.16 - Target *N*-acetylated fluoropiperidines and fluoropyrrolidines 23

Figure 2.1 - Effects of monofluorination 26

Figure 2.2 - Effects of difluorination 27

Figure 2.3 - Mono- and difluorinated matched pairs 28

Figure 2.4 - α-CH_3/CF_3 exchange 29

Figure 2.5 - β-CF_3 and γ-CF_3 alcohols 30

Figure 2.6 - The log*P* of δ-CF_3 alcohols 31

Figure 2.7 - Trifluoromethyl Matched Pairs 32

Figure 2.8 - Trifluoromethyl Matched Pairs 33

Figure 2.9 - Log*P* of CF_3CF_2 motif 34

Figure 2.10 - CF_3CH_2 vs CF_3CF_2 vs HCF_2CF_2 35

Figure 2.11 - CF_2HCF_2R conformations 35

Figure 2.12 - Effect of CF_3/CH_3 exchange on lipophilicity 36

Figure 2.13 - Comparison of the two most abundant conformers of G12 in octanol (left) and water (right)[viii] 37

Figure 2.14 - Reduction of log*P* upon chain elongation 39

Figure 2.15 - Comparison of selected polyfluorinated motifs 40

Figure 2.16 - CF_3CF_2 vs $CF_xH_xCF_2$ 41

Figure 2.17 - Comparison of *vic*-trifluoro motifs 42

Figure 2.18 - *Vic*-difluoro motif 43

Figure 2.19 - 1,4-Butandiol family 44

Figure 2.20 - 1,5-Pent-di-OH family 45

Figure 2.21 - 4-Pentenol family 46

Figure 2.22 - Fluorinated cyclopropanemethanol motifs and their comparisons *=log*P* calculated by MarvinSketch 47

Figure 2.23 - The -SCF_3 motif. L1 value obtained from *Ref*[86] 48

Figure 2.24 - Log*P* values of 2,2,2-trifluoroethan-1-ol and 4,4,4-trifluorobutan-1-ol 49

Figure 2.25 - A total of 66 novel log*P* values. The Δlog*P* values listed are in comparison to the individual compounds respective parent molecule. 52

Figure 3.1 - Electrophilic fluorination reagents 58

Figure 3.2 - Crystal structure of Q4. Thermal ellipsoid – Carbon = black, oxygen = red, fluorine = green and hydrogen = grey. 62

Figure 3.3 - Newly developed nucleophilic fluorination reagents.....63

Figure 3.4 - Popular sulphur-based fluorination reagents.....64

Figure 3.5 - Crystal structure of 3.46 67

Figure 3.6 - Published procedures for the vicinal difluorination of an alkene.....76

Figure 3.7 - All fluorinated alkanols snthesised in Chapter 3 80

Figure 4.1 - SCF_3 analogues 98

Figure 4.2 - Umemoto's Reagent 99

Figure 4.3 - Crystal structure of 4.77 107

Figure 4.4 - All fluorinated alkanols synthesis in Chapter 4.....110

Figure 5.1 - Key lipophilicity lowering trends.....113

Figure 5.2 - Selected alkanols for investigation 114

Figure 5.3 - Evenamide.....115

Figure 5.4 - Log*P*/*D* comparison.....122

Figure 6.1 - Conformer specific log*P* for clenbuterol indicating populations in each layer and their corresponding log*P*'s. Adapted from *Ref*[237].....127

Figure 6.2 - Target *N*-acetyl amide rotamers.....128

Figure 6.3 - ^{1}H NMR of 1.3, acetate signal coalescence (left). ^{19}F NMR of 1.3, fluorine signal coalescence (right). 130

Figure 6.4 - *Trans* and *cis* amide rotamers 131

Figure 6.5 - HSQC spectrum of 1.4 in D_2O, 25.35 °C, Bruker AVII400 FT-NMR Spectrometer.132

Figure 6.6 - NOESY spectrum of compound 1.4 in D_2O, 25.35 °C, Bruker AVII400 FT-NMR Spectrometer. 133

Figure 6.7 - ^{19}F (376 Hz) NMR of *N*-acetyl 3-fluoropyrollidine in $CDCl_3$ and D_2O representing change in chemical shifts in different solvents.....134

Figure 6.8 - ^{1}H NMR (400 Hz) spectrum depicting the comparison of *N*-acetyl-3-fluoropyrrolidine in octanol (Spectrum A) and [1,1-D_2]-octan-1-ol (Spectrum B)......135

Figure 6.9 - HSQC spectrum of *N*-acetyl-3-fluoropyrrolidine in [1,1-D_2]-octan-1-ol, 24.95 °C, Bruker AVII400 FT-NMR Spectrometer. 136

Figure 6.10 - NOESY spectrum of *N*-acetyl-3-fluoropyrrolidine in 1-[1,1-D_2]-octanol, 24.95 °C, Bruker AVII400 FT-NMR Spectrometer. 137

Figure 6.11 - Comparison of overall log*P* values 139

Figure 6.12 - Comparing the log*P* values of the *cis* and *trans* rotamers 140

Figure 9.1 - HSQC spectrum of *N*-acetyl-3,3-difluoropyrrolidine in 1-[1,1-D_2]-octanol. 253

Figure 9.2 - NOESY spectrum of *N*-acetyl-3,3-difluoropyrrolidine in [1,1-D_2]-octan-1-ol. 254

Figure 9.3 - HSQC spectrum of *N*-acetyl-3-fluoropiperidine in [1,1-D_2]-octan-1-ol. 255

Figure 9.4 - NOESY spectrum of *N*-acetyl-3-fluoropiperidine in [1,1-D_2]-octan-1-ol. 256

Figure 9.5 - HSQC spectrum of *N*-acetyl-3-fluoropiperidine in [1,1-D_2]-octan-1-ol 257

Figure 9.6 - ROESY spectrum of *N*-acetyl-3-fluoropiperidine in [1,1-D_2]-octan-1-ol. 258

Research Thesis: Declaration of Authorship

Print name: Benjamin Jeffries

Title of thesis: The Influence of Aliphatic Fluorination on Lipophilicity

I declare that this thesis and the work presented in it are my own and has been generated by me as the result of my own original research.

I confirm that:

1. This work was done wholly or mainly while in candidature for a research degree at this University;
2. Where any part of this thesis has previously been submitted for a degree or any other qualification at this University or any other institution, this has been clearly stated;
3. Where I have consulted the published work of others, this is always clearly attributed;
4. Where I have quoted from the work of others, the source is always given. With the exception of such quotations, this thesis is entirely my own work;
5. I have acknowledged all main sources of help;
6. Where the thesis is based on work done by myself jointly with others, I have made clear exactly what was done by others and what I have contributed myself;
7. Parts of this work have been published as:

Jeffries, B.; Wang, Z.; Graton, J.; Holland, S. D.; Brind, T.; Greenwood, R. D. R.; Le Questel, J.-Y.; Scott, J. S.; Chiarparin, E.; Linclau, B., *J. Med. Chem.* **2018,** *61*, 10602-10618.

Signature: Date:

Acknowledgements

First of all, I would like to thank Professor Bruno Linclau for his continued guidance and support. I am grateful for the opportunity to carry out my PhD under your supervision, your encouragement and assistance has allowed me to develop into a much better organic chemist than I ever dreamed I could be. I would also like to thank my industrial supervisor Dr Elisabetta Chiarparin for her advice, support and enthusiasm for my research. Other members of AstraZeneca I would like to thank are Dr James Scott for his medicinal chemistry knowledge and assistance with the synthesis of my drug scaffolds, Dr Rodrigo Carbajo for advice in relation to NMR and Ryan Greenwood for supervising me in the lab.

I would especially like to thank the ESPRC and AstraZeneca for their funding of this project.

I must thank all past and present members of the Linclau group over the past three years for their support and trips to the Stags. In no particular order: Zhong, Rachel, Gert-Jan, Lucas, Simon, Hannah, Clement, Julien, Joe, David E., Rob, RK, JB, Diego, Mariana, and any others whose names have escaped me. I would also like to thank members of the Brown group, David W. and Victor.

A couple of special memories I would like to mention. Gert-Jan and Lucas for helping me regain my passion for drum and bass, we have shared countless days, nights and festivals together that I will never forget. Rachel, Gemma and Gert-Jan and our love for Taylor Swift. Gemma, Gert-Jan and Joe for introducing me to bouldering. Zhong for his chemistry knowledge and constant advice.

It is worth mentioning that Southampton is my hometown and because of that I had the opportunity to rekindle many friendships over the previous years. They have all been a part of an amazing support network throughout my PhD and have been the focus of many enjoyable memories that I will never forget. I would like to make special mention to my house mate of the past three years Joseph, who has always been there for advice and a drink.

I am very thankful to the University staff within the Chemistry department, in particular Neil for the countless multi-day NMR experiments I have requested over the years. I would also like to mention Mark and Keith for the running of stores and being a pleasure to talk with, Julie for mass spectrometry and finally Mark Light for providing my crystal structures.

Without the support of my family throughout my life I would not be where I was today and for that I am eternally thankful. Finally, I would like to thank Helen, for putting up with hearing about me moan and complain about chemistry for the past few years and always being able to put a smile on my face, even in the darkest of times. You give me a sense of direction in my life.

Definitions and Abbreviations

AIBN	Azobisisobutyronitrile
CI	Chemical ionization
CNS	Central Nervous System
COSY	Correlation Spectroscopy
D1	Relaxation delay
DAST	Diethylaminosulphur trifluoride
DIPEA	*N*,*N*-Diisopropylethylamine
DMAP	4-Dimethylaminopyridine
DMF	Dimethylformamide
DMP	Dess-Martin periodinane
DMPU	*N*,*N*-Dimethylpropyleneurea
EA	EtOAc
EI	Electron ionization
ESI	Electrospray ionization
Et_3N	Triethylamine
FCC	Flash column chromatography
FG	Functional Group
FTIR	Fourier-transform infrared spectroscopy
HMBC	Heteronuclear Multiple Bond Correlation
HPLC	High-performance liquid chromatography
HRMS	High-resolution mass spectrometry
HSQC	Heteronuclear single quantum coherence spectroscopy
IR	Infrared spectroscopy
LRMS	Low resolution mass spectrometry
m.p.	Melting point
*m*CPBA	3-Chloroperbenzoic acid
MPLC	Medium-pressure liquid chromatography
MS	Mass spectrometry

MW	Molecular weight
NFSI	*N*-Fluorobenzenesulphonimide
NMP	*N*-Methyl-2-pyrrolidone
NMR	Nuclear magnetic resonance
NOE	Nuclear Overhauser effect
NOESY	Nuclear Overhauser effect spectroscopy
NS	Number of scans
O/N	Over night
O1P	Frequency offset point
PDC	Pyridinium dichromate
PSA	Polar surface area
*p*TSA	*p*-Toluenesulphonic acid
R_f	Retention factor
ROESY	Rotating-frame overhauser Spectroscopy
RP-HPLC	Reverse phase high-performance liquid chromatography
RTrt	Room temperature
SNR	Signal-to-noise ratio
SW	Spectral width
TCCA	Trichloroisocyanuric acid
TBAF	Tetrabutylammonium fluoride
TBAI	Tetrabutylammonium iodide
TBDMSCl	*tert*-Butyldimethylsilyl chloride
TEMPO	(2,2,6,6-Tetramethylpiperidin-1-yl)oxyl
TFA	Trifluoroacetic acid
THF	Tetrahydrofuran
TLC	Thin layer chromatography
UV	Ultraviolet

Chapter 1 Introduction

1.1 Lipophilicity

Lipophilicity is considered to be one of the most important parameters in drug discovery, influencing a wide range of properties including pharmacodynamic and pharmacokinetic profiles, in addition to drug toxicity.[1] Originally proposed by Hansch and Fujita as a portrayal for biological partition, lipophilicity was defined as the logarithmic partition coefficient (log*P*) of a molecule between a non-polar phase (octanol) and a polar phase (water).[2-3] Essentially, this represents the capability of a molecule to cross a cell membrane (mimicked by octanol) to access the blood stream (mimicked by water) to reach its site of action.[2] The corresponding *P* value is frequently obtained experimentally as the ratio of the concentration for a neutral compound between *n*-octanol and water under equilibrium conditions (Equation 1). It is generally regarded to be the combination of two structural properties, hydrophobicity and polarity.

$$P = \frac{C_{octanol}}{C_{water}} \quad \textbf{(Eq. 1)}$$

For ionisable compounds, the distribution coefficient (log*D*) is used. This parameter is pH dependant, where experimentally the physiological $pH_{7.4}$ is typically used. It refers to the sum of both the ionised and non-ionised species in the water distribution, assuming the charged species will not exist in the octanol phase to a significant extent. The log*D* can be calculated using the following equations (Equation 2 and 3, pK_a is the dissociation equilibrium constant).[2]

$$LogD_{acids} = logP + \log[\frac{1}{(1 + 10^{pH-pK_a})}] \quad \textbf{(Eq. 2)}$$

$$LogD_{bases} = logP + \log[\frac{1}{(1 + 10^{pK_a-pH})}] \quad \textbf{(Eq. 3)}$$

Currently within lead-to-drug development programs, both molecular weight and lipophilicity are often inappropriately increased to improve the potency of drug molecules. This is referred to as "molecular obesity",[4] and generally causes an undesired deterioration of key properties (e.g., solubility, metabolic stability, oral bioavailability) that control a compound's druggability.[5-7] Therefore, the capability to reduce or maintain a low lipophilicity, whilst increasing molecular weight and drug potency is viewed as a fundamental objective for success in drug discovery programs.[7]

As late-stage drug attrition is very costly, an increasing awareness about the importance of lipophilicity on individual ADMET (absorption, distribution, metabolism, elimination and toxicology) parameters has emerged. It is becoming increasingly more obvious that optimum lipophilicity ought to be one of the important targets during drug design and lead optimisation.[8] Therefore methods for the measurement and control of lipophilicity are highly sought after.

1.2 Lipophilicity effects on ADMET properties

1.2.1 Absorption

1.2.1.1 Solubility

At a given temperature, solubility is the measure of the maximum quantity of material that is able to dissolve in a specific amount of solvent.[9] It is critical for both a drug's absorption and bioavailability, making it a key feature within drug discovery.[10-11] Poor solubility is often a problem for medicinal chemists, however this can sometimes be remedied through the use of formulation methodologies, allowing for increased exposure in patients.[4] Low solubility can also reduce the efficacy of a drug because of poor exposure, which can result in delays or failures a drug development program.[12]

The link between solubility and lipophilicity is well established. An equation proposed by Yalkowsky *et al*. in 1980[13] combined both log*P* and melting point (MP) to calculate a molecule's aqueous solubility. The melting point is a measure for the lattice energy which is lost on the molecule dissolving into solution. An updated and simplified equation can be seen below (Equation 4),[14] which links decreasing lipophilicity with increasing solubility for molecules of similar melting points.

$$\log Sol_{aq} = 0.5 - logP - 0.01(MP\,^{\circ}C - 25) \qquad \textbf{(Eq. 4)}$$

A study by Clark *et al*. on a wide range of typically utilized research compounds observed that while only 50% of compounds with log*P* values of <3 were soluble,[i] this figure dramatically decreased to 10% when the log*P* increased to >3.[9] Gleeson's study of 44,584 GSK compounds agreed with this, reporting that if a log*P* value of <3 is targeted, then achieving a high solubility is much more likely.[11] He also observed that on average as the calculated log*P* (Clog*P*, for more information see Section 1.4.3) values increased, solubility decreased.

[i] Kinetic solubility >250 μg/mL, 500 μM for a compound of MW 500 Da

1.2.1.2 Permeability

Permeability is another important parameter in determining a drug's ability to reach the circulatory system through biological membranes found in the gastro-intestinal tract.[15] This can occur *via* various manners, such as paracellular or transcellular diffusion and transport-mediated mechanisms.[10] Lipophilicity plays an important role in the permeability of a drug. One of the original uses of log*P*/*D* measurements was to emulate the distribution of a molecule between a cell membrane and aqueous media.[8] Its relationship with permeability has been documented as hyperbolic,[16] parabolic,[17] linear,[18] bilinear[18-19] and sigmoidal.[20-21] Overall these reports are in agreement that a reduction in lipophilicity will lead to a decrease in permeability. This connection of permeability and lipophilicity was overlooked by Lipinski in his "rule of five"; it was instead linked to other criteria (hydrogen bond donor count <5, H-B acceptor count <10, and MW <500).[22]

The Caco-2 cell line is often used when measuring a molecules permeability.[23] It allows for both active and passive components of permeability to be recognised, because the Caco-2 cells express a range of relevant efflux transports.

Egan *et al*., utilized this Caco-2 cell line in a computational study for the prediction of absorption (permeability) using lipophilicity and other properties such as PSA (polar surface area).[24] This model suggested that a good absorption can be achieved in a log*P* range of -1 to +5.9, with an optimal PSA of <132 Å. A more recent study by Waring utilized AstraZeneca's results from Caco-2 cell permeability datasets, revealing a decrease in permeability for compounds with low log*D*, high PSA and high MW.[23] This reinforces the results from Egan's computational work.[24] Additional statistical analysis revealed that there is a 50% chance for a compound to have high permeability if the log*D* value is >1.7 units, and has a MW between 350 and 400. Furthermore, Waring identifies both lipophilicity and MW as the most important parameters for permeability control, contrary to Egan who proposed lipophilicity and PSA. Finally, despite the fact that issues with low lipophilicity are uncommon, Waring proposed a requirement for a lower lipophilicity limit, due to issues that could be faced with permeability. Overall, it is generally suggested that to improve permeation of a drug molecule through a biological membrane, an increase in lipophilicity, in parallel with a decrease in size (PSA and MW), is recommended.[10]

1.2.1.3 Bioavailability

In drug discovery, bioavailability is a widely used parameter and can be defined as the "fraction of the drug that reaches the systemic circulation after oral administration".[25] It is a complex property, influenced by the previously mentioned solubility and permeability, as well as clearance (See section 1.2.3).[26-27] An acceptable *in-vivo* bioavailability can be accomplished through the

combination of high permeability and solubility, which then allow for improved absorption, together with a low hepatic clearance, to minimise first pass elimination[ii].[8] Therefore, it is predictable that lipophilicity plays a role in the influence of bioavailability: too high and metabolism and solubility will be inadequate; too low, and permeability will be challenging.

Lipinski suggested a log*P* limit of <5, indicating that oral bioavailability was more likely to occur below this limit.[22] Other reports have suggested a log*P* range between 0 and 3,[29] and in the case of log*D*, a range of between 1 and 3.[30] Topliss *et al*. studied oral bioavailability on 232 drugs, with an emphasis on the diversity of the compound properties in regards to physicochemical characteristics and pharmacological data.[31] He reported that 99% of highly bioavailable drugs were in the log$D_{6.5}$ (pH of the small intestine) range of -2 to +3. Gleeson's statistical analysis however, revealed that the relationship between bioavailability and Clog*P* was not statistically significant at a 99.9% confidence level, although he states this may be due to relatively simplistic modelling.[11] Other published studies also agree with this statement, reporting no direct association between bioavailability and lipophilicity.[32] Other parameters such as rotatable bonds, ionisation state and PSA were proposed to be more appropriate forecasters.[10]

1.2.2 Distribution

The volume of distribution is the measure of a drug's dispersal in both plasma and the rest of the body, after dosage and clearance.[10] It is an important parameter within drug development, crucial for determining efficacy.[8] It is typically measured *via* the concentration of the unbound drug in plasma, as only the free drug would be available for distribution and illicit a pharmacological response. Thus, the understanding of a drug's capability to bind specifically or non-specifically to numerous tissues or proteins is important.[8] One particularly important plasma protein is human serum albumin (HSA). It is known to impact the volume of distribution[33], clearance[34] and efficacy of a drug.[11] Hence the ability for the pharmaceutical industry to predict distribution is important.

Various reports have shown that an increase in a drug's lipophilicity will typically cause an increase in plasma protein binding. One publication revealed this relationship to be sigmoidal,[35] whilst another reported it to be linear.[36] This occurs because of an increase in the molecules hydrophobicity (consequence of an elevated lipophilicity), resulting in favourable interactions with the plasma proteins.[10] Furthermore, Valko *et al*. observed that a molecule's binding constant for HSA has a direct correlation to log*P*.[37] It is also important to point out that because the HSA is rich

[ii] Metabolism of the drug prior to reaching the circulatory system.28. Pond, S. M.; Tozer, T. N., *Clin. Pharmacokinet.* **1984,** *9*, 1-25.

in charged proteins and transports endogenous fatty acids, that it is predicted by log*P*, not log*D*. Therefore, both ionised and unionised compounds have comparable affinity.[8] Gleeson *et al*.,[11] reported that while an increase in log*P* leads to an increase in the volume of distribution for either neutral or basic compounds, the same was not observed for zwitterions or acids (HSA has basic residues, thus acids tend to show high levels of binding with little effect from change in log*P*).

Distribution for the central nervous system (CNS) however is different. For a CNS drug to be effective it must permeate an additional hurdle, the blood-brain barrier (BBB).[8] Conversely for non-CNS drugs, the penetration of the BBB should be avoided in order to minimise the chance of unwarranted pharmacological responses.[11] A good distribution within the CNS is considered difficult for two reasons:

1. The BBB consists of a layer of endothelial cells that are connected *via* tight junctions. This is thought be more difficult to cross than other biological membranes.[38]
2. The BBB consists of a variety of efflux transporters, i.e. P-glycoprotein (P-gp), which operates to remove diffusing molecules out of the brain.[39]

Several studies have shown that on average an increase in log*P* leads to an improvement in CNS penetration.[10] Various optimal log*P*/*D* values have subsequently been proposed: Kearns[29] suggested a log*D* range of between 1 and 3 to easily penetrate the BBB, while Meanwell[40] observed that optimum physicochemical properties for oral CNS drugs, is a log*P* of 2.8 and log*D* of 1.7. A study by Peters *et al*.[38] observed that 75% of the studied CNS drugs had log*P* values >2 and that log*P* follows a non-linear fashion in relation to rat brain permeability, plateauing between log*P* values of +2 and +3. Select efflux transporters also showed an improved binding affinity for molecules with high log*P* values.[41-42] The P-gp efflux ratio in particular has been shown to increase in a linear fashion for basic molecules and non-linear for neutral molecules (acidic and zwitterionic were not examined due to a low sample number).[43-44]

Overall, lipophilicity is considered an important parameter in CNS drug discovery programs.[10] The optimum log*P* range for a drug to target the CNS is a complex matter, essentially determined through an act of balance. An increase in lipophilicity increases the capability of a drug to penetrate the BBB (desired), while also increasing efflux ratios and the drug's ability to bind to plasma proteins (undesired).[8, 11]

1.2.3 Metabolism and Excretion

Metabolism and excretion determine the *in vivo* clearance of a drug molecule within the body and are considered to be two of the more difficult processes to control.[10] If drug clearance is too high, it can lead to poor bioavailability, even with candidates with promising permeability and solubility.

It is also a crucial parameter in the decision of the dosing interval of a drug, because it determines the drug's half-life in combination with volume of distribution.[11] For metabolism and excretion to occur, the drug molecule is first metabolised *via* biotransformation processes before excretion *via* hepatic, biliary or renal pathways.[2] These biotransformations include the introduction of polar groups (log*P* decrease) *via* phase I metabolism (reduction, oxidation and hydrolysis) prior to phase II metabolism (conjugation).[2] The enzymes responsible for metabolism often target the more lipophilic molecules because the binding sites of CYP enzymes (responsible for a significant proportion of drug metabolism) are typically lipophilic and thus have an increased affinity for lipophilic molecules.[45-46] Common CYP enzymes can also metabolise low log*P* (0 – 1) molecules.[47]

To avoid a drug molecule interacting with these metabolites, a common strategy to decrease metabolic clearance is with a reduction in lipophilicity.[45, 48] Lipophilicity adjustments from structural modification however are not necessarily the only reason for a change in the metabolic stability of a compound. This change in the molecule's structure can also improve metabolic stability by the removal/blocking of metabolic sites, by decreasing the molecule's recognition by metabolites, or a mixture of the two processes.[8] This is why of the ADMET processes, metabolism and excretion are believed to be the most complicated to predict.[10]

Several reports have indicated an improvement in metabolism and *in-vivo* clearance with a reduction in lipophilicity.[8, 10] Obach *et al*.,[36] recommended log*P* values of <4 if once-daily dosing was to be targeted, and Johnson *et al*.,[49] reported that a log*D* range of between 1 and 3 is desirable. Gleeson observed a weak non-linear relationship between Clog*P* and *in-vivo* clearance, with small differences between ionisation states.[11] Neutral and basic molecules had an increase in clearance for an increase in Clog*P*, while acids and zwitterions observed the inverse. Gleeson further noted that observing the effect of log*P* on metabolism and excretion is challenging due to the changes in chemical structures across a series. This suggests that structural considerations can be more important than physicochemical properties like lipophilicity.

1.2.4 Toxicity

Toxicity is the main source of a drug's preclinical attrition.[50-51] GSK, AZ, Pfizer and Lilly reported that drug candidates that failed Phase I clinical trials due to toxicity had considerably higher mean Clog*P*s (mean Clog*P* +3.8), than those that progressed to Phase II (mean Clog*P* +3.1).[52] Highly lipophilic molecules have the potential to have higher degrees of promiscuity.[8] This promiscuity can lead to binding with anti-targets, resulting in undesired pharmacological responses which have the potential to be toxic.[8] This link between promiscuity and toxicity with lipophilicity has been confirmed by several studies which suggested that a higher degree of toxicological events is likely

to occur at log*P* >3.[40, 54-55] An important rule to mention is the Pfizer 3/75 rule, which highlights the importance of Clog*P* and PSA on toxicity. Their study found that if a compound has a log*P* <3 and PSA of >75 it was 6-fold less toxic than the inverse (clog*P* >3 and PSA <75).[55] Despite a large proportion of approved oral drugs not being in agreement with the 3/75 rule,[56-57] it is still useful to guide drug development during lead-to-drug optimisation.[58] Another rule linked to toxicity is related to Lipophilic Ligand Efficiency (LLE, discussed in Section 1.3), where a result larger than 5 is linked to a reduction in toxicity.[4] In particular, for some local anaesthetic agents, Nava-Ocampo *et al*. found that if the log*P* is ~3, then toxicity was significantly increased.[59] They proposed that this increase came from the compound's excessively high transfer from plasma to the CNS, resulting in an undesired elongated nerve root exposure.

The inhibition of hERG (human ether-à-go-go-gene),[60] a cardiac potassium channel, is extremely undesirable. It can lead to QT prolongation[iii] and thus a potentially fatal heart attack.[61] This process is often targeted for early screening, to avoid late-stage attrition. An increase in lipophilicity and thus drug promiscuity has been linked directly with an increase in hERG binding.[62] This parameter is ionisation class dependent and for a neutral molecule to have a <70% chance of hERG activity, a log*P* of <3.3 is required.[62] Overall minimizing drug attrition rates from hERG is often achieved by identifying lead molecules with low lipophilicity values and high potency.[8]

An increase in lipophilicity has also been directly linked to other toxicological events such as phospholipidosis[63-64] (build-up of phospholipids in cells) and CYP inhibition (enzymes used in metabolism process).[10] A log*P* of <3 has been recommended to avoid either of these events.[11]

1.3 Guidelines for lipophilicity in drug design

Within drug discovery, for a molecule to have improved druglike properties, its log*P* must be taken into consideration. A particularly famous threshold is <5 Clog*P,* published by Lipinski *et al*. in 1997,[22] from the "rule of 5". These rules were initially devised as a set of criteria to improve the likelihood of drug absorption, however they are now widely used as a guide for the design of orally active drugs.[65] The rules are as follows; <5 Clog*P*, <500 molecular weight, <10 hydrogen bond acceptors (O+N atom count) and <5 hydrogen bond donors (OH + NH count). The "rule of 5" is violated if two or more of these criteria are not met. It is important to note that these criteria and the subsequent lipophilicity limit applies to drugs with passive permeation, as opposed to transporter-mediated permeation (e.g. antibiotics, antifungals, vitamins and cardiac glycosides).[52] Furthermore it is

[iii] A measure of delayed ventricular repolarisation – defined as the time in ms between the Q and T-phase on an electrocardiogram

understood that a log*P* of 5 or greater has the potential to lead to unwanted side-effects and is generally associated with toxicological events.[4]

It should be highlighted that the "rule of five" was derived through the empirical investigation of drugs and their respective properties which had reached phase II clinical trials.[22] These rules however may not be ideal for many lead-to-drug research programs. In 1999, Teague *et al*. noted that with the growing popularity of combinatorial chemistry in drug discovery programs, the properties of library compounds should have adjusted rules.[65] The rationale behind this is that many drugs that originate from small molecules identified *via* high-throughput library screens are more likely to find a binding mode with a receptor than a larger druglike molecule. Once a hit has been found with affinity at µM levels, the often small and polar lead molecule is then optimised through chemical modification. This optimisation process from lead-to-drug molecule is commonly accompanied by an increase in both molecular weight and lipophilicity (see Figure 1.1 for selected examples). Thus, if libraries of druglike molecules following Lipinski's "rule of 5" were to be applied initially, then the opportunity for further growth is more limited. Therefore, Teague *et al*. proposed Clog*P* for a library of lead molecules to be between 1 and 3.

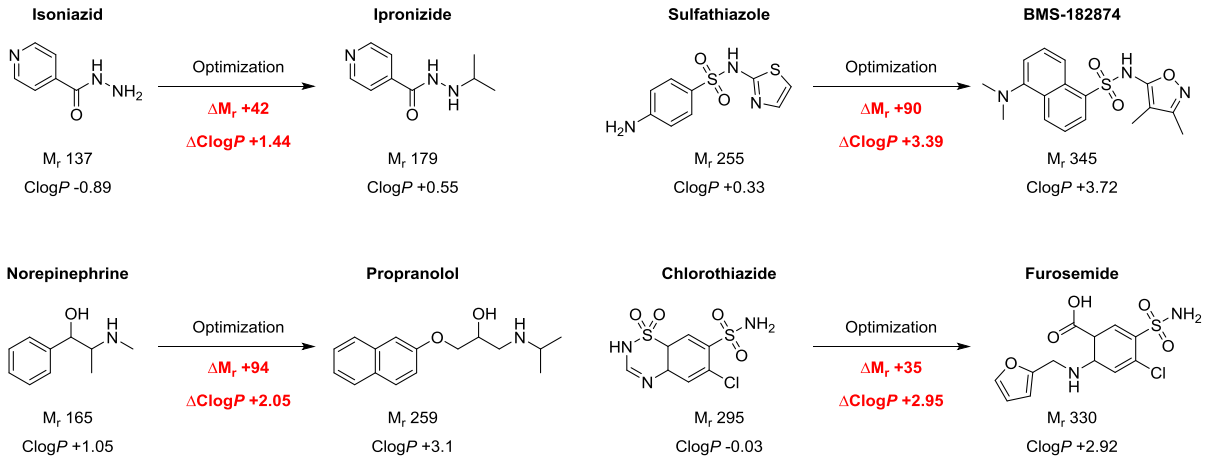

Figure 1.1 - Lead-to-drug optimisation. Adapted from *Ref*[65]

H. Jhoti *et al*. in 2003 arrived at a similar conclusion proposing a "rule of three" based on their examination of a wide range of fragment hits.[66] They proposed that a log*P* of <3 would be a more efficient means for the construction of a fragment library for lead discovery.

Further adjustments have been made to the original "rule of 5" in recent years, as there is now a deeper understanding on the effects of lipophilicity on pharmacokinetic and pharmacodynamic processes, as well as drug toxicity. Overall, the recommended log*P* for drug discovery programs has decreased. Gleeson *et al*. in 2008[11] recommended a log*P* of <4 and Waring in 2010[8] advised a very narrow range of between 1 and 3 for the log*P*/*D* in drug discovery programs.

Strictly following rules and cut off points however is not completely straightforward. When investigating CNS drugs, if a log*P* limit of <3 was set, the synthesis of 30% of the 843 compounds studied, which had full ADME alignment, would not have been performed.[67] Therefore if a log*P* restriction of >3 was applied during the design of drugs, then the amount of useable CNS drugs may be substantially lowered.

LLE (or LiPE, lipophilic ligand efficiency), originally reported by Leeson and Springthorpe, is an important metric also used in drug discovery programs.[54, 68] It is described by Equation 5, and can be used as an "estimate of binding efficiency in the context of lipophilicity", and can therefore be used as an "index of lipophilicity per unit of potency".[40] An ideal range for LLE is between ~5 and 7 units or >7, if achievable, these values correlate to a Clog*P* of between 2.5 and 3 and a potency range of between 1 and 10 nM.[69]

$$LLE = pK_i\ (or\ pIC_{50}) - ClogP\ (or\ ClogD_{7.4}) \quad \textbf{(Eq. 5)}$$

Adaptations of LLE such as LELP[70] ("function to depict the price paid of ligand efficiency[iv] in lipophilicity") and LLE_{AT}[71] (LLE, with heavy atom count considerations) have also been developed within drug discovery.

1.4 The measurement and calculation of lipophilicity

1.4.1 Shake-flask methods

The classic technique for the direct measurement of log*P* is the shake-flask method. It is simple to perform and is the standard procedure according to OECD guidelines.[72] This method utilizes an *n*-octanol and water (or $pH_{7.4}$ buffer solution for log$D_{7.4}$) partition, in which the substrate is added prior to shaking. After equilibrium between all interacting components has been achieved the layers are separated, and the concentration of the substrate is determined in both phases individually utilizing an analytic method, typically UV/VIS spectroscopy. Fundamental issues that arise from this procedure is that it is time consuming and labour intensive, and that the accurate log*P* determination window is roughly between -3 and +3 (confinements of the analytical methods used for concentration determination). Compounds that are either very hydrophobic or hydrophilic have the potential to form emulsions, have issues with solubility or adhere onto vessel walls. Variations of the standard procedure have been developed to overcome these issues, i.e. flow injection analysis, dialysis tubing and ultrasonic agitation.[73-74] Furthermore compounds with high purities are

[iv] Ligand efficiency (LE) reflects the ratio of the affinity of a drug for its target with the heavy atom count (non-hydrogen atoms).

required, especially for UV/VIS spectroscopy which has no means to differentiate between the measured compound and impurities.

Recently, to overcome some of the aforementioned problems, Alelyunas *et al*. had developed a high throughput octanol/water lipophilicity measurement system, which was able to utilize substrates stored in DMSO solutions.[75] The compound in the DMSO solution was first placed into one well of a 96-well plate, then to minimise potential concern for the effect of DMSO on the log*D* values, the solvent is removed *in vacuo* and with gentle heating. Next the octanol and buffer solution are added, and the 96-well plate is mechanically inverted, prior to quantification with LC-UV/APPI-MS. This fully automated method was validated with 72 literature compounds with diverse ionisation and log*D* values ranging from -2 to +6.

1.4.2 Chromatographic methods

Indirect methods to measure lipophilicity rely on chromatographic retention times. These were developed from the 1980s onwards and examples of these methods include reversed phase high performance liquid chromatography (RP-HPLC)[76] and reversed phase thin layer chromatography (RP-TLC).[77] This reversed phase format is essentially energetically analogous to an *n*-octanol/water partition. The stationary phase (chemically bonded hydrocarbon silica) has hydrocarbon chains which have lipophilic 'end-caps' (octanol) and a hydrophilic 'head group' (water), which can be thought of as a phospholipid mimic.[2] Due the convenience, accuracy, speed of experiments and automation, RP-HPLC has become an increasingly popular method that can record log*P* values between 0 and 6 accurately.[78] Compared to direct methods for log*P* measurement, substrates can be measured with impurities present, due to the innate separation occurring during the chromatographic process. To measure log*P* values *via* this method, a calibration curve must first be established using retention times from compounds with known log*P* values. The unknown compound can then be injected, and the retention time recorded, which is then used to then deduce the log*P* value from the calibration curve. The accuracy of log*P* values obtained *via* this method are highly reliant on the calibration curve being established from homologues or closely congeneric compounds.[79] The silica-based stationary phase also has residual silanol groups which can result in interactions (hydrogen bonding or electrostatic) with some polar moieties, leading to asymmetrical peaks.[2] Protection of these silanol groups with polar groups can alleviate these issues, however at the expense of complicating the procedure.

1.4.3 Calculated log*P*

The previous methods mentioned require the synthesised compound for measurement, however the ability to predict the log*P* of a potential substrate is desired in any compound development program. Clog*P* allows one to quickly obtain the value for a wide range of substrates, either utilizing an in-house calculation or commercial software. The log*P* prediction models can be broken into a few major classes.[80]

- The π−Substituent Method – The calculation of log*P* through the substitution of a hydrogen atom on a parent compound of known log*P* with another motif with a corresponding π value.[3]
- Fragment-based methods – Large databases of known log*P* values were statistically analysed to obtain the average contribution from simple chemical fragments. The Clog*P* for a compound was then calculated utilizing correction factors and the sum of the fragment values.[81]
- By atomic contribution and/or surface area – This is similar to the aforementioned fragment-based method however, atomic fragments and/or surface area data are used instead of chemical fragments.[82]
- By molecular properties – A calculation that is based on a function of various calculated molecular properties.[83]

The program MarvinSketch was used throughout this thesis to provide a wide range of Clog*P* values to assist in obtaining estimated values for the log*P* measurement procedure. This program utilizes a fragment-based method derived from a data set data from Viswandahan *et al*[84] (ChemAxon model) or a method constructed from Klopmen *et al*.[85] and ChemAxon models with the PhysProp database (Consensus model).

1.4.4 NMR-based methods

Various NMR methods have been developed in the past. In 1986, N. Muller devised a ^{19}F NMR method for the log*P* measurement of aliphatic fluorinated alcohols.[86] This method relied on the comparison of the height of the compound's signal in the ^{19}F NMR spectra to their respective fluorinated signal in three standard solutions. In the case of the non-fluorinated alcohols, their ^{1}H signals were obscured by octanol. Thus, a benzyl-alcohol/water solvent system was used, and a calibration curve was acquired utilizing literature log*P* values based on an octanol/water system, allowing for the novel log*P* measurement of other alcohols in this study. Kitamura and co-workers were able to relate the ^{19}F spin-lattice relaxation time (T_1) of triflupromazin to the concentration of lecithin small unilamellar liposome (mimicking lipid environment) without layer separation to obtain a partition coefficient.[87] This study relied on the exchange rate of the substrate between the

water and liposome layer to be fast on the ^{19}F NMR time scale,[88] allowing for their correlation equation to operate. Another publication from Kitamura *et al*., determined the lipophilicity of three fluorinated drugs *via* the correlation of the difference in the ^{19}F NMR chemical shift, at varying concentrations of phosphatidylcholine bilayer.[89]

In 2010, Mo *et al*. reported a deuterium-free ^{1}H NMR method for the determination of lipophilicity, based on shake-flask.[90] The water and *n*-octanol partitioning solvents were used as the native references, with neat proton concentrations of 110.7 M and 114 M respectively, allowing for the determination of the concentration of the measured compound. This method however requires both robust solvent suppression and small angle pulse excitation, which are not typical experiments for a multiuser open-access NMR facility. Furthermore, the scope of their recorded compounds is limited, as the chemical shifts are required to not be obscured by *n*-octanol signals, resulting in many aliphatic substrates being unmeasurable.

More recently, other ^{1}H NMR based methodologies for the determination of log*P* based on the shake-flask principle have been published. Soulsby and Chica[91] developed a procedure utilizing CRAFT[v] software, to analyse the ^{1}H NMR spectrum of both the water and *n*-octanol aliquots after the partitioning experiment, with no internal standard required. Herth *et al.*[92] and Rucker *et al.*[93] both published similar methods allowing the lipophilicity partitioning experiment to be performed in an NMR tube. It is important to point out that Rucker's method was developed with the use of a benchtop low-field NMR, and with an educational setting in mind. Both methods had an exact amount of solute dissolved in water and the ^{1}H NMR spectrum recorded. The corresponding solute integral is then compared to the integral of the water signal and an exact amount of octanol is added. The NMR tube is then inverted numerous times and allowed to equilibrate before another ^{1}H NMR spectrum is recorded. The solute integral again is compared to the water integral allowing for a ratio of concentrations to be established, and with some further calculations the log*P* is obtained. Herth established his procedure on a variety of aromatic and aliphatic analytes, whilst Rucker demonstrated his procedure on entirely aliphatic alkanols and solvents, both to great success when compared against literature values. Overall, both methods established a simple log*P* determination method utilizing ^{1}H NMR with easy sample preparation and minimal NMR expertise required for analysis. However, neither procedures accounted for the ~4% solubility of H_2O in octanol, which may affect accurate concentration ratios, although Rucker did mention it briefly.

[v] CRAFT – Complete Reduction to Amplitude-Frequency Table. Available on VnmrJ4.2 (Agilent Technologies) and Assure NMR 2.1™ (Bruker).

Finally, the two methods offered limited log*P* windows: Herth between +0.7 and +3.3 and Rucker with -1 and +1.

Recently, the Linclau group has developed a new method for log*P* determination, which is also based on the shake-flask method, utilizing ^{19}F NMR spectroscopy (Figure 1.2).[94] The method works by using a mixture of an internal reference compound with a known log*P* and an unknown compound which are partitioned between (non-deuterated) octanol and water. An aliquot of each phase is transferred to an NMR tube and its ^{19}F NMR spectrum is taken. The intensity of the subsequent signals in the ^{19}F NMR spectrum relate to the number (n) of fluorine atoms present on the molecule, as well as the compound concentration (C). The integration ratio between the reference compound (R) and the compound being measured (A) is defined as r_o (octanol phase, Eq. 6) and r_w (water phase, Eq. 7). The ratio of the partition coefficient (P) for both A and R is equal to the ratio of the *r* values (r_o/r_w) and relates to the ratio of the respective concentrations (Eq. 8). This results in Eq. 9 and with the log*P* of the reference compound, the log*P* of the unknown compound can be determined.

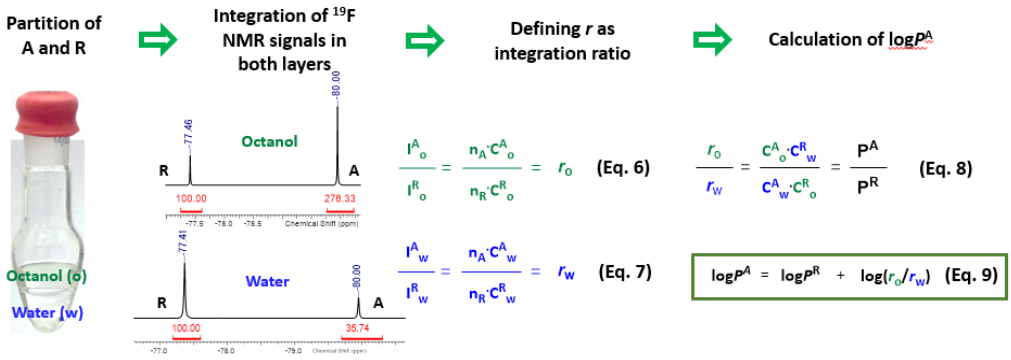

Figure 1.2 - Principle of the log*P* determination method. Adapted from *Ref*[94]

Numerous practical advantages in the application of this method are derived from a compensation effect, inherent to the determination of a ratio of a ratio. This allows systematic errors to be eliminated and that no quantitative measurements are required for the reference or measured compound used, solute volumes or the amount taken for the NMR aliquot. Fluorinated impurities present in the experiment from either the reference or measured compound are also tolerated, provided that they do not overlap or interfere with the accurate integration of the signals of interest. Overall, this method allows for the determination of fluorinated aliphatic (non-UV-active) alkanols and carbohydrates in a log*P* window of ±3.

1.5 Overview of Fluorine Chemistry

One of the first examples of the use of fluorination within medicinal chemistry, is the approval of the first fluorinated drug Fludrocortisone (Figure 1.3).[72] The fluorinated analogue demonstrated excellent potency of more than a factor of 10 when compared to its parent compound hydrocortisone. Subsequent advancements in fluorination techniques and the commercial availability of many fluorinated building blocks[95] has allowed for organofluorine applications within agriculture, polymer and pharmaceutical industries to flourish.[96-98] Traditionally, natural products have been a source of bioactive molecules,[99] therefore it is intriguing that roughly 20% of newly approved pharmaceutical drugs contain at least one fluorine atom,[97] when fluorinated natural products are almost non-existent (only 7 examples).[100] Some examples of commonly used fluorinated drugs include Prozac® (antidepressant) and efavirenz (antiviral).[95]

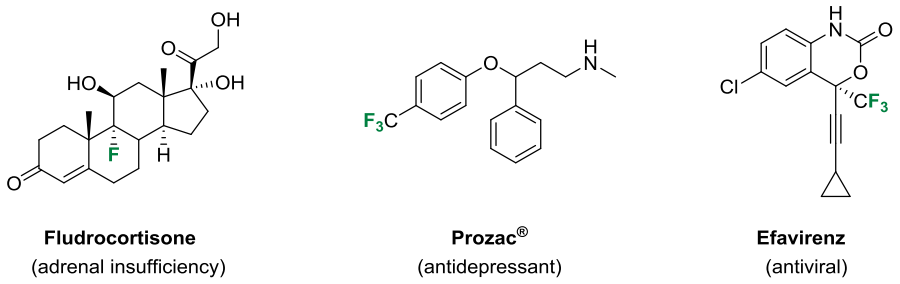

Fludrocortisone (adrenal insufficiency) **Prozac®** (antidepressant) **Efavirenz** (antiviral)

Figure 1.3 - Fludrocortisone, Prozac® and efavirenz.

The extensive use of fluorination within drug discovery programs owes the resulting impact on various physiochemical and pharmacokinetic properties, which can be used to improve the pharmacological profile of a drug candidate.[101] A fluorine atom is a commonly used bioisosteric replacement for a hydrogen atom due to its small size.[102] The high strength of the C-F bond further allows for the modulation of key properties, such as the molecular conformation and the metabolic stability of the molecule.[102] As a result of fluorine's high electronegativity, it also has the ability to influence the acidity or basicity of neighbouring functional groups.[95] Fluorination typically results in an increase in acidity for carboxylic acids and conversely a decrease in basicity for amines (Figure 1.4). In the past, it was commonly believed that "fluorination always increase hydrogen bond acidity", due to fluorine's strong inductive effect.[103] However, the Graton group, utilizing FTIR spectroscopy, reported a series of conformationally restricted monofluorinated cyclohexanols, which demonstrated a reduction in hydrogen bond acidity for certain substrates.[104] This was reported to be a result of competing intramolecular F···HO interactions.

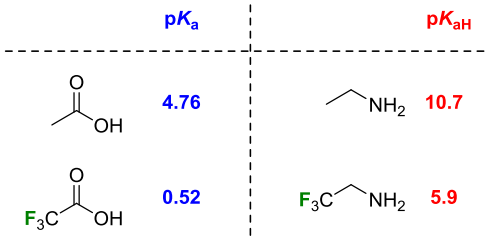

Figure 1.4 - The effect of fluorination on pK_a and pK_{aH} values, adapted from *Ref*[103]

Fluorination has also had a large role in the development of positron emission tomography (PET).[95, 101] This is a result of the half-life of [^{18}F] (110 min) being considerably longer than other frequently used radioactive nuclei. This relatively long half-life tolerates its use in multi-step synthesis, which can allow the incorporation of [^{18}F] into complex drug molecules while allowing for same day imaging.[101] The imaging performed with [^{18}F] provides the ability to determine the distribution and targeting of the drug, as well as providing metabolic information.[95, 101]

In the following section, the impact of fluorine on lipophilicity will be described in greater detail, due to the relevance of the topic to this thesis.

1.6 The effects of fluorination on lipophilicity

As previously discussed, lipophilicity plays an important role within drug discovery programs through its ability to impact ADMET processes.[1-2, 8, 10] Therefore, the ability to easily influence lipophilicity through chemical modification is an attractive strategy. In the past, fluorination has been observed as a tool that can be used to modulate the lipophilicity of a molecule.[95, 103] Statistical analysis reveals that on average, lipophilicity increases by roughly 0.25 log*D* units when a fluorine atom is substituted by a hydrogen atom.[105] However, this is most likely because of the prevalence of fluoroaryl substrates being taken into account.[106] The increase in lipophilicity for fluoroaryl substrates occurs because of the decrease in polarisability of the aromatic π-system due to the fluorine inductive effect. Conversely, hydrogen to fluorine exchange in aliphatic compounds can lead to a decrease in lipophilicity (Figure 1.5).[86, 105] This reduction in log*P* can be attributed to the polarity introduced into the molecule upon fluorination *via* the strong inductive effect of fluorine.[107]

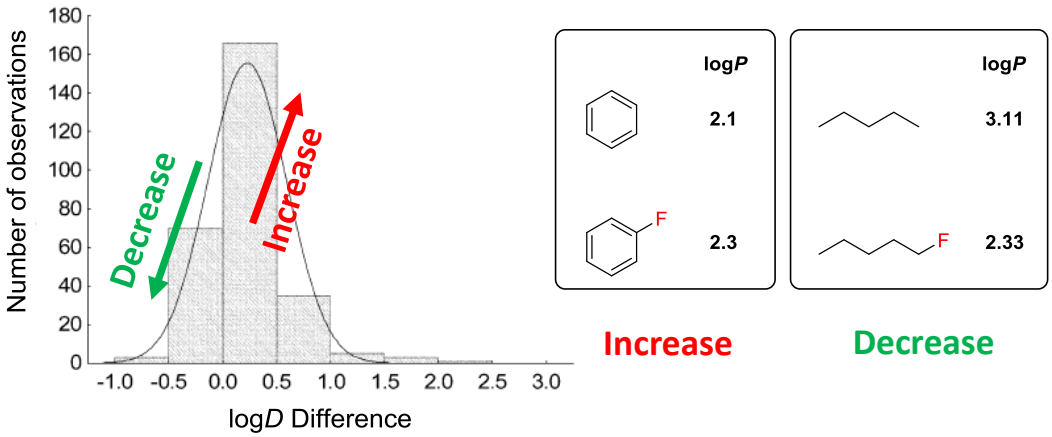

Figure 1.5 - Effect on lipophilicity on the substitution of a hydrogen atom with a fluorine atom, adapted from *Ref*[105] and log*P* values of selected fluorinated compounds[108]

Apart from the aforementioned depolarisation of the aromatic π-system due to the fluorine's electronegativity, other effects that impact lipophilicity include an increase in polarity due to the C-F bond dipole moment, and an increase in hydrophobic surface area as a result of fluorine being larger in size than a hydrogen atom.[103, 109] Therefore as a general rule of thumb, for apolar compounds the effects of fluorine's polarity tends to dominate and fluorination will tend to result in a decrease in lipophilicity, whilst the inverse is observed for polar molecules, due to the increase in hydrophobic surface area being the dominant effect.

Müller *et al.* have published an experimental insight into this, comparing the changes of local hydrophobic surface area (volume) and polarity of fluorinated *N*-propyl indole derivatives (Figure 1.6).[110] This study used simplified bond vector analysis to identity the polarity changes between fluorinated motifs. It was observed that despite the calculated polarity of the difluorinated motif (1.97 D) being higher than that of the monofluorinated motif (1.85 D), it is the monofluorinated motif that had a (slightly) lower log*P* (0.1 log*P* units). It is suggested that this polarity increase from the introduction of the 2nd fluorine is compensated by the concomitant volume increase, thus resulting in the slight increase lipophilicity. Therefore, across the series, aliphatic fluorination resulted in a decrease in lipophilicity following the trend, $RCH_3 > RCF_3 >> RCHF_2 \sim RCH_2F$. Following this, Müller *et al.* observed that *vic*-difluorination exhibited a considerably lower log*P* value than its *gem*-difluorination equivalent.[111] Through the use of vector bond analysis of the *vic*-difluoro motif, this was attributed to its much larger dipole moment in comparison to the *gem*-difluoro motif.

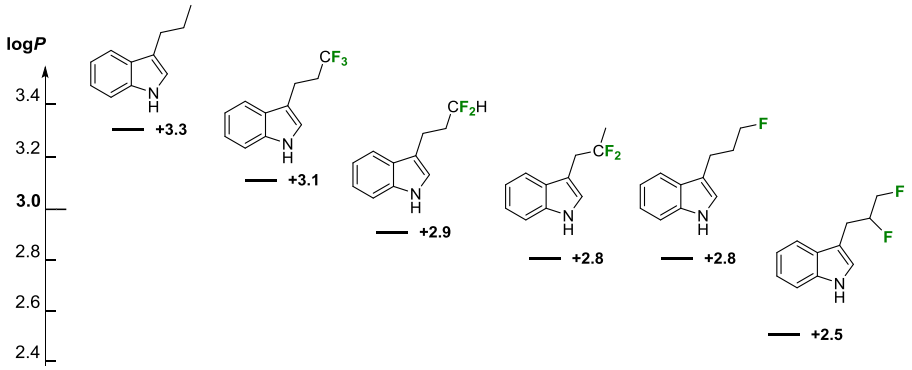

Figure 1.6 - Log*P* of fluorinated *N*-propyl indole analogues[110, 112]

The influence of fluorination on aliphatic lipophilicity is further complicated by the log*P* of the parent compound and the presence of functional groups.[86] An example of this is illustrated in Figure 1.7, where the terminal trifluorination of ethanol, propanol and butanol leads to an increase in lipophilicity as their respective parent compounds are relatively polar. This results in the hydrophobic nature of the CF_3 motif dominating. As the parent compounds become larger and more lipophilic the hydrophobicity introduced through the CF_3 motif is observed less and the polar nature of the motif takes precedence, resulting in the terminal trifluorination of pentanol and hexanol leading to less lipophilic compounds.

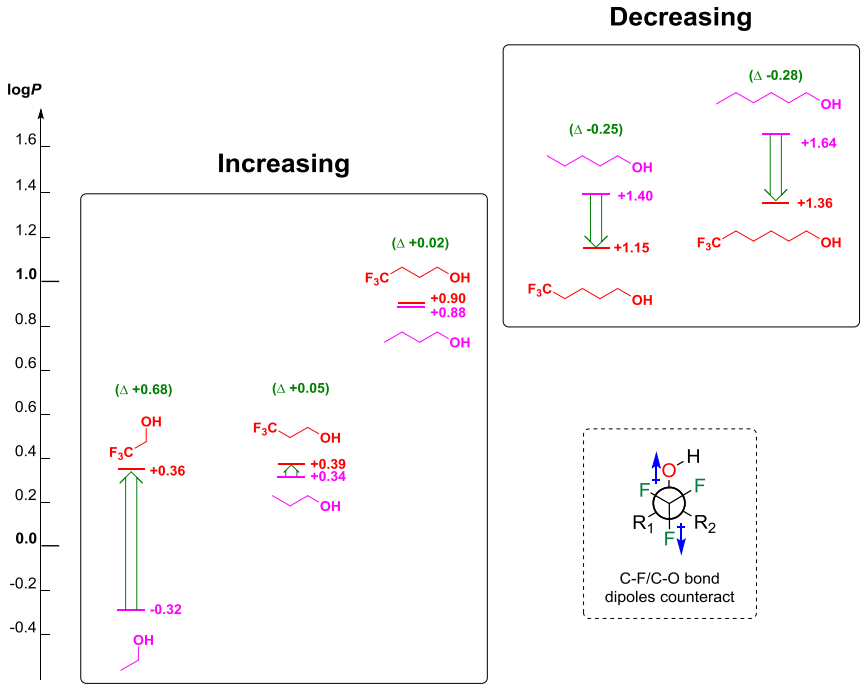

Figure 1.7 - Effects CH_3/CF_3 exchange at varying distances from an alcohol moiety[86]

The surprisingly large increase in lipophilicity for trifluoroethanol when compared to its parent compound ethanol, can be explained through an anti-periplanar orientation which the C-O/C-F bond adopt, allowing for a counteraction of dipole moments, resulting in a reduced effect from the

polarity of the CF_3 group. This results in the hydrophobic nature of the CF_3 group dominating, causing a large increase in lipophilicity. In addition, the strong inductive effect of the CF_3 motif also results in an increase in ethanol's lipophilicity, due to its ability to reduce the polarisability of the neighbouring oxygen's lone pairs.[86]

Another excellent example which displays the importance of the log*P* of the parent compound, is a series of fluorinated ethyl ester proline derivatives (Figure 1.8).[113] Here, the standard lipophilicity pattern of $RCF_3 > RCHF_2 > RCH_2F$, is consistent with previously published results.[94, 110] However, unlike Müller's work on fluorinated *N*-propyl indole derivatives,[110] neither the difluoro- or trifluoroethyl ester observed a decrease in lipophilicity. Instead they exhibited Δ log*P* values similar to their corresponding ethanol analogues.[114] This occurred because the parent compound **1.1** (log*P*= 0.0), is considerably more polar than Müller's *N*-propyl indole parent compound (log*P*= +3.3, Figure 1.6),[110] therefore the polarity introduced by the fluorinated motifs was less important and the impact of fluorine's hydrophobicity dominated. For these examples, C-O/C-F bond dipole counteractions must also be considered due to the proximity of the fluorinated motif to the neighbouring functionality, which results in a large logP increase for **1.4** (Δlog*P* +0.55) in a similar fashion to trifluoroethanol vs ethanol (Δlog*P* +0.68).

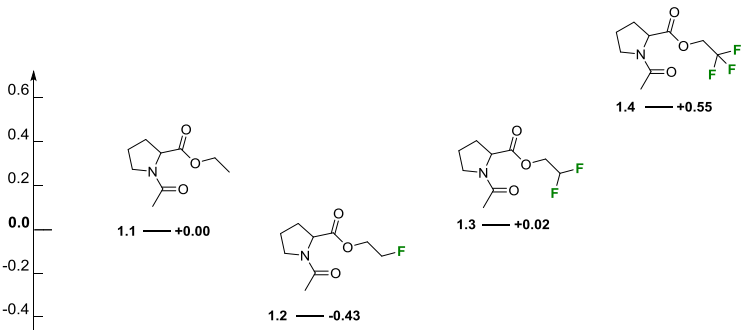

Figure 1.8 - Effects of fluorination on polar molecules

As previously mentioned in Section 1.4.4**,** the Linclau group recently published a paper on a novel ^{19}F NMR based log*P* determination procedure, which also described the effects of fluorination on the lipophilicity of alkanols and carbohydrates.[94] A series of selected fluorinated alkanols and their respective log*P* values from the ethanol, propan-1-ol, butan-2-ol and the petantan-2-ol family can be seen in Figure 1.9. In all cases, monofluorination resulted in the largest log*P* decrease in comparison to their respective parent compound, regardless of the position of fluorination. The *gem*-difluoro motif was then observed to be more lipophilic than the monofluorinated alkanols and more polar than the trifluorinated motif. The *gem*-difluoro motif also resulted in a more polar molecule in respect to its parent compound in all cases, with the exception for ethanol, where a slight increase in lipophilicity was observed (Δlog*P* +0.01). This is a result of the proximity of the *gem*-difluoro motif to the hydroxyl functionality. In accordance to Muller's log*P* results

trifluorination resulted in an increase in log*P* within both the ethanol and propanol family.[86] Within the butan-2-ol family a slight decrease in log*P* was observed (Δlog*P* -0.04), which is likely due to the polarity of the CF_3 motif taking precedence over its respective hydrophobicity on a more lipophilic parent compound. Finally, the pentafluoronated motif was the most lipophilic within their respective families: this is a result of an increase in hydrophobic surface area that accompanies high degrees of fluorination.

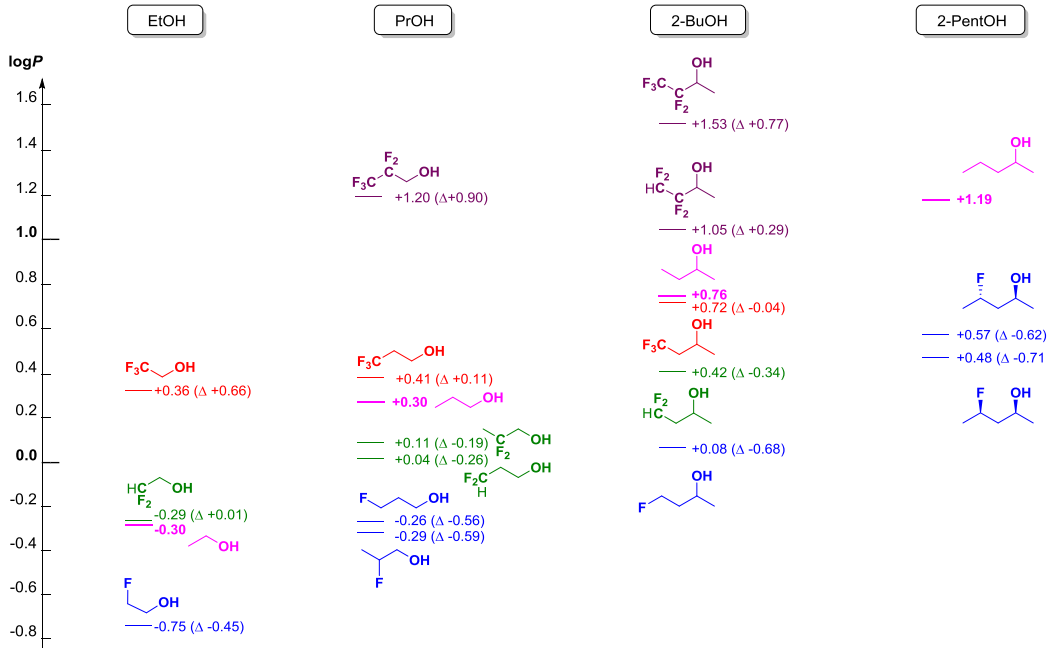

Figure 1.9 - Log*P* values of selected fluorinated alkanols, adapted from Linclau *et al*.[94]

Due to the sensitivity of their ^{19}F NMR based log*P* determination method, Linclau *et al*.[94] were able to determine the log*P* values of a pair of monofluorinated pentan-2-ol diastereoisomers (Figure 1.9).[94] A small log*P* difference (Δlog*P* +0.09) between the two was observed and the *anti*-isomer is the more lipophilic of the pair. It is assumed that within the water layer, that the most polar conformation with aligned C-O/C-F bond dipoles is more stable for the *syn*-isomer than for the anti-isomers (Figure 1.10). This presumably results in the most polar conformation having a higher population for the *syn*-isomer in the water layer, thus resulting in a lower log*P* value.

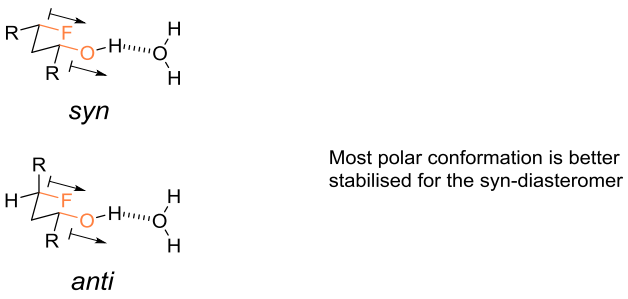

Figure 1.10 - The most polar conformation adoptable by the syn- and anti-isomer

In the same publication, the Linclau group also studied the impact of fluorination on conformationally restricted cyclohexanols, seen in Figure 1.11.[94] The β-monofluorination of parent compound **1.1** resulted in a reduction of log*P* by roughly 0.5 units for both the equatorial and axial analogues. Interestingly, the first example of an increase in log*P* from aliphatic monofluorination was observed for the vicinal *trans* fluorohydrin **1.5**. This unexpected increase in lipophilicity was explained through the unavoidable C-O/C-F bond dipole counteractions, resulting in a more lipophilic molecule in comparison to its parent compound **1.4**. In a similar fashion, the alignment of the C-O/C-F bond dipoles for 1,3-diaxial alkanol **1.6**, resulted in a large decrease in log*P* when compared to its parent compound **1.4**.

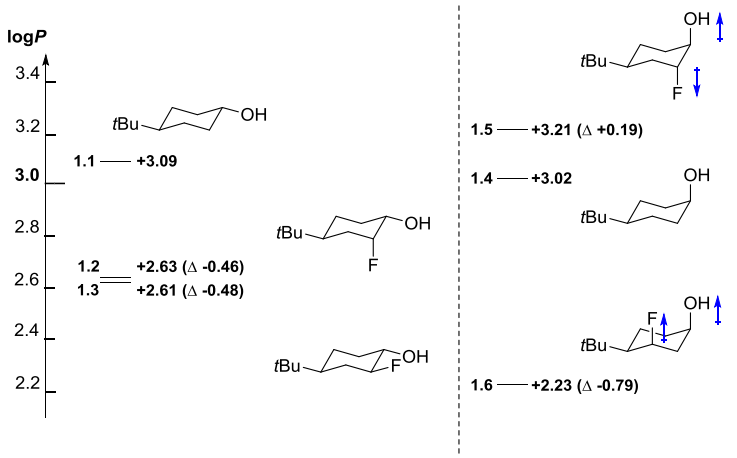

Figure 1.11 - Monofluorination of conformationally restricted cyclohexanol systems. Adapted from *Ref*[94]

Carreira and Müller have also recently published work assessing the effects of fluorination on log*P* and other medicinal properties of pharmacologically relevant compounds.[115] This was achieved by the introduction of various fluorinated motifs into the *N*-propyl chain of ropivacaine, and the *N*-butyl chain of levobupivacaine (Figure 1.12). Their results differ slightly from their previous lipophilicity pattern observed of RCH_3 > RCF_3 >> $RCHF_2$ ~ RCH_2F on their *N*-propyl indole series,[110] which is likely a result of the proximal nitrogen atom to the fluorinated motifs. They instead observed that gem-difluorination resulted in a noticeable increase in lipophilicity in comparison to their respective monofluorinated analogues, as well as an increase in lipophilicity from the non-fluorinated parents to the CF_3 motif. In this publication, they also report the log*P* of various *vic*-difluorinated diastereoisomers, although little difference (~0.1 log*P* units) or no difference in lipophilicity was observed.

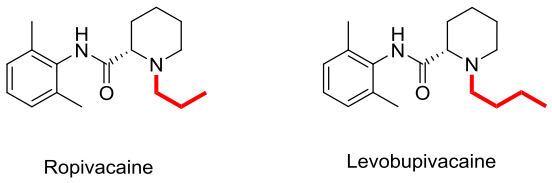

Figure 1.12 - Ropivacaine and levobupivacaine

Recently, O'Hagan published the synthesis of a novel α,β,β-trifluorocyclopropane motif and its respective log*P* value which were compared to similar aryl derivatives (Figure 1.13).[116] Pleasingly, it was observed to have a reduction in log*P* in comparison to its non-fluorinated parent, resulting in the identification of another novel log*P* lowering motif. This is believed to be the result of the fluorine's ability to polarise their neighbouring hydrogens on the cyclopropyl substituent.[116] Interestingly, despite containing two additional carbon atoms, the α,β,β-trifluorocyclopropane motif exhibits the same log*P* value as trifluorotoluene, which suggests that this novel motif could be used as a larger substituent while having the ability to maintain the same lipophilicity.

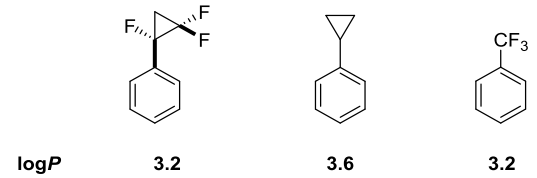

Figure 1.13 - Log*P* of selected aryl derivatives similar to the α,β,β-trifluorocyclopropane motif

1.7 Aims of the project

1.7.1 The investigation of aliphatic fluorination on lipophilicity

Our aim is to synthesise a wide range of novel fluorinated alkanols in order to measure their respective log*P* values using the novel ^{19}F NMR based technique developed by the Linclau group.[94] This will allow for the expansion of the fluorinated alkanol library already obtained by the group. In particular, due to the growing concern of "molecular obesity" within drug discovery programs, the identification of novel fluorinated motifs which reduce the log*P* of the molecule is a high priority for this research.

Furthermore, given that lipophilicity is influenced by both the relative position of a fluorinated motif to a functional group, and also by the actual log*P* of the non-fluorinated substrate itself, it is difficult to compare the same or differing motifs on different "parent" substrates. Hence one of our aims is to prepare "families" of fluorinated analogues based on a few "parent" non-fluorinated compounds, to compare certain motifs at different distances from the functional group.

For example, the *gem*-difluoro family of butan-2-ol will be performed (Figure 1.14). This would allow for an investigation into the effects of α-, β- and γ-difluorination on log*P*. A series of trifluorinated matched pairs will also be synthesised and their respective logP values measured, selected examples of which can be seen in Figure 1.15.

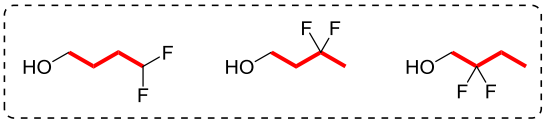

Figure 1.14 - *Gem*-difluorinated butan-1-ol family

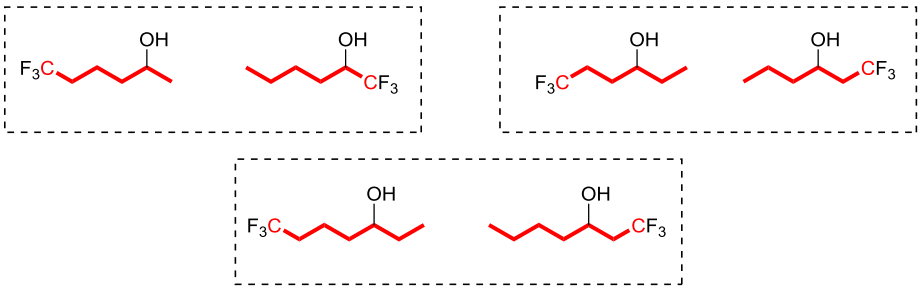

Figure 1.15 - Selected CF_3 matched pairs

As the key topic of this thesis is the influence of aliphatic fluorination on lipophilicity. This will be discussed first, prior to the synthesis of the fluorinated alkanols measured in the chapter.

1.7.2 Investigation of the effects of aliphatic fluorination on a drug scaffold

A common concern with the investigation of fluorination on lipophilicity on simple model alkanols is whether these same trends will be observed on more complex molecules. Therefore, the investigation of whether these lipophilicity lowering trends translate directly from simple alcohols to more complex drug scaffolds is pivotal to the validation of this research. As a portion of this PhD research involves a short placement at AstraZeneca, a series of novel fluorinated alkanols with interesting log*P* results will be taken to their labs to study the effects of fluorination on log*P* and other ADMET properties when incorporated into a drug scaffold.

1.7.3 Measurement of the lipophilicity of amide rotamers

Amide rotamers have characteristically different properties, and since they frequently occur within drugs and other biological compounds, it is of interest to be able to measure or calculate the log*P* values of their different conformations. Unfortunately, the determination of the concentration of rotamers in solution is not straightforward. However, amide rotamers are in slow exchange on the NMR time scale, therefore they are distinguishable *via* NMR, including ^{19}F NMR. We propose to use our ^{19}F NMR based log*P* determination method to measure the log*P* of the individual *cis* and *trans* amide rotamers.

The methodology will be illustrated using simple *N*-acetylated compounds, for example fluoropiperidines and fluoropyrrolidines **1.1**-**1.4** (Figure 1.16), before more complex rotamers or other distinguishable conformers are taken into consideration.

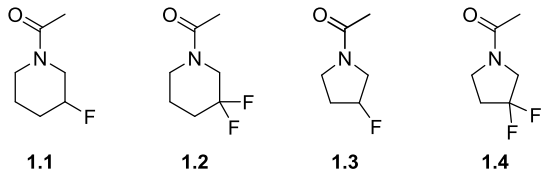

1.1 **1.2** **1.3** **1.4**

Figure 1.16 - Target *N*-acetylated fluoropiperidines and fluoropyrrolidines

Chapter 2 Influence of Aliphatic Fluorination on Lipophilicity

2.1 Introduction

Using the ^{19}F NMR based log*P* determination methodology previously developed and optimized by the group,[94] the lipophilicity of a series of novel fluorinated alkanols was measured. This chapter will include the discussion of the effects monofluorination, difluorination and trifluorination at varying distances from the hydroxyl group on lipophilicity. In addition, the lipophilicity of a range of novel and previously reported fluorinated motifs will also be discussed.

In order to properly assess the effects trace impurities or solvent residues may have on the log*P* procedure, a series of log*P* measurements will be performed with the addition of various common solvents. Previous work performed by Herth *et al*.[92] on the development of a novel ^{1}H NMR based log*P* determination procedure, used D_2O instead of H_2O. With this consideration a small study into the effects of using D_2O in place of H_2O for our ^{19}F NMR based method was performed. If no difference between the two is observed it could allow the group to measure non-fluorinated aliphatic parent compounds by ^{1}H NMR, for comparative studies in the future.

Specific terminology that is used throughout this chapter is defined as follows:

- Parent – The non-fluorinated substrate of a series.
- Family – The whole collection of fluorinated analogues of a given parent, e.g. the pentan-1-ol family.
- Series – A sub-part of members of a family in which logP is compared, e.g. the pentan-1-ol CF_2 series.
- Motif – A particular fluorination pattern.
- Matched Molecular Pairs – Part of a series where two of the same motifs are compared, e.g. the pentan-2-ol CF_3 pairs.

The lipophilicities of alcohols within a Family or Series that had been determined by other members of the group,[94] or that were available in the literature, are also shown in order to provide a picture as complete as possible. All log*P* values underlined and bolded are novel values. Unless mentioned otherwise, all measured compounds were either commercially available or their synthesis will be discussed later in this thesis.

2.2 The influence of simple fluorinated motifs on lipophilicity

2.2.1 Monofluorination

As expected, (Figure 2.1), monofluorination of acyclic alkanols results in a decrease in lipophilicity when compared to their respective parent compound. This decrease in lipophilicity can be quite substantial in some cases (**I2** and **I3**, Δlog*P* -0.99). The β-monofluorination analogues **E2**, **G4**, **H6** and **I10** (with the exception of the PrOH family), all have the highest log*P* values within their respective families. This is explained by the proximity of the fluorination site to the hydroxyl group, resulting in a reduction in polarizability of the oxygen lone pairs, as well as a possible conformation where the C-O/C-F dipoles counteract (See Chapter 1, Section 1.6). Increasing the distance between the fluorine and alcohol functionality results in a greater reduction in lipophilicity (c.f. BuOH family and PentOH family).

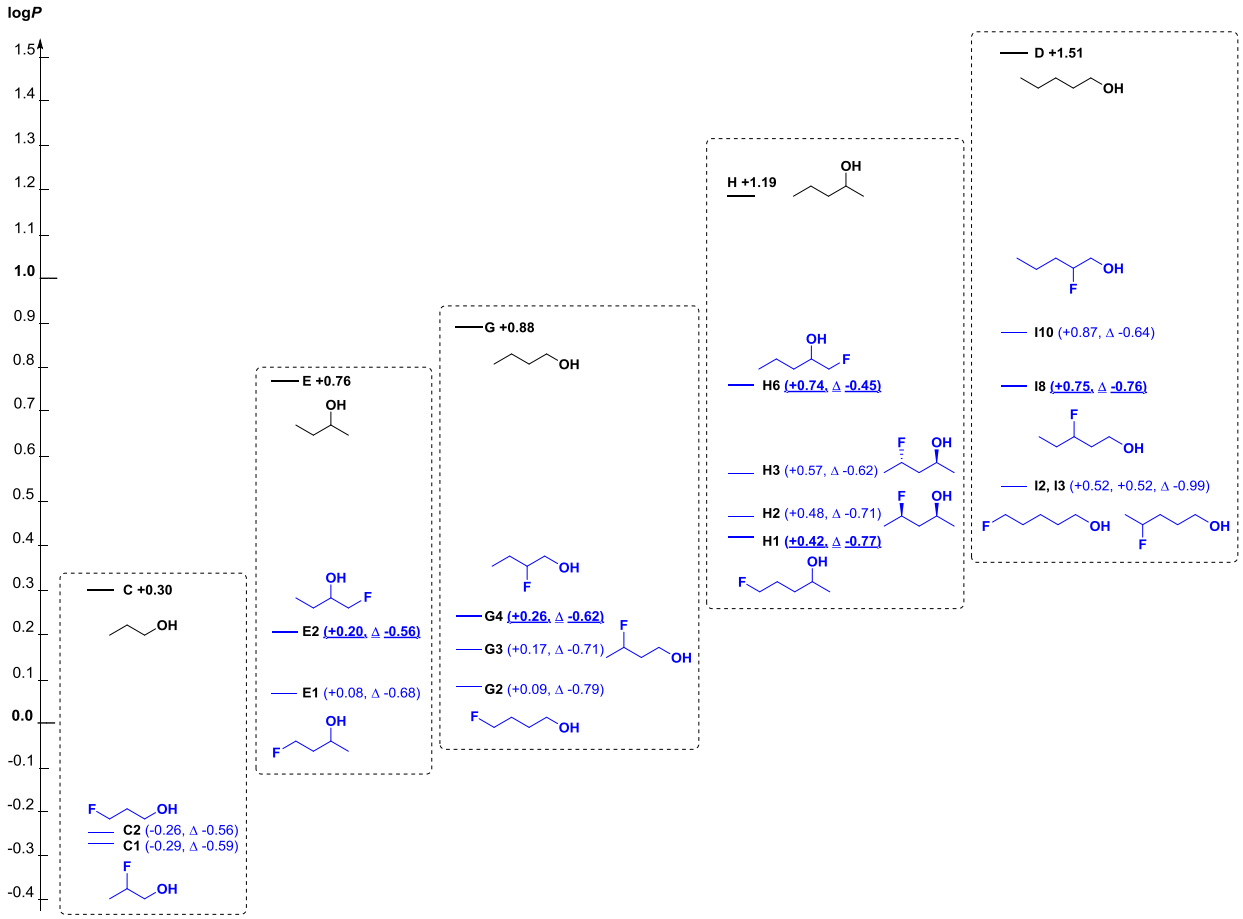

Figure 2.1 - Effects of monofluorination[vi]

[vi] Compound **H6** was synthesised by a previous PhD student Joseph Watts

2.2.2 Difluorination

As shown in Figure 2.2, the incorporation of a *gem*-difluoro moiety results in a reduction of lipophilicity in comparison to their respective parent compound, with the exception of 2,2-difluoroethan-1-ol (Δlog*P* +0.01, not shown), and in a similar fashion to monofluorination the lipophilicity decrease progressively increases with fluorination further from the alcohol group. Indeed, the β-difluorination analogues **C4**, **G11**, **H7**, **H8** and **I14** all have the highest log*P* values within their respective families. In the 2-PentOH family, the internal β-difluorination **H7** causes a larger log*P* decrease compared to its terminal counterpart **H8**, but the influence of the log*P* of the parent compound appears limited, with only a faint trend towards enhanced log*P* reduction with increasing lipophilicity of the parent alcohol. There was little difference in the log*P* between **I6** and **I7** of the PentOH family, **H4** and **H5** of the 2-PentOH family, and **G6** and **G8** in the BuOH family. This suggests that there will be little difference in the log*P* for substrates with γ-difluorination and beyond.

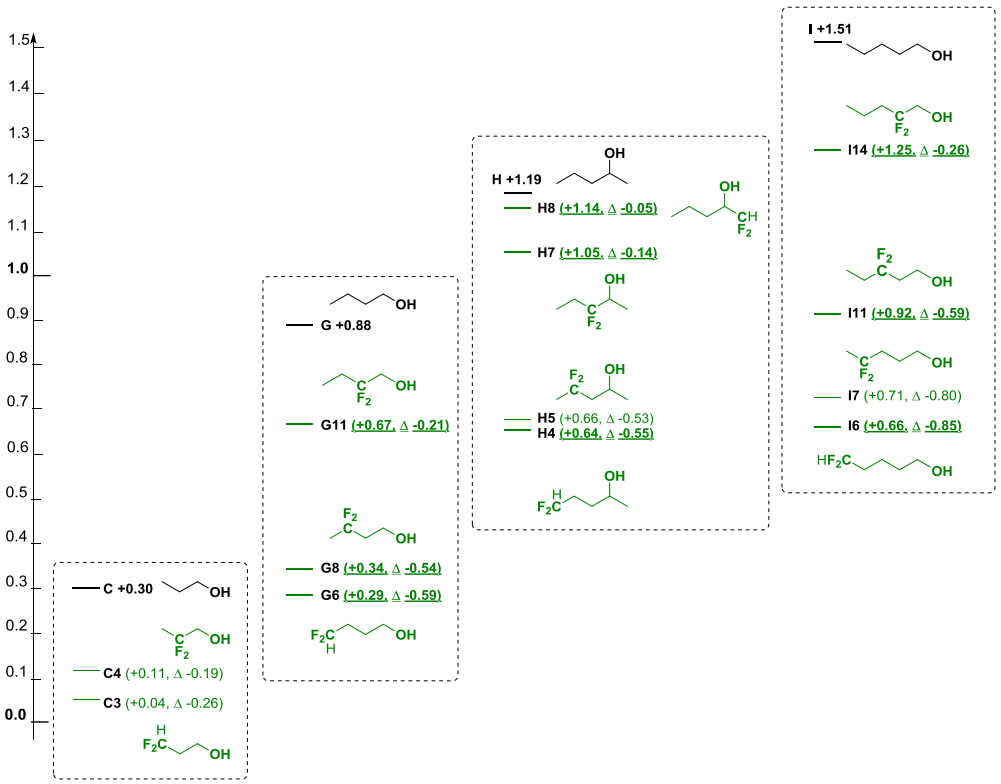

Figure 2.2 - Effects of difluorination[vii]

[vii] Compound **H8** was synthesised by a previous PhD student Joseph Watts

2.2.3 Mono- and difluorination "Matched Pairs"

The use of matched pairs allows for the comparison of the same motif with the same parent compound. This allows for the improved analysis of the effects of fluorination at varying distances from functional groups. As previously discussed (See Section 2.2.1 and 2.2.2), β-mono- and β-difluorination are the most lipophilic within their respective families. This is best showcased in Figure 2.3, through the comparison of ω-monofluorination vs. β-monofluorination within the butan-2-ol family (**E1 → E2,** Δlog*P* +0.12) and the pentan-2-ol family (**H1 → H6**, Δlog*P* +0.32)**.** The same can trend can be observed when for δ-difluorination vs. β-difluorination, within the pentan-2-ol family (**H4 → H8**, Δlog*P* +0.50). As previously discussed in Chapter 1 Section 1.6, β-fluorination exhibits a higher log*P* value, because of the C-F/C-O dipole compensation effect, as well as the reduction in polarizability of the neighbouring oxygen lone pairs.

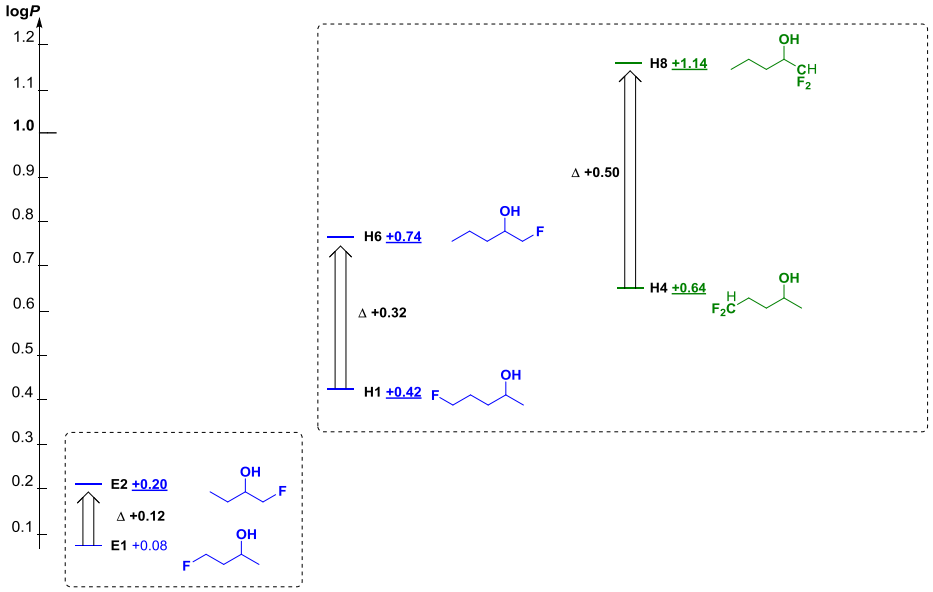

Figure 2.3 - Mono- and difluorinated matched pairs

2.2.4 Trifluorination

Trifluorination can modulate lipophilicity in either direction, depending on the log*P* value of the parent compound and the position of the CF_3 motif in relation to the alcohol group, as discussed in Chapter 1 Section 1.6. With this in mind, an investigation into the effect of CH_3/CF_3 exchange at varying distances from a hydroxyl group on log*P* was performed, with a greater scope of substrates.

As shown in Figure 2.4, alcohols containing an α-trifluoromethyl group exhibit a reasonably consistent increase in lipophilicity when compared to their respective parent compounds. This is consistent with results previously reported by N. Muller.[86] This is rationalised by a compensation of dipole moments, as well as a reduction in the polarizability of the oxygen's lone pairs, previously

discussed in Chapter 1 Section 1.6. This allows for the hydrophobic nature of the CF_3 motif to dominate, thus leading to an increase in lipophilicity. Pleasingly, the same trend was observed when a trifluoromethyl group was already present elsewhere in the molecule. An example of this is **K1**, where an α-CH_3/CF_3 exchange affording **K2** resulted in an increase in lipophilicity (Δlog*P* +0.62) similar to previously observed values.

It was also initially proposed by the group that the impact of an α-trifluoromethyl group was independent of the parent compound and increased the log*P* by roughly 0.65 units (**A → A3**, **B → B3**, **D → D1** and **H → H10**).[94] This is still the case, with the difference between **K1 → K2** (Δlog*P* +0.62) and **K → K3** (Δlog*P* +0.57) close to the value. However, the difference observed between **E → E8** (Δlog*P* +0.49) was slightly smaller.

When performing a second α-CH_3/CF_3 exchange (**D1 → D2** and **B3 → B4**), a further log*P* increase of roughly 1 unit was observed. Hence, double α-CH_3/CF_3 (**D → D2** and **B → B4**) exchange resulted in a dramatic log*P* increase of roughly 1.7 units. All of these results suggest that an increase in lipophilicity will always be observed when performing an α-CH_3/CF_3 exchange.

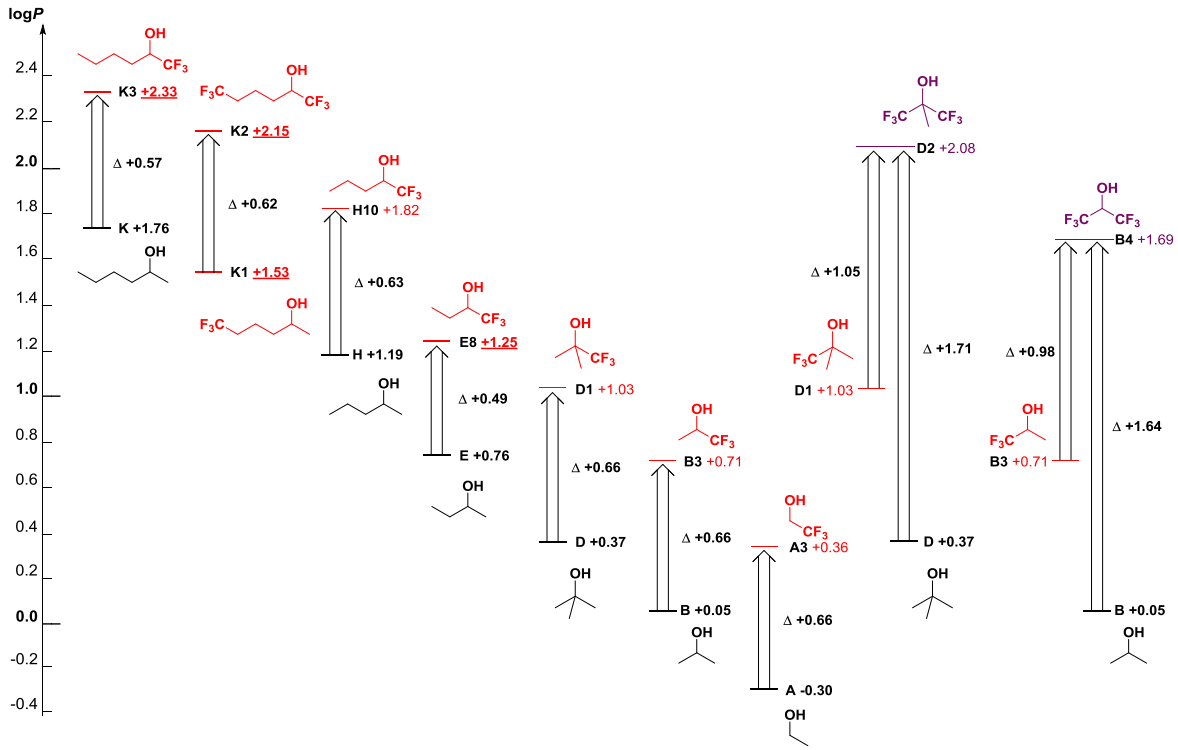

Figure 2.4 - α-CH_3/CF_3 exchange

While the impact of the α-CF_3 motif on lipophilicity was well established within the Linclau group[94] and Muller had already examined the effect of trifluoromethylation on primary alkanols,[86] there were only limited examples of secondary alcohols with a β-, γ- and δ-trifluoromethyl group, which were thus investigated here. For substrates with either a β- or γ-CF_3 motif (Figure 2.5), a small

increase in lipophilicity was observed in comparison to their respective parent compounds (with the exception of **E → E6,** Δlog*P* -0.04). In the case of the β-CF_3 group, the Δlog*P* values are quite similar in relation to increasing the log*P* of the parent compound. The inverse can be observed for γ-CH_3/CF_3 exchange, where the Δlog*P* values increase for the more lipophilic parent compounds.

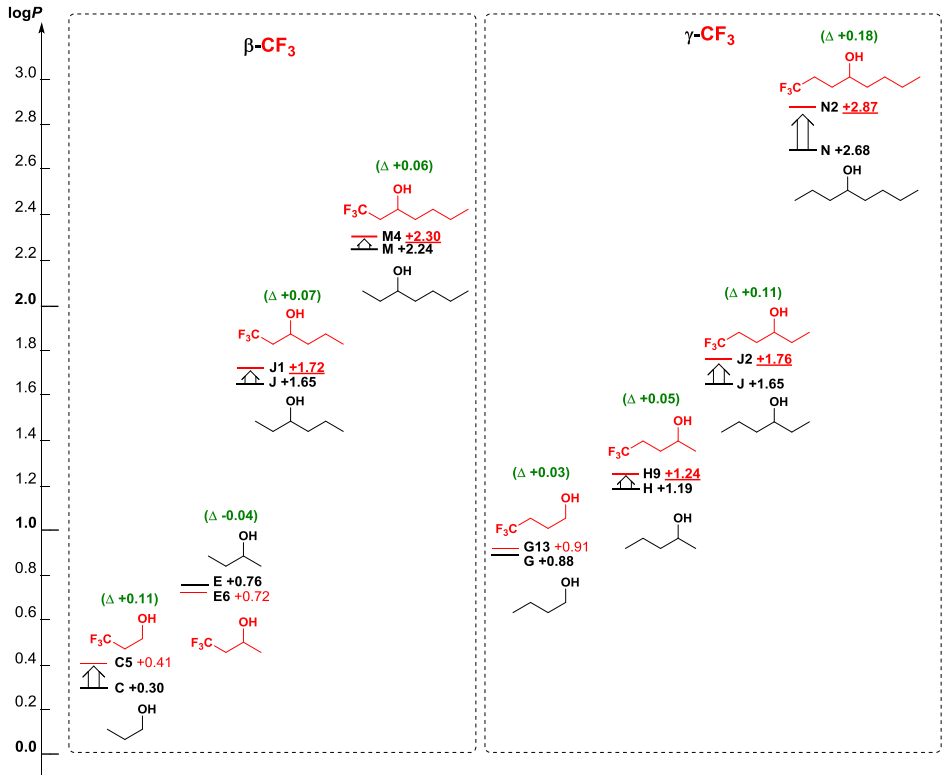

Figure 2.5 - β-CF_3 and γ-CF_3 alcohols

Alcohols containing a δ-CF_3 all exhibited lower log*P* values than their parent compounds (Figure 2.6). However, with increasing log*P* values of the parent compounds, the reduction in lipophilicity decreased. This was surprising, normally as the parent compounds become more lipophilic and larger, the relative effect of the increase in hydrophobic surface decreases, and the impact of the CF_3-dipole increases. Hence, the inverse pattern would be expected: a larger Δlog*P* with increasing log*P* of the parent compound. Due to the distance between the δ-CF_3 and the hydroxyl group, any intramolecular interactions are expected to be minimal and thus little effect on the polarizability of the oxygens lone pairs is expected to occur. With this consideration, and with the increasing conformational flexibility of the alkyl chains, the effects of dipole moments must be important. Within the water phase, aligned dipole conformations are likely to have a greater population, while the reverse is expected in the octanol phase, and the increased conformational flexibility between the functional groups, i.e. small energy differences between conformers, may result in a

'chameleon' effect,[117] in which the conformer population is skewed in each phase according to its dielectric constant. This effect may be important the more lipophilic molecules become.

As observed beforehand with α-CH_3/CF_3 exchange, δ-trifluorination still results in a log*P* reduction when a trifluoromethyl group was already present elsewhere in the molecule. An example of this is **K3**, where an δ-CH_3/CF_3 exchange affording **K3**, resulted in a decrease in lipophilicity similar to previously observed values (Δlog*P* -0.18).

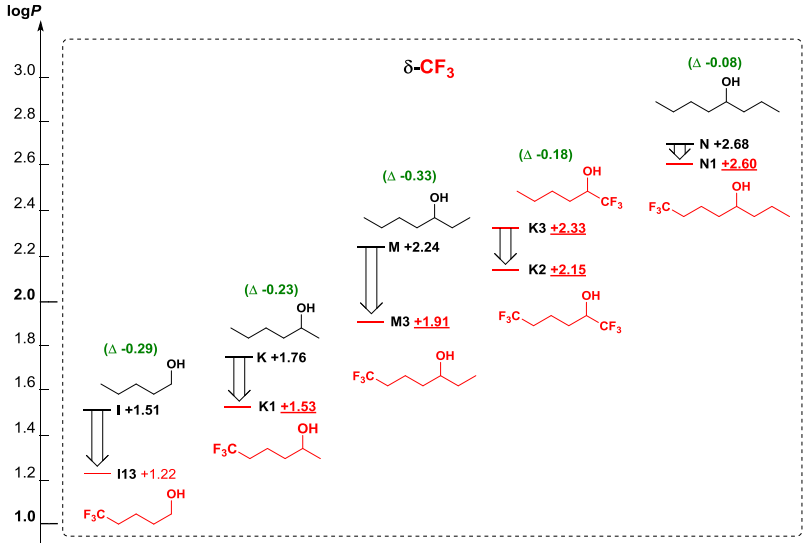

Figure 2.6 - The log*P* of δ-CF_3 alcohols

2.2.5 CF_3 "Matched Pairs"

The results in Figure 2.7 allow for the comparison of the effect of the position of the CF_3 group in matched pair format. Similar to the monofluoro- and difluoro- matched pairs, this was performed in order to compare the effects the given motif on lipophilicity at different distances from the functional group, but with the same non-fluorinated parent reference to avoid any effect arising from lipophilicity differences between parents. The matched pairs for the "-2-ol's" are **E6** and **E8**, **H9** and **H10**, and **K1** and **K3** (Figure 2.7). In all three cases the α-CH_3/CF_3 exchange leads to a more lipophilic compound than the ω-CH_3/CF_3 exchange. This is a result of the unavoidable anti-periplanar orientation of the C-O and C-F bond, resulting in dipole counteraction, and thus leading to a reduced polarity effect from the CF_3 motif. This in combination with the reduction of polarizability of the oxygen's lone pairs allows for hydrophobicity impact from the CF_3 motif to dominate, thus resulting in the increased lipophilicity of α-CH_3/CF_3 exchange.

Comparing the -CF_3 motif in this format allows for the comparison of two trifluoromethyl groups into the same molecule. For **K2**, it can be seen that both the effects of α-CH_3/CF_3 exchange (Δlog*P* +0.62, typically Δlog*P* +0.61) and δ-CH_3/CF_3 exchange (Δlog*P* -0.18, typically Δlog*P* -0.22) are

combined, allowing for the CF_3 motif to exhibit both an increase and decrease in lipophilicity on the same molecule.

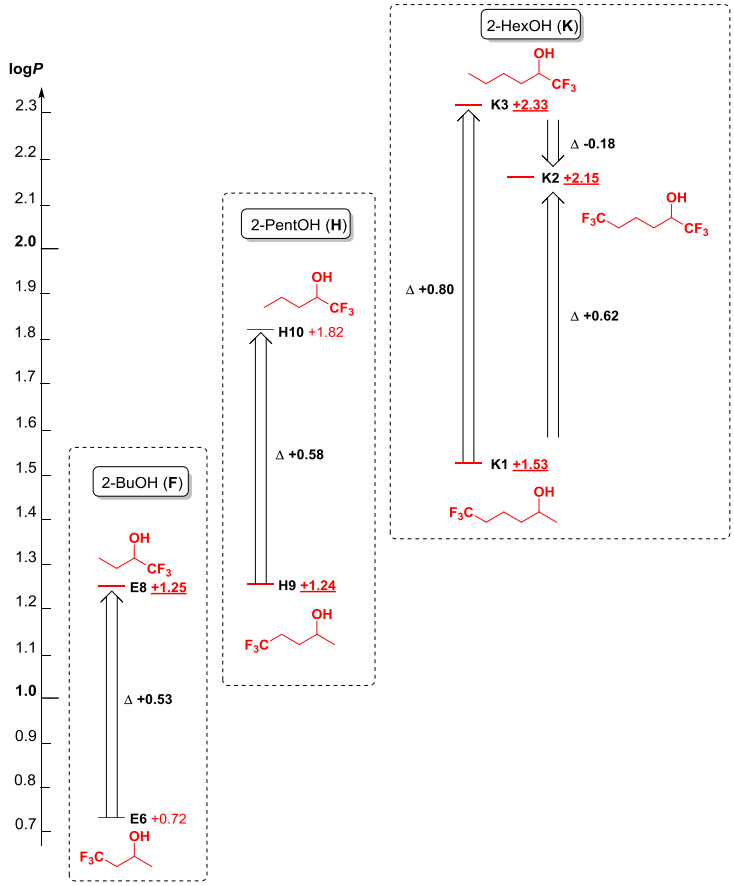

Figure 2.7 - Trifluoromethyl Matched Pairs

The analysis of the matched pairs not involving β-trifluorination is interesting (Figure 2.8). The expectation is that the further the trifluoromethyl group is positioned from the alcohol group, the larger the log*P* reduction will be. This is seen for the **M** and **N** pairs. However, for **J**, showing the effect of β- and γ- CH_3/CF_3 exchange, there is not only no large difference in log*P* between **J1** and **J2**, but also the log*P* of **J2** is larger than that of **J1**. Neither trifluoromethyl groups are in proximity to the alcohol group for C–O/C–F bond dipole counteractions to occur, although **J1** would allow an antiperiplanar C–O/C–CF_3 conformation. However, this would be expected to increase the log*P*, not a decrease. A tentative explanation for the unexpected larger polarity of **J1** could be a conformation as depicted, which features stabilising $\sigma_{C-H} \rightarrow \sigma^*_{C-O}$ and $\sigma_{C-H} \rightarrow \sigma^*_{C-CF3}$ hyperconjugations resulting in the *gauche* arrangement shown.

As previously discussed in Section 2.2.4, the 3-HeptOH **M** and 4-OctOH **N** matched pairs showcase the large difference in log*P* caused by the introduction of the δ-CF_3 group, when compared to both β-CF_3 and γ-CF_3 groups respectively. This further highlights the importance of carefully choosing the position of fluorination, when attempting to modulate the lipophilicity of an aliphatic molecule.

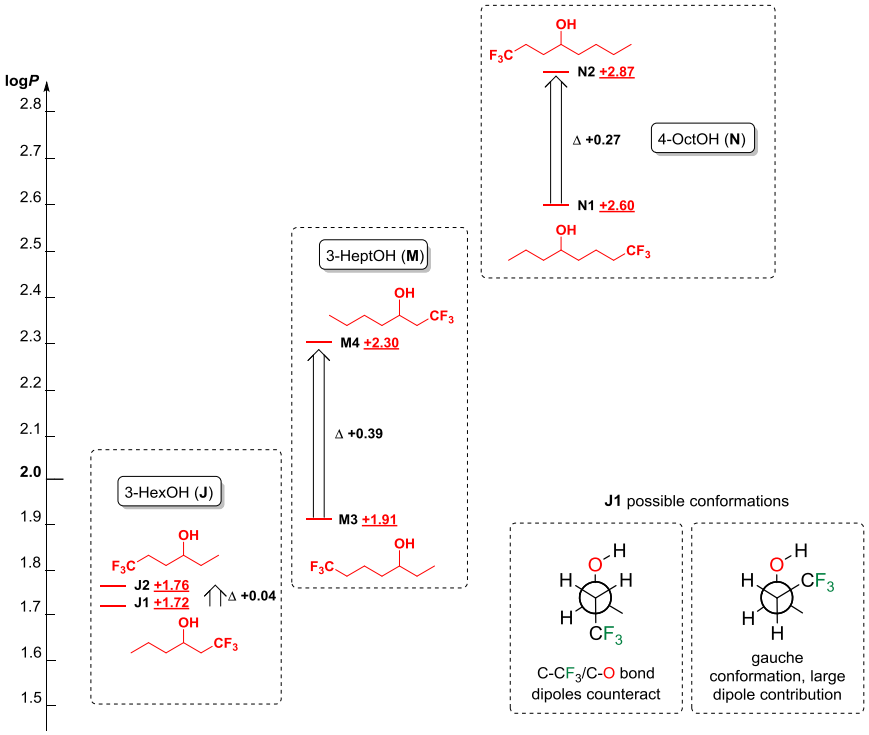

Figure 2.8 - Trifluoromethyl Matched Pairs

2.3 The influence of polyfluorinated motifs on lipophilicity

2.3.1 CF_3CF_2 at varying distances

Following the investigation of the trifluoromethyl motif at varying distances from the alcohol functionality, the CF_3CF_2 series was investigated (Figure 2.9). The large increase for both **C7** (Δlog*P* +0.90) and **E9** (Δlog*P* +0.77), in comparison to their respective parent compounds, is likely due to the proximity of the CF_2 to the alcohol moiety, as well as an increase in volume. A trend of decreasing Δlog*P* values with increasing log*P* of the parent alcohol was also observed. As the motif is further positioned from the alcohol moiety, the Δlog*P* values decrease in a similar fashion to the CF_3 series (See Chapter 1, Section 1.6), eventually resulting in a log*P* decrease when the log*P* of the parent alkanol exceeds 2 (**L → L2**, Δlog*P* -0.06). Hence the dipole contribution of the CF_3CF_2 motif is also outweighing its hydrophobic volume contribution at elevated log*P* values. Yet again, this showcases the importance of comparing fluorinated motifs over various parent compounds, as their influence on lipophilicity may change.

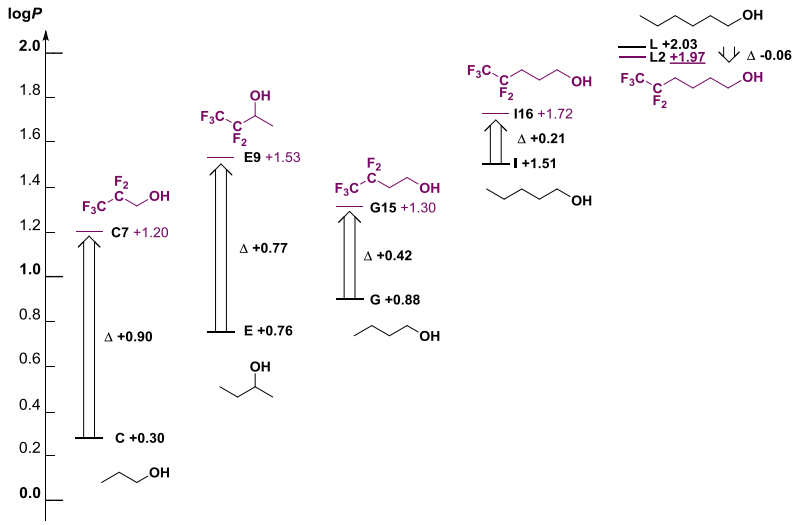

Figure 2.9 - Log*P* of CF_3CF_2 motif

2.3.2 CF_3CH_2 vs CF_3CF_2 vs HCF_2CF_2

As expected, the CF_3CF_2 motif (**C7**, **E9**, **G15** and **I16**) is the most lipophilic of the three motifs being compared in Figure 2.10. This is a likely a result of multiple C-F bond dipole counteractions, allowing fluorine's hydrophobic nature dominate, resulting in large increases in lipophilicity.

Perhaps unsurprisingly, when comparing the CF_3CF_2 with the HCF_2CF_2 motif, a decrease in lipophilicity is observed in all cases, but is substantial for the **G** and **I** series. In addition, while for the PrOH and 2-BuOH families, **C6**/**E7** (HCF_2CF_2) have higher lipophilicities than **C5**/**E6** (CF_3CH_2), this is not the case for the BuOH and PentOH families. Here the CF_3CH_2 motif (**G13** and **I13**) is more lipophilic than the HCF_2CF_2 motif (**G10** and **I12**). It is proposed that the higher log*P* for both **C6** and **E7** compared to that of **C5** and **E6** is due to the former's β-position to the hydroxyl group. As the HCF_2CF_2 motif progresses further away from the alcohol, C-F/C-O bond dipole counteractions no longer occur and despite its increase in hydrophobic surface area, it appears as a more polar functional group than CF_3CH_2.

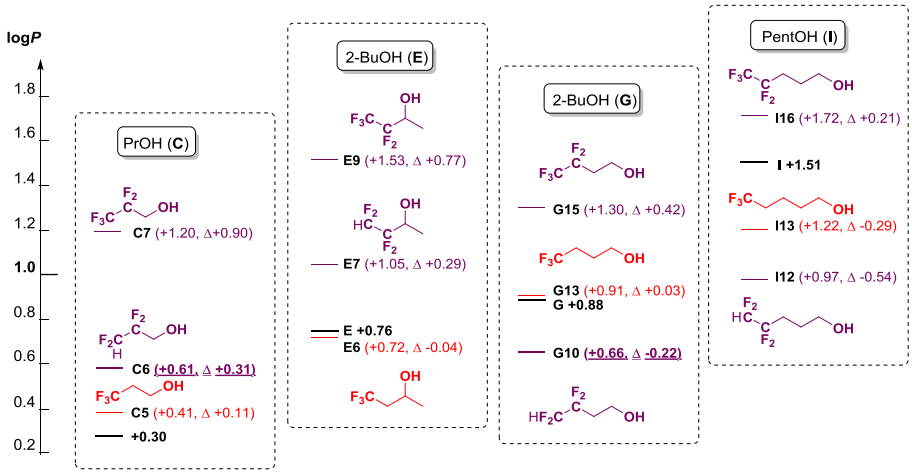

Figure 2.10 - CF_3CH_2 vs CF_3CF_2 vs HCF_2CF_2

It is therefore assumed the terminal CF_2CF_2H group adopts a gauche conformation (Figure 2.11), which is suggested by crystal structures.[118-120] This results in larger dipole contribution when compared to the alternative anti-conformation, where the C-F bond dipoles counteract. It is also pleasing to see that the HCF_2CF_2 group is less lipophilic than its "parent" compound, providing another log*P* lowering motif. Examples like this reveal why it is important to investigate various fluorinated motifs in individual families, as the parent compound plays a large role on fluorine's modulation on lipophilicity.

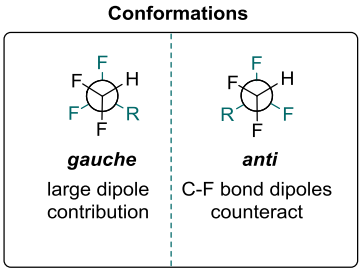

Figure 2.11 - CF_2HCF_2R conformations

2.3.3 CF_3 → CH_3 within different motifs

As discussed earlier in Section 2.2.4, CH_3/CF_3 exchange on an aliphatic substrate can have a wide range effects on the modulation of lipophilicity. Alcohols containing an α-CF_3 group all exhibited higher log*P* values than their parent compounds, however it was established that as the distance between the CF_3 group and the hydroxyl group increased, the Δlog*P* values also decreased and eventually a reduction in log*P* was observed. Therefore, it is interesting to investigate CH_3/CF_3 exchange across other fluorinated motifs. Interestingly, exchange of the CF_3 group for a CH_3 on the pentafluoroethyl (CF_3CF_2-) motif resulted in a surprisingly consistent decrease of one log*P* unit, regardless of the parent compound (Figure 2.12). The considerably higher log*P* values for the

pentafluoroethyl motif can be tentatively explained as a result of a counteraction of the C-F dipoles of the CF_2 and CF_3 moieties, resulting in the hydrophobic nature of the group to dominate. The same trend was observed for changing the CF_3-group into a CH_3 group for both nonafluorobutyl and heptafluopentyl analogues (c.f. **G17 → G12, I18 → I15**). Very unexpectedly, the $MeCF_2(CF_2)_n$- group also had almost identical log*P* values as their parent compounds. Therefore, polyfluorination may not necessarily result in a large increase in lipophilicity, if the terminal position remains nonafluorinated.

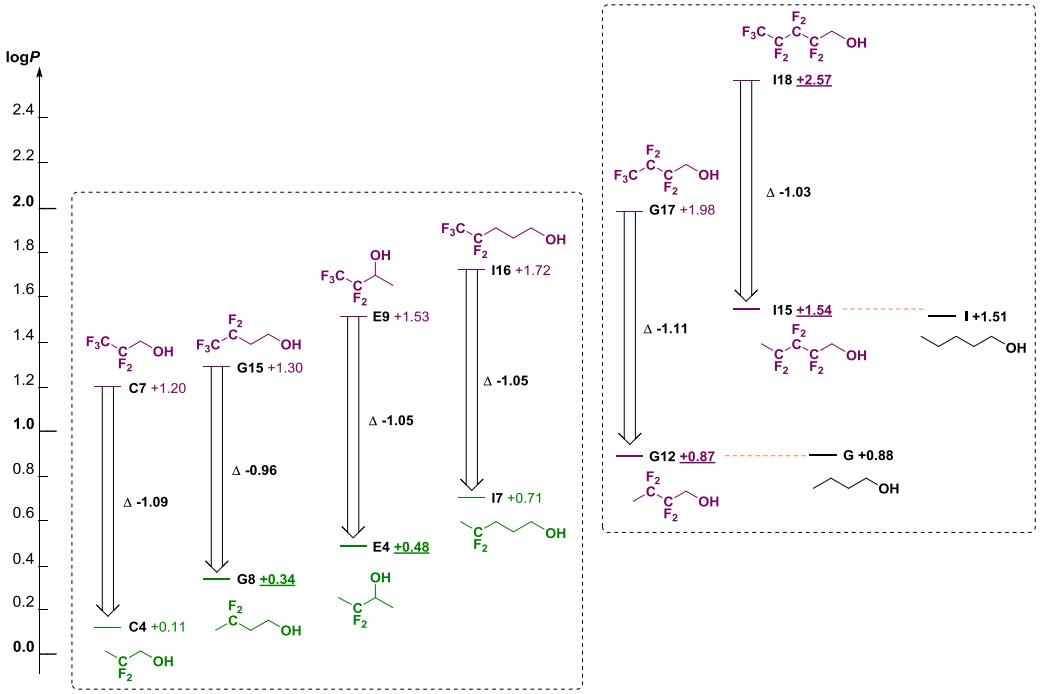

Figure 2.12 - Effect of CF_3/CH_3 exchange on lipophilicity

In an attempt to explain the interesting decrease in log*P* observed for CF_3/CH_3 exchange on perfluoroalkyl groups and the $MeCF_2(CF_2)_n$- groups of similar log*P* value to their respective parent compound, an investigation into the dipole moments of the substrates was performed. This can be achieved through the use of overall molecular dipole moments, which necessitate information on the various conformers the substrates adopt and were calculated by Dr Jerome Graton, University of Nantes, France. The detailed experimental for the following calculations and their subsequent results can be found in *Ref*.[121] In both water and octanol, conformational analysis of **G12**, **G17**, **I15**, **I18** and their respective parent compounds was performed. These calculations indicated that all the compounds were very flexible and that only **G12** has a major conformer with a population greater than 20%. For all compounds, the conformational profiles were different between the octanol and water phases, as shown by the different calculated dipole moments, which typically differed by <0.2 D (Table 2.1). In each case the calculated dipole moments were smaller in octanol, which is anticipated due to the polar conformations being better stabilised in the more polar water.

However, the tetrafluorinated compound **G12** exhibited a much larger difference in dipole moments, roughly 1.0 D, between the water and octanol phase. As mentioned earlier, this was the only compound to have a major conformer with a population greater than 20%. Interestingly, when comparing the two conformers with the highest population in both octanol and water, there is a large difference in dipole moment (Figure 2.13). Hence, **G12** can be referred to as a "lipophilicity chameleon",[117] in which conformers that are close in energy possess markedly different dipole moments, allowing a skewing of the population depending on the medium. Unfortunately, from here it isn't straightforward yet to relate this to a log*P* value, although qualitatively it can be understood that ultimately the level of partitioning will result from the different degrees of stabilisation in a given phase.

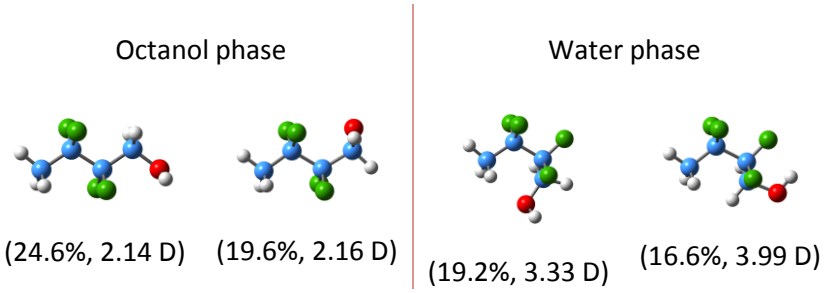

Figure 2.13 - Comparison of the two most abundant conformers of G12 in octanol (left) and water (right)[viii]

Table 2.1 - Calculated dipole moments[viii]

Compound	Phase	μ (D) (weighted)	Compound	Phase	μ (D) (weighted)
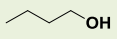 G	oct	2.21	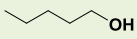 I	oct	2.20
	wat	2.40		wat	2.40
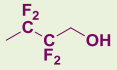 G12	oct	2.87	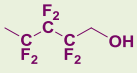 I15	oct	3.37
	wat	3.82		wat	3.57
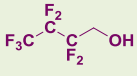 G17	oct	3.34	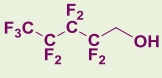 I18	oct	3.12
	wat	3.38		wat	3.31

[viii] Calculated at the SMD/MN15/aug-cc-pVTZ//MN15/cc-pVTZ level of theory in water and octanol medium, and weighted by the relative populations of each conformer, performed by Dr Jerome Graton, University of Nantes, France.

As seen in Table 2.1, fluorination of the parent compound results in an increase in dipole moment. Interestingly, in both octanol and water a higher dipole moment was observed for hexafluorinated **I15** in comparison to its nonafluorinated analogue **I18**, however this was not the case when comparing tetrafluorinated **G12** with its heptafluorinated analogue **G17**. In the octanol layer, **G17** exhibited a lower dipole moment, which can be explained by the very apolar conformers it can adopt as seen in Figure 2.13. These low dipole moments from these conformers exist due to the counteraction of the C-F bond dipoles, however this is not possible for **I15**, which is believed to result in its higher dipole moment in comparison to **I18** in the octanol layer.

The C-H bonds of the CH_3 group on the $MeCF_2(CF_2)_n$- motif are also strongly polarized by an electron withdrawing effect of the neighbouring fluorines. This can be shown through the use of chemical shift analysis showing the resulting deshielding, as well as through partial atomic charge calculations (Table 2.2).[ix] As a result of the fluorine inductive effect, as internal fluorination increased so did the hydrogen positive charge. Therefore, CF_3/CH_3 exchange on a perfluoroalkyl group results in the introduction of a very polar CH_3 group, causing a lipophilicity reducing effect.

Table 2.2 - Chemical shift values and weighted partial atomic charges per hydrogen atom of the methyl group[ix]

Compound	δ_{Me} (ppm) in $CDCl_3$	Water q_H	Octanol q_H
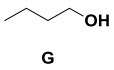 G	0.93	0.2017	0.2012
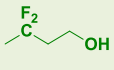 G8	1.67	0.2336	0.2322
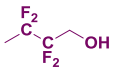 G12	1.78	0.2444	0.2426
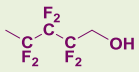 I15	1.83	0.2476	0.2458

Finally, the last factor to consider is the decrease in hydrophobic surface area upon replacement of the CF_3 group for CH_3.

[ix] Calculated at the SMD/MN15/ aug-cc-pVTZ//MN15/cc-pVTZ level of theory using the natural population analysis methodology performed by Dr Jerome Graton, University of Nantes, France.

2.3.4 Chain elongation reduction in log*P*

Another interesting log*P* lowering trend was identified when comparing the lipophilicities of the R-CF_3 group, with its homologue R-CF_2Me (Figure 2.14). Typically, the extension of a carbon chain by one methylene unit on a non-fluorinated alcohol results in a log*P* increase of roughly 0.58 units. Surprisingly, the exchange of a C-F bond on a terminal trifluoromethyl group for a C-Me bond, resulting in the formation of the R-CF_2Me group, leads to a reduction in lipophilicity. This decrease in lipophilicity ranged in Δlog*P* values of -0.06 to -0.44. Pleasingly, this trend was observed in all cases and in both trifluorinated and perfluoroalkyl substrates. O'Hagan *et al*. witnessed a similar trend when comparing the lipophilicities of $ArSCF_3$ (log*P* + 3.70) with $ArSCF_2CH_3$ (log*P* +3.38).[122]

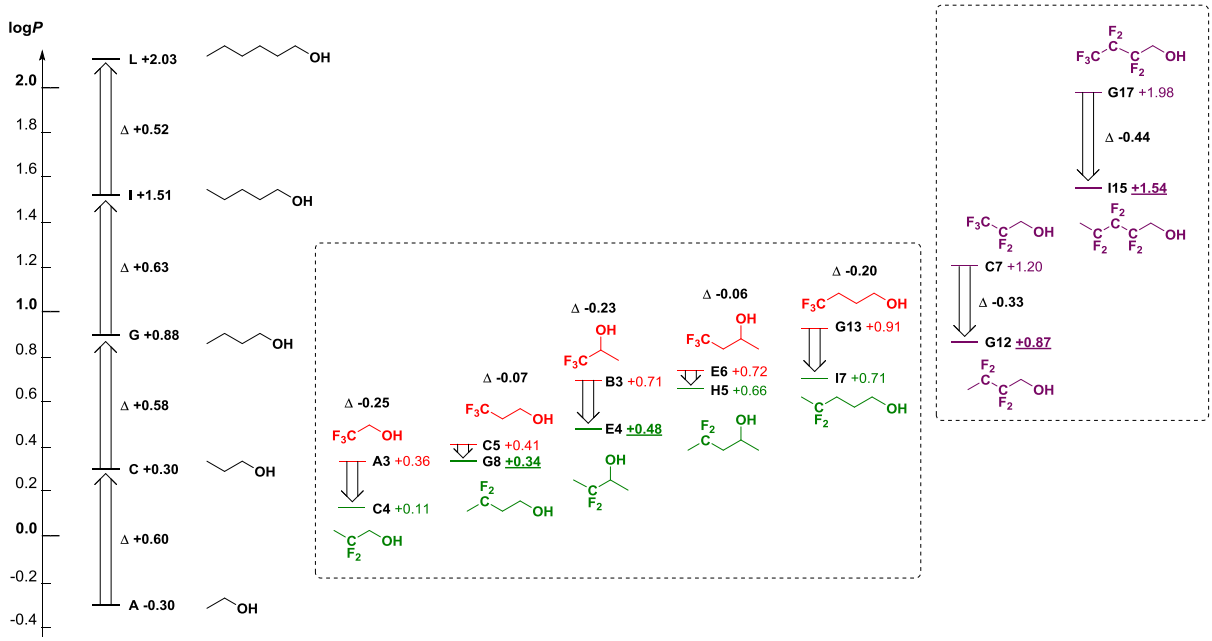

Figure 2.14 - Reduction of log*P* upon chain elongation

2.4 Comparison of partially fluorinated motifs

2.4.1 Comparison of selected partially fluorinated motifs

As expected and consistent with other results, the $CF_3CF_2CF_2$ motif in **G17** is the most lipophilic within this series (Figure 2.15). This is because the high degree of fluorination introduces a large hydrophobic surface, and there is significant C–F dipole compensation in such polyfluoroalkyl moieties. At first sight, the lipophilicity reduction caused by reducing the number of fluorine atoms such as in the hexafluorinated substrate **G16** and the pentafluorinated substrate **G14** is as expected. It is interesting to note that the (substantial) increase in lipophilicity (Δlog*P* +0.65) from **G14** to **G16** is caused by a CH_2→CHF modification, which as a standalone modification virtually always results

in a lower log*P*. However, the lipophilicity trend **G17→G16→G14** can be easily explained by the decrease in dipole compensation, through the removal of fluorine atoms from the central CF_2-group resulting in a log*P* reduction. Overall, this suggests that if a large increase in lipophilicity is required, more than just a high degree of fluorination is required (See Section 2.3.2 and 2.3.3). The fluorination must be adjacent and contain a terminal CF_3. The pentafluorinated substrate **G14** with "skipped" fluorination has only has a small increase of Δlog*P* +0.16 against its parent compound, while the pentafluorinated analogue **G15** with vicinal fluorination has a much larger log*P* (1.30, see Figure 2.12).

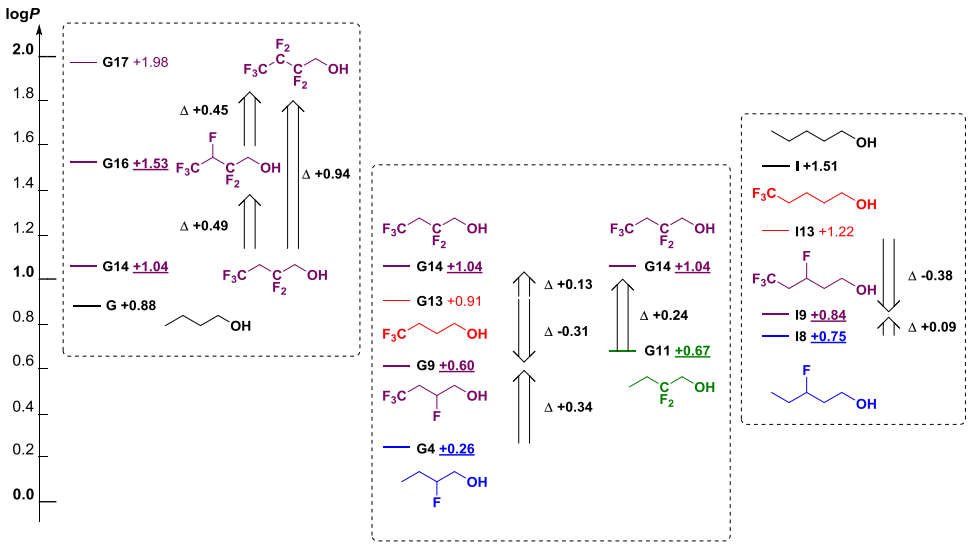

Figure 2.15 - Comparison of selected polyfluorinated motifs

Further examples shown in Figure 2.15 show the different effects of fluorination when introduced within a more complex motif as opposed to a standalone modification. As seen previously (See Chapter 1, Section 1.6), the CH_3/CF_3 exchange on butanol (Δlog*P* +0.03) results in slight log*P* increase, while the inverse is observed on pentanol (Δlog*P* -0.29). When performing the same modification on the terminal CH_3 of a substrate already containing either a monofluoro- or difluoro-motif, an increase in lipophilicity across substrates is observed (**G4 → G9**, **G11 → G14** and **I8 → I9**). This is likely an effect of counteracting C-F and CF_3 dipoles, in conjunction with an increase in hydrophobic surface area.

Interestingly, the introduction of the CF_2 motif (typically log*P* reducing) onto an alcohol containing a CF_3 (**G13 → G14**) results in an increase in lipophilicity, while the inverse is observed for the introduction of a single fluorine atom (**G13 → G9** and **I13 → I9**). With further chain elongation, it is presumed that the $CF_3CH_2CF_2$ motif would result in log*P* reduction.

Despite a large increase in hydrophobic surface area, the tetrafluorinated substrates **G9** and **I9** exhibit a decrease in lipophilicity in comparison to the parent compound, Δlog*P* -0.28 and Δlog*P* -

0.67 respectively. In spite of a potential gauche effect within **G9**, which would result in a C-F/C-O dipole counteraction, a reduction in log*P* inrespect to its parent compound is still observed. The larger Δlog*P* value for **I9** occurs because of the increased lipophilicity of the parent compound and lack of C-O/C-F dipole counteractions, therefore the polar nature of the motif is dominant. Hence, this is the identification of a novel log*P* lowering motif even when β-fluorination occurs.

2.4.2 CF_3CF_2 vs $CF_xH_xCF_2$

As expected and consistent with previous results, the CF_3CF_2 motif **G15** is the most lipophilic (Figure 2.16). A large decrease in log*P* is observed for the HCF_2CF_2 motif **G10** (Δlog*P* +0.64). Interestingly, the H_2CF-CF_2 motif **G5** is slightly less lipophilic than the CH_3CF_2 motif **G8**. This may be due to the increased dipole from the polarity of the monofluoro substituent (polar C—F bond), as well as fluorine polarising its α-hydrogens: a conformation in which the number of $\sigma_{C-H} \rightarrow \sigma^*_{C-F}$ hyperconjugation interactions is maximised will result in all C–F dipoles pointing in a similar direction (see below for discussion). A similar pattern and Δlog*P* values were observed within the pentanol family.

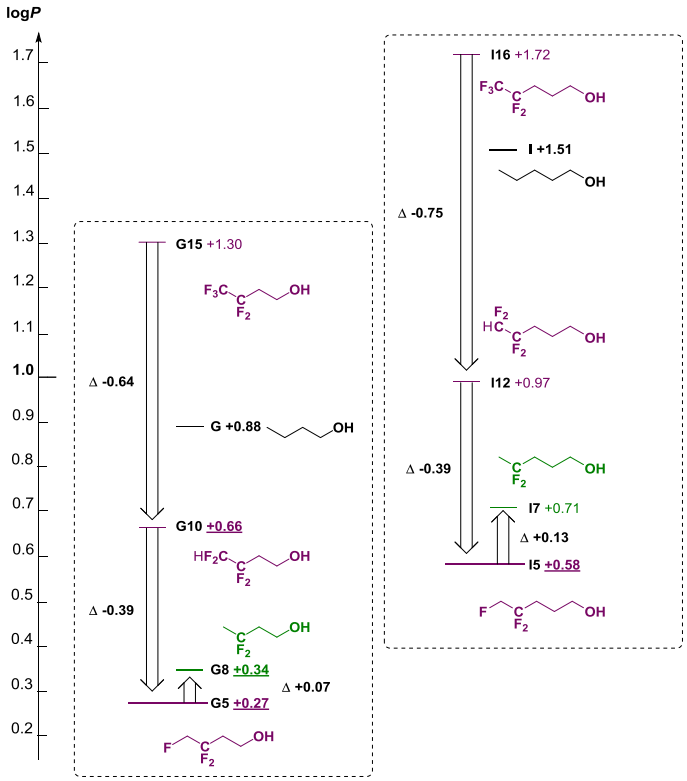

Figure 2.16 - CF_3CF_2 vs $CF_xH_xCF_2$

2.4.3 The effect of the CFH-CF_2 and CF_2-CFH_2 motifs on lipophilicity

Both of the *vic*-trifluorinated motifs, C**F**H-C**F₂** and C**F₂**C-**F**H₂ (Figure 2.17), exhibit rather drastic decreases in lipophilicity in relation to their parent compound (ca. Δlog*P* -0.61 vs. butanol and ca. Δlog*P* -0.95 vs. pentanol), as well as their respective structural isomers **G13** and **I13**. This identifies both as novel log*P* lowering motifs. Interestingly, the C**F**H-C**F₂**H motif is more polar in the butanol family, while the inverse is observed for the pentanol family. However, the Δlog*P* values are relatively small in each case, Δ0.02 within the butanol family and Δ0.06 within the pentanol family.

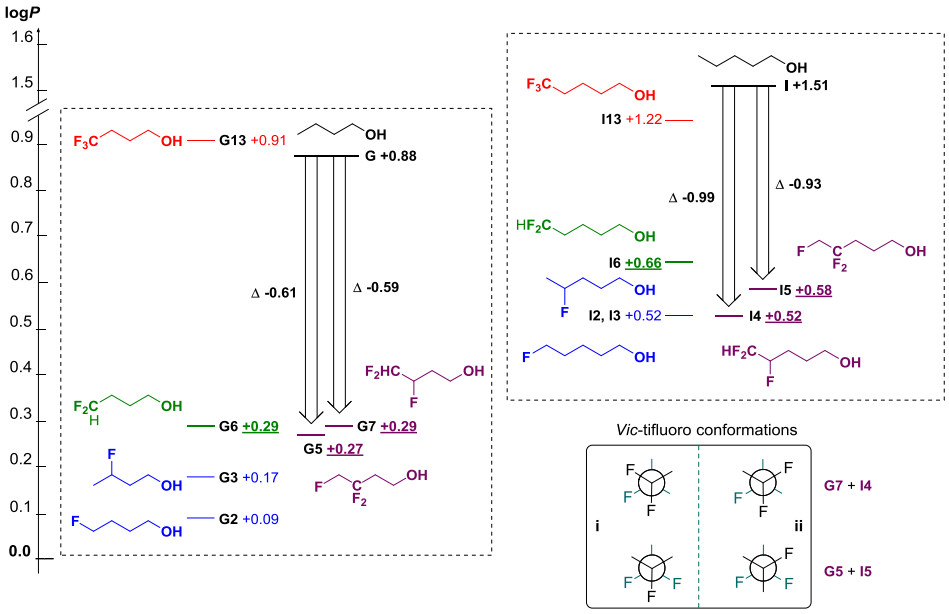

Figure 2.17 - Comparison of *vic*-trifluoro motifs

The introduction of the CF_2 motif (typically observed as log*P* decreasing), onto the monofluorinated substrates within the butanol family exhibit only a slight increase in lipophilicity (**G2 → G5**, Δlog*P* +0.18 and **G3 → G7**, Δlog*P* +0.12). Due to the increased lipophilicity within the pentanol family, the increase is log*P* is not as noticeable (**I3 → I4**, Δlog*P* +0.00 and **I2 → I5**, Δlog*P* +0.06). Another interesting observation is the similarity in log*P* values between the *vic*-trifluoro motifs and gem-difluoro **G6** within the butanol family. These small changes in lipophilicity observed within both the butanol and pentanol family, can be further explained through the analysis of two conformations these motifs may adopt (Figure 2.17).[123]

i. This conformation results in maximising the polarity of the substrate but would also cause an unfavourable clustering of partial charges from the fluorine atoms.

ii. This conformation exhibits a counteraction of two C—F bond dipole moments and would result with an overall polarity similar to the corresponding monofluoro analogue.

Varying populations of these and other potential conformations likely corresponds to the relative log*P* of the substrates. For example, **I4** is isolipophilic to its monofluoro counterpart **I2**, which would typically be unexpected due to the increase in hydrophobic surface area and if it only adopted the presumably favoured conformation **ii**, as this would result in a net log*P* gain. Therefore, the motif must also adopt conformation **i** or similar conformations in order to increase the polarity of the substrate, thus affording an isolipophilic measurement despite an increase in size. Further conformational analysis is required to rationalise these results.

2.4.4 The effect of the *vic*-difluoro motif on lipophilicity

Carreira and Müller have identified the terminal *vic*-difluoro motif as the most polar fluorinated motif, resulting in large log*P* reductions (See Chapter 1, Section 1.6).[111, 115, 124] Gilmour *et al*. also observed the same trend.[125] We were keen to include this motif in the alkanol families as well, for 'calibration' purposes. Pleasingly, the Müller/Gilmour results are consistent with the measured log*P* values of simple terminal vicinal difluorinated alkanols, as both **G1** and **I1** have the lowest log*P* values in their respective families (Figure 2.18). These *vic*-difluoro analogues also hold the two largest reductions in log*P* ever observed in our work in comparison to their parent compound, across all acyclic parents, Δlog*P* -1.00 and Δlog*P* -1.40 respectively.

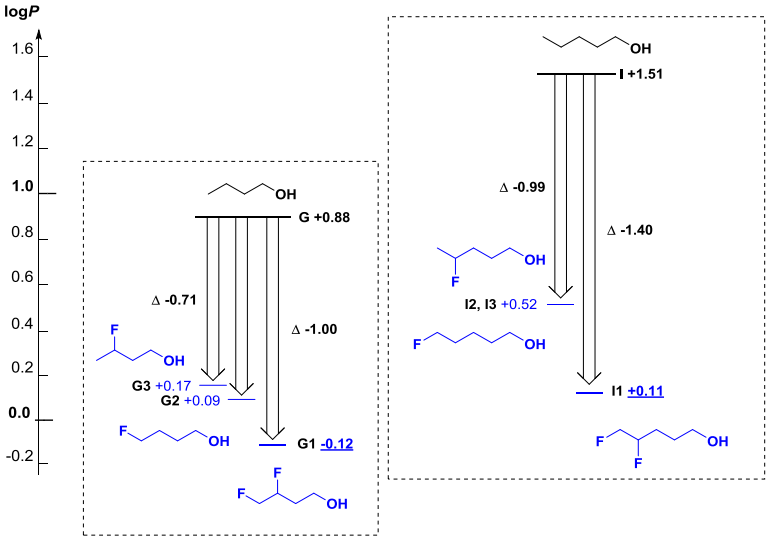

Figure 2.18 - *Vic*-difluoro motif

2.5 The effect of fluorination on the lipophilicity of diols

2.5.1 1,4-Butandiol Family

Utilizing 1,4-butandiol **Q** as a parent compound (log*P* = -0.83) allows for the evaluation of the influence of fluorination on lipophilicity in a much lower lipophilicity range than previously

investigated (Figure 2.19). As expected, the *gem*-difluorinated diol **Q4** has a lower log*P* than the tetrafluorinated **Q5** and a higher log*P* than the monofluorinated diol **Q1**. This trend corresponds nicely with their respective equivalents in the butanol family **G**. Interestingly, lipophilicity increases for **Q4** and **Q5** when compared to their parent compound **Q**, unlike for **G8**, **G11** and **G12**, where a decrease is observed. Commonly, difluorination would show a decrease in lipophilicity when compared to its parent compound, however for **Q4** this is not the case. The dipole contribution from the *gem*-difluoro motif is significantly less pronounced when placed on an already polar parent compound **Q** (log*P* = -0.83) and thus the hydrophobic contribution of fluorine is more prominent. The large increase in lipophilicity for **Q5** (Δlog*P* +0.72) in comparison to its parent compound **Q** is likely due to a counteraction of C-F dipoles with either the neighbouring C-F or C-O dipoles. Therefore, the polarity of this CF_2CF_2 motif is diminished and the contribution of its hydrophobicity dominates, resulting in a more lipophilic molecule. Both of these examples showcase the importance of comparing different fluorinated motifs over various parent compounds.

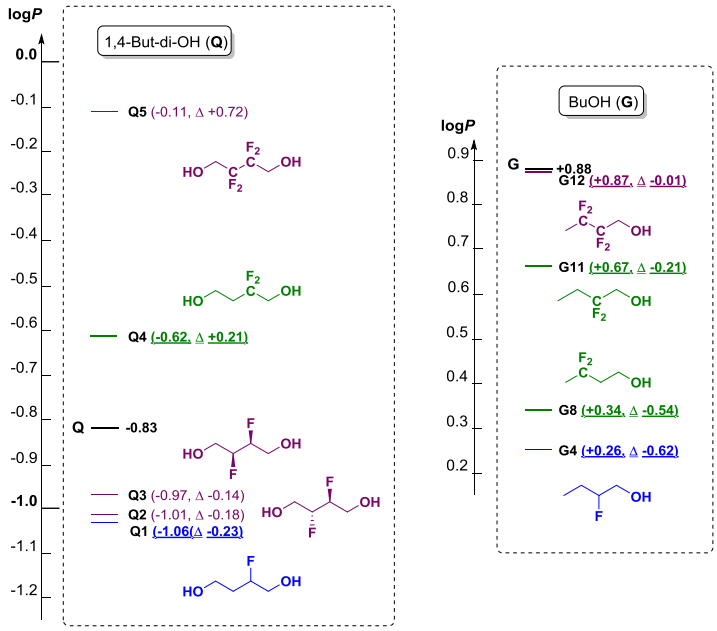

Figure 2.19 - 1,4-Butandiol family

2.5.2 1,5-Pentandiol Family

As expected, the hexafluorinated motif **R4** exhibits the highest log*P* within 1,5-pentandiol family (Figure 2.20). Further observations within the family identify that *gem*-difluorination results in a lipophilicity decrease, which was a commonly observed trend for the CF_2 motif within other families, in contrast to the inverse displayed by **Q4** within its respective family. This is presumably due to the increase in lipophilicity of the parent compound (**R**, log*P* +0.27 vs. **Q**, log*P* -0.83), therefore the dipole from the *gem*-difluoro motif dominates over its hydrophobic contributions,

resulting in an overall log*P* decrease. In a similar fashion to their respective pentan-1-ol analogues, the γ-CF_2 analogue **R1** was less lipophilic than its β-CF_2 counterpart **R2**. Pleasingly, the skipped tetrafluorinated motif **R3** exhibited an increase in log*P* compared to its difluoro- equivalent **R2**, and a reduction in log*P* in relation to its parent compound.

The investigation into the monofluoro- series and other fluorinated motifs within the 1,5-pentandiol family is currently ongoing within the group.

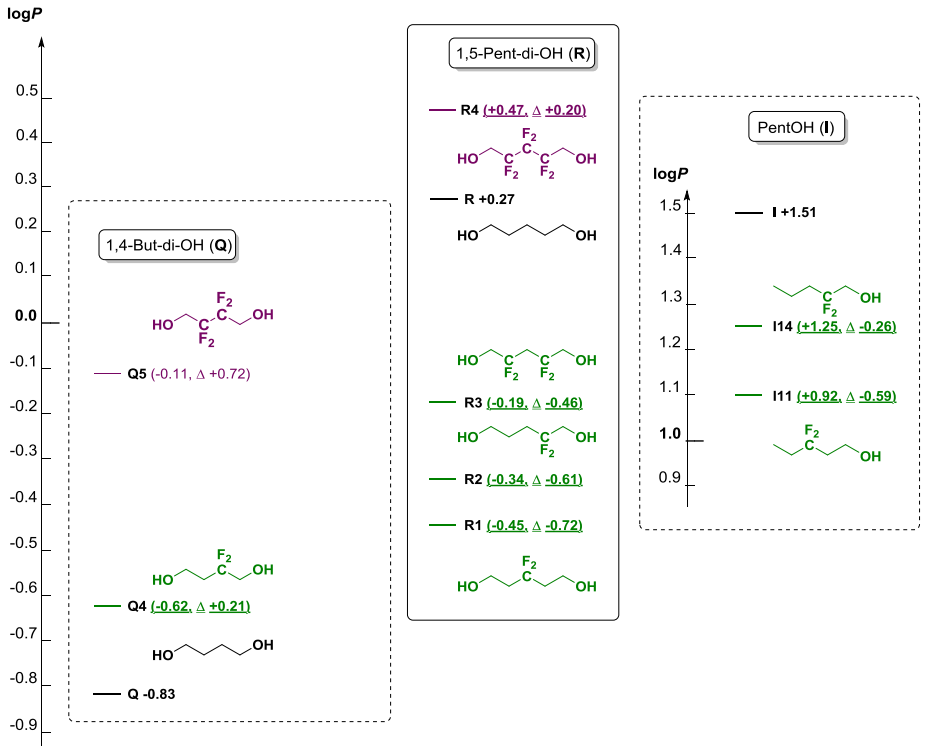

Figure 2.20 - 1,5-Pent-di-OH family[x]

2.6 The effects of fluoroalkenes on lipophilicity

2.6.1 4-Pentenol family

Initial observations show (Figure 2.21) that comparing mono-, di- and trifluorination motifs in fluoroalkenols follow the same trends as in fluoroalkanols, where the monofluorinated substrates are the least lipophilic and the trifluorinated are the most lipophilic. Although surprisingly, this was not the case for *vic*-difluoro substrates **O1** and **O4**, which shared similar log*P* values to their monofluoro counterparts, in stark contrast to the drastic decrease typically observed with the *vic*-difluoro motif on an alkane.

[x] Compounds **R2** and **R3** were synthesised by an MSc student, Eleni Georgiou.

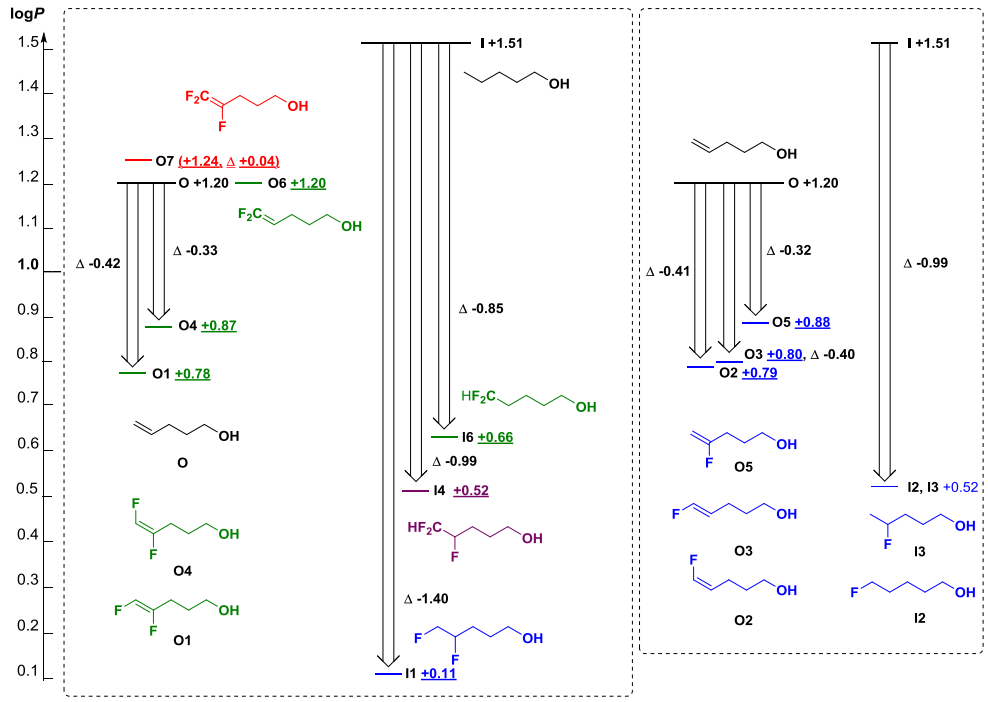

Figure 2.21 - 4-Pentenol family[xi]

Interestingly, it would also appear that the effect of fluorine's polarity has little influence on fluoroalkene substrates, unlike their respective alkane equivalents. This is shown by the monofluoroalkene **O5** having a Δlog*P* -0.32 compared to its parent compound **O** and its monofluoroalkane equivalent **I3** having a Δlog*P* -0.99 compared to its parent **I**. The same can be observed with the corresponding difluoro substrates, where **O6** has a Δlog*P* 0 compared to its parent **O** and **I6** has a Δlog*P* -0.85 to its parent **I**. Tentatively, this can be explained by the decrease in alkene polarisability due to fluorination, similar to what is observed for aromatic rings.

The small lipophilicity difference exhibited between the *vic*-difluoro alkenes **O1** and **O4** was surprising. It was expected that the conformationally fixed counteracting C-F dipoles (increase log*P*) on **O4** and the aligned C-F dipoles (decrease log*P*) on **O1** would result in a larger difference. A similar observation can be made for the comparison of **O7** and **I4**, where previously the log*P* reduction of **I4** was explained through counteracting dipoles (Figure 2.17). Therefore, considering the C-F bonds of **O7** are conformationally fixed, it is assumed that two of the C-F dipoles counteract, resulting in a similar polarity to the monofluoroalkene **O3**. Thus, with an increase in volume, **O7** would be expected it to exhibit only a small increase of log*P* in comparison to **O3**. However, a large difference was observed (**O3 → O7**, Δlog*P* +0.44). Both of these observations may be related to the loss of polarizable hydrogens.

[xi] Compounds **O1**, **O4 – 07** were synthesised by an international MSc summer student, Estelle Meyer. Zhong Wang (PDRA) synthesised and recorded the log*P* values for compounds **O2** and **O3.**

Further studies are currently being performed within the group, through the synthesis of other fluoroalkene analogues and the synthesis of the corresponding fluorinated buten-1-ol family.

2.7 The effects of other motifs on lipophilicity

2.7.1 Fluorinated cyclopropanemethanol and its comparisons

Unfortunately, the log*P* of the parent compound cyclopropanemethanol **P** (Figure 2.22), has not been previously reported in literature and therefore comparisons to it should be approached tentatively. Despite this, comparisons between the other fluorinated motifs can be discussed. The CF_2 motif **P4** is the most lipophilic, followed by the monofluoro- *anti* and *syn* analogues **P3** and **P1** respectively. The *anti*-configured **P3** has the higher log*P* of the pair. Finally the β-F **P2**, has a lipophilicity value in between the *anti* and *syn* analogues **P3** and **P1**. Traditionally, linear β-monofluoro motifs have higher log*P* values than their γ-monofluoro counterparts, therefore it is surprising that **P2** has a higher log*P* value than **P1**. However, this result is also observed within the isopropanol family.

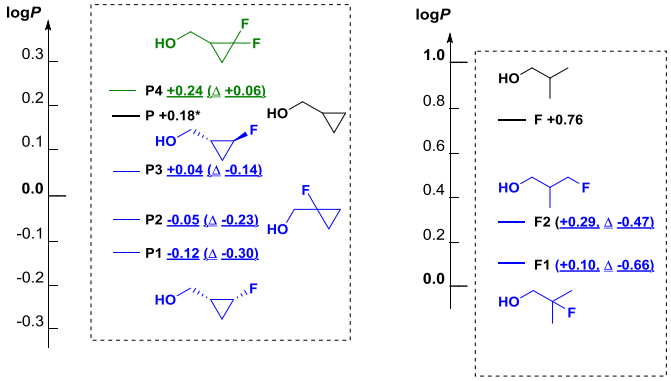

Figure 2.22 - Fluorinated cyclopropanemethanol motifs and their comparisons *=log*P* calculated by MarvinSketch

2.7.2 The effect of the aliphatic -SCF_3 group on lipophilicity

While investigating the effects of the –SCF_3 motif on lipophilicity, both **S1** and **S2** were synthesised and their respective log*P* values recorded (Figure 2.23). Unfortunately, there is no data for their respective parent compounds, however the exchange of the –SCF_3 group for other fluorinated and non-fluorinated motifs will be discussed.

A log*P* increase is observed for CH_3/SCF_3 exchange on both butanol (**G → S1**, Δlog*P* +0.75) and pentanol (**I → S2**, Δlog*P* +0.43). The same trend was observed for the substitution of a CF_3 group for a SCF_3 group (**G13 → S1** and **I13 → S2**, Δlog*P* +0.72). In these two examples, the increase in

lipophilicity is unsurprising considering the presence of an additional heteroatom, thus resulting in an increase in size and subsequent hydrophobicity. This can be further reinforced when their respective Hansch constants are considered, where the $–SCF_3$ (π_x = 1.44) group exhibits a higher lipophilicity value than both CF_3 (π_x = 0.88) and CH_3 (π_x = 0.52).[126] Interestingly, the log*P* increase for CH_3/SCF_3 exchange is smaller on the pentanol scaffold. This can tentatively be explained by the influence of the polarity of the $-SCF_3$ group becoming more prevalent with increasing log*P* of the compared compound, in a similar fashion to the CF_3 and CF_2CF_3 motif seen in Section Chapter 22.2.4 and 2.3.1 respectively.

Next, the exchange of a CH_2CF_3 group for SCF_3 was examined. In this example, while the length of the substrate's backbone is the same, there is a slight decrease in size for **S1** (Van Der Waals surface area = 205.82 Å^2), compared to **I13** (Van Der Waals surface area = 213.16 Å^2) and an increase in PSA (**S1** 45.53 vs. **I13** 20.23). This would be expected to result in a decrease in lipophilicity. Despite this, a log*P* increase is observed in both butanol (**I13 → S1**, Δlog*P* +0.41) and pentanol (**L1**[86] **→ S2**, Δlog*P* +0.30). The increase in lipophilicity can tentatively be explained by the effective compensation of the dipole moments of the C-S and C-F bonds, in a similar fashion to an $–OCF_3$ moiety.[117] The proximity of the CF_3 group to the sulphur also results in a reduction in the polarizability of its lone pairs. Overall, the combination of these two effects results in a highly lipophilic motif.

Work within the group is on-going to synthesise the corresponding $–OCF_3$ analogues and their respective non-fluorinated parent compounds for comparison.

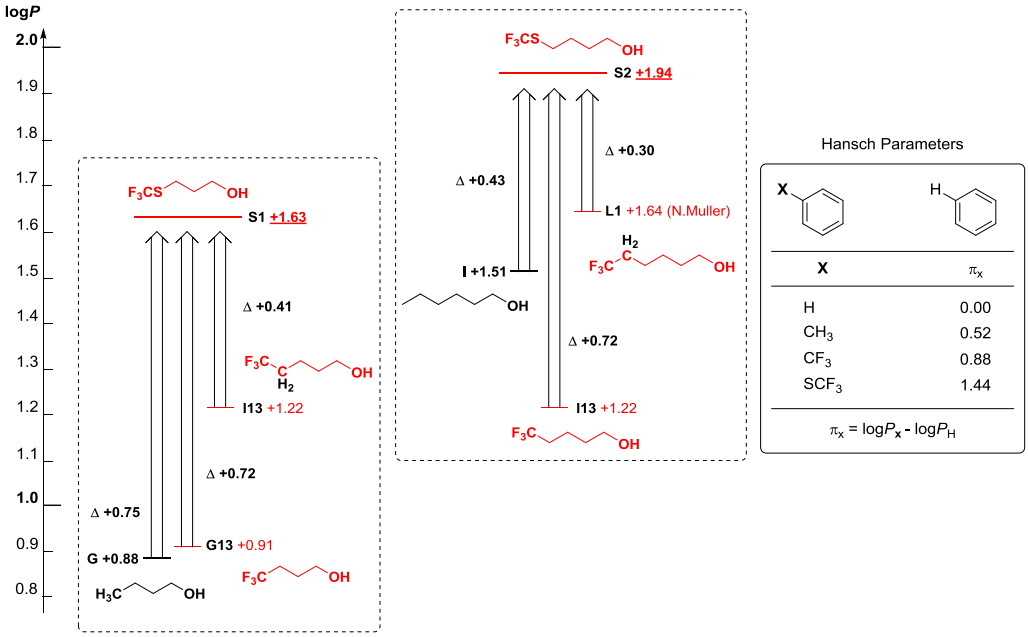

Figure 2.23 - The $-SCF_3$ motif. L1 value obtained from *Ref*[86]

2.8 Methodology development

2.8.1 Effects of impurities on lipophilicity

Occasionally, commercially available compounds are received with trace solvent residues or with an unknown impurity present. In theory, small quantities of these impurities should have little to no effect on the ^{19}F NMR based logP determination method utilized by the Linclau group.[94] This is due the use of ^{19}F NMR, where non-fluorinated material is not visible, and fluorine's large chemical shift dispersion, allowing for a reduced chance of overlap between different fluorine signals. It is assumed that the ability for impurities to interact with either the measured substrate or reference compound is heavily reduced because of low concentrations used in this method (ca. 5-10 mg of material in 4 mL of an octanol/H_2O partition). Therefore, to properly assess the effects of impurities in the Linclau group's log*P* determination methodology, a series of experiments with different solvent impurities was performed.

Trifluorobutanol's log*P* was measured five times with trifluoroethanol as the reference material (Figure 2.24), each with a separate solvent impurity (except the control). This was performed by the addition of a drop of solvent from a Pasteur pipette (~10 mg), to the partition prior to stirring and subsequent equilibration of the biphasic mixture. The solvents used were Et_2O (Entry 1, Table 2.3), CH_2Cl_2 (Entry 2, Table 2.3), THF (Entry 3, Table 2.3), and Et_2O, CH_2Cl_2 and THF (one drop of each, Entry 4, Table 2.3). Finally, a control experiment was also performed with the addition of no impurity (Entry 5, Table 2.3). As observed in Table 2.3 below, all the measured log*P* values with impurities present exhibit very small variations in log*P* value to the control (Entry 5, Table 2.3) and the value published by the Linclau group (Entry 6, Table 2.3).[94] Between all 6 entries, there is an average log*P* value of +0.90 and a standard deviation of ±0.003. This showcases that trace amounts of impurities have little to no effect on the lipophilicity of either the measured substrate or reference material, when using the ^{19}F NMR log*P* determination procedure.

Figure 2.24 - Log*P* values of 2,2,2-trifluoroethan-1-ol and 4,4,4-trifluorobutan-1-ol

Table 2.3 - Effects of impurities on log*P*

Entry	Additive	Log*P*
1	Et_2O	+0.89
2	CH_2Cl_2	+0.89
3	THF	+0.90
4	Et_2O + CH_2Cl_2 + THF	+0.89
5	Control	+0.90
6	Published	+0.91[94]

2.8.2 Log*P* measurements in D_2O

Previous work performed by M. Herth *et al*.,[92] on a novel ^{1}H NMR based log*P* determination procedure used D_2O in place of H_2O.[xii] When describing the methodology, Herth mentions that the difference in the physiological properties between the two solvents were neglected. Through the use of the Linclau group's ^{19}F NMR based log*P* determination methodology,[94] a direct comparison between the use of D_2O and H_2O can be performed, as neither solvent will affect the accurate integration of the measured fluorine signals.

With this in mind, a series of substrates with various fluorinated motifs and a wide range of log*P* values (-2.47 to +1.98, Table 2.4), were selected. The ^{19}F NMR based log*P* determination method was then performed with an *n*-octanol/D_2O partition and the different substrates respective log*P* values were obtained. These values were then directly compared against their corresponding octan-1-ol/H_2O partition values, which had been previously determined by the Linclau group.[94] The Δlog*P* values ranged from 0.001 to 0.052 (Table 2.4). These Δlog*P* values, with the exception of heptafluorobutan-1-ol (Δlog*P* = 0.052), are all within an acceptable range of ±0.015 log*P* units. For the studies of substrates here, it is evident that there is no significant difference in the measured log*P* values, when using either D_2O or H_2O as the polar phase during the partitioning step of the experiment.

[xii] See Chapter 1 Section 1.4.4 for further discussion on this ^{1}H NMR based log*P* determination method.

Table 2.4 - Comparison of log*P* values recorded in both D_2O and H_2O

Compound	Log*P* (D_2O)	Log*P* (H_2O)	ΔLog*P*
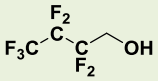	+1.93	+1.98	-0.052
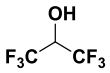	+1.67	+1.69	-0.015
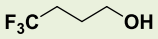	+0.91	+0.91	-0.005
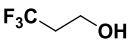	+0.41	+0.42	-0.013
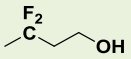	+0.11	+0.11	+0.001
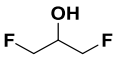	-0.41	-0.42	+0.013
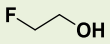	-0.76	-0.75	+0.009
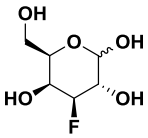	-2.46	-2.47	+0.011

2.9 Conclusion

In conclusion, a total of 66 novel log*P* measurements were performed utilizing the ^{19}F NMR based log*P* determination method developed by the Linclau group (Figure 2.25).[94]

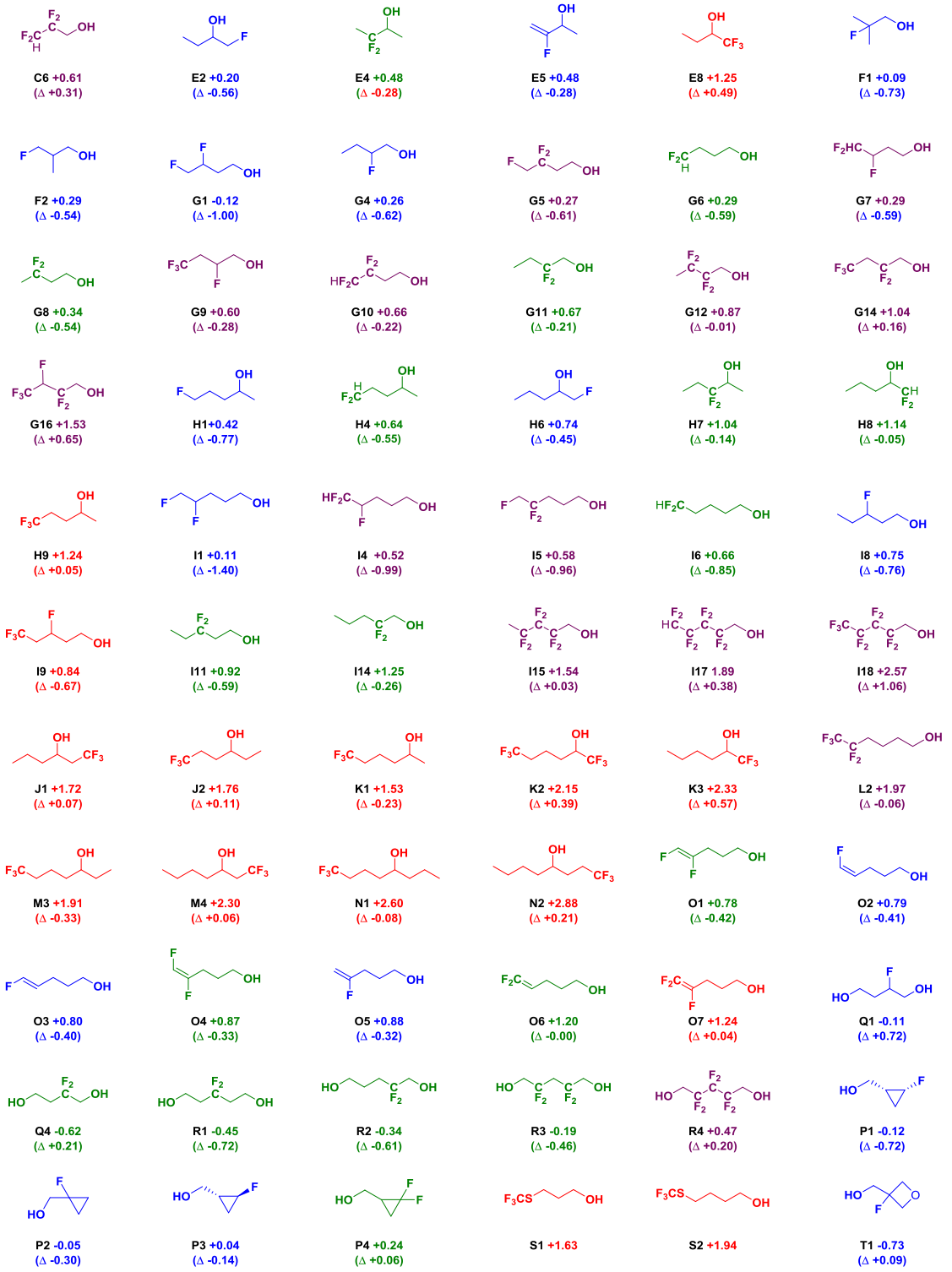

Figure 2.25 - A total of 66 novel log*P* values. The Δlog*P* values listed are in comparison to the individual compounds respective parent molecule.

With this large number of novel fluorinated alkanols, the influence of fluorination on lipophilicity was investigated. In a similar fashion to β-monofluorination, it was found that β-difluorination results in higher log*P* values within their respective families. The impact of the CF_3 motif at varying distances from the alcohol moiety was also investigated through the use of matched pairs. It was found that as the distance between the CF_3 group and the alcohol increases, the Δ log*P* decreased, eventually causing a reduction in lipophilicity. A series of polyfluorinated motifs was also examined and in particular, it was recognised that exchange of the CF_3 group for a CH_3 on the pentafluoroethyl ($CF_3(CF_2)$-) motif or on a perfluoroalkanol, results in a large decrease in lipophilicity. An unexpected decrease in lipophilicity upon exchange of a C-F bond on a terminal trifluoromethyl group for a C-Me bond, resulting in the formation of the R-CF_2Me group was also observed. The partially fluorinated groups, C**F**H-C**F$_2$** and C**F$_2$**-C**F**H_2, were also identified as novel log*P* lowering motifs in comparison to their respective parent compounds. Pleasingly, the *vic*-difluoro motif proved to have the lowest log*P* values recorded within their respective family. The impact of fluorination on diols was also examined, allowing for the investigation of mono- and difluorination on polar molecules. The first log*P* values for fluorinated alkenes and cyclopropanemethanol within the group were also determined. Finally, the impact of the -SCF_3 motif on lipophilicity was evaluated by comparison to other fluorinated and non-fluorinated motifs.

The reproducibility of this method in the presence of trace amount of impurities was confirmed by control experiments. The use of D_2O in place of H_2O was also proven, which would allow for the measurement of non-fluorinated aliphatic parent compounds by ^{1}H NMR, for comparative studies in the future.

Chapter 3 Synthesis of Fluorinated Alkanols by Mono- and Difluorination

3.1 Introduction

In this chapter, fluorinated alkanols, synthesised by either mono- or difluorination, will be discussed. These substrates were synthesised for their use in the investigation of the effects of aliphatic fluorination on lipophilicity (see Chapter 2). The introduction of these mono- and difluoro-motifs will be attempted through the use of either electrophilic fluorination, deoxo/deoxyfluorination, a mixture of these two techniques, or the vicinal difluorination of an alkene. The retrosynthetic analysis of all desired compounds in this chapter will now be performed.

3.1.1 Retrosynthetic analysis and synthetic plan

The synthesis of 2,2-difluorobutanol **G11** and 2,2-difluoropentan-1-ol **I14** can be accomplished *via* electrophilic fluorination with NFSI (Scheme 3.1), starting from their respective commercially available aldehydes **3.1** and **3.2.** The mono- and difluoro-analogues of 1,4-butane diol, **Q1** and **Q4** respectively, can be accessed from the aldehyde **3.3** *via* electrophilic fluorination with NFSI (Scheme 3.1). The aldehyde **3.3**, will be synthesised from 1,4-butane-diol **Q**, following mono protection and subsequent oxidation of the remaining alcohol.

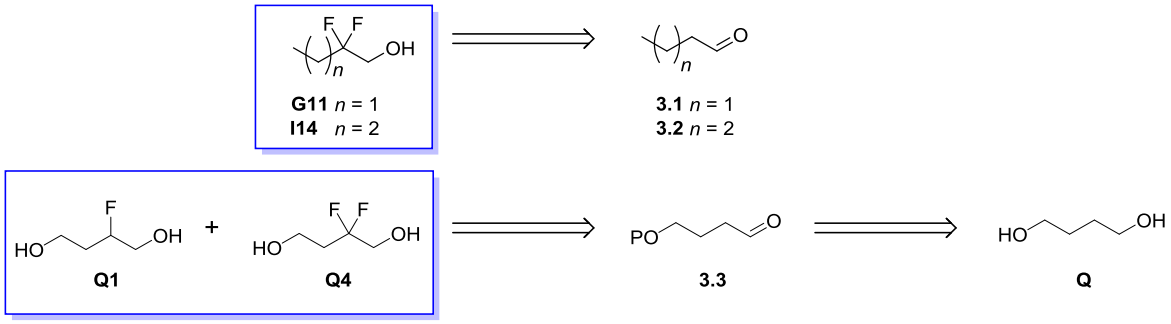

Scheme 3.1 - Planned electrophilic fluorination with NFSI

It was envisioned that the synthesis of **G1** and **I1** (Scheme 3.2) could be achieved through either the vicinal difluorination of the alkenes **3.4** and **I**, or the deoxyfluorination of the advanced intermediates **3.5** and **3.6**, obtained through electrophilic fluorination, as shown in Scheme 3.1. The trifluorinated group R-CHFCHF$_2$ (**G7** and **I4**), could also be synthesised from the same intermediates **3.5** and **3.6**, *via* oxidation to their corresponding fluoroaldehyde, followed by deoxofluorination. The synthesis of the other trifluorinated motif R-CF$_2$CH$_2$F (**G5** and **I5**), will be attempted through the deoxyfluorination of **3.7** and **3.8** respectively.

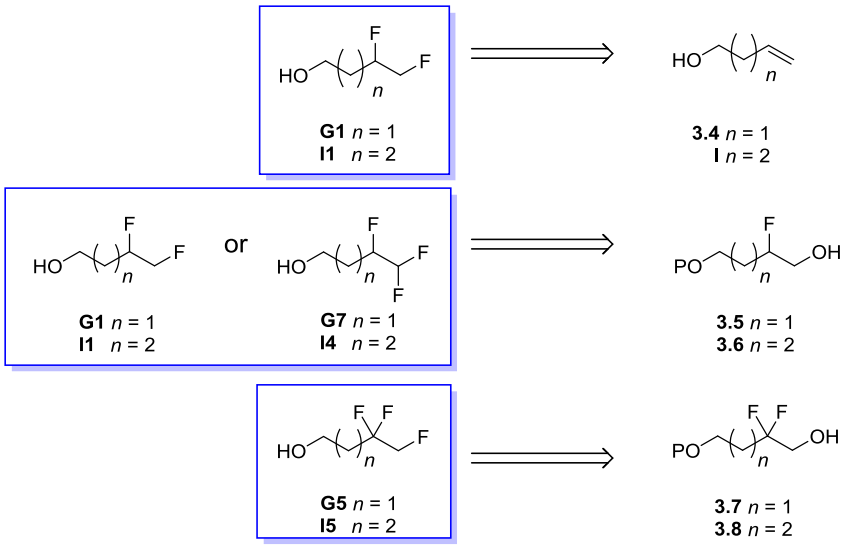

Scheme 3.2 - Proposed route for G1, I1, G7, I4, G5 and I5

Retrosynthetic analysis of the analogues found in Scheme 3.3, reveals that their synthesis can be accomplished *via* either deoxo- or deoxyfluorination of their corresponding commercially available starting materials.

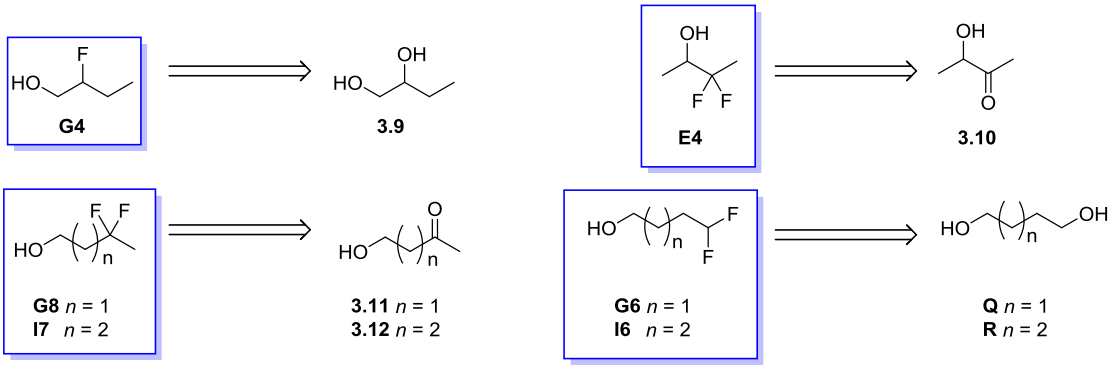

Scheme 3.3 - Synthesis by nucleophilic fluorination

The ketone **3.13** (Scheme 3.4), required for synthesis of either the monofluorinated **I8** or the difluorinated analogue **I11** (after reduction to the corresponding alcohol), is not commercially available. Therefore, **3.13** will be synthesised *via* an oxa-Michael addition from ethyl vinyl ketone **3.14**.[127]

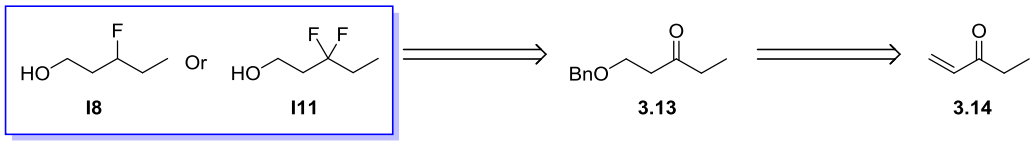

Scheme 3.4 - Retrosynthetic analysis of I8 and I11

While the synthesis of **H1** (Scheme 3.5) has been previously performed by Peterson *et al.*,[128] the synthetic route employed the highly toxic reagent, mercury (II) sulphate ($HgSO_4$). Thus, a safer

alternative route was required. A retrosynthetic analysis of **H1** and **H4**, indicated that γ-valerolactone **3.16** could be employed as a common starting material for both analogues. Their synthesises can be accomplished following the reduction of **3.16** to its corresponding diol and subsequent protection of the secondary alcohol, affording the key intermediate **3.15**. Fluorination with DAST can then be performed, to yield either the 5-fluoropentan-2-ol **H1** or the previously unreported 5,5-difluoropentan-2-ol **H4** (after oxidation of the alcohol to its respective aldehyde).

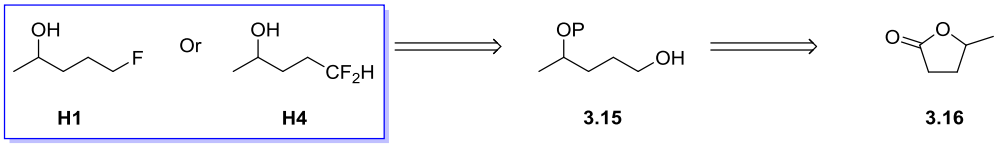

Scheme 3.5 - Retrosynthetic analysis of H1 and H4

Retrosynthetic analysis of **H7** (Scheme 3.6) leads to the ketone **3.17**, which can be obtained from (-)-ethyl L-lactate **3.18** *via* a Weinreb ketone synthesis.[129]

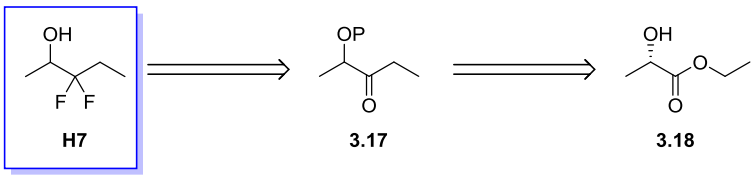

Scheme 3.6 - Retrosynthetic analysis of 3,3-difluoropentan-2-ol H7

3.2 Electrophilic fluorination

3.2.1 Introduction

Electrophilic fluorination is a useful tool to allow for the introduction of the C-F bond into organic molecules. However, the generation of the desired electrophile "F^{+}" is no easy task considering that fluorine is the most electronegative element known.[130] Over the years, a series of reagents have been developed to tackle this issue. These reagents either exploited the inductive effect, withdrawing the electronic charge from fluorine, or utilized the presence of another highly electronegative group, or a combination of the two. Initially, fluorine gas (F_2, first isolated by H. Moissan in 1886[131]) had been employed as the original electrophilic fluorination reagent, however it is highly reactive, toxic and requires specialist equipment for its handling which is not available in Southampton.[132-133] Advancements on the reagent F_2 saw the development of a series of reagents containing an O-F bond (e.g. CF_3OF, HOF and $CsSO_4F$).[134-135] Nevertheless they were still considered too reactive and difficult to handle. Finally, a bench stable, solid source of electrophilic fluorine was

developed, xenon difluoride. Unfortunately, due to its high oxidation potential, many functional groups are unstable towards the reagent.[136]

Fortunately, in the 1980s several N-F bond containing reagents were published, which were crystalline, moisture- and bench-stable (Figure 3.1).[133] Unlike the aforementioned electrophilic fluorination reagents, these required no specialist handling or equipment and were shown to oxidise and fluorinate under mild conditions.[137] Important N-F reagents include *N*-fluorobenzenesulphonimide (NFSI), Selectfluor® and various *N*-fluoropyridinium salts, which have been employed to perform electrophilic fluorination of a range of aromatic rings, Grignard reagents, lithium salts and enolates.[130, 138]

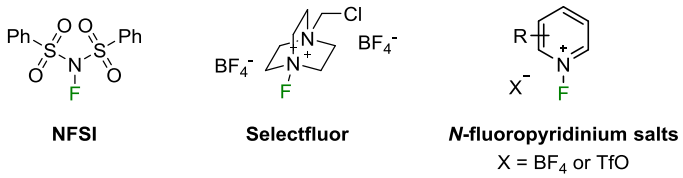

Figure 3.1 - Electrophilic fluorination reagents

Herein, NFSI is covered in greater detail, as a result of the success this reagent has had performing either α-fluorination or α,α-difluorination of aldehydes. These fluorination techniques were developed by D. MacMillan *et al*.[139] *and* C. Barbas *et al*.[140] The introduction of a fluorine in this manner is achieved through the reaction of an aldehyde **3.19** with a secondary amine organocatalyst (Scheme 3.7). This allows for the formation of an enamine **3.20**, followed by electrophilic fluorination with *N*-fluorobenzenesulphonimide (NFSI). The resultant fluoroaldehyde **3.21** can then either be reduced to their corresponding alcohol, undergo a second round of fluorination (if excess of NFSI is used), or functionalised to fluoroamines *via* reductive amination.[141-142]

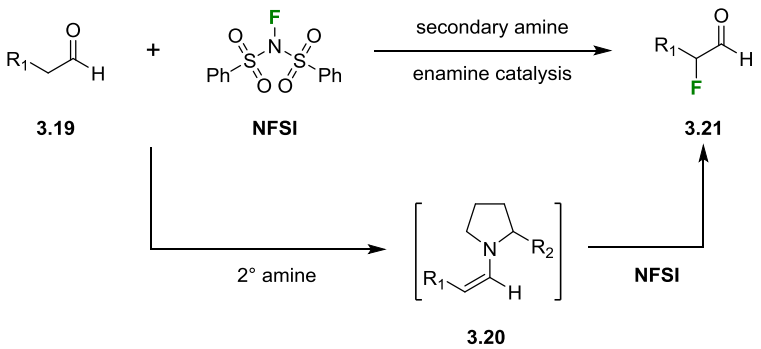

Scheme 3.7 - Organocatalytic α-fluorination adapted from D. MacMillan *et al.*[139]

3.2.2 Synthesis of 2,2-difluorobutan-1-ol and 2,2-difluoropentan-1-ol

The synthesis of both 2,2-difluorobutan-1-ol **G11** and 2,2-difluoropentan-1-ol **I14** was achieved *via* electrophilic fluorination with NFSI (Scheme 3.8), utilizing an adapted procedure from C. Lindsley *et al.*[142] Treatment of the aldehyde **3.1,** with excess NFSI and catalytic proline, allowed for the formation of its corresponding fluoroaldehyde intermediate **3.22**. Reduction with $NaBH_4$ yielded the final product 2,2-difluorobutan-1-ol **G11** in a yield of 28%. The synthesis of 2,2-difluoropentan-1-ol **I14** was achieved in a similar fashion starting from the aldehyde **3.2.**

Several key modifications to the published synthetic procedure were performed due to the presumed volatility of the fluoraldehydes intermediates **3.22** and **3.23**. Traditionally, after the aqueous work up of the electrophilic fluorination, the crude fluoroaldehyde intermediate would be concentrated and then reduced with $NaBH_4$ in a CH_2Cl_2/EtOH solvent system. However, because of the presumed volatility of the fluoraldehydes, after aqueous work up no concentration of the crude mixture was performed. Instead, the resultant crude material, dissolved in a mixture of THF and Et_2O, was treated directly with $NaBH_4$. The reaction was then monitored by ^{19}F NMR, until complete reduction of the fluoroaldehyde intermediate was observed. If the THF were to be removed at this stage, at a reduced pressure *in-vacuo*,[xiii] a considerable loss of product would still occur due to the volatility of the final compounds. Therefore, the THF solvent was removed *via* short path distillation before purification *via* column chromatography.

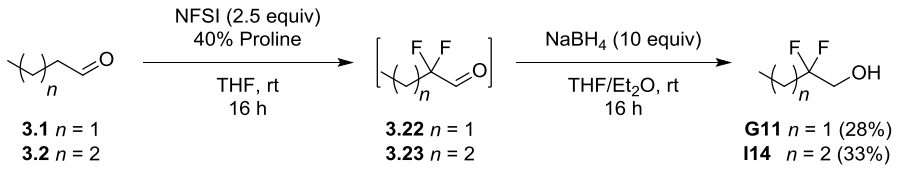

Scheme 3.8 - Synthesis of 2,2-difluorobutan-1-ol and 2,2-difluoropentan-1-ol

3.2.3 Synthesis of 2-fluorobutan-1,4-diol and 2,2-difluorobutan-1,4-diol

The synthesis of both 2-fluorobutan-1,4-diol **Q1** and 2,2-difluorobutan-1,4-diol **Q4** commenced from the commercially available 1,4-butandiol **Q** (Scheme 3.9). An initial mono-benzoylation protection of **Q** was accomplished, affording **3.24** in a yield of 59%. Following this, a Swern oxidation was performed and the resulting aldehyde **3.25** was isolated *via* column chromatography, with a yield of 93%.

[xiii] Procedure often utilized for the removal of commonly used low boiling point solvents (pentane, CH_2Cl_2 and Et_2O).

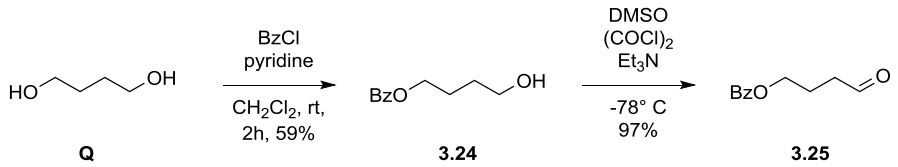

Scheme 3.9 - Synthesis of 4-oxobutyl benzoate

With **3.25** in hand, the organocatalytic fluorination with NFSI and a catalytic secondary amine, as described by C. Lindsley *et al*.[141-142] and D. MacMillan *et al*.,[139] could now be performed. If the correct chiral organocatalyst is employed, the α-fluorination product can be stereo selective to high degrees of *ee*. However, the stereochemistry of the fluorine is not a priority in the synthesis of **Q1**, since enantiomers have the same log*P* value when measured in an octanol/water system. Therefore, L-proline (which was reported to lead to a low enantioselectivity of the fluorination) was the chosen organocatalyst, because of its low cost and commercial availability.

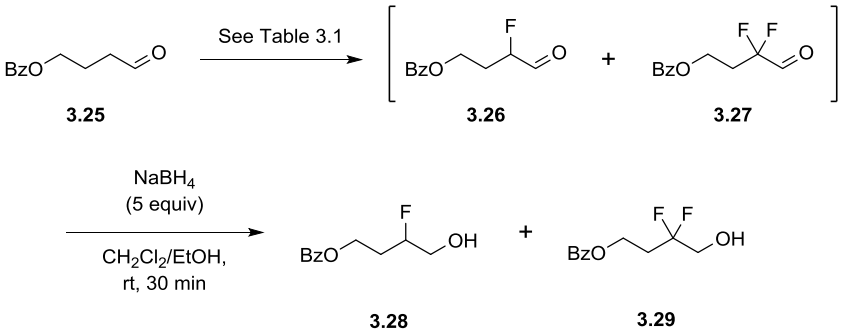

Scheme 3.10 - Optimization of electrophilic fluorination

Initially, standard conditions to afford the α-fluorination product **3.28** were attempted (Scheme 3.10, Entry 1, Table 3.1). This afforded a mixture of the desired mono- and difluorinated substrates **3.26** and **3.27**. These fluoroaldehydes were then reduced as a mixture with sodium borohydride, yielding **3.28** and **3.29** respectively, which were later successfully separated *via* flash column chromatography. Unfortunately, only 7% of the desired α-fluorination product **3.28** was isolated, with 30% of the α,α-difluorinated **3.29** by-product isolated separately. This is thought to have occurred due to the fluorination occurring faster than the enamine aldehyde equilibrium. Therefore, in order to improve the yield, stoichiometric proline was used (Entry 2, Table 3.1). This favoured the α-fluorination product **3.28** with an isolated yield of 49%, however α,α-difluorination still occurred affording **3.29** in a 9% yield. The reaction was repeated once more with more slightly reduced equivalents of NFSI (1 equiv) and an increased isolated yield of 65% of **3.28** was achieved, although **3.29** was still present with a 9% isolated yield (Entry 3, Table 3.1). Finally, one iteration of α,α-difluorination was attempted with excess NFSI and catalytic L-proline (Entry 4, Table 3.1), affording **3.29** in a 40% yield, with no α-monofluorination product observed. Although the yield for the α,α-difluorination reaction was lower than hoped for, the optimization of this reaction was not

investigated further, as sufficient quantities of **3.29** had been isolated through the combining of material obtained from the optimization of **3.28**.

Table 3.1 - Optimization of electrophilic fluorination. Reaction conditions: rt, 16 h, THF/*i*-PrOH (9:1). NFSI and L-Proline equivs, scale and yields can be found in the table.

Entry	Conditions and scale	Isolated yield (over 2 steps)
1	NFSI (1.05 equiv), L-Proline (0.2 equiv), 0.92 g	7% (**3.28**) + 30% (**3.29**)
2	NFSI (1.05 equiv),L-Proline (1.0 equiv), 0.92 g	49% (**3.28**) + 9% (**3.29**)
3	NFSI (1.0 equiv), L-Proline (1.0 equiv), 6.72 g	65% (**3.28**) + 9% (**3.29**)
4	NFSI (2.2 equiv), L-Proline (0.4 equiv), 0.92 g	0% (**3.28**) + 40% (**3.29**)

Following the successful optimisation of the α-fluorination process, both **3.28** and **3.29** were individually deprotected with 25% NaOMe in MeOH (Scheme 3.11). This yielded the desired products **Q1** as an oil and **Q4** as a crystalline solid, with the X-ray crystal structure shown in Figure 3.2.

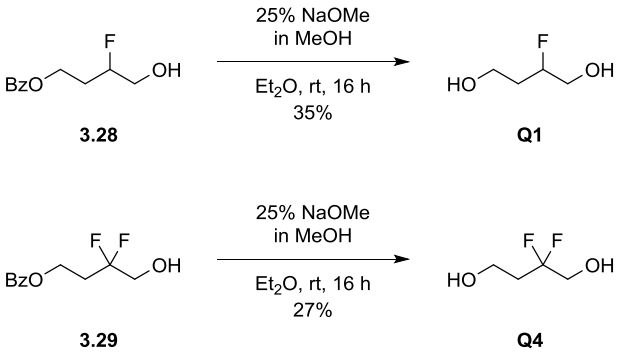

Scheme 3.11 - Synthesis of 2-fluorobutan-1,4-diol and 2,2-difluorobutan-1,4-diol

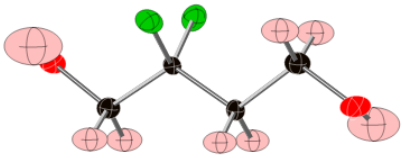

Figure 3.2 - Crystal structure of Q4. Thermal ellipsoid – Carbon = black, oxygen = red, fluorine = green and hydrogen = grey.

3.2.4 Synthesis of advanced fluorinated pentan-1-ol intermediates *via* electrophilic fluorination

The synthesis of **3.30** (Scheme 3.12) was performed in a similar fashion to the synthesis of **3.25** (Scheme 3.9). The subsequent electrophilic fluorination to afford corresponding fluorinated pentyl substrates, utilized the previously optimized α-fluorination conditions. This allowed for the isolation of both **3.33** and **3.34** in sufficient yields for further derivation, 48% and 13% respectively. Unlike **3.28** and **3.29** (Scheme 3.11), **3.33** and **3.34** were not deprotected to afford their corresponding diols, due to another ongoing project within the group, investigating fluorinated 1,5-pentandiol linkers.

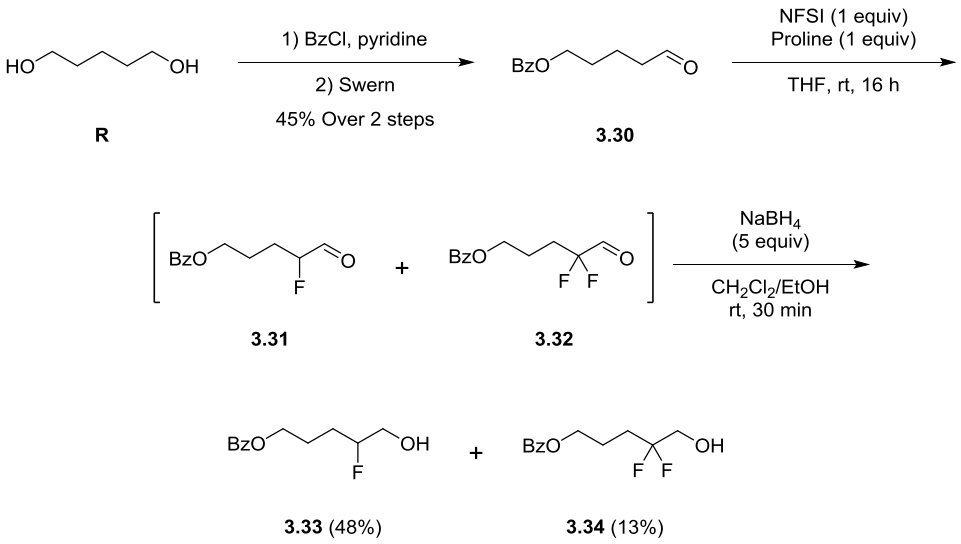

Scheme 3.12 - Synthesis of advanced intermediates 3.33 and 3.34

3.3 Nucleophilic fluorination

3.3.1 Introduction

Nucleophilic fluorination remains a challenging area in organic chemistry. Difficulties in the formation of the C-F bond in this manner arise from fluorine's small size (1.36 Å radius) and low polarizability.[130] These properties allow for fluorine to act as both a nucleophile and as a base, which can lead to unfavourable side reactions, mainly deprotonation and elimination.

Over the years, various fluoride sources have been employed to displace either a halide or sulphonate esters in order to form the C-F bond. HF based reagents (e.g. HF-Pyridine, Et_3N•3HF, DMPU•HF)[134] have been used, although these are corrosive and toxic making them undesirable reagents. Solid sources of fluorine include alkali-metal fluoride salts (e.g., KF and CsF), which were initially employed due to their affordability and commercial availability.[130, 138] Unfortunately, because of their high lattice energy, these reagents behave as weak nucleophiles and have poor solubility in most organic solvents. These issues can be alleviated through the use of crown ethers (improving nucleophilicity), high boiling solvents accompanied with elevated reaction temperatures (aiding solubility), or a combination of the two.[130] Tetralkylammonium fluorides (e.g. TBAF, $TBAF_{anh}$[143], $TBAF(t\text{-BuOH})_4$[144] and TBAT,[145] as seen in Figure 3.3) were developed as a replacement for the alkali-metal fluorides. The use of a bulky organic cation in place of the inorganic M^+ ion, allows for increased solubility in organic solvents, the reduction of ion pairing and the improvement of the nucleophilicity (and basicity) of the fluoride ion.[130] Further advances on one-pot sulphonate displacement deoxyfluorination reagents has taken place in recent years with reagents such as PyFluor[146] and nonafluorosulphonyl fluoride (NfF).[147]

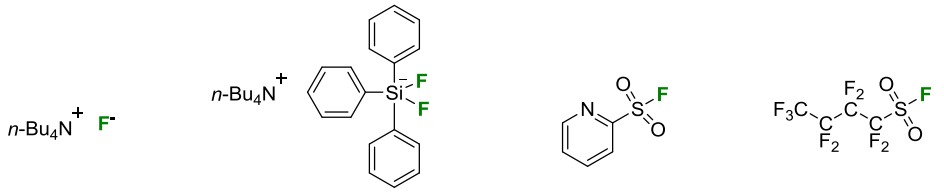

Figure 3.3 - Newly developed nucleophilic fluorination reagents

A series of sulphur-based organic compounds have also been developed, serving as powerful deoxy/deoxofluorination reagents that require no pre-activation of the functional group (i.e. activation of an alcohol *via* its conversion to a mesylate leaving group). The development of these sulphur-based fluorination reagents began with sulphur tetrafluoride (SF_4),[148-149] which has been used for a range of nucleophilic fluorination reactions.[150] However, its high toxicity (similar to that of phosgene) and volatility (b.p. -40 °C) resulted in the requirement of specialist equipment.

Therefore in 1975,[151] DuPont disclosed a bench stable reagent, *N,N*-diethylaminosulphur trifluoride (DAST, Figure 3.4) as an alternative to SF_4. Unfortunately, it was unstable to heat. It is known to rapidly decompose at >60 °C and is explosive at high temperatures (>~155 °C, releasing 1641 J/g),[152] believed to be because of its degradation products (amine and sulphur based compounds).[153] Thus, Deoxo-Fluor® was developed as a safer alternative (>90 °C decomposition temperature).[154] Recently XtalFluor-E®[152], Xtalfluor-M®[152] and Fluolead™[155] have also been developed as a new generation of bench-stable solids with higher degrees of thermal stability. Unfortunately, these sulphur-based reagents also tend to have poor stereoselectivity in deoxyfluorination reactions. This is because they can be prone to S_N1 pathways, as well as the expected S_N2, although, additives can correct this.[156]

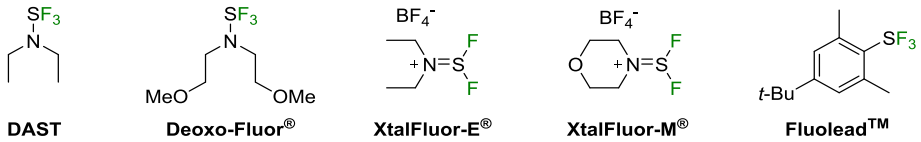

Figure 3.4 - Popular sulphur-based fluorination reagents

3.3.2 Synthesis of 3,4-difluorobutan-1-ol and 4,5-difluoropentan-1-ol

It was envisioned that a simple deoxyfluorination could be performed on the previously synthesised **3.28** and **3.33** (Scheme 3.13), which would yield **3.35** and **3.36** respectively. A scan of the literature revealed a similar deoxyfluorination, performed by Vorberg *et al*., utilizing NfF as their fluorination reagent.[115] The deoxyfluorination of **3.28** and **3.33** with NfF progressed with ease, affording the desired vicinal difluorides **3.35** and **3.36** in good yields. Unfortunately, following the benzoate cleavage of **3.35**, **G1** was isolated in a low 27% yield. Initially, this was presumed to be due to high volatility of **G1**, but upon further consideration it is believed to have undergone a 1,4-cyclisation substituting a fluoride. If the benzoate cleavage was to be repeated, the formation 3-fluorotetrahydrofuran could be confirmed by ^{19}F NMR analysis of the reaction mixture. A similar reaction had occurred previously within the group, when the distillation of 4-fluoropentan-1-ol was attempted (Scheme 3.14), it was discovered that ~20% of the material had cyclised to give 2-methytetrahydrofuran.[94] Following this, to avoid any further 1,4-cyclisations, the deprotection of **3.36** was performed at 0 °C. Analysis of the reaction mixture *via* ^{19}F NMR analysis revealed complete consumption of starting material, with no evolution of fluorinated side products. The final isolated yield for **I1** of 83% further suggests that no side reactions occurred. Therefore, deprotections of substrates where a potential 1,4-cyclisation could occur, should be performed at 0 °C.

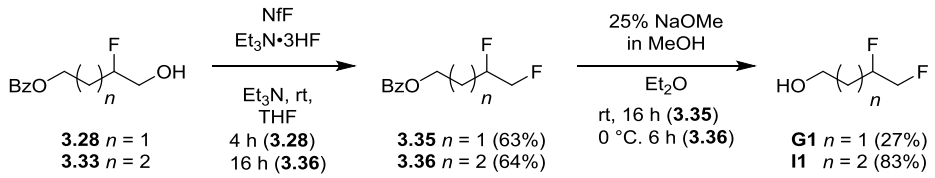

Scheme 3.13 - Synthesis of 3,4-difluorobutan-1-ol and 4,5-difluoropentan-1-ol

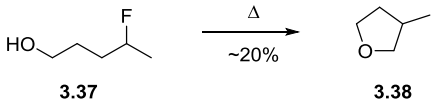

Scheme 3.14 - Undesired thermal degradation of 4-fluoropentan-1-ol

3.3.3 Synthesis of 3,4,4-trifluorobutan-1-ol and 4,5,5-trifluoropentan-1-ol

No synthetic route for the synthesis of the trifluoro-motif R-CHFCHF$_2$, *via* deoxofluorination has previously been reported. Therefore, with the β-monofluorohydrin **3.28** and **3.33** in hand (Scheme 3.15), the synthesis of **G7** and **I5** by deoxofluorination was investigated. While the synthesis of **3.26** and **3.31** was achieved earlier *via* electrophilic fluorination with NFSI, it was decided not to use this route due to the reaction producing both the mono- and difluorinated analogues, which may complicate purification at later stages. Therefore, oxidation of the β-monofluorohydrin to the corresponding aldehyde was performed. Despite the formation of the aldehydes **3.26** and **3.31** earlier, *via* electrophilic fluorination with NFSI (Section 3.2.2), a literature search reveals that this is a relatively uncommon reaction; despite this, standard conditions for either a Swern,[157] Dess-Martin periodinane (DMP)[158] or PCC[159] oxidations have all been reported. Due to the ease of handing and the facile nature of the reaction, DMP was the chosen oxidation reagent.

Both alcohols were successfully oxidised to the corresponding aldehyde, before subsequent deoxofluorination with DAST, providing **3.39** and **3.40** in yields of 34% and 35% over 2 steps respectively (Scheme 3.15). Finally, cleavage of the benzoate afforded the desired novel trifluoro-motif **G7** and **I5** in good yields, 79% and 88% respectively.

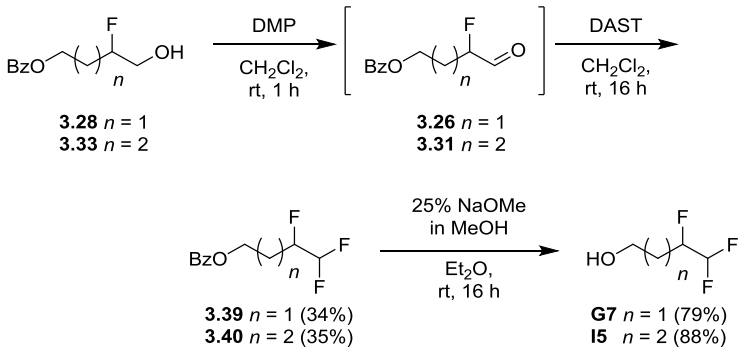

Scheme 3.15 - Synthesis of 3,4,4-trifluorobutan-1-ol and 4,5,5-trifluoropentan-1-ol

3.3.4 Synthesis of 3,3,4-trifluorobutan-1-ol and 4,4,5-trifluoropentanol

The trifluorinated motif R-CF_2CH_2F has little precedence within literature and its synthesis *via* deoxyfluorination has only been performed twice on aromatic substrates; once with nonafluorobutanesulphonyl fluoride (NfF)[160] and once with DAST[161] (Scheme 3.16). Therefore, the introduction of this of this relatively novel motif onto aliphatic substrates will be investigated.

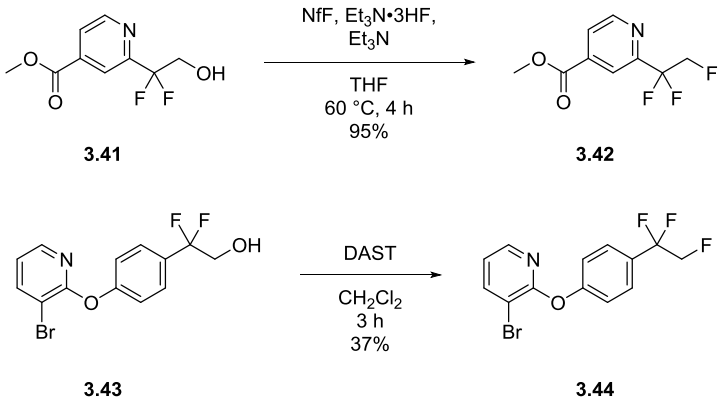

Scheme 3.16 - Previously reported deoxyfluorination to afford the desired trifluorinated motif

With intermediate **3.29** (Scheme 3.17) in hand from the 2,2-difluorobutan-1,4-diol **Q4**, its deoxyfluorination to provide the trifluorinated **3.45** was attempted, employing either NfF or DAST. The first reaction utilized the deoxyfluorination reagent NfF using the originally published conditions by J. Yin *et al.* (Entry 1, Table 3.2).[147] This reaction yielded 10% of the desired trifluorinated product **3.45** and 70% of the sulphonyl intermediate **3.46**, as a crystalline solid (Figure 3.5). The reaction required harsher conditions to progress at a faster rate and therefore the reaction was repeated at 80 °C (Entry 2, Table 3.2). An increased yield of 68% was obtained with no sulphonyl intermediate observed. The second deoxyfluorination reagent employed was DAST, however this reaction was very slow, with TLC analysis indicating an incomplete reaction after 5 days (Entry 3, Table 3.2). Despite this slow reaction, the desired trifluorinated product **3.45** was isolated in a good yield of 60%, with 30% of the starting material being reclaimed. Fortunately, upon heating the reaction to 40 °C, a similar yield of 56% was achieved with a vastly reduced reaction time of 16 h (Entry 4, Table 3.2). Increasing reaction temperature further may improve yields and reduce reaction times, but it is important to note the hazards that can arise when heating DAST (See Section 3.3.1). Thus, it is undesirable to approach these temperatures even for short periods of time, so no further optimization with DAST was performed.

Therefore, if a similar deoxyfluorination is to be performed, NfF should be the reagent of choice. It provided higher yields and the purification of the desired material was easier, due to the lack of DAST degradants that can complicate flash column-chromatography.

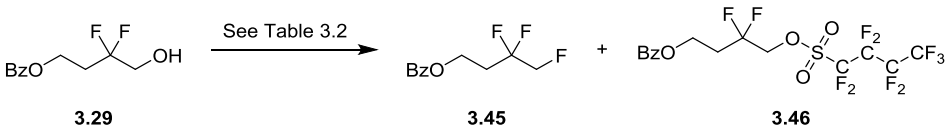

3.29 3.45 3.46

Scheme 3.17 - Synthesis of 3,3,4-trifluorobutyl benzoate

Table 3.2 - Deoxyfluorination optimization

Entry	Conditions	Isolated yield (3.45)
1	NfF, $Et_3N•3HF$, Et_3N, MeCN, rt, 16 h	10% (**3.45**) + 70% (**3.46**)
2	NfF, $Et_3N•3HF$, Et_3N, MeCN, 80 °C, 16 h	68%
3	DAST, CH_2Cl_2, rt, 5 days	60%
4	DAST, CH_2Cl_2, 40 °C 16 h	56%

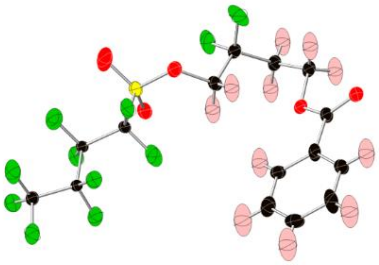

Figure 3.5 - Crystal structure of 3.46

With the sulphonyl intermediate **3.46** (Scheme 3.18) in hand from the previously attempted fluorination of **3.45**, the desired fluorination reaction was driven to completion at 80 °C, in the presence of $Et_3N•3HF$ and Et_3N, to afford the desired deoxyfluorination product **3.45** in an 88% yield. This provided a two-step yield of 62%, slightly lower than that of the 68% yield obtained in the one pot reaction (Entry 2, Table 3.2).

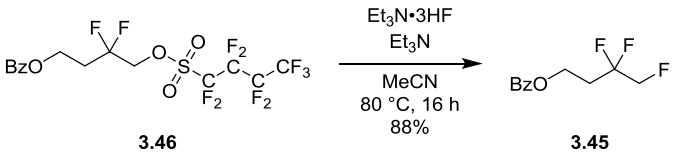

Scheme 3.18 - Synthesis of 3,3,4-trifluorobutyl benzoate

Following the successful optimisation in the synthesis of **3.45** (Scheme 3.19), the fluorination conditions were applied to the pentyl analogue, to afford **3.47** in an in excellent yield of 78%. Finally, deprotection of the benzoate protecting group was performed with 25% NaOMe in MeOH in both cases, to yield the desired final products **G5** and **I4** in a yield of 62% and 87% respectively.

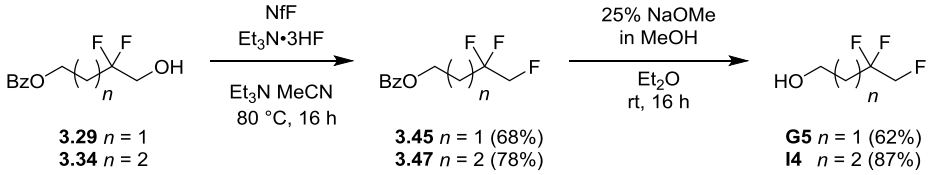

Scheme 3.19 - Synthesis of 3,3,4-trifluorobutan-1-ol and 4,4,5-trifluoropentanol

3.3.5 Synthesis of 2-fluorobutanol

The synthesis of 2-fluorobutanol **G4** was also achieved *via* deoxyfluorination with nonafluorobutanesulphonyl fluoride. Selective protection of the primary alcohol of **3.9** was achieved with benzoyl chloride (Scheme 3.20), affording **3.48** and **3.49** in isolated yields of 79% and 3% respectively after column chromatography.

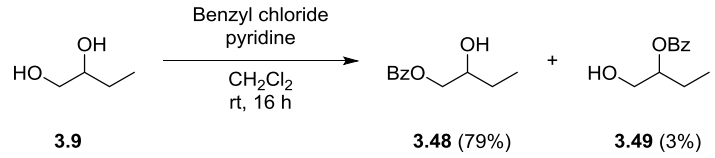

Scheme 3.20 - Selective protection of 3.9 to afford 3.48 and 3.49

With pure **3.48** in hand (Scheme 3.21), the monofluorinated product **3.50** was obtained *via* NfF mediated deoxyfluorination. Subsequent cleavage of the benzoate ester produced the final compound 2-fluorobutanol **G4**, with an overall yield of 34% over 3 steps.

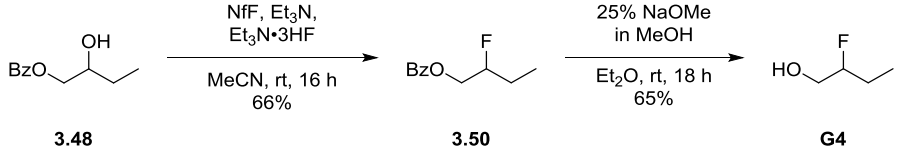

Scheme 3.21 - Synthesis of 2-fluorobutanol

3.3.6 Synthesis towards 3,3-difluorobutan-2-ol

Starting from the commercially available ketone **3.10** (Scheme 3.22), The synthesis of 3,3-difluorobutan-2-ol was successfully performed. Standard conditions were employed for the benzoyl protection of **3.10**, yielding **3.51**. The deoxofluorination of **3.51** was carried out utilizing DAST, although this yielded an inseparable mixture of the desired *gem*-difluoro product **3.52** and the fluoroalkene elimination product **3.53** in a ratio of 9:1. Unfortunately, upon deprotection the two products remained inseparable, yielding a mixture of **E4** and **E5** in a ratio of 85:15.[xiv]

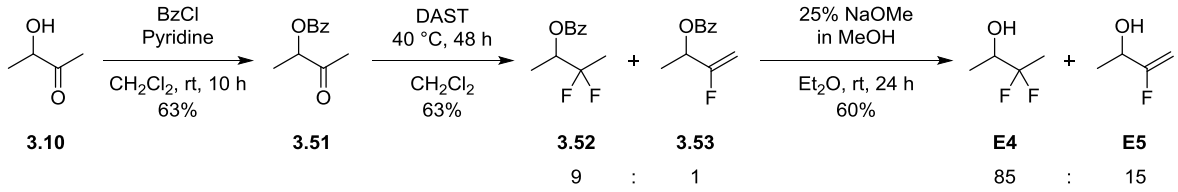

Scheme 3.22 - Synthesis of 3,3-diflurofluorobutan-2-ol

3.3.7 Synthesis of 3,3-difluorobutan-1-ol and 4,4-difluoropentan-1-ol

The synthesis of the 3,3-difluorobutan-1-ol was achieved in three steps from the commercially available 4-hydroxybutan-2-one **3.11** (Scheme 3.23). First, benzoate protection of **3.11** was carried out providing **3.54**. However, after purification by column chromatography, residual benzoic acid was observed *via* ^{1}H NMR analysis. Fortunately, this impurity does not hinder the ensuing fluorination and will only react with DAST to form its respective acyl fluoride, as demonstrated on similar substrates[162] or by the treatment of benzoic acid with Deoxo-Fluor®.[154] The deoxofluorination of **3.54** was therefore performed with no further purification, yielding the *gem*-difluoro product **3.56**. Finally, deprotection was performed with 25% NaOMe in MeOH to yield the desired 3,3-difluorobutan-1-ol, **G8**.[1] Starting from commercially available 5-hydroxypentan-2-one **3.12**, the synthesis of 4,4-difluoropentan-1-ol **I7** was performed in a similar manner as for **G8**.

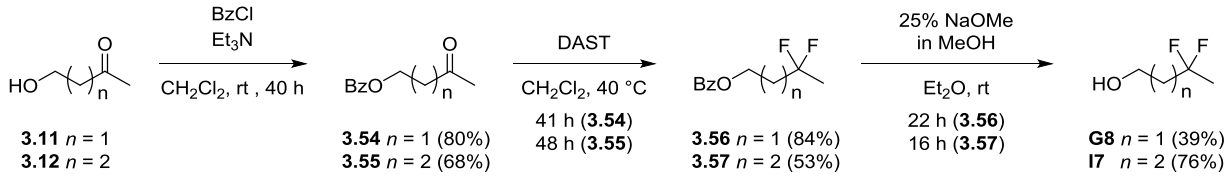

Scheme 3.23 - Synthesis of 3,3-difluorobutan-1-ol and 4,4-difluoropentan-1-ol

[xiv] This synthetic work was performed by Simon Holland (4th year MChem student) under my supervision

3.3.8 Synthesis of 4,4-difluorobutan-1-ol and 5,5-difluoropentanol

The synthesis of 4,4-difluorobutanol-1-ol **G6** (Scheme 3.24) commenced from the advanced intermediate **3.25** (previously synthesised in Section 3.2.3). The deoxofluorination of the aldehyde **3.25** with DAST provided the *gem*-difluorinated product **3.58** in a high yield of 86%. Deprotection of **3.58** was then performed with 25% NaOMe in MeOH to afford the desired 4,4-difluorobutan-1-ol, **G6**.[xv] Starting from the advanced intermediate **3.30** (previously synthesised in Section 3.2.4), the synthesis of 5,5-difluoropentan-1-ol **I6** was performed in a similar manner to **G6**.[xvi]

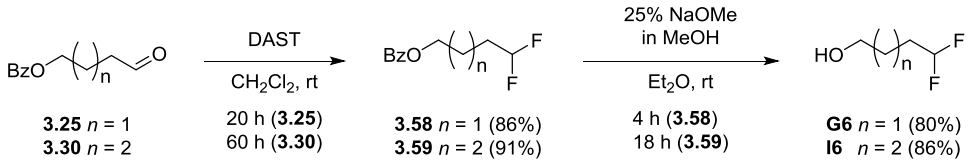

Scheme 3.24 - Synthesis of 4,4-difluorobutan-1-ol and 5,5-difluoropentan-1-ol

3.3.9 Synthesis of 3-fluoropentan-1-ol

The synthesis of 3-fluoropentan-1-ol **I8** was accomplished from the starting material ethyl vinyl ketone **3.14** (Scheme 3.25). The first step of this synthesis is an oxa-Michael addition, promoted by aqueous sodium carbonate as reported by Y. Wang *et al.*[127] Disappointingly, the first attempt to replicate their synthesis provided **3.13** in a yield of 33% (Entry 1, Table 3.3), much lower than the published 73%. Due to similar retention factors, there was also difficulty in the isolation of the target compound **3.13** from unreacted benzyl alcohol *via* column chromatography. In an attempt to ease purification, the reaction was repeated with substantially less equivalents of benzyl alcohol (1.1 equiv vs 4.0 equiv, Entry 2, Table 3.3). This procedural modification facilitated easier purification of **3.13** and conveniently, the same yield as the previous attempt was obtained. As all the starting materials are inexpensive and commercially available, no further reaction optimisation was performed, and a final large-scale reaction was completed with 1.5 equiv of benzyl alcohol (Entry 3, Table 3.3). The isolation of **3.13** was achieved and a slightly improved 42% yield was observed, providing enough substrate to accomplish the synthesis of 3-fluoropentan-1-ol **I8**.

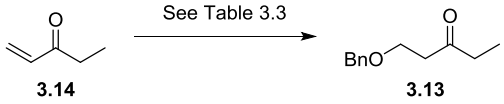

Scheme 3.25 - Synthesis of 3.13

[xv] This synthetic work was performed by Ryan Squire (Summer student) under my supervision
[xvi] This synthetic work was performed by Thomasin Brind (3rd year MChem student) under my supervision

Table 3.3 - Conditions for synthesis of 3.13

Entry	Conditions	Yield
1	BnOH (4.0 equiv), aq. Na_2CO_3 (0.05 M), rt, 16 h	33%
2	BnOH (1.1 equiv), aq. Na_2CO_3 (0.05 M), rt, 16 h	33%
3	BnOH (1.5 equiv), aq. Na_2CO_3 (0.05 M), rt, 16 h	42%

With **3.13** in hand (Scheme 3.26), the reduction of the ketone was performed with $NaBH_4$ and the resultant alcohol **3.60** underwent NfF-mediated deoxyfluorination. This afforded a partially separable mixture of the desired monofluorination product **3.61** and a combination of alkenes **3.62** (elimination products), in a ratio of 1.0:0.4 respectively. To enable a facile isolation of **3.61** from its corresponding alkene side products **3.62**, the mixture was treated with *m*CPBA, resulting in the epoxidation of the alkenes. The epoxides formed were more polar than the desired fluorinated product **3.61**, allowing for its isolation by column chromatography. This provided **3.61** in a yield of 35% over 2 steps. Finally, hydrogenolysis of the benzyl ether protecting group in Et_2O afforded the desired product **I8** in a high yield of 87%.

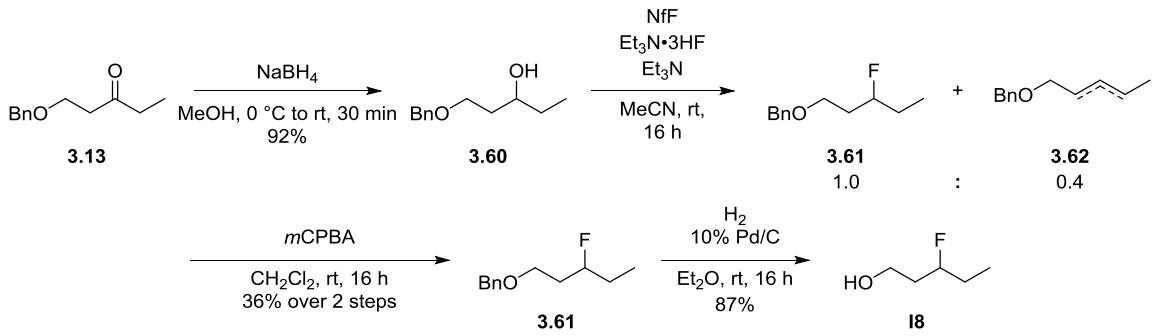

Scheme 3.26 - Synthesis of I8

3.3.10 **Synthesis of 3,3-difluoropentan-1-ol**

With the synthesis of monofluorinated analogue **I8** completed (Scheme 3.26), deoxofluorination of the ketone **3.13** could then be investigated (Scheme 3.27). This was performed *via* the treatment

of **3.13** with DAST at 40 °C. Unfortunately, the reaction progressed at a much lower rate than expected. TLC analysis indicated the presence of starting material **3.13** despite 48 hours elapsing, however, the desired product **3.63** was also observed *via* ^{19}F NMR. Therefore, the reaction was stopped and subsequent column chromatography allowed for **3.63** to be isolated in a 37% yield and ~50% of the starting material **3.13** was reclaimed. The slow rate of conversion and low yield was surprising. Previously performed deoxofluorinations of similar ketones had shown consumption of their respective starting material after ~16 h, with good yields obtained for the *gem*-difluoro products. It is possible that the benzyloxy group could interact with the activated carbonyl but without real formation of the 4-membered ring due to the ring strain, leading to shielding of the carbonyl electrophilic centre from fluoride attack. The reversibility of the DAST-mediated ketone activation step (or any hydrolysis in the workup), would then lead to starting material recovery. Finally, hydrogenolysis of the benzyl ether in Et_2O afforded the desired product **I11** in excellent yield of 86%.

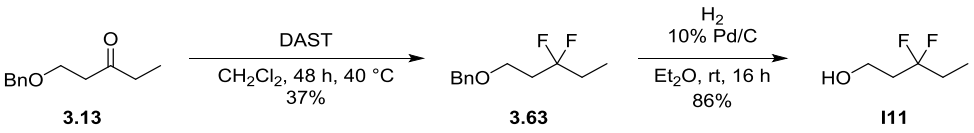

Scheme 3.27 - Synthesis of I11

3.3.11 Synthesis of 5-fluoropentan-2-ol

The synthesis of 5-fluoropentan-2-ol was accomplished starting from γ-valerolactone **3.18** (Scheme 3.28). Following an adapted procedure from Killen *et al.,*[163] **3.18** was reduced with $LiAlH_4$, affording **3.64** in a good yield of 84%. Selective silyl protection of the primary alcohol with TBMSCl was then accomplished, yielding **3.65**, and subsequent basic benzyl ether protection of the secondary alcohol afforded **3.66**. With **3.66** in hand, the deprotection of the silyl group with TBAF was completed, yielding the important intermediate **3.67**, required for deoxyfluorination.

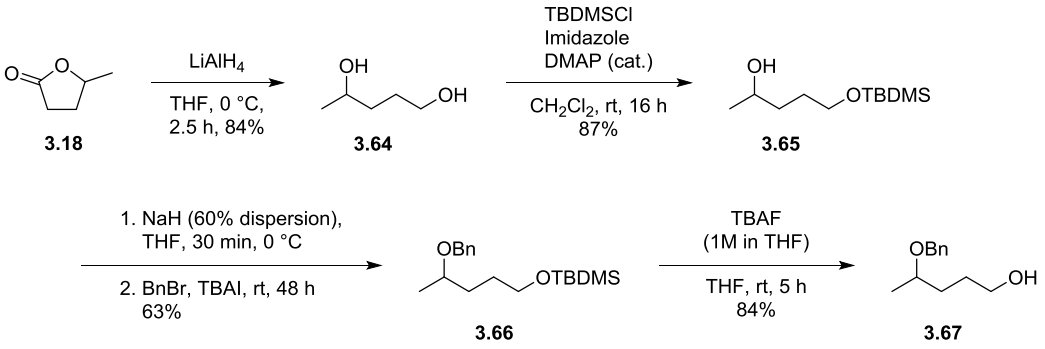

Scheme 3.28 - Synthesis towards key intermediate 3.67

Unfortunately, the fluorination of **3.67** with DAST was unsuccessful (Scheme 3.29), yielding an inseparable mixture of both the presumed desired primary fluorinated substrate **3.68** and the undesired secondary fluorinated substrate **3.69**, with a ratio of 1:10 respectively (^{19}F NMR-analysis).[xvii] No further attempt to purify and characterise **3.68** and **3.69** was performed at this stage and a new route was investigated.

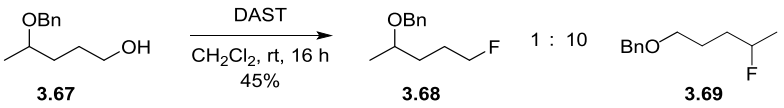

Scheme 3.29 - Fluorination of 3.67

This occurred due to the benzyl ether acting as a nucleophile, resulting in neighbouring group participation and thus the formation of **3.71** (Scheme 3.30). The selectivity towards the formation of **3.69**, is rationalised by the ring opening occurring *via* an S_N1 pathway. The rate determining step in an S_N1 mechanism is the loss of a leaving group, resulting in the formation of a carbocation. The greater the stability of this carbocation, the faster the reaction will occur. Therefore, attack on the secondary carbon of **3.71** is favoured, as its respective carbocation has a greater stability than its corresponding primary carbocation. The selectivity also suggests that the cyclisation pathway is faster than standard fluoride attack on **3.70**.

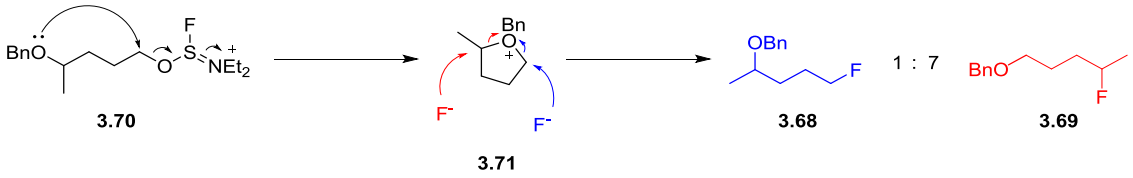

Scheme 3.30 - Mechanism for the formation of 3.68 and 3.69

To avoid any neighbouring group participation during the fluorination reaction, an acetate protecting group was employed instead of the benzyl ether (Scheme 3.31). Standard conditions for the acetylation of the secondary alcohol **3.65** was applied,[164] providing the fully protected substrate **3.72**, in an excellent yield of 97%. The deprotection of the silyl ether of **3.72** was performed again with TBAF, affording the crucial intermediate **3.73**. Deoxofluorination of **3.73** utilizing DAST was successful, providing the desired fluorinated product **3.74** with a yield of 72%. The deprotection of the alcohol was performed using 25% NaOMe in MeOH to afford **H1**.

[xvii] Selected **^{19}F {^{1}H}** (376 MHz, $CDCl_3$) for **3.68**: δ -218.2 (s) ppm; for **3.69**: δ -173.1 (s) ppm.

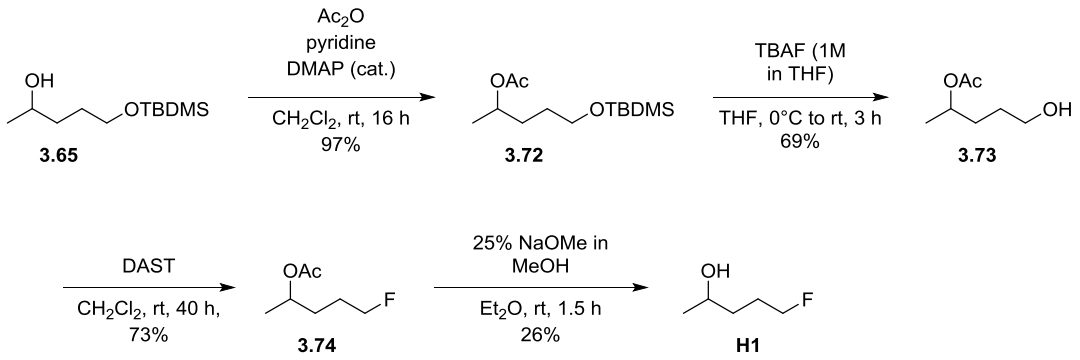

Scheme 3.31 - Synthesis of H1

3.3.12 Synthesis of 5,5-difluoropentan-2-ol

With the key intermediate **3.73** in hand (Scheme 3.32), the synthesis of **H4** could be investigated. However, prior to difluorination, the alcohol of **3.73** must first be oxidised to its corresponding aldehyde **3.75**. This oxidation was achieved utilizing Dess-Martin periodinane, and after purification by column chromatography, the aldehyde **3.75** was immediately treated with DAST. This yielded the desired difluorinated compound **3.76** in a good yield of 73%. The deprotection of **3.76** was performed with 25% NaOMe in MeOH yielding desired final product **H4**.

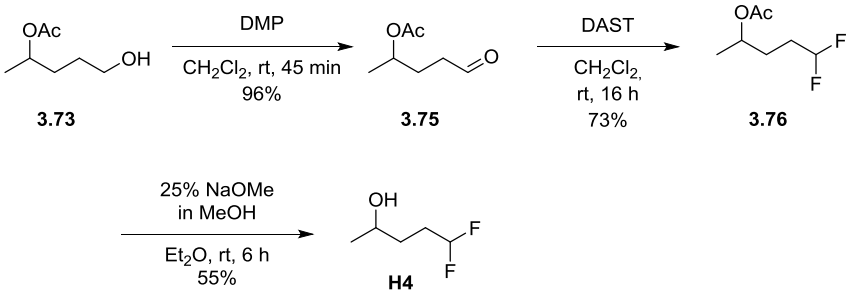

Scheme 3.32 - Synthesis H4

3.3.13 Synthesis of 3,3-difluoropentan-2-ol

The synthesis of 3,3-difluoropentan-2-ol was accomplished from (-)-ethyl L-lactate **3.18**, following its conversion to the protected ketone **3.82,** *via* a Weinreb ketone synthesis (Scheme 3.33). [129, 165] Synthesis of the Weinreb amide **3.77** from **3.18** was performed successfully, with a yield of 89%. Unfortunately, the following Grignard reaction only yielded 33% of the desired Weinreb ketone **3.78**. The low yield was a result of the formation of solid during the reaction (20 g scale). This hampered adequate stirring and resulted in the addition of the Grignard reagent being paused. At this point, TLC analysis indicated complete consumption of the starting material **3.77**. However, after aqueous work up and column chromatography, ~45% of the starting material **3.77** was reclaimed. This suggests that the solid formed may have been a complex of the starting material

and $MgBr_2$. This issue could have been solved with an over-head stirrer. Regardless, a sufficient quantity of the volatile ketone **3.78** had been synthesised, and subsequent benzoate protection of the alcohol with benzoic anhydride, afforded **3.79** in good yield.

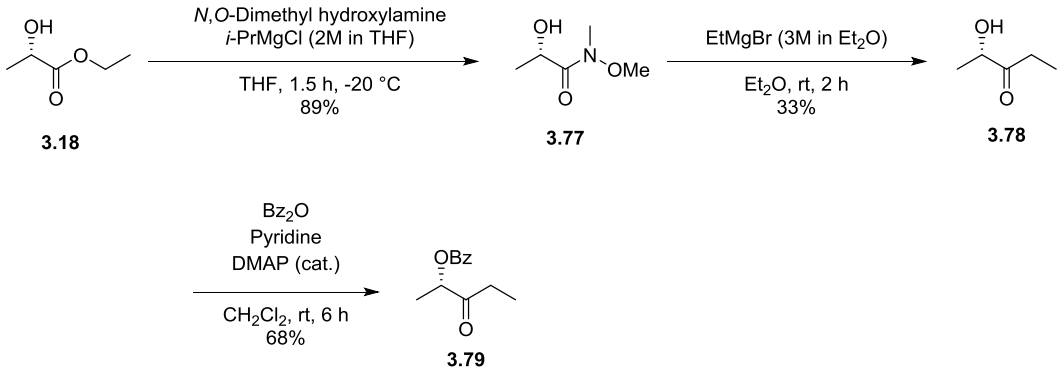

Scheme 3.33 - Synthesis towards 3,3-difluoropentan-2-ol

The difluorination of the key intermediate **3.79** was initially performed with DAST at room temperature (Scheme 3.34). However, TLC analysis of the reaction mixture indicated that the reaction was incomplete after 16 h. Therefore, the reaction mixture was heated to 40 °C and 0.01 equivalents of HF•py was added. After an additional 24 h, the reaction was complete and the formation of the desired *gem*-difluoro product **3.80** and undesired elimination side product **3.81** was observed, in a ratio of 1:0.07 respectively. Unfortunately, the two products were inseparable *via* column chromatography. After cleavage of the benzoyl protecting group, with 25% NaOMe in MeOH, the two compounds were separable with careful column chromatography and **H7** was isolated in a yield of 35% over two steps. The isolation of **3.82** was not attempted due to the small quantity formed.

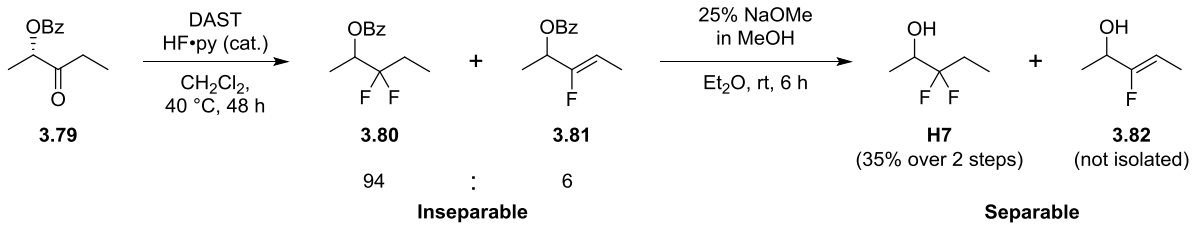

Scheme 3.34 - Synthesis of 3,3-difluoropentan-2-ol

3.4 Vicinal difluorination

3.4.1 Introduction

Despite the previously performed successful 6 step synthesis of **G1** and **I1** (see Section 3.3.2), through a combination of electrophilic and nucleophilic fluorination, it was envisioned that the vicinal difluorination of an alkene could provide the same compounds in fewer steps.

The vicinal difluorination of an alkene with 4-iodotolouene difluoride **3.83** was first investigated in 1998 (Figure 3.6), however the reagents required have limited commercial availability and are required in stoichiometric quantities.[166] In order to overcome these constraints, both R. Gilmour *et al*.[167] and E. Jacobsen *et al*.[168] published procedures on the vicinal difluorination of an alkene with catalytic *p*-iodotoluene. Since then R. Gilmour has further expanded on his research, investigating a procedure for the enantioselective catalytic vicinal difluorination of alkenes[169] and the use of vicinal difluoro-motif as hybrid bioisosteres of trifluoromethyl and ethyl groups.[125]

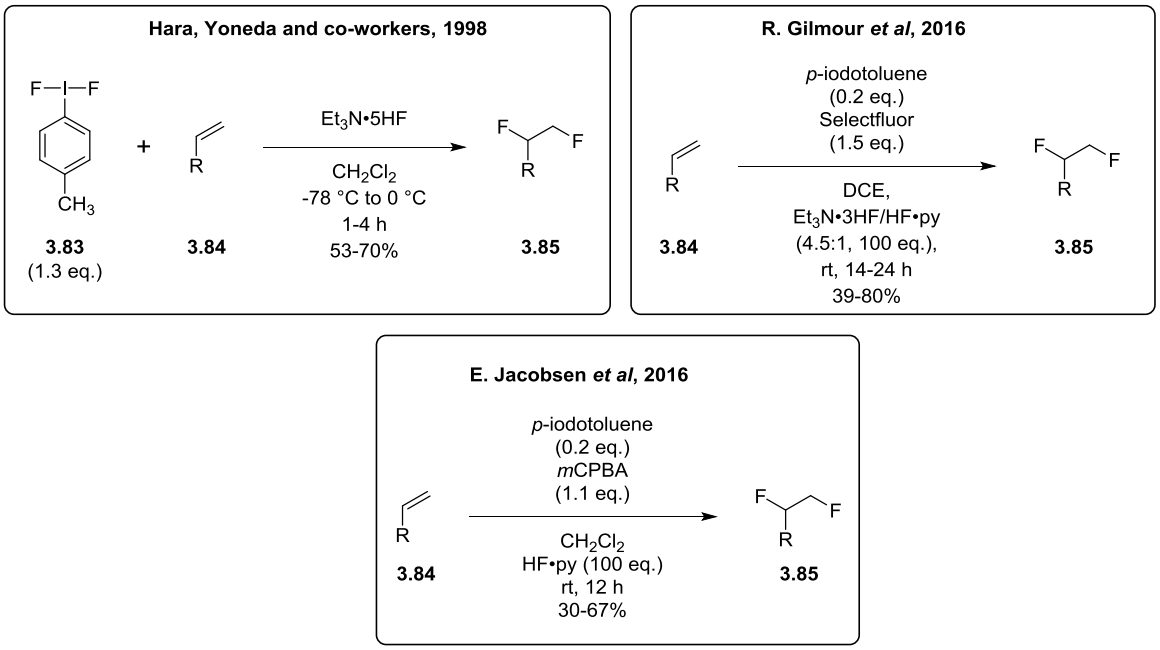

Figure 3.6 - Published procedures for the vicinal difluorination of an alkene

For the following investigation on the vicinal difluorination of buten-1-ol, the procedure by R. Gilmour *et al.*[167] was used. He utilized a mixture of Et_3N•3HF and HF•py (4.5:1, respectively) as the fluoride source, which is marginally safer than neat HF•py (used by E. Jacobsen *et al.*[168]). In an attempt to evaluate the necessity for the excess HF and hopefully improve the safety of the reaction (if scale-up is to be required), the test reactions were performed with both 10 and 100 equivalents of the HF source.

3.4.2 Attempted vicinal difluorination

Initially, the reaction was attempted on buten-1-ol **3.4** with 10 equivalents of the HF source (Scheme 3.35). However, no desired compound was formed, and a large proportion of the starting material remained, as indicated by analysis of the ^{1}H NMR spectrum. A similar reaction was performed by Yoneda *et al*., who observed the cyclization of alkenes (with unprotected hydroxyl groups) analogous to **3.4** when treated with **3.83** (Figure 3.6) and a HF source.[170] Further ^{19}F NMR analysis revealed a multiplet with a similar chemical shift to the cyclization products formed by Yoneda *et al*., at roughly -175 ppm, which became a singlet upon proton decoupling. This suggests the formation of the cyclisation product 3-fluorotetrahydrofuran. If this is the case, the formation of this product likely inhibits any desired fluorination from occurring.

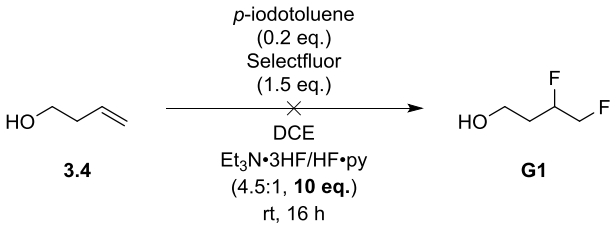

Scheme 3.35 - Synthesis towards 3,4-difluorobutan-1-ol

Instead of attempting increased equivalents of HF (as this would likely promote increased cyclization reactions), buten-1-ol **3.4** was instead benzoate protected, affording **3.86** (Scheme 3.36). The reaction was tried again on **3.86**, with both 10 and 100 equivalents of the HF source. When the reaction was performed with 10 equivalents, no formation of desired product was observed as measured by ^{19}F NMR analysis. However, trace amounts of fluorinated product were observed when the reaction was performed with 100 equivalents. Through subsequent TLC and ^{1}H NMR analysis, it was shown that there was one predominant product. After isolation of the side product by column chromatography and its subsequent analysis by 2D NMR, the by-product was determined to be **3.87**.

The proposed mechanism for the formation of **3.87** is shown in Scheme 3.37. After the formation of the transient cation **3.91**, it is thought that the benzoate protection group undergoes neighbouring group participation to form the 6-membered ring **3.92**, which can then tautomerize to **3.93**. As the reaction progresses through an S_N2 pathway, water preferentially attacks at the less hindered position to re-open the ring and form **3.94**. It is proposed that the source of the water is from the aq. sat. $NaHCO_3$ quench. Finally, the newly introduced hydroxyl ring closes to form **3.87**, while also reforming the catalyst *p*-iodotoluene. The same product was observed by M. Sanford *et al*,[171] when they treated **3.4** (Scheme 3.36) with (dibenzoyloxyiodo)benzene and palladium (II) diacetate, which was formed by a similar mechanism.

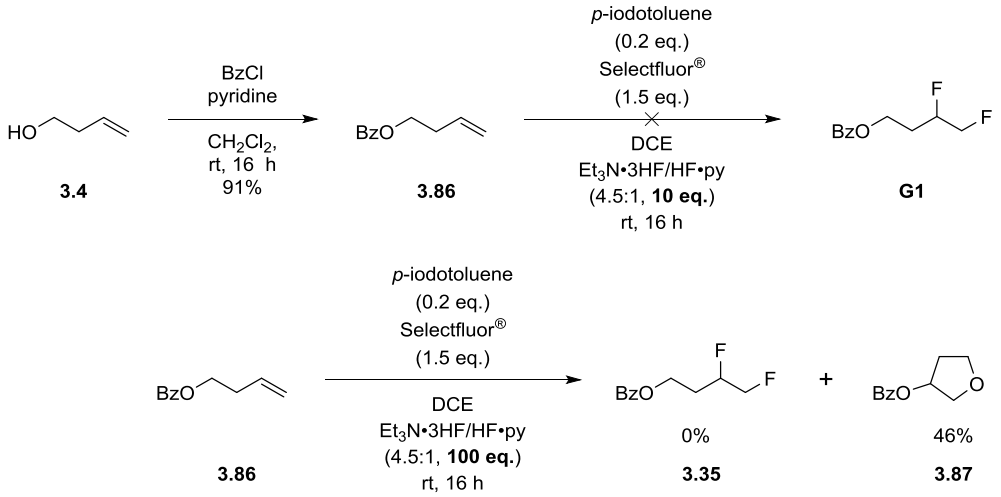

Scheme 3.36 - Synthesis towards 3,4-difluorobutan-1-ol

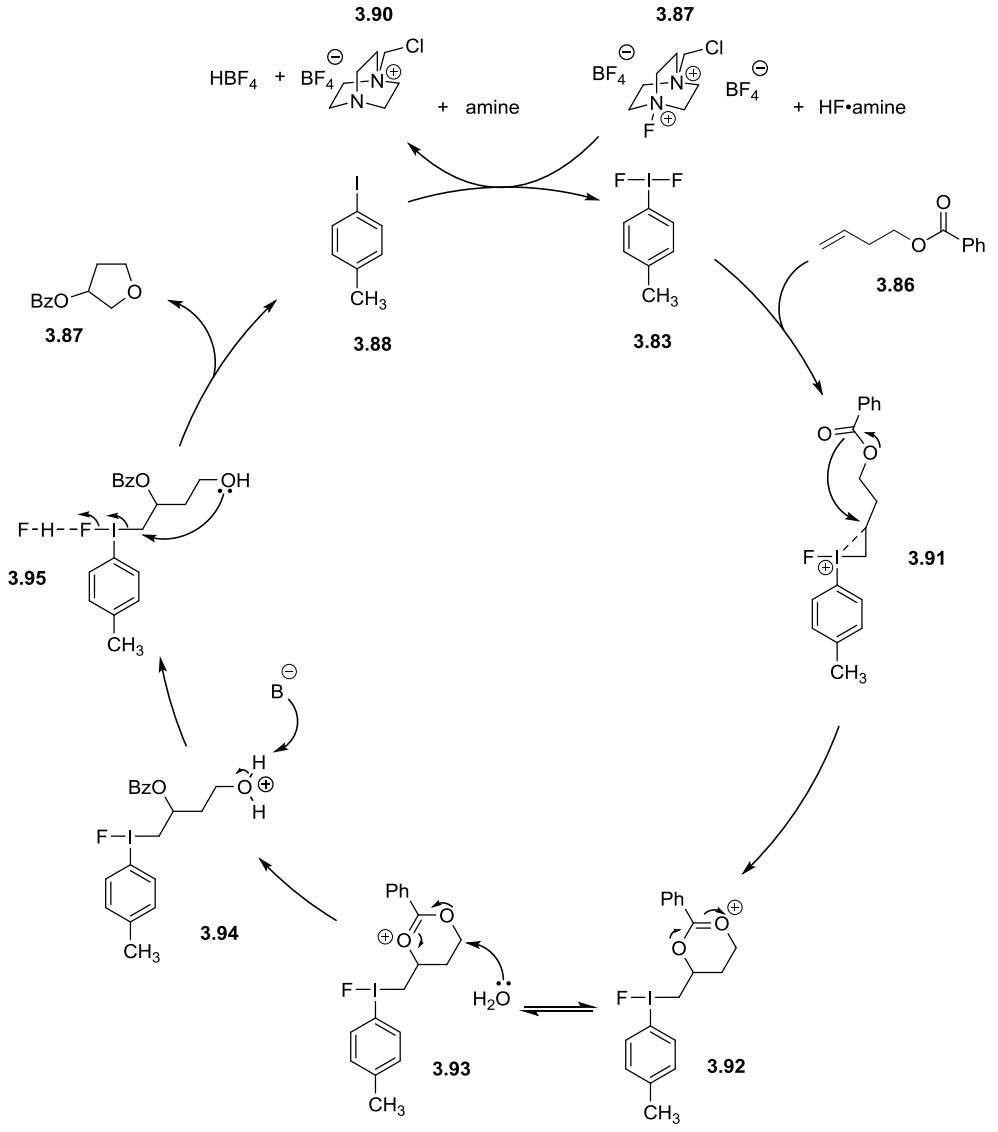

Scheme 3.37 - Proposed mechanism for the formation of 3.87

Despite R. Gilmour's procedure tolerating ester protection groups, the reactions were performed on an undecyl chain, therefore issues with neighbouring group participation would not arise.[167] A different protection group was thus required, and as R. Gilmour *et al.* had success with a tosyl group on a butyl chain, this was attempted next (Scheme 3.38).

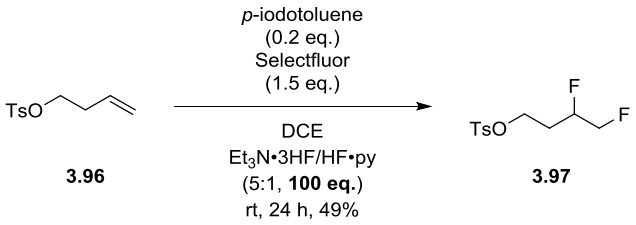

Scheme 3.38 - Vicinal difluorination as reported by R. Gilmour et al.[167]

A tosyl protection group was not originally used, due to the harsh reaction conditions (Na/naphthalene in THF)[172] associated with the deprotection. Unfortunately, when the reaction was trialled with 10 equivalents of the HF source, no reaction *via* ^{19}F NMR was observed and the starting material was completely recovered after aqueous work up (Scheme 3.39). As this reaction failed, no further attempts to reproduce R. Gilmour's procedure was performed, due to the safety concerns of handling large quantities of HF reagents, were scale up was to be performed. It is likely that the high equivalents of the HF source were required to form the reactive intermediate 4-iodotolouene difluoride **3.83** (Figure 3.6).

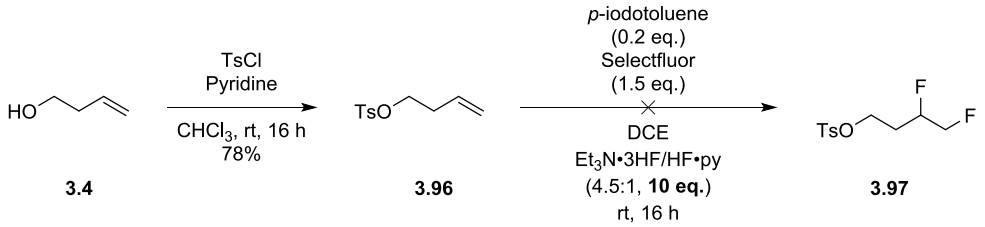

Scheme 3.39 - Synthesis towards 3,4-difluorobutan-1-ol

3.5 Conclusion

A total of twenty-two mono-, di- and trifluorinated analogues of simple alkanols were synthesised through electrophilic, nucleophilic fluorination or a combination of the two (Figure 3.7). All of these substrates were used in the evaluation of the effects of aliphatic fluorination on lipophilicity (Chapter 2).

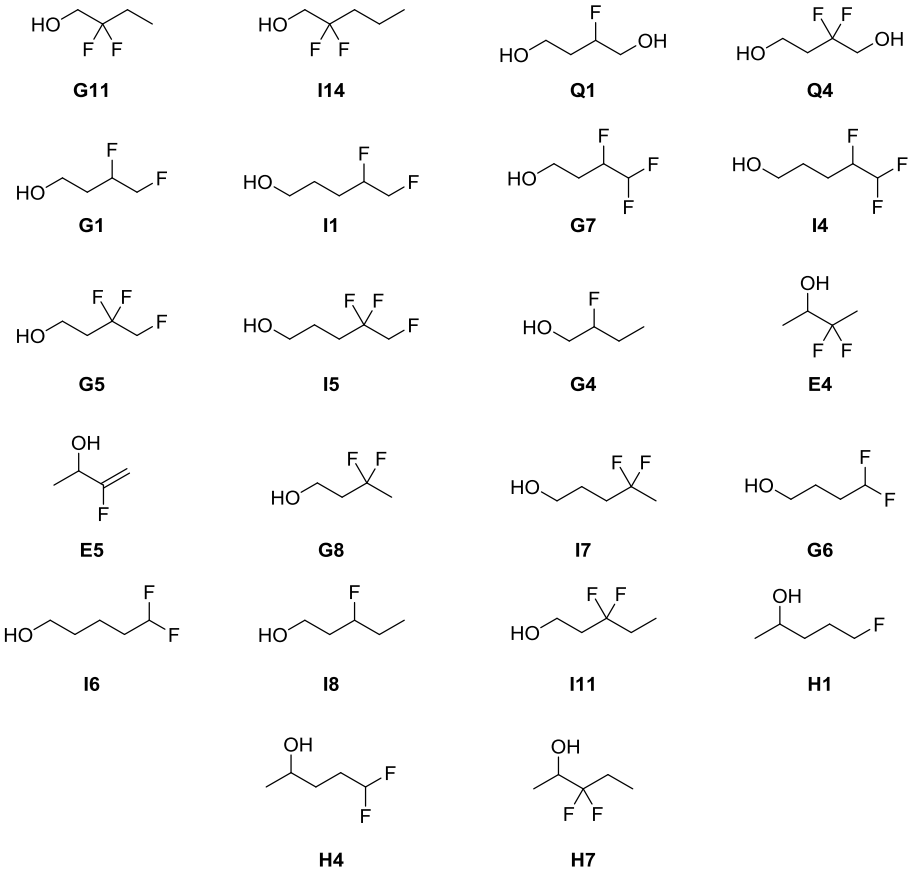

Figure 3.7 - All fluorinated alkanols snthesised in Chapter 3

All three substrates, **G11**, **I14** and **Q4** were synthesised by α,α-difluorination with NFSI and organocatalytic proline from their corresponding aldehydes. In a similar fashion, **Q1** was synthesised after the optimization of electrophilic α-fluorination through the use of stoichiometric proline. With advanced α-fluorinated and α,α-difluorinated intermediates in hand, *via* electrophilic fluorination, the targets **G1**, **I1**, **G7**, **I4**, **G5** and **I5** were successfully synthesised after nucleophilic fluorination of their corresponding alcohol or carbonyl (after oxidation), mediated by either NfF or DAST. While the synthesis of **G1** and **I1** was attempted by vicinal difluorination of an alkene, this route was abandoned due to the safety concerns from the large quantities of HF reagents required to make the reaction work.

Following the appropriate alcohol protection of their respective commercially available starting material, nucleophilic fluorination and subsequent protecting group cleavage afforded **G4**, **E4**, **G8**,

I7, **G6** and **I6**. In a similar manner **I8** and **I11** were synthesised, after the synthesis of their corresponding starting material by an oxa-Michael addition. After the reduction of γ-valerolactone to pentane-1,4-diol and a series of protection and deprotection reactions, the synthesis of advanced intermediate **2.24** was achieved (Scheme 3.31). Treating **2.24** with DAST and subsequent deprotection, afforded **H1**, while oxidising **2.24** to its corresponding aldehyde, treatment with DAST and deprotection yielded **H4**. Finally, **H7** was synthesised by nucleophilic fluorination after the synthesis of the required ketone **2.34** (Scheme 3.33), by a Weinreb ketone synthesis.

Chapter 4 Synthesis of Targets Using Fluorinated Building Blocks

4.1 Introduction

In this chapter, the discussion will focus on the synthesis of a variety of fluorinated motifs through a building-block approach or the use of fluoroalkylating agents. These substrates were produced for their use in the investigation of the effects of fluorine on aliphatic fluorination (see Chapter 2). The retrosynthetic analysis of all desired compounds in this chapter will now be performed.

4.1.1 Retrosynthetic analysis

It was envisioned that **K1**, **H9**, and **J2** could be synthesised through the hydrotrifluoromethylation of their respective unactivated alkenes with CF_3SiMe_3 (Scheme 4.1).[173] In a similar fashion, the tetrafluoro-motif of compound **I9** could be introduced through the fluorotrifluoromethylation of alkene **3.4**.[174] Finally, the synthesis of **J1** could be accomplished through the trifluoromethylaminoxylation of 1-pentene **4.4**, followed by N-O bond cleavage.[175]

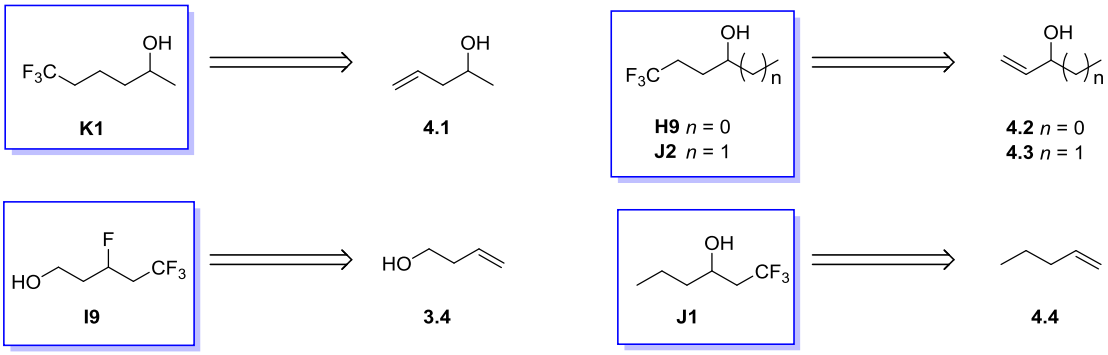

Scheme 4.1 - Proposed radical trifluoromethylation reactions

While designing the synthesis of **G9** and **G14** (Scheme 4.2), compound **4.5** was identified as a potential common advanced intermediate and could be prepared *via* a homologation reaction between the diazoalkane **4.6** and benzyloxyacetaldehyde.[176] Subsequent transformations of the intermediate **4.5** could allow for the synthesis of **G9** to be achieved, *via* the reduction of the ketone, deoxyfluorination and subsequent protecting group hydrogenolysis. In a similar fashion **G14** could be synthesised through deoxofluorination, followed by cleavage of the benzyl ether. However, due to safety concerns associated with the handling of diazoalkanes (explosive and toxic),[177-180] it was envisioned that the key intermediate **4.5** could be synthesised by an oxytrifluoromethylation of the alkene **4.7** utilizing Langlois reagent (CF_3SO_2Na).[181-182]

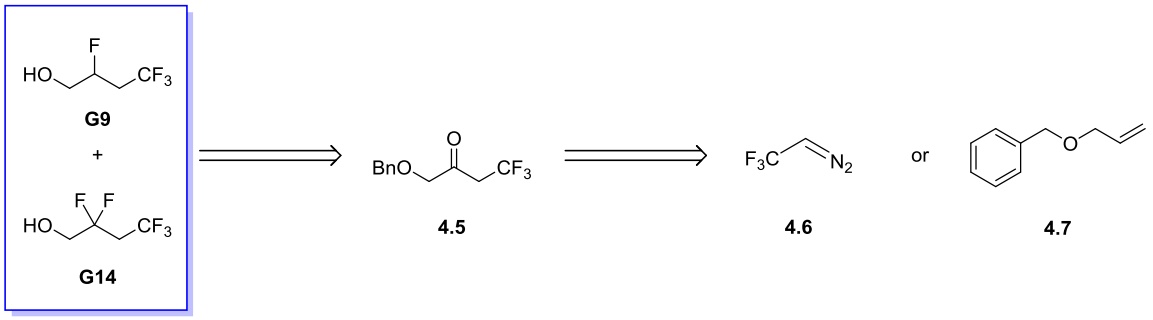

Scheme 4.2 - Proposed route to G9 and G14

It was proposed that **K3** could be synthesised from the aldehyde **3.2** *via* nucleophilic trifluoromethylation with CF_3SiMe_3 (Scheme 4.3). In a similar manner **K2** could be synthesised following the oxidation of **I13** to its corresponding aldehyde.

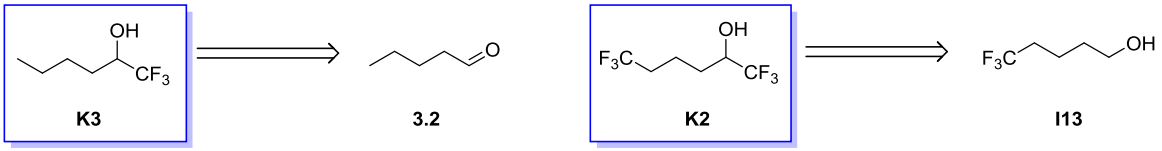

Scheme 4.3 - Nucleophilic trifluoromethylation

Retrosynthetic analysis of the four analogues described in Scheme 4.4 share a common forward synthesis strategy and could be accomplished by Grignard reactions of their respective shorter-chained trifluoromethylated analogues.

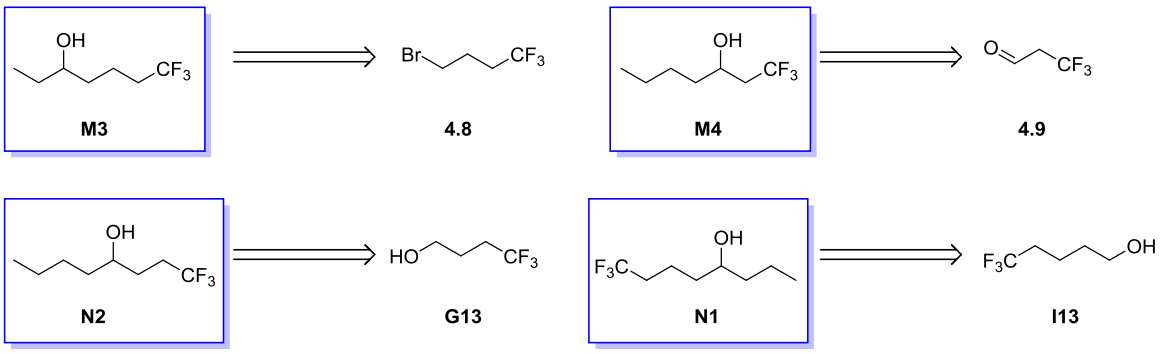

Scheme 4.4 - Synthesis of trifluoro- alkanols *via* the Grignard reaction

Retrosynthetic analysis reveals that **S1** could be synthesised by the treatment of the thiocyanate **4.10** with CF_3SiMe_3 and subsequent protecting group cleavage (Scheme 4.5). The required intermediate **4.10** could be synthesised from its corresponding chloroalkanol **4.12**. The butyl derivate **S2**, could be synthesised in a similar fashion starting from **4.13**.

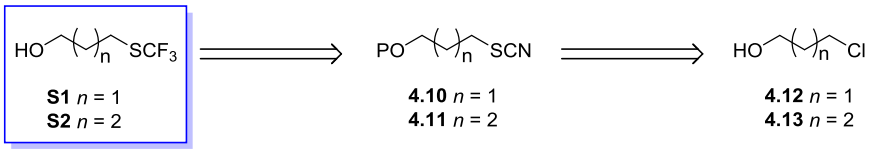

Scheme 4.5 - Retrosynthetic analysis of S1 and S2

The fluorinated cyclopropanemethanol analogues detailed in Scheme 4.6 could all be synthesised by the reduction of their respective commercially available fluorinated carboxylic acids.

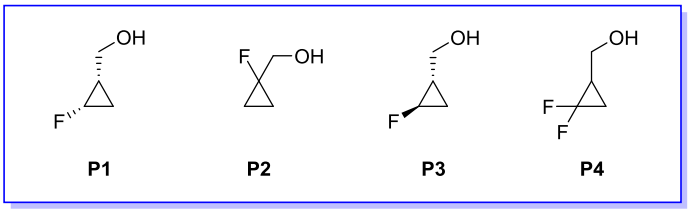

Scheme 4.6 - Fluorinated cyclopropanemethanol analogues

Retrosynthetic analysis for both **4.14** and **G10** (Scheme 4.7) reveals that **4.15** could serve as a common starting material. The analogue **4.14**, could be synthesised by the treatment of **4.15** with MeLi,[183] while radical debromination of **4.15** could synthesise **G10**.

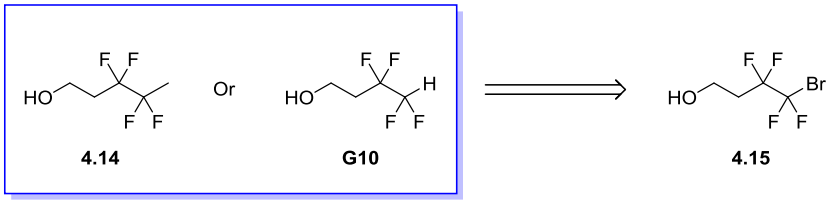

Scheme 4.7 - Proposed synthesis towards tetrafluorinated alkanols

To synthesise the target analogues **G12** and **I15** (Scheme 4.8), retrosynthetic analysis identifies the deoxygenation of their respective commercially available diols, **Q5** and **R4**, as a potentially viable route.

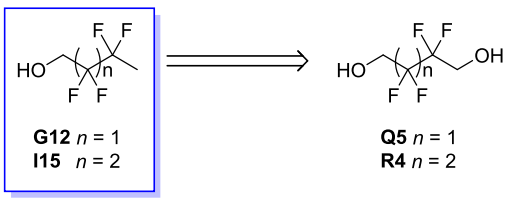

Scheme 4.8 - Retrosynthetic analysis of G12 and I15

4.2 Radical trifluoromethylation

The trifluoromethyl radical was first reported by Haszeldine in 1949 and was a product of subjecting CF_3I to heat or irradiation.[184] Since, the generation of the CF_3 radical has been achieved from a range of precursors (e.g., CF_3SO_2Cl, Me_3SiCF_3 and CF_3SO_2Na)[185] and through a variety of conditions (thermal, oxidative, reductive, electrochemical and photochemical).[186] In the past, reactions involving the CF_3 radical have typically been performed on electron rich aromatic and heteroaromatic substrates, with the study of its interactions at non-aromatic sites being lesser studied.[186] Herein, a range of trifluoromethyl radical additions to unactivated alkene substrates will be discussed.

4.2.1 Synthesis of 6,6,6-trifluorohexan-2-ol, 6,6,6-trifluorohexan-3-ol and 5,5,5-trifluoropentan-2-ol

A silver-catalysed hydrotrifluoromethylation of their respective unactivated alkenes with CF_3SiMe_3 was developed by Qing *et al*. (Scheme 4.9).[173] This methodology was successfully applied in the synthesis of 6,6,6-trifluorohexan-2-ol, 6,6,6-trifluorohexan-3-ol and 5,5,5-trifluoropentan-2-ol. The methodology requires the oxidation of CF_3SiMe_3 to the CF_3 radical by $PhI(OAc)_2$ and/or $AgNO_3$,[185, 187-188] before addition to the alkene. Finally, the resultant secondary radical reacts with 1,4-cyclohexadiene (1,4-CHD), which acts a H-atom source, to furnish the desired product. A proposed mechanism for this reaction can be found in Scheme 4.10.

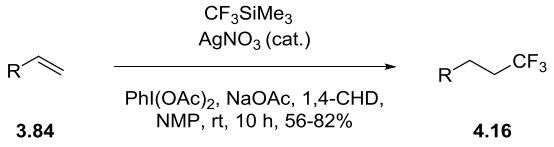

Scheme 4.9 - Hydrotrifluoromethylation of an alkene reported by Qing *et al*.[173]

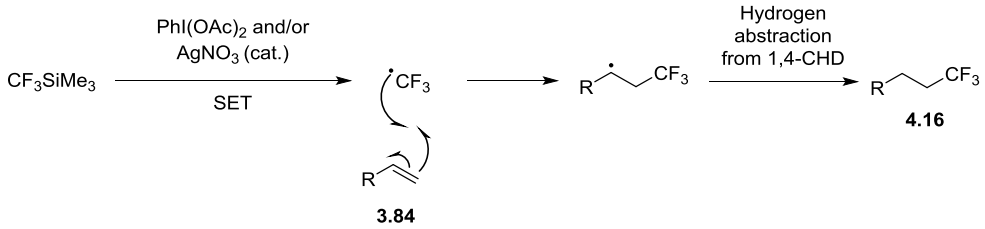

Scheme 4.10 – Proposed mechanism for the hydrotrifluoromethylation of an alkene, adapted from Qing *et al*.[173]

It was reported that this procedure could be performed readily in the presence of alcohols. However, when the reaction was attempted on **4.1** (Scheme 4.11), no trifluorination occurred and instead the silyl ether **4.17** was isolated in a 67% yield. This is likely from following the experimental

procedure in the SI of this publication that contained an error; the reaction was described to use only 1/10th of the actual solvent used, with the correct amount being described within the journal article itself. This likely resulted in the poor solubility of either $PhI(OAc)_2$ and/or $AgNO_3$ required for the formation of the CF_3 radical. Following this observation, it is was decided to protect the alcohol group, prior to the trifluorination, also in order to facilitate the purification and isolation of the volatile final product.

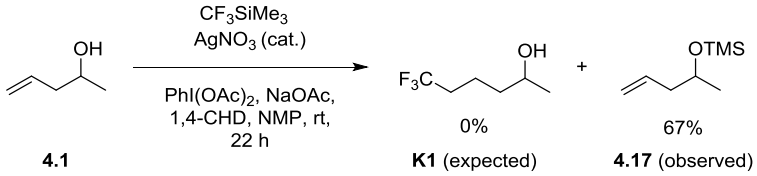

Scheme 4.11 - Attempted synthesis of 6,6,6-trifluorohexan-2-ol

Protection of the alcohol **4.1** was performed with benzoyl chloride afforded **4.18** in quantitative yield (Scheme 4.12). With **4.18** in-hand, the silver-catalysed hydrotrifluoromethylation was trialled using two different silver catalysts concurrently, $AgNO_3$ and AgOTf, resulting in yields of 51% and 58% respectively.

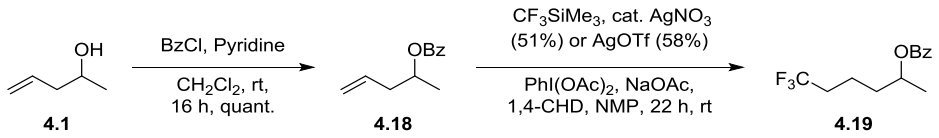

Scheme 4.12 - Synthesis towards 6,6,6-trifluorohexan-2-ol

With the desired trifluorinated compound **4.19** successfully synthesised, the hydrotrifluoromethylation was repeated on a larger scale with AgOTf as the catalyst (Scheme 4.13). Unfortunately, upon scale up, the separation of the trifluoromethylated product **4.19** from the residual starting material **4.18** was problematic. Thus, the alkene **4.18** was removed *via* functionalization with *m*CPBA, affording a pure sample of **4.19** in a 57% yield over 2 steps. Finally, cleavage of the benzoyl group yielded the final compound **K1** in an 80% yield.

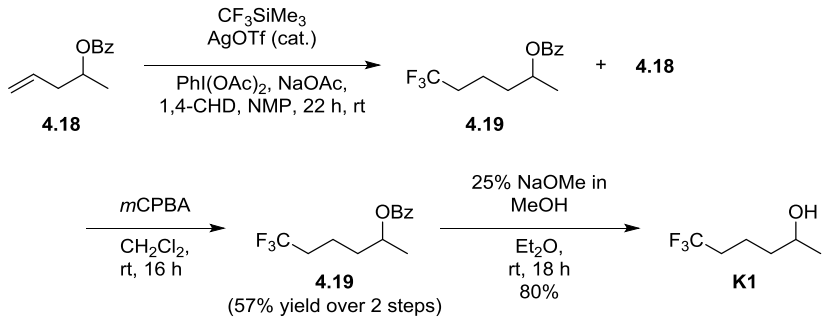

Scheme 4.13 - Synthesis of 6,6,6-trifluorohexan-2-ol

The optimised synthetic procedure employing AgOTf as the catalyst was then repeated on two similar substrates **4.20** and **4.21** (Scheme 4.14), affording both **H9** and **J2** respectively.

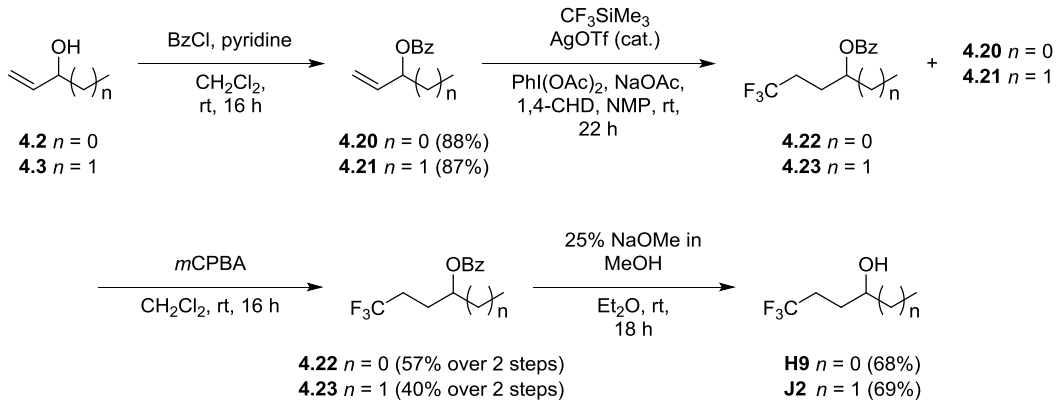

Scheme 4.14 - Synthesis of 5,5,5-trifluoropentan-2-ol and 6,6,6-triflurohexan-3-ol

4.2.2 Synthesis of 3,5,5,5-tetrafluoropentan-1-ol

The synthesis of 3,5,5,5-tetrafluoropentan-1-ol was achieved following a silver-mediated oxidative fluorotrifluoromethylation of unactivated alkenes, developed by Qing *et al.* (Scheme 4.15).[174] The reaction progresses through the generation of a trifluoromethyl anion by CF_3SiMe_3/CsF. The resultant CF_3 anion is then oxidised to a CF_3 radical by $PhI(OAc)_2$ and/or AgOTf,[185, 187-188] before addition to the alkene. Finally, a silver/Selectfluor® mediated addition of a fluorine atom allows for the formation of the desired product.[189-190]

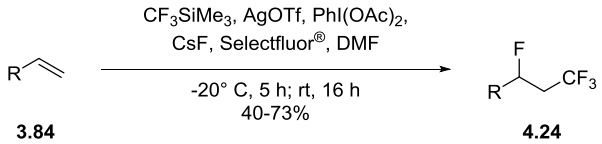

Scheme 4.15 - Fluorotrifluoromethylation of an alkene reported by Qing *et al*.[174]

The paper reported no examples of the methodology being applied to substrates containing benzyl ether protected alcohols. There was also concern that the use of a benzoate protecting group may not be compatible with the required basic conditions. Therefore, a trityl protection group was employed for this synthesis. Trityl protection of **3.4** (Scheme 4.16) progressed with ease affording **4.25** in a high 96% yield. Subsequent silver-mediated oxidative fluorotrifluomethylation was successful, affording **4.26** in a yield of 39%. It is likely that the yield could be improved if a glove-box was used, as recommended by Qing.[174] Finally, acidic cleavage of trityl protection group was completed by the treatment of **4.26** with catalytic *p*TSA.H_2O in CH_2Cl_2/MeOH, yielding **I9** in a good yield of 83%.

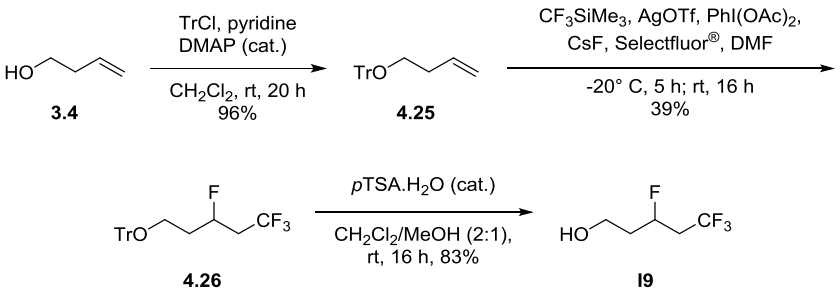

Scheme 4.16 - Synthesis of 3,5,5,5-tetrafluoropentan-1-ol

4.2.3 Synthesis of 1,1,1-trifluorohexan-3-ol

Y. Li and A. Studer[175] reported the successful radical trifluoromethylaminoxylation of unactivated alkenes (Scheme 4.17). This procedure utilized Togni reagent II as the source of the CF_3 radical and TEMPONa as a mild organic reducing reagent (SET), as well as the secondary radical trap. This methodology was successfully applied in the synthesis of 1,1,1-trifluorohexan-2-ol.

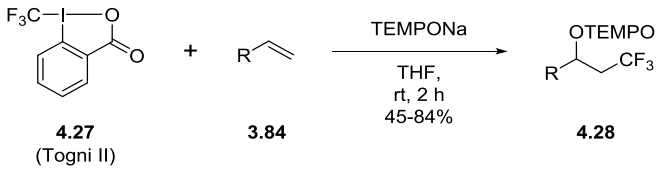

Scheme 4.17 - Trifluoromethylaminoxylation of alkenes reported by Y. Li and A. Studer[175]

Due to the high cost of Togni reagent II[xviii] **4.27** (1 g, £71, 60 wt. % with 40 wt. % stabilizer) and its requirement on a multigram scale. It was synthesised following a one-pot procedure developed by A. Togni *et al*.,[192] which afforded Togni reagent II in a yield of 56% (Scheme 4.18). The yield obtained is slightly lower than the literature value of 72%, however Togni reported that the quality and source of the 2-iodobenzoic acid **4.29** can greatly impact the yield.

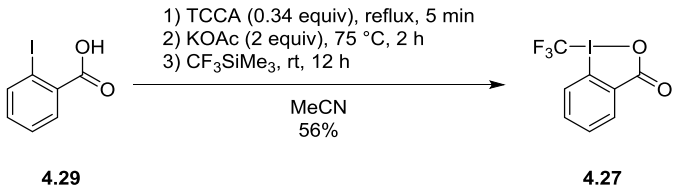

Scheme 4.18 - Synthesis of Togni Reagent II

[xviii] Despite its prevalence in literature since its initial publication in 2006, a paper published in 2013 claimed that some sources of Togni reagent II have an impact sensitiveness of 20 J, similar to that of TNT.191. Fiederling, N.; Haller, J.; Schramm, H., *Org. Process Res. Dev.* **2013,** *17*, 318-319. Although this is likely caused by an impurity from its synthesis, great care should be taken when handling Togni reagent II.

As TEMPONa is not commercially available due to its short shelf life of ~3 days, its synthesis was also required. It was therefore prepared fresh (Scheme 4.19), by first the formation of a sodium mirror, to which THF and catalytic naphthalene is added, followed by a solution of TEMPO in THF.

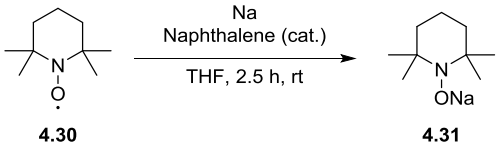

Scheme 4.19 - Synthesis of TEMPONa

With fresh TEMPONa **4.30** and Togni Reagent II in-hand, the radical trifluoromethylaminoxylation of 1-pentene **4.4** was successfully performed (Scheme 4.20). Subsequent column chromatography of the crude material in 100% pentane provided the highly apolar product **4.32** at ~70% purity. As it was reported that the N-O bond cleavage could be performed without purification at this stage, the impure **4.32** was taken forward without any further purification. Unfortunately, the N-O bond cleavage of **4.32** was not as facile as Y. Li and A. Studer[175] described, as only ~32% of the starting material was consumed after 16 hours, indicated by ^{19}F NMR analysis. The reaction was thus heated to 70 °C and carefully monitored by ^{19}F NMR until it reached 93% conversion. The product 1,1,1-trifluorohexan-2-ol **J1** was then isolated in a 24% yield over two steps.

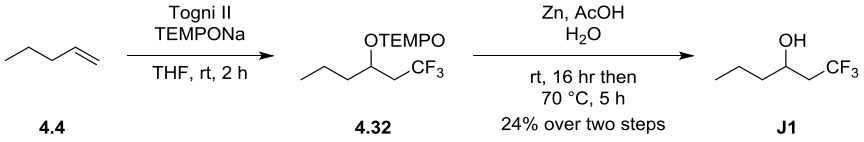

Scheme 4.20 - Synthesis of 1,1,1-trilfuorohexan-3-ol

4.3 Homologation

4.3.1 Synthesis of 2,2,4,4,4-pentafluorobutan-1-ol and 2,4,4,4-tetrafluorobutan-1-ol

As discussed previously in Section 4.1.1, it was envisioned that the synthesis of **G9** and **G14** could be achieved from the common intermediate **4.5** (Scheme 4.21), which had been previously synthesised by E. Carreira *et al*.[176]

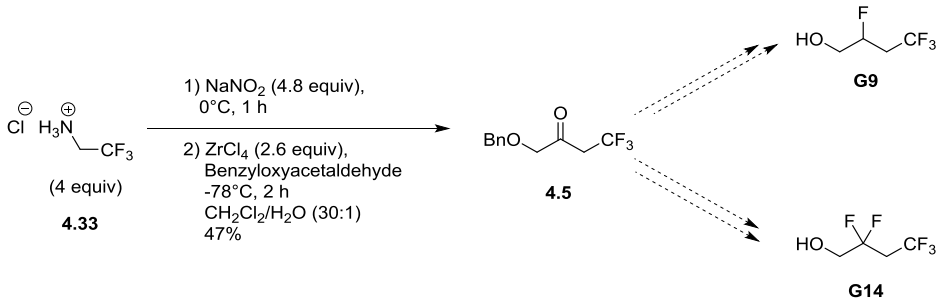

Scheme 4.21 - Synthesis of key intermediate 4.5 performed by Carreira *et al.*[176]

Unfortunately, this route made use of a diazoalkane which are typically considered explosive[177-178] and toxic.[179-180] Therefore, it was hoped that the key intermediate **4.5** could be synthesised *via* an oxytrifluoromethylation of the alkene **4.7** utilizing Langlois reagent (CF_3SO_2Na) as the source of the trifluoromethyl group (Scheme 4.22).[181-182] The required benzyl protected allyl alcohol **4.7** was synthesised using standard conditions in high yields. The first oxytrifluoromethylation reaction performed employed catalytic quantities of $AgNO_3/K_2S_2O_8$.[181] However, limited success was observed with **4.5** isolated in a low yield of 3%. A partially separable mixture of **4.35** and the side product **4.36**, from oxidation of the benzyl ether to its benzoate derivative, was also obtained, in yields of 13% and 13% respectively. Due to the low yield from the previous reaction, a different metal catalyst was employed, $MnCl_2 \bullet 4H_2O$.[182] A moderately improved yield was observed and the desired product **4.5** was isolated in a 7% yield. Again **4.35** was obtained as a partially separable mixture the undesired side product **4.36**, in yields of 20% and 5% respectively.

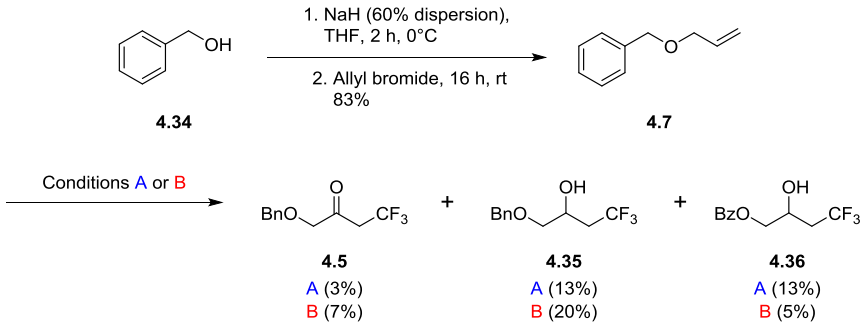

Scheme 4.22 - Conditions A: CF_3SO_2Na, $AgNO_3$ (0.2 eq.), $K_2S_2O_8$ (0.4 eq.), DMF, rt, 24 h. Conditions B: CF_3SO_2Na, $MnCl_2 \bullet 4H_2O$ (0.2 eq.), acetone, rt, 36 h.

In an attempt to convert alcohol **4.35** to the desired ketone **4.5** (Table 4.1), various oxidation reagents were trialled. The reagents employed were TEMPO with (diacetoxyiodo)benzene (BAIB) as the co-oxidant (Entry 1, Table 4.1), Dess-Martin periodinane (DMP, Entry 2, Table 4.1) and pyridinium dichromate (PDC, Entry 3, Table 4.1). The three reactions were conducted in parallel and the progress of the reactions was analysed *via* ^{19}F NMR of the reaction mixture after 24 h. Unfortunately, the conversion of these oxidation reactions was low, with the highest being 33%,

using PDC. The low yield and slow reaction time rendered this route unfeasible and the synthesis of **G9** and **G14** will be investigated *via* the synthesis of **4.5** employing E. Carreira's conditions (Scheme 4.21).[176]

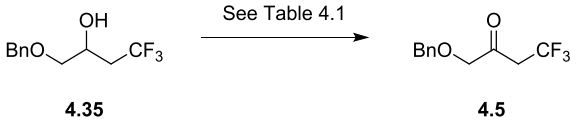

Scheme 4.23 - Oxidation of 4.35

Table 4.1 - Oxidation of 4.35

Entry	Oxidant	Conversion by ^{19}F NMR after 24 h at rt
1	TEMPO/BAIB	15%
2	DMP	10%
3	PDC	33%

In order to repeat Carreira's reaction to obtain **4.5**, the preceding aldehyde **4.39** is first required (Scheme 4.24). This was synthesised first by diol protection of **4.37**, followed by ozonolysis using a literature procedure.[193] This ozonolysis reaction however did not turn the characteristic blue colour (ozone saturation) upon completion as described in the literature and occasionally trace amounts of the side product **4.40** was observed, from oxidation of the benzyl ether due to overreaction. Similar side reactions had been previously reported.[194]

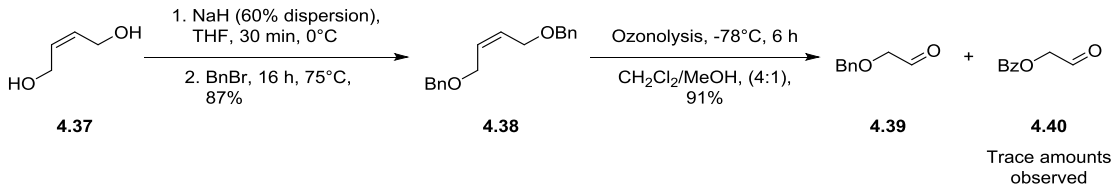

Scheme 4.24 - Ozonolysis to afford 4.42

With the aldehyde **4.39** in hand (Scheme 4.25), the homologation reaction to synthesise **4.5** can be performed. Interestingly the small amount of water that is required and produced in the formation of the diazoalkane is frozen out of the reaction in the second step by lowering the temperature to -78 °C. This leads to essentially an anhydrous reaction media, thus allowing for the use of strong Lewis acids because their decomposition reaction (with ice) is slower than the desired homologation process.[176] Alas, on large scale (> 1g), the layer of ice that formed on the top of the

reaction mixture made the addition of the solid $ZrCl_4$ difficult. The lower yield of 19%, compared to the published 47%, could be explained by this observation (Scheme 4.21). On repetition of this reaction, after the diazo formation, the aqueous and organic phases were separated and the water layer was discarded; only trace amounts of water were therefore present during the addition of the solid $ZrCl_4$, leading to an improved yield of 35%.

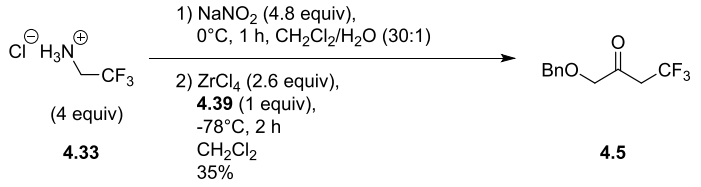

Scheme 4.25 - Synthesis of 4.5

The reaction is believed to follow a mechanism in which the aldehyde is first activated by the Lewis acid (Scheme 4.26), prior to addition of the diazoalkane F_3CCHN_2. The intermediate **4.41** formed, then undergoes a hydride migration to form the desired product **4.5**.

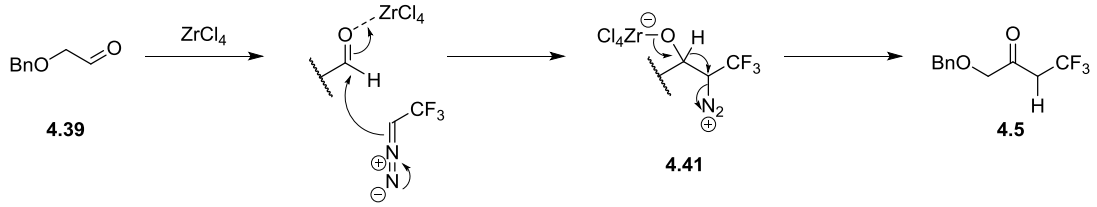

Scheme 4.26 - Mechanism adapted from Carriera *et al.*[176]

The isolated ketone was then subjected to deoxyfluorination with DAST at room temperature overnight. This provided the desired pentafluorinated substrate **4.42** and the in a good yield of 65% with a small inseparable impurity of the fluoroalkene **4.43** (Scheme 4.27), formed by elimination.

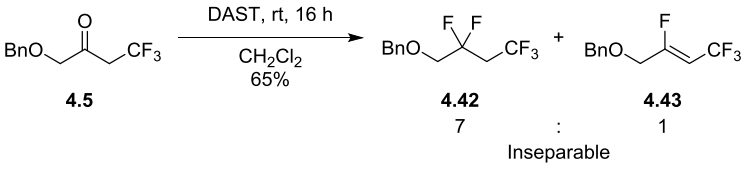

Scheme 4.27 - Deoxofluorination of 4.5

Hydrogenolysis of the benzyl protecting group was initially attempted in CH_2Cl_2, in both batch and flow conditions, in an attempt to circumvent any difficulties in the isolation of the volatile products (Scheme 4.28, Entry 1 and 2, Table 4.2). Neither however were successful. Pleasingly, when the hydrogenation performed in THF, successful cleavage of the benzyl ether group and reduction of the fluoroalkene was observed (Entry 3, Table 4.2). The removal the residual traces of THF proved futile, co-eluting and co-evaporating with the desired products **G14** and **G9.** The hydrogenolysis

was thus repeated in Et_2O instead and **G14** and **G9** were isolated as a mixture in a yield of 61%, with a ratio of 5.5:1 respectively (Entry 4, Table 4.2).

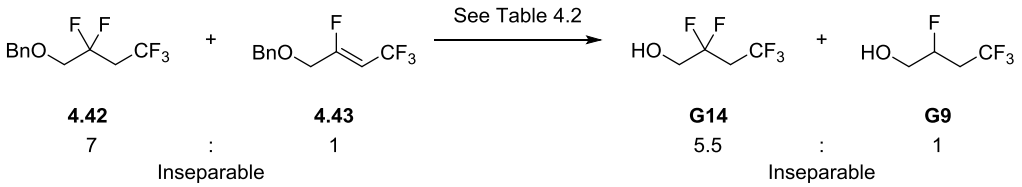

Scheme 4.28 - Synthesis of D14 and D9

Table 4.2 - Hydrogenation conditions

Entry	Conditions	Yield
1	CH_2Cl_2, Pd/C 10% wt., rt, 16 h, Batch	0%
2	CH_2Cl_2, $Pd(OH)_2$, 40 °C, 60 atm, flow	0%
3	THF, Pd/C 10% wt., rt, 16 h, Batch	Not isolated
4	Et_2O, Pd/C 10% wt., rt, 16 h, Batch	61% **G14** + **G9** (5.5:1)

4.4 Nucleophilic trifluoromethylation

4.4.1 Introduction

Nucleophilic trifluoromethylation *via* the trifluoromethyl anion was initially believed to be difficult because of the competing fluoride elimination pathway, which affords the corresponding difluorocarbene (Scheme 4.29).[138] This is a result of the repulsive interaction that exists between the lone-pairs of the fluorine substituents and the filled orbital of the CF_3 anion.

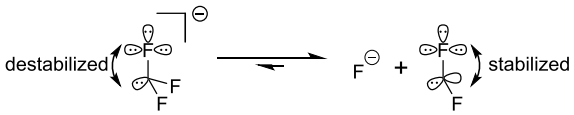

Scheme 4.29 - CF_3 anion fluoride elimination

Fortunately, with an appropriate pronucleophile, the trifluoromethyl anion can be stabilized. Previously this had been performed with Cu(I) forming $CuCF_3$, an air-sensitive reagent and which was required to be prepared fresh or in-situ through the use of the difficult to handle gasses, CF_3I or CF_3Br (banned substance).[195] Fortunately, the Ruppert-Prakash reagent (Me_3SiCF_3)[196] solves

these issues as it is a bench stable, commercially available and an easy to handle liquid. Me_3SiCF_3 itself does not react with carbonyl compounds and first requires a liberation step of the trifluoromethyl anion. This is typically performed through the use of a fluoride initiator where it can then undergo a catalytic reaction with aldehydes, esters, ketones and activated imines (Scheme 4.30).[186, 196]

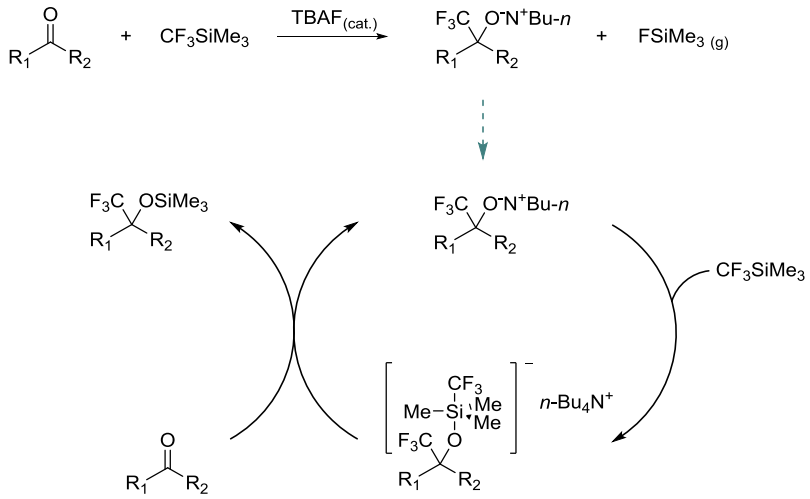

Scheme 4.30 - Catalytic nucleophilic trifluoromethylation of a carbonyl[186, 196]

4.4.2 Synthesis of 1,1,1-trifluorohexan-2-ol

The synthesis of 1,1,1-trifluorohexan-2-ol **K3** was successful and utilised a caesium fluoride catalysed trifluoromethylation of valeraldehyde **3.2** (Scheme 4.31). J. Shreeve *et al.*[197] reported high yields of >85% starting from two similar alkyl aldehydes, however upon repetition of their methodology only 12% of **K3** was isolated. However, this low yield is consistent with previous results within the group; the trifluoromethylation of butanal provided 1,1,1-trifluorobutan-2-ol in only 14% yield.[198] The low yield is believed to have arisen from an incomplete reaction, as crude ^{1}H NMR analysis revealed a large quantity of the starting material **3.2**.

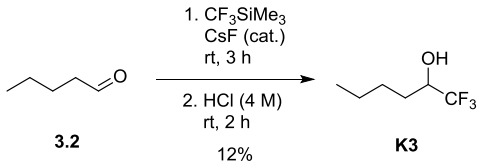

Scheme 4.31 - Synthesis of 1,1,1-trifluorohexan-2-ol

4.4.3 Synthesis of 1,1,1,6,6,6-hexafluorohexan-2-ol

The synthesis of 1,1,1,6,6,6-hexafluorohexan-2-ol **K2** was achieved in a similar fashion to the synthesis of 1,1,1-trifluorohexan-2-ol **K3** (Scheme 4.32). On this occasion, the reaction was

catalysed by TBAF and was performed in CH_2Cl_2, the solvent from preceding reaction, as the aldehyde precursor could not be distilled from the crude mixture.

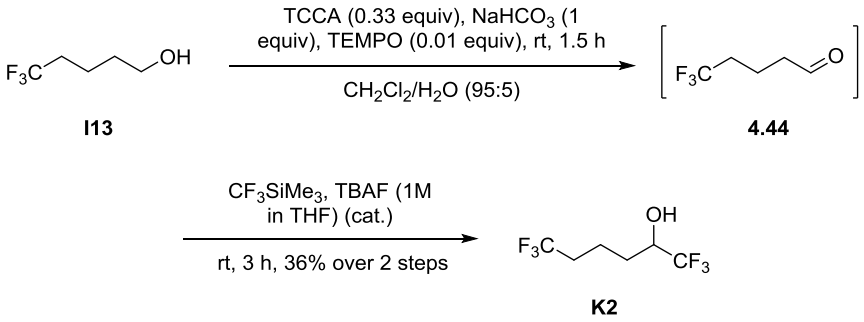

Scheme 4.32 - Synthesis of 1,1,1,6,6,6-hexafluorohexan-2-ol

4.5 Grignard Reactions

4.5.1 Synthesis of 1,1,1-trifluorooctan-4-ol

Despite the availability of various trifluoromethylation methodologies to introduce the CF_3 group, a building block approach was undertaken in the synthesis of **N2** (Scheme 4.34), starting from the commercially available alcohol **G13.** This was achieved through a standard Grignard reaction from the corresponding aldehyde **4.47**. Initially this method appears straightforward, however care must still be taken due to highly volatile nature of the aldehyde intermediate. This means that the solvent used in the oxidation step (CH_2Cl_2), is ideally not removed before the subsequent addition of the Grignard reagent. Dichloromethane is incompatible with the use of organolithium (*n*-BuLi) reagents,[199] however dichloromethane can be used as solvent for Grignard reactions.[200] With this in mind, the Grignard reagent butylmagnesium bromide **4.46** was freshly prepared (Scheme 4.33), in parallel with the TEMPO catalysed oxidation of 4,4,4-trifluorobutan-1-ol **G13** to afford the highly volatile aldehyde intermediate **4.47**. Following aqueous work up and ^{1}H and ^{19}F NMR analysis to confirm the characteristic aldehyde signal, the freshly prepared Grignard reagent **4.46** was then added. This resulted in a successful Grignard reaction with the resultant alcohol product **N2** isolated in a 47% yield over 2 steps.

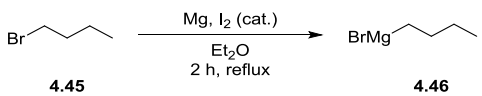

Scheme 4.33 - Synthesis of Grignard reagent 4.49

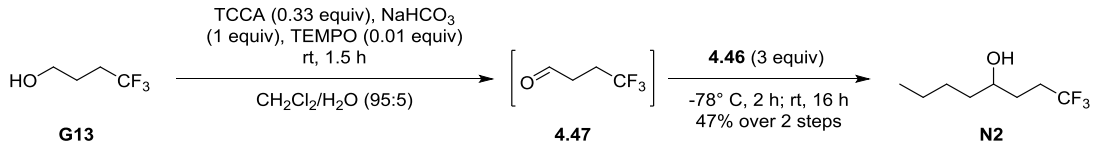

Scheme 4.34 - Synthesis of 1,1,1-trifluorooctan-4-ol

4.5.2 Synthesis of 8,8,8-trifluorooctan-4-ol

The synthesis of 8,8,8-trifluorooctan-4-ol was accomplished in a similar manner to 1,1,1-trifluorooctan-4-ol (Scheme 4.35), employing 5,5,5-trifluoropentan-1-ol as the starting material for the synthesis of the aldehyde **4.44** and the commercially available reagent *n*-PrMgCl for the subsequent Grignard reaction.

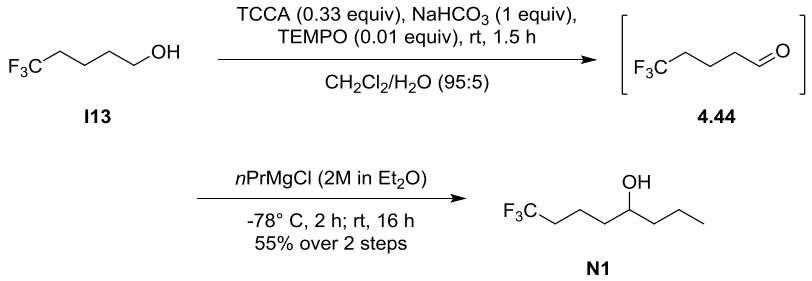

Scheme 4.35 - Synthesis of 8,8,8-trifluorooctan-4-ol

4.5.3 Synthesis of 7,7,7-trifluoroheptan-3-ol

For the synthesis of 7,7,7-trifluoroheptan-3-ol (Scheme 4.36), the Grignard reagent was synthesised from 4-bromo-1,1,1-trifluorobutane and the commercially available propanal was used.

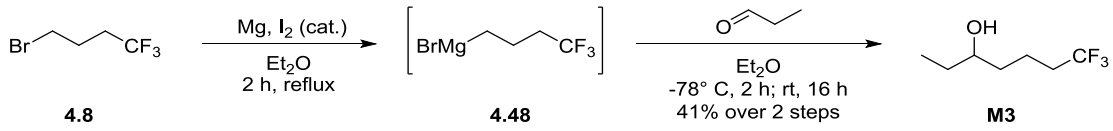

Scheme 4.36 - Synthesis of 7,7,7-trifluoroheptan-3-ol

4.5.4 Synthesis of 1,1,1-trifluoroheptan-3-ol

The synthesis of 1,1,1-trifluoroheptan-3-ol was accomplished in a similar manner to the previous Grignard reactions (Scheme 4.37). The commercially available trifluoropropanal **4.9** was used, while employing *n*BuLi for the addition of a butyl chain in place of a more common Grignard reagent, as used on similar substrates in the past.[30]

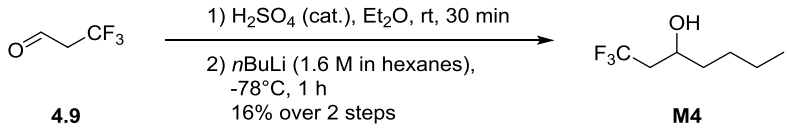

4.9 **M4**

Scheme 4.37 - Synthesis of 1,1,1-trilfuoroheptan-3-ol

Initial analysis of the commercially available trifluoropropanal's **4.9** ^{19}F NMR spectrum, displayed a mixture of the desired compound and unknown impurities was observed, with a ratio of roughly 1:2 respectively. Upon further discussion with the supplier (Fluorochem), it was acknowledged that the substrate exists as a monomer and a mixture of oligomers. It was advised that the desired monomer, could be liberated when treated with a catalytic amount of concentrated acid and that it should be used immediately after. Therefore, the aldehyde was treated with catalytic conc. H_2SO_4, resulting in 2:1 ratio (^{19}F NMR analysis) of compound and unknown impurities, and was immediately used thereafter.

4.6 Synthesis of -SCF_3 analogues

4.6.1 Introduction

As –SCF_3 and –OCF_3 moieties are becoming increasingly more popular in drug discovery programs, due to their similar properties as the trifluoromethyl group (CF_3), [201] the comparison of their log*P* to other similar motifs on aliphatic chains is of interest. Thus, reported herein is the synthesis of the –SCF_3 group incorporated into the propanol and butanol "families", **S1** and **S2** respectively (Figure 4.1).

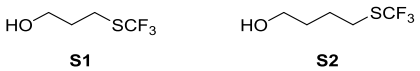

S1 **S2**

Figure 4.1 - SCF_3 analogues

There are many radical, electrophilic and nucleophilic methods to incorporate the -SCF_3 moiety into an organic molecule, however a wide range of these use difficult to handle gaseous reagents, such

as: CF_3I, CF_3Br and CF_3H, or expensive reagents such as Umemoto's Reagent **4.49** or $CuSCF_3$ (Figure 4.2).[201]

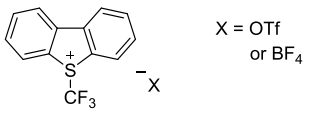

4.49

Figure 4.2 - Umemoto's Reagent

Therefore, a facile nucleophilic trifluoromethylation of a thiocyanate group, developed by Langlois *et al*. utilising easily handled and readily available reagents (Ruppert's reagent and TBAF) was chosen.[202] Furthermore, due to the unavoidable β- elimination of the $-SCF_3$ group in the presence of base, as shown recently by Brigaud *et al.*,[203] a benzyl ether protection group was be employed in synthesis of both **S1** and **S2** instead of a benzoyl protection group.

4.6.2 Synthesis of 4-(trifluoromethylthio)-butanol

The synthesis of **S2** began with a benzyl ether protection of **4.12** (Scheme 4.38). An acidic benzyl ether protection was attempted involving benzyl trichloroacetimidate, due to concerns that the more commonly used basic protection would cause the cyclisation of **4.12** to form THF, but was unsuccessful. A neutral benzyl protection of **4.12** to afford **4.50** with benzyl mesylate has been reported,[204] however this reagent has limited commercial availability.

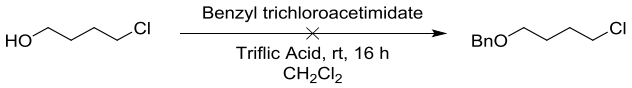

4.12 **4.50**

Scheme 4.38 - Attempted acidic benzyl ether protection

Therefore, it was quickly identified that the benzyl ether protection must be performed prior to introduction of chlorine into the molecule. The benzyl ether protection of 1,4-butane-diol **Q** was then performed (Scheme 4.39), affording the mono-protected compound **4.51**. Successful deoxychlorination of **4.51** with thionyl chloride afforded an inseparable mixture of **4.50** and **4.52**, in a ratio of ~9:1 respectively. This inseparable mixture was carried forward and, using KSCN, the thiocyanate group was installed *via* nucleophilic substation to afford **4.53**. Unfortunately, the benzyl thiocyanate **4.54**, formed from the residual benzyl chloride **4.52**, again proved inseparable from the desired product and the mixture was carried forward to the next reaction.

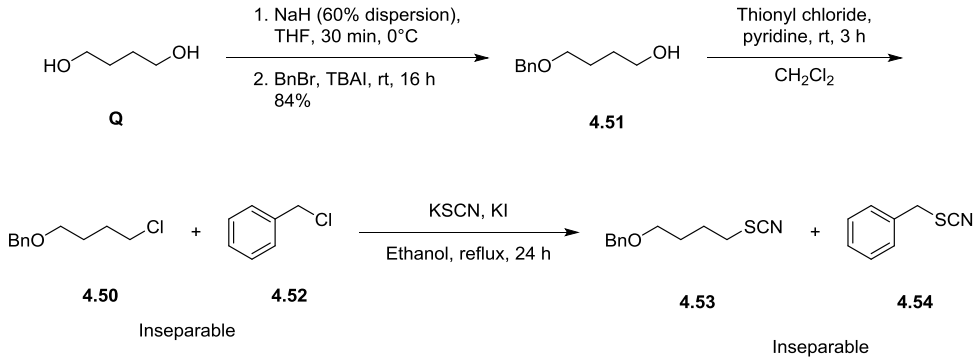

Scheme 4.39 - Synthesis towards 4-(trifluoromethylthio)-butanol

Fortunately, after trifluoromethylation with CF_3SiMe_3 and TBAF (cat.), the desired compound **4.55** proved separable from benzyl impurity **4.56** (Scheme 4.40). Overall, this provided **4.55** in a 39% yield and the undesired molecule **4.56** in an 11% yield, over three steps.

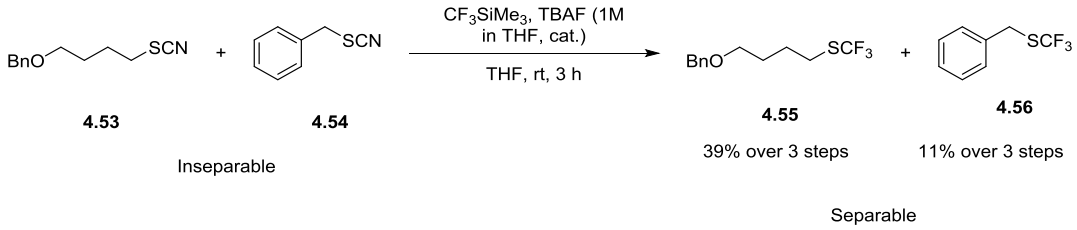

Scheme 4.40 - Synthesis of the $-SCF_3$ motif

As the fluoride source (TBAF) is used catalytic quantities in this reaction, Langlois *et al*. proposed that the CN anion forms a stronger bond with silicon than the trifluoromethyl group (Scheme 4.41). This allows for the generation of the trifluoromethyl anion and thus allows for the catalytic cycle to continue.

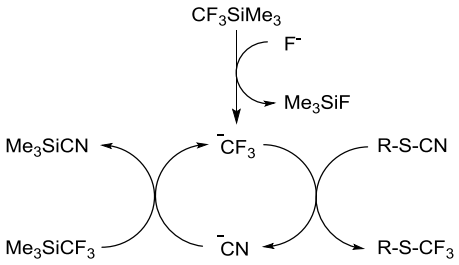

Scheme 4.41 - Catalytic trifluoromethylation, adapted from Langlois *et al*.[202]

With **4.55** now in-hand (Scheme 4.42), hydrogenolysis of the benzyl ether protecting group was possible. Initially Pd/C in MeOH under batch conditions was attempted, however no reaction was observed (Entry 1, Table 4.3). Therefore, a H-Cube Mini™ (continuous-flow hydrogenation reactor) was employed, where much harsher conditions could be tolerated. Success was initially observed on a test run utilizing a $Pd(OH)_2$ catalyst (Entry 2, Table 4.3), where 100% conversion was achieved based on TLC and ^1H NMR analysis. Unfortunately, when this reaction was performed on a larger

scale, only a 27% conversion (based on amount of **4.55** recovered) was observed (Entry 3, Table 4.3). This is likely due to the poisoning of the catalyst from the trace amount of impurity from the trifluoromethylation reaction. Nevertheless, after column chromatography of Entry 3, the two reactions were combined and the final product **S2** was isolated in a combined yield of 39%.

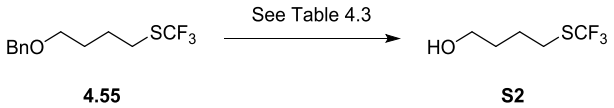

Scheme 4.42 - Hydrogenolysis of 4.55

Table 4.3 - Hydrogenation conditions

Entry	Conditions	Conversion
1	MeOH, Pd/C 10% wt., rt, 16 h, Batch, 1 g	0%
2	CH_2Cl_2, $Pd(OH)_2$, 40 °C, 60 atm, flow, 200 mg	100%
3	CH_2Cl_2, $Pd(OH)_2$, 40 °C, 60 atm, flow, 800 mg	27%

4.6.3 Synthesis of 3-(trifluoromethylthio)-propanol

Following the successful synthesis of 4-(trifluoromethylthio)-butanol, the same synthetic strategy was to be applied for the synthesis of 3-(trifluoromethylthio)-propanol. The benzyl protection of **4.57** progressed smoothly, affording **4.58** (Scheme 4.43)**,** however difficulty arose with the subsequent deoxychlorination reaction to synthesise **4.59**. During the reaction, the complete consumption of the starting material **4.58** was shown *via* TLC, however only starting material **4.58** was observed following an aqueous work up with a sat. aq. $NaHCO_3$ solution.

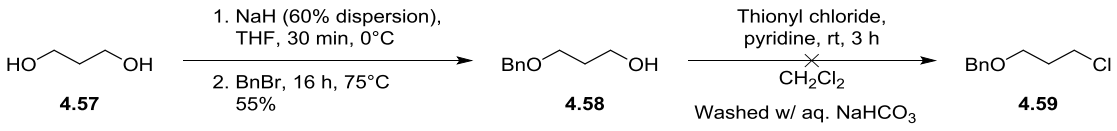

Scheme 4.43 - Synthesis towards 3-(trifluoromethylthio)-propanol

It was originally believed that hydrolysis of the desired chlorinated product **4.59** occurred, reforming the starting material **4.58**. This however was not the case. When the reaction was

repeated with no sat. aq. $NaHCO_3$ wash, the dimerised sulphite **4.60** was isolated in a 52% yield (Scheme 2.5).

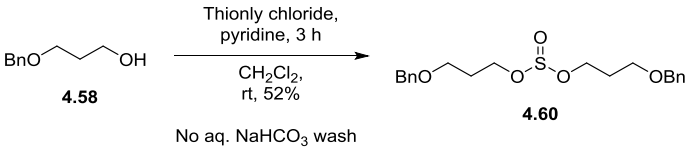

Scheme 4.44 - Synthesis of dimer 4.63

A new procedure towards 3-(trifluoromethylthio)-propanol was thus required. Fortunately, a patent from Smithkline Beecham detailed the protection of 3-chlorobutanol **4.12** with *t*-BuONa and BnBr (Scheme 4.45).[205] This was repeated providing **4.61** in a quantitative yield, allowing for the formation of the key intermediate **4.62**. Trifluoromethylation was then performed according to the above conditions, affording **4.63** in an excellent yield of 94%. The synthesis was then finalised with hydrogenolysis of the benzyl ether using 10% Pd/C in Et_2O, furnishing **S1** in an 89% yield.

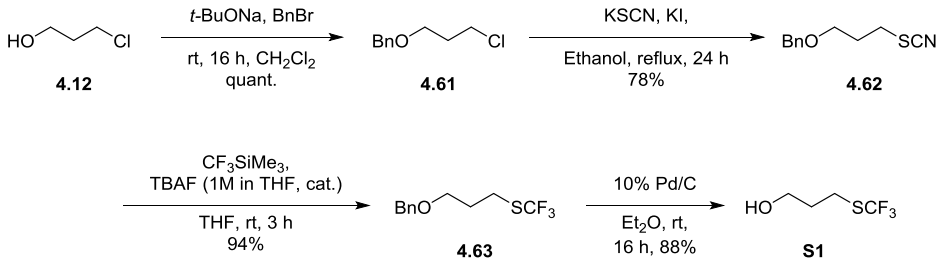

Scheme 4.45 - Synthesis of S1

4.7 Fluorinated cyclopropylmethanol derivatives

4.7.1 Introduction

The synthesis of a cyclopropane ring was first completed in 1882 and since the 1960s, has been used in a wide range of pharmacologically active compounds.[206] It has been used as a replacement for a range of functional groups, such as a phenyl group (reducing Clog*P* and improving potency)[207] and an alkene (improving metabolic stability and other physicochemical properties).[208]

Fluorinated cyclopropane motifs have an expansive history,[209] with the synthesis of various fluorinated cyclopropane derivatives first reported in the 1950s.[210-212] Recently O'Hagan *et al.*,[116] divulged a facile synthesis towards the trifluoro motif **4.65** (Scheme 4.46), without the typical use a mercury based reagent (phenyl(trifluoromethyl)mercury).[213] Interestingly, the substrate exhibited a log*P* of 3.2, which is the same as trifluoromethylbenzene and a reduction in comparison to its non-fluorinated analogues (log*P* = 3.6).

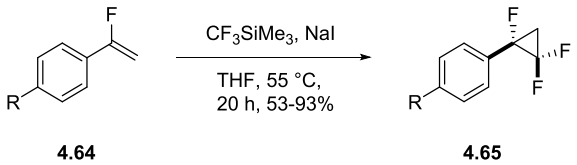

4.64 **4.65**

Scheme 4.46 - Synthesis of a trifluorocyclopropyl derivative

4.7.2 Reduction of fluorinated cyclopropanecarboxylic acid analogues

With this in mind, a systematic study into the effects fluorine has on lipophilicity, when introduced into the simple cyclopropylmethanol ring, is of interest. Therefore, the synthesis of the fluorinated cyclopropanemethanol derivatives **P1**, **P2**, **P3** and **P4** (Scheme 4.47), was achieved by a $LiAlH_4$ mediated reduction of their respective carboxylic acid.

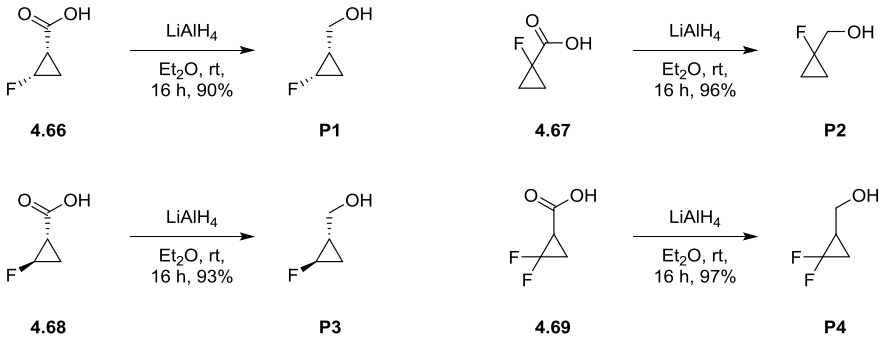

Scheme 4.47 - Carboxylic acid reductions

4.8 Polyfluorinated substrates

4.8.1 Attempted synthesis of 3,3,4,4-tetrafluoropentan-1-ol

Beier *et al.* reported the metalation of the $R^1CF_2CF_2Br$ motif before subjecting it to various electrophiles in an aim to expand the use of CF_2CF_2 containing products.[183] During their initial screening for an appropriate metalation reagent, they observed the reaction of $R^1CF_2CF_2Br$ **4.70** with MeLi, resulting in the formation of the $R^1CF_2CF_2Me$ **4.73** (Scheme 4.48). Similar side reactions have been observed in the past by Linclau *et al*., when investigating anionic cyclization reactions, although the isolated yields of the $R^1CF_2CF_2Me$ containing by-products were considerably lower (0.3% and 1.4%).[214]

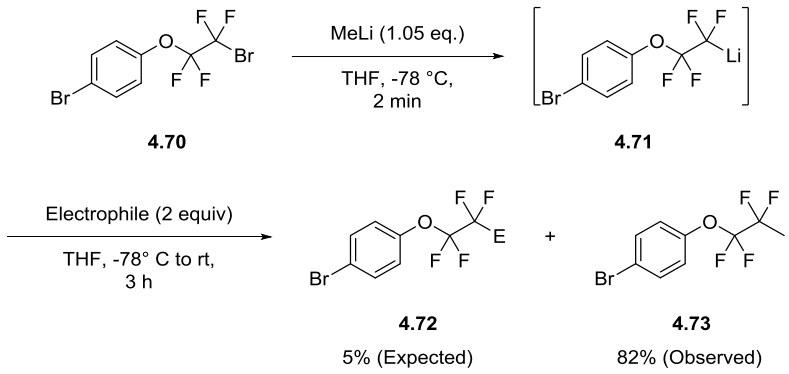

Scheme 4.48 - Methylation of 4.70

With this consideration, the synthesis of 3,3,4,4-tetrafluoropentan-1-ol was attempted utilizing the various conditions employed by Beier *et al*.[183] First, benzyl ether protection of **4.15** was performed to reduce the volatility of any subsequent reaction products (Scheme 4.49), yielding **4.74**. Conditions employing MeLi with and without additive were initially attempted to synthesise the desired **4.75** (Entry 1 and 2,

Table **4.4**). However, based on ^{19}F NMR analysis of the crude reaction mixture, neither were successful with only ~5% of the desired product **4.75** formed.[xix] The major product from this reaction was presumed to be the elimination product **4.76**,[xx] determined by characteristic ^{19}F $\{^1H\}$ signals.[215] Beier observed that the use of the turbo Grignard reagent (*i*PrMgCl.LiCl) afforded a more stable metalated intermediate which, at -78 °C, was stable for 4 h. Therefore, this reagent was employed and after 45 min MeI was added (Entry 3,

Table **4.4**). Unfortunately, the desired product was not observed, suggesting that the organomagenisum intermediate had already degraded *via* fluoride elimination prior to the reaction with MeI. With this in mind, the addition of MeI was performed after 5 min, although only a 5% yield was observed (Entry 4,

Table **4.4**). Finally the reaction was attempted at -90 °C, with the addition of the turbo Grignard to a mixture of **4.74** and MeI, although again, only a 5% yield was observed (Entry 5,

Table **4.4**). It is likely that the metalation product is only stable for very short periods of time and that this reaction would likely benefit from the use of a flow reaction set up, or even lower reaction temperatures.

[xix] Selected data for **4.75** ^{19}F **$\{^1H\}$** (376 MHz, $CDCl_3$) δ -107.7– -107.8 (m, 2F), -114.5– -114.6 (m, 2F) ppm.
[xx] Selected data for **4.76** ^{19}F **$\{^1H\}$** (376 MHz, $CDCl_3$) δ -104.3 (dd, *J*=86.7, 32.1 Hz, 1F), -124.4 (dd, *J*=113.6, 86.7 Hz, 1F), -175.2 (dd, *J*=114.0, 32.5 Hz, 1F) ppm.

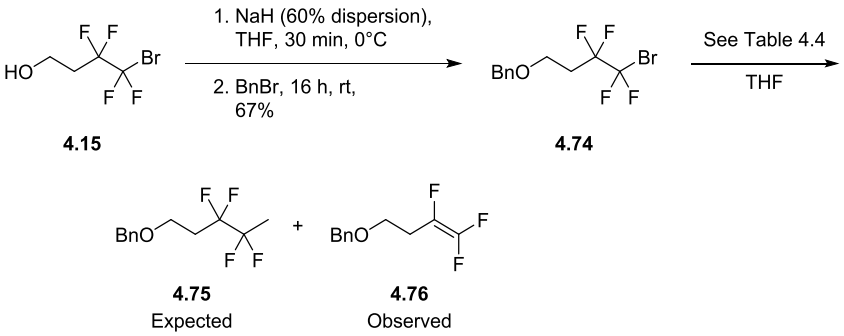

Scheme 4.49 - Attempted synthesis of 4.75

Table 4.4 - Attempted synthesis of 4.75. [A] Additive added after 45 minutes, [B] Additive added after 5 minutes.

Entry	Organometal	Electrophile	Temp	Yield
1	MeLi	N/A	-78 °C	~5%
2	MeLi	MeI[A]	-78 °C	~5%
3	Turbo Grignard	MeI[A]	-78 °C	0%
4	Turbo Grignard	MeI[B]	-90 °C	~5%
5	Turbo Grignard	MeI	-90 °C	~5%

As previously discussed, the major product observed for each of these reactions was a result of fluoride elimination, which was a side reaction Beier only typically observed with *n*BuLi.[183] However, the formation of the alkene product was not surprising, as this motif has previously been synthesised by the group *via* the treatment of $R^1CF_2CF_2Br$ with an excess of MeLi at room temperature. Hence, we did not achieve the synthesis of this compound on sufficient scale.

4.8.2 Synthesis of 3,3,4,4-tetrafluorobutan-1-ol

The radical debromination of **4.15** was successfully performed utilizing Bu_3SnH and AIBN to afford **G10** (Scheme 4.50).[xxi]

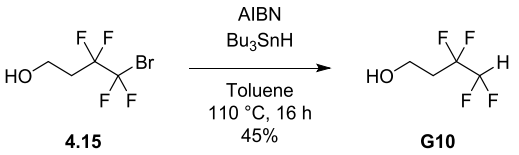

Scheme 4.50 - Synthesis of 3,3,4,4-tetrafluorobutan-1-ol

4.8.3 Synthesis of 2,2,3,3-tetrafluorobutan-1-ol

The deoxygenation of an alcohol with α-CF_2 substitution is a relatively uncommon reaction. The only examples in literature involve the conversion of the alcohol to an iodide *via* a triflate displacement, prior to the radical dehalogenation with *n*-Bu_3SnH/AIBN.[216-217] Due to the highly reactive nature and instability associated with triflate and iodide groups, a Barton-McCombie deoxygenation[218] was chosen. This route still necessitates the activation of the alcohol, this time to either a thiocarbonate, thiocarbamate or a xanthate. The formation of xanthates requires the use of toxic carbon disulphide,[219] thus either a thiocarbonate or thiocarbamate group was trialled.

Initially the deoxygenation of the diol **Q5** (Scheme 4.51), was attempted with the thiocarbonate group and no protecting group on the opposing alcohol. Conversion of **Q5** to the desired thiocarbonate **4.77,** was accomplished using conditions by Girsh *et al*.[219] Successful recrystallization of **4.77** from the slow evaporation of $CHCl_3$ gave crystals that were suitable for X-ray diffraction analysis (Figure 4.3). The reduction of the thiocarbonate **4.77** was then attempted with *n*-Bu_3SnH and AIBN. Despite consumption of the starting material as determined *via* TLC analysis, subsequent investigation of the crude ^{19}F NMR spectrum revealed a complex mixture of undesired fluorinated products.

[xxi] This synthetic work was performed by Simon Holland (4th year MChem student) under my supervision

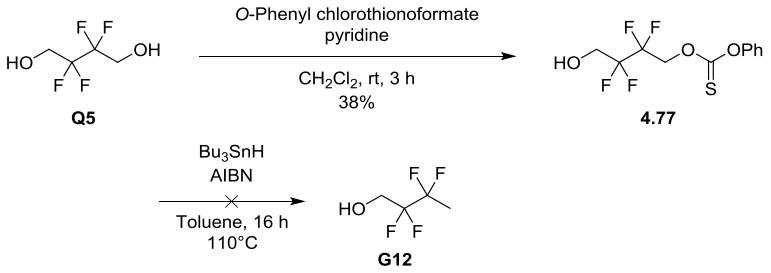

Scheme 4.51 - Attempted Barton–McCombie deoxygenation

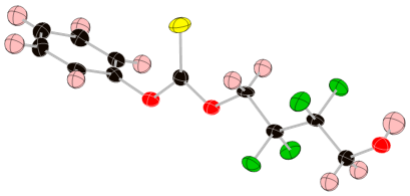

Figure 4.3 - Crystal structure of 4.77

In an effort to reduce the potential for side reactions and reduce the volatility of potential products, a TBDMS protecting group was installed to **Q5**. The selective mono-TBDMS protection reaction was successful and involved NaH and TBDMSCl (Scheme 4.52), affording **4.78** in a high yield of 95%. This was followed by the conversion of **4.78** to its corresponding thiocarbonate containing intermediate **4.79**, with a 76% yield. Again, the deoxygenation reaction was performed with AIBN and *n*-Bu_3SnH (Conditions A), however no desired product was observed as indicated by ^{19}F NMR analysis. Following flash column chromatography, the apolar side products co-eluted with the *n*-Bu_3SnH residues, preventing the identification of any side-reaction products. The deoxygenation of **4.79** was then attempted again, employing triethylsilane with benzoyl peroxide (BPO) as the radical initiator (Conditions B).[220] This resulted in fewer side-products and the crude reaction mixture here proved more useful allowing for an insight into the reaction outcome, in which a tt at 1.76 ppm can be observed, which would be expected from the terminal CH_3 of the $MeCF_2(CF_2)_n$- motif. This suggested the formation of the desired product **4.80**. Unfortunately, this apolar product was inseparable from triethylsilane and its corresponding degradants.

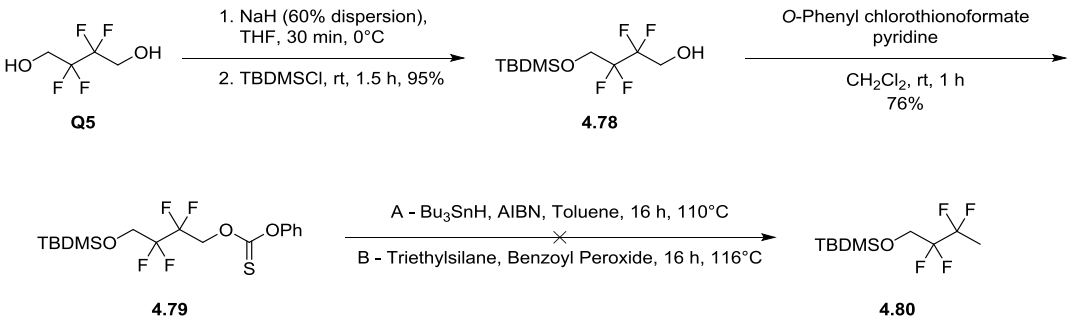

Scheme 4.52 - Synthesis towards 2,2,3,3-tetrafluorobutan-1-ol

Given this encouraging result, the route was repeated with a benzoyl protecting group installed.[xxii] The rationale was to enhance the polarity of the deoxygenated product so to provide a chromatographic handle for separation from triethylsilane and its degradants. The tetrafluorinated diol **Q5** was mono-benzoylated to afford **4.81** (Scheme 4.53), before activation of the free alcohol to the pivotal thiocarbonate intermediate **4.82**. The reduction of thiocarbonate **4.82** with triethylsilane and benzoyl peroxide progressed successfully with an excellent isolated yield of 93%. The deprotection of **4.83** was achieved with 25% NaOMe in MeOH, yielding **G12**.

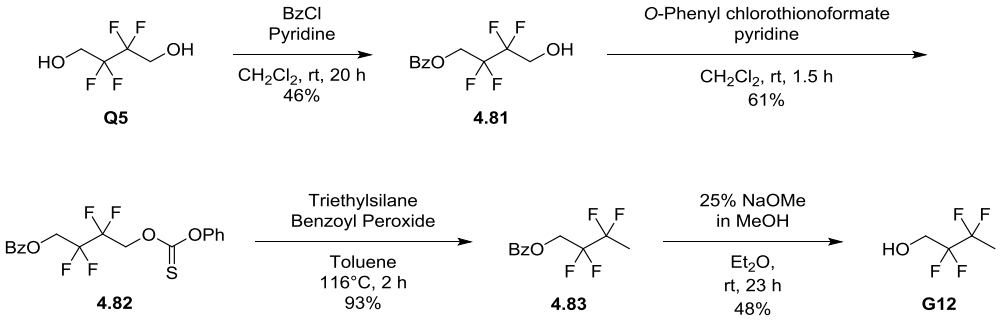

Scheme 4.53 - Synthesis towards 2,2,3,3-tetrafluorobutanol

The mechanism for this radical deoxygenation, which utilises triethylsilane and benzoyl peroxide, can be found in Scheme 4.54.[220]

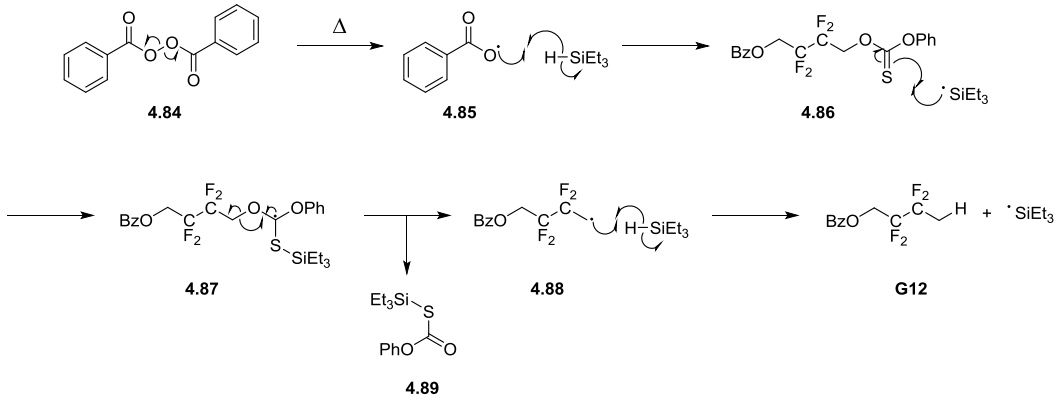

Scheme 4.54 - Mechanism for radical deoxygenation, adapted from Barton *et al*.[220]

[xxii] This synthetic work was performed by Simon Holland (4th year MChem student) under my supervision

4.8.4 Synthesis of 2,2,3,3,4,4-hexafluoropentan-1-ol

Having developed the optimised procedure for alcohol deoxygenation in the presence of an α-CF_2 substituent, the same series of reactions were then applied to hexafluoropentan-1,5-diol **R4** (Scheme 4.55), to afford **I15**.[xxiii] Hexafluoropentan-1,5-diol **R4** was mono-protected with benzyl chloride to afford **4.90** and the thiocarbamate was installed in a good yield of 86%. The reduction of the thiocarbonate **4.91** was performed and **4.92** was obtained in an excellent yield of 91%. Finally, deprotection was performed with 25% NaOMe in MeOH, to obtain the desired deoxygenated compound **I15**.

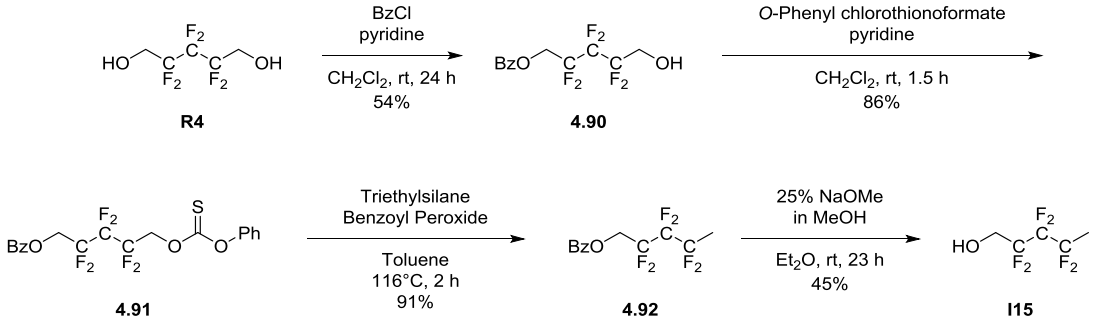

Scheme 4.55 - Synthesis of I15

[xxiii] The following reactions were performed by a 3rd year project student Thomasin Brind under my direct supervision.

4.9 Conclusion

A total of twenty-two fluorinated alkanols were successfully synthesised through the use of building-block and fluoroalkylation reactions (Figure 4.4). These substrates were used in the evaluation of the effects of aliphatic fluorination on lipophilicity, the results of which can be found in Chapter 2.

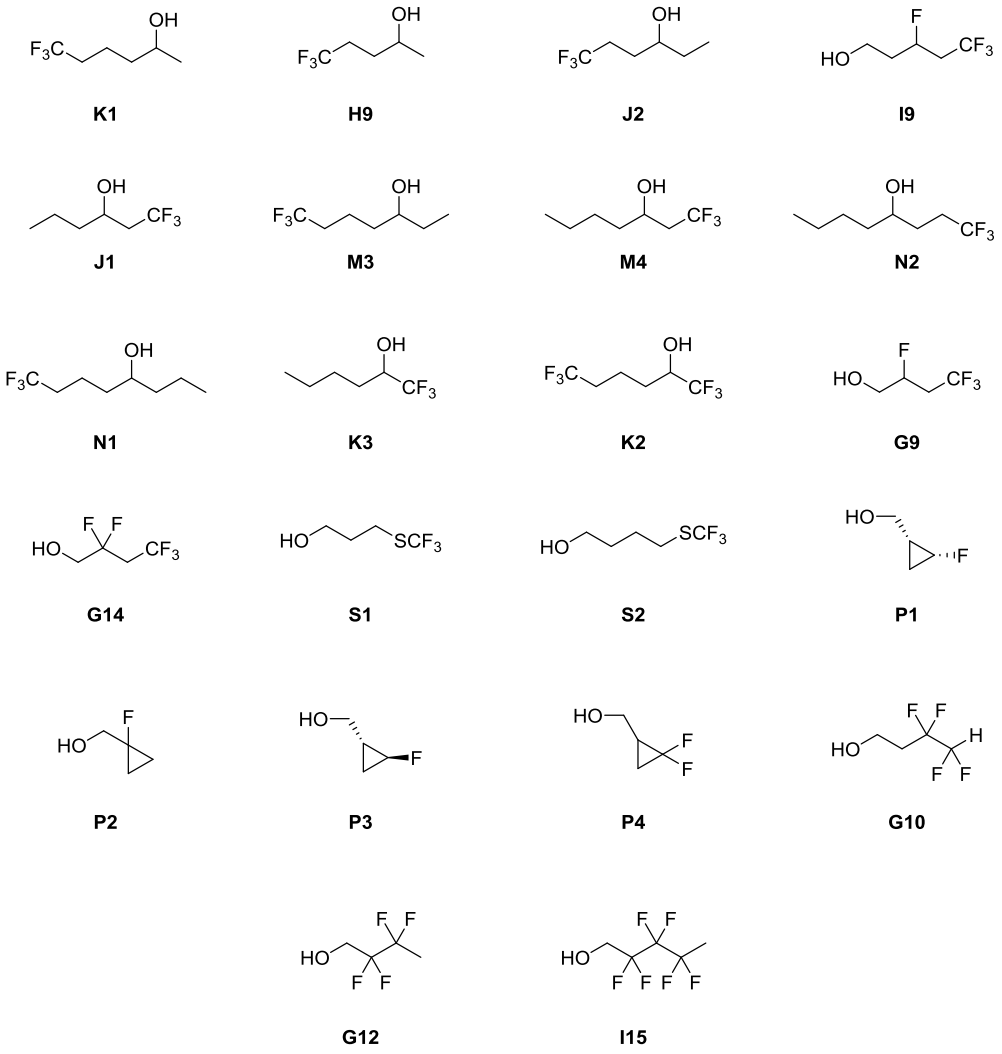

Figure 4.4 - All fluorinated alkanols synthesis in Chapter 4

The trifluorinated analogues **K1**, **H9** and **J2** were all synthesised following the silver catalysed hydrofluoromethylation of their respective alkenes. In a comparable manner, **I9** was synthesised *via* a radical fluorotrifluoromethylation. The trifluoromethylaminoxylation of 1-pentene with Togni II and subsequent N-O bond cleavage, yielded **J1**. The use of the Grignard reaction allowed for the synthesis of **M3**, **M4**, **N2** and **N1**. Nucleophilic trifluoromethylation of their corresponding aldehydes with Ruppert-Prakash reagent, afforded both **K2** and **K3**.

After the limited success of the oxytrifluoromethlation of an alkene, the synthesis of **D9** and **D14** was successfully accomplished. The aforementioned difficulties were overcome by performing a homologation reaction between the diazoalkane F_3CCHN_2 and benzyloxyacetaldehyde, followed by treatment with DAST and finally protecting group hydrogenolysis. Attempts to synthesise **D9** individually by deoxyfluorination was met with failure due to the high degree of alkene formation (elimination product).

The trifluoromethylthio motif of **S1** and **S2**, was successfully incorporated *via* the trifluoromethylation of a thiocyanate. The synthesis of the fluorinated cyclopropylmethanol analogues **P1**, **P2**, **P3** and **P4** was accomplished by the reduction of their corresponding carboxylic acids with $LiAlH_4$. The tetrafluorinated analogue **G10** was synthesised by radical debromination. Finally, a Barton-McCombie deoxygenation afforded both **G12** and **I15**.

Chapter 5 Reducing the Lipophilicity of Perfluoroalkyl Groups by CF_2–F/CF_2-Me or CF_3/CH_3 Exchange

5.1 Introduction

5.1.1 Previous results and Aims

Previous results from the Linclau group would suggest that the polyfluoroalkylation of simple alcohols would typically cause an increase in lipophilicity (**G → G17**, **I → I18,** Figure 5.1).[94] However as discussed earlier in Chapter 2 Section 2.3.3 and 2.3.4, various log*P* lowering trends for perfluoroalkyl groups were established. One of these is the drastic reduction of lipophilicity by roughly a logarithmic unit for the exchange of a trifluoromethyl group for a methyl (*cf.* **G17 → G12**, **I18 → I15**). The other trend observed was the decrease in lipophilicity despite chain elongation (which is typically log*P* increasing, *cf.* **G → I**) for the exchange of a C-F bond of a trifluoromethyl group for a C-Me bond (**G17 → I15**).

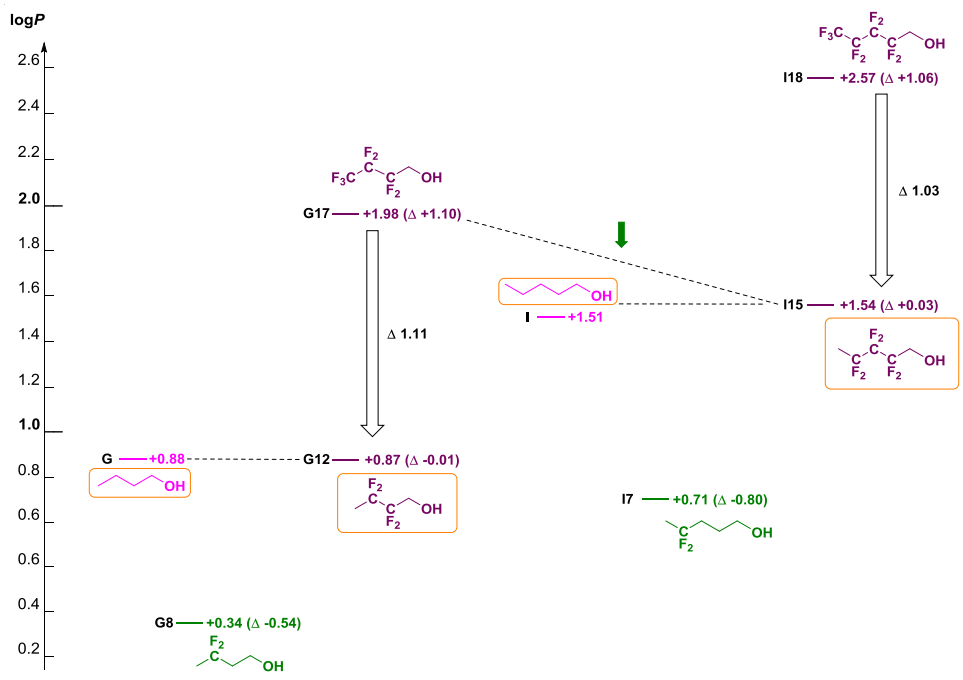

Figure 5.1 - Key lipophilicity lowering trends

Due to these interesting trends, the novel perfluoroalkyl groups (**G12** and **I15**, Figure 5.1) could be of interest in drug discovery programs. The use of $MeCF_2(CF_2)_n$-groups could assist medicinal chemists in the modulation of pharmacokinetic processes, such as metabolism or solubility, while also allowing them to achieve a similar or even reduced lipophilicity in respect to their parent compounds. It could be expected that these fluorinated chains will have a lower metabolic lability

than the corresponding alkyl group. Therefore, the investigation of whether these lipophilicity lowering trends translate directly from simple alcohols to more complex drug scaffolds is pivotal to the validation of this research. With this in mind, the following alcohols **a-h** (Figure 5.2) were selected for their incorporation into a drug scaffold in order to observe whether their effects on lipophilicity, as observed on the butanol/pentanol scaffold, hold when they are part of a more complex structure. The alcohols **a**, **d**, **e** and **h** were commercially available, while the synthesis of **b** and **f** can be found in Chapter 3 Section 3.3.7 and the synthesis of **c** and **g** can be found in Chapter 4 Section 4.8.3 and 4.8.4 respectively.

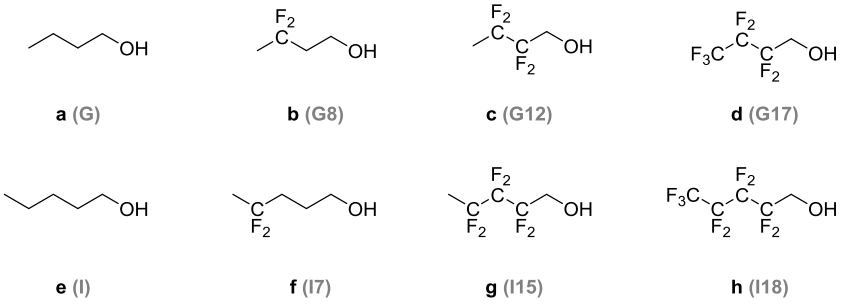

Figure 5.2 - Selected alkanols for investigation[xxiv]

Due to the collaboration with AstraZeneca on this project, the capability to investigate other pharmacological and pharmacokinetic processes is possible. Therefore, metabolism (human microsomes and rat hepatocytes), solubility, hERG inhibition and plasma protein binding will also be examined, as these properties have been known to be modulated by either lipophilicity or fluorination before.[8, 10, 221]

5.1.2 Evenamide

Evenamide **5.1a** (Figure 5.3), is an oral drug developed by Newron Pharmaceuticals designed to target voltage-gated sodium channels to treat schizophrenia as an add-on therapy (to enhance the therapeutic effect of an already prescribed drug).[222] It has recently finished Phase IIa clinical trials with plans to commence Phase III by the end of 2018. Evenamide was specifically chosen because of its butoxy group. The distance of the butoxy side chain in relation to the other functional groups allows for the effects of fluorination on lipophilicity to be observed without the interference of other effects. For example, if fluorine was to be close to a nitrogen containing functional group, it may affect the nitrogen's basicity.[115] This would potentially affect parameters such as solubility and lipophilicity.

[xxiv] To facilitate an easier discussion of the incorporation of these fluorinated alkanols into a drug scaffold within this chapter, they are labelled by a lowercase letter. The original numbering is in brackets.

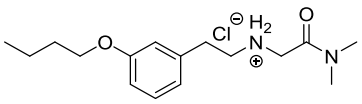

5.1a

Figure 5.3 - Evenamide

5.1.3 Synthetic plan

Newron had developed a simple and robust synthetic route towards evenamide starting from commercially available compound **5.2**•HCl (Scheme 5.1).[18] Ammonium salt **5.2** is first neutralized and the resultant amine is protected with a Boc group. Hydrogenolysis of the benzyl ether is performed, revealing phenol **5.3**. The butoxy group is installed *via* *O*-alkylation with 1-bromobutane, affording **5.4a**. Newron mentioned that other electron withdrawing groups could be used in place of the bromine for the C-O bond formation, such as sulphonate esters, which they demonstrated with other analogues. The dimethylacetamide functional group is then incorporated, providing **5.5a** and finally, Boc cleavage with ethereal HCl furnishes the final drug, evenamide **5.1a**.

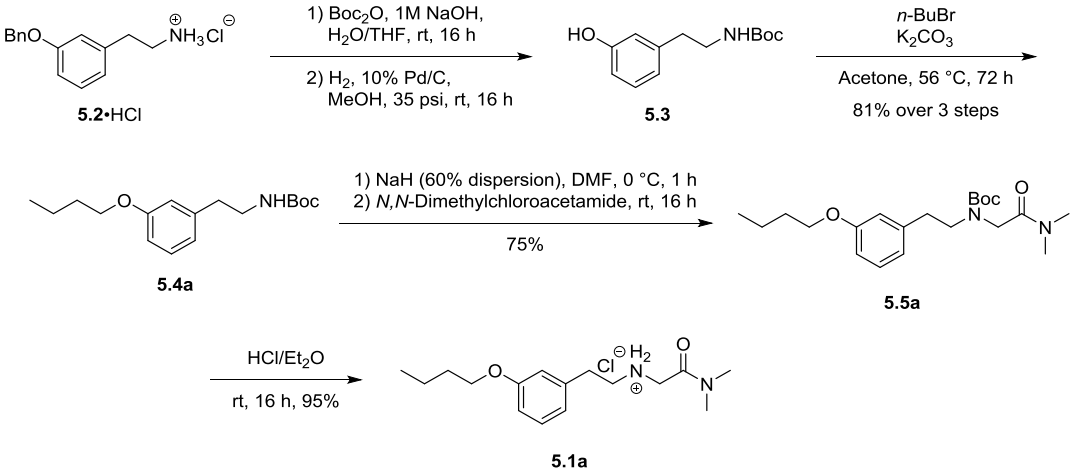

Scheme 5.1 - Newron's synthesis of evenamide

This procedure can be replicated with relative ease. The chosen alkanols (**a**-**h**, Figure 5.2), can be conveniently activated with a sulphonate leaving group for the C-O bond formation. One major procedural modification however will be performed; the dimethylacetamide installation will occur prior to the hydrogenolysis and *O*-alkylation synthetic steps. This is done to minimise the loss of valuable fluorinated material and thus maximise the quantity of the final fluorinated products.

5.2 Synthesis of evenamide and its analogues

5.2.1 Synthesis of scaffold

Despite the commercial availability of **5.2** (Scheme 5.1), its high cost (~£200/g) precluded its use as a starting material. Thus, the synthetic route will start from the vastly cheaper aldehyde **5.6** (~£6/g) which, following a literature procedure,[223] can be easily converted to **5.2** (Scheme 5.2). This was accomplished by performing a Henry reaction on the aldehyde **5.6** and then reducing the resultant nitroalkene **5.7** with $LiAlH_4$, to afford the primary amine. A Boc protection was subsequently performed, which afforded **5.9** in a yield of 42% over 2 steps. This yield was lower than expected and may be improved by performing the nitroalkene reduction at reflux.[224] However, enough material (**5.9**) was synthesised at this stage so there was no need to further investigate and optimise this series of reactions.

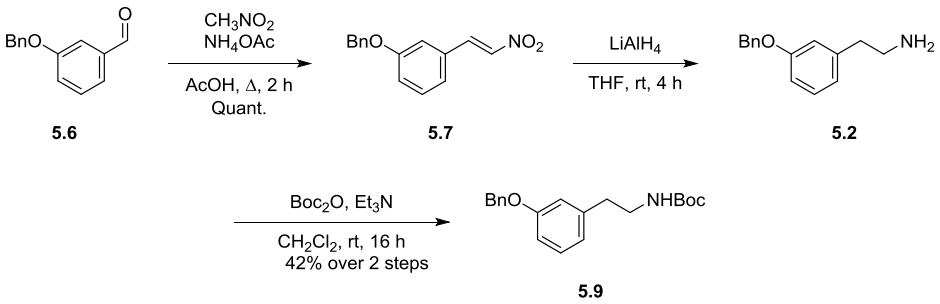

Scheme 5.2 - Synthesis of the required amine starting material

With **5.9** in hand (Scheme 5.3), the deviation from Newron's synthetic procedure was then feasible and the dimethylacetamide functional group was successfully installed. Deprotonation of the BocNH motif was performed with NaH, followed by nucleophilic substitution with *N,N*-dimethyl chloroacetamide, furnishing **5.10** in a yield of 83%. Protecting group hydrogenolysis was then performed, affording **5.11** in excellent yield of 93%, revealing the phenol functionality required for the important C-O bond formation.

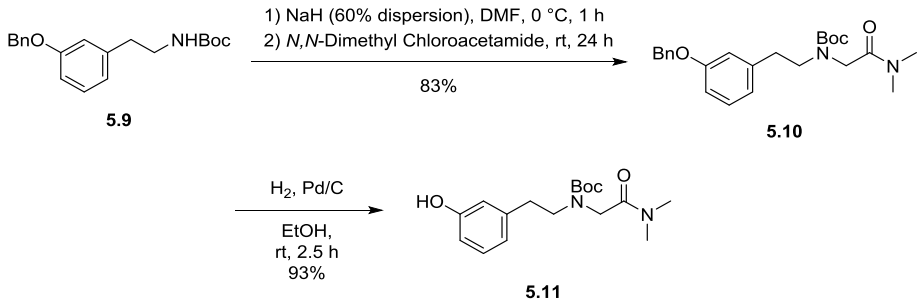

Scheme 5.3 - Synthesis of key phenol intermediate 5.11

5.2.2 *O*-Alkylations *via* a tosylate leaving group

In order to avoid the handling of any volatile sulphonate esters (triflate or mesylate derivatives), it was initially proposed that the introduction of the alkyl chains **a**-**h** (Figure 5.2) would be performed using a tosylate leaving group. The tosylate derivatives of **a**, **b**, **e** and **f**, were synthesised utilizing standard conditions and were used immediately without further purification (Scheme 5.4). The following *O*-alkylation reactions progressed smoothly through the deprotonation of the phenol with Cs_2CO_3, yielding **5.5a**, **5.5b**, **5.5e** and **5.5f** in yields of 43-91%.

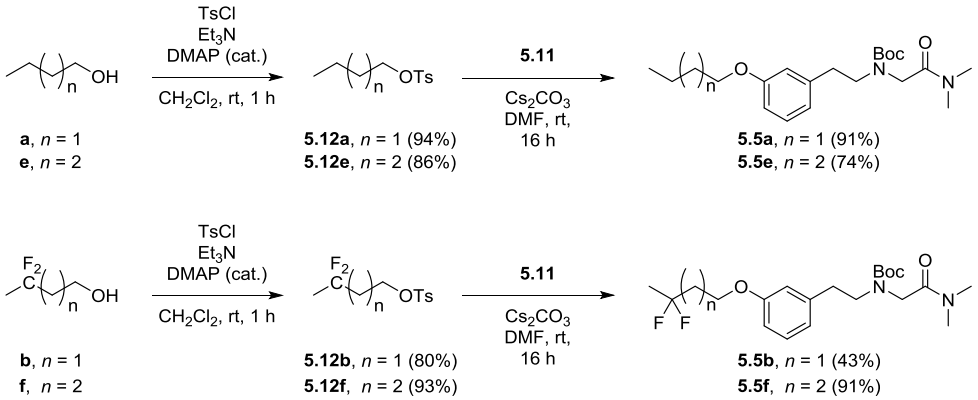

Scheme 5.4 - Key C-O bond formation

Despite the facile nature of the previous C-O bond formations, no reaction could be observed *via* LCMS analysis between the tosyl intermediate **5.12d** and phenol **5.11** at room temperature (Scheme 5.5). The reaction mixture was then heated to 90 °C and instead of the desired *O*-alkylation, tosyl exchange occurred instead, resulting in the formation and subsequent isolation of **5.13** in a yield of 67%. The reduced reactivity of leaving groups attached to perfluoroalkanols is well established.[225-227] This occurs predominantly because of an electronic deactivation effect and because of the neighbouring fluorine atoms causing a destabilizing repulsion to anionic nucleophiles. This leads to either a slow reaction or even no reaction occurring and, in this example, S-O bond cleavage instead of C-O, which is a previously documented side reaction.[228] Fortunately, this problem could be eliminated through the use of a triflate leaving group, which has been reported to be 10^4 more reactive than a tosylate.[229-230] One example of the installation of perfluoroalkanols *via* sulphonate displacement has been performed in literature.[230] In this case, a triflate leaving group was employed, although the other reagents used were NaH and hexamethylphosphoramide (HMPA), which are considered to be relatively forceful and toxic. The investigation and development of a more facile route is thus desired.

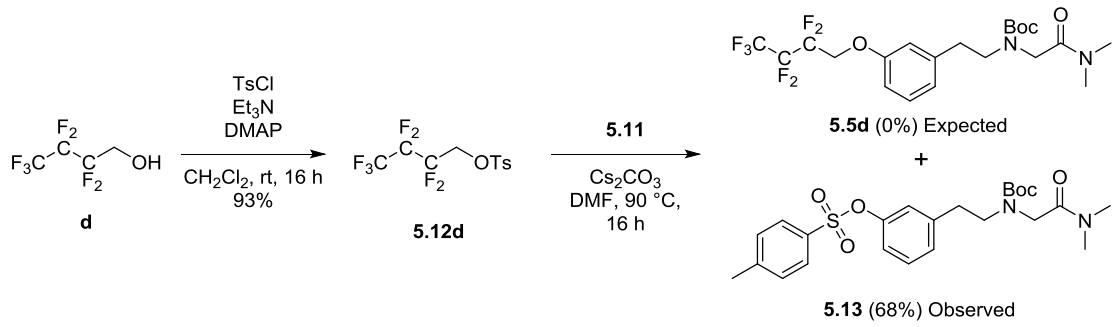

Scheme 5.5 - Attempted *O*-alkylation

5.2.3 *O*-Alkylations *via* a triflate leaving group

It was decided for fluorinated alcohols containing an α-CF_2, that a triflate leaving group would be employed for the *O*-alkylation step, because of its increased reactivity in comparison to the tosylate leaving group.[229-230] Despite the commercial availability of **5.14d** (Scheme 5.6), the triflate derivates of the fluoroalkanols **c**, **g** and **h** (Figure 5.2) are not. Therefore, the development of a procedure for the synthesis and subsequent isolation and handling of these triflate activated alcohols is required.

The optimisation of this process was performed using fluoroalkanol **d** (Scheme 5.6), due to its commercial availability and low cost. As originally expected, **5.14d** was very volatile, with a boiling point of 118-120 °C.[229] Therefore, normal operating protocol was applied for the handling of volatile materials. Standard conditions were applied for the triflate formation and the reaction was successful with complete consumption of the starting material, confirmed *via* crude ^{1}H and ^{19}F NMR analysis. However, a concentrated solution yielded only 38% of the desired material (Scheme 5.6). This low yield was deemed unacceptable, and a different procedure was sought after.

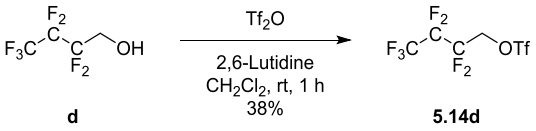

Scheme 5.6 - Triflation reaction

The majority of **5.14d** was presumably lost upon evaporation of the solvent. One way to minimise this loss could be through not attempting its isolation. This can be accomplished by employing a one-pot procedure, where isolation of the desired product occurs only after the C-O bond formation, when the product is no longer volatile (Scheme 5.7). As acetonitrile has been used for both triflation[231] and *O*-alkylation[232] reactions, this was the first solvent utilized for the one-pot procedure (Table 5.1, Entry 1). The triflate formation was performed again using the standard conditions previously employed (Scheme 5.6). After the reaction was deemed complete by ^{19}F NMR (~1 hr), 3 equivalents of Cs_2CO_3 were added to the reaction mixture, followed by **5.11** in a solution

of DMF. After 16 h, crude ^{19}F NMR revealed consumption of the starting material **5.14d** and crude LCMS analysis confirmed the formation of the desired product **5.5d**. Following aqueous work up and column chromatography, **5.5d** was isolated in a good yield of 50%. As there is literature precedent for triflation reactions being performed in neat pyridine,[233] the triflation reaction was attempted in neat 2,6-lutidine (Table 5.1, Entry 2). However, no formation of **5.14d** was observed by ^{19}F NMR. The original solvent for the triflation reaction, CH_2Cl_2, was then trialled and an improved yield of 67% was observed (Table 5.1, Entry 3). In an attempt to further improve this yield, the triflation reaction was repeated in CH_2Cl_2 with an aqueous work up performed prior to the *O*-alkylation (Table 5.1, Entry 4). Unfortunately, the yield decreased to 23%. This is presumably due to the low concentration of the reaction mixture, as a consequence from dilution *via* multiple extractions from the aqueous phase (during the work up procedure of the triflation reaction).

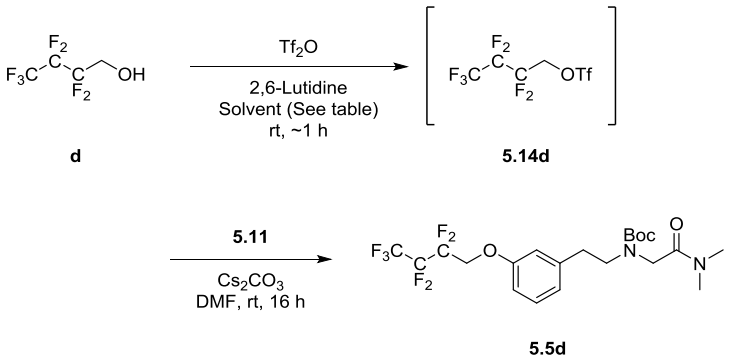

Scheme 5.7 - One-pot *O*-alkylation optimization

Table 5.1 - One-pot *O*-alkylation optimization

Entry	Solvent	Isolated yield of 5.5d over 2 steps
1	MeCN	50%
2	2,6-Lutidine	No triflate formation observed
3	CH_2Cl_2 (No aq. work up)	67%
4	CH_2Cl_2 (w/ aq. work up)	23%

With the synthesis of **5.5d** complete (Scheme 5.7), the same methodology was applied to the fluorinated alkanols which contain an α-CF_2 group **c**, **g** and **h** (Scheme 5.8). This afforded **5.5c**, **5.5g** and **5.5h** in good yields.

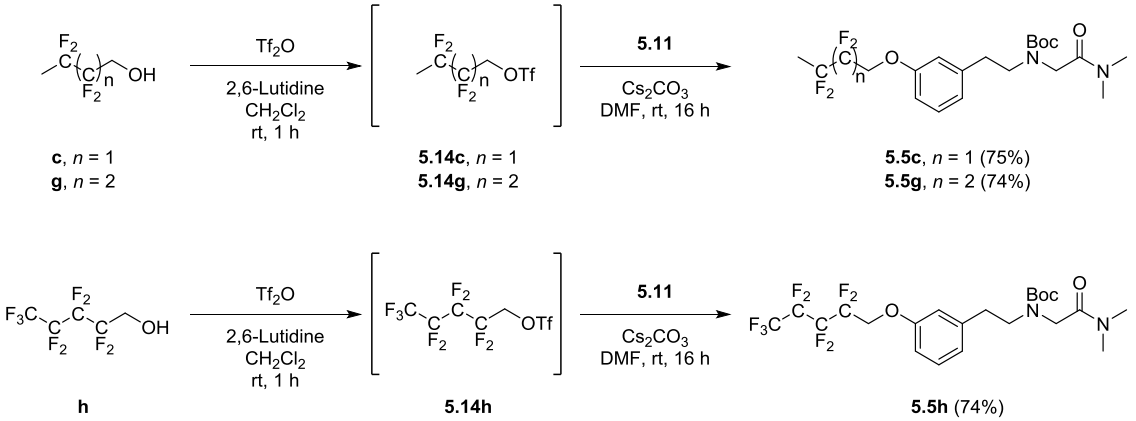

Scheme 5.8 - Application of one-pot procedure to other fluorinated alkanols

5.2.4 Deprotection

With all of the desired Boc-protected evenamide analogues now synthesised, a simple cleavage of the Boc protecting group and subsequent hydrochloric salt formation was accomplished. This was performed with 4M HCl in dioxane, furnishing all of the desired analogues **5.1a-h** in good yields of 87-99% (Scheme 5.9). This reaction was initially attempted with 2M HCl in diethyl ether as the patent described,[222] however the reaction times were found to be considerably longer.

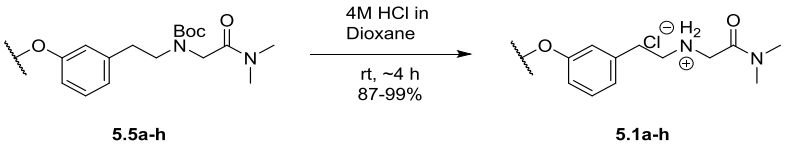

Scheme 5.9 - Acid mediated Boc cleavage

5.3 Results and discussion

5.3.1 Results Table

The data seen in the Table 5.2 was obtained by the PhD sponsors, AstraZeneca, and will be discussed separately in the following sections.

Table 5.2 - Analysis of evenamide 5.1a and analogues 5.1b–h

Structure	Log$D_{7.4}$[a]	Solubility[b] (µM)	Hu Mics Clint[c]	Rat Heps Clint[d]	PPB[e] (% free)	hERG Inhib[f] (%)
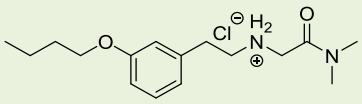 **5.1a**	+1.8	782	13	82	45	31
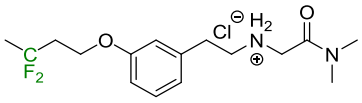 **5.1b**	+1.1	960	7	34	62	35
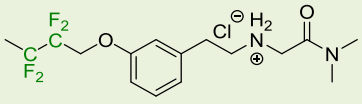 **5.1c**	+1.6	929	10	32	51	41
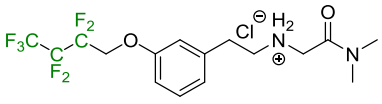 **5.1d**	+2.5	952	8	20	20	57
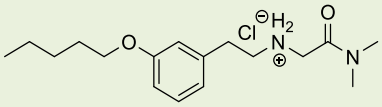 **5.1e**	+2.3	779	29	91	23	70
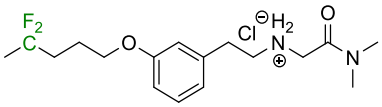 **5.1f**	+1.7	1000	7	38	49	45
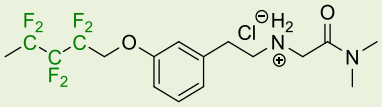 **5.1g**	+2.2	946	9	64	25	63
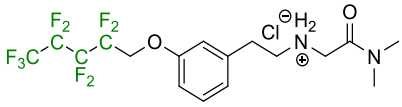 **5.1h**	+3.3	955	7	21	7.6	81

[a]log$D_{7.4}$ determined by shake flask method; [b]Solubility of compounds in aqueous phosphate buffer at pH 7.4 after 24 h at 25 °C; [c]Rate of metabolism (µl/min/mg) determined from DMSO stock

solution in human microsomes; [d]Rate of metabolism (µl/min/10^6 cells) determined from DMSO stock solution in isolated rat hepatocytes diluted to 1x10^6 cells/mL; [e]Determined from DMSO stock solution by equilibrium dialysis in 10% human plasma supplied by Quintiles; [f]% inhibition of hERG ion channel at a concentration of 10 µM. Detailed experimental for how the measurements within this table were performed can be found in *Ref*[121]

5.3.2 Log*D*

The log*D* value for the parent compound evenamide (**5.1a**) is +1.8, and its homologue **5.1e** displays an increased value of +2.3 log*D* units (Figure 5.4 and Table 5.2). This increase in log*D* is a result of the elongation of the carbon chain by one methylene unit. Difluorination at the penultimate position of the alkyl chain (**5.1b** and **5.1f**), leads to a decrease in log*D* by 0.6-0.7 units, in a similar fashion to the trend observed on the model alkanol systems (**G → G8** and **I → I7**). A significant increase in log*D* was observed for the perfluorination of the alkyl chains (**5.1d** and **5.1h**), again in accordance with trends observed on the model alkanol systems (**G17** and **I18** respectively).

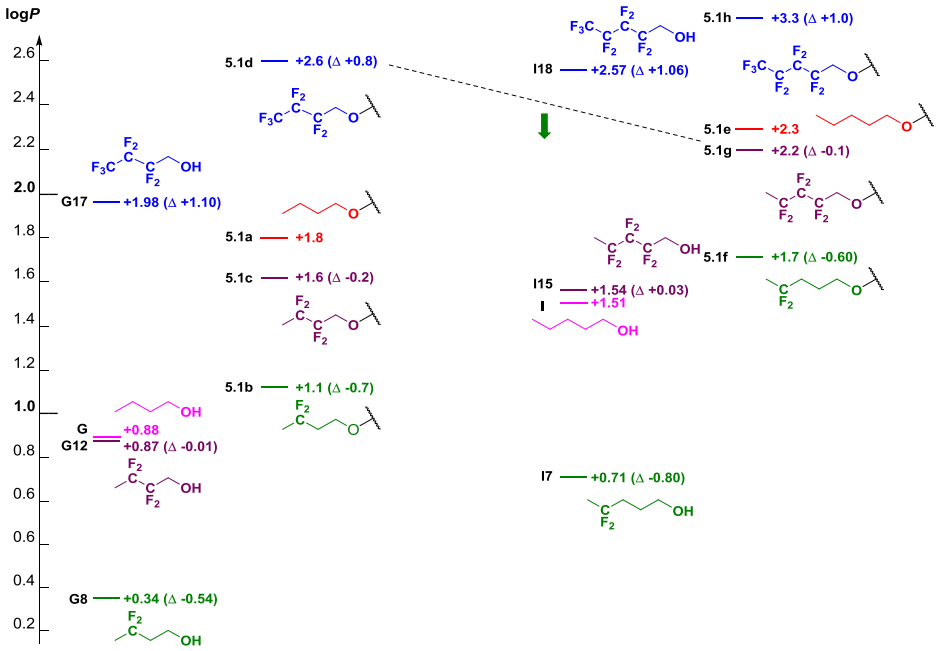

Figure 5.4 - Log*P*/*D* comparison

To our delight, when exchanging a CF_3 for a methyl group on a perfluoroalkyl group of the fluorinated evenamide analogues, a large log*D* reduction of ~1 unit was observed on both the butyl (**5.1d → 5.1c**) and pentyl (**5.1h → 5.1g**) chains. This is similar to what was observed on the simple fluorinated alkanols (**G17 → G12** and **I18 → I15)**. Equally pleasingly, when performed CF_2–F/CF_2-Me exchange on a perfluoroalkyl group (**5.1d → 5.1g**), a decrease in log*P* is observed, consistent with the results from the fluorinated alkanols (**G17 → I15**). Also, when comparing the $MeCF_2(CF_2)_n$- group to its respective parent compound, only a very small decrease in log*P* (Δ-0.01, **G → G12**), or a slight

increase (Δ+0.03 for **I → I15**), was observed. When investigating the $MeCF_2(CF_2)_n$- group on the evenamide analogues, a larger log*D* reduction was observed for the butyl analogue (Δ-0.2, **5.1a → 5.1c**) and in the case of the pentoxy derivative, a log*P* reduction occurred (Δ-0.1, **5.1e → 5.1g**). This can explained through the fact that the evenamide analogues have an increased log*P* in respect to their alkanol counterparts, so the impact of the polarity of the $MeCF_2(CF_2)_n$- group is more pronounced.

Our rationale for this significant log*P* decrease observed for the CF_3/CH_3 exchange on the perfluoroalkyl butoxy and pentoxy groups, which lead to a similar or even reduced log*P* in comparison to their respective parent compounds, can be found in Chapter 2 Section 2.3.3.

Hence, the lipophilicity trends that were observed when comparing the fluorinated motifs on butanol and pentanol models were successfully reproduced when the same motifs were introduced into a pharmaceutical drug candidate as part of an aromatic butoxy/pentoxy chain. This is an important result, which strengthens the relevance of the lipophilicity investigations on these alkanol models.

5.3.3 Solubility

As discussed in Chapter 1 Section 1.2.1.1, an increase in solubility is often attributed to a decrease in lipophilicity. This relationship can be observed for both analogues **5.1b** and **5.1f** (Table 5.2), which possess higher solubility values as well as lower log*D* values than their respective parent compounds. Interestingly, despite an increase in log*D* for **5.1c**, **5.1d**, **5.1g**, and **5.1h**, an increase in solubility was also observed in respect to their parent compound. Typically, the inverse would be expected. As observed in Equation 4 (Chapter 1, Section 1.2.1.1), a decrease in melting point can also be related to an increase in solubility. Therefore, it could be expected that these derivatives (**5.1c**, **5.1d**, **5.1g**, and **5.1h**) with high degrees of fluorination, exhibit lower melting points than their respective parent compounds, which results in their increased solubility.

5.3.4 Metabolic stability

The metabolic stability of all fluorinated substrates improved in comparison to their parent compound against both human microsomes (Hu Mics) and rat hepatocytes (Rat Heps). Evenamide already displayed great stability against Hu Mics, which is of no surprise as it is a lead molecule in a drug discovery program. Thus, little difference was observed in contrast to the fluorinated derivatives. However, for the pentyl series, a much larger increase in metabolic stability can be observed against Hu Mics through the comparison of the parent compound **5.1e** (29 µl/min/mg, Table 5.2), against its fluorinated analogues **5.1f**-**5.1h** (7-9 µl/min/mg). Vastly improved metabolism

can be observed for all fluorinated compounds against Rat Heps when compared to their respective non-fluorinated parent. Fluorination is a commonly employed strategy within drug discovery to block metabolically labile sites,[101, 221] and is presumably the reason behind this observed increase in metabolic stability. It is also important to point out that the fluorine not only blocks the carbon it is situated on, but also neighbouring positions, due to the electronegativity of the fluorine atoms reducing the reactivity of the C-H bonds for oxidation. This is the case for the terminal methyl groups of the $MeCF_2(CF_2)_n$- group, **5.1c** and **5.1g**.

It is also well established that an increase in lipophilicity will typically coincide with a decrease in metabolic stability.[45-46] Thus, it would be expected based on the log*D* values alone that both of the perfluorinated substrates **5.1d** and **5.1h** are the least metabolically stable. However, the inverse is observed, as a result of the high degree of fluorination. This is a good example of why metabolic stability is considered one of the more difficult parameters to predict.

5.3.5 Plasma protein binding (PPB)

Human plasma protein binding is known to correlate with lipophilicity. Therefore, it is of no surprise that for all substrates, the higher the log*D*, the higher the PPB. For example, **5.1e** and **5.1f** are isolipophilic and have the same values for PPB; the same can be observed for **5.1e** and **5.1g** (Table 5.2).

5.3.6 Human *Ether à-go-go*-Related Gene (hERG)

Similar to PPB, hERG inhibition correlated broadly with lipophilicity, where the most lipophilic substrates within each series had the highest hERG inhibition. The only exception to this is evenamide itself which, despite having a higher log*D* than both **5.1b** and **5.1c**, has reduced hERG inhibition in comparison (Table 5.2). This is likely the result of other structural properties, for example, an increase in the MW (size mimic) has also been reported to increase hERG inhibition,[11] which is likely the case here.

5.4 Conclusion

The synthesis of evenamide and its seven analogues was successfully performed, in conjunction with the development of a one-pot *O*-alkylation procedure for polyfluorinated alkanols containing an α-CF_2 group. Pleasingly, both of the key lipophilicity lowering trends for the perfluoroalkyl groups by CF_3/CH_3 and CF_2-F/CF_2-Me exchange were applicable to the drug scaffold. The log*D* values of the fluorinated evenamide analogues also correlate nicely to the log*P* of their respective fluorinated alcohol. This work assists in the validation of other lipophilicity trends that have been observed on simple alkanol systems (See Chapter 2).

In addition to this, the fluorinated analogues exhibited improved aqueous solubility in comparison to their parent compounds, as well as an improvement in metabolic stability against both Hu Mics and Rat Heps assays. Plasma protein binding and hERG inhibition were also investigated, which both correlated well to lipophilicity modulation.

Overall, this chapter showcases the introduction of the novel $MeCF_2(CF_2)_n$- group into a drug scaffold. In a time of lipophilicity control being critical to the drug optimization process, this motif is able to increase the metabolic stability, while maintaining or slightly reducing the lipophilicity of the compound.

Chapter 6 Conformer Specific Lipophilicity

6.1 Introduction

Amide rotamers can have different properties, for example polarity if their dipole moments are different.[234] Amides are often found within drugs and other biological compounds, and it could be of interest to be able to measure or calculate the specific log*P* values of their conformers, in order to refine our understanding of the ADMET properties of the parent molecule.

Conformer-specific lipophilicity has been defined as the partition coefficient of the individual conformers in octanol/water by Davies *et al*. in 1979.[235] Davies also hypothesized that membrane penetration of drugs is due to particular conformers, however they presented neither methodology nor experimental data. Following this, Noszál *et al*. published two papers detailing their work on the log*P* measurement of the individual conformers of amphetamine and clenbuterol (Figure 6.1).[236-237]

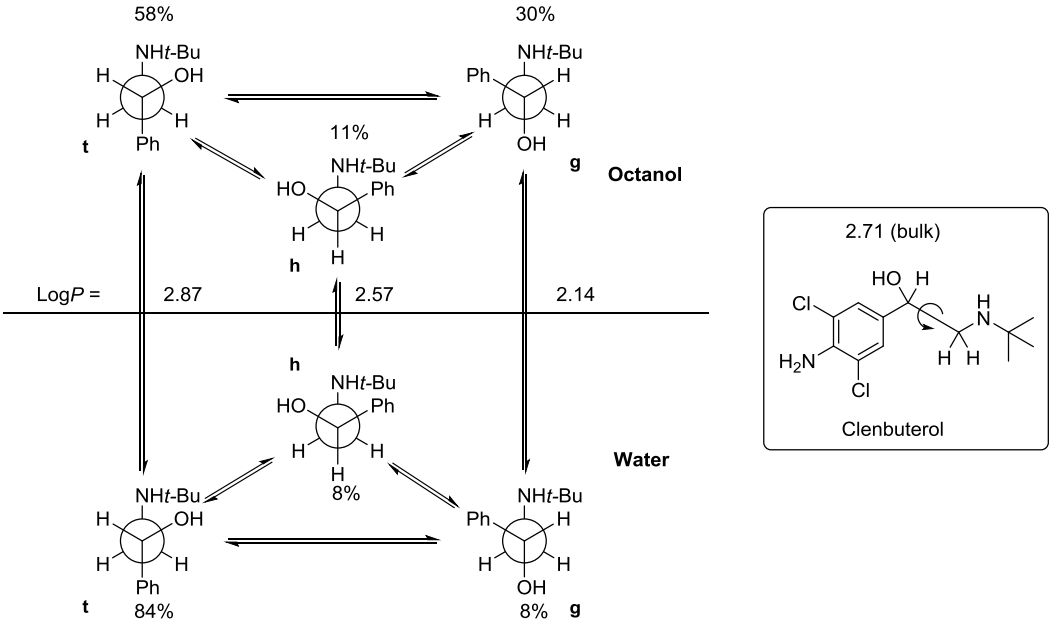

Figure 6.1 - Conformer specific log*P* for clenbuterol indicating populations in each layer and their corresponding log*P*'s. Adapted from *Ref*[237]

The bulk (macroscopic) partition coefficient is defined as the ratio of the concentration of the compound in both the octanol and water phase (Equation 1). The conformer specific partition coefficient for each individual conformer (t = trans, g = gauche and h = hindered) can be seen in Equation 2. Noszál was able to relate Equation 1 and 2 by the rotamer mole fractions (e.g. α_{to} and α_{tw}, calculated through the use of coupling constant analysis in both D_2O and octanol) to derive Equation 3, this enabled him to determine the log*P* of the individual conformers.

$$P = \frac{C_o}{C_w} \quad \textbf{(Eq. 1)}$$

$$P_g = \frac{[g]_o}{[g]_w} \qquad P_t = \frac{[t]_o}{[t]_w} \qquad P_h = \frac{[h]_o}{[h]_w} \quad \textbf{(Eq. 2)}$$

$$P_g = \frac{\alpha_{g_o}}{\alpha_{g_w}} P \qquad P_t = \frac{\alpha_{t_o}}{\alpha_{t_w}} P \qquad P_h = \frac{\alpha_{h_o}}{\alpha_{h_w}} P \quad \textbf{(Eq. 3)}$$

Unfortunately, this method of conformer specific lipophilicity determination is not easily reproducible for a wide range of substrates, as octanol solvent peaks within the ^{1}H NMR spectrum may obscure signals, requiring solvent suppression techniques to obtain *J*-values.

6.2 Aims

The determination of the concentration of rotamers around bonds in solution is not straightforward. However, amide rotamers are unique as their *cis*- and *trans*-conformation are typically in slow exchange on the NMR time scale and therefore are often distinguishable *via* NMR, including ^{19}F NMR. We propose to use our ^{19}F NMR based log*P* determination method to measure the log*P* of the individual *cis* and *trans* amide rotamers.

The methodology will be illustrated using simple *N*-acetylated compounds, for example fluoropiperidines/fluoropyrrolidines **1.1**-**1.4** (Figure 6.2), before more complex rotamers or other distinguishable conformers are taken into consideration.

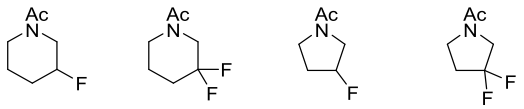

1.1 **1.2** **1.3** **1.4**

Figure 6.2 - Target *N*-acetyl amide rotamers

6.3 Synthesis of amide rotamers

6.3.1 Attempted synthesis of *N*-acetyl 3-fluoropiperidine

Despite the commercial availability of 3-fluoropiperidine, its high cost precluded its use as a starting material. Therefore, the synthesis of *N*-acetyl-3-fluoropiperidine **1.1** was attempted from the cheaper commercially available 3-hydroxypiperidine **6.1** (Scheme 6.1). Following standard procedure a *N*-acetylation was performed yielding **6.2**.[238] The subsequent fluorination of **6.2** with DAST resulted in the formation of an inseparable mixture of the desired monofluorinated product **1.1** and the alkene elimination product **6.3**, in a ratio of 1:1.25 respectively. As discussed earlier in

Chapter 3 Section 3.3.9, *m*CPBA can be used to facilitate the isolation of the desired monofluorinated product from its corresponding alkene side products. This was successfully performed, removing all traces of alkene **6.3** from the desired product **1.1**. Nevertheless, a small amount (~5%) of an unidentified impurity remained with a ^{19}F NMR signal within the region expected of a primary fluoride. It is thought that this may be the 5-membered ring rearrangement product **6.4**.[239] No further attempt to isolate **1.1** was performed at this stage and a different route was investigated.

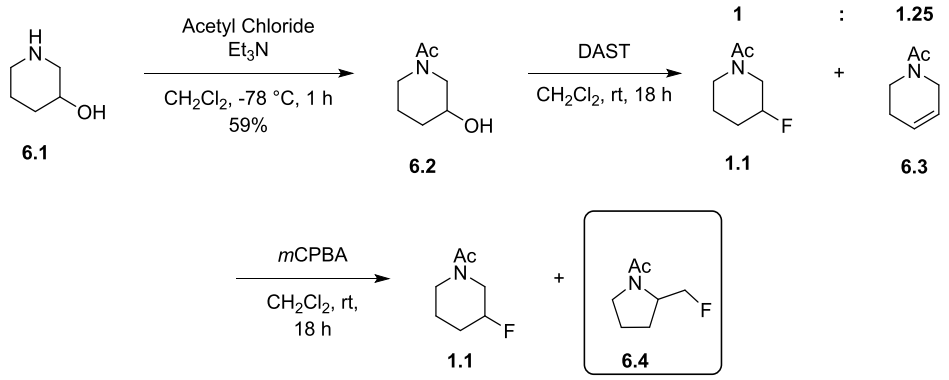

Scheme 6.1 - Attempted synthesis of *N*-acetyl-3-fluoropiperidine

The mechanism for the formation of **6.4** *via* a DAST induced ring contraction can be seen in Scheme 6.2. The reaction progresses through an aziridinium intermediate **6.6**, where fluoride can attack either position of the aziridinium ring to afford either **1.1** or **6.4**.

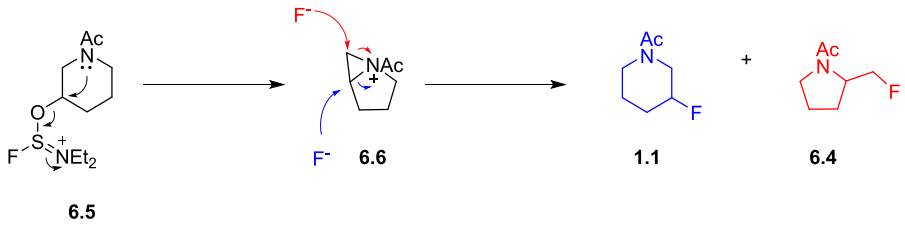

Scheme 6.2 - Ring contraction mechanism adapted from *Ref*[239]

6.3.2 Synthesis of *N*-acetylated fluoropiperidines and fluoropyrroldines

Fortunately, Apollo Scientific subsequently gifted the group 3-fluoropiperidine•HCl **6.7** (Scheme 6.3), 3,3-difluoropiperidine•HCl **6.8**, and 3-fluoropyrrollidine•HCl **6.9**. Finally, 3,3-fluoropyrolidine **6.10** was commercially available at a reasonable cost. With the hydrochloric salts in hand, a series of simple *N*-acetylation reactions was performed yielding the desired compounds **1.1**-**1.4**.

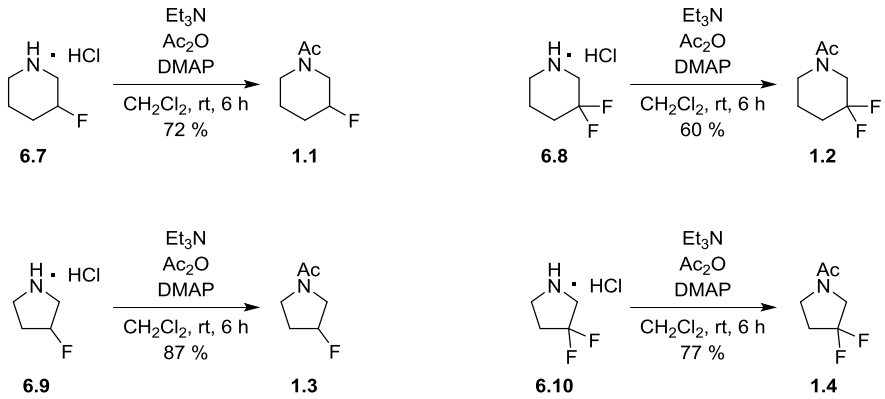

Scheme 6.3 - Synthesis of *N*-acetylated fluoropiperidines and pyrrolidines

6.4 Assignment of amide rotamers

6.4.1 Establishment of amide rotamers

For all the amides **1.1**-**1.4** (Figure 6.2), the fluorine spectrum contains two signals in a variety of NMR solvents. Confirmation that these signals represent a mixture of amide rotamers was performed through variable temperature (VT) ^{1}H and ^{19}F NMR experiments in DMSO-d_6. For example when a VT experiment was performed on **1.3**, the acetate signal occurring within the ^{1}H NMR, displayed line broadening and eventual coalescence (Figure 6.3). The same can be observed for the fluorine signal in the ^{19}F NMR spectrum.

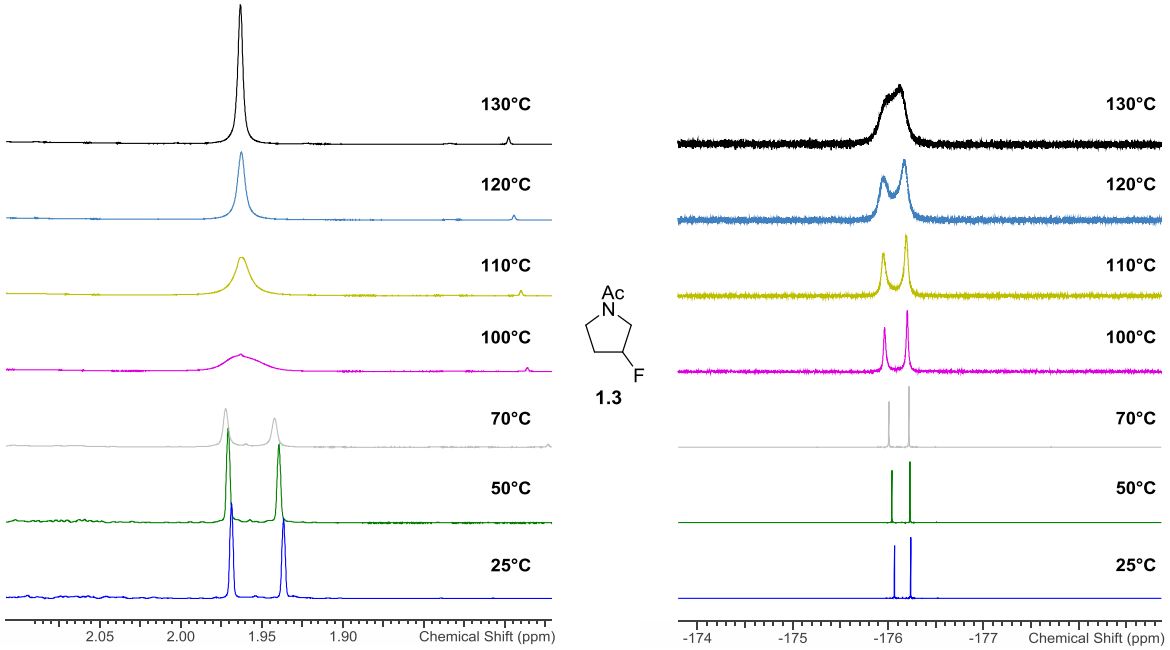

Figure 6.3 - ^{1}H NMR of 1.3, acetate signal coalescence (left). ^{19}F NMR of 1.3, fluorine signal coalescence (right).

6.4.2 Conformer assignment

In order to achieve integration of the fluorine signals for each rotamer, it must first be established which peak corresponds to which rotamer. This is achieved by a NOESY experiment in which the proximity of the methyl group and the ring protons can be established (by the observation of NOE cross peaks) as shown below for compound **1.4** (Figure 6.4):

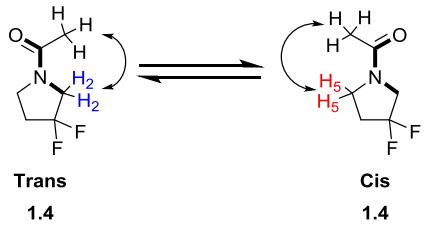

Figure 6.4 - *Trans* and *cis* amide rotamers

A typical procedure to achieve this involves:

1) Assignment of the individual ring proton peaks in the ^{1}H NMR spectrum, especially the protons in the α-position of the amide nitrogen
2) A NOESY experiment as shown above
3) Establish which is the major and which is the minor isomer by integration
4) Assign the fluorine peaks through their relative integration

6.4.3 Rotamer assignment in water (D_2O)

The assignment in water (D_2O) was straightforward and is only illustrated here for **1.4** (Figure 6.5). For the amides under study, the interpretation of the ^{13}C NMR spectrum was facile: C2 can be identified due to the $^{2}J_{C2\text{-}F}$ coupling constants (t, J = 32.2 Hz) and the chemical shift (adjacent to amide), while C5 can be recognised by its much smaller $^{3}J_{C5\text{-}F}$ coupling constants (t, J = 3.3 Hz). An analogous situation occurs for the piperidine compounds. Once the carbons had been assigned, the major and minor signals of H2 and H5 can be assigned *via* HSQC analysis.

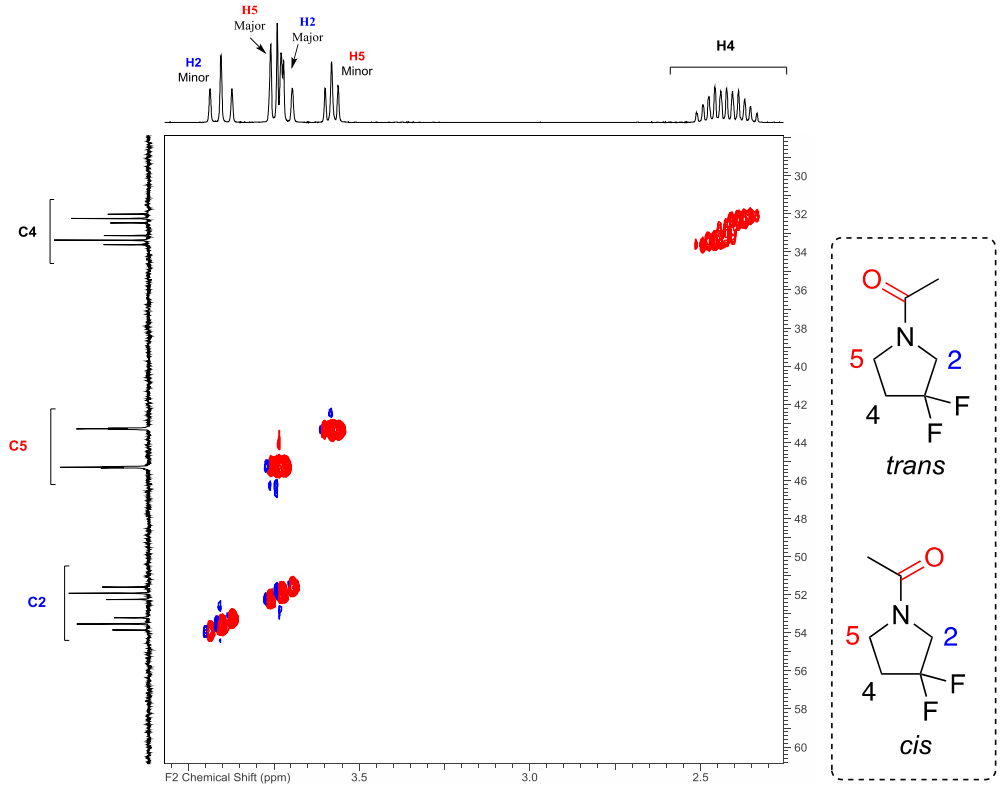

Figure 6.5 - HSQC spectrum of 1.4 in D_2O, 25.35 °C, Bruker AVII400 FT-NMR Spectrometer.

In a NOESY spectrum, a cross-peak will be observed for protons that are close in space. Cross-peaks of the acetate CH_3 with either H2 or H5 will allow to establish the identity of the rotamers (Figure 6.6): the minor acetate signal shows a cross-peak with a previously assigned H2 resonance, which confirms that the minor rotamer has the *trans*-conformation, while the signal for H5 of the minor isomer doesn't show a cross peak. The opposite is expected for the major integration signals and is observed, with the major H5 signal showing a cross-peak with the major acetate signal, and the major H2 signal showing no cross-peak. This confirms that the major rotamer of **1.4** in D_2O is the *cis*-conformation.

In this way the rotamer assignment in D_2O could be achieved for all amides investigated.

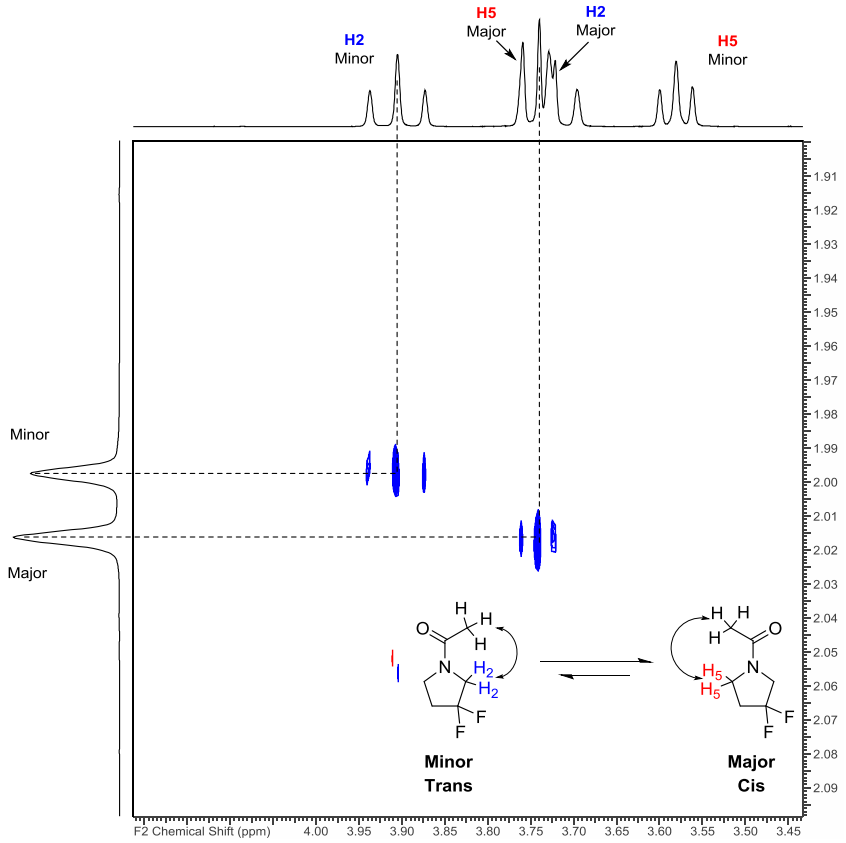

Figure 6.6 - NOESY spectrum of compound 1.4 in D_2O, 25.35 °C, Bruker AVII400 FT-NMR Spectrometer.

6.4.4 Consideration of ^{19}F NMR chemical shifts in different solvents

With the rotamers accurately assigned in D_2O, their respective chemical shifts where compared to $CDCl_3$. It was established that the ^{19}F chemical shift values for the individual rotamers could deviate significantly between solvents. The chemical shifts in some cases even had effectively "reversed". This can be observed for **1.3** where the ^{19}F resonance for the *cis* conformer is more upfield in $CDCl_3$ compared to the resonance of the *trans*-rotamer (Figure 6.7), while in D_2O it is the other way round. Consequently, the assumption that the chemical shift values of the rotamer signals does not change between H_2O to octanol may result in incorrect log*P* values. Therefore, the rotamer assignment within octanol is crucial.

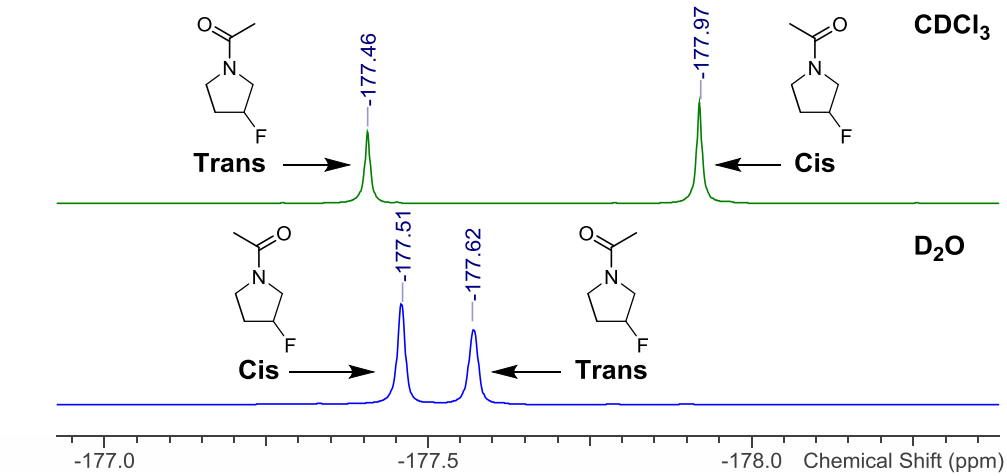

Figure 6.7 - ^{19}F (376 Hz) NMR of *N*-acetyl 3-fluoropyrollidine in $CDCl_3$ and D_2O representing change in chemical shifts in different solvents

6.4.5 Rotamer assignments in octanol

6.4.5.1 Solvent considerations: the use of [1,1-D_2]-octan-1-ol: assignment of *N*-acetyl-3-fluoropyrrolidine in octanol

Given octanol does not contain a deuterium atom, a separate lock solvent is necessary. Given the rotamer ratio is solvent-dependent, the lock solvent (benzene-d_6) was inserted in a flame sealed melting point capillary.

Unfortunately, when dissolving ~5 mg of **1.3** in 0.5 mL of 1-octanol with a capillary insert of benzene-d_6 (Spectrum A, Figure 6.8), the H2 and H5 signals overlap with octanol's α,α-hydrogen signal and its ^{13}C-satellites, preventing rotamer assignment. Hence, it was decided to synthesise [1,1-D_2]-octan-1-ol.

6.4.5.2 Synthesis and evaluation of [1,1-D_2]-octan-1-ol as solvent

A modified Bouveault-Blanc reduction for the synthesis of *α,α*-dideuterio alcohols was developed by J. An *et al*. using Na dispersion and EtOD-d_1.[240] This method was applied to methyl octanoate **6.15** and to afford [1,1-D_2]-octan-1-ol **6.16** in a modest yield of 50% with 97% D_2 incorporation (Scheme 6.4). Upon scale-up (30 g) D_2 incorporation was slightly worse (93%) and the product appeared orange. Despite the product appearing pure by ^{1}H NMR analysis, as this was to be used for NMR studies its high purity was essential and the orange colour is likely from small amounts of undetectable organic or inorganic impurities. To remove the possibility that these impurities could have an effect on the NMR studies, the [1,1-D_2]-octan-1-ol was purified by distillation (8 Mbar, 64–66 °C) to afford a colourless oil in an improved yield of 58%.

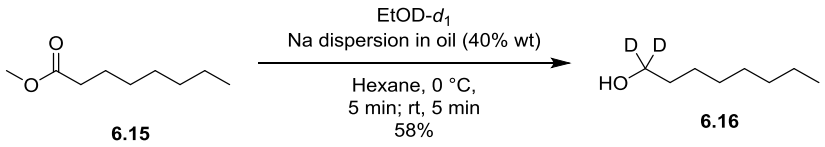

Scheme 6.4 - Synthesis of [1,1-D_2]-octan-1-ol

Hence, [1,1-D_2]-octan-1-ol was used: ~5 mg of **1.3** was dissolved in 0.5 mL of [1,1-D_2]-octan-1-ol and minimal overlapping of these signals is observed (Spectrum B). Following this success, a further ~5 mg of **1.3** was added to the NMR sample B and full characterisation (^{13}C NMR, HSQC and NOESY) was performed to enable the tentative assignment of the rotamers in [1,1-D_2]-octan-1-ol.

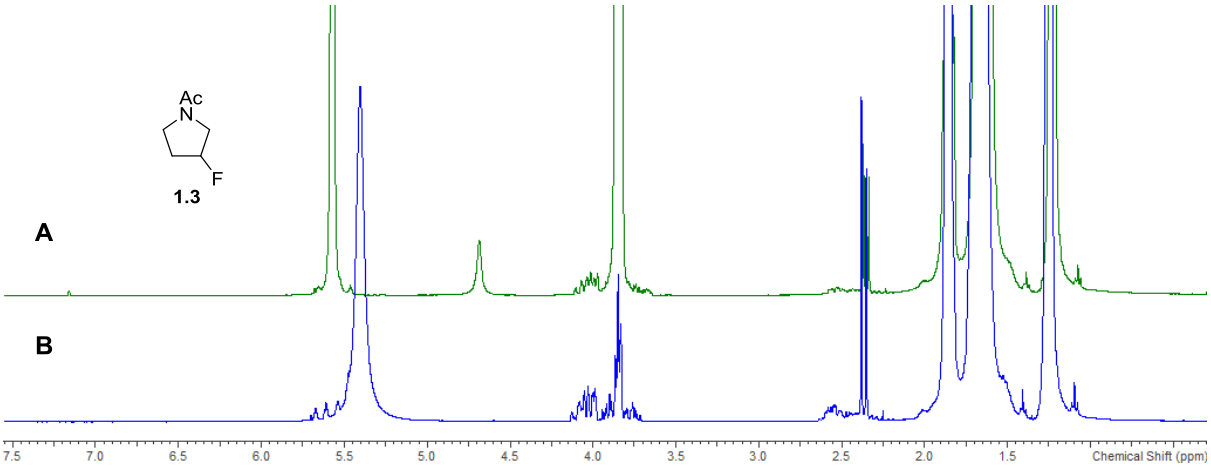

Figure 6.8 - ^{1}H NMR (400 Hz) spectrum depicting the comparison of *N*-acetyl-3-fluoropyrrolidine in octanol (Spectrum A) and [1,1-D_2]-octan-1-ol (Spectrum B).

6.4.5.3 Rotamer assignments in [1,1-D_2]-octan-1-ol

Now, HSQC analysis could be carried out (Figure 6.9). C2 can be identified based on the $^2J_{C2\text{-}F}$ coupling constants (d, J = 23.5 Hz), while C5 can be recognised by its lack of multiplicity. The respective cross peaks indicate the chemical shift values of the corresponding proton resonances.

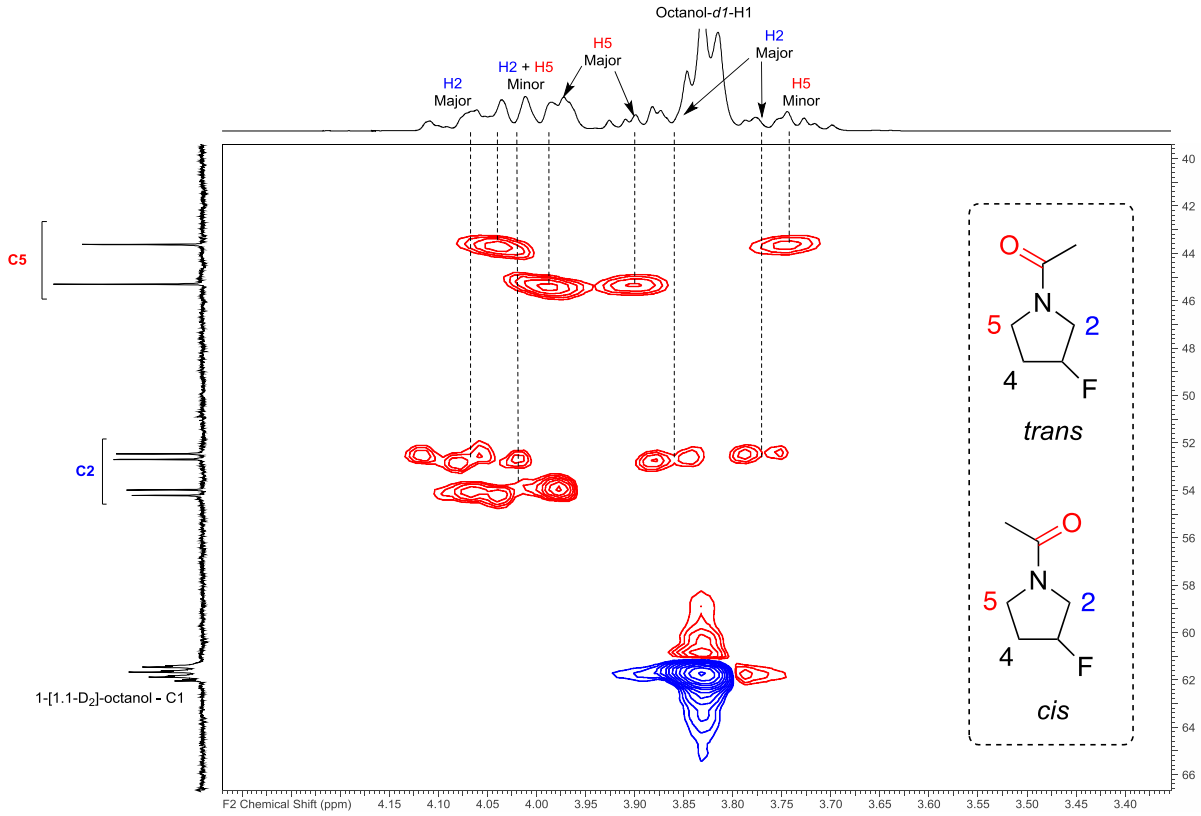

Figure 6.9 - HSQC spectrum of *N*-acetyl-3-fluoropyrrolidine in [1,1-D_2]-octan-1-ol, 24.95 °C, Bruker AVII400 FT-NMR Spectrometer.

In a NOESY spectrum a cross-peak will be observed for protons that are close in space. Therefore in the *trans*-rotamer, the acetate CH_3 will only show a cross-peak with H2 and while in the *cis* rotamer, the acetate CH_3 will only show a cross-peak with H5. In the spectra below H5 has a cross-peak with the major acetate signal, which confirms that the major rotamer has the *cis*-conformation (Figure 6.10). The opposite is expected – and observed – for H2, where H2 only shows a cross-peak with the minor acetate signal.

In this way the rotamer assignment in [1,1-D_2]-octan-1-ol could be achieved for all amides investigated and can be found in Chapter 9 Section 9.4.

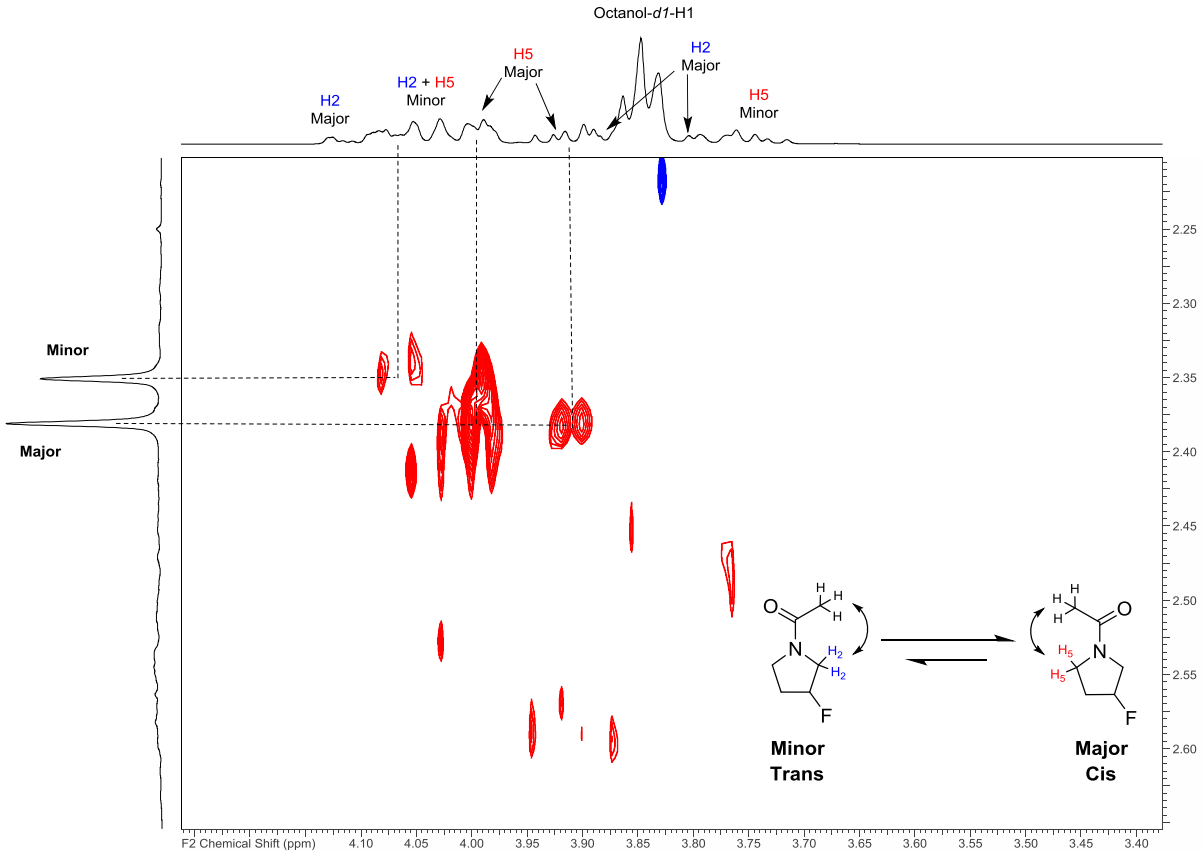

Figure 6.10 - NOESY spectrum of *N*-acetyl-3-fluoropyrrolidine in 1-[1,1-D_2]-octanol, 24.95 °C, Bruker AVII400 FT-NMR Spectrometer.

6.5 Log*P* results and discussion

Lipophilicity determination is performed as per usual, except that the lock solvent ($CDCl_3$ or acetone-d_6) is added to the NMR tube in a capillary. This is necessary in order to not influence the rotamer equilibrium, which is solvent dependent. The use of capillaries occasionally caused the experiments to fail to lock and shim, which required resubmission until successful. This had no effect on the final log*P* result, as shown by the low error values. The results for the amide rotamer specific lipophilicity can be found in Table 6.1, along with the assignment of the major rotamer in both water and octanol. The rotamer ratios within the octanol and water phases can be found in Table 6.2.

Table 6.1 - Amide rotamer-specific lipophilicities. *Defined as logP_{cis} – logP_{trans}

Compound	Overall log*P*	Major isomer in		logP_c	logP_t	Δlog*P**
		oct	wat			
 **1.1**	-0.10	*trans*	*Cis*	-0.20	-0.02	-0.18
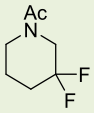 **1.2**	+0.27	*trans*	*cis*	+0.17	+0.38	-0.21
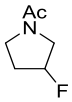 **1.3**	-0.57	*cis*	*cis*	-0.54	-0.60	+0.06
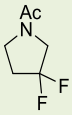 **1.4**	-0.12	*cis*	*cis*	-0.09	-0.15	+0.06

Table 6.2 - Experimental amide rotamer ratio taken from the log*P* determination experiments

Compound	Experimental rotamer ratio (Trans:Cis) in	
	Octanol phase	Water phase
1.1	1.17:1	0.73:1
1.2	1.43:1	0.95:1
1.3	0.72:1	0.84:1
1.4	0.75:1	0.86:1

The overall log*P* values of the amides can be seen in Figure 6.11; the monofluorinated compounds show an overall lower log*P* when compared to the difluorinated compounds. Both fluorinated pyrrolidines also had a lower log*P* compared to the fluorinated piperidines counterparts, as a result of their smaller carbon count which makes them less lipophilic.

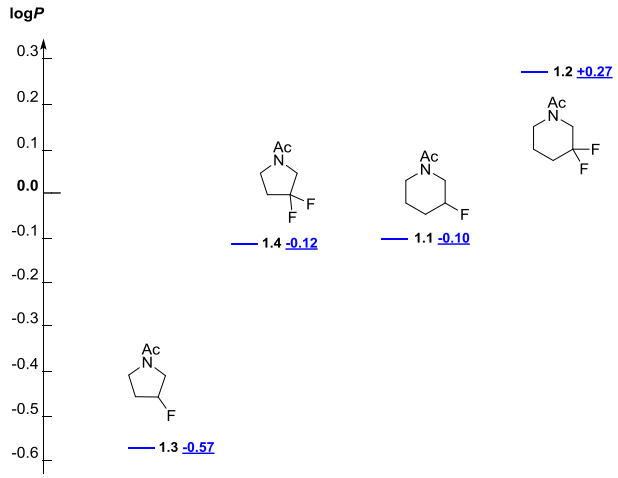

Figure 6.11 - Comparison of overall log*P* values

As the individual *cis* and *trans* rotamers were assigned in both D_2O and [1,1-D_2]-octan-1-ol for the fluorinated *N*-acetyl substrates **1.1–1.4** (Figure 6.12), the effects of amide rotation on lipophilicity can now be observed. While the difference in log*P* value between the two rotamers for the fluoro-pyrrolidines is very small (**1.3** and **1.4**, Δlog*P* +0.06),[xxv] the difference for the fluoro-piperidines is much larger (**1.1** and **1.2**, Δlog*P* -0.18 and Δlog*P* -0.21 respectively).

Preliminary dipole moment calculations[xxvi] performed by Dr Jerome Graton, University of Nantes, France, indicate that the *cis*-rotamer for both **1.1** and **1.2**, exhibits a higher dipole moment than their *trans*-rotamer (

Table **6.3**), which is confirmed by their respective log*P* measurements. The difference in dipole for **1.2** can tentatively be explained by a partial counteraction in dipole moments for the *trans*-rotamer resulting in a more lipophilic conformation, while the inverse is observed for the *cis*-rotamer. However, the difference in log*P* for **1.1** is more difficult to explain as ring inversion can occur resulting in either an axial or equatorial fluorine.

[xxv] Δlog*P* defined as "logP_c – logP_t"
[xxvi] Dipole moments of the energetic minima identified at the SMD/MN15/aug-cc-pVTZ//MN15/cc-pVTZ level of theory in water and *n*-octanol medium.

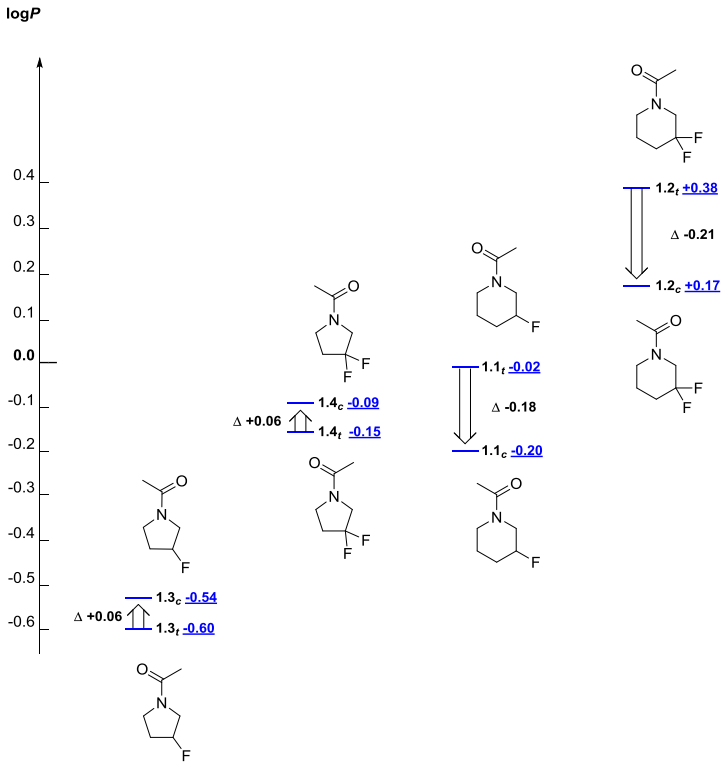

Figure 6.12 - Comparing the log*P* values of the *cis* and *trans* rotamers

Table 6.3 - Calculated dipole moments for 1.1, 1.2 and 1.4[xxvii]

Compound	Conformer	μ D	
		Octanol	Water
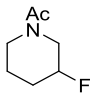 **1.1**	trans	5.37	6.87
	cis	7.20	7.95
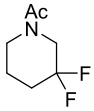 **1.2**	trans	4.63	5.04
	cis	8.00	8.67
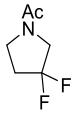 **1.4**	trans	3.83	4.29
	cis	6.20	6.72

Preliminary calculations performed for the *N*-acetyl pyrrolidine **1.4** would suggest that again, the *cis*-rotamer is the more polar of the two conformations, as it exhibits a higher dipole moment.

[xxvii] Dipole moments of the energetic minima identified at the SMD/MN15/aug-cc-pVTZ//MN15/cc-pVTZ level of theory in water and *n*-octanol medium.

Unfortunately, the measured log*P* values did not correlate with these calculations, as the *trans* rotamer had the lower log*P* value. While there is no calculated data for compound **1.3**, it can be observed that it follows the same lipophilicity trend as **1.4**.

Further investigations into the rationale behind these log*P* results is ongoing within our group through the use of calculations and *t*-butyl substituted *N*-acetyl piperidines.

6.6 Conclusion

In this chapter the synthesis of a variety of *N*-acetyl mono- and difluoro pyrrolidines and piperidines was described *via N*-acetylation from their respective amine salts. The individual amide rotamers were first successfully assigned in D_2O allowing for the pairing of the fluorine signals to their respective rotamer. The same assignment was then performed in 1-[1,1-D_2]-octanol, which was synthesised following a modified Bouveault-Blanc reduction for the synthesis of *α,α*-dideuterio alcohols was developed by J. An *et al*. using Na dispersion and EtOD-d_1.[240]

Finally, the Linclau group's ^{19}F NMR based log*P* determination methodology was successfully employed to measure the lipophilicity of simple *cis* and *trans* amide rotamers. This is an important development as amides are often found within drugs and biological conformers. Lipophilicity is known to affect the ADMET properties of drug molecules (See Section 1.2) and thus the ability to connect log*P* values to specfic amide rotamers may allow for a furthering in our understanding of these drug's pharmacological and pharmacokinetic properties. Unfortunately as this procedure utilizes ^{19}F NMR, to be able to apply this methodology and measure the induvial log*P* of compounds which contain rotamers the molecule is required to contain a fluorine atom, which are not always present. Another constraint is that the fluorine signal of each rotamer in both the octanol and water phase must not overlap with each other in order to allow for accurate integration of the ^{19}F signal. This results in this ^{19}F NMR based log*P* determination procedure for induvial rotamers of molecules to be incredibly compound specific and may not be suitable for more complex substrates.

Within the Linclau group, this log*P* determination procedure is also currently succesfully being applied to measure anomer specific log*P* values of sugars. Another equilibrating species that is observable on an NMR timescale are atropisomers, unfortunately these compounds are often highly lipophilic due to the presence of two aromatic rings. Attempts to identify any potential simple atropisomers was unsuccessful as they would not be easily measured by our ^{19}F NMR log*P* determination procedure due to limitations of the technique (only compounds with a logP of ±2.5 are reliably measurable).

While the research presented in this chapter is very fundamental, research within the Linclau group is currently ongoing to rationalise these log*P* results and investigate other slowly equilibrating species which are observable on an NMR timescale.

Chapter 7 Experimental for Lipophilicity

7.1 Detailed logP determination protocols

1) Partitioning

To a 10 mL pear-shaped flash was added octanol (ca. 2 mL), compound A (ca. 1-10 mg), reference compound R (ca. 1-10 mg) and water (ca. 2 mL). The resulting biphasic mixture was stirred at 25 °C (temperature controlled by recirculating chiller) for 2 h and then left to stand at 25 °C overnight to enable complete phase separation. In the case of poor separation, the mixture was transferred to a 4 mL sample vial and centrifuged until the clear separation was observed.

2) Sample Preparation

Using two 1 mL disposable syringes, ca. 0.7 - 0.8 mL was carefully taken from each layer. In the case of the water layer 0.1 mL of air was taken into the syringe before putting the needle into the solution. Whilst moving through the upper octanol layer the air was gently pushed out to avoid contamination from the octanol phase, as small amounts of the octanol phase may enter the needle causing errors for the compounds if not performed. A small amount of the water phase is then discarded (to ensure all traces of octanol are out of the needle), leaving ca. 0.55 mL in the syringe. The needle is then carefully wiped with dry tissue and 0.5 mL is injected into the new NMR tube, followed by addition of 0.1 mL acetonde-d_6 (log*P* alkanols) or a sealed capillary ($CDCl_3$ or acetonde-d_6, log*P* rotamers). The NMR tube was sealed using a blow torch before checking for leaks with tissue and then inverted 20 times to obtain a homogenous solution for NMR measurement.

3) NMR Measurement

^{19}F NMR was run first with standard parameter conditions for chemical shift identification and for the frequency offset point (O1P) which is centered between the two diagnostic F signals. If T1 Values had not been determined, a D1 of 30 sec for the octanol sample, and 60 sec for the water sample are chosen. The spectral width (SW) is set to 100 ppm (however can be widened if required). The number of transients (NS) is left at 64 (but can be increased if higher SNR is required).

4) Data Processing

Data were processed using ACD/Labs NMR software. The obtained FID file was reprocessed using the following conditions: WFunction (LB 2 Exponential). Zero Filling (from 65536 to 262144) and then Fourier transform, followed by mouse phasing and auto baseline correction. The integration

ratio was obtained by manual integration (bias correction can be applied *via* adjusting tilt and slope if integral curve is not parallel to the baseline).

7.2 Detailed experimental data for the log*P* determinations

Unless indicated, the general procedure as detailed above was followed (O1P centered; SW: 100 ppm; D1: oct 30 sec; wat: 60 sec; SR: 295.14 ppm; NMR machine: 400-2 or 400-3; Reference compound: 3,3,3-trifluoroethan-1-ol (log*P*: +0.36).

Compound	Nr	Experiment (octanol/water)	r_o/r_w	log*P*	Average log*P*	error
7.2.1 Propan-1-ol series						
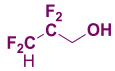	**C6**	jy0416bj2/ jy0416bj3	1.4213/ 0.7770	+0.62	+0.61	+0.613 (±0.007)
		jy0416bj4/ jy0416bj5	1.4735/ 0.8394	+0.60		
		jy0416bj6/ jy0416bj7	1.3372/ 0.7499	+0.61		
C6 – Reference compound: 2,2-difluoroethanol (log*P*: -0.29)						
7.2.2 Butan-2-ol series						
	**E2**	jy0416bj2/ jy0416bj3	1.2800/ 0.9959	+0.20	+0.20	+0.198 (±0.002)
		jy0416bj4/ jy0416bj5	1.1428/ 0.8970	+0.20		
		jy0416bj6/ jy0416bj7	1.2110/ 0.9435	+0.20		
	**E4**	ma1717bj18/ ma1717bj19	0.4520/ 0.3372	+0.49	+0.48	+0.483 (±0.004)
		ma1717bj20/ ma1717bj21	0.5335/ 0.4017	+0.48		
		ma1717bj22/ ma1717bj23	0.4696/ 0.3574	+0.48		
	**E5**	ma1717bj18/ ma1717bj19	0.0318/ 0.0234	+0.49	+0.48	+0.475 (±0.013)
		ma1717bj20/ ma1717bj21	0.0372/ 0.0289	+0.47		
		ma1717bj22/ ma1717bj23	0.0318/ 0.0251	+0.46		

Compound	Nr	Experiment (octanol/water)	r_o/r_w	log*P*	Average log*P*	error
	**E8**	au1916bj11/ au1916bj12	2.7933/ 0.3574	+1.25	+1.25	+1.246 (±0.005)
		au1916bj13/ au1916bj14	3.1764/ 0.4154	+1.24		
		au1916bj15/ au1916bj16	3.8179/ 0.5007	+1.24		

E2 – Reference compound: 4-fluorobutan-1-ol (log*P*: +0.09)

7.2.3 Isobutanol series

	**F1**	au2416bj7/ au2416bj8	0.1647/ 0.2919	+0.11	+0.10	+0.104 (±0.006)
		au2416bj9/ au2416bj10	0.1587/ 0.2902	+0.10		
		au2416bj12/ au2416bj11	0.4046/ 0.7306	+0.10		
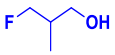	**F2**	au2616bj7/ au2616bj8	0.2390/ 0.2842	+0.28	+0.29	+0.289 (±0.004)
		au2616bj9/ au2616bj10	0.3091/ 0.3649	+0.29		
		au2616bj11/ au2616bj12	0.1631/ 0.1898	+0.29		

7.2.4 Butan-1-ol series

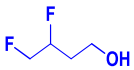	**G1**	dc0917bj5/ dc0917bj6	0.1806/ 0.5405	-0.12	-0.12	-0.123 (±0.005)
		dc0917bj7/ dc0917bj8	0.2152/ 0.6618	-0.13		
		dc0917bj9/ dc0917bj10	0.2742/ 0.8391	-0.13		
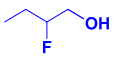	**G4**	ju3017bj9/ ju3017bj10	0.4459/ 0.5539	+0.27	+0.26	+0.264 (±0.008)
		ju3017bj11/ ju3017bj12	0.2798/ 0.3412	+0.27		
		ju3017bj13/ ju3017bj14	0.3550/ 0.4527	+0.25		

Compound	Nr	Experiment (octanol/water)	r_o/r_w	log*P*	Average log*P*	error
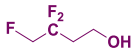	**G5**	ma3117bj5/ ma3117bj6	0.5049/ 0.6277	+0.27	+0.27	+0.270 (±0.004)
		ma3117bj7/ ma3117bj8	0.5548/ 0.6739	+0.28		
		ma3117bj9/ ma3117bj10	0.4339/ 0.5368	+0.27		
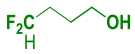	**G6**	au2816bj11/ au2816bj12	0.4880/ 0.5667	+0.30	+0.29	+0.293 (±0.003)
		au2816bj13/ au2816bj14	0.4281/ 0.5034	+0.29		
		au2816bj15/ au2816bj16	0.4442/ 0.5160	+0.29		
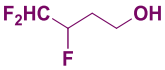	**G7**	dc0917bj11/ dc0917bj12	0.5660/ 0.6508	+0.30	+0.29	+0.289 (±0.007)
		dc0917bj13/ dc0917bj14	0.6910/ 0.8279	+0.28		
		dc0917bj15/ dc0917bj16	0.4877/ 0.5771	+0.29		
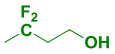	**G8**	au2816bj17/ au2816bj18	0.5334/ 0.5700	+0.33	+0.34	+0.336 (±0.004)
		au2816bj19/ au2816bj20	0.4224/ 0.4487	+0.33		
		au2816bj21/ au2816bj22	0.7951/ 0.8295	+0.34		
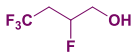	**G9**	ju3017bj15/ ju3017bj16	0.0650/ 0.1384	+0.58	+0.60	+0.597 (±0.011)
		ju3017bj17/ ju3017bj17	0.1062/ 0.2144	+0.60		
		ju3017bj19/ ju3017bj20	0.1322/ 0.2671	+0.60		
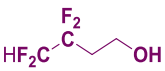	**G10**	nv2516bj18/ nv2516bj19	0.8439/ 0.4211	+0.66	+0.66	+0.660 (±0.003)
		nv2516bj20/ nv2516bj21	0.6944/ 0.3514	+0.66		
		nv2516bj22/ nv2516bj23	0.8755/ 0.4352	+0.66		

Compound	Nr	Experiment (octanol/water)	r_o/r_w	log*P*	Average log*P*	error
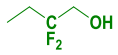	**G11**	ja2917bj1/ ja2917bj2	1.4083/ 0.6939	+0.67	+0.67	+0.668 (±0.001)
		ja2917bj3/ ja2917bj4	1.1056/ 0.5449	+0.67		
		ja2917bj5/ ja2917bj6	1.2902/ 0.6331	+0.67		
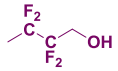	**G12**	se0216bj6/ se0216bj7	1.3084/ 0.3943	+0.88	+0.87	+0.873 (±0.008)
		se0216bj8/ se0216bj9	1.1943/ 0.3759	+0.86		
		se0216bj10/ se0216bj11	1.4106/ 0.4286	+0.88		
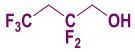	**G14**	ju3017bj15/ ju3017bj16	0.5122/ 0.3726	+1.05	+1.04	+1.044 (±0.006)
		ju3017bj17/ ju3017bj17	0.8506/ 0.6353	+1.04		
		ju3017bj19/ ju3017bj20	1.0486/ 0.7597	+1.05		
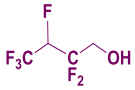	**G16**	ap0116bj5/ ap0116bj6	0.3451/ 0.2252	+1.55	+1.53	+1.534 (±0.009)
		ap0116bj7/ ap0116bj8	0.3113/ 0.2144	+1.52		
		ap0116bj9/ ap0116bj10	0.3241/ 0.2169	+1.53		

G9 and **G14** – Reference compound: 4,4,4-trifluorobutan-1-ol (log*P*: +0.91)

7.2.5 Pentan-2-ol series

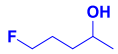	**H1**	ap0116bj5/ ap0116bj6	0.4818/ 0.4181	+0.42	+0.42	+0.424 (±0.002)
		ap0116bj7/ ap0116bj8	0.4723/ 0.4070	+0.42		
		ap0116bj9/ ap0116bj10	0.4976/ 0.4259	+0.43		

Compound	Nr	Experiment (octanol/water)	r_o/r_w	log*P*	Average log*P*	error
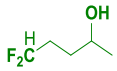	**H4**	au0916bj8/ au0916bj9	1.4365/ 0.7536	+0.64	+0.64	+0.643 (±0.007)
		au0916bj10/ au0916bj11	0.9667/ 0.5104	+0.64		
		au0916bj12/ au0916bj13	0.5937/ 0.3026	+0.65		
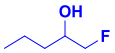	**H6**	se0816bj5/ se0816bj6	0.5100/ 0.2126	+0.74	+0.74	+0.740 (±0.005)
		se1216bj3/ se1216bj4	0.5213/ 0.2202	+0.73		
		se1216bj5/ se1216bj6	0.4437/ 0.1820	+0.75		
	**H7**	se0116bj7/ se0116bj8	1.4984/ 0.3048	+1.05	+1.05	+1.049 (±0.007)
		se0116bj9/ se0116bj10	1.1750/ 0.2459	+1.04		
		se0116bj11/ se0116bj12	1.6069/ 0.3238	+1.06		
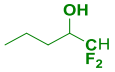	**H8**	se0816bj7/ se0816bj8	0.7028/ 0.1156	+1.14	+1.14	+1.138 (±0.009)
		se1216bj7/ se1216bj8	0.9792/ 0.1684	+1.12		
		se1216bj9/ se1216bj10	0.7531/ 0.1236	+1.15		
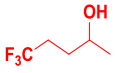	**H9**	ma0317bj6/ ma0317bj7	1.8920/ 0.2542	+1.23	+1.24	+1.236 (±0.003)
		ma0317bj8/ ma0317bj9	2.1248/ 0.2820	+1.24		
		ma0317bj10/ ma0317bj11	1.8764/ 0.2476	+1.24		

7.2.6 Pentan-1-ol series

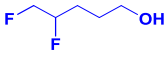	**I1**	se2618bj6/ se2618bj7	0.2379/ 0.4247	+0.11	+0.11	+0.108 (±0.001)
		se2618bj8/ se2618bj9	0.3202/ 0.5700	+0.11		
		se2618bj10/ se2618bj11	0.3091/ 0.5537	+0.11		

Compound	Nr	Experiment (octanol/water)	r_o/r_w	log*P*	Average log*P*	error
	**I4**	se2618bj12/ se2618bj13	0.9075/ 0.6110	+0.53	+0.52	+0.524 (±0.006)
		se2618bj14/ se2618bj15	0.8398/ 0.5835	+0.52		
		se2618bj16/ se2618bj17	0.7705/ 0.5320	+0.52		
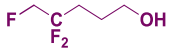	**I5**	se0418bj13/ se0418bj14	0.8046/ 0.4783	+0.59	+0.58	+0.578 (±0.005)
		se0418bj15/ se0418bj16	0.7838/ 0.4782	+0.57		
		se0418bj17/ se0418bj18	0.7407/ 0.4531	+0.57		
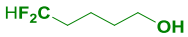	**I6**	nv2516bj12/ nv2516bj13	0.6295/ 0.3138	+0.66	+0.66	+0.661 (±0.002)
		nv2516bj14/ nv2516bj15	0.6413/ 0.3231	+0.66		
		nv2516bj16/ nv2516bj17	0.7242/ 0.3612	+0.66		
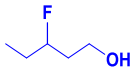	**I8**	dc0117bj11/ dc0117bj12	0.3727/ 0.1501	+0.76	+0.75	+0.752 (±0.007)
		dc0117bj13/ dc0117bj14	0.5548/ 0.2212	+0.76		
		dc0117bj15/ dc0117bj16	0.5106/ 0.2116	+0.74		
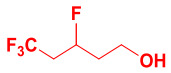	**I9**	se0518bj3/ se0518bj4	1.9447/ 0.6484	+0.84	+0.84	+0.842 (±0.004)
		se0518bj5/ se0518bj6	1.7701/ 0.5811	+0.84		
		se0518bj7/ se0518bj8	1.4755/ 0.4813	+0.85		
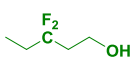	**I11**	dc0117bj5/ dc0117bj6	0.2149/ 0.2076	+0.93	+0.92	+0.919 (±0.005)
		dc0117bj8/ dc0117bj7	0.3772/ 0.3743	+0.91		
		dc0117bj9/ dc0117bj10	0.4899/ 0.4800	+0.92		

Compound	Nr	Experiment (octanol/water)	r_o/r_w	log*P*	Average log*P*	error
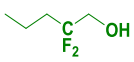	**I14**	ja2917bj7/ ja2917bj8	0.6946/ 0.0893	+1.25	+1.25	+1.249 (±0.001)
		ja2917bj9/ ja2917bj10	0.6751/ 0.0890	+1.24		
		ja2917bj11/ ja2917bj12	0.7650/ 0.0972	+1.25		
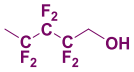	**I15**	ma2217bj7/ ma2217bj8	2.8478/ 0.6565	+1.55	+1.54	+1.544 (±0.011)
		ma2217bj9/ ma2217bj10	2.7277/ 0.6166	+1.56		
		ma2217bj11/ ma2217bj12	2.7190/ 0.6529	+1.53		
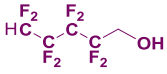	**I17**	se2118bj14/ se2118bj15	0.3488/ 0.2191	+1.89	+1.89	+1.892 (±0.004)
		se2118bj16/ se2118bj17	0.4447/ 0.2824	+1.89		
		se2118bj18/ se2118bj19	0.4135/ 0.2571	+1.90		
	**I18**	dc0516bj12/ ap0717njwbj1	1.1421/ 0.0149	+2.57	+2.57	+2.574 (±0.000)*

I11 and **I15** – Reference compound: 4,4,4-trifluorobutan-1-ol (log*P*: +0.91)
I17 and **I18** – Reference compound: hexafluoro-2-propanol (log*P*: +1.69)
I18 – Water layer, 8192 scans

7.2.7 Hexan-3-ol series

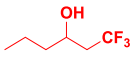	**J1**	ma3117bj11/ ma3117bj12	0.3839/ 0.3532	+1.73	+1.72	+1.722 (±0.003)
		ma3117bj13/ ma3117bj14	0.4597/ 0.4275	+1.72		
		ma3117bj15/ ma3117bj16	0.4406/ 0.4129	+1.72		
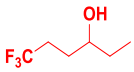	**J2**	ma0317bj12/ ma0317bj13	2.4893/ 0.0981	+1.76	+1.76	+1.757 (±0.006)
		ma0317bj14/ ma0317bj15	2.8464/ 0.1146	+1.76		
		ma0317bj16/ ma0317bj17	2.3683/ 0.0963	+1.75		

J1 – Reference compound: hexafluoro-2-propanol (log*P*: +1.69)

Compound	Nr	Experiment (octanol/water)	r_o/r_w	log*P*	Average log*P*	error

7.2.8 Hexan-2-ol series

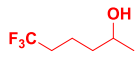	**K1**	ma1717bj7/ ma1717bj8	2.0960/ 0.1449	+1.52	+1.53	+1.533 (±0.010)
		ma1717bj9/ ma1717bj10	2.8816/ 0.1880	+1.55		
		ma1717bj11/ ma1717bj12	2.3456/ 0.1576	+1.53		
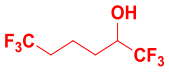	**K2**	se1418bj10/ se1418bj11	1.8039/ 0.6278	+2.15	+2.15	+2.148 (±0.0004)
		se1418bj12/ se1418bj13	1.8010/ 0.6266	+2.15		
		se1418bj14/ se1418bj15	1.9257/ 0.6713	+2.15		
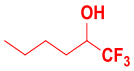	**K3**	se1418bj16/ se1418bj17	1.4700/ 0.3247	+2.35	+2.33	+2.328 (±0.026)
		se1418bj18/ se1418bj19	1.4412/ 0.3606	+2.29		
		se1418bj20/ se1418bj21	1.4882/ 0.3277	+2.34		

K3 – Reference compound: hexafluoro-2-propanol (log*P*: +1.69)

7.2.9 Hexan-1-ol series

	**L2**	se2118bj8/ se2118bj9	1.3277/ 0.6808	+1.98	+1.97	+1.973 (±0.011)
		se2118bj10/ se2118bj11	0.8964/ 0.4571	+1.98		
		se2118bj12/ se2118bj13	0.8832/ 0.4775	+1.96		

L2 – Reference compound: hexafluoro-2-propanol (log*P*: +1.69)

7.2.10 Septan-3-ol series

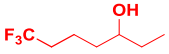	**M3**	nv2017bj5/ nv1717bj2	1.0958/ 0.6723	+1.90	+1.91	+1.909 (±0.006)
		nv2017bj7/ nv2017bj8	0.7765/ 0.4624	+1.92		
		nv2017bj9/ nv2017bj10	0.7117/ 0.4381	+1.90		

Compound	Nr	Experiment (octanol/water)	r_o/r_w	log*P*	Average log*P*	error
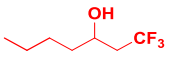	**M4**	nv1717bj3/ nv2717bj1	0.7238/ 0.1737	+2.31	+2.30	+2.298 (±0.009)
		nv1717bj5/ nv2717bj2	1.1295/ 0.2857	+2.29		
		nv1717bj6/ nv2717bj3	0.8396/ 0.2068	+2.30		

M3 and **M4** – Reference compound: hexafluoro-2-propanol (log*P*: +1.69)

7.2.11 Octan-4-ol series

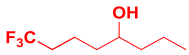	**N1**	oc1617bj13/ oc2017bj3	1.1607/ 0.1369	+2.61	+2.60	+2.604 (±0.013)
		oc1717bj15/ oc2017bj4	113.26/ 0.1422	+2.59		
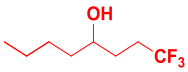	**N2**	jy2117bj7/ jy2417bj1	1.9774/ 0.0125	+2.89	+2.87	+2.873 (±0.015)
		jy2117bj11/ oc2017bj2	1.1818/ 0.0802	+2.86		

N1 and **N2** – Reference compound: hexafluoro-2-propanol (log*P*: +1.69)
N1 – Water layer, 4096 scans, D1 (10 seconds)
N2 – Water layer, 8192 scans, D1 (10 seconds)

7.2.12 4-Penten-1-ol series

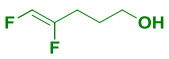	**O1**	se0117bj13/ se0117bj14	0.3151/ 0.1152	+0.80	+0.78	+0.784 (±0.011)
		se0117bj15/ se0117bj16	0.3197/ 0.1198	+0.79		
		se0117bj17/ se0117bj18	0.6071/ 0.2355	+0.77		
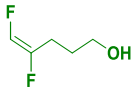	**O4**	se0117bj7/ se0117bj8	0.5272/ 0.1640	+0.87	+0.87	+0.866 (±0.010)
		se0117bj9/ se0117bj10	0.6032/ 0.1831	+0.88		
		se0117bj11/ se0117bj12	0.2768/ 0.0888	+0.85		

Compound	Nr	Experiment (octanol/water)	r_o/r_w	log*P*	Average log*P*	error
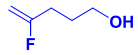	**O5**	ju3017bj3/ ju3017bj4	0.3522/ 0.1029	+0.89	+0.88	+0.879 (±0.011)
		ju3017bj5/ ju3017bj6	0.2604/ 0.0798	+0.87		
		ju3017bj7/ ju3017bj8	0.3215/ 0.0997	+0.87		
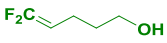	**O6**	my1917bj8/ my1917bj9	2.4147/ 0.3606	+1.19	+1.20	+1.201 (±0.011)
		my1917bj10/ my1917bj11	1.4195/ 0.2009	+1.21		
		my1917bj12/ my1917bj13	0.5909/ 0.0834	+1.21		
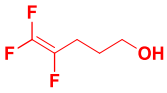	**O7**	ju2917bj7/ jy2917bj25	0.2132/ 0.0282	+1.24	+1.24	+1.243 (±0.005)
		ju2917bj9/ jy2917bj26	0.2134/ 0.0276	+1.25		

O7 – Water layer, 2048 scans

7.2.13 1,4-Butanediol series

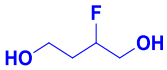	**Q1**	ja1017bj8/ ja1017bj9	0.5367/ 1.0639	-1.05	-1.06	-1.063 (±0.013)
		ja1017bj10/ ja1017bj11	0.4619/ 0.9455	-1.06		
		ja1017bj13/ ja1017bj12	0.4750/ 1.0154	-1.08		
	**Q4**	jy2117bj13/ jy2117bj14	0.2384/ 2.2534	-0.62	-0.62	-0.620 (±0.004)
		jy2117bj15/ jy2117bj16	0.2093/ 2.0197	-0.62		

Q1 – Reference compound: 2-fluoroethan-1-ol (log*P*: -0.75)
Q4 – Only 2 runs due to limited material

7.2.14 1,5-Pentanediol series

	**R1**	ma1618bj3/ ma2118bj3	0.1663/ 1.1001	-0.46	-0.45	-0.451 (±0.006)
		ma1618bj5/ ma1618bj6	0.1021/ 0.6518	-0.45		
		ma1618bj7/ ma1618bj8	0.1294/ 0.8356	-0.45		

Compound	Nr	Experiment (octanol/water)	r_o/r_w	log*P*	Average log*P*	error
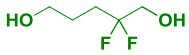	**R2**	ap1118bj3/ ap1118bj4	0.1094/ 0.5438	-0.34	-0.34	-0.338 (±0.008)
		ap1118bj5/ ap1118bj6	0.0673/ 0.3289	-0.33		
		ap1118bj7/ ap1118bj8	0.0785/ 0.4007	-0.35		
	**R3**	se0418bj7/ se0418bj8	1.1074/ 3.9416	-0.19	-0.19	-0.185 (±0.005)
		se0418bj9/ se0418bj10	0.8333/ 2.9110	-0.18		
		se0418bj11/ se0418bj12	0.6847/ 2.3783	-0.18		
	**R4**	dc0516bj14/ dc0516bj15	3.6483/ 2.7859	+0.47	+0.47	+0.4718 (±0.017)
		dc0516bj16/ dc0516bj17	6.7794/ 5.0330	+0.49		
		dc0516bj18/ dc0516bj19	7.1141/ 5.7983	+0.45		

7.2.15 Cyclopropylmethanol series

	**P2**	ma0818bj16/ ma0818bj17	0.3196/ 0.8280	-0.05	-0.05	-0.054 (±0.004)
		ma0818bj18/ ma0818bj19	0.2721/ 0.7142	-0.06		
		ma0818bj20/ ma0818bj21	0.3051/ 0.7854	-0.05		
	**P1**	ma0918bj12/ ma0918bj13	0.1806/ 0.5405	-0.12	-0.12	-0.123 (±0.005)
		ma0918bj14/ ma0918bj15	0.2152/ 0.6618	-0.13		
		ma0918bj16/ ma0918bj17	0.2742/ 0.8391	-0.13		
	**P3**	ma0918bj6/ ma0918bj7	2.8391/ 0.4521	+0.05	+0.04	+0.042 (±0.004)
		ma0918bj8/ ma0918bj9	2.6565/ 0.4317	+0.04		
		ma0918bj10/ ma0918bj11	2.4055/ 0.3919	+0.04		

Compound	Nr	Experiment (octanol/water)	r_o/r_w	log*P*	Average log*P*	error
	**P4**	ma0818bj9/ ma0818bj10	0.6074/ 0.8029	+0.24	+0.24	+0.242 (±0.004)
		ma0818bj11/ ma0818bj12	0.6010/ 0.7946	+0.24		
		ma0818bj13/ ma0818bj14	0.6163/ 0.7988	+0.25		

P2 and **P3** – Reference compound: 2-fluoroethan-1-ol (log*P*: -0.75)

7.2.16 –SCF_3 motif

	**S1**	oc1617bj7/ oc1617bj8	1.3935/ 0.0750	+1.63	+1.63	+1.627 (±0.004)
		oc1617bj9/ oc1617bj10	1.2674/ 0.0693	+1.62		
		oc1617bj11/ oc1617bj12	1.7192/ 0.0919	+1.63		
	**S2**	ju2817bj7/ ju2817bj8	2.5790/ 0.2410	+1.94	+1.94	+1.936 (±0.014)
		ju2817bj9/ ju2817bj10	2.5191/ 0.2286	+1.95		
		ju2817bj11/ ju2817bj12	2.7141/ 0.2669	+1.92		

S2 – Reference compound: 4,4,4-trifluorobutan-1-ol (log*P*: +0.91)

7.2.17 Oxetan-3-ylmethanol series

	**Exp1**	au2416bj13/ au2416bj14	0.2429/ 2.8355	-0.70	-0.73	-0.729 (±0.016)
		au2416bj15/ au2416bj16	0.1157/ 1.4632	-0.74		
		au2416bj17/ au2416bj18	0.2416/ 3.0274	-0.74		

7.3 Methodology Development

Compound	Solvent	Experiment (octanol/water)	r_o/r_w	log*P*	Average log*P*	error
7.3.1 Impurity screening						
	**CH_2Cl_2**	ju0417bj3/ ju0417bj4	1.0095/ 0.2981	+0.89	+0.89	-0.893 (±0.004)
	Et_2O	ju0417bj5/ ju0417bj6	0.8376/ 0.2454	+0.89		
	THF	ju0417bj7/ ju0417bj8	1.0700/ 0.3087	+0.90		
	CH_2Cl_2 + Et_2O + THF	ju0417bj9/ ju0417bj10	1.0300/ 0.3022	+0.89		
	Control	ma3116bj5/ ma3116bj6	188.01/ 0.5397	+0.90		

Standard log*P* measurement procedure seen in Section 7.2 was followed as normal, except for an addition of 1 drop from a Pasteur pipette added of the indicated solvent (~10-15 mg). A control experiment performed at an earlier date was used as a comparison.

Compound	Nr	Experiment (octanol/D_2O)	r_o/r_{D_2O}	log*P* (D_2O)	Average log*P* (D_2O)	Log*P* (H_2O)	ΔLog*P*
7.3.2 Use of D_2O in place of H_2O for log*P* determination procedure							
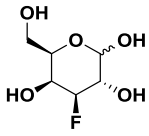	**Exp2**	dc0916bj6/ dc0916bj7	0.1037/ 5.3170	-2.46	-2.46	-2.47	+0.011
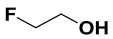	**A1**	nv2916bj9/ nv2916bj10	0.6474/ 4.6303	-0.76	-0.76	-0.75	+0.009
		nv2916bj11/ nv2916bj12	0.5382/ 3.7571	-0.75			
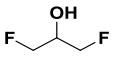	**B1**	nv2916bj13/ nv2916bj14	0.1886/ 1.1064	-0.41	-0.41	-0.42	-0.013
		nv2916bj15/ nv2916bj16	0.2373/ 1.3875	-0.41			
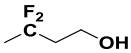	**G8**	dc0916bj12/ dc0916bj13	0.4490/ 0.8005	+0.11	+0.11	+0.11	+0.001
		dc0916bj14/ dc0916bj15	0.4754/ 0.8400	+0.11			
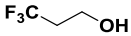	**C5**	nv0816bj7/ nv0816bj8	1.0897/ 0.9506	+0.42	+0.42	+0.41	+0.009
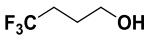	**G13**	nv0816bj9/ nv0816bj10	1.0906/ 0.3105	+0.91	+0.91	+0.91	-0.005
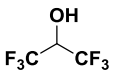	**B4**	dc1516bj11/ dc1516bj12	9.4272/ 0.4549	+1.68	+1.67	+1.69	-0.015
		dc1516bj13/ dc1516bj14	6.4124/ 0.3116	+1.67			
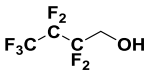	**G17**	dc0916bj8/ dc0916bj9	6.9597/ 0.1964	+1.91	+1.93	+1.98	-0.052
		dc0916bj10/ dc0916bj11	6.5857/ 0.1703	+1.95			

Standard log*P* measurement procedure seen in Section 7.2 was followed as normal, except for the use of D_2O instead of water and experiments were performed in duplicate.

Exp2 – Reference compound: 2-fluoroethan-1-ol (log*P*: -0.75)

A1 – Reference compound: 4-fluorobutan-1-ol (log*P*: +0.09)

C5 and **G13** – Only one iteration ran due to lack of D_2O in the lab at the time

Chapter 8 Experimental for Synthesis

8.1 General methods

All chemical reagents were obtained from commercial sources and used without further purification. Anhydrous solvents were purchased from commercial sources. All glassware was flame-dried under vacuum and cooled under Ar prior to use. Water or air sensitive reactions were performed under inert atmosphere, using dry solvents.

Reactions were monitored by TLC (Merck Kieselgel 60 F_{254}, aluminium sheet) and spots were visualized by UV and/or by exposure to a basic solution of $KMnO_4$, followed by brief heating. Flash column chromatography was performed on silica gel (Merck silica gel 60, particle size 40–63 μm). All reported solvent mixtures are volume measures. $KMnO_4$ reagent – A solution of 3 g $KMnO_4$, 20 g K_2CO_3 and 5 mL NaOH (aq., 5%) in 300 mL H_2O.

Nuclear magnetic resonance spectra were recorded using either a Bruker Ultrashield 400 MHz or 500 MHz spectrometer. The chemical shift (δ) is given in ppm using the residual solvent peak as an internal standard. The coupling constants (*J*) are given in Hertz (Hz). ^{19}F spectra were internally referenced to $CFCl_3$. The proton, fluorine and when appropriate carbon NMR signals were designated as follows: s (singlet), d (doublet), t (triplet), q (quartet), quin (quintet), sxt (sextet), spt (septet), m (multiplet) or a combination of the above.

IR spectra were recorded on a Thermo Scientific™ Nicolet iS5 as a film and absorption peaks are given in cm^{-1} and the intensities were designated as follows: w (weak), m (medium), s (strong), br (broad). Optical rotations were recorded on an OPTICAL ACTIVITY POLAAR 2001 polarimeter at 589 nm. Melting points were recorded on a Reichert melting point apparatus, equipped with a Reichert microscope. Low-resolution electrospray mass spectra were recorded with a Waters Acquity TQD mass tandem quadrupole mass spectrometer. HRMS were measured on a Bruker Daltonics MaXis time of flight (TOF) mass spectrometer or, for volatile compounds, a Thermo MAT900 XP double focusing sector mass spectrometer.

8.2 Synthesis of fluorinated alkanols by mono- and difluorination

Synthesis of 2,2-difluorobutan-1-ol (G11)

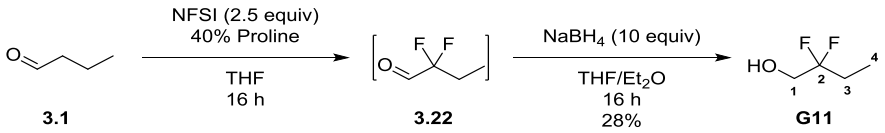

A solution of NFSI (21.88 g, 2.5 equiv) and proline (1.27 g, 0.4 equiv) in THF (45 mL) was stirred for 15 min before the addition of a solution of butyraldehyde (2.50 mL, 1 equiv) in THF (5 mL). After 16 h, Et_2O (50 mL) was added and the reaction mixture was cooled to -78 °C. After 30 min the reaction mixture was filtered through a silica plug, eluting with cold Et_2O (100 mL). The organic mixture was washed with sat. aq. $NaHCO_3$ (3×100 mL), brine and dried over $MgSO_4$ and filtered. $NaBH_4$ (10.48 g, 10 equiv) was then added portion wise to the resultant crude solution. After 16 h, the reaction mixture was cooled to 0 °C and quenched with sat. aq. NH_4Cl (300 mL), stirring vigorously for 30 min. The layers were then separated, and the aqueous phase was extracted with Et_2O (3×75 mL). The combined organic phases were washed with $NaHCO_3$ (3×100 mL), brine and dried over $MgSO_4$. The crude was carefully concentrated at 750 mbar/30 °C, and then concentrated further by short path distillation (to remove THF), before purification by column chromatography (CH_2Cl_2 to 9:1, CH_2Cl_2/Et_2O) to yield **G11** as a yellow oil (0.86 g, 28%).

^{1}H NMR (400 MHz, $CDCl_3$) δ 3.75 (td, *J*=12.8, 6.8 Hz, 2H, H1), 1.96 (tq, *J*=17.1, 7.5 Hz, 2H, H3), 1.84-1.90 (m, 1H, OH), 1.05 (t, *J*=7.5 Hz, 3H, H4) ppm; **^{13}C NMR** (101 MHz, $CDCl_3$) δ 123.5 (t, *J*=241.4 Hz, C2), 63.8 (t, *J*=31.9 Hz, C1), 26.5 (t, *J*=24.6 Hz, C3), 6.1 (t, *J*=5.5 Hz, C4) ppm; **^{19}F NMR** (376 MHz, $CDCl_3$) δ -111.0 (tt, *J*=17.3, 12.1 Hz, 2F) ppm; **^{19}F {^{1}H} NMR** (376 MHz, $CDCl_3$) δ -111.0 (s, 2F) ppm; **IR** (neat) 3337 (br. w), 2987 (w), 2893 (w), 1072 (s), 1050 (m), 903 (s) cm^{-1}; **HRMS** (CI) for $C_4H_7F_2O$ $[M-H]^-$, calculated 109.0470, found 109.0489 (+2.91 ppm error).

Synthesis of 2,2-difluoropentan-1-ol (I14)

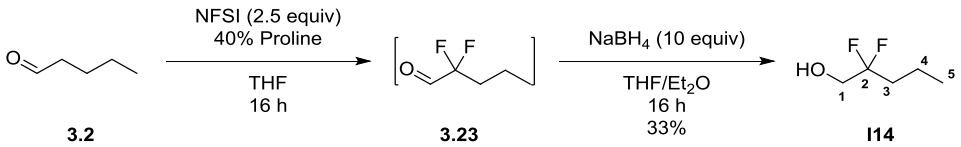

A solution of NFSI (18.31 g, 2.5 equiv) and proline (1.07 g, 0.4 equiv) in THF (45 mL) was stirred for 15 min before the addition of a solution of valeraldehyde (2.47 mL, 1 equiv) in THF (5 mL). After 16 h, Et_2O (50 mL) was added and the reaction mixture was cooled to -78 °C. After 30 min the reaction mixture was filtered through a silica plug, eluting with cold Et_2O (100 mL). The organic mixture was washed with sat. aq. $NaHCO_3$ (3×100 mL), brine and dried over $MgSO_4$ and filtered. $NaBH_4$ (10.48 g,

10 equiv) was then added portion wise to the resultant crude solution. After 16 h, the reaction mixture was cooled to 0 °C and quenched with sat. aq. NH_4Cl (300 mL), stirring vigorously for 30 min. The layers were then separated, and the aqueous phase was extracted with Et_2O (3×75 mL). The combined organic phases were washed with $NaHCO_3$ (3×100 mL), brine and dried over $MgSO_4$. The crude was carefully concentrated at 750 mbar/30 °C, and then concentrated further by short path distillation (to remove THF), before purification by column chromatography (CH_2Cl_2 to 9:1, CH_2Cl_2/Et_2O) to yield **I14** as a yellow oil (0.95 g, 33%).

^{1}H NMR (400 MHz, $CDCl_3$) δ 3.74 (td, *J*=12.8, 6.6 Hz, 2H, H1), 1.99–1.88 (m, 2H, H3), 1.81 (br. t, *J*=6.7 Hz, 1H, OH), 1.54 (tq, *J*=8.2, 7.5 Hz, 2H, H4), 0.99 (t, *J*=7.4 Hz, 3H, H5) ppm; **^{13}C NMR** (101 MHz, $CDCl_3$) δ 123.2 (t, *J*=241.4, C2), 64.1 (t, *J*=31.9 Hz, C1), 35.3 (t, *J*=23.8 Hz, C3), 15.3 (t, *J*=5.1 Hz, C4), 13.9 (C5) ppm; **^{19}F NMR** (376 MHz, $CDCl_3$) δ -108.8 (tt, *J*=17.3, 13.9 Hz, 2F) ppm; **^{19}F {^{1}H} NMR** (376 MHz, $CDCl_3$) δ -108.9 (s, 2F) ppm; **IR** (neat) 3349 (br. w), 2968 (m), 2880 (w), 1164 (m), 1068 (s), 1010 (s) cm^{-1}; **HRMS** (CI) for $C_5H_{11}F_2O$ $[M+H]^+$, calculated 125.0773, found 125.0777 (+0.47 ppm error).

Synthesis of 4-hydroxybutyl benzoate (3.24)

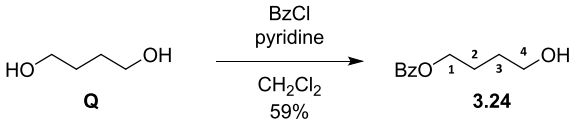

To a solution of butane-1,4-diol **Q** (4.90 mL, 1 equiv) and pyridine (120 mL), benzoyl chloride (6.43 mL, 1 equiv) was added dropwise at 0 °C. The reaction was allowed to warm to room temperature and after 2 h, the reaction mixture was quenched with aq. HCl (2 M, 30 mL) and the aqueous phase was then extracted with $CHCl_3$ (3×30 mL). The combined organic phases were dried over Na_2SO_4 and concentrated *in vacuo*. The crude oil was purified by flash column chromatography (3:7, EtOAc/petroleum ether 40–60 °C) to afford **3.24** as a colourless oil (6.39 g, 59%).

^{1}H NMR (400 MHz, $CDCl_3$) δ 8.08–8.03 (m, 2H, H_{Ar}), 7.60–7.53 (m, 1H, H_{Ar}), 7.48–7.41 (m, 2H, H_{Ar}), 4.38 (t, *J*=6.5 Hz 2H, H1), 3.75 (t, *J*=6.4 Hz, 2H, H4), 1.96–1.84 (m, 2H, H2), 1.81–1.70 (m, 2H, H3), 1.58 (br. s, 1H, OH) ppm; **^{13}C NMR** (101 MHz, $CDCl_3$) δ 166.7 (C=O), 132.9 (C_{Ar}), 130.4 (C_{Ar}), 129.5 (C_{Ar}×2), 128.4 (C_{Ar}×2), 64.7 (C1), 62.5 (C4), 29.3 (C3), 25.2 (C2) ppm.

Data consistent with literature.[241]

Synthesis of 4-oxobutyl benzoate (3.25)

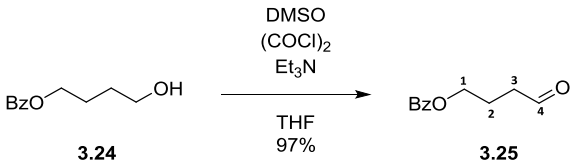

A solution of dimethyl sulphoxide (3.18 mL, 1.1 equiv) in CH_2Cl_2 (50 mL) was added to a stirring solution of oxalyl chloride (3.98 mL, 1.2 equiv) in CH_2Cl_2 (50 mL) at -78 °C. After 15 min, a solution of **3.24** (7.50 g, 1 equiv) in CH_2Cl_2 (50 mL) was added dropwise to the reaction mixture. After 30 min, Et_3N (26.9 mL, 5 equiv) was added at -78 °C. After 30 min, the reaction mixture was allowed to warm to room temperature. The reaction mixture was quenched with sat. aq. NH_4Cl (100 mL) and the organic phase was washed with brine (2×50 mL). The organic phase was dried over $MgSO_4$ and concentrated *in vacuo*. The crude oil was purified by column chromatography (CH_2Cl_2) to afford **3.25** as a colourless oil (7.22 g, 97%).

^{1}H NMR (400 MHz, $CDCl_3$) δ 9.85 (t, *J*=1.2 Hz, 1H, H4), 8.06–8.01 (m, 2H, H_{Ar}), 7.61–7.55 (m, 1H, H_{Ar}), 7.50–7.42 (m, 2H, H_{Ar}), 4.38 (t, *J*=6.3 Hz, 2H, H1), 2.66 (td, *J*=7.2, 1.2 Hz, 2H, H3), 2.14 (br. quin, *J*=6.8 Hz, 2H, H2) ppm.

Data consistent with literature.[241]

Synthesis of 3-fluoro-4-hydroxybutyl benzoate (3.28) and 3,3-difluoro-4-hydroxybutyl benzoate (3.29)

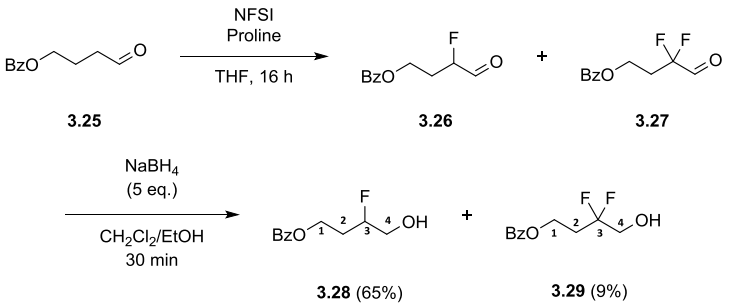

A solution of NFSI (10.73 g, 1 equiv) and proline (4.02 g, 1 equiv) in THF (40 mL) and *i*-PrOH (5 mL) was stirred for 15 min before the addition of a solution of **3.25** (6.72 g, 1 equiv) in THF (5 mL). After 16 h, Et_2O (50 mL) was added and the reaction mixture was cooled to -78 °C. After 30 min, the reaction mixture was filtered through a silica plug, eluting with cold Et_2O (75 mL). The organic mixture was washed with sat. aq. $NaHCO_3$ (3×50 mL), brine and dried over $MgSO_4$ and concentrated. The resultant crude oil was dissolved in EtOH (48 mL) and CH_2Cl_2 (72 mL), before the addition of $NaBH_4$ (6.62 g, 5 equiv) in one portion. After 30 min, the reaction mixture was cooled to 0 °C and quenched with sat. aq. NH_4Cl (300 mL) stirring vigorously for 30 min. The reaction mixture

was then diluted with CH_2Cl_2 (250 mL) and the layers separated. The aqueous phase was extracted with CH_2Cl_2 (3×150 mL) and the combined organic phases washed with $NaHCO_3$ (2×150 mL), brine and dried over $MgSO_4$. The crude was concentrated and purified by column chromatography (3:7, acetone/petroleum ether 40–60 °C) to yield **3.28** as a colourless oil (4.83 g, 65%) and **3.29** as a pale-yellow oil (0.72 g, 9%).

Data for 3.28: ^{1}H NMR (400 MHz, $CDCl_3$) δ 8.09–8.00 (m, 2H, H_{Ar}), 7.65-7.56 (m, 1H, H_{Ar}), 7.53–7.43 (m, 2H, H_{Ar}), 4.85 (ddddd, *J*=49.3, 8.7, 5.9, 3.9, 3.0 Hz, 1H, H3), 4.59–4.39 (m, 2H, H1), 3.94–3.68 (m, 2H, H4), 2.28–2.00 (m, 2H, H2), 1.89 (br. t, *J*=7.1, 1H, OH) ppm; **^{13}C NMR** (101 MHz, $CDCl_3$) δ 166.4 (C=O), 133.1 (C_{Ar}), 130.0 (C_{Ar}), 129.6 (C_{Ar}×2), 128.4 (C_{Ar}×2), 91.5 (d, *J*=168.7 Hz, C3), 64.8 (d, *J*=22.0 Hz, C4), 60.7 (d, *J*=5.1 Hz, C1), 30.4 (d, *J*=20.5 Hz, C2) ppm; **^{19}F NMR** (376 MHz, $CDCl_3$) δ -192.7 (app. dddq, *J*=49.3, 26.0, 23.4, 15.6 Hz, 1F) ppm; **^{19}F {1H} NMR** (376 MHz, $CDCl_3$) δ -192.7 (s, 1F) ppm; **IR** (neat) 3447 (br. w), 2965 (w), 2945 (w), 1716 (s), 1271 (s), 1111 (s), 1070 (s) cm^{-1}; **HRMS** (CI) for $C_{11}H_{14}FO_3$ $[M+H]^+$, calculated 213.0922, found 213.0921 (-0.03 ppm error).

Data for 3.29: ^{1}H NMR (400 MHz, $CDCl_3$) δ 8.11–8.00 (m, 2H, H_{Ar}), 7.61–7.54 (m, 1H, H_{Ar}), 7.49–7.42 (m, 2H, H_{Ar}), 4.56 (t, *J*=6.5 Hz, 2H, H1), 3.86 (td, *J*=12.8, 6.8 Hz, 2H, H4), 2.48 (tt, *J*=16.3, 6.4 Hz, 2H, H2), 1.94 (br. t, *J*=7.0 Hz, 1H, OH) ppm; **^{13}C NMR** (101 MHz, $CDCl_3$) δ 166.4 (C=O), 133.2 (C_{Ar}), 129.8 (C_{Ar}), 129.6 (C_{Ar}×2), 128.5 (C_{Ar}×2), 122.2 (t, *J*=242.1 Hz, C3), 64.3 (t, *J*=31.9 Hz, C4), 58.7 (t, *J*=5.9 Hz, C1), 32.8 (t, *J*=24.6 Hz, C2) ppm; **^{19}F NMR** (376 MHz, $CDCl_3$) δ -107.6 (tt, *J*=16.13, 12.8 Hz, 2F) ppm; **^{19}F {1H} NMR** (376 MHz, $CDCl_3$) δ -107.6 (s, 2F) ppm; **IR** (neat) 3444 (br. w), 2961 (w), 2938 (w), 1714 (s), 1271 (s), 1110 (m), 1069 (m) cm^{-1}; **HRMS** (CI) for $C_{11}H_{13}F_2O_3$ $[M+H]^+$, calculated 231.0827, found 231.0825 (-0.24 ppm error).

Synthesis of 2-fluorobutane-1,4-diol (Q1)

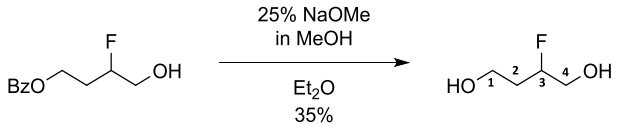

3.28 **Q1**

To a solution of **3.28** (0.5 g, 1 equiv) in Et_2O (25 mL), NaOMe (25% w/w in MeOH, 1.07 mL, 2 equiv) was added dropwise. After 16 h, reaction mixture was neutralised with aq. HCl (2 M) and the aqueous phase was washed with Et_2O (3×20 mL). The combined organic phases were washed with brine and then dried over $MgSO_4$, and carefully concentrated (30 °C, 750 mbar). The crude mixture was purified by column chromatography (95:5, Et_2O/acetone) to afford **Q1** as a pale-yellow oil (89 mg, 35%).

^{1}H NMR (400 MHz, $CDCl_3$) δ 4.87 4.81 (ddddd, *J*=48.9, 7.9, 5.5, 4.6, 3.4 Hz, 1H, H3), 3.94–3.66 (m, 4H, H1 + H4), 2.16–1.77 (m, 2H, H2), ppm; **^{13}C NMR** (101 MHz, $CDCl_3$) δ 92.2 (d, *J*=168.0 Hz, C3),

64.8 (d, *J*=22.7 Hz, C4), 58.5 (d, *J*=5.9 Hz, C1), 33.9 (d, *J*=20.5 Hz, C2) ppm; **^{19}F NMR** (376 MHz, $CDCl_3$) δ -191.5– -192.0 (m, 1F) ppm; **^{19}F {1H} NMR** (376 MHz, $CDCl_3$) δ -191.8 (s, 1F) ppm; **IR** (neat) 3313 (br. m), 2954 (m), 2892 (m), 1394 (w), 1254 (w), 1054 (s) cm^{-1}; **HRMS** (EI) for $C_4H_9FO_2$ [$M^{\cdot+}$], calculated 108.0581, found 108.0580 (-0.16 ppm error).

Synthesis of 2,2-difluorobutane-1,4-diol (Q4)

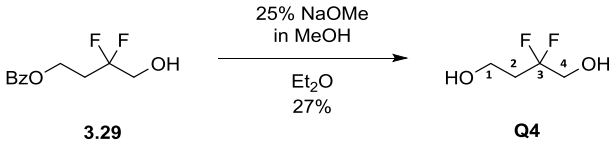

3.29 **Q4**

To a solution of **3.29** (150 mg, 1 equiv) in Et_2O (10 mL), NaOMe (25% w/w in MeOH, 0.30 mL, 2 equiv) was added dropwise. After 16 h, the reaction mixture was neutralised with aq. HCl (2 M) and the aqueous phase was washed with CH_2Cl_2 (3×5 mL). The combined organic phases were washed with brine, dried over $MgSO_4$, and carefully concentrated (30 °C, 750 mbar). The crude mixture was first purified by column chromatography (1:1, acetone/petroleum ether 40–60 °C) and then by HPLC (95:5, Et_2O/pentane) to afford **Q4** as colourless crystals (22 mg, 27%).

^{1}H NMR (400 MHz, $CDCl_3$) δ 3.90 (td, *J*=5.6, 4.8 Hz, 2H, H1), 3.83 (td, *J*=12.6, 7.3 Hz, 2H, H4), 2.69 (t, *J*=7.3 Hz, 1H, $\underline{H}OCH_2CF_2$), 2.25 (tt, *J*=15.8, 5.6 Hz, 2H, H2), 1.98 (t, *J*=4.8 Hz, 1H, $\underline{H}OCH_2CH_2$) ppm; **^{13}C NMR** (126 MHz, $CDCl_3$) δ 122.9 (t, *J*=242.6 Hz, C2), 64.4 (t, *J*=33.1 Hz, C1), 56.0 (t, *J*=6.6 Hz, C4), 36.8 (t, *J*=24.4 Hz, C3) ppm; **^{19}F NMR** (471 MHz, $CDCl_3$) δ -105.1 (tt, *J*=15.6, 12.7 Hz, 2F) ppm; **^{19}F {1H} NMR** (471 MHz, $CDCl_3$) δ -105.1 (s, 2F) ppm; **IR** (thin film, $CDCl_3$) 3352 (br. w), 2962 (w), 1374 (w), 1262 (m), 1066 (s), 904 (s) cm^{-1}; **HRMS** (CI) for $C_4H_9F_2O_2$ [M+H]$^+$, calculated 127.0565, found 127.0566 (+0.05 ppm error); **m.p.** 37-39 °C; **Crystal Structure**

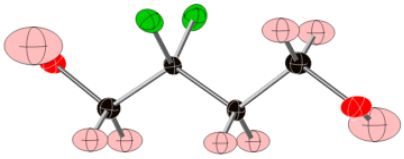

Synthesis of 5-hydroxylpentyl benzoate

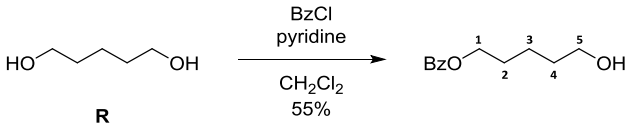

R

To a solution of pentane-1,5-diol (5.00 g, 1 equiv) and pyridine (7.77 mL, 2 equiv) in THF (50 mL), benzoyl chloride (6.13 mL, 1.1 equiv) was added drop wise at 0 °C. The reaction mixture was allowed to warm to room temperature and after 16 h, was quenched with water (75 mL). The aqueous

phase was extracted with CH_2Cl_2 (2×50 mL) and the combined organic phases were washed with aq. HCl (100 mL, 2M), sat. aq. $NaHCO_3$ (100 mL), brine, dried over $MgSO_4$, filtered and concentrated. The crude was purified by column chromatography (3:7, EtOAc/heptane) to yield 5-hydroxylpentyl benzoate as a colourless oil (5.51 g, 55%).

^{1}H NMR (400 MHz, $CDCl_3$) δ 8.11–8.02 (m, 2H, H_{Ar}), 7.59–7.52 (m, 1H, H_{Ar}), 7.47–7.41 (m, 2H, H_{Ar}), 4.34 (t, *J*=6.5 Hz, 2H, H1), 3.68 (t, *J*=6.4 Hz, 2H, H5), 1.87–1.77 (m, 2H, H2), 1.71–1.62 (m, 2H, H4), 1.60–1.51 (m, 2H, H3), 1.48 (s, 1H, OH) ppm; **^{13}C NMR** (101 MHz, $CDCl_3$) δ 166.7 (C=O), 132.8 (C_{Ar}), 130.4 (C_{Ar}), 129.5 (C_{Ar}×2), 128.3 (C_{Ar}×2), 64.9 (C1), 62.7 (C5), 32.3 (C4), 28.5 (C2), 22.3 (C3) ppm.

Data consistent with literature.[242]

Synthesis of 5-oxopentyl benzoate (3.30)

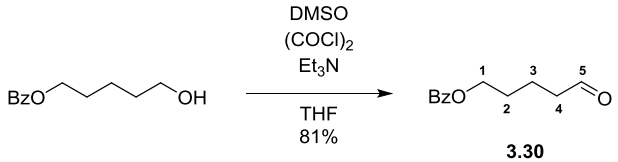

3.30

To a solution of DMSO (1.87 mL, 1.1 equiv) in CH_2Cl_2 (30 mL), a solution of oxalyl chloride (2.52 mL, 1.15 equiv) in CH_2Cl_2 (30 mL) was added at -78 °C. After 15 min, a solution of 5-hydroxylpentyl benzoate (5.00 g, 1 equiv) in CH_2Cl_2 (2.5 mL) was added dropwise to the reaction mixture. After 30 min, Et_3N (16.73 mL, 5 equiv) was added and the reaction mixture was warmed to room temperature and quenched with sat. aq. NH_4Cl (100 mL). The organic phase was dried over $MgSO_4$, filtered and concentrated. The crude was purified by column chromatography (CH_2Cl_2) to afford 3.30 as a pale-yellow oil (4.00 g, 81%).

^{1}H NMR (400 MHz, $CDCl_3$) δ 9.81 (t, *J*=1.5 Hz, 1H, H5), 8.08–8.01 (m, 2H, H_{Ar}), 7.63–7.52 (m, 1H, H_{Ar}), 7.49–7.42 (m, 2H, H_{Ar}), 4.36 (t, *J*=6.1 Hz, 2H, H1), 2.63–2.50 (m, 2H, H4), 1.90–1.75 (m, 4H, H2 + H3) ppm; **^{13}C NMR** (101 MHz, $CDCl_3$) δ 202.2 (C5), 166.9 (Ph<u>C</u>=O), 133.3 (C_{Ar}), 129.9 (C_{Ar}×2), 128.7 (C_{Ar}×2), 64.7 (C1), 43.7 (C4), 28.9 (C2), 19.0 (C3) ppm.

Data consistent with literature.[243]

Synthesis of 4-fluoro-5-hydroxypentyl benzoate (3.33) and 4,4-difluoro-5-hydroxypentyl benzoate (3.34)

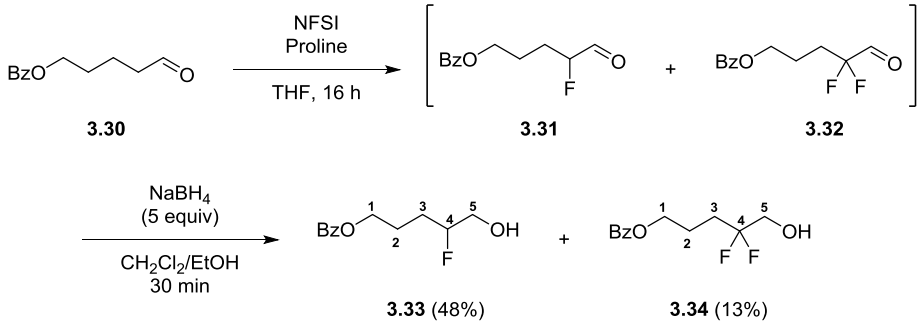

A solution of NFSI (6.12 g, 1 equiv) and proline (2.23 g, 1 equiv) in THF (45 mL) and *i*-PrOH (5 mL) was stirred for 15 min before the addition of a solution of **3.30** (4.00 g, 1 equiv) in THF (5 mL). After 16 h, Et_2O (50 mL) was added and the reaction mixture was cooled to -78 °C. After 30 min the reaction mixture was filtered through a silica plug, eluting with cold Et_2O (50 mL). The organic mixture was washed with sat. aq. $NaHCO_3$ (2×50 mL), brine and dried over $MgSO_4$ and concentrated. The resultant crude oil was dissolved in EtOH (40 mL) and CH_2Cl_2 (60 mL) before the addition of $NaBH_4$ (3.67 g, 5 equiv) in one portion. After 30 min, the reaction mixture was cooled to 0 °C and quenched with sat. aq. NH_4Cl (50 mL) stirring vigorously for 30 min. The reaction mixture was then diluted with CH_2Cl_2 (100 mL) and the layers separated. The aqueous phase was extracted with CH_2Cl_2 (3×50 mL) and the combined organic phases washed with $NaHCO_3$ (50 mL), brine and dried over $MgSO_4$. The crude was concentrated and purified by column chromatography (3:7, EtOAc/heptane) to yield **3.33** as a colourless oil (2.12 g, 48%) and **3.34** as a pale-yellow oil (0.60 g, 13%).

Data for 3.33: ^{1}H NMR (500 MHz, $CDCl_3$) δ 8.07–8.00 (m, 2H, H_{Ar}), 7.59–7.54 (m, 1H, H_{Ar}), 7.47–7.42 (m, 2H, H_{Ar}), 4.74–4.57 (m, 1H, H4), 4.44–4.31 (m, 2H, H1), 3.83–3.66 (m, 2H, H5), 2.10–1.59 (m, 5H, H2 + H3 + OH) ppm; **^{13}C NMR** (126 MHz, $CDCl_3$) δ 166.6 (C=O), 133.0 (C_{Ar}), 130.2 (C_{Ar}), 129.5 (C_{Ar}×2), 128.4 (C_{Ar}×2), 94.1 (d, *J*=169.1 Hz, C4), 64.9 (d, *J*=22.1 Hz, C5), 64.4 (C1), 27.7 (d, *J*=21.1 Hz, C3), 24.5 (d, *J*=4.6 Hz, C2) ppm; **^{19}F NMR** (471 MHz, $CDCl_3$) δ -190.4– -190.9 (m, 2F) ppm; **^{19}F {^{1}H} NMR** (471 MHz, $CDCl_3$) δ -190.6 (s, 2F) ppm; **IR** (neat) 3427 (br. w), 2955 (m), 2876 (w), 1714 (s), 1271 (s), 1110 (m), 709 (s) cm^{-1}; **HRMS** (ESI+) for $C_{12}H_{15}FNaO_3$ $[M+Na]^+$, calculated 249.0897, found 249.0898 (-0.2 ppm error).

Data for 3.34: ^{1}H NMR (500 MHz, $CDCl_3$) δ 8.06–8.02 (m, 2H, H_{Ar}), 7.60–7.53 (m, 1H, H_{Ar}), 7.47–7.42 (m, 2H, H_{Ar}), 4.38 (t, *J*=6.3 Hz, 2H, H1), 3.78 (t, *J*=12.6 Hz, 2H, H5), 2.20–1.98 (m, 4H, H2 + H3), 1.93 (br. s, 1H, OH) ppm; **^{13}C NMR** (126 MHz, $CDCl_3$) δ 166.5 (C=O), 133.0 (C_{Ar}), 130.1 (C_{Ar}), 129.6 (C_{Ar}×2), 128.4 (C_{Ar}×2), 122.9 (t, *J*=241.8 Hz, C4), 64.2 (t, *J*=32.2 Hz, C5), 64.1 (C1), 30.1 (t, *J*=24.4 Hz, C3), 21.4 (t, *J*=4.6 Hz, C2) ppm; **^{19}F NMR** (471 MHz, $CDCl_3$) δ 109.0 (tt, *J*=17.3, 12.6 Hz, 2 F) ppm; **^{19}F {^{1}H} NMR**

(471 MHz, $CDCl_3$) δ -109.0 (s, 2F) ppm; **IR** (neat) 3445 (br. w), 2959 (w), 2941 (w), 1716 (s), 1271 (s), 1111 (m), 709 (s) cm^{-1}; **HRMS** (ESI+) for $C_{12}H_{14}F_2NaO_3$ $[M+Na]^+$, calculated 267.0803, found 267.0802 (+0.4 ppm error).

Synthesis of 3,4-difluorobutyl benzoate (3.35)

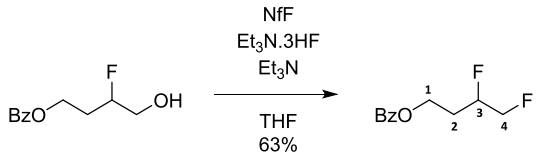

3.28 **3.35**

To a solution of **3.28** (1.00 g, 1 equiv) in THF (20 mL) was added Et_3N (3.94 mL, 6 equiv), $Et_3N{\bullet}3HF$ (1.50 mL, 2 equiv) and nonafluorobutane-1-sulphonic fluoride (1.70 mL, 2 equiv). After 4 h, the reaction was quenched with sat. aq. $NaHCO_3$ until pH 7 and the aqueous layer was extracted with Et_2O (3×30 mL). The combined organic layers were washed with brine, dried over $MgSO_4$ and concentrated. The resulting crude was purified by column chromatography (7:3, CH_2Cl_2/petroleum ether 40–60 °C) to yield **3.35** as a colourless oil (0.64 g, 63%).

^{1}H NMR (400 MHz, $CDCl_3$) δ 8.08–8.03 (m, 2H, H_{Ar}), 7.62–7.56 (m, 1H, H_{Ar}), 7.49–7.43 (m, 2H, H_{Ar}), 5.06–4.80 (m, 1H, H3), 4.75–4.42 (m, 4H, H1 + H4), 2.30–2.02 (m, 2H, H2) ppm; **^{13}C NMR** (101 MHz, $CDCl_3$) δ 166.3 (C=O), 133.2 (C_{Ar}), 129.9 (C_{Ar}), 129.6 (C_{Ar}×2), 128.4 (C_{Ar}×2), 88.8 (dd, *J*=173.9, 19.8 Hz, C3), 83.8 (dd, *J*=174.6, 22.7 Hz, C4), 60.3 (d, *J*=5.1 Hz, C1), 29.7 (dd, *J*=21.3, 6.6 Hz, C2) ppm; **^{19}F NMR** (376 MHz, $CDCl_3$) δ -191.7– -192.2 (m, 1F, F3), -230.9 (tdd, *J*=47.3, 21.7, 13.0 Hz, 1F, F4) ppm; **^{19}F {^{1}H} NMR** (376 MHz, $CDCl_3$) δ -191.9 (d, *J*=13.0 Hz, 1F, F3), -230.9 (br. d, *J*=13.0 Hz, 1F, F4) ppm; **IR** (neat) 2964 (w), 2908 (w), 1715 (s), 1452 (m), 1270 (s), 1109 (s) cm^{-1}; **HRMS** (ESI+) $C_{11}H_{12}F_2NaO_2$ $[M+Na]^+$, calculated 237.0698, found 237.0698 (-0.3 ppm error).

Synthesis of 3,4-difluorobutan-1-ol (G1)

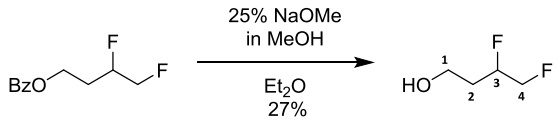

3.35 **G1**

To a solution of **3.35** (0.59 g, 1 equiv) in Et_2O (20 mL), MeONa (25% in MeOH, 1.26 mL, 2 equiv) was added. After 16 h, the reaction was quenched with aq. HCl (2M) until pH 7. The aqueous layer was extracted with CH_2Cl_2 (3×10 mL) and the organic phases were collected washed with brine and dried over $MgSO_4$. The crude was carefully concentrated at 750 mbar/30 °C and was purified by column chromatography (1:9, CH_2Cl_2/Et_2O) to afford **G1** as a pale-yellow oil (81 mg, 27%).

^{1}H NMR (400 MHz, $CDCl_3$) δ 4.93 (dddddd, *J*=48.9, 22.0, 8.9, 5.1, 4.2, 2.3 Hz, 1H, H3), 4.72–4.38 (m, 2H, H4), 3.85 (br. t, *J*=4.9 Hz, 2H, H1), 2.08–1.77 (m, 2H, H2), 1.59 (br. s, 1H, OH) ppm; **^{13}C NMR** (101

MHz, $CDCl_3$) δ 89.6 (dd, *J*=172.4, 19.8 Hz, C3), 84.2 (dd, *J*=173.9, 22.0 Hz, C4), 58.3 (d, *J*=5.1 Hz, C1), 32.8 (dd, *J*=20.5, 6.6 Hz, C2) ppm; **^{19}F NMR** (376 MHz, $CDCl_3$) δ -191.6– -192.2 (m, 1F, F3), -230.1 (tdd, *J*=47.6, 21.9, 13.0 Hz, 1F, F4) ppm; **^{19}F {^{1}H} NMR** (376 MHz, $CDCl_3$) δ -191.9 (d, *J*=13.0 Hz, 1F, F3), -230.1 (d, *J*=13.0 Hz, 1F, F4) ppm; **IR** (neat) 3371 (br. w), 2931 (m), 2853 (w), 1152 (m), 1072 (s), 1045 (s), 688 (s) cm^{-1}; **HRMS** (CI) for $C_4H_9F_2O$ $[M+H]^+$, calculated 111.0616, found 111.0621 (+0.47 ppm error).

Synthesis of 4,5-difluoropentyl benzoate (3.36)

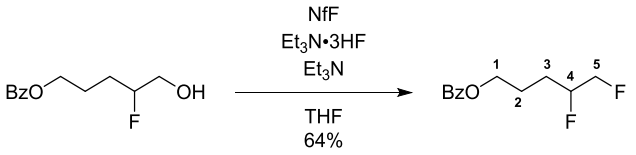

3.33 **3.36**

To a solution of **3.33** (1.00 g, 1 equiv) in THF (15 mL) was added Et_3N (3.70 mL, 6 equiv), Et_3N•3HF (1.44 mL, 2 equiv) and nonafluorobutane-1-sulphonic fluoride (1.59 mL, 2 equiv). After 16 h, the reaction was quenched with sat. aq. $NaHCO_3$ (40 mL) and diluted with Et_2O (50 mL). The organic phase was collected and the aqueous layer was extracted with Et_2O (3×40 mL). The combined organic layers were washed with aq. HCl (2M, 30 mL), brine, dried over $MgSO_4$, filtered and concentrated. The resulting crude was purified by column chromatography (1:19, EtOAc/heptane) to yield **3.36** as a colourless oil (0.65 g, 64%).

^{1}H NMR (400 MHz, $CDCl_3$) δ 8.13–7.97 (m, 2H, H_{Ar}), 7.64–7.56 (m, 1H, H_{Ar}), 7.53–7.41 (m, 2H, H_{Ar}), 4.96–4.67 (m, 1H, H4), 4.67–4.45 (m, 2H, H5), 4.46–4.33 (m, 2H, H1), 2.18–1.66 (m, 4H, H2 + H3) ppm; **^{13}C NMR** (101 MHz, $CDCl_3$) δ 166.5 (C=O), 133.0 (C_{Ar}), 130.1 (C_{Ar}), 129.5 (C_{Ar}×2), 128.4 (C_{Ar}×2), 91.2 (dd, *J*=173.5, 19.4 Hz, C4), 83.9 (dd, *J*=174.6, 23.5 Hz, C5), 64.2 (C1), 26.9 (dd, *J*=21.3, 6.6 Hz, C3), 24.3 (d, *J*=4.4 Hz, C2) ppm; **^{19}F NMR** (376 MHz, $CDCl_3$) δ -190.0– -190.6 (m, 1F, F4), -230.6 (tdd, *J*=46.8, 20.8, 13.9 Hz, 1F, F5) ppm; **^{19}F {^{1}H} NMR** (376 MHz, $CDCl_3$) δ -190.3 (d, *J*=13.9 Hz, 1F, F4), -230.6 (d, *J*=13.9 Hz, 1F, F5) ppm; **IR** (neat) 2959 (w), 2906 (w), 1714 (s), 1270 (s), 1109 (m), 709 (s) cm^{-1}; **HRMS** (ESI+) for $C_{12}H_{14}F_2NaO_2$ $[M+Na]^+$, calculated 251.0854, found 251.0850 (+1.7 ppm error).

4,5-difluoropentan-1-ol (I1)

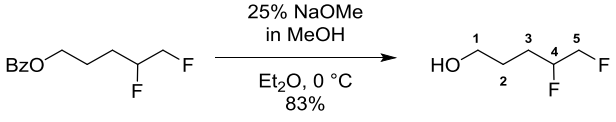

3.36 **I1**

To a solution of **3.36** (0.58 g, 1 equiv) in Et_2O (10 mL), NaOMe (25% in MeOH, 0.86 mL, 1.5 equiv) was added at 0 °C. After 6 h, the reaction was quenched with aq. HCl (2M) until pH 7. The aqueous layer was extracted with CH_2Cl_2 (3×10 mL) and the organic phases were collected washed with brine

and dried over $MgSO_4$. The crude was carefully concentrated at 750 mbar/30 °C and was purified by column chromatography (1:9, Et_2O/CH_2Cl_2) to afford **I1** as a colourless oil (0.26 g, 83%).

^{1}H NMR (400 MHz, $CDCl_3$) δ 4.88–4.64 (m, a doublet with 49.2 Hz can be observed, 1H, H4), 4.65–4.35 (m, 2H, H5), 3.78–3.65 (m, 2H, H1), 1.91–1.64 (m, 4H, H2 + H3), 1.44 (br. s, 1H, OH) ppm; **^{13}C NMR** (101 MHz, $CDCl_3$) δ 91.7 (dd, *J*=172.8, 19.4 Hz, C4), 84.0 (dd, *J*=173.9, 23.5 Hz, C5), 62.2 (C1), 27.9 (d, *J*=4.4 Hz, C2), 26.6 (dd, *J*=23.1, 6.6 Hz, C3) ppm; **^{19}F NMR** (376 MHz, $CDCl_3$) δ -189.3– -189.9 (m, 1F, F4), -230.4 (tdd, *J*=47.5, 20.4, 13.9 Hz, 1F, F5) ppm; **^{19}F {^{1}H} NMR** (376 MHz, $CDCl_3$) δ -189.4 (d, *J*=13.9 Hz, 1F, F4), -230.2 (d, *J*=13.9 Hz, 1F, F5) ppm; **IR** (neat) 3349 (br. w), 2955 (w), 2881 (w), 1456 (w), 1038 (s), 916 (m) cm^{-1}; **HRMS** (CI) for $C_5H_{11}F_2O$ $[M+H]^+$, calculated 125.0773, found 125.0758 (-1.49 ppm error).

Synthesis of 3,4,4-trifluorobutyl benzoate (3.29)

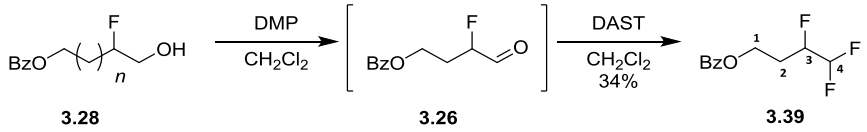

3.28 **3.26** **3.39**

To a solution of **3.28** (1.00 g, 1 equiv) in CH_2Cl_2 (20 mL) was added DMP (2.99 g, 1.5 equiv). After 1 h, the reaction was quenched with sat. aq. $Na_2S_2O_3$ (10 mL) and sat. aq. $NaHCO_3$ (10 mL). The layers were separated and the aqueous was extracted with CH_2Cl_2 (3×20 mL). The combined organic layers were dried over Na_2SO_4, filtered and concentrated. The crude was purified by column chromatography (2:1, Et_2O/petroleum ether 40–60 °C) to afford the intermediate **3.26**, which was immediately dissolved in CH_2Cl_2 before the dropwise addition of DAST (1.10 mL, 2.5 equiv) at 0 °C. The reaction mixture was allowed to warm to room temperature and after 16 h, was quenched with sat. aq. $NaHCO_3$ until pH 7. The aqueous layer was then extracted with CH_2Cl_2 (3×20 mL) and the combined organic layers were washed with brine, dried over $MgSO_4$, filtered and concentrated. The crude was purified by column chromatography (7:3, CH_2Cl_2/petroleum ether 40–60 °C) to afford **3.39** (0.38 g, 34% over 2 steps) as a pale-yellow oil.

^{1}H NMR (400 MHz, $CDCl_3$) δ 8.11–8.01 (m, 2H, H_{Ar}), 7.63–7.56 (m, 1H, H_{Ar}), 7.50–7.43 (m, 2H, H_{Ar}), 5.91 (tdd, *J*=54.7, 5.6, 3.7 Hz, H4), 4.95–4.64 (m, a doublet with 46.9 Hz can be observed, 1H, H3), 4.63–4.42 (m, 2H, H1), 2.36–2.14 (m, 2H, H2) ppm; **^{13}C NMR** (101 MHz, $CDCl_3$) δ 166.2 (C=O), 133.2 (C_{Ar}), 129.8 (C_{Ar}), 129.6 (C_{Ar}×2), 128.5 (C_{Ar}×2), 113.3 (td, *J*=244.5, 31.2 Hz, C4), 87.5 (dt, *J*=177.5, 27.1 Hz, C3), 59.6 (d, *J*=3.7 Hz, C1), 27.7 (dt, *J*=20.5, 2.9 Hz, C2) ppm; **^{19}F NMR** (376 MHz, $CDCl_3$) δ -129.6 (dddd, *J*=297.8, 54.7, 12.1, 8.7 Hz, 1F, F4'), -133.3 (ddt, *J*=297.8, 54.7, 12.1 Hz, 1F, F4''), -203.26– -203.72 (m, 1F, F3) ppm; **^{19}F {^{1}H} NMR** (376 MHz, $CDCl_3$) δ -129.6 (dd, *J*=297.8, 11.7 Hz, 1F, F4'), -133.3 (dd, *J*=297.8, 13.4 Hz, 1F, F4''), -203.5 (t, *J*=13.4 Hz, 1F, F3) ppm; **IR** (neat) 2975 (w), 2910 (w),

1717 (s), 1270 (s), 1069 (s), 1069 (s) cm^{-1}; **HRMS** (EI) for $C_{11}H_{11}F_3O_2$ [$M^{\cdot+}$], calculated 232.0706, found 232.0722 (+1.60 ppm error).

Synthesis of 3,4,4-trifluorobutan-1-ol (G7)

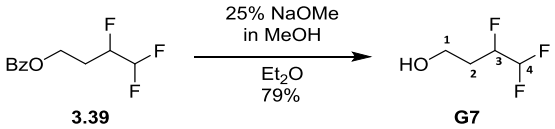

3.39 **G7**

To a solution of **3.39** (0.35 g, 1 equiv) in Et_2O (15 mL), MeONa (25% in MeOH, 0.69 mL, 2 equiv) was added. After 16 h, the reaction was quenched with aq. HCl (2M) until pH 7. The aqueous layer was extracted with CH_2Cl_2 (3×10 mL) and the organic phases were collected washed with brine and dried over $MgSO_4$. The crude was carefully concentrated at 750 mbar/30 °C and was purified by column chromatography (1:9, CH_2Cl_2/Et_2O) to afford **G7** as a pale-yellow oil (0.15 g, 79%).

^{1}H NMR (400 MHz, $CDCl_3$) δ 5.89 (tdd, *J*=55.0, 6.1, 3.7 Hz, 1H, H4), 4.94–4.65 (m, 1H, H3), 3.95–3.80 (m, 2H, H1), 2.09–1.87 (m, 2H, H2), 1.53–1.44 (m, 1H, OH) ppm; **^{13}C NMR** (101 MHz, $CDCl_3$) δ 113.6 (td, *J*=243.9, 30.8 Hz, C4), 87.7 (dt, *J*=175.7, 27.0 Hz, C3), 57.5 (d, *J*=4.1 Hz, C1), 30.8 (dt, *J*=20.5, 2.9 Hz, C2) ppm; **^{19}F NMR** (376 MHz, $CDCl_3$) δ -130.1 (ddt, *J*=296.5, 55.5, 10.4 Hz, 1F, F4'), -133.0 (ddt, *J*=296.5, 55.5, 12.1 Hz, 1F, F4''), -204.2– -204.6 (m, 1F, F3) ppm; **^{19}F {^{1}H} NMR** (376 MHz, $CDCl_3$) δ -130.1 (dd, *J*=296.5, 12.1 Hz, 1F, F4'), -133.0 (dd, *J*=296.5, 13.9 Hz, 1F, F4''), -204.4 (t, *J*=13.0 Hz, 1F, F3) ppm; **IR** (neat) 3362 (br. w), 2971 (w), 2900 (w), 1152 (m), 1068 (s), 1042 (s), 968 (s) cm^{-1}; **HRMS** (CI) for $C_4H_8F_3O$ [M+H]$^+$, calculated 129.0522, found 129.0529 (+0.76 ppm error).

4,5,5-trifluoropentyl benzoate (3.40)

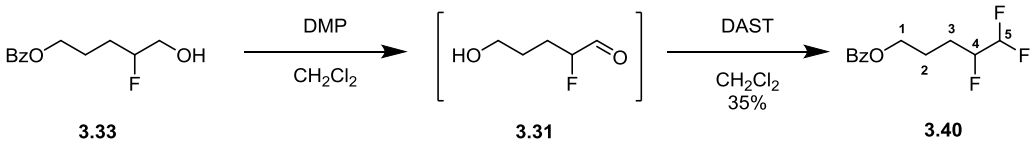

3.33 **3.31** **3.40**

To a solution of **3.33** (0.90 g, 1 equiv) in CH_2Cl_2 (15 mL) was added DMP (2.53 g, 1.5 equiv). After 1 h, the reaction was quenched with sat. aq. $Na_2S_2O_3$ (8 mL) and sat. aq. $NaHCO_3$ (8 mL). The layers were separated and the aqueous was extracted with CH_2Cl_2 (3×15 mL). The combined organic layers were dried over Na_2SO_4, filtered and concentrated. The crude was purified by column chromatography (3:1, Et_2O/petroleum ether 40–60 °C) to afford the intermediate **3.31**, which was immediately dissolved in CH_2Cl_2 before the dropwise addition of DAST (1.62 mL, 3 equiv) at 0 °C. The reaction mixture was allowed to warm to room temperature and after 16 h, was quenched with sat. aq. $NaHCO_3$ until pH 7. The aqueous layer was then extracted with CH_2Cl_2 (3×20 mL) and the combined organic layers were washed with brine, dried over $MgSO_4$, filtered and concentrated. The

crude was purified by column chromatography (1:1, CH_2Cl_2/petroleum ether 40–60 °C) to afford **3.40** (0.34 g, 35% over 2 steps) as a pale-yellow oil.

^{1}H NMR (400 MHz, $CDCl_3$) δ 8.07–8.02 (m, 2H, H_{Ar}), 7.62–7.54 (m, 1H, H_{Ar}), 7.49–7.43 (m, 2H, H_{Ar}), 5.83 (tdd, *J*=54.9, 5.5, 3.8 Hz, 1H, H5), 4.74–4.49 (m, 1H, H4), 4.47–4.32 (m, 2H, H1), 2.17–1.78 (m, 4H, H2 + H3) ppm; **^{13}C NMR** (101 MHz, $CDCl_3$) δ 166.5 (C=O), 133.0 (C_{Ar}), 130.1 (C_{Ar}), 129.5 (C_{Ar} x 2), 128.4 (C_{Ar} x 2), 113.5 (td, *J*=244.3, 31.5 Hz, C5), 89.9 (dt, *J*=176.8, 26.8 Hz, C4), 64.0 (C1), 25.0 (dt, *J*=20.5, 3.3 Hz, C3), 23.8 (d, *J*=2.9 Hz, C2) ppm; **^{19}F NMR** (376 MHz, $CDCl_3$) δ -129.5 (dddd, *J*=297.4, 55.0, 11.7, 9.5 Hz, 1F, F5), -132.9 (ddt, *J*=297.4, 55.0, 12.1 Hz, 1F, F5'), -201.9– -201.4 (m, 1F, F4) ppm; **^{19}F {^{1}H} NMR** (376 MHz, $CDCl_3$) δ -129.5 (dd, *J*=297.4, 12.1 Hz, 1F, F5), -132.9 (dd, *J*=297.6, 13.7 Hz, 1F, F5'), -201.7 (t, *J*=12.6 Hz, 1F, F4) ppm; **IR** (neat) 2967 (w), 1715 (s), 1270 (s), 1069 (s), 709 (s) cm^{-1}; **HRMS** (EI) for $C_{12}H_{13}F_3O_2$ [$M^{\cdot+}$], calculated 246.0862, found 246.0843 (-1.97 ppm error).

4,5,5-trifluoropentan-1-ol (I4)

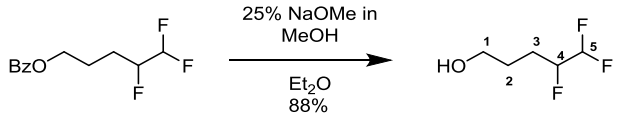

3.40 **I4**

To a solution of **3.40** (0.31 g, 1 equiv) in Et_2O (5 mL), NaOMe (25% in MeOH, 0.58 mL, 2 equiv) was added at 0 °C. After 16 h, the reaction was quenched with aq. HCl (2M) until pH 7. The aqueous layer was extracted with CH_2Cl_2 (3×5 mL) and the organic phases were collected washed with brine and dried over $MgSO_4$. The crude was carefully concentrated at 750 mbar/30 °C and was purified by column chromatography (CH_2Cl_2) to afford **I4** as a colourless oil (0.16 g, 88%).

^{1}H NMR (400 MHz, $CDCl_3$) δ 5.80 (tdd, *J*=54.9, 5.8, 3.8 Hz, 1H, H5), 4.72–4.45 (m, 1H, H4), 3.82–3.64 (m, 2H, 2H, H1), 2.04–1.66 (m, 4H, H2 + H3), 1.43 (br. s, 1H, OH) ppm; **^{13}C NMR** (101 MHz, $CDCl_3$) δ 113.6 (td, *J*=244.3, 31.5 Hz, C5), 90.3 (dt, *J*=176.1, 26.8 Hz, C4), 62.1 (C1), 27.3 (d, *J*=2.9 Hz, C2), 24.7 (dt, *J*=20.5, 2.9 Hz, C3) ppm; **^{19}F NMR** (376 MHz, $CDCl_3$) δ -129.7 (dddd, *J*=296.5, 55.5, 12.1, 9.5 Hz, 1F, F5), -132.8 (dddd, *J*=296.5, 54.6, 13.0, 11.3 Hz, 1F, F5'), -201.3– -201.8 (m, 1F, F4) ppm; **^{19}F {^{1}H} NMR** (376 MHz, $CDCl_3$) δ -129.7 (dd, *J*=296.5, 12.1 Hz, 1F, F5), -132.8 (dd, *J*=296.5, 13.9 Hz, 1F, F5'), -201.5 (t, *J*=12.1 Hz, 1F, F4) ppm; **IR** (neat) 3349 (br. w), 2960 (w), 2884 (w), 1152 (m), 1058 (s), 980 (w) cm^{-1}; **HRMS** (CI) for $C_5H_{10}F_3O$ [M+H]$^+$, calculated 143.0678, found 143.0667 (-1.17 ppm error).

Synthesis of 3,3,4-trifluorobutyl benzoate (3.45)

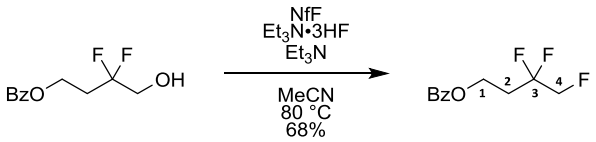

3.29 **3.45**

To a solution of **3.29** (570 mg, 1 equiv) in MeCN (15 mL) was added Et_3N (2.07 mL, 6 equiv), Et_3N•3HF (0.83 mL, 2 equiv) and nonafluorobutane-1-sulphonic fluoride (0.89 mL, 2 equiv). The reaction was heated to 80 °C and after 16 h, was quenched with sat. aq. $NaHCO_3$ (50 mL). The aqueous layer was extracted with CH_2Cl_2 (3×50 mL) and the combined organic layers were washed with brine, dried over $MgSO_4$ and concentrated. The resulting crude was purified by column chromatography (3:7, Et_2O/pentane) to yield **3.45** as a pale-yellow oil (391 mg, 68%).

Data for 3.45: ^{1}H NMR (400 MHz, $CDCl_3$) δ 8.11–7.97 (m, 2H, H_{Ar}), 7.65–7.54 (m, 1H, H_{Ar}), 7.51–7.41 (m, 2H, H_{Ar}), 4.57 (t, *J*=6.2 Hz, 2H, H1), 4.54 (dt, *J*=46.1, 11.7 Hz, 2H, H4), 2.50 (ttd, *J*=16.4, 6.5, 2.4 Hz, 2H, H2) ppm; **^{13}C NMR** (101 MHz, $CDCl_3$) δ 166.2 (C=O), 133.2 (C_{Ar}), 129.7 (C_{Ar}), 129.6 (C_{Ar}×2), 128.5 (C_{Ar}×2), 119.9 (td, *J*=243.0, 23.1 Hz, C3), 81.5 (dt, *J*=179.0, 36.7 Hz, C4), 58.2 (t, *J*=5.9 Hz, C1), 32.6 (t, *J*=24.2 Hz, C2) ppm; **^{19}F NMR** (376 MHz, $CDCl_3$) δ -108.1 (tdt, *J*=16.4, 15.4, 12.1 Hz, 2F, F3), -234.2 (tt, *J*=46.2, 15.4 Hz, 1F, F4) ppm; **^{19}F {^{1}H} NMR** (376 MHz, $CDCl_3$) δ -108.1 (d, *J*=15.6 Hz, 2F, F3), -234.2 (t, *J*=15.6 Hz, 1F, F4) ppm; **IR** (neat) 2971 (w), 2912 (w), 1718 (s), 1268 (s), 1110 (m), 1053 (m) cm^{-1}; **HRMS** (ESI+) for $C_{11}H_{11}F_3NaO_2$ $[M+Na]^+$, calculated 255.0603, found 255.0605 (-0.5 ppm error).

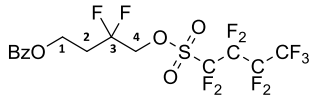

3.46

This compound was observed when the previous rection was performed at rt

Data for 3.46: ^{1}H NMR (400 MHz, $CDCl_3$) δ 8.08–8.01 (m, 2H, H_{Ar}), 7.65–7.56 (m, 1H, H_{Ar}), 7.51–7.44 (m, 2H, H_{Ar}), 4.68 (t, *J*=11.5 Hz, 2H, H4), 4.58 (t, *J*=6.1 Hz, 2H, H1), 2.52 (tt, *J*=16.0, 6.1 Hz, 2H, H2) ppm; **^{13}C NMR** (101 MHz, $CDCl_3$) δ 166.1 (C=O), 133.4 (C_{Ar}), 129.6 (C_{Ar}×2), 129.4 (C_{Ar}), 128.5 (C_{Ar}×2), 118.7 (t, *J*=245.0 Hz, C3), 73.0 (t, *J*=34.8 Hz, C4), 57.8 (t, *J*=5.9 Hz, C1), 33.0 (t, *J*=23.5 Hz, C2) ppm (nonafluorobutyl sulphonate carbons not visible due to multiple fluorine-fluorine couplings); **^{19}F NMR** (376 MHz, $CDCl_3$) δ -80.9 (t, *J*=8.7 Hz, 3F), -105.7 (tt, *J*=15.6, 12.1 Hz, 2F, F3), -110.3 (t, *J*=13.9 Hz, 2F), -121.3– -121.5 (m, 2F), -126.0– -126.2 (m, 2F) ppm; **^{19}F {1H} NMR** (376 MHz, $CDCl_3$) δ -80.9 (br. t, *J*=9.5 Hz, 3F), -105.7 (s, 2F, F3), -110.3 (t, *J*=13.9 Hz, 2F), -121.3– -121.5 (m, 2F), -126.0– -126.1 (m, 2F) ppm; **IR** (neat) 2964 (w), 2918 (w), 1722 (s), 1422 (s), 1238 (s), 1199 (m), 1142 (s) cm^{-1}; **HRMS** (ESI+) for $C_{15}H_{11}F_{11}NaO_5S$ $[M+Na]^+$, calculated 535.0044, found 535.0055 (-2.1 ppm error); **m.p.**: 55-57 °C; **Crystal Structure**

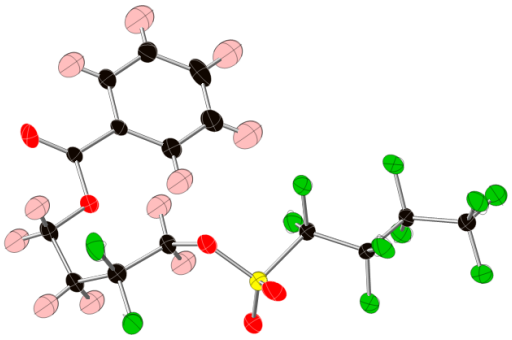

Synthesis of 3,3,4-trifluorobutan-1-ol (G5)

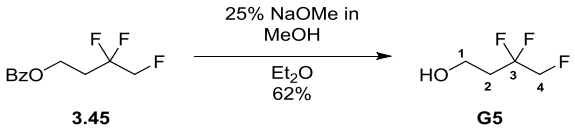

3.45 **G5**

To a solution of **3.45** (500 mg, 1 equiv) in Et_2O (15 mL), NaOMe (25% in MeOH, 0.99 mL, 2 equiv) was added dropwise. After 16 h, the reaction was quenched with aq. HCl (1M) until pH 7. The aqueous layer was extracted with CH_2Cl_2 (3×10 mL) and the organic phases were collected and dried over $MgSO_4$. The crude was carefully concentrated at 750 mbar/30 °C and was then purified by column chromatography (CH_2Cl_2) to afford **G5** as a pale-yellow oil (171 mg, 62%).

^{1}H NMR (400 MHz, $CDCl_3$) δ 4.52 (dt, *J*=46.6, 11.9 Hz, 2H, H4), 3.92 (t, *J*=5.9 Hz, 2H, H1), 2.26 (ttd, *J*=16.7, 6.0, 2.3 Hz, 2H, H2), 1.64 (br. s, 1H, OH) ppm; **^{13}C NMR** (101 MHz, $CDCl_3$) δ 120.7 (td, *J*=242.3, 22.4 Hz, C3), 81.8 (dt, *J*=178.1, 35.7 Hz, C4), 56.4 (t, *J*=5.9 Hz, C1), 36.0 (t, *J*=22.7 Hz, C2) ppm; **^{19}F NMR** (376 MHz, $CDCl_3$) δ -108.1 (tdt, *J*=16.7, 15.4, 11.9 Hz, 2F, F3), -234.6 (ttt, *J*=46.2, 15.4, 2.3 Hz, 1F, F4) ppm; **^{19}F {^{1}H} NMR** (376 MHz, $CDCl_3$) δ -108.1 (d, *J*=13.9 Hz, 2F, F3), -234.6 (t, *J*=13.9 Hz, 1F, F4) ppm; **IR** (neat) 3365 (br. w), 2974 (w), 2905 (w), 1105 (m), 1049 (s), 917 (s) cm^{-1}; **HRMS** (CI) for $C_4H_8F_3O$ $[M+H]^+$, calculated 129.0522, found 129.0528 (+0.60 ppm error).

Synthesis of 4,4,5-trifluoropentyl benzoate (3.47)

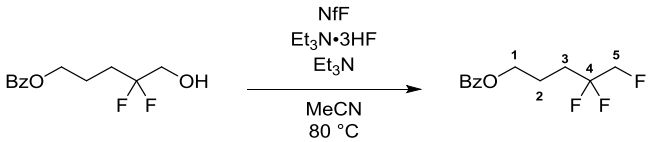

3.34 **3.47**

To a solution of **3.34** (0.54 g, 1 equiv) in MeCN (15 mL) was added Et_3N (1.85 mL, 6 equiv), HF•Et_3N (0.72 mL, 2 equiv) and nonafluorobutane-1-sulphonic fluoride (0.79 mL, 2 equiv). The reaction was heated to 80 °C and after 16 h, was quenched with sat. aq. $NaHCO_3$ (50 mL). The aqueous layer was extracted with Et_2O (3×50 mL) and the combined organic layers were washed with brine, dried over $MgSO_4$, filtered and concentrated. The resulting crude was purified by column chromatography (1:19, EtOAc/heptane) to yield **3.47** as a pale-yellow oil (0.42 g, 78%).

^{1}H NMR (400 MHz, $CDCl_3$) δ 8.10–8.01 (m, 2H, H_{Ar}), 7.62–7.55 (m, 1H, H_{Ar}), 7.49–7.43 (m, 2H, H_{Ar}), 4.48 (dt, *J*=46.5, 11.5 Hz, 2H, H5), 4.40 (t, *J*=6.2 Hz, 2H, H1), 2.26–1.95 (m, 4H, H3 + H4) ppm; **^{13}C NMR** (101 MHz, $CDCl_3$) δ 166.4 (C=O), 133.1 (C_{Ar}), 130.0 (C_{Ar}), 129.6 (C_{Ar}×2), 128.4 (C_{Ar}×2), 120.7 (td, *J*=241.4, 22.0 Hz, C5), 81.6 (dt, *J*=178.3, 37.4 Hz, C4), 63.9 (C2), 29.9 (t, *J*=23.8 Hz, C3) 21.2 (t, *J*=4.8 Hz, C2) ppm; **^{19}F NMR** (376 MHz, $CDCl_3$) δ -109.6 (tdt, *J*=16.5, 15.6, 11.5 Hz, 2F, F4), -234.3 (tt, *J*=46.2, 15.4 Hz, 1F, F5) ppm; **^{19}F {^{1}H} NMR** (376 MHz, $CDCl_3$) δ -109.6 (d, *J*=15.6 Hz, 2F, F4), -234.3 (t, *J*=15.6 Hz, 1F, F5) ppm; **IR** (neat) 2969 (w), 2901 (w), 1716 (s), 1269 (s), 1110 (m), 709 (s) cm^{-1}; **HRMS** (ESI+) for $C_{12}H_{13}F_3NaO_2$ $[M+Na]^+$, calculated 269.0760, found 269.0760 (-0.0 ppm error).

4,4,5-trifluoropentan-1-ol (I5)

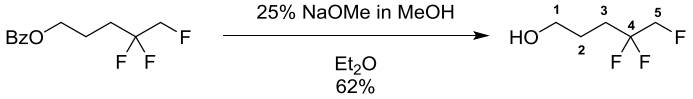

3.47 **I5**

To a solution of **3.47** (0.40 g, 1 equiv) in Et_2O (5 mL), NaOMe (25% in MeOH, 0.55 mL, 1.5 equiv) was added. After 16 h, the reaction was quenched with aq. HCl (2M) until pH 7. The aqueous layer was extracted with CH_2Cl_2 (3×5 mL) and the organic phases were collected washed with brine and dried over $MgSO_4$. The crude was carefully concentrated at 750 mbar/30 °C and was purified by column chromatography (1:9, Et_2O/CH_2Cl_2) to afford **I5** as a pale-yellow oil (202 mg, 87%).

^{1}H NMR (400 MHz, $CDCl_3$) δ 4.46 (dt, *J*=46.5, 11.5 Hz, 2H, H5), 3.74 (t, *J*=6.2 Hz, 2H, H1), 2.18–1.98 (m, 2H, H3), 1.88–1.75 (m, 2H, H2), 1.33 (br. s, 1H, OH) ppm; **^{13}C NMR** (101 MHz, $CDCl_3$) δ 120.9 (td, *J*=242.1, 22.7 Hz, C4), 81.6 (dt, *J*=178.3, 37.0 Hz, C5), 61.9 (C1), 29.6 (t, *J*=23.8 Hz, C3), 24.6 (t, *J*=4.0 Hz, C2) ppm; **^{19}F NMR** (376 MHz, $CDCl_3$) δ -109.5 (tdt, *J*=17.3, 15.2, 11.5 Hz, 2F, F4), -234.5 (ttt, *J*=46.0, 15.2, 2.6 Hz, 1F, F5) ppm; **^{19}F {^{1}H} NMR** (376 MHz, $CDCl_3$) δ -109.5 (d, *J*=15.2 Hz, 2F, F4), -234.5 (t, *J*=15.2 Hz, 1F, F5) ppm; **IR** (neat) 3363 (br. w), 2970 (w), 2885 (w), 1197 (m), 1054 (s), 1017 (s), 930 (s) cm^{-1}; **HRMS** (CI) for $C_5H_{10}F_3O$ $[M+H]^+$, calculated 143.0678, found 143.0674 (-0.46 ppm error).

Synthesis of 2-hydroxybutyl benzoate (3.48)

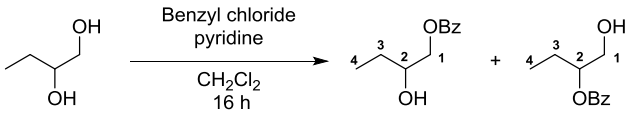

3.9 **3.48** (79%) **3.49** (3%)

To a solution 1,2-butandiol **3.9** (1 g, 1 equiv) and pyridine (1.79 mL, 2 equiv) in CH_2Cl_2 (30 mL), was added benzoyl chloride (1.28 mL, 1 equiv). After 16 h, the reaction mixture was quenched with aq. HCl (2 M, 10 mL). The layers were separated, and the aqueous phase was extracted with CH_2Cl_2 (3×10 mL). The combined organic layers were washed with sat. aq. $NaHCO_3$ (10 mL) and brine before

being dried over $MgSO_4$ and concentrated *in vacuo*. The crude oil was purified by flash column chromatography (3:7, EtOAc/petroleum ether 40–60 °C) to **3.48** as a colourless oil (1.70 g, 79%) and **3.49** as a colourless oil (0.06 g, 3%).

Data for 3.48: ^{1}H NMR (400 MHz, $CDCl_3$) δ 8.12–8.02 (m, 2H, H_{Ar}), 7.64–7.55 (m, 1H, H_{Ar}), 7.54–7.42 (m, 2H, H_{Ar}), 4.42 (dd, *J*=11.5, 3.2 Hz, 1H, H1''), 4.26 (dd, *J*=11.5, 7.0 Hz, 1H, H1'), 4.00–3.88 (m, 1H, H2), 2.13 (br. s, 1H, OH), 1.72–1.53 (m, 2H, H3), 1.05 (t, *J*=7.5 Hz, 3H, H4) ppm; **^{13}C NMR** (101 MHz, $CDCl_3$) δ 166.8 (C=O), 133.2 (C_{Ar}), 129.9 (C_{Ar}), 129.6 (C_{Ar}×2), 128.4 (C_{Ar}×2), 71.5 (C1), 68.9 (C2), 26.5 (C3), 9.8 (C4) ppm.
Proton consistent with literature.[244]

Data for 3.49: ^{1}H NMR (400 MHz, $CDCl_3$) δ 8.12–8.01 (m, 2H, H_{Ar}), 7.66–7.53 (m, 1H, H_{Ar}), 7.50–7.41 (m, 2H, H_{Ar}), 5.12 (qd, *J*=6.4, 3.4 Hz, 1H, H2), 3.90–3.73 (m, 2H, H1), 2.12–1.99 (m, 1H, OH), 1.85–1.73 (m, 2H, H3), 1.02 (t, *J*=7.5 Hz, 3H, H4) ppm; **^{13}C NMR** (101 MHz, $CDCl_3$) δ 167.0 (C=O), 133.1 (C_{Ar}), 130.2 (C_{Ar}), 129.7 (C_{Ar}×2), 128.4 (C_{Ar}×2), 77.6 (C2), 64.7 (C1), 23.8 (C3), 9.8 (C4) ppm.
Data consistent with literature.[245]

Synthesis of 2-fluorobutyl benzoate (3.50)

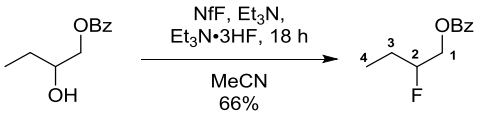

3.48 **3.50**

To a solution of **3.48** (1.60 g, 1 equiv) in MeCN (25 mL) was added Et_3N (6.89 mL, 6 equiv), Et_3N•3HF (2.68 mL, 2 equiv) and nonafluorobutane-1-sulphonic fluoride (2.96 mL, 2 equiv). After 16 h, was quenched with sat. aq. $NaHCO_3$ (70 mL) and diluted with CH_2Cl_2 (100 mL). The organic phase was collected and washed with 2M HCl (70 mL), sat. aq. $NaHCO_3$ (70 mL) and brine. The organic layer was dried over $MgSO_4$ and concentrated. The resulting crude was purified by column chromatography (5:95, acetone/hexane) to yield **3.50** as a colourless oil (1.06 g, 66%).

^{1}H NMR (400 MHz, $CDCl_3$) δ 8.09 (dd, *J*=8.1, 1.0 Hz, 2H, H_{Ar}), 7.63–7.55 (m, 1H, H_{Ar}), 7.46 (t, *J*=7.6 Hz, 2H, H_{Ar}), 4.86–4.65 (m, 1H, H2), 4.57–4.33 (m, 2H, H1), 1.91–1.65 (m, 2H, H3), 1.07 (t, *J*=7.5 Hz, 3H, H4) ppm; **^{13}C NMR** (101 MHz, $CDCl_3$) δ 166.3 (C=O), 133.2 (C_{Ar}), 129.8 (C_{Ar}), 129.7 (C_{Ar}×2), 128.4 (C_{Ar}×2), 92.5 (d, *J*=172.4 Hz, C2), 65.9 (d, *J*=22.7 Hz, C1), 24.7 (d, *J*=21.3 Hz, C3), 9.2 (d, *J*=5.9 Hz, C4) ppm; **^{19}F NMR** (376 MHz, $CDCl_3$) δ -188.1 (dtdd, *J*=48.6, 27.0, 22.5, 17.3 Hz, 1F) ppm; **^{19}F {^{1}H} NMR** (376 MHz, $CDCl_3$) δ -188.1 (s, 1F) ppm; **IR** (neat) 2972 (w), 2883 (w), 1719 (s), 1451 (m), 1267 (s), 707 (s) cm^{-1}; **HRMS** (CI) for $C_{11}H_{14}FO_2$ $[M+H]^+$, calculated 197.0972, found 197.0960 (-1.19 ppm error).

Synthesis of 2-fluorobutanol (G4)

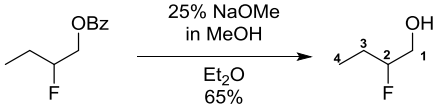

3.50 **G4**

To a solution of **3.50** (0.98 g, 1 equiv) in Et_2O (15 mL), NaOMe (25% in MeOH, 2.28 mL, 2 equiv) was added. After 18 h, the reaction was quenched with aq. HCl (2M) until pH 7. The aqueous layer was extracted with CH_2Cl_2 (3×20 mL) and the organic phases were collected washed with brine and dried over $MgSO_4$. The crude was carefully concentrated at 750 mbar/30 °C and was purified by column chromatography (CH_2Cl_2) to afford **G4** as a pale-yellow oil (297 mg, 65%).

^{1}H NMR (400 MHz, $CDCl_3$) δ 4.51 (ddddd, *J*=49.4, 7.93, 6.2, 5.1, 3.0 Hz, 1H, H2), 3.80–3.58 (m, 2H, H1), 1.94 (br. s, 1H), 1.80–1.49 (m, 2H, H3), 1.00 (t, *J*=7.5 Hz, 3H, H4) ppm; **^{13}C NMR** (101 MHz, $CDCl_3$) δ 95.9 (d, *J*=167.3 Hz, C2), 64.7 (d, *J*=22.0 Hz, C1), 24.1 (d, *J*=20.5 Hz, C3), 9.2 (d, *J*=5.9 Hz, C4) ppm; **^{19}F NMR** (376 MHz, $CDCl_3$) δ -190.7 (dtdd, *J*=49.4, 27.7, 23.4, 16.5 Hz, 1F) ppm; **^{19}F {^{1}H} NMR** (376 MHz, $CDCl_3$) δ -190.7 (s, 1F) ppm; **IR** (neat) 3346 (br. w), 2972 (w), 2884 (w), 1464 (w), 1058 (s), 843 (s) cm^{-1}; **HRMS** (CI) for $C_4H_{10}FO$ $[M+H]^+$, calculated 93.0710, found 93.0705 (-0.56 ppm error).

Synthesis of 3-oxobutan-2-yl benzoate (3.51)

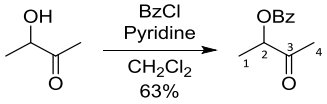

3.10 **3.51**

To a solution of acetoin **3.10** (7.30 g, 1 equiv), pyridine (12.8 mL, 2 equiv) and DMAP (1.07 g, 0.1 equiv) in CH_2Cl_2 (100 mL) was added benzoic anhydride (19.68 g, 1.1 equiv). After 10 h, the reaction mixture was quenched with water (250 mL) under vigorous stirring. The layers were separated and the aqueous phase was extracted with CH_2Cl_2 (3×200 mL). The combined organic extracts were washed with aq. HCl (2 M, 50 mL) followed by sat. aq. $NaHCO_3$ (200 mL), dried over $MgSO_4$ and concentrated. The crude was purified by column chromatography (1:2, Et_2O/petroleum ether 40–60 °C) to afford **3.51** as a colourless oil (10.37 g, 63 %).

^{1}H NMR (400 MHz, $CDCl_3$) δ 8.08–8.12 (m, 2H, H_{Ar}), 7.61 (tt, *J*=7.5, 1.34 Hz, 1H, H_{Ar}), 7.45–7.51 (m, 2H, H_{Ar}), 5.34 (q, *J*=7.1 Hz, 1H, H2), 2.26 (s, 3H, H4), 1.55 (d, *J*=7.1 Hz, 3H, H1) ppm; **^{13}C NMR** (101 MHz, $CDCl_3$) δ 205.8 (C3), 165.9 (C=O), 133.4 (C_{Ar}), 129.8 (C_{Ar}×2), 129.4 (C_{Ar}), 128.5 (C_{Ar}×2), 75.5 (C2), 25.7 (C4), 16.2 (C1) ppm.

Data consistent with literature.[246]

Synthesis of 3,3-difluorobutan-2-yl benzoate (3.52)

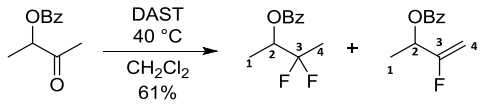

3.51 **3.52** **3.53**

To a solution of **3.51** (2.99 g, 1 equiv) in CH_2Cl_2 (50 mL) was added DAST (4.10 mL, 2 equiv) was added at 0 °C. The reaction mixture was allowed to warm to room temperature and the reaction mixture was refluxed at 40 °C for 48 h. The reaction was cooled to 0 °C and quenched with sat. aq. $NaHCO_3$ till pH 7. The layers were then separated, and the aqueous phase was extracted with CH_2Cl_2 (2×150 mL), dried over $MgSO_4$ and concentrated. The crude was purified by column chromatography (1:9, Et_2O/petroleum ether 40–60 °C) to afford mixture of **3.52** and **3.53** as a pale-yellow oil (2.02 g, 61 % ~9:1 mix).

Data for 3.52: **^{1}H NMR** (400 MHz, $CDCl_3$) δ 8.10–8.05 (m, 2H, H_{Ar}), 7.64–7.57 (m, 1H, H_{Ar}), 7.51–7.44 (m, 2H, H_{Ar}), 5.33 (ddq, *J*=12.9, 7.6, 6.5 Hz, 1H, H2), 1.70 (t, *J*=18.7 Hz, 3H, H4), 1.45 (d, *J*=6.6 Hz, 3H, H1) ppm; **^{13}C NMR** (101 MHz, $CDCl_3$) δ 165.3 (C=O), 133.4 (C_{Ar}), 129.8 (C_{Ar}×2), 129.6 (C_{Ar}), 128.5 (C_{Ar}×2), 121.9 (dd, *J*=243.2, 241.0 Hz, C3), 71.0 (dd, *J*=33.0, 30.1 Hz, C2), 20.0 (t, *J*=26.4 Hz, C4), 13.7 (t, *J*=3.3 Hz, C1) ppm; **^{19}F NMR** (376 MHz, $CDCl_3$) δ -100.4 (dqd, *J*=251.4, 19.1, 6.9 Hz, 1F, F3), -104.8 (dqd, *J*=251.4, 18.5, 12.1 Hz, 1F, F3') ppm; **^{19}F {^{1}H} NMR** (376 MHz, $CDCl_3$) δ -100.4 (d, *J*=251.4 Hz, 1F, F3), -104.8 (d, *J*=251.4 Hz, 1F, F3') ppm; **IR** (neat) 3076 (w), 2999 (w), 2961 (w), 1723 (s), 1268 (s), 1246 (s), 1105, 1071 (s) cm^{-1}; **HRMS** (EI) for $C_{11}H_{12}F_2O_2$ [$M^{\cdot+}$], calculated 214.0800, found 214.0796 (-0.39 ppm error).

Data for 3.53: **^{1}H NMR** (400 MHz, $CDCl_3$) δ 8.10–8.05 (m, 2H, H_{Ar}), 7.64–7.57 (m, 1H, H_{Ar}), 7.51–7.44 (m, 2H, H_{Ar}), 5.66 (dq, *J*=13.4, 6.6 Hz, 1H, H2), 4.77 (dd, *J*=16.6, 3.3 Hz, 1H, $H4_{cis}$), 4.67 (ddd, *J*=48, 3.3, 0.4 Hz, 1H, $H4_{trans}$), 1.55 (d, *J*=6.6, 2H, H1) ppm; **^{13}C NMR** (101 MHz, $CDCl_3$) δ (C_{Ar}, C=O, C-F not observed likely due to overlap with **3.55** and low concentration) 91.7 (d, *J*=17.6 Hz, CH_2), 68.1 (d, *J*=32.3 Hz, CH), 17.5 (d, *J*=2.2 Hz, CH_3) ppm; **^{19}F NMR** (376 MHz, $CDCl_3$) δ -110.5 (ddd, *J*=48.6, 16.5, 13.0 Hz, 1F) ppm; **^{19}F {^{1}H} NMR** (376MHz, $CDCl_3$) δ -110.5 (s, 1F) ppm; **HRMS** (EI) for $C_{11}H_{12}FO_2$ $[M+H]^+$, calculated 195.0816, found 195.0800 (-1.59 ppm error).

Synthesis of 3,3-difluorobutan-2-ol (E4)

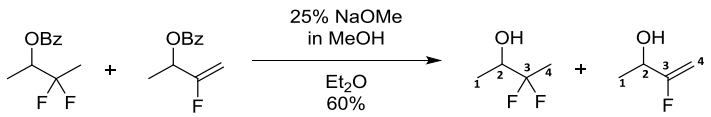

3.52 **3.53** **E4** 85 : **E5** 15

To the mixture of **3.52** and **3.53** (800 mg, 1 equiv) in Et_2O (20 mL) was added NaOMe in MeOH (25 %, 16 mL, 2 equiv). After 24 h, the reaction mixture was neutralised with aq. HCl (2 M) until pH 7. The aqueous phase was extracted with Et_2O (3×30 mL) and the combined organic layers were dried over $MgSO_4$ and carefully concentrated (30 °C, 750 mbar). The crude mixture was purified by column chromatography (9:1 to 1:1, pentane/Et_2O) to yield **E4** and **E5** as a mixture (247 mg, 60%, ~85:15 mix).

Data for E4: **^{1}H NMR** (400 MHz, $CDCl_3$) δ 3.90 (tqd, *J*=9.5, 6.5, 5.6 Hz, 1H, H2), 1.92 (d, *J*=5.6 Hz, 1H, OH), 1.62 (t, *J*=18.9 Hz, 3H, H4), 1.28 (d, *J*=6.5 Hz, 3H, H1) ppm; **^{13}C NMR** (101 MHz, $CDCl_3$) δ 123.9 (dd, *J*=241.4, 239.9 Hz, C3), 69.8 (dd, *J*=30.1, 28.6 Hz, C2), 18.6 (t, *J*=26.8 Hz, C4), 16.3 (dd, *J*=4.4, 2.2 Hz, C1) ppm; **^{19}F NMR** (376 MHz, $CDCl_3$) δ -102.5 (dqd, *J*=248.0, 19.1, 8.7 Hz, 1F, F3), -105.7 (dqd, *J*=248.0, 19.1, 10.0 Hz, 1F, F3') ppm; **^{19}F {^{1}H} NMR** (376 MHz, $CDCl_3$) δ -102.6 (d, *J*=275.7 Hz, 1F, F3), -105.7 (d, *J*=248.0 Hz, 1F, F3') ppm; **IR** (neat) 3390 (br. w), 2988 (w), 2924 (w), 1111 (s), 1081 (s), 918 (m) cm^{-1}; **HRMS** (CI) for $C_4H_7OF_2$ $[M-H]^-$, calculated 109.0470, found 109.0473 (+2.75 ppm error).

Data for E5: **^{1}H NMR** (400 MHz, $CDCl_3$) δ 4.64 (d, *J*=17.4, 3.6 Hz, 1H, $H4_{cis}$), 4.50 (ddd, *J*=49.0, 3.2, 0.6 Hz, 1H, $H4_{trans}$), 4.33 (dqd, *J*=17.2, 6.0, 0.6 Hz, 1H, H2), 1.84 (d, *J*=1.84 Hz, 1H, O*H*), 1.39 (dd, *J*=6.6, 0.5 Hz, 3H, H1) ppm; **^{13}C NMR** (101 MHz, $CDCl_3$) δ 167.7 (d, *J*=259.7, C3), 89.2 (d, *J*=18.4 Hz, C4), 66.1 (d, *J*=32.3 Hz, C2), 20.3 (d, *J*=1.5 Hz, C1) ppm; **^{19}F NMR** (376 MHz, $CDCl_3$) δ -110.8 (ddd, *J*=49.0, 17.8, 9.5 Hz, 1F) ppm; **^{19}F {^{1}H} NMR** (376 MHz, $CDCl_3$) δ -110.8 (s, 1F) ppm; **HRMS** (CI) for C_4H_8FO $[M+H]^+$, calculated 91.0554, found 91.0560 (+0.6 ppm error).

Synthesis of 3-oxobutyl benzoate (3.54)

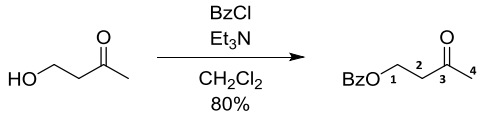

3.11 **3.54**

To a solution of benzoyl chloride (8.6 mL, 1.3 equiv), CH_2Cl_2 (30 mL) and pyridine (9.2 mL, 2 equiv) was added 4-hydroxy butan-2-one (4.9 mL, 1 equiv) dropwise at 0 °C. The reaction mixture was allowed to warm to rt and after 19 h, additional benzoyl chloride (3 mL, 0.45 equiv) was added. After 21 h, the reaction mixture was quenched with aq. HCl (2 M, 50 mL) and the organic phase was

washed with sat. aq. $NaHCO_3$ (2×50 mL) and water (50 mL). The organic phase was dried over $MgSO_4$ and concentrated to afford **3.54** as a colourless oil (6.72 g, 80%)

^{1}H NMR (400 MHz, $CDCl_3$) δ 7.99 (dd, *J*=8.2, 1.0 Hz, 2H, H_{Ar}), 7.61–7.51 (m, 1H, H_{Ar}), 7.47–7.36 (m, 2H, H_{Ar}), 4.58 (t, *J*=6.3, 2H, H1), 2.90 (t, *J*=6.3 Hz, 2H, H2), 2.22 (s, 3H, H4) ppm; **^{13}C NMR** (101 MHz, $CDCl_3$) δ 205.5 (C3), 166.3 (C=O), 133.0 (C_{Ar}), 129.9 (C_{Ar}), 129.5 (C_{Ar}×2), 128.3 (C_{Ar}×2), 59.8 (C1), 42.3 (C2), 30.2 (C4) ppm.

Data consistent with literature.[247]

Synthesis of 3,3-difluorobutyl benzoate (3.56)

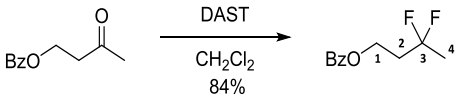

3.54 **3.56**

To a solution of **3.54** (9.50 g, 1 equiv) in CH_2Cl_2 (40 mL), DAST (13.06 mL, 2 equiv) was added dropwise at 0 °C. The reaction mixture was heated to 40 °C and after 41 h was cooled to 0 °C, diluted with CH_2Cl_2 (50 mL) and neutralised with sat. aq. $NaHCO_3$ until pH 7. The aqueous phase was washed with CH_2Cl_2 (3×100 mL) and the combined organic phases were dried over $MgSO_4$ and concentrated *in vacuo*. The crude oil was purified by column chromatography (1:9, Et_2O/pentane) to afford **3.56** as a pale-yellow oil (8.90 g, 84%).

^{1}H NMR (400 MHz, $CDCl_3$) δ 8.05 (dd, *J*=8.1, 1.0 Hz, 2H, H_{Ar}), 7.66–7.53 (m, 1H, H_{Ar}), 7.50–7.42 (m, 2H, H_{Ar}), 4.53 (t, *J*=6.5 Hz, 2H, H1), 2.38 (tt, *J*=15.4, 6.6 Hz, 2H, H2), 1.71 (t, *J*=18.6 Hz, 3H, H4) ppm; **^{13}C NMR** (101 MHz, $CDCl_3$) δ 166.3 (C=O), 133.1 (C_{Ar}), 129.9 (C_{Ar}), 129.6 (C_{Ar}×2), 128.4 (C_{Ar}×2), 123.0 (t, *J*=237.7 Hz, C3), 59.2 (t, *J*=6.2 Hz, C1), 37.1 (t, *J*=26.0 Hz, C2), 23.8 (t, *J*=27.5 Hz, C4) ppm; **^{19}F NMR** ($CDCl_3$, 376 MHz) δ -89.7– -90.0 (m, 2F) ppm; **^{19}F {^{1}H} NMR** (376 MHz, $CDCl_3$) δ -89.8 (s, 2F) ppm; **IR** (neat) 2980 (w), 1710 (s), 1270 (s), 700 (s) cm^{-1}; **HRMS** (ESI+) for $C_{11}H_{12}F_2NaO_2$ $[M+Na]^+$, calculated 237.0698, found 237.0698 (-0.1 ppm error).

Synthesis of 3,3-difluorobutan-1-ol (G8)

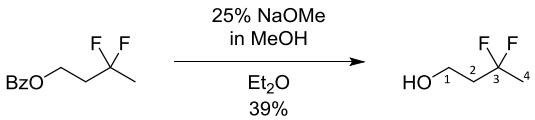

3.56 **G8**

To a solution of **3.56** (8.90 g, 1 equiv) in Et_2O (90 mL), NaOMe (25% w/w in MeOH, 21.52 mL, 2 equiv) was added dropwise. After 22 h, the reaction mixture was neutralised with aq. HCl (2 M) and the aqueous phase was washed with Et_2O (3x50 mL). The combined organic phases were washed with water (2×100 mL), dried over $MgSO_4$, and carefully concentrated (30 °C, 750 mbar). The crude

mixture was purified by column chromatography (1:4, Et_2O/CH_2Cl_2) to afford **G8** as a pale-yellow oil (1.78 g, 39%).

^{1}H NMR (400 MHz, $CDCl_3$) δ 3.87 (q, *J*=6.0 Hz, 2H, H1), 2.16 (tt, *J*=16.3, 6.2 Hz, 2H, H2), 1.65 (br. s, 1 H, O*H*), 1.67 (t, *J*=18.8 Hz, 3H, H4) ppm; **^{13}C NMR** (101 MHz, $CDCl_3$) δ 124.1 (t, *J*=236.2 Hz, C3) 57.3 (t, *J*=5.5 Hz, C1) 40.4 (t, *J*=24.6 Hz, C2) 23.9 (t, *J*=26.4 Hz, C4) ppm; **^{19}F NMR** (376 MHz, $CDCl_3$) δ -89.8 (qt, *J*=18.8, 16.3 Hz, 2F) ppm; **^{19}F {^{1}H} NMR** (376 MHz, $CDCl_3$) δ -89.8 (s, 2F) ppm; **IR** (neat) 3387 (br. w), 2972 (w), 2947 (w), 2899 (w), 1124 (s) cm^{-1}; **HRMS** (EI) for $C_4H_8F_2O$ [$M^{\cdot+}$], calculated 110.0538, found 110.0531 (-0.65 ppm error).

Synthesis of 4-oxopentyl benzoate (3.55)

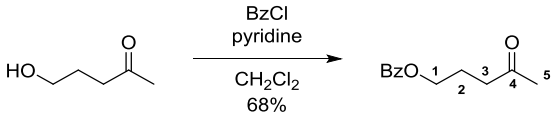

3.12 **3.55**

To a solution 5-hydroxypentan-2-one **3.12** (1.00 g, 1 equiv) and pyridine (1.58 mL, 2 equiv) in CH_2Cl_2 (30 mL), benzoyl chloride (1.14 mL, 1 equiv) was added dropwise at 0 °C. The reaction was allowed to warm to room temperature and after 40 h, the reaction mixture was quenched with water (15 mL). The organic layer was collected and washed with aq. HCl (2M, 20 mL), sat. aq. $NaHCO_3$ (20 mL) and brine before being dried over $MgSO_4$, filtered and concentrated *in vacuo*. The crude oil was purified by flash column chromatography (15:85, EtOAc/heptane) to afford **3.55** as a colourless oil (1.37 g, 68%).

^{1}H NMR (400 MHz, $CDCl_3$) δ 8.07–7.99 (m, 2H, H_{Ar}), 7.62–7.54 (m, 1H, H_{Ar}), 7.52–7.43 (m, 2H, H_{Ar}), 4.35 (t, *J*=6.4 Hz, 2H, H1), 2.62 (t, *J*=7.2 Hz, 2H, H3), 2.19 (s, 3H, H5), 2.07 (quin, *J*=6.8 Hz, 2H, H2) ppm; **^{13}C NMR** (101 MHz, $CDCl_3$) δ 207.6 (C4) 166.5 (C=O), 133.0 (C_{Ar}), 130.2 (C_{Ar}), 129.5 (C_{Ar}×2), 128.4 (C_{Ar}×2), 64.1 (C1), 40.0 (C3), 30.0 (C5), 22.9 (C2) ppm.

Data consistent with literature.[94]

Synthesis of 4,4-difluoropentyl benzoate (3.57)

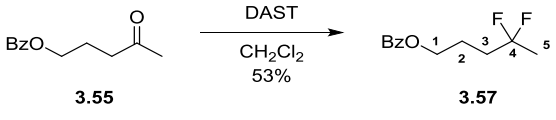

3.55 **3.57**

To a solution of the **3.55** (1.36 g, 1 equiv) in CH_2Cl_2 (20 mL), DAST (2.17 mL, 2.5 equiv) was added dropwise at 0 °C. The reaction was then refluxed for 40 °C for 48 h. The reaction mixture was then cooled to 0 °C and quenched with sat. aq. $NaHCO_3$ until pH 7. The aqueous phase was extracted with CH_2Cl_2 (3×30 mL), the organic phases were combined, dried over $MgSO_4$, filtered over a plug

of silica gel and concentrated *in vacuo*. The crude product was purified by column chromatography (1:19, EtOAc/heptane) to afford **3.57** as a colourless oil (0.80 g, 53%).

^{1}H NMR (400 MHz, $CDCl_3$) δ 8.09–8.01 (m, 2H, H_{Ar}), 7.61–7.55 (m, 1H, H_{Ar}), 7.50–7.42 (m, 2H, H_{Ar}), 4.38 (t, *J*=6.0 Hz, 2H, H1), 2.11–1.94 (m, 4H, H2 + H3), 1.65 (t, *J*=18.3 Hz, 3H, H5) ppm; **^{13}C NMR** (101 MHz, $CDCl_3$) δ 166.5 (C=O), 133.0 (C_{Ar}), 130.1 (C_{Ar}), 129.5 (C_{Ar}×2), 128.4 (C_{Ar}×2), 123.8 (t, *J*=237.7 Hz, C4), 64.1 (C1), 34.7 (t, *J*=25.7 Hz, C3), 23.5 (t, *J*=27.9 Hz, C5), 22.2 (t, *J*=4.8 Hz, C2) ppm; **^{19}F NMR** (376 MHz, $CDCl_3$) δ -91.4– -91.7 (m, 2F) ppm; **^{19}F {^{1}H} NMR** (376 MHz, $CDCl_3$) δ -91.5 (s, 2F) ppm.

Data consistent with literature.[94]

Synthesis of 4,4-difluoropentan-1-ol (I7)

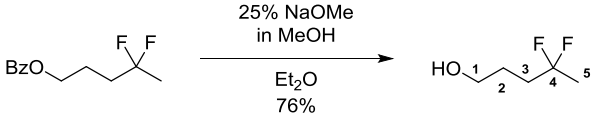

3.57 **I7**

To a solution of **3.57** (0.40 g, 1 equiv) in Et_2O (6 mL), MeONa (25% in MeOH, 0.60 mL, 2 equiv) was added. After 16 h, the reaction was quenched with aq. HCl (2M) until pH 7. The aqueous layer was extracted with CH_2Cl_2 (3×5 mL) and the organic phases were collected washed with brine and dried over $MgSO_4$. The crude was carefully concentrated at 750 mbar/30 °C and was purified by column chromatography (1:9, CH_2Cl_2/Et_2O) to afford **I7** as a pale-yellow oil (0.18 g, 76%).

^{1}H NMR (400 MHz, $CDCl_3$) δ 3.71 (q, *J*=6.0 Hz, 2H, H1), 2.05–1.88 (m, 2H, H3), 1.81–1.71 (m, 2H, H2), 1.62 (t, *J*=18.5 Hz, 3H, H5), 1.38 (br. t, *J*=5.1 Hz, 1H, OH) ppm; **^{13}C NMR** (101 MHz, $CDCl_3$) δ 124.2 (t, *J*=237.7 Hz, C4), 62.2 (C1), 34.4 (t, *J*=25.7 Hz, C3), 25.9 (t, *J*=4.4 Hz, C2), 23.4 (t, *J*=28.2 Hz, C5) ppm; **^{19}F NMR** (376 MHz, $CDCl_3$) δ -91.2 (app. sxt, *J*=17.3 Hz, 2F) ppm; **^{19}F {^{1}H} NMR** (376 MHz, $CDCl_3$) δ -91.2 (s 2F) ppm.

Data consistent with literature.[94]

Synthesis of 4,4-difluorobutyl benzoate (3.58)

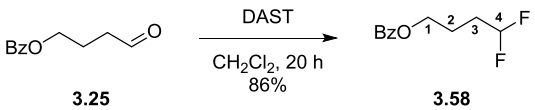

3.25 **3.58**

To a solution of **3.25** (8.93 g, 1 equiv) in CH_2Cl_2 (60 mL), DAST (12.24 mL, 2 equiv) was added dropwise at 0 °C. The reaction as allowed to warm to room temperature and after 20 h, was quenched with sat. aq. $NaHCO_3$ (300 mL) at 0 °C. The aqueous phase was extracted with CH_2Cl_2 (3×150 mL) and the combined organic phases were dried over $MgSO_4$ and concentrated. The crude oil was purified by column chromatography (1:9, Et_2O/pentane) to yield **3.58** as a pale-yellow oil (8.51 g, 86%).

^{1}H NMR (400 MHz, $CDCl_3$) δ 8.15–7.98 (m, 2H, H_{Ar}), 7.65–7.52 (m, 1H, H_{Ar}), 7.65–7.52 (m, 2H, H_{Ar}), 5.92 (tt, *J*=56.9, 4.1 Hz, 1H, H4), 4.39 (t, *J*=6.0 Hz, 2H, H1), 2.17–1.88 (m, 4H, H2 + H3) ppm; **^{13}C NMR** (101 MHz, $CDCl_3$) δ 166.4 (C=O), 133.1 (C_{Ar}), 130.1 (C_{Ar}), 129.6 (C_{Ar}×2), 128.4 (C_{Ar}×2), 116.7 (t, *J*=239.2 Hz, C4), 63.9 (C1), 31.0 (t, *J*=21.6 Hz, C3), 21.6 (t, *J*=5.5 Hz, C2) ppm; **^{19}F NMR** (376 MHz, $CDCl_3$) δ -116.5 (dt, *J*=57.2, 17.3 Hz, 2F) ppm; **^{19}F {1H} NMR** (376 MHz, $CDCl_3$) δ -116.5 (s, 2F) ppm; **IR** (neat) 2920 (w), 1720 (m), 1250 (m), 900 (s), 710 (s) cm^{-1}; **HRMS** (ESI+) for $C_{11}H_{12}F_2NaO_2$ $[M+Na]^+$, calculated 237.0698, found 237.0699 (-0.27 ppm error).

Data consistent with literature.[248]

Synthesis of 4,4-difluorobutan-1-ol (G6)

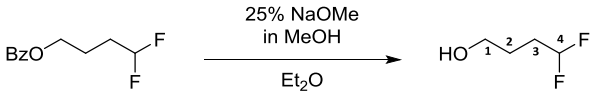

3.58 **G6**

To a solution of **3.58** (3.00 g, 1 equiv) in Et_2O (30 mL), NaOMe (25% w/w in MeOH, 6.41 mL, 2 equiv) was added dropwise. After 4 h, the reaction was neutralised with aq. HCl (2M, 20 mL) and the aqueous phase was washed with CH_2Cl_2 (3×30 mL). The combined organic phases were dried ($MgSO_4$), filtered and concentrated (750 mbar, 30 °C). The crude oil was purified by column chromatography (CH_2Cl_2) to **G6** as a pale-yellow oil (1.24 g, 80%).

^{1}H NMR (400 MHz, $CDCl_3$) δ 5.89 (tt, *J*=57.0, 4.0 Hz, 1H H4), 3.72 (td, *J*=5.6, 4.9, 2H, H1), 2.11–1.86 (m, 2H, H3), 1.81–1.66 (m, 2H, H2), 1.41 (br. t, *J*=4.9, 1H, OH) ppm; **^{13}C NMR** (101 MHz, $CDCl_3$) δ 117.2 (t, *J*=238.8 Hz, C4), 61.9 (C1), 30.7 (t, *J*=21.3 Hz, C3), 25.1 (t, *J*=5.1 Hz, C2) ppm; **^{19}F NMR** (376 MHz, $CDCl_3$) δ -116.2 (dt, *J*=57.2, 18.2 Hz, 2F) ppm; **^{19}F {1H} NMR** (376 MHz, $CDCl_3$) δ -116.2 (s, 2F) ppm; **IR** (neat) 3300 (br, w), 2950 (w), 2900 (w), 980 (s), 1010 (s), 1060 (s), 1110 (s) cm^{-1}; **HRMS** (EI) for $C_4H_8F_2O$ $[M^{\cdot+}]$, calculated 110.0538, found 110.0535 (-0.27 ppm error).

Synthesis of 5,5-difluoropentyl benzoate (3.59)

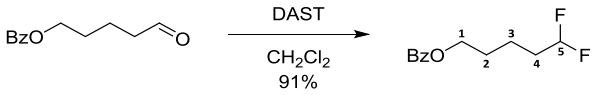

3.30 **3.59**

To a solution of **3.30** (3.27 g, 1 equiv) in CH_2Cl_2 (30 mL), DAST (4.0 mL, 1.9 equiv) was added dropwise at 0 °C. After 60 h the reaction was quenched with sat. aq. $NaHCO_3$ until pH 7. The aqueous phase was extracted with CH_2Cl_2 (2×150 mL), the organic phases were combined, dried over $MgSO_4$ and concentrated *in vacuo*. The crude product was purified by column chromatography (5:95, EtOAc/petroleum ether 40–60 °C) to afford **3.59** as a pale-yellow oil (3.23 g, 91%).

^{1}H NMR (400 MHz, $CDCl_3$) δ 8.07–8.03 (m, 2H, H_{Ar}), 7.58 (tt, *J*=7.4, 1.3 Hz, 1H, H_{Ar}), 7.49–7.43 (m, 2H, H_{Ar}), 5.85 (tt, *J*=57.6, 4.4 Hz, 1H, H5), 4.36 (t, *J*=6.4 Hz, 2H, H1), 2.01–1.81 (m, 4H, H2 + H3), 1.71–

1.60 (m, 2H, H4) ppm; **^{13}C NMR** (101 MHz, $CDCl_3$) δ 166.9 (C=O), 133.3 (C_{Ar}), 130.6 (C_{Ar}), 129.8 (C_{Ar}×2), 128.7 (C_{Ar}×2), 117.4 (t, *J*=239.3 Hz, C5), 64.7 (C1), 34.0 (t, *J*=20.9 Hz, C4), 28.5 (C2), 19.2 (t, *J*=5.5 Hz, C3) ppm; **^{19}F NMR** (376 MHz, $CDCl_3$) δ -116.3 (dt, *J*=57.2, 17.3 Hz, 2F) ppm; **^{19}F {^{1}H} NMR** (376 MHz, $CDCl_3$) δ -116.3 (s, 2F) ppm; **IR** (neat) 2959(w), 1714 (s), 1451 (m), 1269 (s), 1094 (s), 1026 (s) cm^{-1}; **HRMS** (ESI+) for $C_{12}H_{14}F_2NaO_2$ $[M+Na]^+$, calculated 251.0854, found 251.0853 (+0.3 ppm error).

Synthesis of 5,5-difluoropentan-1-ol (I6)

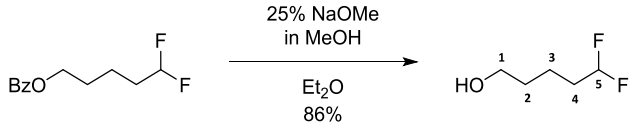

3.59 **I6**

To a solution of **3.59** (3.19 g, 1 equiv) in Et_2O (30 mL), NaOMe (25% w/w in MeOH, 6.60 mL, 2 equiv). After 18 h, the reaction was quenched with aq. HCl (1M) until pH 7. The aqueous layer was extracted with CH_2Cl_2 (3×30 mL) and the organic phases were collected and dried over $MgSO_4$. The crude was carefully concentrated at 750 mbar/30 °C and was purified by column chromatography (CH_2Cl_2 to 9:1, CH_2Cl_2/Et_2O) to afford **I6** as a pale-yellow oil (1.50 g, 86%).

^{1}H NMR (400 MHz, $CDCl_3$) δ 5.82 (tt, *J*=56.9, 4.4 Hz, 1H, H5), 3.68 (t, *J*=6.5 Hz, 2 H, H1), 1.95–1.80 (m, 2H, H4), 1.68–1.52(m, 4H, H2 + H3), 1.34 (br. s, 1H, OH) ppm; **^{13}C NMR** (101 MHz, $CDCl_3$) δ 117.2 (t, J=238.8 C5), 62.4 (C1), 33.7 (t, *J*=20.91 Hz, C4), 32.0 (C2), 18.5 (t, *J*=5.5 Hz, C3) ppm; **^{19}F NMR** (376 MHz, $CDCl_3$) δ -116.2 (dt, *J*=55.9, 18.0 Hz, 2F) ppm; **^{19}F {^{1}H} NMR** (376 MHz, $CDCl_3$) δ -116.2 (s, 2F) ppm; **IR** (neat) 3333 (br. w), 2940 (w), 2873 (w), 1404 (m), 1121 (s), 1087 (s), 994 (s) cm^{-1}; **HRMS** (EI) for $C_5H_{10}F_2O$ $[M^{\cdot+}]$, calculated 124.0694, found 124.0662 (-3.26 ppm error).

Synthesis of 1-(benzyloxy)pentan-3-one (3.13)

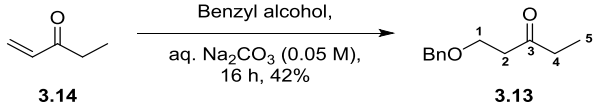

3.14 **3.13**

To a suspension of **3.14** (5.87 mL, 1 equiv) and aq. Na_2CO_3 (0.05 M, 50 mL) was added benzyl alcohol (8.88 mL, 1.5 equiv). After 16 h, the reaction mixture was diluted with EtOAc (50 mL) and the aqueous phase was extracted with EtOAc (3×50 mL). The combined organic phases were washed with brine, dried over Na_2SO_4 and concentrated. The crude oil was purified by column chromatography (1:9, acetone/petrol ether 40–60 °C) to yield **3.13** as a colourless oil (4.78 g, 42%).

^{1}H NMR (400 MHz, $CDCl_3$) δ 7.39–7.28 (m, 5H, H_{Ar}), 4.52 (s, 2H, PhC$\underline{H}_2$), 3.76 (t, *J*=6.3 Hz, 2H, H1), 2.71 (t, *J*=6.3 Hz, 2H, H2), 2.48 (q, *J*=7.3 Hz, 2H, H4), 1.07 (t, *J*=7.3 Hz, 3H, H5) ppm; **^{13}C NMR** (101 MHz, $CDCl_3$) δ 209.8 (C3), 138.1 (C_{Ar}), 128.4 (C_{Ar}×2), 127.7 (C_{Ar}×2), 127.6 (C_{Ar}), 73.2 (Ph$\underline{C}H_2$), 65.4 (C1), 42.5 (C2), 36.6 (C4), 7.6 (C5) ppm.

Data consistent with literature.[127]

Synthesis of 1-(benzyloxy)pentan-3-ol (3.60)

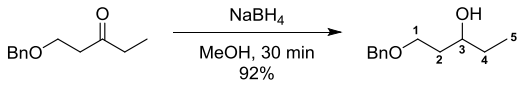

3.13 **3.60**

To a solution of **3.13** (2.33 g, 1 equiv) in MeOH (40 mL), $NaBH_4$ (0.92 g, 2 equiv) was added portion wise at 0 °C. The reaction mixture was allowed to warm to room temperature and after 30 min, the reaction mixture was quenched with water (30 mL) at 0 °C. The aqueous phase was extracted with EtOAc (3×30 mL) and the combined organic phases were dried over Na_2SO_4 and concentrated to afford **3.60** as a colourless oil (2.16 g, 92%).

^{1}H NMR (400 MHz, $CDCl_3$) δ 7.42–7.28 (m, 5H, H_{Ar}), 4.54 (s, 2H, PhC$\underline{H}_2$), 3.81–3.62 (m, 3H, H1 + H3), 2.85 (s, 1H, OH), 1.82–1.68 (m, 2H, H2), 1.56–1.43 (m, 2H, H4), 0.95 (t, *J*=7.5 Hz, 3H, H5) ppm; **^{13}C NMR** (101 MHz, $CDCl_3$) δ 137.9 (C_{Ar}), 128.4 (C_{Ar}×2), 127.7 (C_{Ar}), 127.6 (C_{Ar}×2), 73.3 (Ph$\underline{C}H_2$), 72.8 (C3), 69.3 (C1), 35.9 (C2), 30.2 (C4), 9.9 (C5) ppm.

Data consistent with literature.[249]

Synthesis of 3-fluoropentyl benzylether (3.61)

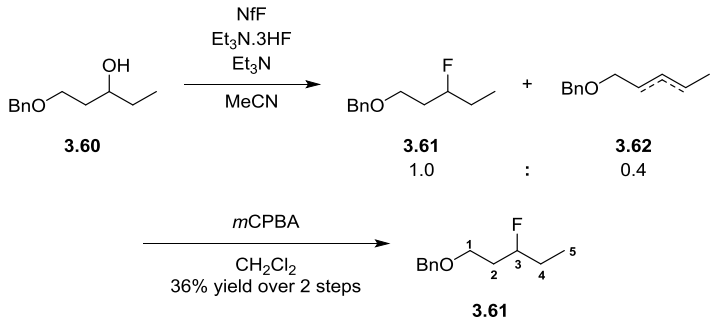

To a solution of **3.60** (2.08 g, 1 equiv) in MeCN (32 mL) was added Et_3N (8.99 mL, 6 equiv), Et_3N•3HF (3.50 mL, 2 equiv) and nonafluorobutane-1-sulphonic fluoride (3.20 mL, 2 equiv). After 16 h, the reaction was quenched with sat. aq. $NaHCO_3$ until pH 7 and the aqueous layer was extracted with CH_2Cl_2 (3×30 mL). The combined organic layers were washed with brine, dried over $MgSO_4$ and concentrated. The resulting crude was purified by column chromatography (1:19, acetone/petroleum ether 40–60 °C) to yield **3.61** and **3.62** as a mixture (1.31 g, 1:0.4 respectively). The mixture of **3.61** (~0.93 g) and **3.62** (~0.38 g, 1 equiv) was dissolved in CH_2Cl_2 (25 mL), followed by portion wise addition of *m*CPBA (0.97 g, 2 equiv) at 0 °C. After 16 h, the reaction was quenched with sat. aq. $NaHCO_3$ (20 mL) and the aqueous layer was extracted with CH_2Cl_2 (3×30 mL). The combined organic layers were washed with brine, dried over $MgSO_4$ and concentrated. The resulting crude was purified by column chromatography (1:19, Et_2O/petroleum ether 40–60 °C) to yield **3.61** as a colourless oil (0.75 g, 36%).

^{1}H NMR (400 MHz, $CDCl_3$) δ 7.41–7.28 (m, 5H, H_{Ar}), 4.73–4.54 (m, a doublet with 49.5 Hz can be observed, 1H, H3), 4.55 (d, *J*=11.9 Hz, 1H, PhC<u>H</u>H'), 4.51 (d, *J*=11.9 Hz, 1H, PhCH<u>H</u>'), 3.68–3.57 (m, 2H, H1), 1.96–1.78 (m, 2H, H2), 1.72–1.59 (m, 2H, H4), 0.99 (t, *J*=7.5 Hz, 3H, H5) ppm; **^{13}C NMR** (101 MHz, $CDCl_3$) δ 138.4 (C_{Ar}), 128.4 (C_{Ar}×2), 127.6 (C_{Ar}×2), 127.6 (C_{Ar}), 92.7 (d, *J*=167.3 Hz, C3), 73.1 (Ph<u>C</u>H$_2$), 66.3 (d, *J*=4.4 Hz, C1), 35.1 (d, *J*=21.3 Hz, C2), 28.3 (d, *J*=20.5 Hz, C4), 9.3 (d, *J*=5.9 Hz, C5) ppm; **^{19}F NMR** (376 MHz, $CDCl_3$) δ -184.4– -184.0 (m, 1F) ppm; **^{19}F {^{1}H} NMR** (376 MHz, $CDCl_3$) δ -184.1 (s, 1F) ppm; **IR** (neat) 3065 (w), 2967 (m), 2879 (m), 1363 (m), 1097 (s), 930 (s) cm^{-1}; **HRMS** (ESI+) for $C_{12}H_{17}FNaO$ $[M+Na]^+$, calculated 219.1156, found 219.1156 (-0.1 ppm error).

Synthesis of 3-fluoropentan-1-ol (I8)

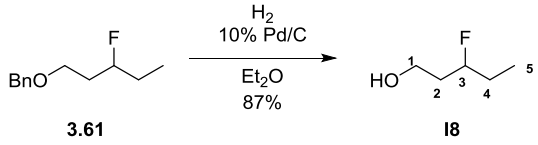

To a solution of **3.61** (0.70 g, 1 equiv) in Et_2O (20 mL) was added a suspension of Pd/C 10 wt. % (300 mg) in Et_2O (10 mL). The reaction mixture was degassed with nitrogen and one balloon of hydrogen. The reaction mixture was stirred at room temperature under a hydrogen atmosphere. After 16 h,

the reaction was then filtered over Celite, which was then rinsed with CH_2Cl_2 (30 mL). The crude was carefully concentrated at 750 mbar/30 °C and purified by column chromatography (9:1, CH_2Cl_2/Et_2O) to afford **I8** as a colourless oil (0.33 g, 87%).

^{1}H NMR (400 MHz, $CDCl_3$) δ 4.79–4.53 (m, a doublet with 49.2 Hz can be observed, 1H, H3), 3.82 (t, *J*=5.8 Hz, 2H, H1), 1.99–1.48 (m, 5H, H2 + H4 + OH), 1.00 (t, *J*=7.5 Hz, 3H, H5) ppm; **^{13}C NMR** (101 MHz, $CDCl_3$) δ 93.8 (d, *J*=165.8 Hz, C3), 59.5 (d, *J*=3.7 Hz, C1), 37.4 (d, *J*=20.5 Hz, C2), 28.3 (d, *J*=20.5 Hz, C4), 9.3 (d, *J*=6.6 Hz, C5) ppm; **^{19}F NMR** (376 MHz, $CDCl_3$) δ -183.5– -184.0 (m, 1F) ppm; **^{19}F {^{1}H} NMR** (376 MHz, $CDCl_3$) δ -183.7 (s, 1F) ppm; **IR** (neat) 3341 (br. w), 2969 (m), 2884 (m), 1463 (m), 1056 (s), 927 (s) cm^{-1}; **HRMS** (CI) for $C_5H_{12}FO$ $[M+H]^+$, calculated 107.0867, found 107.0863 (-0.37 ppm error).

Synthesis of 3,3-difluoropentyl benzylether (3.63)

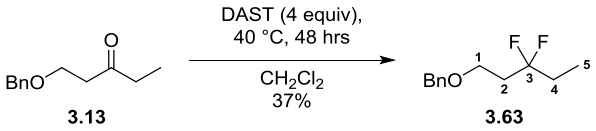

3.13 **3.63**

To a solution of **3.13** (2.23 g, 1 equiv) in CH_2Cl_2 (35 mL), DAST (3.07 mL, 2 equiv) was added dropwise at 0 °C. The reaction mixture was heated 40 °C and after 48 h, the reaction mixture was quenched with sat. aq. $NaHCO_3$ until pH 7. The aqueous phase was extracted with CH_2Cl_2 (3×100 mL) and the combined organic phases were washed with brine and dried over $MgSO_4$ and concentrated. The crude oil was purified by column chromatography (5:95, acetone/petrol ether 40–60 °C) to yield **3.63** as a pale-yellow oil (0.91 g, 37%).

^{1}H NMR (400 MHz, $CDCl_3$) δ 7.40–7.28 (m, 5H, H_{Ar}), 4.53 (s, 2H, PhC$\underline{H}_2$), 3.67 (t, *J*=6.7 Hz, 2H, H1), 2.20 (tt, *J*=16.2, 6.7 Hz, 2H, H2), 1.90 (tq, *J*=16.8, 7.6 Hz, 2H, H4), 1.03 (t, *J*=7.5, 3H, H5) ppm; **^{13}C NMR** (101 MHz, $CDCl_3$) δ 138.0 (C_{Ar}), 128.4 (C_{Ar}×2), 127.7 (C_{Ar}), 127.6 (C_{Ar}×2), 124.8 (t, *J*=240.3 Hz, C3), 73.2 (Ph$\underline{C}H_2$), 64.3 (t, *J*=5.9 Hz, C1), 36.2 (t, *J*=25.7 Hz, C2), 30.0 (t, *J*=25.7, C4), 6.6 (t, *J*=5.5, C5) ppm; **^{19}F NMR** (376 MHz, $CDCl_3$) δ -98.9 (quin, *J*=16.5 Hz, 2F) ppm; **^{19}F {^{1}H} NMR** (376 MHz, $CDCl_3$) δ -98.9 (s, 2F) ppm; **IR** (neat) 2982 (br. w), 2888 (w), 1374 (m), 1102 (s), 940 (s), 737 (s) cm^{-1}; **HRMS** (ESI+) for $C_{12}H_{16}F_2NaO$ $[M+Na]^+$, calculated 237.1061, found 237.1055 (+2.6 ppm error).

Synthesis of 3,3-difluoropentan-1-ol (I11)

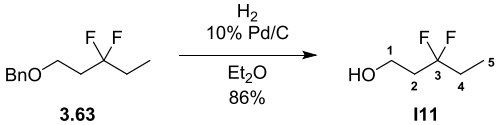

3.63 **I11**

To a solution of **3.63** (0.64 g, 1 equiv) in Et_2O (20 mL) was added a suspension of Pd/C 10% (300 mg) in Et_2O (10 mL). The reaction mixture was degassed with nitrogen and one balloon of hydrogen. The reaction mixture was stirred at room temperature under a hydrogen atmosphere. After 16 h, the

reaction was then filtered over Celite, which was then rinsed with CH_2Cl_2 (30 mL). The crude was carefully concentrated at 750 mbar/30 °C and was purified by column chromatography (9:1, CH_2Cl_2/Et_2O) to afford **I11** as a colourless oil (0.32 g, 86%).

^{1}H NMR (400 MHz, $CDCl_3$) δ 3.89 (q, *J*=5.9 Hz, 2H, H1), 2.14 (tt, *J*=17.0, 6.2 Hz, 2H, H2), 1.91 (tq, *J*=16.8, 7.5 Hz, 2H, H4), 1.61 (br. t, *J*=7.1 Hz, 1H, OH), 1.04 (t, *J*=7.5 Hz, 3H, H5) ppm; **^{13}C NMR** (101 MHz, $CDCl_3$) δ 125.4 (t, *J*=240.3 Hz, C3), 57.2 (t, *J*=5.5 Hz, C1), 38.5 (t, *J*=24.2 Hz, C2), 30.2 (t, *J*=26.0 Hz, C4), 6.5 (t, *J*=5.9 Hz, C5) ppm; **^{19}F NMR** (376 MHz, $CDCl_3$) δ -99.5 (quin, *J*=16.9 Hz, 2F) ppm; **^{19}F {^{1}H} NMR** (376 MHz, $CDCl_3$) δ -99.5 (s, 2F) ppm; **IR** (neat) 3351 (br. w), 2984 (m), 2893 (w), 1375 (m), 1144 (s), 1052 (s), 936 (s) cm^{-1}; **HRMS** (CI) for $C_5H_{11}F_2O$ $[M+H]^+$, calculated 125.0773, found 125.0768 (-0.44 ppm error).

Synthesis of Pentan-1,4-diol (3.64)

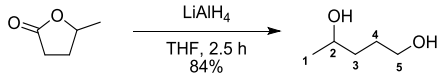

3.18 **3.64**

To a solution of lithium aluminium hydride (10.32 g, 2.5 equiv) in THF (250 mL) was added γ-valerolactone **3.18** (9.83 mL, 1 equiv) dropwise at 0 °C. The reaction was stirred at 0 °C for 30 min before being allowed to warm to room temperature. After 2 h, the reaction was then cooled to 0 °C and water (30 mL) was added dropwise, followed by aq. NaOH (15% wt., 10 mL) then water (30 mL). $MgSO_4$ (10 g) was added to the quenched reaction mixture and stirred for 30 min. The reaction mixture was then filtered over Celite and the filter cake was rinsed with EtOAc (5×200 mL). The combined organic phases were dried over $MgSO_4$ and concentrated *in vacuo*. The resulting oil was purified by column chromatography (EtOAc) to yield **3.64** as a colourless oil (8.63 g, 84%).

^{1}H NMR (400 MHz, $CDCl_3$) δ 3.90–3.82 (m, 1H, H2), 3.74–3.63 (m, 2H, H5), 2.40 (br. s, 1H, OH), 2.17 (br. s, 1H, OH), 1.74–1.47 (m, 4H, H3 + H4), 1.22 (d, *J*=6.2 Hz, 3H, H1) ppm; **^{13}C NMR** (101 MHz, $CDCl_3$) δ 68.0 (C2), 62.9 (C5), 36.2 (C3 or C4), 29.1 (C3 or C4), 23.6 (C1) ppm.

Data consistent with literature.[163]

Synthesis of 5-((*tert*-butyldimethylsilyl)oxy)pentan-2-ol (3.65)

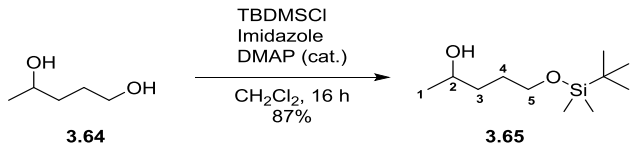

3.64 **3.65**

To a stirred solution of **3.64** (8.50 g, 1 equiv), imidazole (6.67 g, 1.2 equiv) and DMAP (0.50 g, 0.05 equiv) in CH_2Cl_2 (100 mL) was added TBDMSCl (12.54 g, 1.02 equiv) portion wise at 0 °C. The reaction mixture was allowed to warm to rt. After 16 h, the reaction was quenched with aq. HCL (2 M, 40

mL) and water (40 mL) and the layers separated. The aqueous phase was extracted with CH_2Cl_2 (3×100 mL) and the combined organic layers were washed with brine (100 mL), dried over $MgSO_4$ and concentrated *in vacuo*. The resulting oil was purified with column chromatography (1:9, EtOAc/petrol ether 40–60 °C) to yield **3.65** as a colourless oil (15.52 g, 87%)

^{1}H NMR (400 MHz, $CDCl_3$) δ 3.86–3.78 (m, 1H, H2), 3.72–3.63 (m, 2H, H5), 2.63 (br. s, 1H, OH), 1.72–1.44 (m, 4H, H3 + H4), 1.20 (d, *J*=6.2 Hz, 3H, H1), 0.91 (s, 9H, $SiC(CH_3)_3$), 0.08 (s, 6H, $Si(CH_3)_2$) ppm; **^{13}C NMR** (101 MHz, $CDCl_3$) δ 67.7 (C2), 63.6 (C5), 36.7 (C3 or C4), 29.4 (C3 or C4), 25.9 ($SiC(\underline{C}H_3)_3$), 23.4 (C1), 18.3 ($Si\underline{C}(CH_3)_3$), -5.41 ($Si(\underline{C}H_3)_2$) ppm.

Data consistent with literature.[163]

Synthesis of ((4-(benzyloxy)pentyl)oxy)(*tert*-butyl)dimethylsilane (3.66)

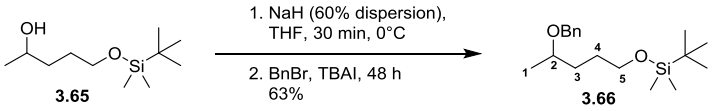

To a solution of **3.65** (640 mg, 1 equiv) in THF, NaH in 60% mineral oil (602 mg, 5 equiv) was added portion wise at 0 °C. After 30 min, BnBr (0.47 mL, 1.3 equiv) and TBAI (340 mg, 0.3 equiv) were added at 0 °C. After 48 h, the reaction mixture was cooled to 0 °C and sat. aq. NH_4Cl (10 mL) was added dropwise. After 10 min, the reaction mixture was diluted with brine (50 mL) and Et_2O (100 mL). The layers were separated and the aqueous phase was extracted with Et_2O (2×100 mL). The combined organic layers were washed with brine (100 mL), dried over $MgSO_4$ and concentrated *in vacuo*. The crude oil was purified with column chromatography (1:19, EtOAc/petrol ether 40–60 °C) to afford **3.66** as a colourless oil (0.57 g, 63%).

^{1}H NMR (400 MHz, $CDCl_3$) δ 7.40–7.25 (m, 5H, H_{Ar}), 4.57 (d, *J*=11.9 Hz, 1H, PhC$\underline{H}$H'), 4.47 (d, *J*=11.9 Hz, 1H, PhCH$\underline{H}$'), 3.64–3.60 (m, 2H, H5), 3.54 (br. sxt, *J*=6.1 Hz, 1H, H2), 1.70–1.49 (m, 4H, H3 + H4), 1.21 (d, *J*=6.1 Hz, 3H, H1), 0.90 (s, 9H, $SiC(C\underline{H}_3)_3$), 0.05 (s, 6H, $Si(CH_3)_2$) ppm; **^{13}C NMR** (101 MHz, $CDCl_3$) δ 139.1 (C_{Ar}), 128.3 (C_{Ar}×2), 127.6 (C_{Ar}×2), 127.4 (C_{Ar}), 74.7 (C2), 70.3 (Ph$\underline{C}H_2$), 63.2 (C5), 32.8 (C3 or C4), 28.8 (C3 or C4), 26.0 ($SiC(\underline{C}H_3)_3$), 19.7 (C1), 18.4 ($Si\underline{C}(CH_3)_3$), -5.3 ($Si(\underline{C}H_3)_2$) ppm; **IR** (thin film, $CDCl_3$) 2952 (w), 2927 (w), 2856 (w), 1254 (w), 1093 (s), 835 (s) cm^{-1}; **MS** (ESI+) m/z 309.2 $[M+H]^+$, 331.2 $[M+Na]^+$; **HRMS** (ESI+) for $C_{18}H_{33}O_2Si$ $[M+H]^+$, calculated 309.2244, found 309.2252 (-2.6 ppm error).

Synthesis of 4-(benzyloxy)pentan-1-ol (3.67)

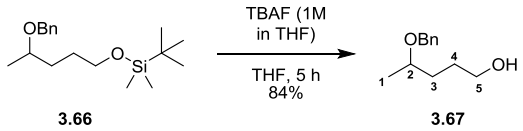

3.66 3.67

To a stirred solution of **3.66** (450 mg, 1 equiv) in THF (3 mL), was added TBAF (1M in THF, 2.18 mL, 1.5 equiv) dropwise at 0 °C over 30 min. The reaction was stirred at 0 °C for 30 min before allowing to warm to room temperature. After 4 h, the reaction mixture was quenched with the dropwise addition of sat. aq. NH_4Cl (10 mL) at 0 °C. After vigorous stirring for 30 min, the aqueous phase was extracted with EtOAc (3×10 mL) and the combined organic layers were dried over $MgSO_4$ and concentrated *in vacuo*. The crude oil was purified with column chromatography (1:9, acetone/petrol ether 40–60 °C) to afford **3.67** as a pale orange oil (237 mg, 84%).

^{1}H NMR (400 MHz, $CDCl_3$) δ 7.37–7.28 (m, 5H, H_{Ar}), 4.62 (d, *J*=11.6 Hz, 1H, PhC<u>H</u>H'), 4.47 (d, *J*=11.6, 1H, PhCH<u>H</u>'), 3.64 (t, *J*=5.7 Hz, 2H, H5), 3.59 (br. sxt, *J*=6.1 Hz, 1H, H2), 1.99 (br. s, 1H, OH), 1.74–1.56 (m, 4H, H3 + H4), 1.24 (d, *J*=6.1 Hz, 3H, H1) ppm; **^{13}C NMR** (101 MHz, $CDCl_3$) δ 138.6 (C_{Ar}), 128.4 (C_{Ar}×2), 127.7 (C_{Ar}×2), 127.5 (C_{Ar}), 74.7 (C2), 70.4 (Ph<u>C</u>H_2), 63.0 (C5), 33.2 (C3 or C4), 28.8 (C3 or C4), 19.4 (C1) ppm.

Proton consistent with literature.[250]

Synthesis of 5-((*tert*-butyldimethylsilyl)oxy)pentan-2-yl acetate (3.72)

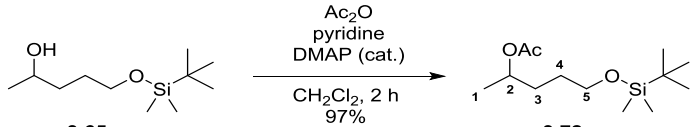

3.65 3.72

To a solution of **3.65** (14.50 g, 1 equiv), pyridine (13.15 mL, 2.5 equiv) and DMAP (0.83 g, 0.1 equiv) was added acetic anhydride (7.6 mL, 1.2 equiv) at 0 °C. The reaction was allowed to warm to room temperature and after 2 h, was quenched with aq. HCl (2M, 100 mL). The aqueous phase was extracted with CH_2Cl_2 (3×100 mL) and the combined organic layers were washed with brine (100 mL), dried over $MgSO_4$ and concentrated *in vacuo* to afford **3.72** as a colourless oil (16.98 g, 97%).

^{1}H NMR (400 MHz, $CDCl_3$) δ 4.92 (br. sxt, *J*=6.2, 1H, H2), 3.61 (br. t, *J*=6.0, 2H, H5), 2.03 (s, 3H, CH_3, Ac), 1.69–1.40 (m, 4H, H3 + H4), 1.22 (d, *J*=6.2 Hz, 3H, H1), 0.90 (s, 9H, $SiC(CH_3)_3$), 0.05 (s, 6H, $Si(CH_3)_2$) ppm; **^{13}C NMR** (101 MHz, $CDCl_3$) δ 170.8 (C=O), 70.8 (C2), 62.8 (C5), 32.4 (C3 or C4), 28.7 (C3 or C4), 25.9 ($SiC(\underline{C}H_3)_3$), 21.4 (CH_3, Ac), 20.0 (C1), 18.3 ($Si\underline{C}(CH_3)_3$), -5.3 ($Si(\underline{C}H_3)_2$) ppm.

Data consistent with literature.[251]

Synthesis of 5-hydroxypentan-2-yl acetate (3.73)

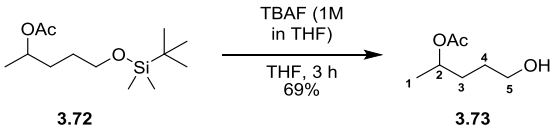

3.72 **3.73**

To a stirred solution of **3.72** (16.80 g, 1 equiv) in THF (100 mL), was added TBAF (1M in THF, 92 mL, 1.1 equiv) dropwise at 0 °C over 30 min. The reaction was stirred at 0 °C for 30 min, before allowing to warm to room temperature. After 2 h, the reaction mixture was quenched by the dropwise addition of sat. aq. NH_4Cl (150 mL) at 0 °C. After 30 min of vigorous stirring, the aqueous phase was extracted with EtOAc (3×300 mL) and the combined organic layers were dried over $MgSO_4$. The crude oil was purified with column chromatography (1:9, acetone/petrol ether 40–60 °C) to afford **3.73** as a slightly orange oil (7.80 g, 69%).

^{1}H NMR (400 MHz, $CDCl_3$) δ 4.90–4.87 (m, 1H, H2), 3.67 (t, *J*=6.0 Hz, 2H, H5), 2.04 (s, 3H, CH_3, Ac), 1.71–1.50 (m, 4H, H3 + H4), 1.42 (br. s, 1H, OH), 1.23 (d, *J*=6.4 Hz, 3H, H1) ppm; **^{13}C NMR** (101 MHz, $CDCl_3$) δ 170.8 (C=O), 70.7 (C2), 62.5 (C5), 32.2 (C3 or C4), 28.5 (C3 or C4), 21.3 (CH_3, Ac), 20.0 (C1) ppm.

Data consistent with literature.[252]

Synthesis of 5-Fluoropentan-2-yl acetate (3.74)

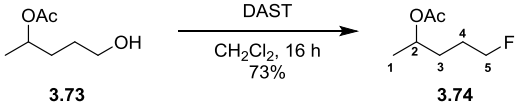

3.73 **3.74**

To a stirred solution of DAST (2.50 mL, 2.5 equiv) in CH_2Cl_2 (3 mL), was added **3.73** (1.08 g, 1 equiv) dissolved in CH_2Cl_2 (3 mL) dropwise at -78 °C. The reaction was allowed to warm to room temperature and after 16 h, DAST (1 mL) was added at 0 °C. After 24 h, the reaction mixture was quenched with sat. aq. $NaHCO_3$ (60 mL) dropwise at 0 °C and left to stir for 15 min until evolution of CO_2 ceased. The aqueous was extracted with CH_2Cl_2 (3×40 mL) and the combined organic layers were dried over $MgSO_4$. The crude was carefully concentrated at 750 mbar/30 °C and was purified with column chromatography (1:9, Et_2O/pentane) to afford a slightly yellow solution (calculated yield based on ^{1}H NMR, 790 mg, 73%). Due to the presumed volatility of this fluorinated product, **3.74** (containing eluting solvents) was used directly for next step without complete removal of the solvent residue.

^{1}H NMR (400 MHz, $CDCl_3$) δ 4.95 (sxt, *J*=6.2 Hz, 1H, H2), 4.57–4.35 (m, a doublet with *J*=47.1 was observed, 2H, H5), 2.04 (s, 3H, CH_3, Ac), 1.89–1.61 (m, 4H, H3 + H4), 1.25 (d, *J*=6.2 Hz, 3H, H1) ppm;

^{19}F NMR (376 MHz, $CDCl_3$) δ -218.9 (tt, *J*= 46.7, 24.3 Hz, 1F) ppm; **^{19}F {1H} NMR** (376 MHz, $CDCl_3$) δ -218.9 (s, 1F) ppm.

Synthesis of 5-Fluoropentan-2-ol (H1)

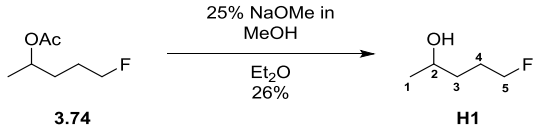

3.74 **H1**

To a stirred solution of **3.74** (593 mg, 1 equiv) in Et_2O (5 mL) was added NaOMe (25% w/w in MeOH, 1.8 mL, 2 equiv). After 1.5 h, the reaction was neutralized with aq. HCl (1 M) until 7 pH. The aqueous layer was extracted with CH_2Cl_2 (3×10 mL) and the combined organic layers were dried over $MgSO_4$. The crude was carefully concentrated at 750 mbar/30 °C and purified by column chromatography (1:9, Et_2O/CH_2Cl_2) to afford **H1** as a slightly yellow oil (110 mg, 26%).

^{1}H NMR (400 MHz, $CDCl_3$) δ 4.61–4.38 (m, a doublet with *J*=47.3 was observed, 2H, H5), 3.87 (sxt, *J*=6.2 Hz, 1H, H2), 1.98–1.67 (m, 2H, H4), 1.67–1.47 (m, 2H, H3), 1.34 (br. s, 1H, OH), 1.24 (d, *J*=6.2 Hz, 3H, H1) ppm; **^{13}C NMR** (101 MHz, $CDCl_3$) δ 84.2 (d, *J*=164.3 Hz, C5), 67.6 (C2), 34.8 (d, *J*=5.1 Hz, C3), 26.8 (d, *J*=19.8 Hz, C4), 23.6 (C1) ppm; **^{19}F NMR** (376 MHz, $CDCl_3$) δ -218.2 (tt, *J*=46.8, 26.0 Hz, 1F) ppm; **^{19}F {1H} NMR** (376 MHz, $CDCl_3$) δ -218.0 (s, 1F) ppm; **IR** (thin film, $CDCl_3$) 3486 (br. w), 2965 (w), 2893 (w), 1424 (s), 1371 (s), 1134 (s) cm^{-1}; **HRMS** (EI) for $C_5H_{11}FO$ [$M^{\cdot+}$], calculated 106.0788, found 106.0779 (-0.93) ppm error.

Synthesis of 5-oxopentan-2-yl acetate (3.75)

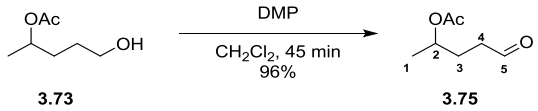

3.73 **3.75**

To a solution of **3.73** (2.02 g, 1 equiv) in CH_2Cl_2 (20 mL) was added DMP (8.40 g, 1.4 equiv) portion wise at 0 °C. The reaction mixture was allowed to warm to room temperature and after 45 min, the reaction mixture was quenched with sat. aq. $Na_2S_2O_3$ (20 mL). The organic layer was washed with sat. aq. $NaHCO_3$ (20 mL) and the aqueous layer was extracted with CH_2Cl_2 (3×30 mL). The combined organic phases were dried over $MgSO_4$, concentrated *in vacuo* and the crude oil was purified with column chromatography (1:3, EtOAc/pentane) to afford **3.75** as a colourless oil (1.89 g, 96%).

^{1}H NMR (400 MHz, $CDCl_3$) δ 9.77 (t, *J*=1.3 Hz, 1H, H5), 4.93 (sxt, *J*=6.3 Hz, 1H, H2), 2.50 (td, *J*=7.3, 1.3 Hz, 2H, H4), 2.03 (s, 3H, CH_3, Ac), 1.95–1.84 (m, 2H, H3), 1.25 (d, *J*=6.2 Hz, 3H, H1) ppm.

Synthesis of 5,5-difluoropentan-2-yl acetate (3.76)

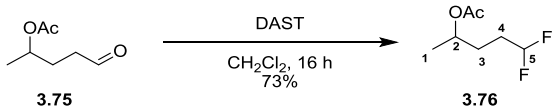

3.75 **3.76**

To a stirred solution of **3.75** (1.89 g, 1 equiv) in CH_2Cl_2 (50 mL) was added DAST (3.46 mL, 2 equiv) dropwise at 0 °C. The reaction was allowed to warm to room temperature and after 16 h, was quenched with sat. aq. $NaHCO_3$ until pH 7. The aqueous phase was extracted with CH_2Cl_2 (3×50 mL), dried over $MgSO_4$ and carefully concentrated at 750 mbar/30 °C. The crude was purified with column chromatography (1:19 to 1:9, Et_2O/pentane) to afford a colourless solution (calculated yield based on ^{1}H NMR, 1.60 g, 73%). Due to the presumed volatility of this fluorinated product, **3.76** (containing eluting solvents) was used directly for next step without complete removal of the solvent residue.

^{1}H NMR (400 MHz, $CDCl_3$) δ 5.84 (tt, *J*=56.7, 4.3 Hz, 1H, H5), 4.28 (sxt, *J*=6.24 Hz, 1H, H2), 2.05 (s, 3H, CH_3, Ac), 2.00–1.79 (m, 2H, H4), 1.77–1.67 (m, 2H, H3), 1.25 (d, *J*=6.24 Hz, 3H, H1) ppm; **^{19}F NMR** (376 MHz, $CDCl_3$) δ -116.4 (dt, *J*=57.2, 17.3 Hz, 2F) ppm; **^{19}F {1H} NMR** (376 MHz, $CDCl_3$) δ -116.4 (s, 2F) ppm.

Synthesis of 5,5-Difluoropentan-2-ol (H4)

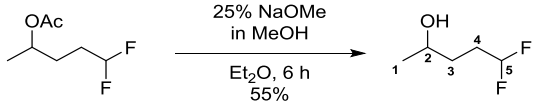

3.79 **H4**

To a stirred solution of **3.76** (1.60 g, 1 equiv) in Et_2O (30 mL) was added NaOMe (25% w/w in MeOH, 4.40 mL, 2 equiv). After 6 h, the reaction was neutralized with aq. HCl (1 M) until 7 pH. The aqueous layer was extracted with CH_2Cl_2 (3×30 mL) and the combined organic layers were dried with $MgSO_4$. The crude was carefully concentrated at 750 mbar/30 °C and purified by column chromatography (CH_2Cl_2) to afford **H4** as a colourless oil (633 mg, 53%).

^{1}H NMR (400 MHz, $CDCl_3$) δ 5.88 (tt, *J*=57.0, 4.3 Hz, 1H, H5), 3.87 (qtd, *J*=6.1, 6.0, 4.7 Hz, 1H, H2), 2.16–1.79 (m, 2H, H4), 1.73–1.48 (m, 2H, H3), 1.38 (d, *J*=4.6 Hz, 1H, OH), 1.24 (d, *J*=6.1 Hz, 3H, H1) ppm; **^{13}C NMR** (101 MHz, $CDCl_3$) δ 117.3 (t, *J*=238.8 Hz, C5), 67.3 (C2), 31.2 (t, *J*=4.8 Hz, C3), 30.5 (t, *J*=21.3 Hz, C4), 23.7 (C1) ppm; **^{19}F NMR** (376 MHz, $CDCl_3$) δ -115.7 (ddt, *J*=279.2, 55.5, 17.3 Hz, 1F, F5'), -116.7 (ddt, *J*=280.0, 57.2, 17.3 Hz, 1F, F5'') ppm; **^{19}F {1H} NMR** (376 MHz, $CDCl_3$) δ -115.7 (d, *J*=279.2 Hz, 1F, F5'), -116.7 (d, *J*=280.0 Hz, 1F, F5'') ppm; **IR** (neat) 3346 (br. w), 2971 (w), 2936 (w), 2875 (w), 1120 (s), 1003 (s), 928 (m) cm^{-1}; **HRMS** (EI) for $C_5H_{10}F_2O$ [$M^{\cdot+}$], calculated 124.0694, found 124.0700 (+0.53 ppm error).

Synthesis of (S)-2-hydroxy-N-methoxy-N-methylpropanamide (3.77)

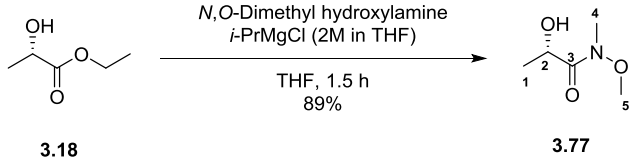

3.18 **3.77**

To a solution of (-)-ethyl L-lactate **3.18** (20.1 g, 1 equiv) and *N*,*O*-dimethyl hydroxylamine (41.73 g, 6 equiv) in THF (100 mL) at -20 °C, *i*-PrMgCl (2M in THF, 400 mL, 5 equiv) was added dropwise over 30 min. The reaction was then allowed to stir for a further 30 min at -20 °C and then an additional 30 min at 0 °C. The reaction mixture was then quenched with sat. aq. NH_4Cl solution (500 mL) at 0 °C. The aqueous phase was extracted with Et_2O (3×300 mL), followed by CH_2Cl_2 (3×300 mL). The combined organic layers were dried over $MgSO_4$ and concentrated *in vacuo*. The crude oil was purified by column chromatography (3:7, acetone/petrol ether 40–60 °C) to afford **3.77** as a colourless oil (20.03 g, 89%).

^{1}H NMR (400 MHz, $CDCl_3$) δ 4.49 (quin, *J*=6.9 Hz, 1H, H2), 3.73 (s, 3H, H5), 3.34 (d, *J*=7.7 Hz, 1H, OH), 3.26 (s, 3H, H4), 1.37 (d, *J*=6.6 Hz, 3H, H1) ppm; **^{13}C NMR** (101 MHz, $CDCl_3$) δ 175.8 (C3), 65.0 (C2), 61.3 (C5), 32.4 (C4), 21.0 (C1) ppm.

Data consistent with literature.[165]

Synthesis of (S)-2-hydroxypentan-3-one (3.81)

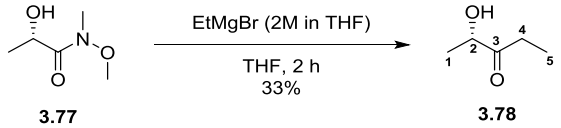

3.77 **3.78**

To a solution of **3.77** (20.03 g, 1 equiv) in Et_2O (500 mL) at 0 °C, EtMgBr (3M in Et_2O, 90 mL, 1.5 equiv) was added dropwise and the reaction was allowed to warm to room temperature. After 2 h, the reaction was quenched with sat. aq. NH_4Cl solution (600 mL). The aqueous phase was extracted with Et_2O (200 mL) and CH_2Cl_2 (3×200 mL). The combined organic layers were dried over $MgSO_4$ and concentrated carefully at 750 mbar/30 °C. The crude oil was purified with column chromatography (1:1, Et_2O/pentane) to produce **3.78** as a colourless liquid (5.01 g, 33%).

^{1}H NMR (400 MHz, $CDCl_3$) δ 4.25 (qd, *J*=7.1, 4.6 Hz, 1H, H2), 3.56 (d, *J*=4.6 Hz, 1H, OH), 2.56 (dq, *J*=17.9, 7.3 Hz, 1H, H4'), 2.44 (dq, *J*=17.9, 7.3 Hz, 1H, H4''), 1.38 (d, *J*=7.1 Hz, 3H, H1), 1.12 (t, *J*=7.3 Hz, 3H, H5) ppm; **^{13}C NMR** (101 MHz, $CDCl_3$) δ 213.0 (C3), 72.4 (C2), 30.7 (C4), 19.9 (C1), 7.5 (C5) ppm.

Data consistent with literature.[253]

Synthesis of (S)-3-oxopentan-2-yl benzoate (3.79)

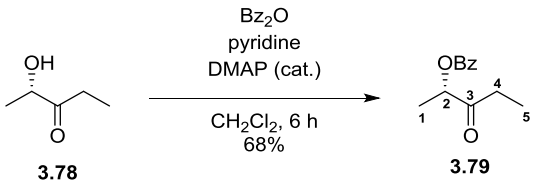

To a solution of **3.78** (4.74 g, 1 equiv) in CH_2Cl_2 (100 mL) was added benzoic anhydride (15.74 g, 1.5 equiv), DMAP (560 mg, 0.1 equiv) and *i*-$PrNEt_2$ (16.2 mL, 2 equiv). After 6 h, the reaction was quenched with water (250 mL) and the aqueous layer was extracted with CH_2Cl_2 (3×200 mL). The organic layers were combined, dried over $MgSO_4$ and the crude oil was purified by column chromatography (1:4, acetone/petrol ether 40–60 °C) to produce **3.79** as a colourless oil (6.50 g, 68%).

^{1}H NMR (400 MHz, $CDCl_3$) δ 8.15–8.06 (m, 2H, H_{Ar}), 7.66–7.57 (m, 1H, H_{Ar}), 7.53–7.43 (m, 2H, H_{Ar}), 5.37 (q, *J*=7.0 Hz, 1H, H2), 2.67 (dq, *J*=18.3, 7.3 Hz, 1H, H4'), 2.54 (dq, *J*=18.3, 7.3 Hz, 1H, H4''), 1.54 (d, *J*=7.1 Hz, 3H, H1), 1.11 (t, *J*=7.3 Hz, 3H, H5) ppm; **^{13}C NMR** (101 MHz, $CDCl_3$) δ 208.5 (C3), 165.9 (C=O), 133.4 (C_{Ar}), 129.8 (C_{Ar}×2), 129.5 (C_{Ar}), 128.5 (C_{Ar}×2), 75.1 (C2), 31.5 (C4), 16.5 (C1), 7.2 (C5) ppm; **$[\alpha]_D$** 24.66 (c = 1.7, $CHCl_3$, 22°C).

Data consistent with literature.[165]

Synthesis of 3,3-difluoropentan-2-yl benzoate (3.80)

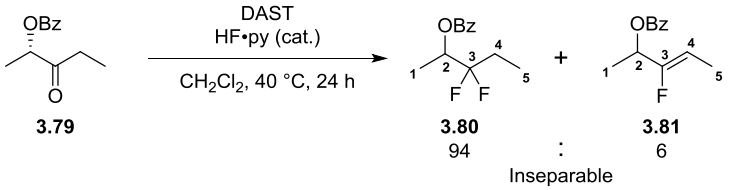

To a solution of **3.79** (5.0 g, 1 equiv) in CH_2Cl_2 (15 mL) was added DAST (6.4 mL, 2 equiv) dropwise at 0 °C. The reaction was heated to 40 °C and after 24 h, 10 drops of HF•py was added. The reaction was heated to 40 °C for 24 h, then cooled to 0 °C and quenched with sat. aq. $NaHCO_3$ until pH 7 is reached. The aqueous layer was then extracted with CH_2Cl_2 (3×75 mL), and the combined organic layers were dried over $MgSO_4$ and concentrated. The crude oil was purified by column chromatography (1:19, Et_2O/pentane) to afford **3.80** and **3.81** as a mix of the inseparable products with a 94:6 ratio by ^{19}F NMR.

Data for 3.80: ^{1}H NMR (400 MHz, $CDCl_3$) δ 8.13–8.02 (m, 2H, H_{Ar}), 7.67–7.56 (m, 1H, H_{Ar}), 7.52–7.44 (m, 2H, H_{Ar}), 5.48–5.23 (m, 1H, H2), 2.10–1.83 (m, 2H, H4), 1.45 (d, *J*=6.6 Hz, 3H, H1), 1.07 (t, *J*=7.5 Hz, 3H, H5) ppm; **^{13}C NMR** (101 MHz, $CDCl_3$) δ 165.3 (C=O), 133.4 (C_{Ar}), 129.8 (C_{Ar}×2), 129.6 (C_{Ar}), 128.5 (C_{Ar}×2), 122.7 (dd, *J*=246.5, 242.8 Hz, C3), 70.0 (dd, *J*=34.5, 28.6 Hz, C2), 26.5 (t, *J*=24.9 Hz,

C4), 13.4 (t, *J*=2.9 Hz, C1), 5.7 (dd, *J*=6.6, 5.1 Hz, C5)ppm; **^{19}F NMR** (376 MHz, $CDCl_3$) δ -111.2– -112.2 (m, 1F, F3'), -113.8– -115.0 (m, 1F, F3'') ppm; **^{19}F NMR** (376 MHz, $CDCl_3$) δ -111.8 (d, *J*=250.6 Hz, 1F, F3'), -114.4 (d, *J*=251.42 Hz, 1F, F3'') ppm; **IR** (neat) 2990 (w), 2948 (w), 1723 (s), 1265 (s), 1097 (s), 965 (s) cm^{-1}; **HRMS** (ESI+) for $C_{12}H_{14}F_2NaO_2$ $[M+Na]^+$, calculated 251.0854, found 251.0853 (+0.5 ppm error).

Data for 3.81: ^{1}H NMR (400 MHz, $CDCl_3$) δ benzoyl group not visible due to overlap with major product, 5.63 (dq, *J*=17.6, 6.6 Hz, 1H, H2), 5.02 (dq, *J*=36.3, 6.8 Hz, 1H, H4), 1.65 (dd, *J*=7.2, 2.3 Hz, 1H, H5), 1.52 (d, *J*=6.7 Hz, 1H, H1) ppm; **^{13}C NMR** (101 MHz, $CDCl_3$) δ not visible due to low concentration; **^{19}F NMR** (376 MHz, $CDCl_3$) δ -126.4 (ddd, *J*=36.4, 17.3, 3.5 Hz, 1F) ppm; **^{19}F NMR** (376 MHz, $CDCl_3$) δ -126.4 (s, 1F) ppm; **HRMS** (ESI+) for $C_{12}H_{13}FNaO_2$ $[M+Na]^+$, calculated 231.0792, found 231.0791 (+0.4 ppm error).

Synthesis of 3,3-difluoropentan-2-ol (H7)

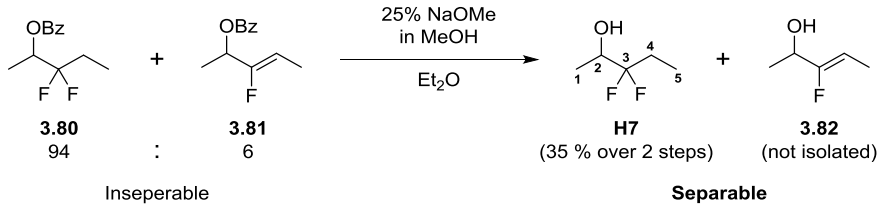

To a stirred solution of **3.80** and **3.81** in Et_2O (30 mL) was added NaOMe (25% w/w in MeOH, 11.0 mL). After 6 h, the reaction was neutralized with aq. HCl (1 M) until 7 pH. The aqueous layer was extracted with CH_2Cl_2 (3×30 mL) and the combined organic layers were dried over $MgSO_4$. The crude was carefully concentrated at 750 mbar/30 °C and purified by column chromatography (CH_2Cl_2) to afford **H7** as a colourless oil (1.05 g, 35% over 2 steps).

^{1}H NMR (400 MHz, $CDCl_3$) δ 3.93 (ddq, *J*=18.5, 8.7, 6.5 Hz, 1H, H2), 2.09–1.85 (m, 2H, H4), 1.85–1.80 (m, 1H, OH), 1.29 (d, *J*=6.6 Hz, 3H, H1), 1.06 (t, *J*=7.5 Hz, 3H, H5) ppm; **^{13}C NMR** (101 MHz, $CDCl_3$) δ 124.3 (t, *J*=243.9 Hz, C3), 68.9 (t, *J*=29.3 Hz, C2), 25.3 (t, *J*=24.9 Hz, C4), 16.1 (t, *J*=3.7 Hz, C1), 5.7 (t, *J*=5.5 Hz, C5) ppm; **^{19}F NMR** (376 MHz, $CDCl_3$) δ -113.7– -115.0 (m, 1F, F3'), -116.7 (ddt, *J*=246.2, 23.4, 12.1 Hz, 1F, F3'') ppm; **^{19}F NMR** (376 MHz, $CDCl_3$) δ -114.3 (d, *J*=246.2 Hz, 1F, F3'), -116.7 (d, *J*=246.2 Hz, 1F, F3'') ppm; **IR** (neat) 3356 (br. w), 2989 (w), 2949 (w), 2882 (w), 1468 (m), 1106 (s), 957 (s) cm^{-1}; **HRMS** (CI) for $C_5H_{11}F_2O$ $[M+H]^+$, calculated 125.0773, found 125.0777 (+0.48 ppm error).

Synthesis of but-3-en-1-yl benzoate (3.86)

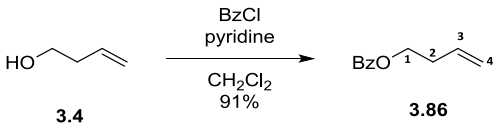

To a solution of 3-buten-1-ol **3.4** (500 mg, 1 equiv) and pyridine (1.12 mL, 2 equiv) in CH_2Cl_2 (10 mL) was added benzoyl chloride (0.97 mL, 1.2 equiv) dropwise. After 16 h, the reaction was quenched with water (30 mL) and layers were separated. The organic layer was washed with aq. 2M HCl (30 mL), sat. aq. $NaHCO_3$ (30 mL), brine and dried over $MgSO_4$. The crude mixture was concentrated *in vacuo* and purified by column chromatography (1:4, EtOAc/petroleum ether 40–60 °C) to yield **3.86** as a colourless oil (1.11 g, 91%).

^{1}H NMR (400 MHz, $CDCl_3$) δ 8.16–7.95 (m, 2H, H_{Ar}) 7.60–7.54 (m, 1H, H_{Ar}), 7.49–7.40 (m, 2H, H_{Ar}), 5.89 (ddt, *J*=17.1, 10.3, 6.7 Hz, 1H, H3), 5.19 (dq, *J*=17.2, 1.6 Hz, 1H, $H4_{cis}$), 5.14 (dq, *J*=10.3, 1.6 Hz, 1H, $H4_{trans}$), 4.39 (t, *J*=6.7 Hz, 2H, H1), 2.54 (qt, *J*=6.7, 1.3 Hz, 2H, H2) ppm; **^{13}C NMR** (101 MHz, $CDCl_3$) δ 166.6 (C=O), 134.0 (C3), 132.9 (C_{Ar}), 130.4 (C_{Ar}), 129.6 (C_{Ar}×2), 128.3 (C_{Ar}×2), 117.3 (C4), 64.0 (C1), 33.2 (C2) ppm.

Data consistent with literature.[254]

Attempted synthesis of tetrahydrofuran-3-yl benzoate (3.90)

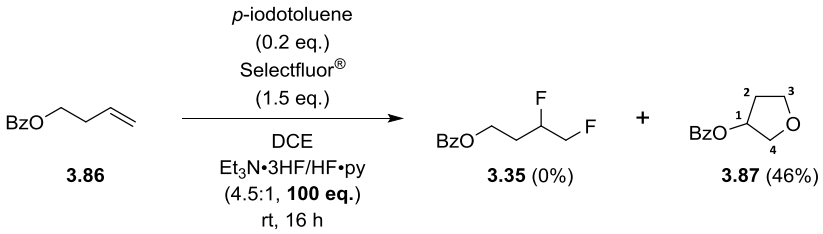

To a Teflon tube was added a solution of **3.86** (100 mg, 1 equiv) and *p*-iodotoluene (24 mg, 0.2 equiv) in DCE (1.3 mL). A solution of Et_3N•3HF (0.76 mL) and HF•Py (0.55 mL) was then added, followed by Selectfluor® (302 mg, 1.5 equiv). After 16 h, the reaction was quenched with sat. aq. $NaHCO_3$ until pH 7. The aqueous phase was extracted with CH_2Cl_2 (3×5 mL) and the combined organic layers were dried over $MgSO_4$. The crude mixture was concentrated and purified by column chromatography (1:4, acetone/petroleum ether 40–60 °C) to yield **3.87** as a colourless oil (0.50 mg, 46%).

Data for 3.87: ^{1}H NMR (400 MHz, $CDCl_3$) δ 8.20–7.97 (m, 2H, H_{Ar}), 7.66–7.54 (m, 1H, H_{Ar}), 7.51–7.42 (m, 2H, H_{Ar}), 5.57 (ddt, *J*=6.4, 4.3, 2.0Hz, 1H, H1), 4.08–3.96 (m, 3H, H3' + H4), 3.93 (td, *J*=8.3, 4.4 Hz, 1H, H3''), 2.37–2.24 (m, 1H, H2'), 2.23–2.12 (m, 1H, H2'') ppm; **^{13}C NMR** (101 MHz, $CDCl_3$) δ 166.3 (C=O), 133.1 (C_{Ar}), 130.0 (C_{Ar}), 129.63 (C_{Ar}×2), 128.4 (C_{Ar}×2), 75.4 (C1), 73.2 (C4), 67.2 (C3), 33.0 (C2) ppm.

Data consistent with literature.[255]

Synthesis of 4-tosyl(oxy)but-1-ene (3.96)

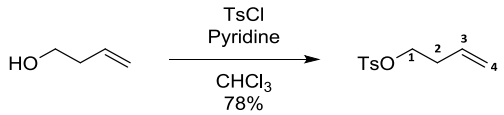

3.4 **3.96**

To a solution of 3-buten-1-ol **3.4** (500 mg, 1 equiv) and pyridine (1.12 mL, 2 equiv) in $CHCl_3$ (50 mL) was added a solution of tosyl chloride (1.58 g, 1.2 equiv) in $CHCl_3$ (5 mL) dropwise. After 16 h, the reaction was quenched with water (50 mL) and layers were separated. The organic layer was washed with aq. 2M HCl (2×50 mL), sat. aq. $NaHCO_3$ (50 mL), brine and dried over $MgSO_4$. The crude mixture was concentrated *in vacuo* and purified by column chromatography (1:4, acetone/petroleum ether 40–60 °C) to yield **3.96** as a colourless oil (1.22 g, 78%).

^{1}H NMR (400 MHz, $CDCl_3$) δ 7.84–7.76 (m, 2H, H_{Ar}), 7.38–7.33 (d, *J*=7.9 Hz, 2H, H_{Ar}), 5.68 (ddt, *J*=17.1, 10.3, 6.7 Hz, 1H, H3), 5.12–5.08 (m, 2H, H4), 4.07 (t, *J*=6.8 Hz, 2H, H1), 2.46 (s, 3H, PhC$\underline{H}_3$), 2.41 (qt, *J*=6.7, 1.3 Hz, 2 H, H2) ppm; **^{13}C NMR** (101 MHz, $CDCl_3$) δ 144.7 (C_{Ar}), 133.2 (C_{Ar}), 132.4 (C3), 129.8 (C_{Ar}×2), 127.9 (C_{Ar}×2), 118.2 (C4), 69.4 (C1), 33.1 (C2), 21.6 (Ph$\underline{C}H_3$) ppm.
Data consistent with literature.[167]

8.3 Synthesis of targets using fluorinated building blocks

Synthesis of 4-(Trimethylsilyloxy)-1-penten (4.17)

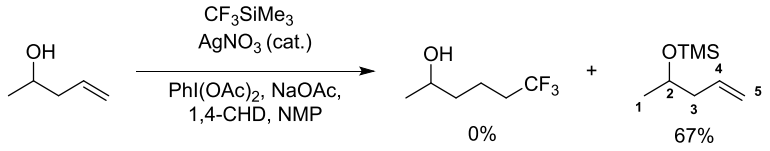

4.1 **K1** (expected) **4.17** (observed)

To a round bottom flask was added (diacetoxyiodo)benzene (3.74 g, 2 equiv), NaOAc (0.95 g, 2 equiv) and $AgNO_3$ (0.11 mg, 0.1 equiv) under an inert atmosphere. NMP (1.74 mL), **4.1** (0.5 g, 1 equiv), 1,4-cyclohexadiene (1.10 mL, 1 equiv) and CF_3SiMe_3 (3.43 mL, 4 equiv) were then added. After 6 h, a second portion of CF_3SiMe_3 (3.43 mL, 4 equiv), (diacetoxyiodo)benzene (3.74 g, 2 equiv), NaOAc (0.95 g, 2 equiv) and 1,4-cyclohexadiene (1.10 mL, 1 equiv) was added. After 16 h, the reaction was filtered over a pad of Celite, diluted with Et_2O (100 mL) and washed with water (100 mL), brine and dried over $MgSO_4$. The crude is then purified *via* column chromatography (1:1, CH_2Cl_2/pentane) to afford a **4.17** as a colourless oil (0.61 g, 67%).

^{1}H NMR (400 MHz, $CDCl_3$) δ 5.80 (ddt, *J*=17.2, 10.1, 7.1 Hz, 1H, H4), 4.99-5.09 (m, 2H, H5), 3.83 (sxt, *J*=6.1 Hz, 1H, H2), 2.09-2.30 (m, 2H, H3), 1.15 (d, *J*=6.1 Hz, 3H, H1), 0.12 ppm (s, 9H, $Si(CH_3)_3$) ppm; **^{13}C NMR** (101 MHz, $CDCl_3$) δ 135.5 (C4), 116.6 (C5), 68.3 (C2), 44.1 (C3), 23.4 (C1), 0.2 ($Si(CH_3)_3$) ppm.

Data consistent with literature.[256]

Synthesis of pent-4-en-2-yl benzoate (4.18)

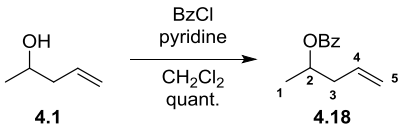

To a solution pent-4-ene-2-ol **4.1** (0.60 mL, 1 equiv) and pyridine (1.4 mL, 3 equiv) in CH_2Cl_2 (20 mL), benzoyl chloride (1.01 mL, 1 equiv) was added dropwise at 0 °C. The reaction was allowed to warm to room temperature and after 16 h, the reaction mixture was diluted with CH_2Cl_2 (10 mL) and quenched with aq. HCl (2 M, 10 mL). The organic layer was collected and washed with sat. aq. $NaHCO_3$ (10 mL) and brine, before being dried over $MgSO_4$ and concentrated *in vacuo*. The crude oil was purified by flash column chromatography (1:9, EtOAc/petroleum ether 40-60 °C) to afford **4.18** as a colourless oil (1.22 g, quant.).

^{1}H NMR (400 MHz, $CDCl_3$) δ 8.09–8.02 (m, 2H, H_{Ar}), 7.59–7.52 (m, 1H, H_{Ar}), 7.49–7.41 (m, 2H, H_{Ar}), 5.85 (ddt, *J*=17.1, 10.1, 7.1 Hz, 1H, H4), 5.23 (sxt, *J*=6.3 Hz, 1H, H1), 5.15 (dq, *J*=17.1, 1.5 Hz, 1H, $H5_{cis}$), 5.10 (ddt, *J*=10.1, 1.9, 1.0 Hz, 1H, $H5_{trans}$), 2.59–2.35 (m, 2H, H3), 1.37 (d, *J*=6.4 Hz, 3H, H1) ppm; **^{13}C NMR** (101 MHz, $CDCl_3$) δ 166.1 (C=O), 133.6 (C4), 132.7 (C_{Ar}), 130.8 (C_{Ar}), 129.5 (C_{Ar}×2), 128.3 (C_{Ar}×2), 117.9 (C5), 70.7 (C2), 40.4 (C3), 19.6 (C1) ppm.

Proton consistent with literature.[257] No carbon available.

Synthesis of 6,6,6-trifluorohexan-2-yl benzoate (4.19)

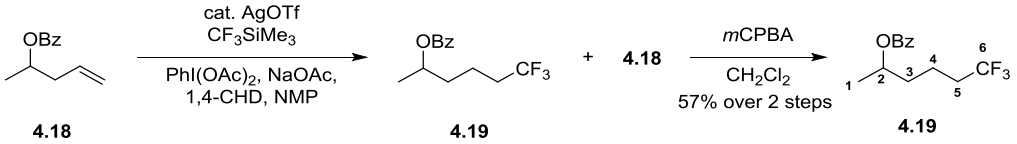

To a round bottom flask was added (diacetoxyiodo)benzene (2.13 g, 2 equiv), NaOAc (0.54 g, 2 equiv) and AgOTf (85 mg, 0.1 equiv) under an inert atmosphere. NMP (9.94 mL), **4.18** (0.63 g, 1 equiv), 1,4-cyclohexadiene (0.31 mL, 1 equiv) and CF_3SiMe_3 (1.95 mL, 4 equiv) were then added. After 6 h, a second portion of CF_3SiMe_3 (1.95 mL, 4 equiv), (diacetoxyiodo)benzene (2.13 g, 2 equiv), NaOAc (0.54 g, 2 equiv) and 1,4-cyclohexadiene (0.31 mL, 1 equiv) was added. After 16 h, the reaction was filtered over a pad of Celite, diluted with Et_2O (100 mL) and washed with water (100 mL), 2M HCl (100 mL), brine and dried over $MgSO_4$. The crude is then purified *via* column chromatography (1:19, EtOAc/petroleum ether 40-60 °C) to afford a mixture of the desired product and starting material.

The inseparable mixture of **4.19** (546 mg) and **4.18** (174 mg, 1 equiv) was dissolved in CH_2Cl_2 (20 mL) before the addition of *m*CPBA (0.39 g, 1.25 equiv). After 16 h, the reaction was quenched with sat. aq. $NaHCO_3$ (30 mL), the aqueous layer was extracted with CH_2Cl_2 (3×20 mL). The combined organic layers were washed with brine and dried over $MgSO_4$, before purification *via* column chromatography (1:19, EtOAc/petroleum ether 40-60 °C) to afford **4.19** as a colourless oil (480 mg, 57% over 2 steps).

^{1}H NMR (400 MHz, $CDCl_3$) δ 8.06–8.02 (m, 2H, H_{Ar}), 7.61–7.53 (m, 1H, H_{Ar}), 7.50–7.41 (m, 2H, H_{Ar}), 5.25–5.12 (m, 1H, H2), 2.24–2.04 (m, 2H, H5), 1.91–1.61 (m, 4H, H3 + H4), 1.38 (d, *J*=6.4 Hz, 3H, H1) ppm; **^{13}C NMR** (101 MHz, $CDCl_3$) δ 166.1 (C=O), 132.9 (C_{Ar}), 130.5 (C_{Ar}), 129.5 (C_{Ar}×2), 128.4 (C_{Ar}×2), 127.0 (q, *J*=275.1 Hz, C6), 70.7 (C2), 35.0 (C3), 33.5 (q, *J*=28.6 Hz, C5), 20.0, (C1), 18.0 (q, *J*=2.9 Hz, C4) ppm; **^{19}F NMR** (376 MHz, $CDCl_3$) δ -66.6 (t, *J*=10.4 Hz, 3F) ppm; **^{19}F {^{1}H} NMR** (376 MHz, $CDCl_3$) δ -66.6 (s, 3F) ppm; **IR** (neat) 2979 (w), 2953 (w), 1714 (s) 1271 (s), 1251 (m), 1110 (s), 711 (s) cm^{-1}; **HRMS** (ESI+) for $C_{13}H_{15}F_3NaO_2$ $[M+Na]^+$, calculated 283.0916, found 283.0921 (-1.6 ppm error)

Synthesis of 6,6,6-trifluorohexan-2-ol (K1)

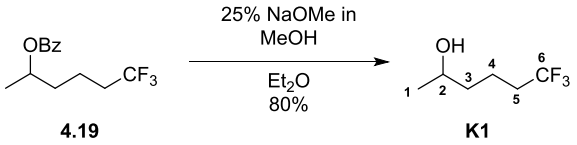

4.19 **K1**

To a solution of **4.19** (0.54 g, 1 equiv) in Et_2O (20 mL), NaOMe (25% in MeOH, 0.95 mL, 2 equiv) was added. After 18 h, the reaction was quenched with aq. HCl (1M) until pH 7. The aqueous layer was extracted with CH_2Cl_2 (3×30 mL), and the organic phases were collected and dried over $MgSO_4$. The crude was carefully concentrated at 750 mbar/30 °C and purified by column chromatography (100% to 9:1, CH_2Cl_2/Et_2O) to afford **K1** as a pale-yellow oil (259 mg, 80%).

^{1}H NMR (400 MHz, $CDCl_3$) δ 3.83 (sxt, *J*=6.1 Hz, 1H, H2), 2.12 (qt, J=10.9, 7.9 Hz, 2H, H5), 1.81–1.45 (m, 5H, H3 + H4 + OH), 1.23 (d, *J*=6.2 Hz, 3H, H1) ppm; **^{13}C NMR** (101 MHz, $CDCl_3$) δ 127.1 (q, *J*=276.6 Hz, C6), 67.6 (C2), 37.9 (C3), 33.7 (q, *J*=28.6 Hz, C5), 23.7 (C1), 18.3 (q, *J*=2.9 Hz, C4) ppm; **^{19}F NMR** (376 MHz, $CDCl_3$) δ -66.7 (t, *J*=10.4 Hz, 3F) ppm; **^{19}F {^{1}H} NMR** (376 MHz, $CDCl_3$) δ -66.7 (s, 3F) ppm; **IR** (neat) 3345 (br. w), 2971 (w), 2884 (w), 1248 (m), 1137 (s), 1044 (m), 974 (m) cm^{-1}; **HRMS** (CI) for $C_6H_{12}F_3O$ $[M+H]^+$, calculated 157.0835, found 157.0842 (+0.68 ppm error).

Synthesis of but-3-en-2-yl benzoate (4.20)

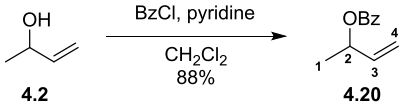

To a solution 3-buten-2-ol **4.2** (1.20 mL, 1 equiv) and pyridine (3.35 mL, 3 equiv) in CH_2Cl_2 (20 mL), benzoyl chloride (2.41 mL, 1.5 equiv) was added dropwise at 0 °C. The reaction was allowed to warm to room temperature and after 16 h, was diluted with CH_2Cl_2 (10 mL) and quenched with aq. HCl (2 M, 20 mL). The organic layer was collected washed with sat. aq. $NaHCO_3$ (20 mL) and brine before being dried over $MgSO_4$ and concentrated *in vacuo*. The crude oil was purified by flash column chromatography (1:19, EtOAc/petroleum ether 40-60 °C) to afford **4.20** as a colourless oil (2.15 g, 88%).

^{1}H NMR (400 MHz, $CDCl_3$) δ 8.18–8.02 (m, 2H, H_{Ar}), 7.61–7.52 (m, 1H, H_{Ar}), 7.50–7.39 (m, 2H, H_{Ar}), 5.98 (ddd, *J*=17.2, 10.5, 5.7 Hz, 1H, H3), 5.62 (quint, *J*=6.3, 1.3 Hz, 1H, H2), 5.35 (dt, *J*=17.3, 1.3 Hz, 1H, $H4_{cis}$), 5.20 (dt, *J*=10.5, 1.2 Hz, 1H, $H4_{trans}$), 1.46 (d, *J*=6.6 Hz, 3H, H1) ppm; **^{13}C NMR** (101 MHz, $CDCl_3$) δ 165.8 (C=O), 137.7 (C3), 132.8 (C_{Ar}), 130.6 (C_{Ar}), 129.6 (C_{Ar}×2), 128.3 (C_{Ar}×2), 115.8 (C4), 71.5 (C2), 20.1 (C1) ppm.

Data consistent with literature.[258]

Synthesis of 5,5,5-trifluoropentan-2-yl benzoate (4.22)

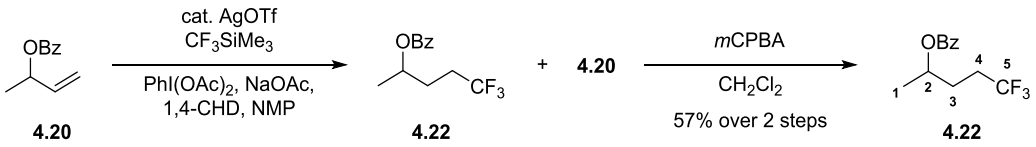

To a round bottom flask was added (diacetoxyiodo)benzene (7.32 g, 2 equiv), NaOAc (1.86 g, 2 equiv) and AgOTf (0.29 g, 0.1 equiv) under an inert atmosphere. NMP (34 mL), **4.20** (2 g, 1 equiv), 1,4-cyclohexadiene (1.07 mL, 1 equiv) and CF_3SiMe_3 (6.71 mL, 4 equiv) were then added. After 6 h, a second portion of CF_3SiMe_3 (6.71 mL, 4 equiv), (diacetoxyiodo)benzene (7.32 g, 2 equiv), NaOAc (1.86 g, 2 equiv) and 1,4-cyclohexadiene (1.07 mL, 1 equiv) was added. After 16 h, the reaction was filtered over a pad of Celite, diluted with Et_2O (100 mL) and washed with water (100 mL), 2M HCl (100 mL), brine and dried over $MgSO_4$. The crude is then purified *via* column chromatography (1:19, EtOAc/petroleum ether 40-60 °C) to afford a mixture of the desired product and starting material.

The inseparable mixture of **4.22** (2.10 g) and **4.20** (500 mg, 1 equiv) was dissolved in CH_2Cl_2 (40 mL) before the addition of *m*CPBA (1.13 g, 2 equiv). After 16 h, the reaction was quenched with sat. aq. $NaHCO_3$ (30 mL), the aqueous layer was extracted with CH_2Cl_2 (3×30 mL). The combined organic layers were washed with brine and dried over $MgSO_4$, before purification *via* column

chromatography (1:19, EtOAc/petroleum ether 40-60 °C) to afford **4.22** as a colourless oil (1.60 g, 57% over 2 steps).

^{1}H NMR (400 MHz, $CDCl_3$) δ 8.09–7.99 (m, 2H, H_{Ar}), 7.63–7.54 (m, 1H, H_{Ar}), 7.52–7.42 (m, 2H, H_{Ar}), 5.23 (sxt, *J*=6.4 Hz, 1H, H2), 2.37–2.10 (m, 2H, H4), 2.06–1.87 (m, 2H, H3), 1.41 (d, *J*=6.2 Hz, 3H, H1) ppm; **^{13}C NMR** (101 MHz, $CDCl_3$) δ 165.9 (C=O), 133.0 (C_{Ar}), 130.2 (C_{Ar}), 129.5 (C_{Ar}×2), 128.4 (C_{Ar}×2), 126.9 (q, *J*=275.8 Hz, C5), 69.8 (C2), 30.2 (q, *J*=29.1 Hz, C4), 28.4 (q, *J*=2.9 Hz, C3), 20.0 (C1) ppm; **^{19}F NMR** (376 MHz, $CDCl_3$) δ -66.8 (t, *J*=10.4 Hz, 3F) ppm; **^{19}F {^{1}H} NMR** (376 MHz, $CDCl_3$) δ -66.8 (s, 3F) ppm; **IR** (neat) 2983 (w), 2939 (w), 1716 (s), 1243 (m), 1025 (s) cm^{-1}; **HRMS** (ESI+) for $C_{12}H_{13}F_3NaO_2$ $[M+Na]^+$, calculated 269.0760, found 269.0757 (+0.9 ppm error).

Synthesis of 5,5,5-trifluoropentan-2-ol (H9)

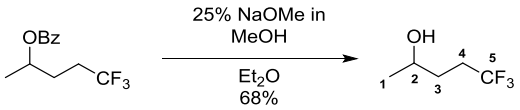

4.22 **H9**

To a solution of **4.22** (1.49 g, 1 equiv) in Et_2O (30 mL), NaOMe (25% in MeOH, 2.76 mL, 2 equiv) was added. After 18 h, the reaction was quenched with aq. HCl (1M) until pH 7. The aqueous layer was extracted with CH_2Cl_2 (3×10 mL), and the organic phases were collected and dried over $MgSO_4$. The crude was carefully concentrated at 750 mbar/30 °C and purified by column chromatography (100% to 9:1, CH_2Cl_2/Et_2O) to afford **H9** as a pale-yellow oil (583 mg, 68%).

^{1}H NMR (400 MHz, $CDCl_3$) δ 3.87 (br. sxt, *J*=6.2 Hz, 1H, H2), 2.40–2.23 (m, 1H, H4'), 2.23–2.07 (m, 1H, H4''), 1.80–1.57 (m, 2H, H3), 1.39 (br. s, 1H, OH), 1.25 (d, *J*=6.2 Hz, 3H, H1) ppm; **^{13}C NMR** (101 MHz, $CDCl_3$) δ 127.3 (q, *J*=275.8 Hz, C5), 66.6 (C2), 31.1 (q, *J*=2.9 Hz, C3), 30.2 (q, *J*=28.9 Hz, C4), 23.7 (C1) ppm; **^{19}F NMR** (376 MHz, $CDCl_3$) δ -66.6 (t, *J*=10.4 Hz, 3F) ppm; **^{19}F {^{1}H} NMR** (376 MHz, $CDCl_3$) δ -66.6 (s, 3F) ppm; **IR** (neat) 3354 (br. w), 2974 (w), 2879 (w), 1252(s), 1152(m), 1035 (s) cm^{-1}; **HRMS** (CI) for $C_5H_{10}F_3O$ $[M+H]^+$, calculated 143.06783, found 143.0726 (-0.56 ppm error).

Synthesis of pent-1-en-3-yl benzoate (4.21)

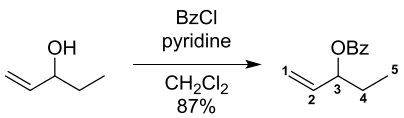

4.3 **4.21**

To a solution 1-penten-3-ol **4.3** (1.19 mL g, 1 equiv) and pyridine (2.8 mL, 3 equiv) in CH_2Cl_2 (20 mL), benzoyl chloride (2.02 mL, 1 equiv) was added dropwise at 0 °C. The reaction was allowed to warm to room temperature and after 16 h, was diluted with CH_2Cl_2 (10 mL) and quenched with aq. HCl (2 M, 20 mL). The organic layer was collected, washed with sat. aq. $NaHCO_3$ (10 mL) and brine before being dried over $MgSO_4$ and concentrated *in vacuo*. The crude oil was purified by flash column

chromatography (1:19, EtOAc/petroleum ether 40-60 °C) to afford **4.21** as a colourless oil (1.93 g, 87%).

^{1}H NMR (400 MHz, $CDCl_3$) δ 8.16–7.95 (m, 2H, H_{Ar}), 7.62–7.51 (m, 1H, H_{Ar}), 7.50–7.41 (m, 2H, H_{Ar}), 5.90 (ddd, *J*=17.1, 10.7, 6.2 Hz, 1H, H2), 5.45 (qt, *J*=6.2, 1.2 Hz, 1H, H3), 5.34 (dt, *J*=17.3, 1.3 Hz, 1H, $H1_{cis}$), 5.23 (dt, *J*=10.6, 1.2 Hz, 1H, $H1_{trans}$), 1.90–1.72 (m, 2H, H4), 1.00 (t, *J*=7.4 Hz, 3H, H5) ppm; **^{13}C NMR** (101 MHz, $CDCl_3$) δ 165.9 (C=O), 136.3 (C1), 132.8 (C_{Ar}), 130.6 (C_{Ar}), 129.6 (C_{Ar}×2), 128.3 (C_{Ar}×2), 116.7 (C1), 76.4 (C3), 27.3 (C4), 9.4 (C5) ppm.

Proton consistent with literature.[259] No carbon available.

Synthesis of 6,6,6-trifluorohexan-3-yl benzoate (4.23)

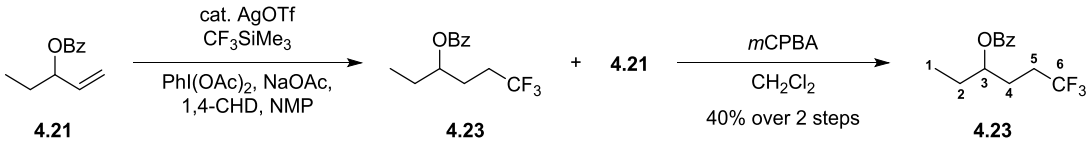

To a round bottom flask was added (diacetoxyiodo)benzene (5.08 g, 2 equiv), NaOAc (1.29 g, 2 equiv) and AgOTf (0.20 g, 0.1 equiv) under an inert atmosphere. NMP (23 mL), **4.21** (1.5 g, 1 equiv), 1,4-cyclohexadiene (0.75 mL, 1 equiv) and CF_3SiMe_3 (4.66 mL, 4 equiv) were then added. After 6 h, a second portion of CF_3SiMe_3 (4.66 mL, 4 equiv), (diacetoxyiodo)benzene (5.08 g, 2 equiv), NaOAc (1.29 g, 2 equiv) and 1,4-cyclohexadiene (0.75 mL, 1 equiv) was added. After 16 h, the reaction was filtered over a pad of Celite, diluted with Et_2O (100 mL) and washed with water (100 mL), 2M HCl (100 mL), brine and dried over $MgSO_4$. The crude is then purified *via* column chromatography (1:19, EtOAc/petroleum ether 40-60 °C) to afford a mixture of the desired product and starting material.

The inseparable mixture of **4.23** (1.39 g) and **4.21** (470 mg, 1 equiv) was dissolved in CH_2Cl_2 (40 mL) before the addition of *m*CPBA (1.02 g, 2 equiv). After 16 h, the reaction was quenched with sat. aq. $NaHCO_3$ (30 mL), the aqueous layer was extracted with CH_2Cl_2 (3×30 mL). The combined organic layers were washed with brine and dried over $MgSO_4$, before purification *via* column chromatography (1:19, EtOAc/petroleum ether 40-60 °C) to afford **4.23** as a colourless oil (0.82 g, 40% over 2 steps).

^{1}H NMR (400 MHz, $CDCl_3$) δ 8.08–8.05 (m, 2H, H_{Ar}), 7.62–7.56 (m, 1H, H_{Ar}), 7.51–7.43 (m, 2H, H_{Ar}), 5.14 (quin, *J*=6.2 Hz, 1H, H3), 2.29–2.11 (m, 2H, H5), 2.00–1.92 (m, 2H, H4), 1.87–1.63 (m, 2H, H2), 0.99 (t, *J*=7.5 Hz, 3H, H1) ppm; **^{13}C NMR** (101 MHz, $CDCl_3$) δ 166.2 (C=O), 133.1 (C_{Ar}), 130.1 (C_{Ar}), 129.6 (C_{Ar}×2), 128.4 (C_{Ar}×2), 127.0 (q, *J*=275.8 Hz, C6), 74.3 (C3), 30.2 (q, *J*=28.9 Hz, C5), 27.1 (C2), 26.2 (q, *J*=2.9 Hz, C4), 9.5 (C1) ppm; **^{19}F NMR** (376 MHz, $CDCl_3$) δ -66.8 (t, *J*=10.4 Hz, 3F) ppm; **^{19}F {^{1}H} NMR** (376 MHz, $CDCl_3$) δ -66.8 (s, 3F) ppm; **IR** (neat) 2972 (w), 2941 (w), 1716 (s), 1252 (m),

1098 (s) cm^{-1}; **HRMS** (ESI+) for $C_{13}H_{15}F_3NaO_2$ $[M+Na]^+$, calculated 283.0916, found 283.0914 (+0.7 ppm error).

Synthesis of 6,6,6-trifluorohexan-3-ol (J2)

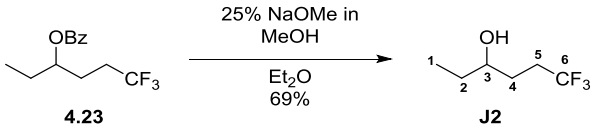

4.23 **J2**

To a solution of **4.23** (0.77 g, 1 equiv) in Et_2O (30 mL), NaOMe (25% in MeOH, 1.77 mL, 2 equiv) was added. After 18 h the reaction was quenched with aq. HCl (1M) until pH 7. The aqueous layer was extracted with CH_2Cl_2 (3×10 mL), and the organic phases were collected and dried over $MgSO_4$. The crude was carefully concentrated at 750 mbar/30 °C and purified by column chromatography (100% to 9:1, CH_2Cl_2/Et_2O) to afford **J2** as a pale-yellow oil (319 mg, 69%).

^{1}H NMR (400 MHz, $CDCl_3$) δ 3.65–3.53 (m, 1H, H3), 2.43-2.25 (m, 1H, H5'), 2.24–2.07 (m, 1H, H5''), 1.83–1.70 (m, 1H, H4'), 1.68–1.57 (m, 1H, H4''), 1.57–1.45 (m, 2H, H2), 1.38 (br. d, *J*=4.8 Hz, 1H, OH), 0.97 (t, *J*=7.5 Hz, 3H, H1) ppm; **^{13}C NMR** (101 MHz, $CDCl_3$) δ 127.4 (q, *J*=276.1 Hz, C6), 71.9 (C3), 30.4 (C2), 30.2 (q, *J*=28.6 Hz, C5), 28.9 (q, *J*=2.9 Hz, C4), 9.8 (C1) ppm; **^{19}F NMR** (376 MHz, $CDCl_3$) δ -66.6 (t, *J*=10.4 Hz, 3F) ppm; **^{19}F {^{1}H} NMR** (376 MHz, $CDCl_3$) δ -66.6 (s, 3F) ppm; **IR** (neat) 3350 (br. w), 2969 (w), 2883 (w), 1252 (m), 1149 (m), 1104 (m), 1042 (m) cm^{-1}; **HRMS** (CI) for $C_6H_{12}F_3O$ $[M+H]^+$, calculated 157.0835, found 157.0826 (-0.90 ppm error).

Trityl-(but-3-en-1-yl)-aether (4.25)

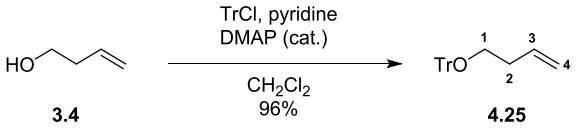

3.4 **4.25**

To a solution 3-buten-1-ol **3.4** (0.80 g, 1 equiv) and pyridine (1.35 mL, 1.05 equiv) in CH_2Cl_2 (33 mL), was added trityl chloride (3.40 g, 1.1 equiv). After 20 h, the reaction mixture was washed with sat. aq. NaHCO3 (2×30 mL), water and brine. The organic layer was dried over $MgSO_4$ and concentrated *in vacuo*. The crude oil was purified by flash column chromatography (1:19, CH_2Cl_2/petroleum ether 40-60 °C) to **4.25** as a colourless oil (3.34 g, 96%).

^{1}H NMR (400 MHz, $CDCl_3$) δ 7.50–7.43 (m, 6H, H_{Ar}), 7.34–7.27 (m, 6H, H_{Ar}), 7.26–7.20 (m, 3H, H_{Ar}), 5.86 (ddt, *J*=17.1, 10.2, 6.8 Hz, 1H, H3), 5.13–4.98 (m, 2H, H4), 3.13 (t, *J*=6.8 Hz, 2H, H1), 2.38 (q, *J*=6.8 Hz, 2H, H2) ppm; **^{13}C NMR** (101 MHz, $CDCl_3$) δ 144.3 (C_{Ar}×3), 135.6 (C3), 128.7 (C_{Ar}×6), 127.7 (C_{Ar}×6), 126.9 (C_{Ar}×3), 116.3 (C4), 86.4 ($\underline{C}Ph_3$), 63.2 (C1), 34.6 (C2) ppm; **IR** (neat) 3058 (w), 2924 (w), 1448 (s), 1068 (s), 695 (s) cm^{-1}; **HRMS** (EI) for $C_{23}H_{22}O$ $[M^{\cdot+}]$, calculated 314.1665, found 314.1656 (-0.97 ppm error).

3,5,5,5-tetrafluoropentyl trityl ether (4.26)

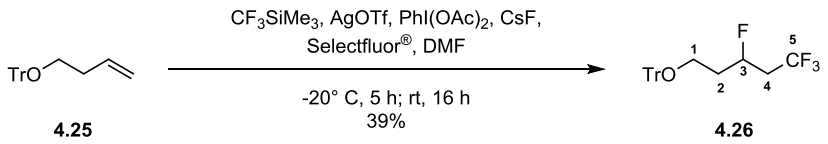

4.25 **4.26**

To a solution of Selectfluor® (6.08 g, 3 equiv) in DMF (70 mL) was added $PhI(OAc)_2$ (1.85 g, 1 equiv), AgOTf (2.94 g, 2 equiv) and CsF (1.73 g, 2 equiv) at -50 °C. A solution of **4.25** (1.80 g, 1 equiv) in DMF (10 mL) was added, followed by CF_3SiMe_3 (2.52 mL, 3 equiv). The reaction was allowed to warm to -20 °C and after 5 h was allowed to warm to room temperature. After 16 h, the reaction was quenched with water (80 mL) and the aqueous phase was extracted with Et_2O (3×100 mL). The combined organic phases were washed with water, brine, dried over Na_2SO_4 and concentrated. The crude oil was purified by flash column chromatography (1:4, CH_2Cl_2/petroleum ether 40-60 °C) to **4.26** as a colourless oil (0.90 g, 39%).

^{1}H NMR (400 MHz, $CDCl_3$) δ 7.52–7.45 (m, 6H, H_{Ar}), 7.39–7.32 (m, 6H, H_{Ar}), 7.31–7.26 (m, 3H, H_{Ar}), 5.12 (dtt, *J*=49.0, 8.0, 4.0 Hz, 1H, H3), 3.39–3.20 (m, 2H, H1), 2.63–2.24 (m, 2H, H4), 2.11–1.81 (m, 2H, H2) ppm; **^{13}C NMR** (101 MHz, $CDCl_3$) δ 143.9 (C_{Ar} x 3), 128.5 (C_{Ar} x 6), 127.8 (C_{Ar} x 6), 127.1 (C_{Ar} x 3), 125.4 (qd, *J*=277.3, 2.9 Hz, C5), 86.9 ($\underline{C}Ph_3$), 85.4 (dq, *J*=172.1, 3.3 Hz, C3), 58.8 (d, *J*=5.1 Hz, C1), 39.4 (qd, *J*=28.5, 22.4 Hz, C4), 35.4 (d, *J*=21.3 Hz, C2) ppm; **^{19}F NMR** (376 MHz, $CDCl_3$) δ -64.2 (q, *J*=10.4 Hz, 3F, F5), -183.4–-182.9 (m, 1F, F3) ppm; **^{19}F {^{1}H} NMR** (376 MHz, $CDCl_3$) δ -64.2 (d, *J*=8.1 Hz, 3F, F5), -183.2 (q, *J*=8.1 Hz, 1F, F3) ppm; **IR** (neat) 3059 (w), 2932 (w), 1449 (s), 1256 (s), 1135 (s), 1072 (s), 697 (s) cm^{-1}; **HRMS** (EI) for $C_{24}H_{22}F_4O$ [$M^{\cdot+}$], calculated 402.1601, found 402.1617 (+0.47 ppm error).

3,5,5,5-tetrafluoropentan-1-ol (I9)

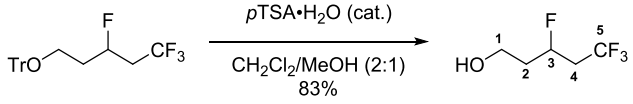

4.26 **I9**

To a solution of **4.26** (0.90 g, 1 equiv) in CH_2Cl_2 (4.4 mL) and MeOH (2.2 mL), *p*-TsOH•H_2O (207 mg, 0.05 equiv) was added. After 16 h, the reaction was quenched with sat. aq $NaHCO_3$ (5 mL). The aqueous layer was extracted with CH_2Cl_2 (3×5 mL) and the organic phases were collected washed with brine and dried over Na_2SO_4. The crude was carefully concentrated at 750 mbar/30 °C and was purified by column chromatography (CH_2Cl_2) to afford **I9** as a colourless oil (298 mg, 83%).

^{1}H NMR (400 MHz, $CDCl_3$) δ 5.07 (dtt, *J*=49.0, 8.5, 3.7 Hz, 1H, H3), 3.86 (dt, *J*=6.8, 5.0 Hz, 2H, H1), 2.69–2.31 (m, 2H, H4), 2.09–1.79 (m, 2H, H2), 1.47 (td, *J*=5.0, 0.7 Hz, 1H, OH) ppm; **^{13}C NMR** (101 MHz, $CDCl_3$) δ 125.4 (qd, *J*=276.6, 2.9 Hz, C5), 85.5 (dq, *J*=171.3, 3.3 Hz, C3), 58.2 (d, *J*=4.4 Hz, C1), 39.5 (qd, *J*=28.6, 22.7 Hz, C4), 37.4 (d, *J*=20.5 Hz, C2) ppm; **^{19}F NMR** (376 MHz, $CDCl_3$) δ -64.3 (td,

J=10.4, 7.4 Hz, 3F, F5), -184.3–-184.8 (m, 1F, F3) ppm; **^{19}F {^{1}H} NMR** (376 MHz, $CDCl_3$) δ -64.3 (d, *J*=7.4 Hz, 3F, F5), -184.5 (q, *J*=7.4 Hz, 1F, F3) ppm; **IR** (neat) 3364 (br. w), 2962 (w), 2898 (w), 1257 (s), 1151 (s), 1130 (s), 1053 (s) cm^{-1}; **HRMS** (CI) for $C_5H_9F_4O$ $[M+H]^+$, calculated 161.0584, found 161.0555 (-2.90 ppm error).

Synthesis of Togni Reagent II (4.27)

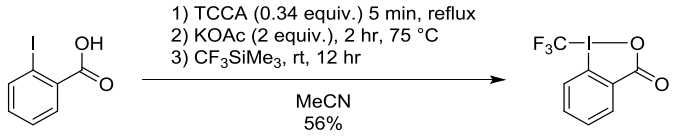

4.29 **4.27**

To a solution of 2-iodobenzoic acid (4.8 g, 1 equiv) in MeCN (40 mL) at 75 °C, was added a solution of TCCA (1.53 g, 0.34 equiv) in MeCN (10 mL) dropwise. After 5 min, the reaction was allowed to cool to room temperature and KOAc (3.8 g, 2 equiv) was added. The reaction was then heated to 75 °C for 2 h. Once the reaction had cooled to room temperature, CF_3SiMe_3 (4 mL, 1.4 equiv) was added. After 14 h, MeCN (15 mL) was added and the reaction was brought to reflux, before filtering over a pad of Celite. The filtrate was then concentrated to 1/3 of its volume, cooled to -20 °C and filtered. The resultant crystals were washed with a small amount of cold MeCN. The filtrate for a second time was concentrated to 1/3 of its volume, cooled to -20 °C and filtered. The resultant crystals were washed with cold MeCN and combined with the first batch of crystals. The combined material was dried *in vacuo* to yield Togni Reagent II **4.27** as white crystals (3.45 g, 56%).

^{1}H NMR (400 MHz, $CDCl_3$) δ 8.49 (dd, *J*=7.0, 1.8 Hz, 1H, H_{Ar}), 7.88–7.74 (m, 3H, H_{Ar}) ppm; **^{19}F NMR** (376 MHz, $CDCl_3$) δ -34.3 (s, 3F) ppm.

Data consistent with literature.[260]

Synthesis of TEMPONa (4.31)

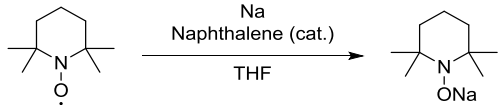

4.30 **4.31**

Under an inert atmosphere, freshly cleaned elemental sodium (320 mg, 2 equiv) was melted to form a mirror. Once cooled, THF (8 mL), naphthalene (89 mg, 0.1 equiv) were added followed by TEMPO (1.08 g, 1 equiv). After 2.5 h, the solution of TEMPONa was used directly in the next experiment with no further purification.

Synthesis of 2,2,6,6-tetramethyl-1-((1,1,1-trifluorohexan-3-yl)oxy)piperidine (4.32)

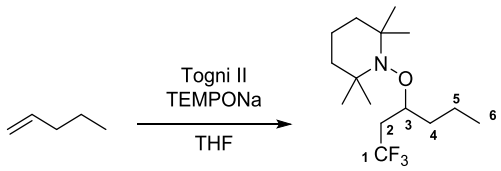

4.4 **4.32**

To a solution of 1-pentene (5.47 mL, 10 equiv) and Togni Reagent II (1.58 g, 1 equiv) in THF (10 mL), was added TEMPONa (7 mL, 1.2 equiv) *via* syringe pump over 2 h. After complete addition, the reaction was quenched with sat. aq. $NaHCO_3$ (100 mL) and the aqueous phase was extracted with CH_2Cl_2 (3×200 mL). The combined organic layers were dried over $NaSO_4$ and concentrated *in-vacuo*. The crude was purified by column chromatography (pentane) to afford **4.32** (~70% pure). The impure **4.32** was then taken to the next step with no further purification.

^{1}H NMR (400 MHz, $CDCl_3$) δ 4.18–4.07 (m, 1H, H3), 3.12–2.95 (m, 1H, H2'), 2.12–1.92 (m, 1H, H2''), 1.80–1.23 (m, 10H, H3 + H4 + TEMPO-$(CH_2)_3$), 1.14 (s, 6H, TEMPO-$(CH_3)_2$), 1.09 (s, 3H, TEMPO-CH_3), 1.06 (s, 3H, TEMPO-CH_3), 0.96 (t, *J*=7.2, 3H, H6) ppm; **^{19}F NMR** (376 MHz, $CDCl_3$) δ -62.8 (t, *J*=11.3 Hz, 3F) ppm; **^{19}F {^{1}H} NMR** (376 MHz, $CDCl_3$) δ -62.8 (s, 3F) ppm; **MS** (ESI+) m/z 297.4 $[M+H]^+$.

Synthesis of 1,1,1-trifluorohexan-3-ol (J1)

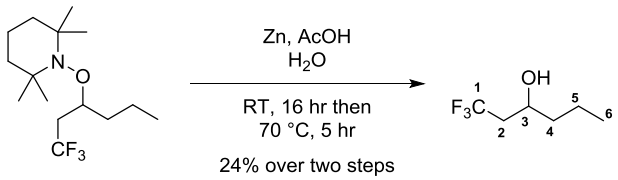

4.32 **J1**

The impure product **4.32** was dissolved in water (10 mL) and AcOH (31 mL) before the addition of Zn dust (1.11 g, 5 equiv) in two portions, 2 h apart. After 16 h, Zn dust (1.11 g, 5 equiv) was added in two portions, 2 h apart and the reaction was heated to 70 °C. After 5 h, the reaction was cooled to room temperature and NaOH powder was added till a pH of 14 was achieved. The resulting mixture was extracted with CH_2Cl_2 (3×200 mL) and the combined organic layers were dried over $MgSO_4$. The crude was carefully concentrated at 750 mbar/30 °C, before purification by column chromatography (100% to 9:1, CH_2Cl_2/Et_2O) to afford **J1** as a pale-yellow oil (187 mg, 24% over 2 steps).

^{1}H NMR (400 MHz, $CDCl_3$) δ 4.04 (tq, *J*=7.7, 4.0 Hz, 1H, H3), 2.38–2.15 (m, 2H, H2), 1.82 (d, *J*=4.2 Hz, 1H, OH), 1.58–1.30 (m, 4H, H4 + H5), 0.96 (t, *J*=6.8 Hz, 3H, H6) ppm; **^{13}C NMR** (101 MHz, $CDCl_3$) δ 126.5 (q, *J*=276.8 Hz, C1), 65.9 (q, *J*=2.9 Hz, C3), 41.1 (q, *J*=26.4 Hz, C2), 39.2 (C4), 18.4 (C5), 13.8 (C6) ppm; **^{19}F NMR** (376 MHz, $CDCl_3$) δ -63.8 (t, *J*=10.4 Hz, 3F) ppm; **^{19}F {^{1}H} NMR** (376 MHz, $CDCl_3$)

δ -63.8 (s, 3F) ppm; **IR** (neat) 3370 (br. w), 2964 (w), 2878 (w), 1251 (s), 1135 (s), 1086 (m) cm^{-1}; **HRMS** (CI) for $C_6H_{12}F_3O$ $[M+H]^+$, calculated 157.0835, found 157.0859 (+2.38 ppm error).

Allyl Benzyl Ether (4.7)

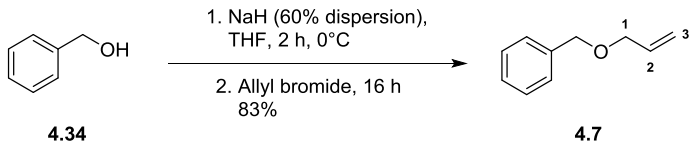

4.34 **4.7**

To NaH in 60% mineral oil (0.88 g, 1.2 equiv) in DMF (30 mL) was added a solution of benzyl alcohol (2 g, 1 equiv) in DMF (10 mL) dropwise at 0 °C. After 1 h, a solution of allyl bromide (3.36 g, 1.5 equiv) in DMF (5 mL) was added dropwise at 0 °C. The reaction was allowed to warm to room temperature and after 3 h was concentrated. The residue was dissolved in EtOAc (50 mL) and was then washed with brine (2×50 mL). The organic layer was then dried over Na2SO4, filtered and concentrated. The crude oil was purified with column chromatography (1:9, EtOAc/petrol ether 40 – 60 °C) to afford **4.7** as a colourless oil (2.27 g, 83%).

^{1}H NMR (400 MHz, $CDCl_3$) δ 7.44–7.27 (m, 5H), 5.98 (ddt, *J*=17.2, 10.4, 5.6 Hz, 1H, H2), 5.33 (qd, *J*=17.2, 1.7 Hz, 1H, $H3_{cis}$), 5.22 (dq, *J*=10.4, 1.4 Hz, 1H, $H3_{trans}$), 4.54 (s, 2H, Ph$C\underline{H}_2$), 4.05 (td, *J*=1.4, 5.6 Hz, 2H, H1) ppm; **^{13}C NMR** (101 MHz, $CDCl_3$) δ 138.3 (C_{Ar}), 134.7 (C2), 128.4 (C_{Ar}×2), 127.7 (C_{Ar}×2), 127.6 (C_{Ar}), 117.1 (C3), 72.1 (Ph$\underline{C}H_2$), 71.1 (C1) ppm.

Data consistent with literature.[261]

Synthesis of 1-(benzyloxy)-4,4,4-trifluorobutan-2-one (4.5) 1-(benzyloxy)-4,4,4-trifluorobutan-2-ol (4.35) and 4,4,4-trifluoro-2-hydroxybutyl benzoate (4.36)

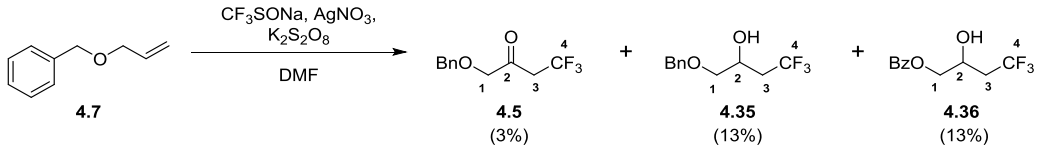

4.7 **4.5** (3%) **4.35** (13%) **4.36** (13%)

To a solution of **4.7** (0.1 g, 1 equiv) in DMF (8 mL), was added CF_3SO_2Na, $AgNO_3$ and $K_2S_2O_8$. After 24 h, the reaction mixture was diluted with Et_2O (10 mL) and filtered over a pad of Celite. The solution was then washed with water (15 mL). The aqueous phase was extracted with Et_2O (3×10 mL), dried over Na_2SO_4 and concentrated. The crude oil was purified by column chromatography (15:85, Et_2O/hexane) to yield **4.5** as a colourless oil (5 mg, 3%), **4.35** as a colourless oil (20 mg, 13%) and **4.36** as a colourless oil (20 mg, 13%).

Data for 4.35: ^{1}H NMR (400 MHz, $CDCl_3$) δ 7.47–7.28 (m, 5H, H_{Ar}), 4.61 (s, 2H, Ph$C\underline{H}_2$), 4.10 (s, 2H, H1), 3.40 (q, *J*=10.3 Hz, 2H, H3) ppm; **^{13}C NMR** (101 MHz, $CDCl_3$) δ 198.8 (q, *J*=2.9 Hz, C2), 136.5 (C_{Ar}), 128.6 (C_{Ar}×2), 128.3 (C_{Ar}), 128.0 (C_{Ar}×2), 123.6 (q, *J*=276.6 Hz, C4), 74.9 (q, *J*=2.2 Hz, C1), 73.6

(Ph<u>C</u>H$_2$), 42.7 (q, *J*=29.1 Hz, C3) ppm; **^{19}F NMR** (376 MHz, $CDCl_3$) δ -62.6 (t, *J*=9.5 Hz, 3F) ppm; **^{19}F {^{1}H} NMR** (376 MHz, $CDCl_3$) δ -62.6 (s, 3F) ppm.

Data consistent with literature.[176]

Data for 4.5: ^{1}H NMR (400 MHz, $CDCl_3$) δ 7.40–7.27 (m, 5H, H_{Ar}), 4.60 (d, *J*=12.1 Hz, 1H, PhC<u>H</u>'H), 4.57 (d, *J*=12.1 Hz, 1H, PhCH<u>H</u>'), 4.22–4.12 (m, 1H, H2), 3.57 (dd, *J*=9.4, 3.7 Hz, 1H, H1'), 3.45 (dd, *J*=9.5, 6.5 Hz, 1H, H1''), 2.45 (d, *J*=4.6 Hz, 1H, OH), 2.43–2.23 (m, 2H, H3) ppm; **^{13}C NMR** (101 MHz, $CDCl_3$) δ 137.4 (C_{Ar}), 128.5 (C_{Ar}×2), 128.0 (C_{Ar}), 127.8 (C_{Ar}×2), 126.1 (q, *J*=276.7 Hz, C4), 73.5 (Ph<u>C</u>H$_2$), 73.0 (C1), 65.1 (q, *J*=3.1 Hz, C2), 37.7 (q, *J*=27.9 Hz, C3) ppm; **^{19}F NMR** (376 MHz, $CDCl_3$) δ -63.8 (t, *J*=12.1 Hz, 3F) ppm; **^{19}F {^{1}H} NMR** (376 MHz, $CDCl_3$) δ -63.8 (s, 3F) ppm; **IR** (neat) 3430 (br. w), 3033 (w), 2867 (w), 1251 (s), 1132 (s) cm^{-1}; **HRMS** (ESI+) for $C_{11}H_{13}F_3NaO_2$ $[M+Na]^+$, calculated 257.0760, found 257.0765 (-2.2 ppm error).

Data for 4.36: ^{1}H NMR (400 MHz, $CDCl_3$) δ 8.09–8.01 (m, 2H, H_{Ar}), 7.65–7.56 (m, 1H, H_{Ar}), 7.51–7.43 (m, 2H, H_{Ar}), 4.47 (dd, *J*=10.8, 3.1 Hz, 1H, H1'), 4.44–4.37 (m, 1H, H2), 4.36 (dd, *J*=11.1, 5.7 Hz, 1H, H1''), 2.58–2.36 (m, 3H, H3 + OH) ppm; **^{13}C NMR** (101 MHz, $CDCl_3$) δ 166.5 (C=O), 133.5 (C_{Ar}), 129.7 (C_{Ar}×2), 129.3 (C_{Ar}), 128.6 (C_{Ar}×2), 126.0 (q, *J*=277.3 Hz, C4), 67.7 (C1), 64.9 (q, *J*=2.9 Hz, C2), 34.0 (q, *J*=27.9 Hz, C3) ppm; **^{19}F NMR** (376 MHz, $CDCl_3$) δ -63.7 (t, *J*=11.3 Hz, 3F) ppm; **^{19}F {^{1}H} NMR** (376 MHz, $CDCl_3$) δ -63.7 (s, 3F) ppm; **IR** (thin film, $CDCl_3$) 3461 (br. w), 2955 (w), 1719 (s), 1272 (s), 1120 (s) cm^{-1}; **m.p.** 46-48 °C; **HRMS** (ESI+) for $C_{11}H_{11}F_3NaO_3$ $[M+Na]^+$, calculated 271.0552, found 271.0550 (+0.9 ppm error); **Crystal Structure**

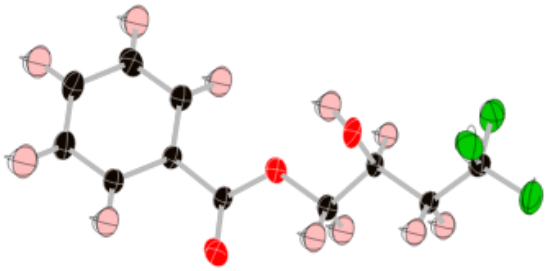

Synthesis of (Z)-1,4-bis(benzyloxy)but-2-ene (4.38)

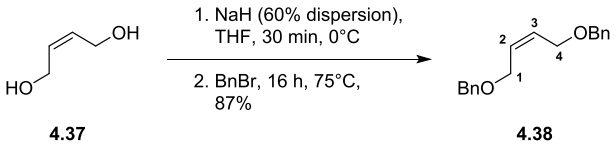

4.37 **4.38**

To a solution of *cis*-2-butene-1,4-diol **4.37** (3 g, 1 equiv) in THF (40 mL), NaH in 60% mineral oil (2.85 g, 2.1 equiv) was added portion wise at 0 °C. After 1 hr, BnBr (12.14 mL, 3 equiv) was added and the reaction was heated to 75 °C and after 16 h, quenched sat. aq. NH_4Cl (100 mL). The aqueous phase was extracted with CH_2Cl_2 (3×50 mL) and the combined organic layers were collected dried over

$MgSO_4$ and concentrated *in vacuo*. The crude oil was purified with column chromatography (1:9, acetone/petrol ether 40 – 60 °C) to afford **4.38** as a colourless oil (7.98 g, 87%).

^{1}H NMR (400 MHz, $CDCl_3$) δ 7.41–7.28 (m, 10H, H_{Ar}), 5.87–5.75 (m, 2H, H2 + H3), 4.51 (s, 4H), 4.08 (d, *J*=4.8 Hz, 4H, H1+H4) ppm; **^{13}C NMR** (101 MHz, $CDCl_3$) δ 138.1 (C_{Ar}×2), 129.5 (C2 + C3), 128.4 (C_{Ar}×4), 127.8 (C_{Ar}×4), 127.7 (C_{Ar}×2), 72.2 (Ph<u>C</u>H_2), 65.8 (C1 + C4) ppm.

Data consistent with literature.[262]

Synthesis of 2-(benzyloxy)acetaldehyde (4.39)

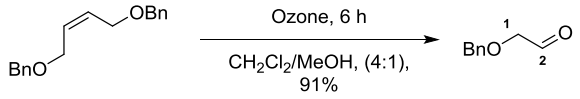

4.38 **4.39**

Ozone was bubbled through a solution of **4.38** (4.87 g) in CH_2Cl_2 (37.5 mL) and MeOH (12.5 mL) at -78 °C. After 4 h, oxygen was bubbled through the reaction mixture followed by argon. The reaction mixture was then quenched DMS (5.51 mL, 4 equiv) and was allowed to warm to room temperature. After 16 h, the reaction mixture was concentrated, and the crude oil was purified by column chromatography (1:1, acetone/ petrol ether 40 – 60 °C) to yield **4.39** as a pale-yellow oil (4.94 g, 91 %).

^{1}H NMR (400 MHz, $CDCl_3$) δ 9.66 (s, 1H, H2), 7.33–7.21 (m, 5H, H_{Ar}), 4.57 (s, 2H, $PhCH_2$), 4.03 (d, *J*=0.7 Hz, 2H, H1) ppm.

Data consistent with literature.[193]

Synthesis of 1-(benzyloxy)-4,4,4-trifluorobutan-2-one (4.5)

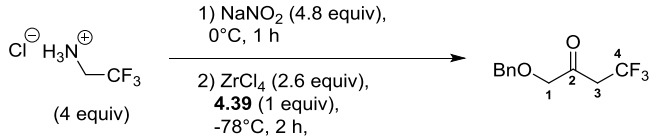

4.33 **4.5**

To a solution of **4.33** (14.0 g, 4 equiv) in CH_2Cl_2 (630 mL) and water (21 mL), $NaNO_2$ (8.55 g mL, 4.8 equiv) was added at 0 °C. After 1 h, the reaction was added to a separatory funnel and the aqueous layer was discarded. The organic phase was then cooled to -78 °C and **4.39** (4.50 g, 1 equiv) and $ZrCl_4$ (15.64 g, 2.6 equiv) was added. After 2 h, the reaction was quenched with MeOH (200 mL) and sat. aq. $NaHCO_3$ (200 mL). The aqueous phase was extracted with CH_2Cl_2 (3×300 mL) and the combined organic phases were dried over $MgSO_4$ and concentrated. The crude oil was purified by column chromatography (1:9, EA/petrol ether 40 – 60 °C) to yield **4.5** as a pale-yellow oil (2.41 g, 35%).

^{1}H NMR (400 MHz, $CDCl_3$) δ 7.47–7.28 (m, 5H, H_{Ar}), 4.61 (s, 2H, PhC$\underline{H}_2$), 4.10 (s, 2H, H1), 3.40 (q, *J*=10.3 Hz, 2H, H3) ppm; **^{13}C NMR** (101 MHz, $CDCl_3$) δ 198.8 (q, *J*=2.9 Hz, C2), 136.5 (C_{Ar}), 128.6 (C_{Ar}×2), 128.3 (C_{Ar}), 128.0 (C_{Ar}×2), 123.6 (q, *J*=276.6 Hz, C4), 74.9 (q, *J*=2.2 Hz, C1), 73.6 (Ph$\underline{C}H_2$), 42.7 (q, *J*=29.1 Hz, C3) ppm; **^{19}F NMR** (376 MHz, $CDCl_3$) δ -62.6 (t, *J*=9.5 Hz, 3F) ppm; **^{19}F {^{1}H} NMR** (376 MHz, $CDCl_3$) δ -62.6 (s, 3F) ppm.

Data consistent with literature.[176]

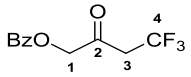

Exp3

Was occasionally observed if ozonolysis (previous reaction) resulted in over oxidation

Data for Exp3: **^{1}H NMR** (400 MHz, $CDCl_3$) δ 8.15–8.05 (m, 2H, H_{Ar}), 7.69–7.60 (m, 1H, H_{Ar}), 7.52–7.46 (m, 2H, H_{Ar}), 4.97 (s, 2H, H1), 3.39 (q, *J*=10.3 Hz, 2H, H3) ppm; **^{13}C NMR** (101 MHz, $CDCl_3$) δ 193.8 (q, *J*=2.4 Hz, C2), 165.7 (Ph$\underline{C}$=O), 133.8 (C_{Ar}), 129.9 (C_{Ar}×2), 128.6 (C_{Ar}×3, overlapped), 123.3 (q, *J*=276.8 Hz, C4), 68.2 (q, *J*=2.4 Hz, C1), 43.4 (q, *J*=29.8 Hz, C3) ppm; **^{19}F NMR** (376 MHz, $CDCl_3$) δ -62.2 (t, *J*=10.4 Hz, 3F) ppm; **^{19}F {^{1}H}; NMR** (376 MHz, $CDCl_3$) δ -62.2 (s, 3F) ppm; **m.p.** 95-97 °C (lit. 98-100 °C).[263] **Crystal Structure**

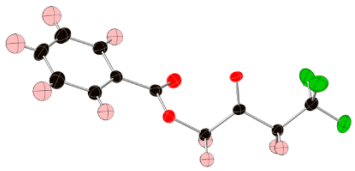

^{1}H, ^{13} C and ^{19}F NMR data consistent with literature.[263]

Synthesis of 2,2,4,4,4-pentafluorobutyl benzyl ether (4.42)

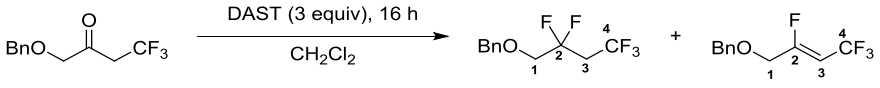

4.5 **4.42** 7 : **4.43** 1

Inseparable

To a solution of **4.5** (2.3 g, 1 equiv) in CH_2Cl_2 (35 mL), DAST (4.37 mL, 3 equiv) was added dropwise at 0 °C. The reaction mixture was allowed to warm to room temperature and after 16 h, was quenched with sat. aq. $NaHCO_3$ until pH 7. The aqueous phase was extracted with CH_2Cl_2 (3×30 mL) and the combined organic phases were dried over $MgSO_4$ and concentrated. The crude oil was purified by column chromatography (1:4, CH_2Cl_2/hexane) to yield an inseparable mixture of **4.42** and **4.43** as a pale-yellow oil in a ratio of 7:1 respectively (1.64 g, 65%).

Data for 4.42: ^{1}H NMR (500 MHz, $CDCl_3$) δ 7.44–7.31 (m, 5H, H_{Ar}), 4.64 (s, 2H, PhC$\underline{H}_2$), 3.72 (t, *J*=12.4 Hz, 2H, H1), 2.90 (tq, *J*=14.6, 10.2 Hz, 2H, H3) ppm; **^{13}C NMR** (126 MHz, $CDCl_3$) δ 136.7 (C_{Ar}), 128.6 (C_{Ar}×2), 128.2 (C_{Ar}), 127.9 (C_{Ar}×2), 123.7 (qt, *J*=276.7, 5.8 Hz, C4), 118.9 (tq, *J*=244.7, 3.1 Hz, C2), 73.9 (Ph$\underline{C}H_2$), 70.0 (tq, *J*=31.7, 1.4 Hz, C1), 37.8 (qt, *J*=30.1, 26.5 Hz, C3) ppm; **^{19}F NMR** (471 MHz, $CDCl_3$) δ -61.9 (tt, *J*=10.2, 8.9 Hz, 3F, F4), -103.0 (ttq, *J*=14.6, 12.4, 8.9 Hz, 3F, F2) ppm; **^{19}F {^{1}H} NMR** (471 MHz, $CDCl_3$) δ -62.1 (t, *J*=8.7 Hz, 3F), -103.2 (q, *J*=8.7 Hz, 2F) ppm; **IR** (neat) 2926 (w), 2876 (w), 1389 (s), 1171 (s), 1119 (s), 1095 (s), 698 (s) cm^{-1}; **HRMS** (CI) for $C_{11}H_{12}F_5O$ $[M+H]^+$, calculated 255.0803, found 255.0827 (+2.44 ppm error).

Data for 4.43: ^{1}H NMR (500 MHz, $CDCl_3$) δ 7.44–7.31 (m, 5H, H_{Ar}), 5.41 (dqt, *J*=33.4, 7.5, 1.0 Hz, 1H, H3), 4.62 (s, 2H, $PhCH_2$), 4.12–4.04 (m, 2H, H1) ppm; **^{13}C NMR** (126 MHz, $CDCl_3$) δ 97.9 (qd, *J*=35.8, 5.7 Hz, C3), 73.3 (PhC$\underline{H}_2$), 65.9 (d, *J*=34.1 Hz, C1) ppm (other carbons not visible due to overlap with **4.42**); **^{19}F NMR** (471 MHz, $CDCl_3$) δ -57.9 (ddt, *J*=16.7, 7.5, 2.2 Hz, 3F, F4), -101.0 (dqt, *J*=33.5, 16.7, 6.4 Hz, 1F, F2) ppm; **^{19}F {^{1}H} NMR** (471 MHz, $CDCl_3$) δ -57.9 (d, *J*=16.5 Hz, 3F, F4), -101.0 (q, *J*=16.8 Hz, 1F, F2); **HRMS** (EI) for $C_{11}H_{10}F_4O$ $[M^{\cdot+}]$, calculated 234.0662, found 234.0666 (+0.36 ppm error).

Synthesis of 2,2,4,4,4-pentafluorobutan-1-ol (G14) and 2,4,4,4-tetrafluorobutan-1-ol (G9)

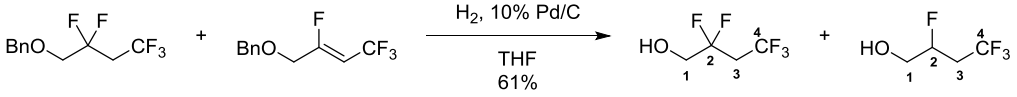

4.42 **4.43** **G14** 5.5 : **G9** 1

Inseparable

To a solution of **4.42** and **4.43** (0.6 g, 1 equiv) in THF (8 mL) was added a suspension of Pd/C 10% (300 mg) in THF (2 mL). The reaction mixture was degassed with argon and one balloon of hydrogen. The reaction mixture was stirred at room temperature under a hydrogen atmosphere for 5 h. The reaction was then filtered over Celite, which was then rinsed with CH_2Cl_2 (30 mL). The crude was carefully concentrated at 750 mbar/30 °C and was purified by column chromatography (9:1, CH_2Cl_2/pentane) to afford **G14** and **G9** as a pale-yellow oil in a 5.5:1 ratio respectively (225 mg, 61%).

Data for D14: ^{1}H NMR (400 MHz, $CDCl_3$) δ 3.86 (td, *J*=12.5, 7.1 Hz, 2H, H1), 2.89 (tq, *J*=14.5, 10.2 Hz, 2H, H3), 1.93 (br. t, *J*=7.0 Hz, 1H, OH) ppm; **^{13}C NMR** (126 MHz, $CDCl_3$) δ 123.6 (qt, *J*=276.6, 6.0 Hz, C4), 119.1 (tq, *J*=244.5, 2.9 Hz, C2), 63.6 (tq, *J*=31.5, 1.4 Hz, C1), 37.4 (qt, *J*=30.3, 26.7 Hz, C3) ppm; **^{19}F NMR** (376 MHz, $CDCl_3$) δ -62.1 (quin, *J*=9.5 Hz, 3F), -106.2 (ttq, *J*=14.5, 12.6, 9.3 Hz, 2F) ppm; **^{19}F {^{1}H} NMR** (376 MHz, $CDCl_3$) δ -62.1 (t, *J*=8.7 Hz, 3F), -106.2 (q, *J*=9.2 Hz, 2F) ppm; **IR** (neat) 3364 (br. w), 2953 (w), 2887 (w), 1389 (s), 1161 (s), 1076 (s), 890 (s) cm^{-1}; **HRMS** (CI) for $C_4H_6F_5O$ $[M+H]^+$, calculated 165.0333, found 165.0315 (-1.80 ppm error).

Data for D9: ^{1}H NMR (400 MHz, $CDCl_3$) δ 4.91 (dsxt, *J*=48.3, 3.9 Hz, 1H, H2), 3.97–3.63 (m, 2H, H1), 2.72–2.38 (m, 2H, H3), 1.81 (br. t, *J*=6.6 Hz, 1H, OH) ppm; **^{13}C NMR** (126 MHz, $CDCl_3$) δ 125.4 (qd, *J*=276.3, 4.8 Hz, C4), 87.8 (dq, *J*=172.9, 3.1 Hz, C2), 64.0 (d, *J*=22.9 Hz, C1), 35.7 (qd, *J*=29.3, 23.0 Hz, C3) ppm; **^{19}F NMR** (376 MHz, $CDCl_3$) δ -64.3 (td, *J*=10.6, 6.9 Hz, 3F), -191.0– -191.4 (m, 1F) ppm; **^{19}F {^{1}H} NMR** (376 MHz, $CDCl_3$) δ -64.3 (d, *J*=6.9 Hz, 3F), -191.2 (q, *J*=6.9 Hz, 1F) ppm; **IR** (neat) 3364 (br. w), 2953 (w), 2887 (w), 1389 (s), 1161 (s), 1076 (s), 890 (s) cm^{-1}; **HRMS** (CI) for $C_4H_5F_4O$ $[M-H]^-$, calculated 145.0282, found 145.0261 (-1.04 ppm error).

Synthesis of 1,1,1-trifluorohexan-2-ol (K3)

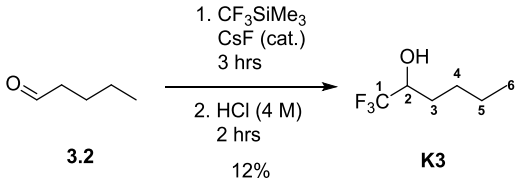

To a solution of valeraldehyde (3.71 mL, 1 equiv) and CF_3SiMe_3 (5.4 mL, 1.05 equiv) was added caesium fluoride (53 mg, 0.01 equiv) in one portion. After 3 h, aq. HCl (4M, 24 mL) was added. After a further 2 h, the reaction was quenched with water (20 mL) and the aqueous solution was extracted with Et_2O (3×30 mL). The combined organic layers were dried over $MgSO_4$, and the crude was carefully concentrated at 750 mbar/30 °C before purification by column chromatography (100% to 1:4, pentane/CH_2Cl_2), to afford **K3** as a colourless oil (0.64 g, 12%)

^{1}H NMR (400 MHz, $CDCl_3$) δ 3.92 (tqd, *J*=9.7, 6.5, 6.2 Hz, 1H, H2), 1.98 (d, *J*=6.2 Hz, 1H, OH), 1.81–1.66 (m, 1H, H3'), 1.66–1.50 (m, 2H, H3'' + H4'), 1.47–1.29 (m, 3H, H4'' + H5), 0.94 (t, *J*=7.2 Hz, 3H, H6) ppm; **^{13}C NMR** (101 MHz, $CDCl_3$) δ 125.2 (q, *J*=281.7 Hz, C1), 70.6 (q, *J*=30.8 Hz, C2), 29.3 (q, *J*=1.5 Hz, C3), 27.0 (C4), 22.3 (C5), 13.8 (C6) ppm; **^{19}F NMR** (376 MHz, $CDCl_3$) δ -80.3 (d, *J*=6.9 Hz, 3F) ppm; **^{19}F {^{1}H} NMR** (376 MHz, $CDCl_3$) δ -80.3 (s, 3F) ppm; **IR** (neat) 3361 (br. w), 2961 (w), 2867 (w), 1140 (m), 1086 (s) cm^{-1}; **HRMS** (CI) for $C_6H_{12}F_3O$ $[M+H]^+$, calculated 157.0835, found 157.0828(-0.66 ppm error).

Synthesis of 1,1,1,6,6,6-hexafluorohexan-2-ol (K2)

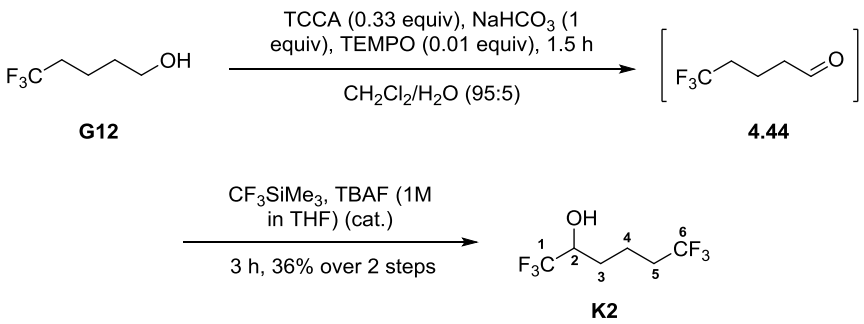

To a solution of 5,5,5-trifluoropentanol (0.62 g, 1 equiv) and TEMPO (6 mg, 0.01 equiv) in CH_2Cl_2 (7.5 mL) and water (0.25 mL), was added $NaHCO_3$ (0.37 g, 1 equiv) followed by TCCA (0.34 g, 0.33 equiv) portion wise over 1 h. After 30 min, the reaction mixture is filtered over a plug of silica gel, dried over $MgSO_4$ and filtered. To the resulting filtrate was added CF_3SiMe_3 (0.71 mL, 1.1 equiv) and the reaction mixture cooled to 0 °C before the dropwise addition of TBAF (1M in THF, 0.48 mL, 0.1 equiv). The reaction mixture was allowed to warm to room temperature and after 1 h, TBAF (1M in THF, 4.8 mL, 1 equiv) was added. After 18 h, the reaction was quenched with aq. 2M HCl (10 mL) for 1 h. The layers were separated, and the organic phase was washed with sat. aq. $NaHCO_3$ (10 mL), brine, dried over $MgSO_4$, filtered over a plug of silica gel and carefully concentrated at 750 mbar/30 °C. The crude was purified by column chromatography (1:1, CH_2Cl_2/pentane) to afford **K2** (0.33 g, 36% over 2 steps) as a colourless oil.

^{1}H NMR (400 MHz, $CDCl_3$) δ 4.06–3.84 (m, 1H, H2), 2.24 (d, *J*=5.4 Hz, 1H, OH), 2.22–2.09 (m, 2H, H5), 1.99–1.65 (m, 4H, H3 + H4) ppm; **^{13}C NMR** (101 MHz, $CDCl_3$) δ 126.8 (q, *J*=276.6 Hz, C6), 124.9 (q, *J*=281.9 Hz, C1), 70.2 (q, *J*=31.3 Hz, C2), 33.4 (q, *J*=28.9 Hz, C5), 28.4 (C3), 17.8 (q, *J*=2.9 Hz, C4) ppm; **^{19}F NMR** (376 MHz, $CDCl_3$) δ -66.6 (t, *J*=10.6 Hz, 3F, F6), -80.4 (d, *J*=6.5 Hz, 3F, F1) ppm; **^{19}F {^{1}H} NMR** (376 MHz, $CDCl_3$) δ -66.6 (s, 3F, F6), -80.4 (s, 3F, F1) ppm; **IR** (neat) 3389 (br. w), 2952 (w), 2893 (w), 1392 (m), 1252 (s), 1113 (s) cm^{-1}; **HRMS** (CI) for $C_6H_9F_6O$ $[M+H]^+$, calculated 211.0552, found 211.0545 (-0.75 ppm error).

Synthesis of *n*-Butylmagnesium bromide (4.46)

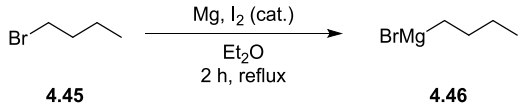

To a slurry of Mg turnings (1.16 g, 3.15 equiv) in Et_2O (14 mL) was added iodine (19 mg, 0.01 equiv) and the flask was heated with a heat gun (~80 °C) until bubbles from Mg were evolved. To the reaction mixture was added *n*-bromobutane (2.58 mL, 3 equiv) and heating with a heat gun was continued until the iodine colour disappeared. The reaction mixture was then refluxed for 2 h before cooling to room temperature before use in the next step with no further purification.

Synthesis of 1,1,1-trifluorooctan-4-ol (N2)

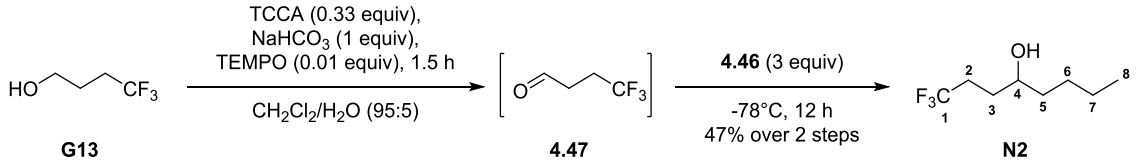

To a solution of 4,4,4-trifluorobutanol (1 g, 1 equiv) and TEMPO (14 mg, 0.01 equiv) in CH_2Cl_2 (12 mL) and water (0.4 mL) was added $NaHCO_3$ (0.66 g, 1 equiv) followed by TCCA (0.60 g, 0.33 equiv)

portion wise over 1 h. After 30 min, the reaction mixture is filtered over a plug of silica gel, dried over $MgSO_4$ and filtered. The resulting solution was used in the next step with no further purification.

The freshly prepared Grignard reagent **4.46** in a solution of Et_2O was then added dropwise over 10 min to a -78 °C solution of **4.47** in CH_2Cl_2. After 2 h, the reaction mixture was allowed to warm to room temperature and after a further 16 hr, was quenched with NH_4Cl (30 mL). The aqueous was then extracted with CH_2Cl_2 (3×20 mL) and the combined organics are washed with brine, dried over $MgSO_4$, filtered and carefully concentrated at 750 mbar/30 °C. The crude was purified by column chromatography (2:3, pentane/CH_2Cl_2) to afford **N2** as a colourless oil (0.68 g, 47% over 2 steps).

^{1}H NMR (400 MHz, $CDCl_3$) δ 3.71–3.58 (m, 1H, H4), 2.42–2.07 (m, 2H, H2), 1.83–1.69 (m, 1H, H3'), 1.65–1.55 (m, 1H, H3''), 1.53–1.25 (m, 7H, H5 + H6 + H7 + OH), 0.92 (t, *J*=7.0 Hz, 3H, H8) ppm; **^{13}C NMR** (101 MHz, $CDCl_3$) δ ppm: 127.4 (q, *J*=275.8 Hz, C1), 70.5 (C4), 37.3 (C5), 30.2 (q, *J*=28.6 Hz, C2), 29.4 (q, *J*=2.7 Hz, C3), 27.7 (C6 or C7), 22.6 (C6 or C7), 14.0 (C8) ppm; **^{19}F NMR** (376 MHz, $CDCl_3$) δ -66.6 (t, *J*=10.4 Hz) ppm; **^{19}F {^{1}H} NMR** (376 MHz, $CDCl_3$) δ -66.6 (s) ppm; **IR** (neat) 3344 (br. w), 2959 (m), 2864 (w), 1454 (w), 1253 (s), 1147 (s) cm^{-1}; **HRMS** (CI) for $C_8H_{16}F_3O$ $[M+H]^+$, calculated 185.1148, found 185.1128 (-1.96 ppm error).

Synthesis of 8,8,8-trifluorooctan-4-ol (N1)

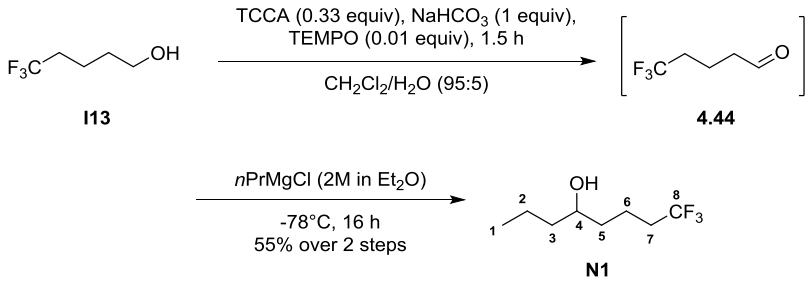

To a solution of 5,5,5-trifluoropentanol (1 g, 1 equiv) and TEMPO (10 mg, 0.01 equiv) in CH_2Cl_2 (12 mL) and water (0.4 mL) was added $NaHCO_3$ (0.59 g, 1 equiv), followed by TCCA (0.54 g, 0.33 equiv) portion wise over 1 h. After 30 min, the reaction mixture is filtered over a plug of silica gel, dried over $MgSO_4$ and filtered. The resulting solution was used in the next step with no further purification.

To a -78 °C solution of **4.44** in CH_2Cl_2 was added *n*PrMgCl (10.71 mL, 3 equiv, 2M in Et_2O). After 2 h, the reaction mixture was allowed to warm to room temperature and after an additional 16 h, was quenched with NH_4Cl (30 mL). The aqueous was then extracted with CH_2Cl_2 (3×20 mL) and the combined organics are washed with brine, dried over $MgSO_4$, filtered and carefully concentrated at 750 mbar/30 °C. The crude was purified by column chromatography (2:3, pentane/CH_2Cl_2) to afford **N1** as a colourless oil (0.71 g, 55% over 2 steps).

^{1}H NMR (400 MHz, $CDCl_3$) δ 3.74–3.50 (m, 1H, H4), 2.21–2.01 (m, 2H, H7), 1.83–1.28 (m, 9H, H2 + H3 + H5 + H6 + OH), 0.95 (t, *J*=6.8 Hz, 3H, H1) ppm; **^{13}C NMR** (101 MHz, $CDCl_3$) δ 127.2 (q, *J*=276.1 Hz, C8), 71.2 (C4), 39.7 (C3 or C5), 36.2 (C3 or C5), 33.7 (q, *J*=28.1 Hz, C7), 18.8 (C2), 18.3 (q, *J*=3.2 Hz, C6), 14.0 (C1) ppm; **^{19}F NMR** (376 MHz, $CDCl_3$) δ -66.6 (t, *J*=10.4 Hz) ppm; **^{19}F {^{1}H} NMR** (376 MHz, $CDCl_3$) δ -66.6 (s) ppm; **IR** (neat) 3350 (br. w), 2960 (m), 2876 (w), 1390 (m), 1255 (s), 1137 (s) cm^{-1}; **HRMS** (CI) for $C_8H_{16}F_3O$ $[M+H]^+$, calculated 185.1148, found 185.1161 (+1.30 ppm error).

Synthesis of 7,7,7-trifluoroheptan-3-ol (M3)

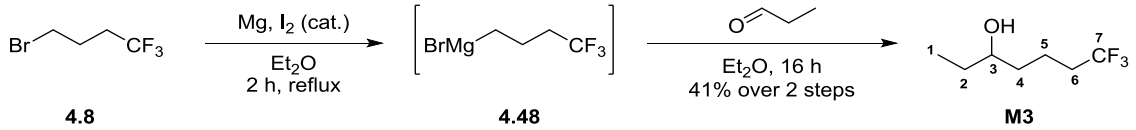

4.8 **4.48** **M3**

To a slurry of Mg turnings (0.13 g, 1.1 equiv) in Et_2O (10 mL) was added iodine (7 mg, 0.01 equiv). The reaction was heated with a heat gun (~80 °C) until bubbles from Mg are evolved. To the reaction mixture was then added 4-bromo-1,1,1-trifluorobutane (1 g, 1 equiv) and heating was continued with the heat gun (~80 °C) until the iodine colour disappeared. The reaction mixture was then refluxed for 2 h before cooling to room temperature. The freshly prepared Grignard reagent **4.48** was then added dropwise over 10 min to a -78 °C solution of propanal (0.32 mL, 0.9 equiv) in Et_2O (10 mL). After 2 h, the reaction mixture was allowed to warm to room temperature and after an additional 16 h, was quenched with NH_4Cl (30 mL). The aqueous was then extracted with CH_2Cl_2 (3×20 mL) and the combined organics are washed with brine, dried over $MgSO_4$, filtered and carefully concentrated at 750 mbar/30 °C. The crude was purified by column chromatography (CH_2Cl_2) to afford **M3** as a colourless oil (0.36 g, 41% over 2 steps).

^{1}H NMR (400 MHz, $CDCl_3$) δ 3.55 (br. tq, *J*=7.4, 3.9 Hz, 1H, H3), 2.21–2.00 (m, 2H, H6), 1.85–1.41 (m, 6H, H2 + H4 + H5), 1.38 (br. s, 1H, OH), 0.96 (t, *J*=7.5 Hz, 3H, H1) ppm; **^{13}C NMR** (101 MHz, $CDCl_3$) δ 127.2 (q, *J*=276.1 Hz, C7), 72.8 (C3), 35.7 (C4), 33.7 (q, *J*=28.1 Hz, C6), 30.3 (C2), 18.3 (q, *J*=2.9 Hz, C5), 9.8 (C1) ppm; **^{19}F NMR** (376 MHz, $CDCl_3$) δ -66.6 (t, *J*=10.8 Hz, 3F) ppm; **^{19}F {^{1}H} NMR** (376 MHz, $CDCl_3$) δ -66.6 (s, 3F) ppm; **IR** (neat) 3355 (br. w), 2967 (m), 2893 (m), 1390 (m), 1253 (s), 1136 (s) cm^{-1}; **HRMS** (CI) for $C_7H_{14}F_3O$ $[M+H]^+$, calculated 171.0991, found 171.0978 (-1.32 ppm error).

Synthesis of 1,1,1-trifluoroheptan-3-ol (M4)

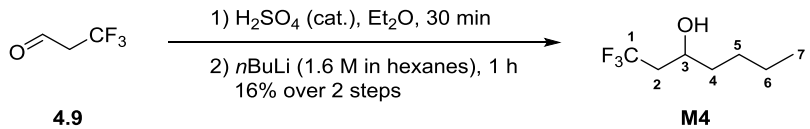

4.9 **M4**

To a solution of trifluoropropanal (0.9 mL, 0.1 equiv) in Et_2O (19 mL) was added a solution of H_2SO_4 (39 mg, 0.05 equiv) in Et_2O (1 mL). After 30 min, the reaction was cooled to -78 °C and *n*BuLi (1.6 M

in hexanes, 7.53 mL, 1.5 equiv) was added dropwise. After 1 h, the reaction was allowed to warm to room temperature and quenched with sat. aq. NH_4Cl (20 mL). The aqueous was extracted with Et_2O (3×20 mL) and the combined organic phases were washed with brine, dried over $MgSO_4$, filtered and carefully concentrated at 750 mbar/30 °C. The crude was purified by column chromatography (1:1, pentane/CH_2Cl_2) to afford **M4** as a colourless oil (0.20 g, 16% over 2 steps).

^{1}H NMR (400 MHz, $CDCl_3$) δ 4.07–3.95 (m, 1H, H3), 2.37–2.16 (m, 2H, H2), 1.80 (d, *J*=4.3 Hz, 1H, OH), 1.57–1.22 (m, 6H, H4 + H5 + H6), 0.93 (t, *J*=7.1 Hz, 3H, H7) ppm; **^{13}C NMR** (101 MHz, $CDCl_3$) δ 126.5 (q, *J*=277.3 Hz, C1), 66.2 (q, *J*=2.9 Hz, C3), 41.1 (q, *J*=26.4 Hz, C2), 36.9 (C4), 27.3 (C5), 22.5 (C6), 13.9 (C7) ppm; **^{19}F NMR** (376 MHz, $CDCl_3$) δ -63.8 (t, *J*=11.4 Hz, 3F) ppm; **^{19}F {^{1}H} NMR** (376 MHz, $CDCl_3$) δ -63.8 (s, 3F) ppm; **IR** (neat) 3370 (br. w), 2960 (m), 2865 (w), 1382 (m), 1253 (s), 1137 (s), 1091 (s) cm^{-1}; **HRMS** (CI) for $C_7H_{14}F_3O$ $[M+H]^+$, calculated 171.0991, found 171.0996 (+0.48 ppm error).

Synthesis of 4-Benzyloxy-1-butanol (4.51)

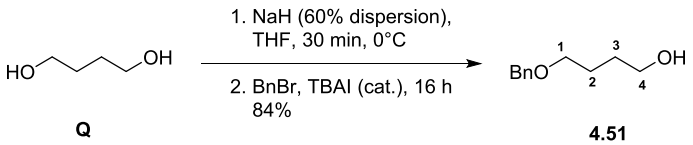

Q 4.51

To a solution of 1,4-butandiol **Q** (10.74 mL, 2 equiv) in THF (25 mL), NaH in 60% mineral oil (2.4 g, 1 equiv) was added portion wise at 0 °C. After 30 min, a solution of BnBr (7.25 mL, 1 equiv) in THF (15 mL) was added at 0 °C dropwise, followed by TBAI (60 mg, 0.01 equiv). The reaction and was allowed to warm to room temperature and after 16 h, the reaction mixture was quenched with water (75 mL). The aqueous phase was extracted with Et_2O (3×50 mL) and the combined organic layers were collected washed with brine (100 mL), dried over $MgSO_4$ and concentrated *in vacuo*. The crude oil was purified with column chromatography (3:7, EtOAc/petrol ether 40–60 °C) to afford **4.51** as a colourless oil (9.24 g, 84%).

^{1}H NMR (400 MHz, $CDCl_3$) δ 7.41–7.27 (m, 5H, H_{Ar}), 4.53 (s, 2H, Ph$C\underline{H}_2$), 3.66 (t, *J*=5.6 Hz, 2H, H4), 3.54 (t, *J*=5.7 Hz, 2H, H1), 2.19 (br. s, 1H, OH), 1.80–1.62 (m, 4H, H2 + H3) ppm; **^{13}C NMR** (101 MHz, $CDCl_3$) δ 138.1 (C_{Ar}), 128.4 (C_{Ar}×2), 127.7 (C_{Ar}×2), 127.7 (C_{Ar}), 73.1 (Ph$\underline{C}H_2$), 70.3 (C1), 62.7 (C4), 30.2 (C3), 26.7 (C2) ppm.

Data consistent with literature.[264]

Synthesis of 4-chlorobutyl benzyl ether (4.50)

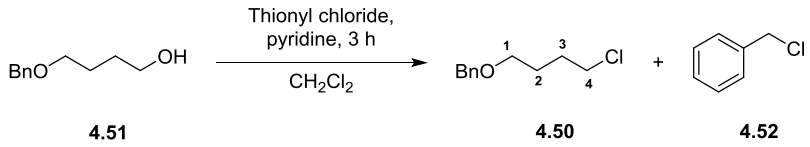

4.51 **4.50** **4.52**

To a solution of **4.51** (2.33 g, 1 equiv) and pyridine (2.25 mL, 1 equiv) in CH_2Cl_2 (100 mL), thionyl chloride (3.03 mL, 1.5 equiv) was added dropwise at 0 °C. The reaction mixture was allowed to warm to room temperature and after 3 h, the reaction mixture was quenched with sat. aq. $NaHCO_3$ (150 mL) at 0 °C. The organic phase was washed with water (100 mL) and brine (100 mL) and then dried over $MgSO_4$ and concentrated. The crude oil was purified with column chromatography (1:19, acetone/petrol ether 40–60 °C) to afford **4.50** and **4.52** as an inseparable pale-yellow oil (3.05 g, ~9:1, respectively).

Data for 4.50: ^{1}H NMR (400 MHz, $CDCl_3$) δ 7.44–7.28 (m, 5H, H_{Ar}), 4.52 (s, 2H, PhC$\underline{H}_2$), 3.58 (t, *J*=6.6 Hz, 2H, H4), 3.52 (t, *J*=6.2 Hz, 2H, H1), 1.96–1.86 (m, 2H, H3), 1.82–1.73 (m, 2H, H2) ppm; **^{13}C NMR** (101 MHz, $CDCl_3$) δ 138.4 (C_{Ar}), 128.4 (C_{Ar}×2), 127.6 (C_{Ar}×2), 127.6 (C_{Ar}), 72.9 (Ph$\underline{C}H_2$), 69.4 (C1), 45.0 (C4), 29.52 (C3), 27.1 (C2) ppm.

Proton consistent with literature.[265]

Data for 4.52: Selected ^{1}H NMR (400 MHz, $CDCl_3$) δ 4.61 (s, 2H, PhC$\underline{H}_2$Cl), (phenyl proton signals overlap with **4.50**).

Selected signals consistent with literature.[266]

Synthesis of 4-(thiocyanate)butyl benzyl ether (4.53)

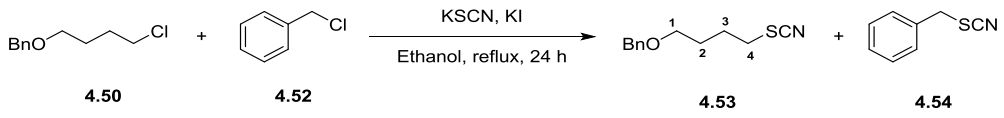

4.50 **4.52** **4.53** **4.54**

To a solution of **4.50** and **4.52** (2.87 g, 1 equiv, ratio of ~9:1 respectively) and KI (0.481 g, 0.2 equiv) in ethanol (45 mL) was added potassium thiocyanate (9.15 g, 6.5 equiv). The reaction mixture was refluxed for 24 h and then concentrated *in-vacuo*. The residue was dissolved in EtOAc (50 mL) and washed with water (2×50 mL), brine, dried over $MgSO_4$ and concentrated. The crude oil was purified with column chromatography (1:4, acetone/petrol ether 40–60 °C) to afford **4.53** and **4.54** as an inseparable pale-yellow oil (2.91 g, ~6:1, respectively).

Data for 4.53: ^{1}H NMR (400 MHz, $CDCl_3$) δ 7.44–7.28 (m, 5H, H_{Ar}), 4.51 (s, 2H, PhC$\underline{H}_2$), 3.53 (t, *J*=6.1 Hz, 2H, H1), 2.99 (t, *J*=7.2 Hz, 2H, H4), 1.97 (quin, *J*=7.3 Hz, 2H, H3), 1.86–1.73 (m, 2H, H2) ppm; **^{13}C NMR** (101 MHz, $CDCl_3$) δ 138.2 (C_{Ar}), 128.4 (C_{Ar}×2), 127.7 (C_{Ar}), 127.6 (C_{Ar}×2), 112.3 (SCN), 73.1

(Ph<u>C</u>H$_2$), 69.2 (C1), 34.0 (C4), 28.0 (C3), 27.1 (C2) ppm; **IR** (neat) 2940 (m), 2958 (m), 2153 (s), 1453 (m), 1102 (s), 697 (s) cm^{-1}; **MS** (ESI+) m/z 244.3 [M+Na]$^+$; **HRMS** (ESI+) for $C_{12}H_{15}NNaOS$ [M+Na]$^+$, calculated 244.0770, found 244.0767 (-1.5 ppm error).

Data for 4.54: ^{1}H NMR (400 MHz, $CDCl_3$) δ 4.18 (s, 2H, PhC<u>H</u>$_2$SCN) (phenyl proton signals overlap with **4.53**); **^{13}C NMR** (101 MHz, $CDCl_3$) δ 134.3 (C_{Ar}), 129.1 (C_{Ar}×2), 129.0 (C_{Ar}×2), 128.9 (C_{Ar}), 111.9 (SCN), 38.3 (Ph<u>C</u>H$_2$SCN).

Data consistent with literature.[267]

Synthesis of 4-(trifluoromethylthio)butyl benzyl ether (4.55)

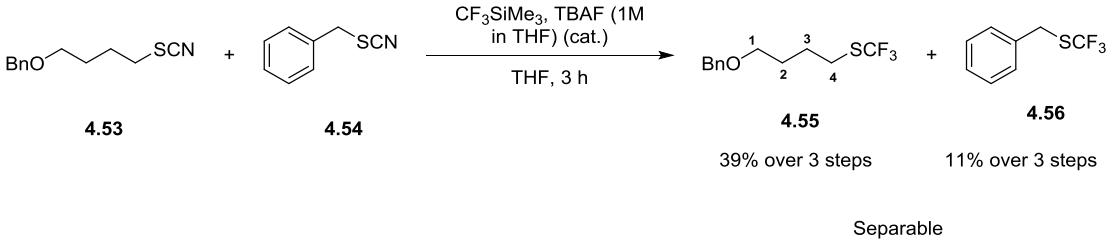

To a solution of **4.53** and **4.54** (2.81 g, 1 equiv, ratio of ~6:1 respectively), CF_3SiMe_3 (6.06 mL, 3 equiv) in THF (60 mL) was added TBAF (1M in THF, 1.36 mL, 0.1 equiv) at 0 °C. The reaction mixture was allowed to warm to room temperature and after 3 h the reaction mixture was concentrated *in-vacuo*. The crude oil was purified with column chromatography (1:19, acetone/petrol ether 40 – 60 °C) to afford **4.55** as a colourless oil (2.78 g, 39% over 3 steps) and **4.56** as a colourless oil (0.58 g, 11% yield over 3 steps).

Data for 4.55: ^{1}H NMR (400 MHz, $CDCl_3$) δ 7.39–7.28 (m, 5H, H_{Ar}), 4.51 (s, 2H, PhC<u>H</u>$_2$), 3.51 (t, *J*=6.0 Hz, 2H, H2), 2.92 (t, *J*=7.3 Hz, 2H, H4), 1.88–1.68 (m, 4H, H2 + H3) ppm; **^{13}C NMR** (101 MHz, $CDCl_3$) δ 138.3 (C_{Ar}), 131.1 (q, *J*=305.9 Hz, S<u>C</u>F$_3$), 128.4 (C_{Ar}×2), 127.6 (C_{Ar}×3, Overlapped), 73.0 (Ph<u>C</u>H$_2$), 69.3 (C2), 29.7 (q, *J*=2.2 Hz, C4), 28.6 (C2), 26.5 (C3) ppm; **^{19}F NMR** (376 MHz, $CDCl_3$) δ -41.4 (s, 3F) ppm; **IR** (neat) 2945 (w), 2857 (w), 1454 (m), 1146 (s), 1100 (s), 734 (s) cm^{-1}; **HRMS** (ESI+) for $C_{12}H_{15}F_3NaOS$ [M+Na]$^+$, calculated 287.0688, found 287.0684 (-1.3 ppm error).

Data for 4.56: ^{1}H NMR (400 MHz, $CDCl_3$) δ 7.29–7.17 (m, 5H, H_{Ar}), 4.03 (s, 2H, PhC<u>H</u>$_2$) ppm; **^{13}C NMR** (101 MHz, $CDCl_3$) δ 135.0 (C_{Ar}), 130.6 (q, *J*=306.6 Hz), 128.9 (C_{Ar}×2), 128.9 (C_{Ar}×2), 128.0 (C_{Ar}) ppm. **^{19}F NMR** (376 MHz, $CDCl_3$) δ -41.9 (s, 3F) ppm.

Proton and fluorine consistent with literature.[268]

Synthesis of 4-(trifluoromethylthio)-butanol (S2)

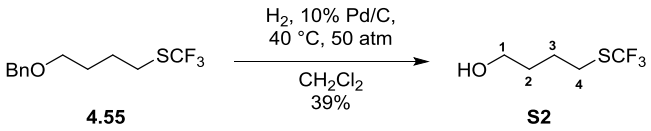

4.55 **S2**

A solution of **4.55** (800 mg, 1 equiv) in CH_2Cl_2 (60 mL) was passed through a HCube Mini (40 °C, 50 atm, 1 mL/min) with a 10% Pd/C cartridge. The resulting solution was washed with brine and dried over $MgSO_4$. The crude was combined with another reaction on a 200 mg scale and was carefully concentrated at 750 mbar/30 °C. The crude was purified by column chromatography (1:9, Et_2O/CH_2Cl_2) to afford **S2** as a colourless oil (256 mg, 39%).

^{1}H NMR (400 MHz, $CDCl_3$) δ 3.69 (t, *J*=6.2 Hz, 2H, H1), 2.94 (t, *J*=7.3 Hz, 2H, H4), 1.87–1.75 (m, 2H, H3), 1.74–1.63 (m, 2H, H2) ppm; **^{13}C NMR** (101 MHz, $CDCl_3$) δ 131.1 (q, *J*=305.9 Hz, S<u>C</u>F_3), 62.0 (C1), 31.3 (C2), 29.7 (q, *J*=2.2 Hz, C4), 26.0 (C3) ppm; **^{19}F NMR** (376 MHz, $CDCl_3$) δ -41.4 (s, 3F) ppm; **IR** (neat) 3332 (br. w), 2944 (m), 2880 (m), 1436 (w), 1099 (s), 1055 (s), 755 (s) cm^{-1}; **HRMS** (CI) for $C_5H_{10}F_3OS$ $[M+H]^+$, calculated 175.0399, found 175.0391 (-0.76 ppm error).

Synthesis of 3-(benzyloxy)propan-1-ol (4.58)

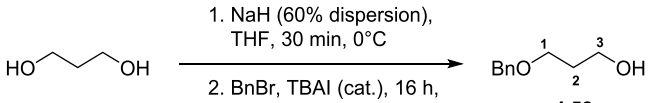

4.57 **4.58**

To a solution of 1,3-propandiol **4.57** (5 g, 1 equiv) in THF (50 mL), NaH in 60% mineral oil (2.62 g, 1 equiv) was added portion wise at 0 °C. After 30 min, BnBr (7.82 mL, 1 equiv) and TBAI (243 mg, 0.01 equiv) were added at 0 °C. The reaction and was allowed to warm to room temperature and after 16 h, the reaction mixture was quenched with water (100 mL). The aqueous phase was extracted with Et_2O (3×100 mL) and the combined organic layers were washed with brine (100 mL), dried over $MgSO_4$ and concentrated *in vacuo*. The crude oil was purified with column chromatography (3:7, EtOAc/petrol ether 40–60 °C) to afford **4.58** as a colourless oil (5.97 g, 55%).

^{1}H NMR (400 MHz, $CDCl_3$) δ 7.44–7.29 (m, 5H, H_{Ar}), 4.55 (s, 2H, Ph<u>C</u>H_2), 3.82 (q, *J*=5.6 Hz, 2H, H3), 3.70 (t, *J*=5.7 Hz, 2H, H1), 2.27 (t, *J*=5.5 Hz, 1H, OH), 1.90 (quin, *J*=5.7 Hz, 2H, H2) ppm; **^{13}C NMR** (101 MHz, $CDCl_3$) δ 138.1 (C_{Ar}), 128.4 (C_{Ar}×2), 127.7 (C_{Ar}), 127.6 (C_{Ar}×2), 73.3 (Ph<u>C</u>H_2), 69.4 (C1), 62.0 (C3), 32.1 (C2) ppm.

Data consistent with literature.[269]

Synthesis of bis(3-(benzyloxy)propyl) sulphite (4.60)

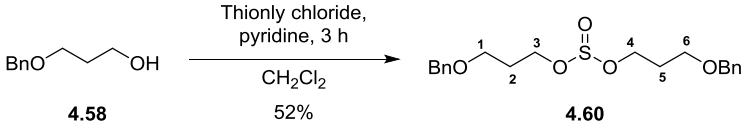

To a solution of **4.58** (2.69 g, 1 equiv) and pyridine (1.31 mL, 1 equiv) in CH_2Cl_2 (70 mL), thionyl chloride (1.77 mL, 1.5 equiv) was added dropwise at 0 °C. The reaction mixture was allowed to warm to room temperature and after 3 h, the reaction mixture was quenched with brine (100 mL) at 0 °C. The organic phase was dried over $MgSO_4$ and concentrated. The crude oil was purified with column chromatography (1:9, acetone/petrol ether 40–60 °C) to afford **4.60** as a yellow oil (3.19 g, 52%).

^{1}H NMR (400 MHz, $CDCl_3$) δ 7.39–7.28 (m, 10H, H_{Ar}), 4.51 (s, 4H, PhC$\underline{H}_2$×2), 4.20–4.03 (m, 4H, H3 + H4), 3.57 (t, *J*=6.0 Hz, 4H, H1 + H6), 1.97 (quin, *J*=6.2 Hz, 4H, H2 + H5) ppm; **^{13}C NMR** (101 MHz, $CDCl_3$) δ 138.2 (C_{Ar}×2), 128.4 (C_{Ar}×4), 127.6 (C_{Ar}×6, Overlapped), 73.1 (Ph$\underline{C}H_2$), 66.2 (C1 + C6), 59.5 (C3 + C4), 29.9 (C2 + C5) ppm;; **IR** (neat) 3031 (w), 2861 (w), 1454 (m), 1203 (s), 1099 (s) cm^{-1}; **MS** (ESI+) m/z 401.4 $[M+Na]^+$; **HRMS** (ESI+) for $C_{20}H_{26}NaO_5S$ $[M+Na]^+$, calculated 401.1393, found 401.1403 (-2.5 ppm error).

Synthesis of 3-chloropropyl benzyl ether (4.61)

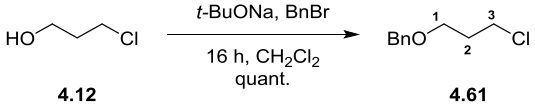

To a solution of 3-chloropropanol **4.12** (1 g, 1 equiv) and *t*-BuONa (1.07 g, 1.05 equiv) in THF (12 mL), benzyl bromide (1.77 mL, 1.5 equiv) was added dropwise at 0 °C. The reaction mixture was allowed to warm to room temperature and after 16 h, the reaction mixture was quenched with aq. HCl (2M) till pH 2. The aqueous phase was then extracted with Et_2O (3×10 mL). The combined organic phases are then washed with brine, dried over $MgSO_4$ and concentrated to afford **4.61** as a colourless oil (1.99 g, quant.).

^{1}H NMR (400 MHz, $CDCl_3$) δ 7.44–7.28 (m, 5H, H_{Ar}), 4.53 (s, 2H, PhC$\underline{H}_2$), 3.69 (t, *J*=6.5 Hz, 2H, H3), 3.63 (t, *J*=5.9 Hz, 2H, H1), 2.07 (quin, *J*=6.2 Hz, 2H, H2) ppm; **^{13}C NMR** (101 MHz, $CDCl_3$) δ 138.3 (C_{Ar}), 128.4 (C_{Ar}×2), 127.7 (C_{Ar}), 127.6 (C_{Ar}×2), 73.1 (Ph$\underline{C}H_2$), 66.7 (C1), 42.0 (C3), 32.8 (C2) ppm.

Data consistent with literature.[270]

Synthesis of 4-(thiocyanate)propyl benzyl ether (4.62)

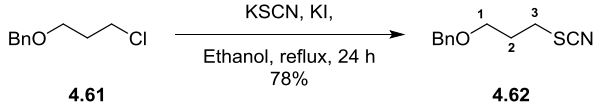

4.61 **4.62**

To a solution of **4.61** (1.88 g, 1 equiv) and KI (0.34 g, 0.2 equiv) in ethanol (30 mL) was added potassium thiocyanate (6.45 g, 6.5 equiv). The reaction mixture was refluxed for 24 h and then concentrated *in-vacuo*. The residue was dissolved in EtOAc (50 mL) and washed with water (2×50 mL), brine, dried over $MgSO_4$ and concentrated. The crude oil was purified with column chromatography (1:4, acetone/petrol ether 40 – 60 °C) to afford **4.62** as a pale-yellow oil (1.64 g, 78%).

^{1}H NMR (400 MHz, $CDCl_3$) δ 7.42–7.28 (m, 5H, H_{Ar}), 4.52 (s, 2H, PhC$\underline{H}_2$), 3.63 (t, *J*=5.6 Hz, 2H, H1), 3.11 (t, *J*=7.0 Hz, 2H, H3), 2.12 (tt, *J*=6.9, 5.7 Hz, 2H, H2) ppm; **^{13}C NMR** (101 MHz, $CDCl_3$) δ 137.9 (C_{Ar}), 128.5 (C_{Ar}×2), 127.8 (C_{Ar}), 127.7 (C_{Ar}×2), 112.3 (S$\underline{C}$N), 73.2 (Ph$\underline{C}H_2$), 66.9 (C1), 31.2 (C3), 30.0 (C2) ppm; **IR** (neat) 2943 (w), 2861 (m), 2153 (s), 1454 (s), 1080 (s), 1073 (s), 736 (s) cm^{-1}; **HRMS** (ESI+) for $C_{11}H_{13}NNaOS$ $[M+Na]^+$, calculated 230.0610, found 230.0613 (-1.1 ppm error).

Synthesis of 4-(trifluoromethylthio)propyl benzyl ether (4.63)

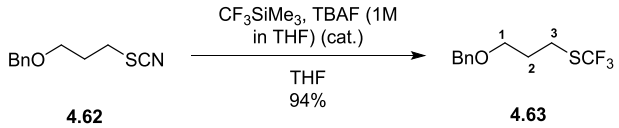

4.62 **4.63**

To a solution of **4.62** (1.50 g, 1 equiv), CF_3SiMe_3 (3.20 mL, 3 equiv) in THF (22 mL) was added TBAF (1M in THF, 0.72 mL, 0.1 equiv) at 0 °C. The reaction mixture was allowed to warm to room temperature and after 3 h, the reaction mixture was concentrated *in-vacuo*. The crude oil was purified with column chromatography (1:19, acetone/petrol ether 40–60 °C) to afford **4.63** as a colourless oil (1.70 g, 94%).

^{1}H NMR (400 MHz, $CDCl_3$) δ 7.41–7.28 (m, 5H, H_{Ar}), 4.52 (s, 2H, PhC$\underline{H}_2$), 3.59 (t, *J*=5.9 Hz, 2H, H1), 3.03 (t, *J*=7.2 Hz, 2H, H3), 2.01 (quin, *J*=6.4 Hz, 2H, H2) ppm; **^{13}C NMR** (101 MHz, $CDCl_3$) δ 138.1 (C_{Ar}), 128.4 (C_{Ar}×2), 127.7 (C_{Ar}), 127.6 (C_{Ar}×2), 131.1 (q, *J*=305.9 Hz, S$\underline{C}F_3$), 73.1 (Ph$\underline{C}H_2$), 67.7 (C1), 29.7 (C2), 26.9 (q, *J*=1.5 Hz, C3) ppm; **^{19}F NMR** (376 MHz, $CDCl_3$) δ -41.4 (s, 3F) ppm; **IR** (neat) 2943 (w), 2861 (m), 1455 (m), 1147 (s), 1096 (s), 734 (s) cm^{-1}; **HRMS** (EI) for $C_{11}H_{13}F_3OS$ $[M^{\cdot+}]$, calculated 250.0634, found 250.0623 (-1.04 ppm error).

Synthesis of 4-(trifluoromethylthio)-propanol (S1)

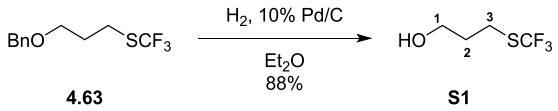

4.63 S1

To a solution of **4.63** (1.50 g, 1 equiv) in Et_2O (20 mL) was added a suspension of Pd/C 10% (300 mg) in Et_2O (5 mL). The reaction mixture was degassed with argon and one balloon of hydrogen. The reaction mixture was stirred at room temperature under a hydrogen atmosphere and after 16 h, the reaction was then filtered over Celite, which was then rinsed with CH_2Cl_2 (30 mL). The crude was carefully concentrated at 750 mbar/30 °C and purified by column chromatography (CH_2Cl_2) to afford **S1** as a colourless oil (0.85 g, 88%).

^{1}H NMR (400 MHz, $CDCl_3$) δ 3.79 (td, *J*=5.8, 4.3 Hz, 2H, H1), 3.03 (t, *J*=7.2 Hz, 2H, H3), 2.08–1.88 (m, 2H, H2), 1.41 (br. t, *J*=4.3 Hz, 1H, OH) ppm; **^{13}C NMR** (101 MHz, $CDCl_3$) δ 131.1 (q, *J*=305.4 Hz, SCF_3), 60.6 (C1), 32.1 (C2), 26.4 (q, *J*=1.5 Hz, C3) ppm; **^{19}F NMR** (376 MHz, $CDCl_3$) δ -41.5 (s, 3F) ppm; **IR** (neat) 3330 (br. w), 2950 (w), 2886 (w), 1442 (w), 1098 (s), 1053 (s), 755 (s) cm^{-1}; **HRMS** (EI) for $C_4H_7F_3OS$ [$M^{\cdot+}$], calculated 160.0164, found 160.0178 (+1.37 ppm error).

Synthesis of ((1R,2R)-2-fluorocyclopropyl)methanol (P1)

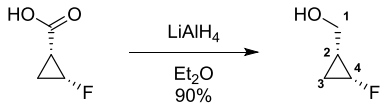

4.66 P1

A solution of **4.66** (250 mg, 1 equiv) in Et_2O (2 mL) was added to a slurry of $LiAlH_4$ (273 mg, 3 equiv) in Et_2O (6 mL) at 0 °C dropwise. The reaction was allowed to warm to room temperature and stirred for 16 h. It was then cooled to 0 °C and water (0.27 mL) was added dropwise, followed by aq. NaOH (15% wt., 0.27 mL) then water (0.81 mL). To this $MgSO_4$ was added and after stirring for 15 min the mixture was filtered and the resultant filtrate was carefully concentrated at 750 mbar/30 °C to afford **P1** as a colourless oil (195 mg, 90%).

^{1}H NMR (400 MHz, $CDCl_3$) δ 4.74 (dtd, *J*=65.2, 5.9, 2.7 Hz, 1H, H4), 3.94 (br. d, *J*=4.3 Hz, 1H, H1'), 3.69–3.60 (m, 1H, H1''), 1.52 (br. s, 1H, OH), 1.34–1.15 (m, 1H, H2), 0.92–0.71 (m, 2H, H3) ppm; **^{13}C NMR** (101 MHz, $CDCl_3$) δ 72.3 (d, *J*=218.8 Hz, C4), 61.1 (d, *J*=9.2 Hz, C1), 18.7 (d, *J*=11.0 Hz, C2), 9.4 (d, *J*=10.1 Hz, C3) ppm; **^{19}F NMR** (471 MHz, $CDCl_3$) δ -227.4 (dddd, *J*=65.0, 23.4, 11.3, 5.2 Hz, 1F) ppm; **^{19}F {^{1}H} NMR** (471 MHz, $CDCl_3$) δ -227.4 (s, 1 F) ppm; **IR** (neat) 3334 (br. w), 2943 (w), 2888 (w), 1445 (m), 1200 (s), 1016 (s), 982 (s) cm^{-1}; **HRMS** (CI) for C_4H_8FO [M+H]$^+$, calculated 91.0554, found 91.0544 (-0.98 ppm error).

Synthesis of (1-fluorocyclopropyl)methanol (P2)

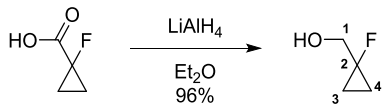

4.67 **P2**

A solution of **4.67** (250 mg, 1 equiv) in Et_2O (2 mL) was added to a slurry of $LiAlH_4$ (273 mg, 3 equiv) in Et_2O (6 mL) at 0 °C dropwise. The reaction was allowed to warm to room temperature and stirred for 16 h. It was then cooled to 0 °C and water (0.27 mL) was added dropwise, followed by aq. NaOH (15% wt., 0.27 mL) then water (0.81 mL). To this $MgSO_4$ was added and after stirring for 15 min the mixture was filtered and the resultant filtrate was carefully concentrated at 750 mbar/30 °C to afford **P2** as a colourless oil (208 mg, 96%).

^{1}H NMR (400 MHz, $CDCl_3$) δ 3.63 (d, *J*=22.0 Hz, 2H, H1), 1.66 (br. s, 1H, OH), 0.95–0.83 (m, 2H, H3' + H4'), 0.55–0.44 (m, 2H, H3'' + H4'') ppm; **^{13}C NMR** (101 MHz, $CDCl_3$) δ 79.9 (d, *J*=216.4 Hz, C2), 66.1 (d, *J*=22.0 Hz, C1), 9.2 (d, *J*=11.7 Hz, C3 and C4 overlapped) ppm; **^{19}F NMR** (376 MHz, $CDCl_3$) δ -191.3 (ttt, *J*=22.0, 18.6, 8.7 Hz, 1F) ppm; **^{19}F {^{1}H} NMR** (376 MHz, $CDCl_3$) δ -191.3 (s, 1F) ppm; **IR** (neat) 3339 (br. w), 2931 (w), 2872 (w), 1416 (m), 1200 (m), 1038 (s), 1013 (s) cm^{-1}; **HRMS** (CI) for C_4H_8FO $[M+H]^+$, calculated 91.0554, found 91.0544 (-0.94 ppm error).

Synthesis of ((1R,2S)-2-fluorocyclopropyl)methanol (P3)

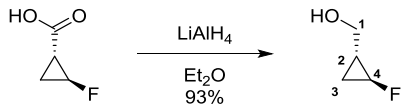

4.68 **P3**

A solution of **4.68** (250 mg, 1 equiv) in Et_2O (2 mL) was added to a slurry of $LiAlH_4$ (273 mg, 3 equiv) in Et_2O (6 mL) at 0 °C dropwise. The reaction was allowed to warm to room temperature and stirred for 16 h. It was then cooled to 0 °C and water (0.27 mL) was added dropwise, followed by aq. NaOH (15% wt., 0.27 mL) then water (0.81 mL). To this $MgSO_4$ was added and after stirring for 15 min the mixture was filtered and the resultant filtrate was carefully concentrated at 750 mbar/30 °C to afford **P3** as a colourless oil (201 mg, 93%).

^{1}H NMR (400 MHz, $CDCl_3$) δ 4.47 (ddt, *J*=64.1, 6.2, 2.3 Hz, 1H, H4), 3.55–3.42 (m, 2H, H1), 1.63–1.51 (m, 1H, H2), 1.48 (br. t, *J*=4.5 Hz, 1H, OH), 1.15–1.04 (m, 1H, H3'), 0.62 (app. dq, *J*=10.3, 6.7 Hz, 1H, H3') ppm; **^{13}C NMR** (101 MHz, $CDCl_3$) δ 72.5 (d, *J*=220.6 Hz, C4), 62.7 (C1), 20.2 (d, *J*=10.1 Hz, C2), 9.7 (d, *J*=11.0 Hz, C3) ppm; **^{19}F NMR** (376 MHz, $CDCl_3$) δ -210.2 (dtdd, *J*=64.2, 20.8, 10.4, 1.7 Hz, 1F) ppm; **^{19}F {^{1}H} NMR** (471 MHz, $CDCl_3$) δ -210.2 (s, 1F) ppm; **IR** (neat) 3335 (br. w), 2930 (w), 2881 (w), 1453 (m), 1135 (s), 1031 (s), 982 (s) cm^{-1}; **HRMS** (CI) for C_4H_8FO $[M+H]^+$, calculated 91.0554, found 91.0545 (-0.83 ppm error).

Synthesis of (2,2-difluorocyclopropyl)methanol (P4)

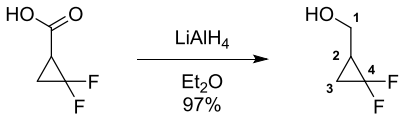

4.69 **P4**

A solution of **4.69** (250 mg, 1 equiv) in Et_2O (2 mL) was added to a slurry of $LiAlH_4$ (233 mg, 3 equiv) in Et_2O (6 mL) at 0 °C dropwise. The reaction was allowed to warm to room temperature and stirred for 16 h. It was then cooled to 0 °C and water (0.23 mL) was added dropwise followed by aq. NaOH (15% wt., 0.23 mL) then water (0.69 mL). To this $MgSO_4$ was added and after stirring for 15 min the mixture was filtered and the resultant filtrate was carefully concentrated at 750 mbar/30 °C to afford **P4** as a colourless oil (214 mg, 97%).

^{1}H NMR (400 MHz, $CDCl_3$) δ 3.98–3.54 (m, 2H, H1), 1.99–1.83 (m, 1H, H2), 1.48 (tdd, *J*=11.9, 7.6, 4.2 Hz, 1H, H3'), 1.18 (dtd, *J*=13.3, 7.6, 3.8 Hz, 1H, H3'') ppm; **^{13}C NMR** (101 MHz, $CDCl_3$) δ 113.6 (t, *J*=281.7 Hz, C4), 60.1 (d, *J*=5.9 Hz, C1), 24.3 (t, *J*=10.6 Hz, C2), 14.5 (t, *J*=11.4 Hz, C3) ppm; **^{19}F NMR** (376 MHz, $CDCl_3$) δ -128.8 (app. dtt, *J*=161.3, 12.1, 3.5 Hz, 1F, F4'), -144.5 (app. ddd, *J*=160.8, 13.4, 4.3 Hz, 1F, F4'') ppm; **^{19}F {^{1}H} NMR** (376 MHz, $CDCl_3$) δ -128.8 (d, *J*=161.3 Hz, 1F, F4''), -144.5 (d, *J*=161.3 Hz, 1F, F4'') ppm.

Data consistent with literature.[271]

4-bromo-3,3,4,4-tetrafluorobutyl benzyl ether (4.74)

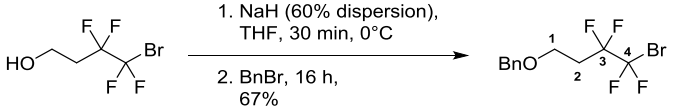

4.15 **4.74**

To a solution of 4-bromo-3,3,4,4-tetrafluoro-butan-1-ol (1 g, 1 equiv) in THF (15 mL), NaH in 60% mineral oil (195 mg, 1.1 equiv) was added portion wise at 0 °C. After 30 min, BnBr (0.79 mL, 1.5 equiv) was added after 16 h, quenched with sat. aq. NH_4Cl (15 mL). The aqueous phase was extracted with Et_2O (3×20 mL). The combined organic layers were collected, washed with water, brine, dried over $MgSO_4$ and concentrated *in vacuo*. The crude oil was purified with column chromatography (7:3, CH_2Cl_2/petrol ether 40 – 60 °C) to afford **4.74** as a colourless oil (0.94 g, 67%).

^{1}H NMR (400 MHz, $CDCl_3$) δ 7.42–7.27 (m, 5H), 4.56 (s, 2H, PhC$\underline{H}_2$), 3.78 (t, *J*=6.8 Hz, 2H, H1), 2.47 (tt, *J*=18.0, 6.9 Hz, 2H, H2) ppm; **^{13}C NMR** (101 MHz, $CDCl_3$) δ 137.6 (C_{Ar}), 128.5 (C_{Ar}×2), 127.8 (C_{Ar}), 127.6 (C_{Ar}×2), 117.5 (tt, *J*=311.0, 39.6 Hz, C4), 116.7 (tt, *J*=254.6, 31.5 Hz, C3), 73.3 (Ph$\underline{C}H_2$), 62.4 (t, *J*=4.0 Hz, C1), 31.1 (t, *J*=22.0 Hz, C2) ppm; **^{19}F NMR** (376 MHz, $CDCl_3$) δ -66.3 (t, *J*=3.5 Hz, 2F, F4), -111.2 (tt, *J*=17.4, 3.5 Hz, 2F, F3) ppm; **^{19}F {^{1}H} NMR** (376 MHz, $CDCl_3$) δ -66.3 (t, *J*=3.5 Hz, 2F, F3), -

111.2 (t, *J*=3.5 Hz, 2F, F4) ppm; **IR** (neat) 3033 (w), 2875 (w), 1368 (m), 1139 (s), 1088 (s), 903 (s), 755 (s) cm^{-1}; **HRMS** (EI) for $C_{11}H_{11}{}^{79}BrF_4O$ [$M^{\cdot+}$], calculated 313.9924, found 313.9914 (-1.03 ppm error).

Synthesis of 3,3,4,4-tetrabutan-1-ol (G10)

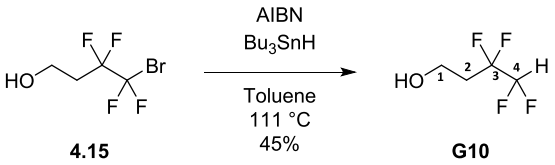

To a solution of 3,3,4,4-tetrafluoro-4-bromobutan-1-ol **4.15** (3.00 g, 1 equiv) and AIBN (219 mg, 0.1 equiv) in degassed toluene (15 mL) was added Bu_3SnH (5.4 mL, 1.5 equiv). The reaction mixture was refluxed for 16 h, before purification by column chromatography (100:0 to 0:100, Pentane/ CH_2Cl_2). The resulting crude was carefully concentrated 750 mbar/30 °C and purified again by column chromatography (10:0 to 8:2, CH_2Cl_2, Et_2O) on a silica gel/K_2CO_3 mix (9:1). The combined fractions were concentrated at 750 mbar/30 °C and combined with the concentrate from a reaction on a 2 g scale to yield **G10** as a colourless oil (1.47 g, 45 %).

^{1}H NMR (500 MHz, $CDCl_3$) δ 5.83 (tt, *J*=53.8, 3.5 Hz, 1H, H4), 3.95 (q, *J*=5.9 Hz, 2H, H1), 2.29 (ttt, *J*=17.5, 6.2, 1.5 Hz, 2H, H2), 1.65 (t, *J*=5.1 Hz, 1H, OH) ppm; **^{13}C NMR** (126 MHz, $CDCl_3$) δ 117.7 (tt, *J*=246.9, 28.9 Hz, C3), 110.1 (tt, *J*=248.9, 39.3 Hz, C4), 55.7 (t, *J*=5.5 Hz, C1), 33.2 (t, *J*=21.7 Hz, C2) ppm; **^{19}F NMR** (471 MHz, $CDCl_3$) δ -115.8 (tdt, *J*=17.5, 3.7, 1.8 Hz, 2F, F3), -136.2 (ddt, *J*=53.8, 3.5, 1.8 Hz, 2F, F4) ppm; **^{19}F {^{1}F} NMR** (471 MHz, $CDCl_3$) δ -115.7 (t, *J*=1.8 Hz, 2F, F3), -136.2 (t, *J*=1.8 Hz, 2F, F4) ppm; **IR** (neat) 3370 (br. w), 2982 (w), 2908 (w), 1091 (s), 1047 (s), 986 (s) cm^{-1}; **HRMS** (EI) for $C_4H_6F_4O$ [$M^{\cdot+}$], calculated 146.0349, found 146.0346 (-0.30 ppm error).

Synthesis of O-phenyl O-(2,2,3,3-tetrafluoro-4-hydroxybutyl) carbonothioate (4.77)

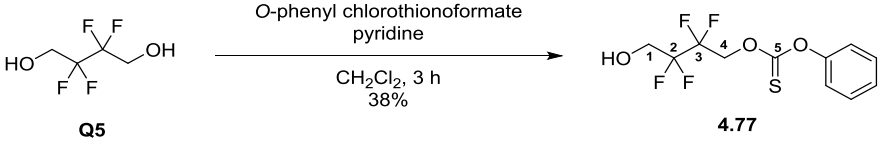

O-phenyl chlorothionoformate (0.28 mL, 1.1 equiv) was added dropwise to a solution of 2,2,3,3,tetrafluoro-1,4-butandiol (297 mg, 1 equiv) in Et_2O (10 mL) and pyridine (0.15 mL) at -50 °C. After 3 h, the reaction mixture was quenched with water (2 mL) and aq. HCl (2 M, 2 mL). The aqueous was extracted with Et_2O (2×10 mL) and CH_2Cl_2 (10 mL). The combined organic layers were dried over $MgSO_4$ and was concentrated *in vacuo*. The crude oil was purified by flash column chromatography (CH_2Cl_2). The resultant solid was washed with pentane and recrystallized by slow evaporation of CH_3Cl_3 to afford pure **4.77** as white crystals (0.29 g, 52%).

^{1}H NMR (400 MHz, $CDCl_3$) δ 7.48–7.41 (m, 2H, H_{Ar}), 7.36–7.30 (m, 1H, H_{Ar}), 7.17–7.12 (m, 2H, H_{Ar}), 5.01 (tt, *J*=13.8, 1.1 Hz, 2H, H4), 4.14 (tdt, *J*=13.8, 7.3, 1.4 Hz, 2H, H1), 1.94 (t, *J*=7.3 Hz, 1H, OH) ppm; **^{13}C NMR** (126 MHz, $CDCl_3$) δ 194.1 (C5), 153.4 (C_{Ar}), 129.7 (C_{Ar}×2), 126.9 (C_{Ar}), 121.6 (C_{Ar}×2), 115.8 (tt, *J*=252.7, 31.7 Hz, C2 or C3), 114.9 (tt, *J*=254.2, 33.0 Hz, C2 or C3), 68.1 (t, *J*=26.2 Hz, C4), 60.3 (t, *J*=26.8 Hz, C1) ppm; **^{19}F NMR** (376 MHz, $CDCl_3$) δ -121.2 (t, *J*=13.9 Hz, 2F, F3), -123.9 (t, *J*=13.9 Hz, 2F, F2) ppm; **^{19}F {^{1}H} NMR** (376 MHz, $CDCl_3$) δ -121.2 (s, 2F, F3), -123.9 (s, 2F, F2) ppm; **IR** (neat) 3368 (br. w), 2966 (w), 2939 (w), 2866 (w), 1189 (s), 1084 (s) cm^{-1}; **HRMS** (ESI+) for $C_{11}H_{10}F_4NaO_3S$ $[M+Na]^+$, calculated 321.0179, found 321.0179 (+0.1 ppm error); **Crystal Structure**

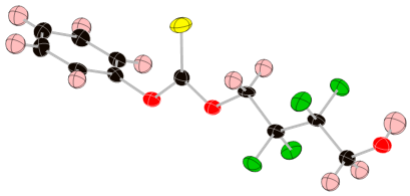

Synthesis of 4-((*tert*-butyldimethylsilyl)oxy)-2,2,3,3-tetrafluorobutan-1-ol (4.78)

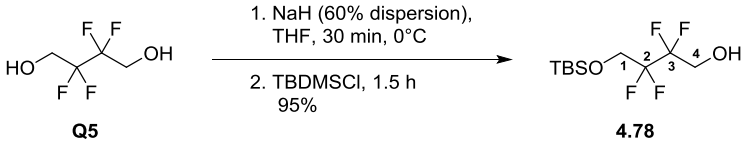

Q5 **4.78**

To a solution of 2,2,3,3-tetrafluoro-1,4-butandiol (0.987 mg, 1 equiv) in THF (20 mL) was added NaH (60% oil dispersion, 178 mg, 0.7 equiv) at 0 °C. After 30 min, TBDMSCl (660 mg, 0.7 equiv) was added portion wise. After 1.5 h, the reaction mixture was quenched with sat. aq. NH_4Cl (10 mL) and the aqueous phase was extracted with Et_20 (3×20 mL) and CH_2Cl_2 (20 mL). The combined organic layers were washed with brine, dried over $MgSO_4$ and concentrated *in vacuo*. The crude oil was purified by column chromatography (1:9, acetone/petrol ether 40–60 °C) to afford **4.78** as a colourless oil (1.08 g, 95%).

^{1}H NMR (400 MHz, $CDCl_3$) δ 4.02 (tt, *J*=12.6, 1.7 Hz, 2H, H1), 3.98 (tdt, *J*=13.4, 7.5, 1.5 Hz, 2H, H4), 2.81 (t, *J*=7.5 Hz, 1H, OH), 0.93 (s, 9H, $SiC(CH_3)_3$), 0.15 (s, 6H, $Si(CH_3)_2$) ppm; **^{13}C NMR** (126 MHz, $CDCl_3$) δ 116.0 (tt, *J*=253.3, 29.9 Hz, C2 or C3), 115.7 (tt, *J*=253.2, 29.1 Hz, C2 or C3), 61.2 (t, *J*=29.9 Hz, C1), 60.7 (t, *J*=27.4 Hz, C4), 25.6 ($SiC(\underline{C}H_3)_3$), 18.2 ($Si\underline{C}(CH_3)_3$), -5.7 ($Si(\underline{C}H_3)_2$) ppm; **^{19}F NMR** (376 MHz, $CDCl_3$) δ -124.4 (t, *J*=13.0 Hz, 2F, F2 or F3), -125.4 (t, *J*=13.9 Hz, 2F, F2 or F3) ppm; **^{19}F {^{1}H} NMR** (376 MHz, $CDCl_3$) δ -124.4 (s, 2F, F2 or F3), -125.4 (s, 2F, F2 or F3) ppm; **IR** (neat) 3362 (br. w), 2953 (w), 2859 (w), 1257 (m), 1116 (s), 1091 (s) 836 (s) cm^{-1}; **MS** and **HRMS**: Unsuccessful after multiple attempts, HRMS was successful on the next compound in the series **4.79**.

Synthesis of O-(4-((*tert*-butyldimethylsilyl)oxy)-2,2,3,3-tetrafluorobutyl) O-phenyl carbonothioate (4.79)

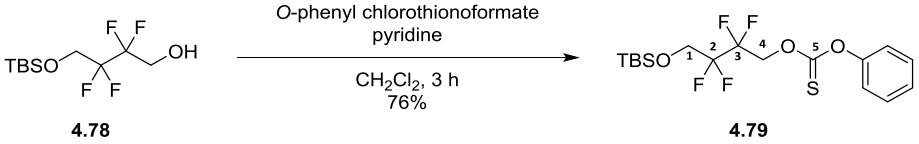

To a solution of **4.78** (1.01 g, 1 equiv) in CH_2Cl_2 was added *O*-phenyl chlorothionoformate (0.8 mL, 1.2 equiv) and pyridine (0.59 mL, 2 equiv). After 1 h, the reaction was diluted with EtOAc (50 mL) and washed with sat. aq. $NaHCO_3$ (50 mL). The organic layer was dried over $MgSO_4$ and the crude oil was purified by flash column chromatography (1:9, acetone/petrol ether 40–60 °C) to a yield **4.79** as a colourless oil (1.14g, 76%).

^{1}H NMR (400 MHz, $CDCl_3$) δ 7.50–7.40 (m, 2H, H_{Ar}), 7.37–7.29 (m, 1H, H_{Ar}), 7.18–7.09 (m, 2H, H_{Ar}), 4.99 (t, *J*=14.6 Hz, 2H, H4), 4.06 (tt, *J*=13.0, 1.7 Hz, 2H, H1), 0.93 (s, 9H, $SiC(C\underline{H}_3)_3$), 0.15 (s, 6H, $Si(CH_3)_2$) ppm; **^{13}C NMR** (126 MHz, $CDCl_3$) δ 194.3 (C5), 153.5 (C_{Ar}), 129.6 (C_{Ar}×2), 126.8 (C_{Ar}), 121.7 (C_{Ar}×2), 115.7 (tt, *J*=253.5, 29.8 Hz, C2 or C3), 114.8 (tt, *J*=255.0, 31.7 Hz, C2 or C3), 68.8 (t, *J*=24.0 Hz, C4), 61.1 (t, *J*=29.1 Hz, C1), 25.6 ($SiC(\underline{C}H_3)_3$), 18.3 ($Si\underline{C}(CH_3)_3$), -5.7 ($Si(CH_3)_2$) ppm; **^{19}F NMR** (376 MHz, $CDCl_3$) δ -122.0 (t, J=14.7 Hz, 2F, F3), -123.6 (t, J=13.0 Hz, 2F, F2) ppm; **^{19}F {^{1}H} NMR** (376 MHz, $CDCl_3$) δ -122.0 (s, 2F, F3), -123.6 (s, 2F, F2) ppm; **IR** (neat) 2954 (w), 2931 (w), 2859 (w), 1296 (s), 1127 (s), 837 (s) cm^{-1}; **HRMS** (ESI+) for $C_{17}H_{24}F_4NaO_3SSi$ $[M+Na]^+$, calculated 435.1044, found 435.1044 (-0.1 ppm error).

Synthesis of 2,2,3,3-tetrafluoro-4-hydroxybutyl benzoate (4.81)

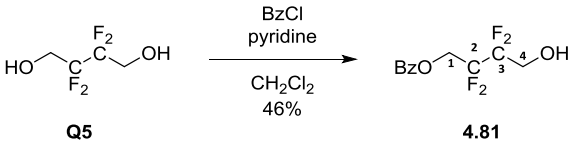

To a solution of benzoyl chloride (1.46 mL, 1.05 equiv) and pyridine (1.94 mL, 2 equiv) in CH_2Cl_2 was added **Q5** (1.945 g, 1 equiv) portion wise at 0 °C. After 20 h, the reaction was quenched with aq. HCl (2M, 15 mL) and the aqueous phase was extracted with CH_2Cl_2 (2×15 mL). The combined organic phases were washed with sat. aq. $NaHCO_3$ (2×40 mL) and water (40 mL), dried over $MgSO_4$ and concentrated *in vacuo*. The crude oil was purified by column chromatography (CH_2Cl_2) to afford **4.81** as a colourless oil (1.26 g, 46%)

^{1}H NMR (500 MHz, $CDCl_3$) δ 8.12–8.03 (m, 2H, H_{Ar}), 7.68–7.57 (m, 1H, H_{Ar}), 7.52–7.42 (m, 2H, H_{Ar}), 4.82 (tt, *J*=14.0, 1.1 Hz, 2H, H1), 4.10 (t, *J*=13.9 Hz, 2H, H4) ppm; **^{13}C NMR** (126 MHz, $CDCl_3$) δ 165.4 (C=O), 133.7 (C_{Ar}), 123.0 (C_{Ar}×2), 128.7 (C_{Ar}), 128.6 (C_{Ar}×2), 116.0 (tt, *J*=252.3, 32.2 Hz, C2 or C3), 115.4 (tt, *J*=252.8, 32.9 Hz, C2 or C3), 60.3 (t, *J*=26.3 Hz, C1 and C4, overlapped) ppm; **^{19}F NMR** (376

MHz, $CDCl_3$) δ -121.4 (t, *J*=13.9 Hz, 2F, F2), -123.9 (t, *J*=13.9 Hz, 2F, F3) ppm; **^{19}F {^{1}H} NMR** (376 MHz, $CDCl_3$) δ -121.4 (s, 2F, F2), -123.9 (t, *J*=5.2 Hz, 2F, F3) ppm; **IR** (neat) 3454 (br. w), 3082 (w), 2967 (w), 1730 (s), 1272 (s), 1111 (s), 1072 (s) cm^{-1}; **HRMS** (ESI+) for $C_{11}H_{10}F_4NaO_3$ $[M+Na]^+$, calculated 289.0458, found 289.0465 (-2.3 ppm error).

Synthesis of 2,2,3,3-tetrafluoro-4-((phenoxycarbonothioyl)oxy)butyl benzoate (4.82)

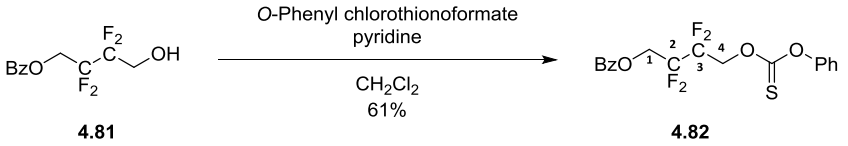

4.81 **4.82**

To a solution of **4.81** (1.26 g, 1 equiv) and pyridine (0.9 mL, 2 equiv) in CH_2Cl_2 (25 mL) was added *O*-phenyl chlorothionoformate (0.93 mL, 1.2 equiv) dropwise. After 1.5 h, the reaction was diluted with CH_2Cl_2 and washed with sat. aq. $NaHCO_3$ (50 mL) and dried over $MgSO_4$. The crude was concentrated *in vacuo* and purified by column chromatography (3:97, Et_2O/pentane) to afford **4.82** as a colourless oil (1.37 g, 61%).

^{1}H NMR (500 MHz, $CDCl_3$) δ 8.14–8.07 (m, 2H, H_{Ar}), 7.67–7.60 (m, 1H, H_{Ar}), 7.52–7.47 (m, 2H, H_{Ar}), 7.47–7.42 (m, 2H, H_{Ar}), 7.35–7.30 (m, 1H, H_{Ar}), 7.15–7.08 (m, 2H, H_{Ar}), 5.03 (tt, *J*=31.4, 1.3 Hz, 2H, H4), 4.85 (tt, *J*=13.5, 1.2 Hz, 2H, H1) ppm; **^{13}C NMR** (126 MHz, $CDCl_3$) δ 194.0 (C=S), 165.1 (C=O), 153.4 (C_{Ar}), 133.8 (C_{Ar}), 130.0 (C_{Ar}×2), 129.7 (C_{Ar}×2), 128.6 (C_{Ar}×2), 128.6 (C_{Ar}), 126.9 (C_{Ar}), 121.6 (C_{Ar}×2), 115.1 (tt, *J*=254.9, 31.7 Hz, C2), 114.6 (tt, *J*=255.0, 33.0 Hz, C3), 67.7 (t, *J*=26.7 Hz, C4), 59.9 (t, *J*=27.4 Hz, C1) ppm; **^{19}F NMR** (471 MHz, $CDCl_3$) δ -120.4– -120.5 (m, 2F, F3), -120.5– -120.6 (m, 2F, F2) ppm; **^{19}F {^{1}H} NMR** (471 MHz, $CDCl_3$) δ -120.3– -120.5 (m, 2F, F3), -120.5– -120.7 (m, 2F, F2) ppm; **IR** (neat) 3064 (w), 2963 (w), 1734 (s), 1266 (s), 1244 (s), 1228 (s), 1196 (s) cm^{-1}; **HRMS** (ESI+) for $C_{18}H_{14}F_4NaO_4S$ $[M+Na]^+$, calculated 425.0441, found 425.0447 (-1.5 ppm error).

Synthesis of 2,2,3,3-tetrafluorobutyl benzoate (4.83)

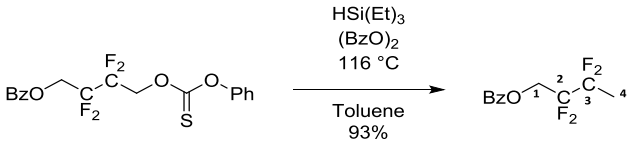

4.82 **4.83**

To a solution of **4.82** (1.36 g, 1 equiv) in toluene (20 mL, degassed) was added triethylsilane (2.7 mL, 5 equiv) and benzoyl peroxide (0.17 g, 0.2 equiv). The reaction was then brought to reflux. After 90 min, another addition of triethylsilane (2.7 mL, 5 equiv) and benzoyl peroxide (0.17 g, 0.2 equiv) was performed, and the reaction was bought back to reflux. After 2 h, the reaction mixture was concentrated *in vacuo* and purified by column chromatography (1:99, Et_2O/pentane) to afford **4.83** as a colourless oil (0.79 g, 93%).

^{1}H NMR (500 MHz, $CDCl_3$) δ 8.15–8.03 (m, 2H, H_{Ar}), 7.64–7.58 (m, 1H, H_{Ar}), 7.51–7.46 (m, 2H, H_{Ar}), 4.78 (tt, *J*=13.9, 1.2 Hz, 2H, H1), 1.82 (tt, *J*=19.1, 1.8 Hz, 3H, H4) ppm; **^{13}C NMR** (126 MHz, $CDCl_3$) δ 165.4 (C=O), 133.6 (C_{Ar}), 130.0 (C_{Ar}×2), 128.9 (C_{Ar}), 128.5 (C_{Ar}×2), 118.5 (tt, *J*=247.2, 34.6 Hz, C3), 115.0 (tt, *J*=251.7, 35.6 Hz, C2), 59.8 (t, *J*=26.8 Hz, C1), 17.4 (t, *J*=24.6 Hz, C4) ppm; **^{19}F NMR** (471 MHz, $CDCl_3$) δ -107.1– -107.3 (m, 2F, F3) -120.9– -121.1 (m, 2F, F2) ppm; **^{19}F {^{1}H} NMR** (471 MHz, $CDCl_3$) δ -107.2– -107.3 (m, 2F, F3) -120.9– -121.1 (m, 2F, F2) ppm; **IR** (neat) 3070 (w), 2968 (w), 1733 (s), 1452 (m), 1273 (s), 1108 (s), 1066 (s) cm^{-1}; **HRMS** (ESI+) for $C_{11}H_{10}F_4NaO_2$ $[M+Na]^+$, calculated 273.0509, found 273.0515 (-2.1 ppm error).

Synthesis of 2,2,3,3-tetrafluorobutanol (G12)

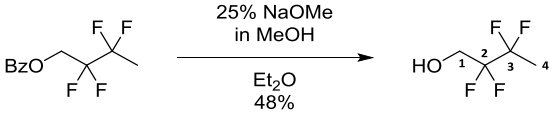

4.83 **G12**

To a solution of **4.83** (0.67 g, 1 equiv) in Et_2O (50 mL), NaOMe (25% w/w in MeOH, 1.20 mL, 2 equiv) was added dropwise. After 23 h, the reaction was neutralised with aq. HCl (2M, 15 mL) and the aqueous phase was washed with Et_2O (3×90 mL). The combined organic phases were dried over $MgSO_4$, filtered and concentrated (750 mbar, 30 °C). The crude mixture was purified by column chromatography (CH_2Cl_2) to **G12** as a pale-yellow oil (186 mg, 48%).

^{1}H NMR (400 MHz, $CDCl_3$) δ 4.04 (tdt, *J*=14.2, 7.1, 1.3 Hz, 2H, H1), 1.83 (t, *J*=7.3 Hz, 1H, OH), 1.78 (tt, *J*=19.3, 1.7 Hz, 3H, H4) ppm; **^{13}C NMR** (126 MHz, $CDCl_3$) δ 118.8 (tt, *J*=246.3, 34.8 Hz, C3), 115.8 (tt, *J*=250.5, 35.0 Hz, C2), 60.0 (t, *J*=26.3 Hz, C1), 17.6 (t, *J*=24.6 Hz, C4) ppm; **^{19}F NMR** (376 MHz, $CDCl_3$) δ -107.3– -107.5 (m, F3), -124.0– -124.1 (m, F2) ppm; **^{19}F {^{1}H} NMR** (376 MHz, $CDCl_3$) δ -107.3– -107.4 (m, F3), -124.0– -124.1 (m, F2) ppm; **IR** (thin film) 3367 (br. w), 2929 (w), 1174 (s), 1118 (s), 1084 (s), 1064 (s) cm^{-1}; **HRMS** (CI) for $C_4H_7F_4O$ $[M+H]^+$, calculated 147.0428, found 147.0434 (+0.69 ppm error).

Synthesis of 2,2,3,3,4,4-hexafluoro-5-hydroxypentyl benzoate (4.90)

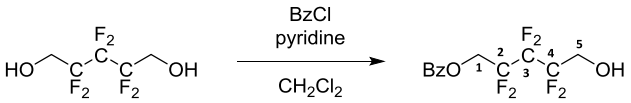

R4 **4.90**

To a solution of 2,2,3,3,4,4-hexafluoropentane-1,5-diol **R4** (5.00 g, 1 equiv) and pyridine (3.81 mL, 2 equiv) in CH_2Cl_2 (50 mL), was added a solution of benzoyl chloride (3.29 mL, 1.2 equiv) in CH_2Cl_2 (100 mL) dropwise over 30 min at 0 °C. The reaction was allowed to warm to room temperature and was quenched after 24 h with water (75 mL). The aqueous phase was washed with CH_2Cl_2 (2×30 mL), and the combined organic phases were washed with aq. HCl (1M, 50 mL) and sat. aq. $NaHCO_3$

(100 mL). The organic phase was dried over $MgSO_4$ and concentrated *in vacuo*. The crude product was purified by column chromatography (CH_2Cl_2) to afford **4.90** as a colourless oil (4.02 g, 54%).

^{1}H NMR (500 MHz, $CDCl_3$) δ 8.12–8.05 (m, 2H, H_{Ar}), 7.66–7.59 (m, 1H, H_{Ar}), 7.51–7.45 (m, 2H, H_{Ar}), 4.82 (t, *J*=13.9 Hz, 2H, H1), 4.11 (t, *J*=13.8 Hz, 2H, H5), 2.34 (br. s, 1H, OH) ppm; **^{13}C NMR** (126 MHz, $CDCl_3$) δ 165.2 (C=O), 133.8 (C_{Ar}), 130.0 (C_{Ar}×2), 128.6 (C_{Ar}×2), 128.5 (C_{Ar}), 115.6 (tt, *J*=255.6, 29.8 Hz, C4), 114.8 (tt, *J*=256.4, 31.0 Hz, C2), 111.5 (tquin, *J*=263.5, 33.1 Hz, C3), 60.6 (t, *J*=25.5 Hz, C5), 60.3 (t, *J*=26.7 Hz, C1) ppm; **^{19}F NMR** (471 MHz, $CDCl_3$) δ -119.7 (tt, *J*=13.9, 10.3 Hz, F2), -122.5 (tt, *J*=14.7, 9.9 Hz, F4), -125.7 (s, F3) ppm; **^{19}F {^{1}H} NMR** (471 MHz, $CDCl_3$) δ -119.7 (t, *J*=10.0 Hz, F2), -122.5 (t, *J*=10.0 Hz, F4), -125.7 (s, F3) ppm; **IR** (neat) 3459 (br. w), 2997 (w), 1733 (s), 1268 (s), 1147 (s) cm^{-1}; **HRMS** (ESI+) for $C_{12}H_{10}F_6NaO_3$ $[M+Na]^+$, calculated 339.0426, found 339.0425 (+0.3 ppm error).

Synthesis of 2,2,3,3,4,4-hexafluoro-5-((phenoxycarbonothioyl)oxy)pentyl benzoate (4.91)

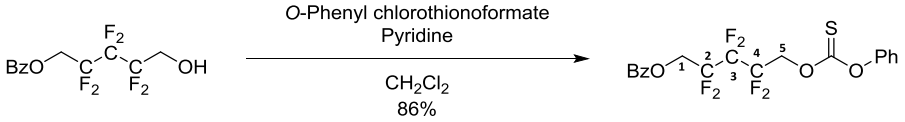

4.90 **4.91**

To a solution of **4.90** (3.10 g, 1 equiv) in CH_2Cl_2 (110 mL) was added pyridine (3.37 mL, 4.25 equiv) then *O*-phenyl chlorothioformate (1.62 mL, 1.2 equiv) at 0 °C. The reaction was allowed to warm to room temperature and after 1.5 h, the reaction mixture was diluted with CH_2Cl_2 (50 mL) and quenched with sat. aq. $NaHCO_3$ (50 mL). The aqueous phase was extracted with CH_2Cl_2 (3×50 mL) and the combined organic phases were dried over $MgSO_4$ and concentrated *in vacuo*. The crude product was purified by column chromatography (3:97, Et_2O/petroleum ether 40-60 °C) to afford **4.91** as a pale-yellow oil (3.81 g, 86%).

^{1}H NMR (500 MHz, $CDCl_3$) δ 8.14–8.06 (m, 2H, H_{Ar}), 7.64 (tt, *J*=7.5, 1.3 Hz, 1H, H_{Ar}), 7.53–7.47 (m, 2H, H_{Ar}), 7.48–7.42 (m, 2H, H_{Ar}), 7.37–7.30 (m, 1H, H_{Ar}), 7.17–7.12 (m, 2H, H_{Ar}), 5.03 (t, *J*=13.4 Hz, 2H, H5), 4.87 (t, *J*=13.6 Hz, 2H, H1) ppm; **^{13}C NMR** (126 MHz, $CDCl_3$) δ 193.9 (C6), 165.0 (C=O), 153.4 (C_{Ar}), 133.8 (C_{Ar}), 130.0 (C_{Ar}×2), 129.7 (C_{Ar}×2), 128.6 (C_{Ar}×2), 128.5 (C_{Ar}), 126.9 (C_{Ar}), 121.6 (C_{Ar}×2), 114.8 (tt, *J*=256.8, 31.3 Hz, C2), 114.3 (tt, *J*=259.1, 31.3 Hz, C4), 111.1 (tquin, *J*=263.7, 32.4 Hz, C3), 67.8 (t, *J*=26.2 Hz, C5), 60.2 (t, *J*=26.9 Hz, C1) ppm; **^{19}F NMR** (471 MHz, $CDCl_3$) δ -119.0– -119.2 (m, 2F, F4), -119.2– -119.4 (m, 2F, F2), -125.2 (s, 2F, F3) ppm; **^{19}F {^{1}H} NMR** (471 MHz, $CDCl_3$) δ -119.1 (t, *J*=10.7 Hz, 2F, F4), -119.3 (t, *J*=10.4 Hz, 2F, F2), -125.2 (s, 2F, F3) ppm; **IR** (neat) 3065 (w), 2964 (w), 1735 (s), 1490 (m), 1265 (s), 1196 (s), 1150 (s) cm^{-1}; **HRMS** (ESI+) for $C_{19}H_{14}F_6NaO_4S$ $[M+Na]^+$ calculated 475.0409, found 475.0420 (-2.3 ppm error).

Synthesis of 2,2,3,3,4,4-hexafluoropentyl benzoate (4.92)

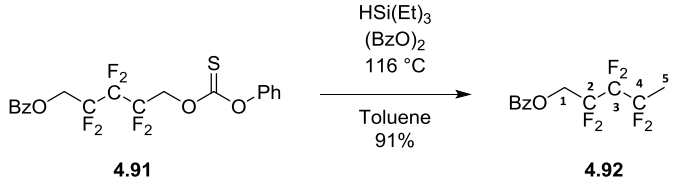

A solution of **4.91** (3.60 g, 1 equiv) in toluene (40 mL, degassed) and triethylsilane (6.36 mL, 5 equiv) was heated to reflux and benzoyl peroxide (387.0 mg, 0.2 equiv) was added. Benzoyl peroxide (387.0 mg, 0.2 equiv) and triethylsilane (6.36 mL, 5 equiv) were then added every 30 min to the refluxing reaction mixture until all the starting material had been consumed (3 additions). The reaction mixture was then concentrated *in vacuo* and the crude oil was purified by column chromatography (2:98, Et_2O/petroleum ether 40-60 °C) to afford **4.92** as a pale-yellow oil (2.17 g, 91%).

^{1}H NMR (400 MHz, $CDCl_3$) δ 8.13–8.06 (m, 2H, H_{Ar}), 7.66–7.58 (m, 1H, H_{Ar}), 7.52–7.43 (m, 2H, H_{Ar}), 4.81 (t, *J*=13.9 Hz, 2H, H1), 1.94–1.77 (m, 3H, H5) ppm; **^{13}C NMR** (126 MHz, $CDCl_3$) δ 165.1 (C=O), 133.7 (C_{Ar}), 130.0 (C_{Ar}×2), 128.6 (C_{Ar}), 128.6 (C_{Ar}×2), 117.9 (tt, *J*=250.2, 31.9 Hz, C4), 114.9 (tt, *J*=256.3, 30.9 Hz, C2), 111.2 (ttt, *J*=261.5, 34.3, 31.5 Hz, C3), 60.5 (t, *J*=26.5 Hz, C1), 18.5 (t, *J*=24.2 Hz, C5) ppm; **^{19}F NMR** (376 MHz, $CDCl_3$) δ -106.4 (qt, *J*=19.1, 9.5 Hz, 2F, F4), -119.5 (tt, *J*=13.9, 10.4 Hz, 2F, F2), -126.4 (s, 2F, F3) ppm; **^{19}F {^{1}H} NMR** (376 MHz, $CDCl_3$) δ -106.4 (t, *J*=9.5 Hz, 2F, F4), -119.5 (t, *J*=10.4 Hz, 2F, F2), -126.4 (s, 2F, F3) ppm; **IR** (neat) 3065 (w), 2964 (w), 1735 (s), 1267 (s), 1151 (s), 1107 (s) cm^{-1}; **HRMS** (ESI+) for $C_{12}H_{10}F_6NaO_2$ $[M+Na]^+$, calculated 323.0477, found 323.0483 (-1.7 ppm error).

Synthesis of 2,2,3,3,4,4-hexafluoropentan-1-ol (I15)

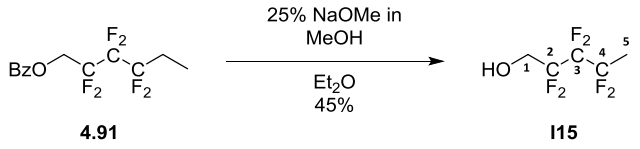

To a solution of **4.92** (0.91 g, 1 equiv) in Et_2O (6.6 mL), NaOMe (25% w/w in MeOH, 1.33 mL, 2 equiv) was added dropwise. After 23 h, the reaction was neutralised with aq. HCl (2M, 15 mL) and the aqueous phase was washed with CH_2Cl_2 (3×30 mL). The combined organic phases were dried ($MgSO_4$), filtered and concentrated (750 mbar, 30 °C). The crude mixture was purified by column chromatography (CH_2Cl_2) to **I15** as a pale-yellow oil (256 mg, 45%).

^{1}H NMR (400 MHz, $CDCl_3$) δ 4.08 (tdt, *J*=14.5, 7.5, 1.3 Hz, 2H, H1), 1.89 (tt, *J*=7.1, 0.9 Hz, 1H, OH), 1.83 (ttt, *J*=19.3, 1.9, 0.9 Hz, 3H, H5) ppm; **^{13}C NMR** (126 MHz, $CDCl_3$) δ 118.0 (tt, *J*=249.6, 32.2 Hz, C4), 115.7 (ttt, *J*=254.6, 30.3, 1.2 Hz, C2), 111.4 (ttt, *J*=261.1, 34.3, 31.5 Hz, C3), 60.8 (ttt, *J*= 25.4,

2.5, 1.5 Hz, C1), 18.4 (t, *J*=24.3 Hz, C5) ppm; **^{19}F NMR** (376 MHz, $CDCl_3$) δ -106.5 (qt, *J*=19.4, 9.1 Hz, 2F, F4), -122.6 (tt, *J*=14.3, 10.0 Hz, 2F, F2), -126.8 (s, 2F, F3) ppm; **^{19}F {^{1}H} NMR** (376 MHz, $CDCl_3$) δ -106.5 (t, *J*=9.5 Hz, 2F, F4), -122.6 (t, *J*=9.5 Hz, 2F, F2), -126.8 (s, 2F, F3) ppm; **IR** (thin film) 3354 (br. w), 2962 (w), 2888 (w), 1397 (m), 1149 (s), 1119 (s), 955 (s) cm^{-1}; **HRMS** (CI) for $C_5H_7F_6O$ $[M+H]^+$, calculated 197.0396, found 197.0402 (+0.64 ppm error).

8.4 Synthesis of evenamide analogues

Synthesis of 1-(benzyloxy)-3-[(E)-2-nitroethenyl]benzene (5.7)

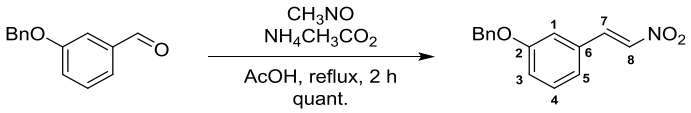

5.6 **5.7**

To a solution of 3-(benzyloxy)benzaldehyde **5.6** (3.00 g, 1 equiv) and ammonium acetate (2.40 g, 2.2 equiv) in acetic acid (25 mL) was added nitromethane (2.10 mL, 2.75 equiv). The reaction mixture was then brought up to reflux. After 2 h, the reaction mixture was allowed to cool, diluted with water (20 mL) and extracted with CH_2Cl_2 (3×40 mL). The combined organic layers were dried over $MgSO_4$, filtered and concentrated. The resultant solid residue was then stirred over heptane for 30 min, filtered and dried, to yield **5.7** as a green solid (3.61 g, quant.).

^{1}H NMR (400 MHz, $CDCl_3$) δ 7.97 (d, *J*=13.7 Hz, 1H, H7), 7.56 (d, *J*=13.7 Hz, 1H, H8), 7.48–7.33 (m, 6H, H4 + H_{Ar}×5 ($OCH_2\underline{Ph}$)), 7.20–7.14 (m, 1H, H5), 7.13 (d, *J*=1.2 Hz, 1H, H1), 7.13–7.10 (m, 1H, H3), 5.12 (s, 2H, $OC\underline{H}_2Ph$) ppm; **^{13}C NMR** (101 MHz, $CDCl_3$) δ 159.3 (C2), 139.0 (C7), 137.4 (C8), 136.2 ($C_{Ar,}$ $OCH_2\underline{Ph}$), 131.4 (C6), 130.5 (C4), 128.7 (C_{Ar}×2, $OCH_2\underline{Ph}$), 128.3 ($C_{Ar,}$ $OCH_2\underline{Ph}$), 127.4 (C_{Ar}×2, $OCH_2\underline{Ph}$), 122.0 (C5), 118.8 (C3), 115.0 (C1), 70.2 ($O\underline{C}H_2Ph$) ppm; **m.p.** 82-84 °C.

Data consistent with literature.[224]

Synthesis of (3-(benzyloxy)phenethyl)-*N*-Boc-amine (5.9)

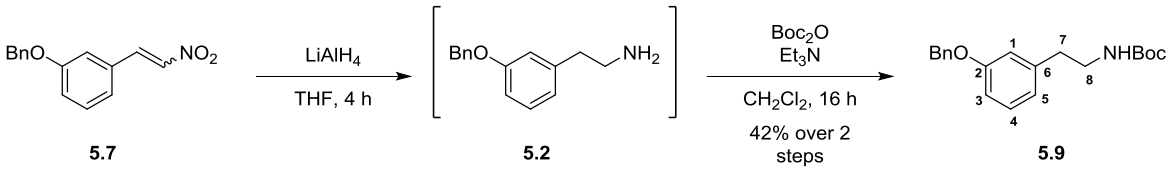

5.7 **5.2** **5.9**

To a solution of **5.7** (3.61 g, 1 equiv) in THF (30 mL) was added, a slurry of $LiAlH_4$ (1.21 g, 2 equiv) in Et_2O (30 mL) dropwise at 0 °C. The reaction was allowed to warm to room temperature and after 4 h was cooled to 0 °C, before the dropwise addition of water (1.2 mL), followed by 15% w.t. aq. NaOH (1.2 mL) and finally water (3.6 mL). The mixture is allowed to warm to room temperature and $MgSO_4$ is then added. The resultant slurry is stirred for 15 min, before filtration. The filter cake is then

washed with EtOAc (50 mL) and the combined filtrates are concentrated to afford the intermediate **5.2** (3.21 g, assumed quant.). To a solution of **5.2** (3.21 g, 1 equiv), Et_3N (1.97 mL, 1 equiv) in CH_2Cl_2 (30 mL) was added Boc_2O (3.39 g, 1.1 equiv) dissolved in CH_2Cl_2 (10 mL). After 16 h, the reaction mixture was concentrated and the crude was purified by column chromatography (1:4, EtOAc/heptane) to afford **5.9** as a colourless oil (1.92 g, 42% over 2 steps).

^{1}H NMR (400 MHz, $CDCl_3$) δ 7.49–7.30 (m, 5H, $H_{Ar,}OCH_2\underline{Ph}$), 7.23 (t, *J*=8.0 Hz, 1H, H4), 6.88–6.78 (m, 3H, H1 + H3 + H5), 5.07 (s, 2H, $OC\underline{H}_2Ph$), 4.54 (br. s, 1H, NH), 3.39 (q, *J*=6.2 Hz, 2H, H8), 2.78 (t, *J*=6.9 Hz, 2H, H7), 1.45 (s, 9H, $CH_3\times3$, Boc) ppm; **^{13}C NMR** (101 MHz, $CDCl_3$) δ 159.0 (C2), 155.8 (C=O), 140.7 (C6), 137.0 ($C_{Ar,}OCH_2\underline{Ph}$), 129.6 (C4), 128.6 ($C_{Ar}\times2$, $OCH_2\underline{Ph}$), 128.0 ($C_{Ar,}OCH_2\underline{Ph}$), 127.5 ($C_{Ar}\times2$, $OCH_2\underline{Ph}$), 121.4 (C5), 115.4 (C1), 112.7 (C3), 79.2 ($\underline{C}\text{-}(CH_3)_3$), 69.9 ($Ph\underline{C}H_2$), 41.6 (C8), 36.2 (C7), 28.4 ($CH_3\times3$, Boc) ppm.

Data consistent with literature.[272]

Synthesis of 2-((3-(Benzyloxy)phenethyl)-*N*-Boc-amino)-*N*,*N*-dimethylacetamide (5.10)

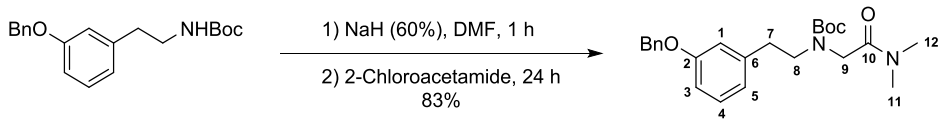

5.9 **5.10**

To a suspension of sodium hydride 60% in mineral oil (0.57 g, 2 equiv) in DMF (35 mL) at 0 °C, was added a solution of **5.9** (2.35 g, 1 equiv) in DMF (35 mL) dropwise. The reaction mixture was allowed to warm to room temperature and after 1 h, 2-chloroacetamide (1.47 mL, 2 equiv) was added. After 24 h, the reaction was quenched with water (5 mL) and the solvent removed *in vacuo*. The residue was dissolved in water (40 mL) and extracted with EtOAc (3×50 mL). The combined organic layers were washed with brine (50 mL), dried over Na_2SO_4 and concentrated. The crude was purified by column chromatography (1:1, EtOAc/heptane) to afford **5.10** as a colourless gum (2.46 g, 83%).

^{1}H NMR (400 MHz, $CDCl_3$, mixture of rotamers) δ 7.46–7.41 (m, 2H, $H_{Ar,}OCH_2\underline{Ph}$), 7.40–7.35 (m, 2H, $H_{Ar,}OCH_2\underline{Ph}$), 7.35–7.29 (m, 1H, $H_{Ar,}OCH_2\underline{Ph}$), 7.19 (t, *J*=7.7 Hz, 1H, H4), 6.93–6.71 (m, 3H, H1 + H3 + H5), 5.04 (s, 2H, $OC\underline{H}_2Ph$), 3.94 (s, 2H, H9 major), 3.82 (s, 2H, H9 minor), 3.51 (m, *J*=7.4 observed br. t, 2H, H8 major and minor), 2.97–2.88 (m, 6H, H11 + H12), 2.82 (m, *J*=7.4 observed br. t, 2H, H7 major and minor), 1.52–1.39 (m, 9H, $CH_3\times3$, Boc) ppm; **^{13}C NMR** (101 MHz, $CDCl_3$) δ (only major rotamer reported) 168.6 (C10), 158.9 (C2), 155.9 (C=O, Boc), 141.2 (C6), 137.1 ($C_{Ar,}OCH_2\underline{Ph}$), 129.4 (C4), 128.6 ($C_{Ar}\times2$, $OCH_2\underline{Ph}$), 127.9 ($C_{Ar,}OCH_2\underline{Ph}$), 127.5 ($C_{Ar}\times2$, $OCH_2\underline{Ph}$), 121.6 (C5), 115.6 (C1), 112.4 (C3), 80.0 ($\underline{C}\text{-}(CH_3)_3$), 69.9 ($Ph\underline{C}H_2$), 50.0 (C8), 48.7 (C9), 36.2 (C11 or C12), 35.7 (C11 or C12), 35.0 (C7), 28.4 ($CH_3\times3$, Boc) ppm; **IR** (neat) 2974 (m), 1691 (s), 1663 (s), 1252 (s), 1156 (s) cm^{-1}; **MS** (ESI+)

m/z 413.4 $[M+H]^+$, 435.4 $[M+Na]^+$; **HRMS** (ESI+) for $C_{24}H_{33}N_2O_4$ $[M+H]^+$, calculated 413.2435, found 413.2435 (+0.1 ppm error), for $C_{24}H_{32}N_2NaO_4$ $[M+Na]^+$, calculated 435.2254, found 435.2256 (-0.4 ppm error).

Synthesis of 2-((3-Hydroxyphenethyl)-*N*-Boc-amino)-N,N-dimethylacetamide (5.11)

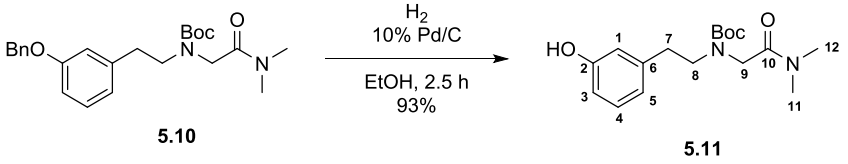

5.10 5.11

To a solution of **5.10** (2.37 g, 1 equiv) in EtOH (18 mL) was added a slurry of 10% Pd/C (0.50 g) in EtOH (2 mL). The reaction was degassed and placed under a H_2 environment. After 2.5 h the reaction mixture was filtered over a pad of Celite and concentrated. The crude was purified by column chromatography (3:7, acetone/heptane) to afford **5.11** as a colourless gum (1.73 g, 93%). **^{1}H NMR** (400 MHz, $CDCl_3$, mixture of rotamers) δ 7.13 (t, *J*=7.5 Hz, 1H, H4), 6.75–6.64 (m, 3H, H1 + H3 + H5), 6.40 (s, 1H, OH minor), 6.21 (s, 1H, OH major), 3.95 (s, 2H, H9, major), 3.86 (s, 2H, H9 minor), 3.49 (br. t, *J*=7.3 Hz, 2H, H8), 3.01–2.87 (m, 6H, H11 + H12), 2.78 (t, *J*=7.3 Hz, 2H, H7), 1.51–1.40 (m, 9H, CH_3×3, Boc) ppm; **^{13}C NMR** (101 MHz, $CDCl_3$) δ (only major rotamer reported) 168.9 (C10), 156.5 (C2), 156.0 (C=O, Boc), 141.0 (C6), 129.5 (C4), 120.6 (C5), 115.9 (C1), 113.4 (C3), 80.2 (C-$(CH_3)_3$), 50.1 (C8), 48.7 (C9), 36.3 (C11 or C12), 35.8 (C11 or C12), 34.8 (C7), 28.3 (CH_3×3, Boc) ppm; **IR** (neat) 3274 (br. w), 2975 (m), 1646 (s), 1249 (m), 1156 (s) cm^{-1}; **MS** (ESI+) m/z 323.4 $[M+H]^+$, 345.3 $[M+Na]^+$; **HRMS** (ESI+) for $C_{17}H_{27}N_2O_4$ $[M+H]^+$, calculated 323.1965, found 323.1961 (+1.4 ppm error), for $C_{17}H_{26}N_2NaO_4$ $[M+Na]^+$, calculated 345.1785, found 345.1782 (+0.5 ppm error).

8.4.1 General procedure A for tosylate formation

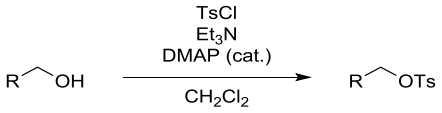

To a solution of alcohol (1 equiv) in CH_2Cl_2 was added Et_3N (1.1 equiv), DMAP (0.05-0.1 equiv) and tosyl chloride (1.1 equiv). After 1 h, the reaction was quenched with 2M aq. HCl and the layers were separated. The organic layer was washed with aq. sat. $NaHCO_3$, dried over Na_2SO_4 and concentrated to afford the tosylate **5.12**, which was used immediately without further purification.

Synthesis of Butyl tosylate (5.12a)

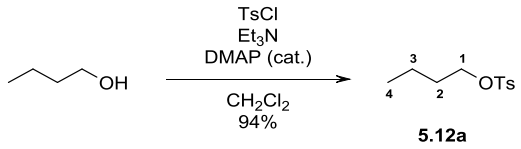

5.12a

Using general procedure A with butan-1-ol (0.3 g) in CH_2Cl_2 (10 mL), **5.12a** was obtained as a colourless oil (0.87 g, 94%). **^{1}H NMR** (500 MHz, $CDCl_3$) δ 7.82–7.75 (m, 2H, H_{Ar}), 7.37 - 7.30 (m, 2H, H_{Ar}), 4.03 (t, *J*=6.5 Hz, 2H, H1), 2.45 (s, 3H, PhC$\underline{H}_3$), 1.66–1.57 (m, 2H, H2), 1.39–1.29 (m, 2H, H3), 0.86 (t, *J*=7.4 Hz, 3H, H4) ppm;

Data consistent with literature.[273]

Synthesis of Pentyl tosylate (5.12e)

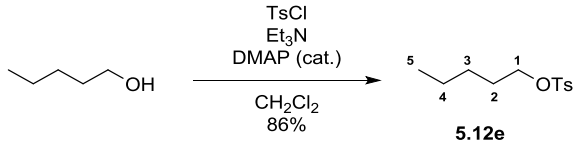

5.12e

Using general procedure A with pentan-1-ol (0.1 g) in CH_2Cl_2 (5 mL), **5.12e** was obtained as a colourless oil (0.24 g, 86%). **^{1}H NMR** (400 MHz, $CDCl_3$) δ 7.83–7.74 (m, 2H, H_{Ar}), 7.39–7.30 (m, 2H, H_{Ar}), 4.02 (t, *J*=6.6 Hz, 2H, H1), 2.45 (s, 3H, PhC$\underline{H}_3$), 1.68–1.60 (m, 2H, H2), 1.33–1.21 (m, 4H, H3 + H4), 0.85 (t, *J*=7.2 Hz, 3H, H5) ppm;

Data consistent with literature.[274]

Synthesis of 3,3-Difluorobutyl tosylate (5.12b)

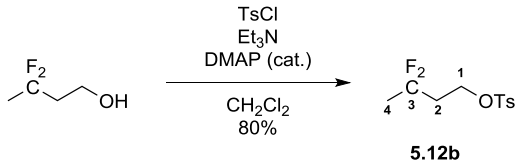

5.12b

Using general procedure A with 3,3-difluorobutan-1-ol (45 mg) in CH_2Cl_2 (5 mL), **5.12b** was obtained as a colourless oil (86 mg, 80%). **^{1}H NMR** (500 MHz, $CDCl_3$) δ 7.84–7.76 (m, 2H, H_{Ar}), 7.36 (d, *J*=8.6 Hz, 2H, H_{Ar}), 4.20 (t, *J*=6.7 Hz, 2H, H1), 2.46 (s, 3H, PhC$\underline{H}_3$), 2.26 (tt, *J*=15.2, 6.7 Hz, 2H, H2), 1.60 (t, *J*=18.7 Hz, 3H, H4) ppm; **^{19}F NMR** (471 MHz, $CDCl_3$) δ -90.2 (qt, *J*=18.7, 15.2, 2F) ppm; **^{19}F {^{1}H} NMR** (471 MHz, $CDCl_3$) δ -90.2 (s, 2F) ppm.

Synthesis of 4,4-Difluoropentyl tosylate (5.12f)

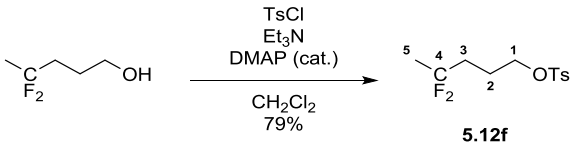

Using general procedure A with 4,4-difluoropentan-1-ol (30 mg) in CH_2Cl_2 (2 mL), **5.12f** was obtained as a colourless oil (53 mg, 79%). **^{1}H NMR** (400 MHz, $CDCl_3$) δ 7.84–7.75 (m, 2H, H_{Ar}), 7.36 (dd, *J*=8.6, 0.6 Hz, 2H, H_{Ar}), 4.08 (t, *J*=5.9 Hz, 2H, H1), 2.47 (s, 3H, PhC$\underline{H}_3$), 2.00–1.80 (m, 4H, H2 + H3), 1.58 (t, *J*=18.3 Hz, 3H, H5) ppm; **^{19}F NMR** (376 MHz, $CDCl_3$) δ -92.1 (qt, *J*=18.3, 15.6 Hz, 2F) ppm; **^{19}F {^{1}H} NMR** (376 MHz, $CDCl_3$) δ -92.1 (s, 2F) ppm.

Synthesis of 2,2,3,3,4,4,4-Heptafluorobutyl tosylate (5.12d)

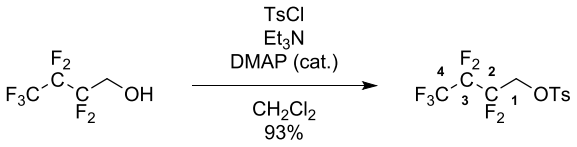

Using general procedure A with 2,2,3,3,4,4,4-heptafluorobutan-1-ol (0.11 g) in CH_2Cl_2 (5 mL), **5.12d** was obtained as a colourless oil (0.181 g, 93%). **^{1}H NMR** (500 MHz, $CDCl_3$) δ 7.85–7.78 (m, 2H, H_{Ar}), 7.39 (d, *J*=8.6 Hz, 2H, H_{Ar}), 4.45 (tt, *J*=12.9, 1.2 Hz, 2H, H1), 2.48 (s, 3H, PhC$\underline{H}_3$) ppm; **^{19}F NMR** (471 MHz, $CDCl_3$) δ -80.8 (t, *J*=9.1 Hz, 3F), -120.3– -120.4 (m, 2F), -127.2– -127.4 (m, 2F) ppm; **^{19}F {^{1}H} NMR** (471 MHz, $CDCl_3$) δ -80.8 (t, *J*=9.1 Hz, 3F), -120.3– -120.5 (m, 2F), -127.2– -127.4 (m, 2F) ppm.

8.4.2 General procedure B for aryl ether formation *via* the tosylate

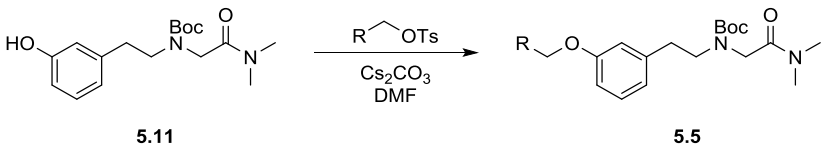

To a solution of **5.11** (1 equiv) and the tosylate **5.12** (1.1 equiv) in DMF was added Cs_2CO_3 (2 equiv). After 16 h the solvent was removed *in vacuo*. The residue was dissolved in water (30% v/v of DMF volume) and extracted with EtOAc. The combined organic layers were dried over Na_2SO_4 and concentrated. The crude was purified by column chromatography (1:1, EtOAc/heptane) to afford the ether **5.5**.

8.4.3 General procedure C for Boc-deprotection

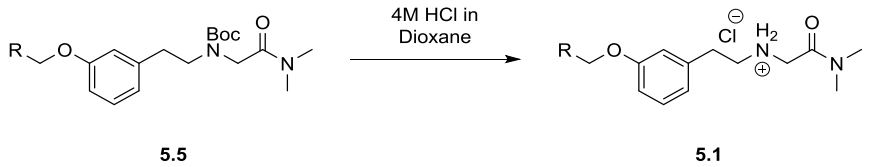

5.5 **5.1**

To the Boc protected amine **5.5** was added 4M HCl in dioxane (0.5 mL). The reaction was concentrated after complete consumption of starting material as confirmed by mass-spec analysis (roughly 4 h). The residue is then dissolved in CH_2Cl_2 (5 mL) and concentrated 3 times. The salt is then stirred in Et_2O (10 mL), filtered and further rinsed with Et_2O (10 mL). The resultant solid is then dissolved in CH_2Cl_2 and washed through the filter and concentrated to afford the evenamide analogues **5.1** as the pure HCl salt.

Synthesis of 2-((3-Butoxyphenethyl)amino)-*N*,*N*-dimethylacetamide•HCl (5.1a)

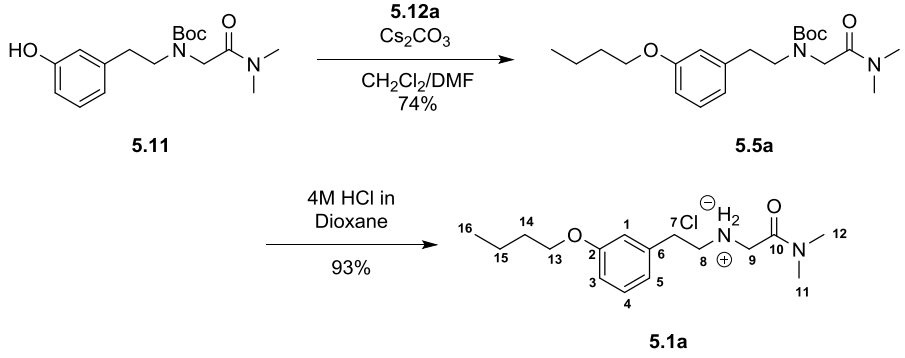

5.11 **5.5a** **5.1a**

Using general procedure B with **5.11** (61 mg) and **5.12a** (48 mg) in DMF (1 mL), **5.5a** was obtained as a colourless gum (53 mg, 74%). According to general procedure C, *N*-Boc cleavage of **5.5a** (97 mg, 1 equiv) yielded **5.1a** as an off white solid (75 mg, 93%). **^{1}H NMR** (400 MHz, $CDCl_3$) δ 9.54 (br. s, 2H, NH_2^+), 7.20 (t, *J*=7.8 Hz, 1H, H4), 6.86 (d, *J*=7.6 Hz, 1H, H5), 6.83 (s, 1H, H1), 6.77 (d, *J*=8.2 Hz, 1H, H3), 4.00 (s, 2H, H9), 3.93 (t, *J*=6.4 Hz, 2H, H13), 3.44–3.33 (m, 2H, H8), 3.31–3.21 (m, H7), 2.96 (s, 3H, H11 or H12), 2.94 (s, 3 H, H11 or H12), 1.74 (tt, *J*=7.5, 6.4, 2H, H14), 1.48 (qt, *J*=7.5, 7.4 Hz, 2H, H15), 0.97 (t, *J*=7.4 Hz, 3H, H16) ppm; **^{13}C NMR** (101 MHz, $CDCl_3$) δ 164.5 (C10), 159.6 (C2), 137.8 (C6), 129.8 (C4), 120.8 (C5), 114.9 (C1), 113.4 (C3), 67.7 (C13), 49.7 (C8), 48.0 (C9), 36.3 (C11 or C12), 35.8 (C11 or C12), 32.5 (C7), 31.3 (C14), 19.2 (C15), 13.8 (C16) ppm; **IR** (neat) 2930 (br. m), 2745 (br. m), 1665 (s), 1253 (s), 1161 (s) cm^{-1}; **MS** (ESI+) m/z 279.3 $[M+H]^+$, 301.3 $[M+Na]^+$; **HRMS** (ESI+) for $C_{16}H_{27}N_2O_2$ $[M+H]^+$, calculated 279.2067, found 279.2073 (-2.3 ppm error), for $C_{16}H_{26}N_2NaO_2$ $[M+Na]^+$, calculated 301.1886, found 301.1887 (-0.3 ppm error).

Synthesis of 2-((3-Pentoxyphenethyl)amino)-*N*,*N*-dimethylacetamide•HCl (5.1e)

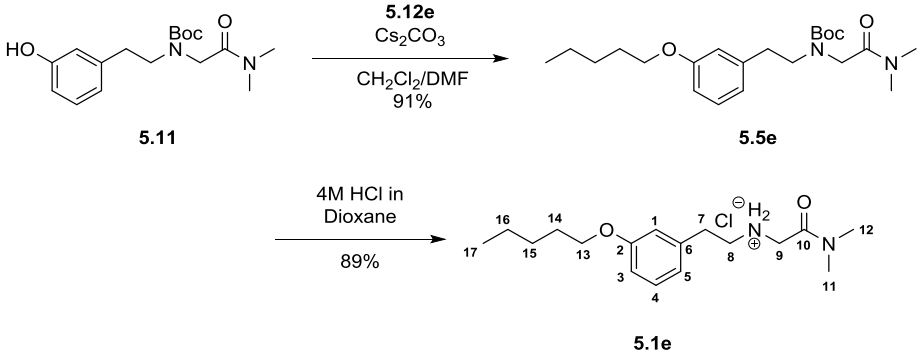

Using general procedure B with **5.11** (114 mg) and **5.12e** (90 mg) in DMF (2 mL), **5.5e** was obtained as a colourless gum (126 mg, 91%). According to general procedure C, *N*-Boc cleavage of **5.5e** (90 mg, 1 equiv) yielded **5.1e** as an off white solid (67 mg, 89%). **^{1}H NMR** (400 MHz, $CDCl_3$) δ 9.55 (br. s, 2 H, NH_2^+), 7.20 (t, *J*=7.8 Hz, 1H, H4), 6.86 (d, *J*=7.5 Hz, 1H, H5), 6.83 (s, 1H, H1), 6.77 (dd, *J*=8.2, 1.8 Hz, 1H, H3), 4.00 (s, 2H, H9), 3.93 (t, *J*=6.5 Hz, 2H, H13), 3.44–3.31 (m, 2H, H8), 3.31–3.21 (m, 2H, H7), 2.96 (s, 3H, H11 or H12), 2.94 (s, 3H, H11 or H12), 1.76 (tt, *J*=7.3, 6.5 Hz, 2H, H14), 1.51–1.30 (m, 4H, H15 + H16), 0.93 (t, *J*=7.1 Hz, 3H, H17) ppm; **^{13}C NMR** (101 MHz, $CDCl_3$) δ 164.5 (C10), 159.6 (C2), 137.8 (C6), 129.9 (C4), 120.8 C5), 114.9 (C1), 113.4 (C3), 68.0 (C13), 49.7 (C8), 48.0 (C9), 36.2 (C11 or C12), 35.8 (C11 or C12), 32.5 (C7), 28.9 (C14), 28.2 (C15), 22.4 (C16), 14.0 (C17) ppm; **IR** (neat) 2929 (br. s), 2744 (br. m), 1668 (s), 1252 (s), 1162 (s) cm^{-1}; **MS** (ESI+) m/z 293.3 $[M+H]^+$, 315.3 $[M+Na]^+$; **HRMS** (ESI+) for $C_{17}H_{29}N_2O_2$ $[M+H]^+$, calculated 293.2224, found 293.2226 (-0.7 ppm error), for $C_{17}H_{28}N_2NaO_2$ $[M+Na]^+$, calculated 315.2043, found 315.2043 (+0.1 ppm error).

Synthesis of 2-((3-(3,3-Difluorobutoxy)phenethyl)amino)-*N*,*N*-dimethylacetamide•HCl (5.1b)

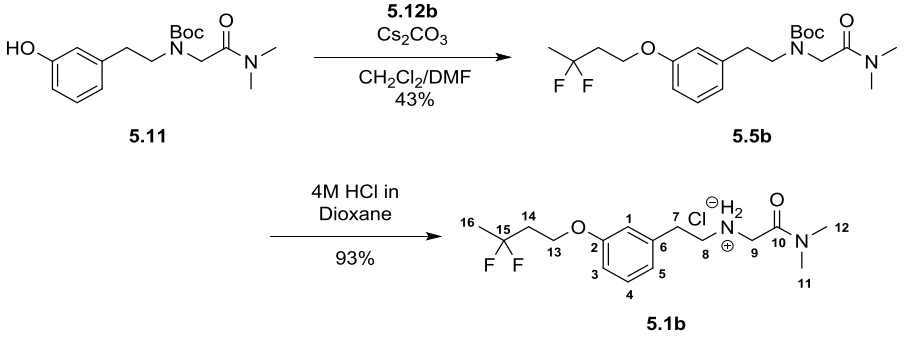

Using general procedure B with **5.11** (1 equiv) and **5.12b** (80 mg) in DMF (2 mL), **5.5b** was obtained as a colourless gum (54 mg, 43%). According to general procedure C, *N*-Boc cleavage of **5.5b** (51 mg, 1 equiv) yielded **5.1b** as an off white solid (40 mg, 93%). **^{1}H NMR** (400 MHz, $CDCl_3$) δ 9.57 (br. s, 2H, NH_2^+), 7.22 (t, *J*=7.8 Hz, 1H, H4), 6.90 (br. d, *J*=7.5 Hz, 1H, H5), 6.86 (s, 1H, H1), 6.78 (dd, *J*=8.1, 1.5 Hz, 1H, H3), 4.13 (t, *J*=6.4 Hz, 2H, H13), 4.01 (br. s, 2H, H9), 3.44–3.32 (m, 2H, H8), 3.32–3.23 (m, 2H, H7), 2.96 (s, 3H, H11 or H12), 2.93 (s, 3H, H11 or H12), 2.35 (tt, *J*=15.1, 6.4, 2H, H14), 1.70 (t,

J=18.8 Hz, 3H, H16) ppm; **^{13}C NMR** (101 MHz, $CDCl_3$) δ 164.5 (C10), 158.8 (C2), 138.0 (C6), 130.0 (C4), 121.5 (C5), 123.3 (t, *J*=238.1 Hz, C15), 115.0 (C1), 113.3 (C3), 62.2 (t, *J*=6.2 Hz, C13), 49.6 (C8), 48.0 (C9), 37.6 (t, *J*=26.0 Hz, C14), 36.3 (C11 or C12), 35.8 (C11 or C12), 32.4 (C7), 23.9 (t, *J*=27.1 Hz, C16) ppm; **^{19}F NMR** (376 MHz, $CDCl_3$) δ -89.3 (qt, *J*=18.8, 15.1 Hz, 2F) ppm; **^{19}F {^{1}H} NMR** (376 MHz, $CDCl_3$) δ -89.3 (s, 2F) ppm; **IR** (neat) 2921 (br. m), 2746 (br. m), 1667 (s), 1255 (w), 1160 (m) cm^{-1}; **MS** (ESI+) m/z 315.3 $[M+H]^+$, 337.3 $[M+Na]^+$; **HRMS** (ESI+) for $C_{16}H_{25}F_2N_2O_2$ $[M+H]^+$, calculated 315.1879, found 315.1882 (-1.2 ppm error), for $C_{16}H_{24}F_2N_2NaO_2$ $[M+Na]^+$, calculated 337.1698, found 337.1701 (-0.8 ppm error).

Synthesis of 2-((3-(4,4-Difluoropentoxy)phenethyl)amino)-*N*,*N*-dimethylacetamide•HCl (5.1f)

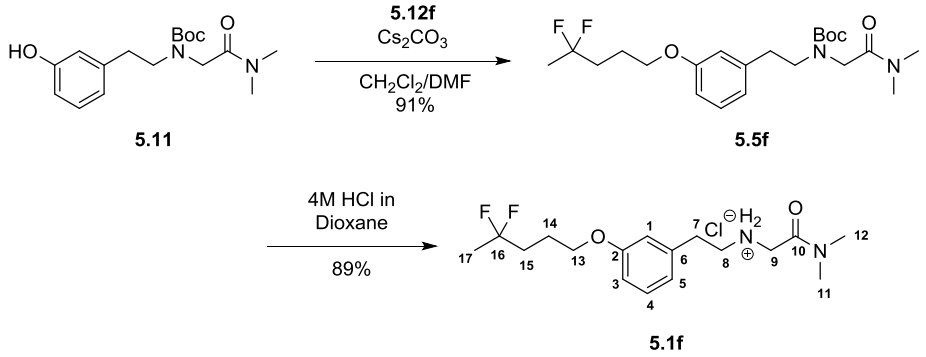

Using general procedure B with **5.11** (74 mg) and **5.12f** (53 mg) in DMF (2 mL), **5.5f** was obtained as a colourless gum (74 mg, 91%). According to general procedure C, *N*-Boc cleavage of **5.12f** (74 mg, 1 equiv) yielded **5.1f** as an off white solid (56 mg, 89%). **^{1}H NMR** (400 MHz, $CDCl_3$) δ 9.58 (br. s, 2H, NH_2^+), 7.20 (t, *J*=7.6 Hz, 1H, H4), 6.88 (d, *J*=7.3 Hz, 1H, H5), 6.85 (s, 1H, H1), 6.77 (d, *J*=8.1 Hz, 1H, H3), 4.02 (br. s, 2H, H9), 3.97 (t, *J*=5.5 Hz, 2H, H13), 3.38 (br. s, 2H, H8), 3.28 (br. s, 2H, H7), 2.96 (s, 3H, H11 or H12), 2.94 (s, 3H, H11 or H12), 2.14–1.86 (m, 4H, H14 + H15), 1.63 (t, *J*=18.3 Hz, 3H, H17); **^{13}C NMR** (101 MHz, $CDCl_3$) δ 164.5 (C10), 159.2 (C2), 138.0 (C6), 129.9 (C4), 124.1 (t, *J*=238.1 Hz, C16), 121.2 (C5), 115.0 (C1), 113.3 (C3), 67.0 (C13), 49.7 (C8), 48.1 (C9), 36.4 (C11 or C12), 35.8 (C11 or C12), 34.6 (t, *J*=25.7 Hz, C15), 32.5 (C7), 23.5 (t, *J*=27.9 Hz, C15), 22.7 (t, *J*=4.4 Hz, C14) ppm; **^{19}F NMR** (376 MHz, $CDCl_3$) δ -91.4 (sxt, *J*=17.3 Hz, 2F) ppm; **^{19}F {^{1}H} NMR** (376 MHz, $CDCl_3$) δ -91.4 (s, 2F) ppm; **IR** (neat) 2914 (br. m), 2743 (br. m), 1669 (s), 1251 (m), 1163 (m) cm^{-1}; **MS** (ESI+) m/z 329.3 $[M+H]^+$, 351.3 $[M+Na]^+$; **HRMS** (ESI+) for $C_{17}H_{27}F_2N_2O_2$ $[M+H]^+$, calculated 329.2035, found 329.2033 (+0.7 ppm error), for $C_{17}H_{26}F_2N_2NaO_2$ $[M+Na]^+$, calculated 351.1855, found 351.1847 (+2.0 ppm error).

Synthesis of 2-((3-(Tosyloxy)phenethyl)-*N*-Boc-amino)-*N*,*N*-dimethylacetamide (5.13)

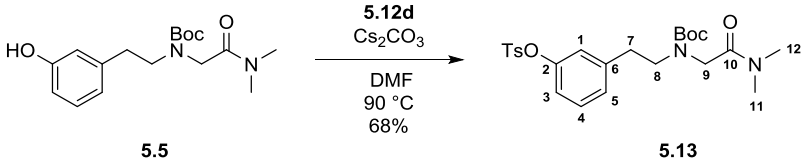

5.5 5.13

Using general procedure B with **5.5** (0.150 g) and **5.12d** (0.181 g) in DMF (2 mL), **5.13** was obtained as a colourless oil (0.15 g, 68%). **^{1}H NMR** (400 MHz, $CDCl_3$, mixture of rotamers) δ 7.70 (d, *J*=8.1 Hz, 2H, $H_{Ar(o)}$), 7.32 (d, *J*=7.9 Hz, 2H, $H_{Ar(m)}$), 7.19 (t, *J*=7.9 Hz, 1H, H4), 7.14–7.01 (m, 1H, H5), 6.86 (br. s, 1H, H1), 6.80 (br. d, *J*=8.1 Hz, 1H, H3), 3.91 (s, 2H, H9, major), 3.79 (s, 2H, H9 minor), 3.42 (t, *J*=7.3 Hz, 2H, H8), 2.94 (s, 6H, H11 + H12), 2.86–2.74 (m, 2H, H7), 2.46 (s, 3H, $PhC\underline{H}_3$), 1.55–1.37 (m, 9H, $C\underline{H}_3\times3$, Boc) ppm; **^{13}C NMR** (101 MHz, $CDCl_3$) δ (only major rotamer reported) 168.4 (C10), 155.7 ($\underline{C}$=O, Boc), 149.6 (C2), 145.3 ($C_{Ar(i)}$), 141.6 (C6), 132.5 ($C_{Ar(p)}$), 129.7 ($C_{Ar(m)}\times2$), 129.5 (C4), 128.4 ($C_{Ar(o)}\times2$), 127.7 (C5), 122.8 (C1), 120.1 (C3), 80.1 ($\underline{C}$-$(CH_3)_3$), 49.9 (C8), 48.9 (C9), 36.2 (C11 or C12), 35.7 (C11 or C12), 34.7 (C7), 28.4 ($CH_3\times3$, Boc), 21.7 ($PhC\underline{H}_3$) ppm; **IR** (neat) 2930 (m), 1695 (s), 1663 (s), 1367 (s), 1178 (s) cm^{-1}; **MS** (ESI+) m/z 477.4 $[M+H]^+$, 499.4 $[M+Na]^+$; **HRMS** (ESI+) for $C_{24}H_{33}N_2O_6S$ $[M+H]^+$, calculated 477.2054, found 477.2058 (-1.0 ppm error), for $C_{24}H_{32}N_2NaO_6S$ $[M+Na]^+$, calculated 499.1873, found 499.1880 (-1.3 ppm error).

8.4.4 General procedure D for aryl ether formation *via* the triflate

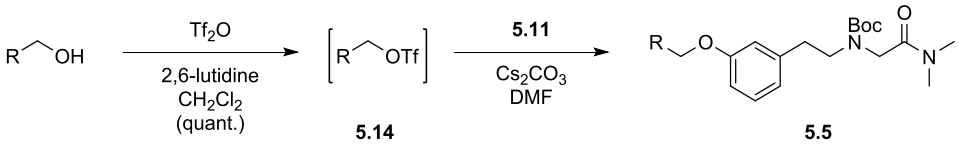

5.14 5.5

To a solution of the alcohol (1 equiv) in CH_2Cl_2 was added triflic anhydride (1.05 equiv) and 2,6-lutidine (1.1 equiv). Once complete consumption of the alcohol was shown by ^{19}F NMR analysis (roughly 1 h), Cs_2CO_3 (3 equiv) was added to the reaction mixture followed by a solution of **5.11** (1.2 equiv) in DMF. After 16 h the solvent was removed *in vacuo*. The residue was dissolved in water (similar volume as DMF) and extracted with EtOAc. The combined organic layers were dried over Na_2SO_4 and concentrated. The crude mixture was purified by column chromatography (1:1 EtOAc/heptane) to afford the ether **5.5**.

Synthesis of 2-((3-(2,2,3,3-Tetrafluorobutoxy)phenethyl)amino)-*N*,*N*-dimethylacetamide•HCl (5.1c)

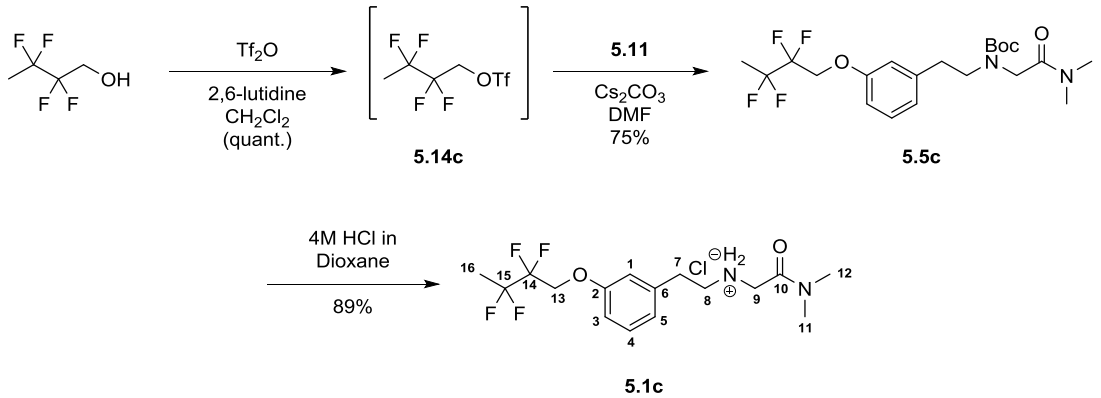

Using general procedure D with 2,2,3,3-tetrafluorobutan-1-ol (30 mg) in CH_2Cl_2 (0.5 mL), and **5.11** (79 mg) in DMF (0.6 mL), **5.5c** was obtained as a colourless gum (69 mg, 75%). According to general procedure C, *N*-Boc cleavage of **5.5c** (69 mg, 1 equiv) yielded **5.1c** as an off white solid (53 mg, 89%).

^{1}H NMR (400 MHz, $CDCl_3$) δ 9.59 (br. s, 2 H, NH_2^+), 7.24 (t, *J*=7.9 Hz, 1H, H4), 6.97 (d, *J*=7.5 Hz, 1H, H5), 6.93 (s, 1H, H1), 6.83 (dd, *J*=8.3, 1.9 Hz, 1H, H3), 4.39 (t, *J*=13.4 Hz, 2H, H13), 4.02 (s, 2H, H9), 3.46–3.34 (m, 2H, H8), 3.34–3.25 (m, 2H, H7), 2.96 (s, 3H, H11 or H12), 2.92 (s, 3H, H11 or H12), 1.82 (tt, *J*=19.3, 1.5 Hz, 3H, H16) ppm; **^{13}C NMR** (101 MHz, $CDCl_3$) δ 164.5 (C10), 158.1 (C2), 138.3 (C6), 130.1 (C4), 122.6 (C5), 115.4 (C1), 113.5 (C3), 64.7 (t, *J*=26.8 Hz, C13), 49.4 (C8), 48.0 (C9), 36.3 (C11 or C12), 35.7 (C11 or C12), 32.3 (C7), 17.8 (t, *J*=24.2 Hz, C16) ppm (C14 and C15 were not observed due to multiple fluorine-fluorine couplings); **^{19}F NMR** (376 MHz, $CDCl_3$) δ -107.2– -107.7 (m, 2F, F15), -121.7– -122.1 (m, 2F, F14) ppm; **^{19}F {^{1}H} NMR** (376 MHz, $CDCl_3$) δ -107.4– -107.5 (m, 2F, F15), -121.8– -122.0 (m, 2F, F14) ppm; **IR** (neat) 2943 (br. m), 2784 (br. m), 1663 (s), 1269 (w), 1161 (s), 1141 (s) cm^{-1}; **MS** (ESI+) m/z 351.3 $[M+H]^+$, 373.3 $[M+Na]^+$; **HRMS** (ESI+) for $C_{16}H_{23}F_4N_2O_2$ $[M+H]^+$, calculated 351.1690, found 351.1693 (-0.9 ppm error), for $C_{16}H_{22}F_4N_2NaO_2$ $[M+Na]^+$, calculated 373.1510, found 373.1512 (-0.5 ppm error).

Synthesis of 2-((3-(2,2,3,3,4,4,4-Heptafluorobutoxy)phenethyl)amino)-*N*,*N*-dimethylacetamide•HCl (5.1d)

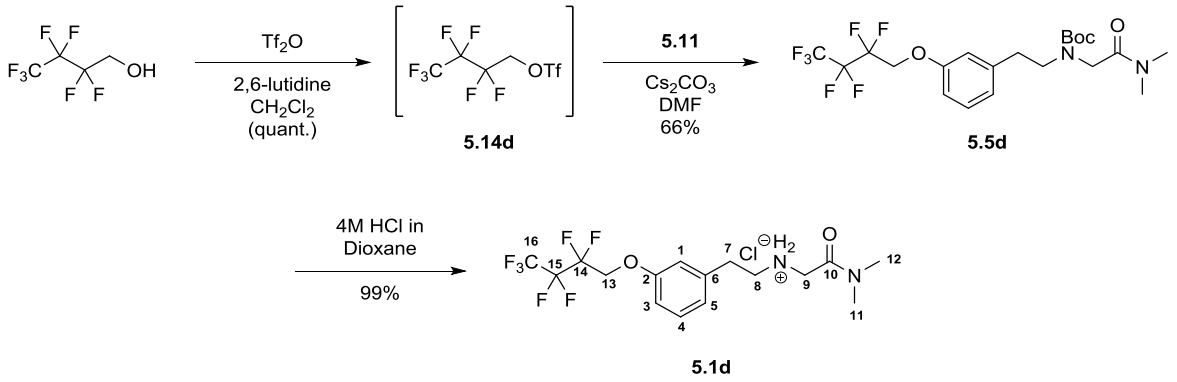

Using general procedure D with 2,2,3,3,4,4,4-heptafluorobutan-1-ol (20 mg) in CH_2Cl_2 (0.3 mL), **5.11** (32 mg) in DMF (0.2 mL), but only 2 equiv of Cs_2CO_3, **5.5d** was obtained as a colourless gum (33 mg, 66%). According to general procedure C, *N*-Boc cleavage of **5.5d** (57 mg, 1 equiv) yielded **5.1d** as an off white solid (49 mg, 99%).

^{1}H NMR (400 MHz, $CDCl_3$) δ 9.53 (br. s, 2 H, NH_2^+), 7.26 (t, *J*=7.8 Hz, 1H, H4), 6.99 (d, *J*=7.2 Hz, 1H, H5), 6.95 (s, 1H, H1), 6.83 (d, *J*=7.9 Hz, 1H, H3), 4.47 (t, *J*=12.7 Hz, 2H, H13), 4.03 (s, 2H, H9), 3.38 (s, 2H, H8), 3.31 (br. s, 2H, H7), 2.97 (s, 2H, H11 or H12), 2.93 (s, 3H, H11 or H12) ppm; **^{13}C NMR** (101 MHz, $CDCl_3$) δ 164.5 (C10), 157.7 (C2), 138.5 (C6), 130.2 (C4), 123.0 (C5), 115.4 (C1), 113.7 (C3), 65.0 (t, *J*=27.1 Hz, C13), 49.5 (C8), 48.1 (C9), 36.3 (C11 or C12), 35.7 (C11 or C12), 32.3 (C7) ppm (C14, C15, and C16 were undetected due to multiple fluorine-fluorine couplings); **^{19}F NMR** (376 MHz, $CDCl_3$) δ -81.0 (t, *J*=9.5 Hz, 3F, F16), -120.3– -120.9 (m, 2F, F14), -127.1– -127.8 (m, 2F, F15) ppm; **^{19}F {^{1}H} NMR** (376 MHz, $CDCl_3$) δ -81.0 (br. t, *J*=9.5 Hz, 3F, F16), -120.5– -120.7 (m, 2F, F14), -127.4– -127.5 (m, 2F, F15) ppm; **IR** (neat) 2892 (br. w), 2744 (br. w), 1666 (s), 1227 (s), 1185 (s), 1162 (s) cm^{-1}; **MS** (ESI+) m/z 405.2 $[M+H]^+$, 427.2 $[M+Na]^+$; **HRMS** (ESI+) for $C_{16}H_{20}F_7N_2O_2$ $[M+H]^+$, calculated 405.1408, found 405.1413 (-1.5 ppm error), for $C_{16}H_{19}F_7N_2NaO_2$ $[M+Na]^+$, calculated 427.1227 found 427.1231 (-1.0 ppm error).

Synthesis of 2-((3-(2,2,3,3,4,4-Hexafluoropentoxy)phenethyl)amino)-*N*,*N*-dimethylacetamide•HCl (5.1g)

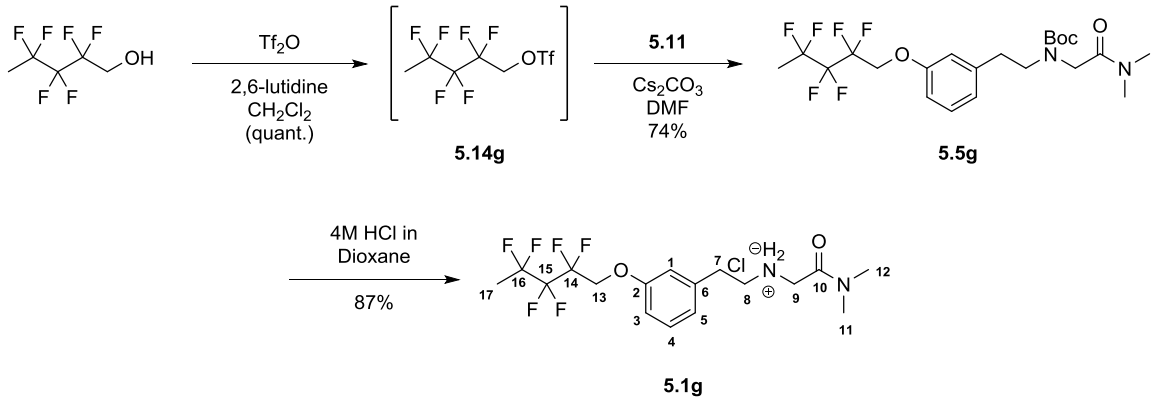

Using general procedure D with 2,2,3,3,4,4-hexafluoropentan-1-ol (30 mg) in CH_2Cl_2 (0.5 mL), and **5.11** (79 mg) dissolved in DMF (0.5 mL), **5.5g** was obtained as a colourless gum (58 mg, 74%). According to general procedure C, *N*-Boc cleavage of **5.5g** (58 mg, 1 equiv) yielded **5.1g** as an off white solid (44 mg, 87%).

^{1}H NMR (400 MHz, $CDCl_3$) δ 9.61 (br. s, 2 H, NH_2^+), 7.25 (t, *J*=7.9 Hz, 2H, H4), 6.98 (br. d, *J*=7.5 Hz, 1H, H5), 6.93 (s, 1H, H1), 6.83 (dd, *J*=8.0, 1.8 Hz, 1H, H3), 4.44 (t, *J*=13.6 Hz, 2H, H13), 4.01 (s, 2H, H9), 3.49–3.33 (m, 2H, H8), 3.33–3.25 (m, 2H, H7), 2.96 (s, 3H, H11 or H12), 2.92 (s, 3H, H11 or H12), 1.85 (t, *J*=19.3 Hz, 3H, H17); **^{13}C NMR** (101 MHz, $CDCl_3$) δ 164.5 (C10), 158.0 (C2), 138.3 (C6), 130.1 (C4),122.8 (C5), 115.5 (C1), 113.7 (C3), 65.4 (t, *J*=25.7 Hz, C13), 49.5 (C8), 48.0 (C9), 36.2 (C11 or C12), 35.7 (C11 or C12), 32.3 (C7), 18.6 (br. t, *J*=24.2 Hz, C17) ppm (C14, C15 and C16 were undetected due to multiple fluorine-fluorine couplings); **^{19}F NMR** (376 MHz, $CDCl_3$) δ -106.3 (qt, *J*=19.6, 9.5 Hz, 2F, F16), -119.6 (tt, *J*=13.6, 9.5 Hz, 2F, F14), -126.4 (s, 2F, F15) ppm; **^{19}F {^{1}H} NMR** (376 MHz, $CDCl_3$) δ -106.3 (t, *J*=9.5 Hz, 2F, F16), -119.9 (t, *J*=9.5 Hz, 2F, F14), -126.4 (s, 2F, F15) ppm; **IR** (neat) 2915 (br. m), 2745 (br. m), 1666 (s), 1160 (s), 1123 (m) cm^{-1}; **MS** (ESI+) m/z 401.3 $[M+H]^+$, 423.3 $[M+Na]^+$; **HRMS** (ESI+) for $C_{17}H_{23}F_6N_2O_2$ $[M+H]^+$, calculated 401.1658, found 401.1660 (-0.5 ppm error), for $C_{17}H_{22}F_6N_2NaO_2$ $[M+Na]^+$, calculated 423.1478, found 423.1476 (+0.5 ppm error).

Synthesis of 2-((3-(2,2,3,3,4,4,5,5,5-nonafluoropentoxy)phenethyl)amino)-*N*,*N*-dimethylacetamide•HCl (5.1h)

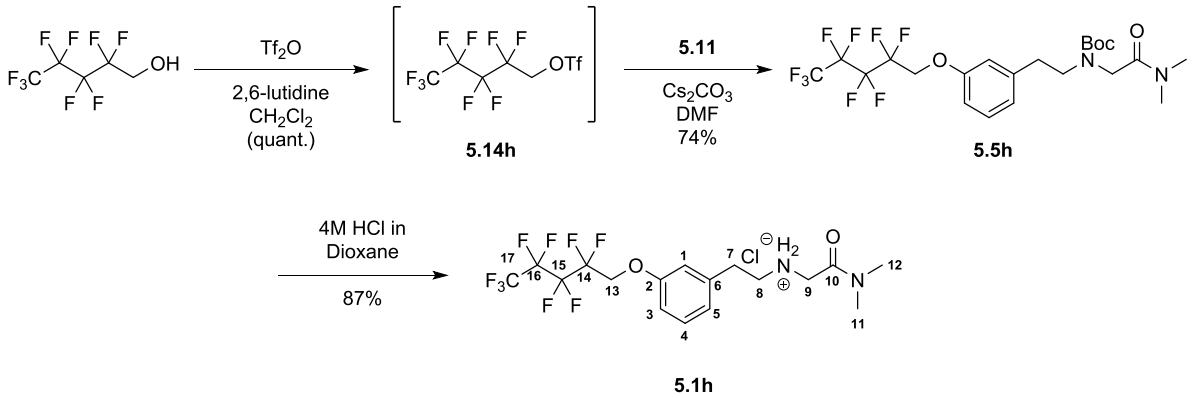

Using general procedure D with 2,2,3,3,4,4,5,5,5-nonafluoropentan-1-ol (20 mg) in CH_2Cl_2 (0.3 mL) and **5.11** (31 mg) dissolved in DMF (0.2 mL), **5.5h** was obtained as a colourless gum (31 mg, 70%). According to general procedure C, *N*-Boc cleavage of **5.5h** (57 mg, 1 equiv) yielded **5.1h** as an off white solid (46 mg, 91%).

^{1}H NMR (500 MHz, $CDCl_3$) δ 9.58 (br. s, 2H, NH_2^+), 7.23 (t, *J*=7.9 Hz, 2H, H4), 6.98 (d, *J*=7.4 Hz, 1H, H5), 6.94 (s, 1H, H1), 6.81 (dd, *J*=9.2, 2.1 Hz, 1H, H3), 4.46 (t, *J*=12.9 Hz, 2H, H13), 4.05 (s, 2H, H9), 3.46–3.35 (m, 2H, H8), 3.35–3.25 (m, 2H, H7), 2.96 (s, 3H, H11 or H12), 2.91 (s, 3H, H11 or H12); **^{13}C NMR** (101 MHz, $CDCl_3$) δ 164.6 (C10), 157.7 (C2), 138.6 (C6), 130.1 (C4), 123.0 (C5), 115.4 (C1), 113.6 (C3), 65.2 (t, *J*=27.1 Hz, C13), 49.3 (C8), 48.1 (C9) 36.3 (C11 or C12), 35.7 (C11 or C12), 32.2 (C7) ppm (C14, C15, C16 and C17 undetected due to multiple fluorine-fluorine couplings); **^{19}F NMR** (471 MHz, $CDCl_3$) δ -80.9 (tt, *J*=9.7, 2.5 Hz, 3F, F17), -119.6– -119.8 (m, 2F, F14), -124.0– -124.1 (m, 2F, F16), -126.2– -126.4 (m, 2F, F15) ppm; **^{19}F {^{1}H} NMR** (471 MHz, $CDCl_3$) δ -80.9 (tt, *J*=9.7, 2.5 Hz, 3F, F17), -119.6– -119.8 (m, 2F, F14), -124.0– -124.1(m, 2F, F16), -126.2– -126.5 (m, 2F, F15) ppm; **IR** (neat) 2942 (br. w), 1664 (m), 1231 (s), 1163 (s), 1134 (s) cm^{-1}; **MS** (ESI+) m/z 455.3 $[M+H]^+$, 477.3 $[M+Na]^+$; **HRMS** (ESI+) for $C_{17}H_{20}F_9N_2O_2$ $[M+H]^+$, calculated 455.1376, found 455.1387 (-2.6 ppm error), for $C_{17}H_{19}F_9N_2NaO_2$ $[M+Na]^+$, calculated 477.1195, found 477.1206 (-2.3 ppm error).

Chapter 9 Conformer Specific Lipophilicity Experimental

9.1 Synthesis of amide rotamers

Synthesis of *N*-acetyl-3-hydroxypiperdine (6.2)

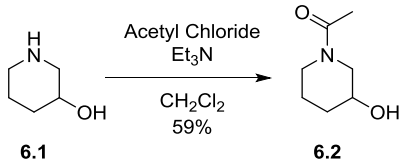

6.1 **6.2**

To a solution of 3-hydroxypiperidine (3.00 g, 29.7 mmol, 1 equiv) and triethylamine (10.3 mL, 73.8 mmol, 2.46 equiv) in THF (40 mL) and CH_2Cl_2 (40 mL) was added acetyl chloride (2.2 mL, 28.0 mmol, 0.95 equiv) dropwise at -78 °C. The reaction was allowed to warm to room temperature and stirred for 1 h. The reaction was then concentrated *in vacuo*, diluted with CH_2Cl_2 (20 mL) and water (20 mL) and the aqueous was extracted with CH_2Cl_2 (3×40 mL), Et_2O (3×50 mL) and EA (3×50 mL). The combined organic layers were collected, dried over $MgSO_4$ and concentrated *in vacuo.* The crude oil was purified by column chromatography (acetone) to afford a pale-yellow oil (2.51 g, 59%).

^{1}H NMR (400 MHz, $CDCl_3$) δ (mixture of rotamers) 3.95–3.13 (m, 5H), 2.11 (s, 3H, CH_3), 2.02–1.70 (m, 2H), 1.67–1.55 (m, 1H), 1.55–1.43 (m, 1H) ppm; **^{13}C NMR** (101 MHz, $CDCl_3$) δ (Major Rotamer) 169.9, 65.7, 48.5, 46.8, 31.9, 22.8, 21.4 ppm; (Minor Rotamer) 169.8, 66.4, 53.1, 41.8, 32.8, 21.7, 21.5 ppm.

Proton consistent with literature.[238] Carbon consistent with literature.[275]

***N*-acetyl-3-fluoropiperidine (1.1)**

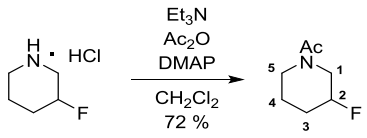

6.7 **1.1**

To a solution of 3-fluoropiperidine hydrochloride of (296 mg, 1 equiv) in CH_2Cl_2 (10 mL) was added Et_3N (0.9 mL, 3.1 equiv) and DMAP (17 mg, 0.05 equiv). Once all of 3-fluoropiperidine hydrochloride had dissolved, acetic anhydride (0.33 mL, 1.2 equiv) was added dropwise. After 6 h the reaction was quenched with sat. aq. NH_4Cl (10 mL) and washed with CH_2Cl_2 (10 mL). The organic layer is then washed with aq. 2 M HCl (2×10 mL) and sat. aq. $NaHCO_3$ (2×10 mL). The organic layer is then washed with brine and dried over $MgSO_4$ and concentrated *in vacuo*. The crude oil was then purified by

column chromatography (3:7, acetone/petrol ether 40–60 °C) to afford a pale-yellow oil (223 mg, 72%).

Rotamer ratio 1:0.8 ($CDCl_3$), undetermined (acetate overlap); **^{1}H NMR** (400MHz, $CDCl_3$) δ (mixture of rotamers) 4.83–4.48 (m, 1H, major + minor, H2), 4.11–4.01 (m, 1H, major, H'5), 3.90 (ddd, *J*=13.8, 8.8, 6.2 Hz, 1H, minor, H'1), 3.75 (ddd, *J*=14.2, 9.0, 5.1 Hz, 1H, major, H'1), 3.65 (ddd, *J*=24.7, 13.7, 3.3 Hz, 1H, minor, H''1), 3.54–3.40 (m, 2H, major, H''1 and major, H'5), 3.40–3.29 (m, 1H, major H''5), 3.11 (tt, *J*=8.9, 4.0 Hz, 1H, major, H''5), 2.11 (s, 3H, major + minor, CH_3), 2.05–1.73 (m, 3H, major + minor, H3 and major + minor H'4), 1.63–1.44 (m, 1H, major + minor, H''4) ppm; **^{13}C NMR** (101MHz, $CDCl_3$) δ (mixture of rotamers) 169.7 (major, C=O), 169.7 (minor, C=O), 86.4 (d, *J*=175.3 Hz, major, C2), 86.1 (d, *J*=174.6 Hz, minor, C2), 50.6 (d, *J*=22.7 Hz, major, C1), 46.2 (minor, C5), 45.4 (d, *J*=24.9 Hz, minor, C1), 41.7 (major, C5), 29.6 (d, *J*=20.5 Hz, minor, C3), 29.5 (d, *J*=21.3 Hz, major, C3), 21.8 (d, *J*=4.4 Hz, minor C4), 21.4 (major + minor, CH_3), 20.5 (d, *J*=2.9 Hz, major, C4) ppm; **^{19}F NMR** (376MHz, $CDCl_3$) δ -184.2– -184.6 (m, 1F, minor), -185.8 (app. tddd, *J*=45.8, 36.7, 28.0, 9.8 Hz, 1F, major) ppm; **^{19}F {H} ^{277}NMR** (376MHz, $CDCl_3$) δ -184.4 (s, 1F, minor), -185.8 (s, 1F, major) ppm; **IR** (neat) 2947 (w), 2864 (w), 1625 (s), 1427 (m), 1200 (s), 1123 (s) cm^{-1}; **MS** (ESI+) m/z 146.2 $[M+H]^+$, 168.2 $[M+Na]^+$; **HRMS** (ESI+) $C_7H_{12}FNO$ $[M+H]^+$, calculated 146.0976, found 146.0973 (+1.9 ppm error). $C_7H_{13}FNNaO$ $[M+Na]^+$, calculated 168.0795, found 168.0793 (+1.0 ppm error.)

***N*-acetyl-3,3-difluoropiperidine (1.2)**

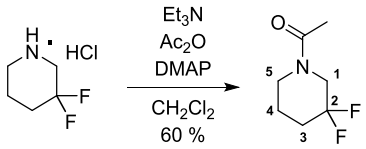

6.8 **1.2**

To a solution of 3,3-difluoropiperidine hydrochloride (312 mg, 1 equiv) in CH_2Cl_2 (10 mL) was added Et_3N (0.58 mL, 2.2 equiv) and DMAP (10 mg, 0.05 equiv). Once all of 3,3-difluoropiperidine hydrochloride had dissolved, acetic anhydride (0.22 mL, 1.2 equiv) was added dropwise. After 6 h the reaction was quenched with sat. aq. NH_4Cl (10 mL) and washed with CH_2Cl_2 (10 mL). The organic layer is then washed with aq. 2 M HCl (2×10 mL) and sat. aq. $NaHCO_3$ (2×10 mL). The organic layer is then washed with brine and dried over $MgSO_4$ and concentrated *in vacuo*. The crude oil was then purified by column chromatography (30% acetone/petrol ether 40–60 °C) to afford a pale-yellow oil (187 mg, 60%).

Rotamer ratio 1:0.72 ($CDCl_3$), Cis Major; **^{1}H NMR** (400MHz, $CDCl_3$) δ (mixture of rotamers) 3.86–3.36 (m, 4H, major + minor, H1 + H5), 2.12 (s, 3H, CH_3) + 2.11 (s, 3H, major, CH_3), 2.09–1.97 (m, 2H, major + minor, H3), 1.84–1.66 (m, 2H, major + minor, H4) ppm; **^{13}C NMR** (101MHz, $CDCl_3$) δ (mixture of rotamers) 169.6 (major, C=O), 169.4 (minor, C=O), 119.1 (t, *J*=244.7 Hz, C2), 52.2 (t, *J*=31.5 Hz, major, C1), 46.9 (t, *J*=32.6 Hz, minor, C1), 45.5 (minor, C5), 41.0 (major, C5), 32.6 (t, *J*=23.8 Hz, minor,

C3), 32.5 (t, *J*=23.1 Hz, major, C3), 22.6 (t, *J*=4.4 Hz, minor, C4), 21.7 (t, *J*=4.4 Hz, major, C4), 21.4 (minor, CH_3), 21.3 (major, CH_3) ppm; **^{19}F NMR** (376MHz, $CDCl_3$) δ -103.3 (quin, *J*=12.6 Hz, 2F, minor), -103.8 (quin, *J*=12.6 Hz, 2F, major) ppm; **^{19}F {H} NMR** (376MHz, $CDCl_3$) δ -103.3 (s, 2F, minor), -103.8 (s, 2F, major) ppm; **IR** (neat) 2941 (w), 2869 (w), 1641 (s), 1427 (m), 1243 (s), 1103 (s) cm^{-1}; **MS** (ESI+) m/z 164.2 $[M+H]^+$, 186.2 $[M+Na]^+$; **HRMS** (ESI+) $C_7H_{12}F_2NO$ $[M+H]^+$, calculated 164.0885, found: 164.0881 (-2.0 ppm error), $C_7H_{13}FNNaO$ $[M+Na]^+$, calculated 186.0705, found 186.0701 (-2.4 ppm error.)

***N*-acetyl-3-fluoropyrrolidine (1.3)**

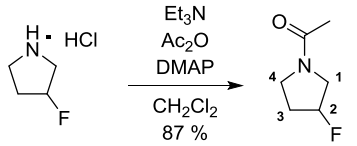

6.9 **1.3**

To a solution of 3-fluoropyrrolidine hydrochloride (315 mg, 1 equiv) in CH_2Cl_2 (10 mL) was added Et_3N (0.75 mL, 2.2 equiv) and DMAP (15 mg, 0.05 equiv). Once all of 3-fluoropyrrolidine hydrochloride had dissolved, acetic anhydride (0.28 mL, 1.2 equiv) was added dropwise. After 6 h the reaction was quenched with sat. aq. NH_4Cl (10 mL) and washed with CH_2Cl_2 (10 mL). The organic layer is then washed with aq. 2 M HCl (2×10 mL) and sat. aq. $NaHCO_3$ (2×10 mL). The organic layer is then washed with brine and dried over $MgSO_4$ and concentrated *in vacuo*. The crude oil was then purified by column chromatography (3:7, acetone/petrol ether 40–60 °C) to afford a pale-yellow oil (272 mg, 87%).

Rotamer ratio: 1:0.73 ($CDCl_3$), Cis Major; **^{1}H NMR** (400MHz, $CDCl_3$) δ (mixture of rotamers) 5.33–5.15 (m, 1H, major, H2), 5.29 (td, *J*=3.7, 52.6 Hz, 1H, minor, H2), 3.96–3.31 (m, 4H, major + minor, H1 + H4), 2.40–1.85 (m, 2H, major + minor, H3), 2.08 (s, 3H, major, CH_3), 2.05 (s, 3H, minor, CH_3) ppm; **^{13}C NMR** (101MHz, $CDCl_3$) δ (mixture of rotamers) 169.5 (major, C=O), 169.3 (minor, C=O), 92.9 (d, *J*=176.8 Hz, minor, C2), 91.6 (d, *J*=176.1 Hz, major, C2), 53.8 (d, *J*=23.5 Hz, minor C1), 52.2 (d, *J*=23.5 Hz, major, C1), 45.0 (major, C4), 43.3 (minor, C4), 32.8 (d, *J*=22.0 Hz, major, C3), 31.2 (d, *J*=21.3 Hz, minor, C3), 22.4 (minor, CH_3), 22.3 (major, CH_3) ppm; **^{19}F NMR** (376MHz, $CDCl_3$) δ -177.2– -177.7 (m, 1F, minor), -177.7– -178.4 (m, 1F, major) ppm; **^{19}F NMR** (376MHz, $CDCl_3$) δ -177.5 (s, 1F, minor), -178.0 (s, 1F, major) ppm; **IR** (neat) 2982 (w), 2886 (w), 1623 (s), 1420 (m), 1204 (s), 1093 (s) cm^{-1}; **MS** (ESI+) m/z 132.1 $[M+H]^+$, 154.2 $[M+Na]^+$; **HRMS** (ESI+) $C_6H_{11}FNO$ $[M+H]^+$, calculated 132.0819 found 132.0818 (+1.0 ppm error), $C_6H_{11}FNNaO$ $[M+Na]^+$, calculated 154.0639, found 154.0636 (+1.8 ppm error.)

_N_-acetyl-3,3-difluoropyrrolidine (1.4)

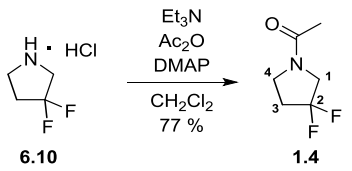

To a solution of 3,3-difluoropyrrolidine hydrochloride (305 mg, 1 equiv) in CH_2Cl_2 (10 mL) was added Et_3N (0.65 mL, 2.2 equiv) and DMAP (20 mg, 0.05 equiv). Once all of 3,3-difluoropyrrolidine hydrochloride had dissolved, acetic anhydride (0.24 mL, 1.2 equiv) was added dropwise. After 6 h the reaction was quenched with sat. aq. NH_4Cl (10 mL) and washed with CH_2Cl_2 (10 mL). The organic layer is then washed with aq. 2 M HCl (2×10 mL) and sat. aq. $NaHCO_3$ (2×10 mL). The organic layer is then washed with brine and dried over $MgSO_4$ and concentrated *in vacuo*. The crude oil was then purified by column chromatography (3:7, acetone/petrol ether 40–60 °C) to afford a pale-yellow oil (243 mg, 77%).

Rotamer ratio 1:0.81 ($CDCl_3$), Cis Major; **^{1}H NMR** (400MHz, $CDCl_3$) δ (mixture of rotamers) 3.80 (t, *J*=13.1 Hz, 2H, major, H1), 3.79 (t, *J*=12.6 Hz, 2H, minor, H1), 3.73–3.64 (m, 2H, major + minor, H4), 2.57–2.26 (m, 2H, major + minor, H3), 2.06 (s, 3H, major, CH_3), 2.04 (s, 3H, minor, CH_3) ppm; **^{13}C NMR** (101MHz, $CDCl_3$) δ (mixture of rotamers) 169.4 (major, C=O), 169.2 (minor, C=O), 126.5 (t, *J*=247.2 Hz, minor, C2), 127.5 (t, *J*=249.4 Hz, major, C2), 54.0 (t, *J*=31.9 Hz, minor, C3), 52.2 (t, *J*=31.9 Hz, major, C3), 44.8 (t, *J*=3.3 Hz, major, C4), 42.9 (t, *J*=2.9 Hz minor, C4), 34.5 (t, *J*=24.6 Hz, major, C1), 33.1 (t, *J*=23.5 Hz, minor, C1), 22.2 (major, CH_3), 21.2 (minor, CH_3) ppm; **^{19}F NMR** (376MHz, $CDCl_3$) δ -101.2 (quin, *J*=13.0 Hz, 2F, minor), -102.2 (quin, *J*=13.0 Hz, 2F, major) ppm; **^{19}F NMR** (376MHz, $CDCl_3$) δ -101.2 (s, 2F, minor), -102.2 (s, 2F, major) ppm; **IR** (neat) 2963 (w), 2866 (w), 1626 (s), 1422(m), 1213 (s), 1118 (s) cm^{-1}; **MS** (ESI+) m/z 150.2 $[M+H]^+$, 172.2 $[M+Na]^+$; **HRMS** (ESI+) $C_6H_{10}F_2NO$ $[M+H]^+$, calculated 150.0725, found 150.0725 (+0.2 ppm error).

9.2 Synthesis of [1,1-D_2]-octan-1-ol

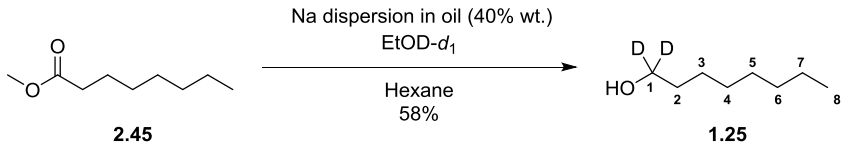

To a solution of methyl octanoate (31.6 g, 1 equiv) in hexane (1 L) was added EtOD-d_1 (52.4 mL 4.5 equiv), followed by an Na dispersion in oil (40% wt., 28.8 g, 4.5 equiv) at 0 °C. After 5 minutes, the reaction is allowed to warm to room temperature and then after a further 5 minutes, the reaction is quenched with aq. HCl (3M, 450 mL). The mixture was diluted with Et_2O (200 mL) and brine (200 mL) and the aqueous layer was extracted with Et_2O (2×800 mL) before the combined organic layers

were dried over $MgSO_4$. The solution was then filtered over a plug of silica gel. The crude was purified by flash column chromatography (3:7, Et_2O/Pentane) to afford a light orange oil which was then further purified by distillation (64 – 66 °C, 8 mbar) to yield a colourless oil (15.3 g, 58%).

^{1}H NMR (400 MHz, $CDCl_3$) δ 1.56 (t, *J*=6.8 Hz, 2H, H2), 1.17-1.43 (m, 11H, H3 + H4 + H5 + H6 +H7 + OH), 0.89 ppm (t, *J*=6.8 Hz, 2H, H8) ppm; **^{13}C NMR** (101 MHz, $CDCl_3$) δ 62.4 (quin, *J*=21.8 Hz, C1), 32.6 (C2), 31.8 (C6), 29.4 (C4), 29.3 (C5), 25.7 (C3), 22.6 (C7), 14.1 (C8) ppm.

Data consistent with literature.[276]

9.3 Detailed experimental data for the log*P* determination

Unless indicated, the general procedure seen in Chapter 7 Section 7.1 above was followed (O1P centered; SW: 100 ppm; D1: oct 30 sec; wat: 60 sec; SR: 295.14 ppm; NMR machine: 400-2 or 400-3. Trifluoroethanol was used as primary reference.

Overall log*P* of *N*-acetyl-3,3-difluoropiperdine

Compound	Experimental (octanol/water)	ρ_{oct}/ρ_{wat}	Log*P*	Average Log *P*	Error
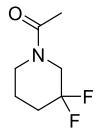	ju2916bj2/ ju2916bj3	0.5618/0.6711	+0.28	+0.27	+0.272 (±0.007)
	ju2916bj4/ ju2916bj5	0.4532/0.5554	+0.27		
	ju2916bj6/ ju2916bj7	0.7613/0.9494	+0.26		

Ratio of trans/cis rotamers:
Octanol phase: 1.17/1 = $K_{1.17}$
Water phase: 0.73/1 = $K_{0.73}$

Conformer Specific Log*P*

Conformation	ρ_{oct}/ρ_{wat}	Log*P*	Average Log*P*	Error
Trans	0.3027/0.2843	+0.39	+0.38	+0.378 (±0.008)
	0.2456/0.2340	+0.38		
	0.4097/0.4027	+0.37		

Conformation	ρ_{oct}/ρ_{wat}	Log*P*	Average Log*P*	Error
Cis	0.2591/0.3868	+0.18	+0.17	+0.174 (±0.008)
	0.2076/0.3214	+0.17		
	0.3516/0.5467	+0.17		

Overall log*P* of *N*-acetyl-3-fluoropiperdine

Compound	Experimental (octanol/water)	ρ_{oct}/ρ_{wat}	Log*P*	Average Log*P*	Error
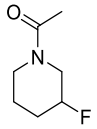	oc0616bj3/ oc0616bj4	1.9574/1.3281	-0.09	-0.10	-0.100 (±0.008)
	oc0616bj5/ oc0716bj3	1.5753/1.1101	-0.11		
	oc0616bj7/ oc0716bj2	2.6861/1.8871	-0.11		

Reference - 4-Fluorobutan-1-ol

Ratio of trans/cis rotamers:
Octanol phase: 1.43/1 = $K_{1.43}$
Water phase: 0.95/1 = $K_{0.95}$

Conformer Specific Log*P*

Conformation	ρ_{oct}/ρ_{wat}	Log*P*	Average Log*P*	Error
Trans	1.1397/0.6440	-0.01	-0.02	-0.015 (±0.003)
	0.9366/0.5367	-0.02		
	1.5800/0.9229	-0.03		

Conformation	ρ_{oct}/ρ_{wat}	Log*P*	Average Log*P*	Error
Cis	0.8177/0.6841	-0.18	-0.20	-0.198 (±0.015)
	0.6387/0.5734	-0.21		
	1.1061/0.9642	-0.20		

Overall log*P* of *N*-acetyl-3,3-difluoropyrrolidine

Compound	Experimental (octanol/water)	ρ_{oct}/ρ_{wat}	Log*P*	Average Log*P*	Error
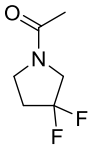	ju1016bj9/ ju1016bj10	0.0798/0.2410	-0.12	-0.12	-0.117 (±0.004)
	ju1016bj11/ ju2916bj4	0.1373/0.4144	-0.12		
	ju1016bj13/ ju1016bj14	0.0975/0.2887	-0.11		

Ratio of trans/cis rotamers:
Octanol phase: 0.72/1 = $K_{0.72}$
Water phase: 0.84/1 = $K_{0.84}$

Conformer Specific Log*P*

Conformation	ρ_{oct}/ρ_{wat}	Log*P*	Average Log*P*	Error
Trans	0.0330/0.1093	-0.16	-0.15	-0.153 (±0.006)
	0.0579/0.1895	-0.15		
	0.0411/0.1314	-0.15		

Conformation	ρ_{oct}/ρ_{wat}	Log*P*	Average Log*P*	Error
Cis	0.0468/0.1319	-0.09	-0.09	-0.089 (±0.003)
	0.0794/0.2249	-0.09		
	0.0411/0.1314	-0.09		

Overall log*P* of N-acetyl-3-fluoropyrrolidine

Compound	Experimental (octanol/water)	ρ_{oct}/ρ_{wat}	Log*P*	Average Log*P*	Error
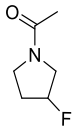	my2716bj6/my2716b7	0.2483/0.4086	-0.57	-0.57	-0.568 (±0.002)
	my2716bj8/my2716b9	0.5189/0.8615	-0.57		
	my2716bj10/my2716b11	0.2140/0.3520	-0.57		

Reference - 1-Fluoropropan-2-ol

Ratio of trans/cis rotamers:
Octanol phase: 0.75/1 = $K_{0.75}$
Water phase: 0.86/1 = $K_{0.86}$

Conformer Specific Log*P*

Conformation	ρ_{oct}/ρ_{wat}	Log*P*	Average Log*P*	Error
Trans	0.1062/0.1892	-0.60	-0.60	-0.602 (±0.001)
	0.2228/0.3985	-0.60		
	0.0908/0.1631	-0.60		

Conformation	ρ_{oct}/ρ_{wat}	Log*P*	Average Log*P*	Error
Cis	0.1424/0.2194	-0.54	-0.54	-0.538 (±0.003)
	0.2967/0.4626	-0.54		
	0.1234/0.1887	-0.53		

9.4 Assignment of amide rotamers in [1,1-D_2]-octan-1-ol

Rotamer assignment of *N*-acetyl-3,3-difluoropyrrolidine

HSQC analysis in [1,1-D_2]-octan-1-ol (benzene-d_6 capillary) was carried out similarly to that of the previous example seen in Chapter 6 Section 6.4.5.3: C2 can be identified due to the $^2J_{C2\text{-}F}$ coupling constants (t, *J* = 32.3 Hz, Figure 9.1), while C5 can be recognised by its much smaller $^3J_{C5\text{-}F}$ coupling constants (t, *J* = 2.9 Hz). Once the carbons had been assigned, the major and minor signals of H2 and H5 can be assigned via the cross-peaks, clearly visible adjacent to the residual resonance of octanol, that is present as trace impurity in [1,1-D_2]-octan-1-ol.

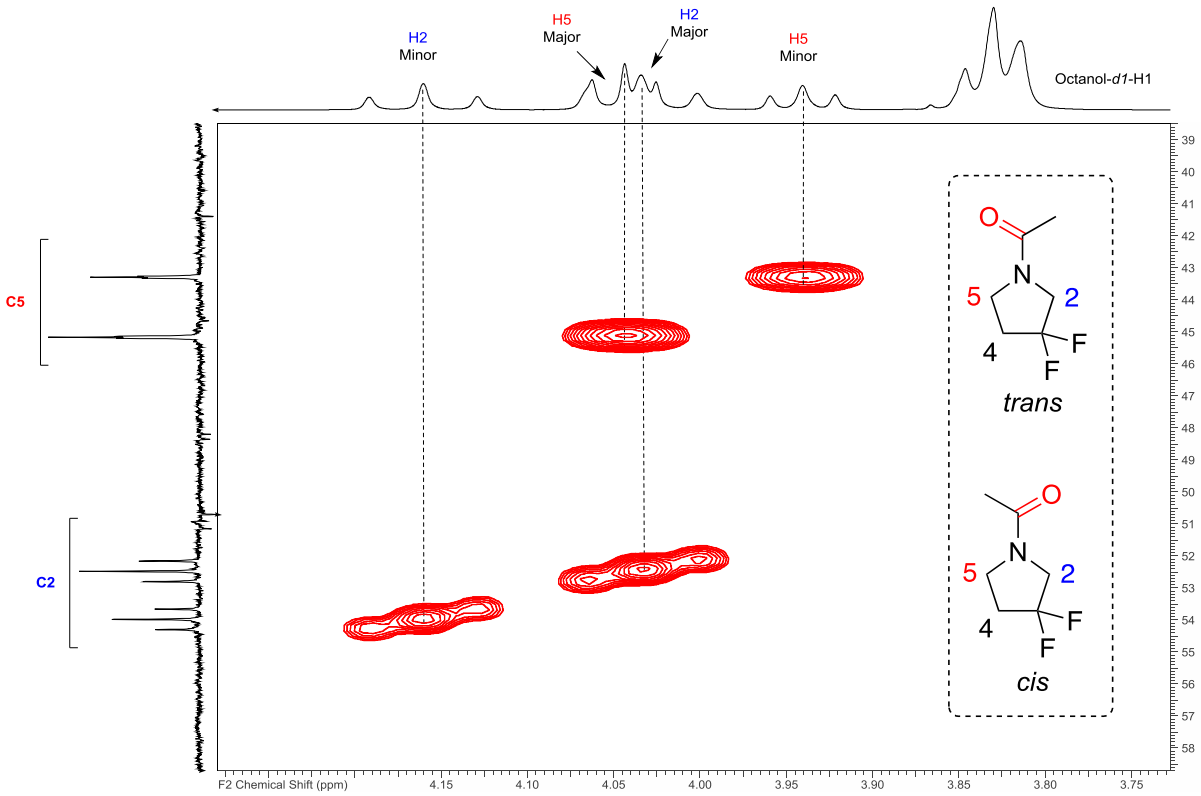

Figure 9.1 - HSQC spectrum of *N*-acetyl-3,3-difluoropyrrolidine in 1-[1,1-D_2]-octanol.

Despite the overlapping of the H2 and H5 resonances of the major rotamer in the ^{1}H NMR spectrum, the configuration of the rotamers can still be assigned via HSQC analysis (Figure 9.1). The acetate CH_3 resonance of the minor rotamer shows a cross-peak with an H2 signal (Figure 9.2), indicating that the minor confirmation has *trans*-configuration. Therefore it can be determined that the major acetate resonance is displaying a cross-peak to the H5 signal of the major rotamer, and not the H2 signal.

Thus, the major rotamer of *N*-acetyl-3,3-difluoropyrrolidine in octanol also has the *cis*-conformation.

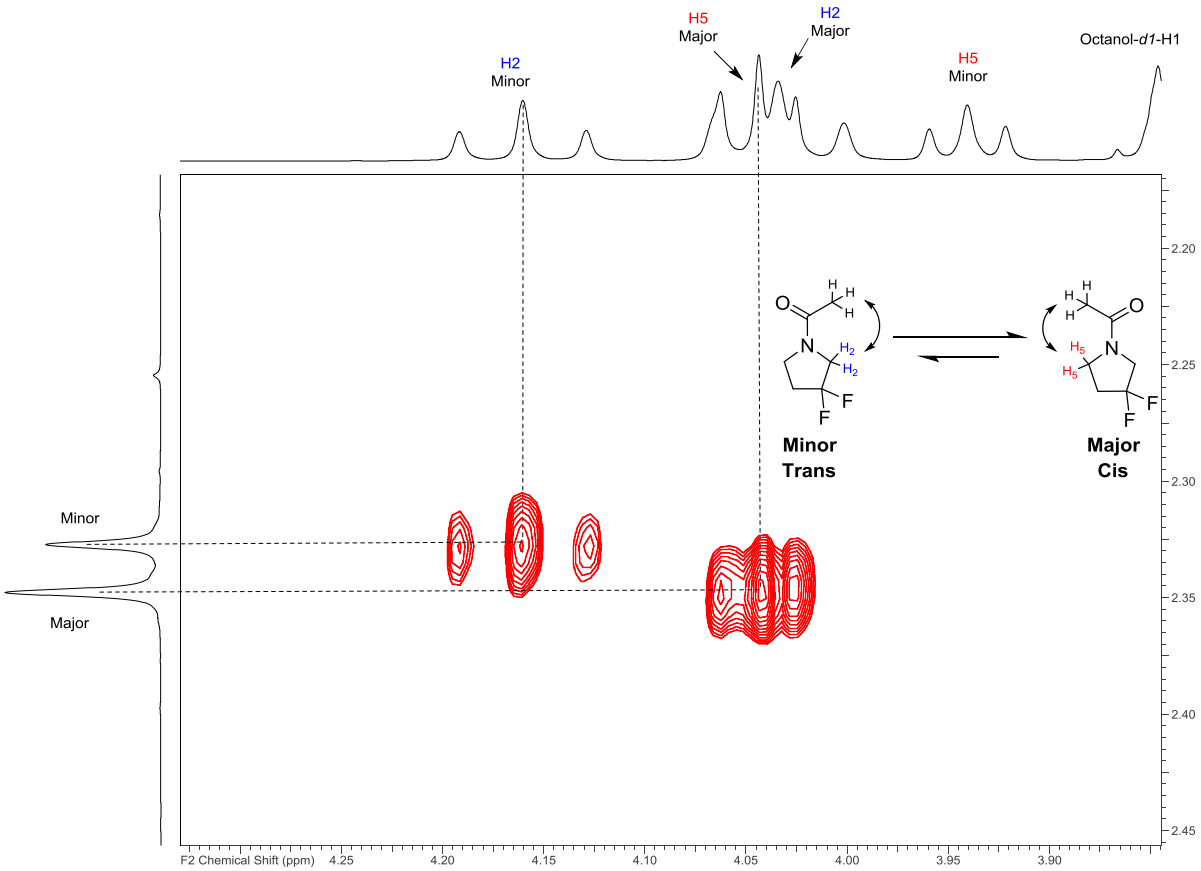

Figure 9.2 - NOESY spectrum of *N*-acetyl-3,3-difluoropyrrolidine in [1,1-D_2]-octan-1-ol.

Rotamer assignment of *N*-acetyl-3-fluoropiperidine 4 in octanol

The HSQC spectrum in [1,1-D_2]-octan-1-ol is shown in Figure 9.3. The correlation of the C6 resonance of the major rotamer with its two protons, which now have a different chemical shift, is easily seen. The other assignments are more difficult, but still clear, as indicated.

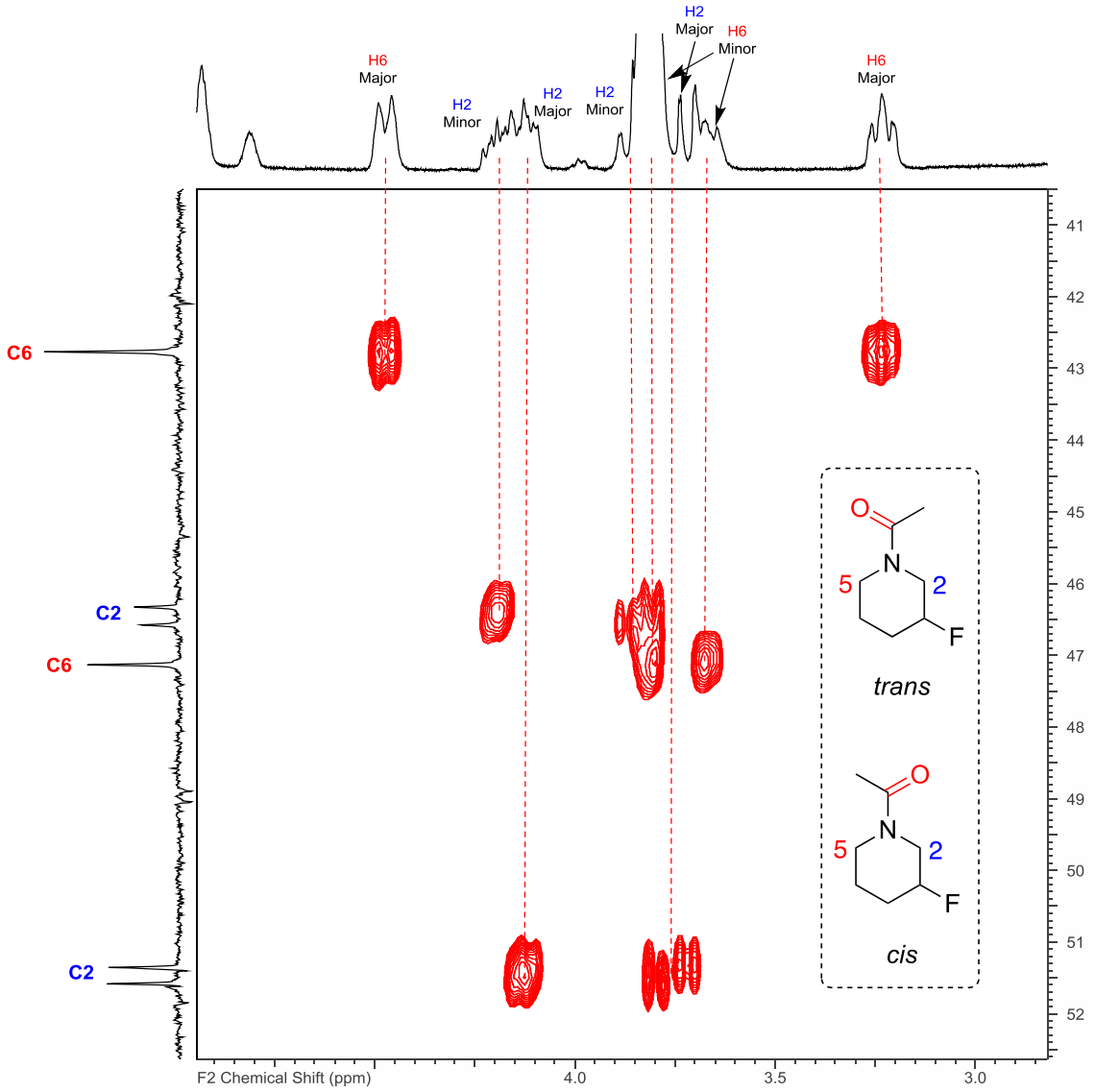

Figure 9.3 - HSQC spectrum of *N*-acetyl-3-fluoropiperidine in [1,1-D_2]-octan-1-ol.

In the NOESY spectrum (Figure 9.4), it is observed that the H6 signals of the major rotamer do not show a cross peak to an acetate resonance. Hence, by inference the major rotamer must have the *trans*-conformation. This can be confirmed by inspection of the cross peaks, despite the slight overlap of the acetate peaks: the major acetate peak shows a cross peak to the H2 resonances of the major rotamer, while the minor acetate peak shows a cross peak with the H6 resonances of the minor rotamer.

Hence the major rotamer for *N*-acetyl-3-fluoropiperidine in octanol has the *trans*-conformation.

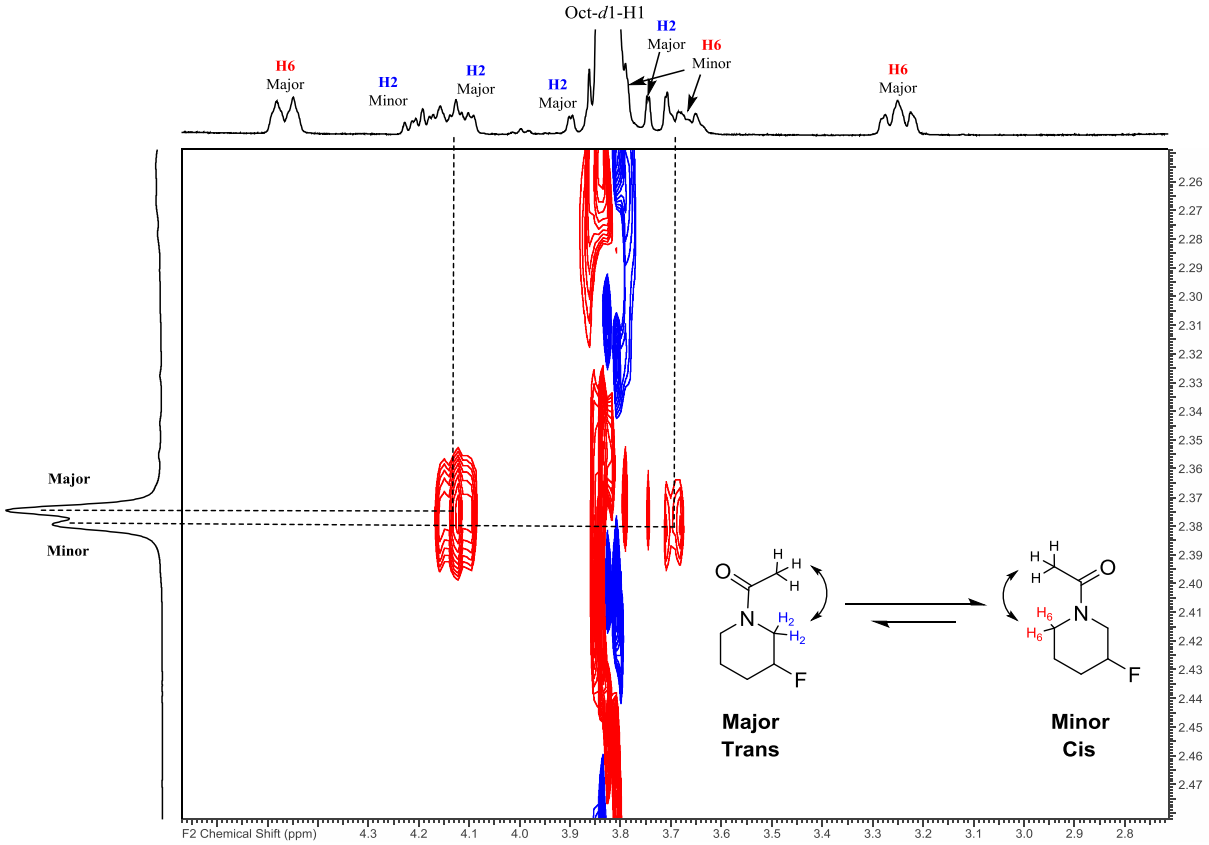

Figure 9.4 - NOESY spectrum of *N*-acetyl-3-fluoropiperidine in [1,1-D_2]-octan-1-ol.

Rotamer assignment of *N*-acetyl-3,3-difluoropiperidine in octanol

The HSQC spectrum in [1,1-D_2]-octan-1-ol is shown in Figure 9.5. Similar to that of previous examples the C2 can be identified due to $^2J_{C2\text{-}F}$ coupling constants (t, J = 31.5 Hz), while C6 can be recognised by its lack of multiplicity. The respective cross peaks indicate the chemical shift values of the corresponding proton resonances, with the minor H6 partially overlapping with residual oct-*d1*-H1.

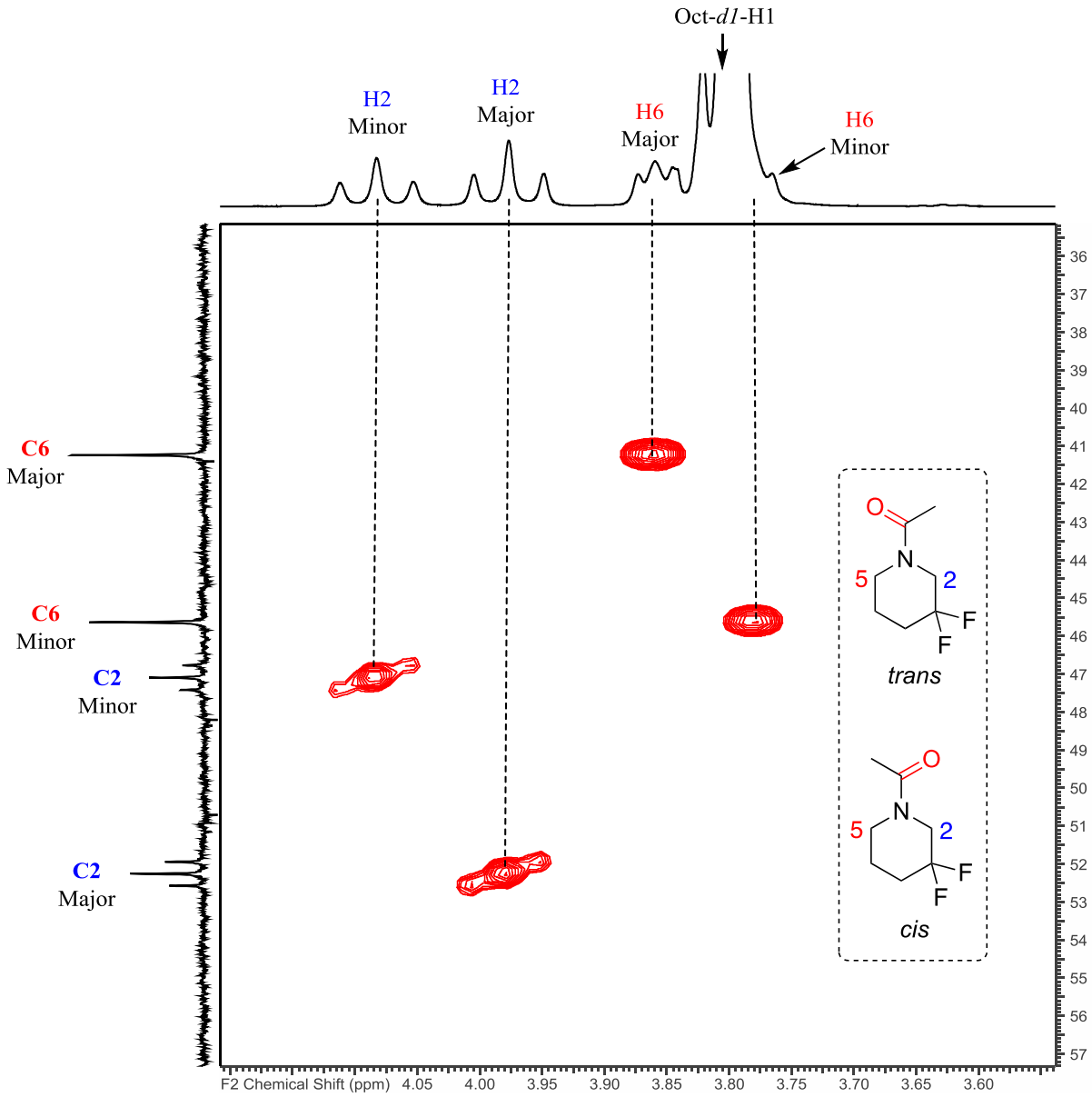

Figure 9.5 - HSQC spectrum of *N*-acetyl-3-fluoropiperidine in [1,1-D_2]-octan-1-ol

In this case a ROESY experiment was used because of t_1 noise in the NOESY spectrum from the residual oct-*d1*-H1 signal, causing difficulty in accurately assigning cross peaks. In the ROESY spectrum (Figure 9.6), it can be seen that the major H2 signal shows a cross peak with the corresponding major acetate resonance. In the case of the minor acetate resonance, a cross peak can be observed with the minor H6 signal which partially overlaps with the oct-*d1*-H1.

Hence the major rotamer for *N*-acetyl-3,3-difluoropiperidine in octanol has the *trans*-conformation.

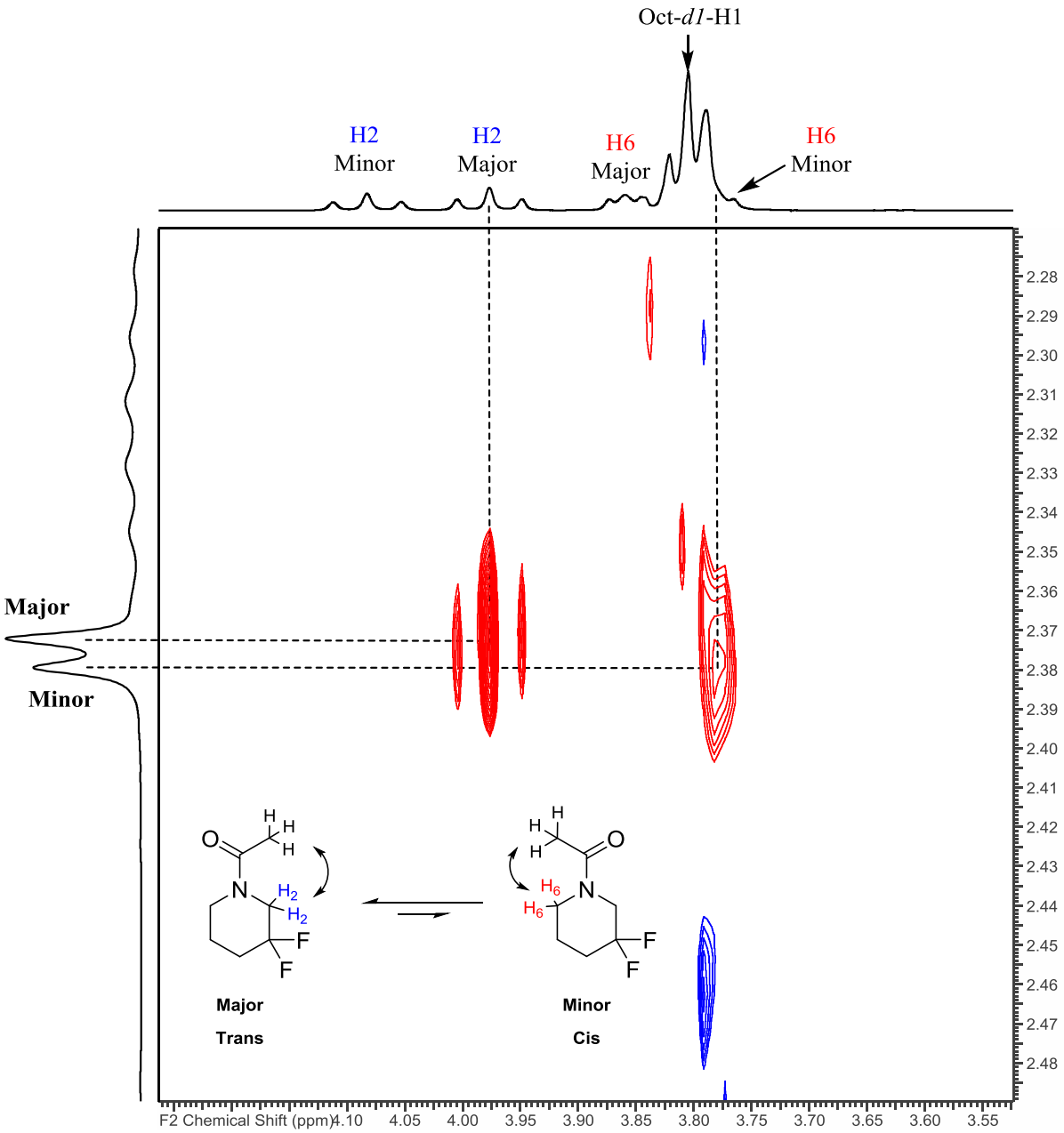

Figure 9.6 - ROESY spectrum of *N*-acetyl-3-fluoropiperidine in [1,1-D_2]-octan-1-ol.

9.5 Calculations

The calculations found within Chapter 6 were peformed by Dr Jerome Graton, University of Nantes, France. Density Functional Theory (DFT) calculations were carried out with the Gaussian16 program[277] to estimate the conformational dependence of dipole moment within the amide series under study. The conformational analysis of the various compounds investigated was performed with the MN15 functional[278] in combination with the triple-zeta quality cc-pVTZ basis set. The solvent effects (octanol and water) were taken into account using the SMD solvation continuum model.[279] The vibrational spectrum of each optimized conformer was computed to confirm its nature of true minimum and to obtain the correction to the free energies. Single point calculations

at the SMD/MN15/aug-cc-pVTZ were finally carried out to obtain refined electronic energy values. The relative populations, p_i, of the various conformers were evaluated at 298K from the computed free energies through a Boltzmann distribution. The theoretical molecular dipole moments were calculated then for each conformer, and used as is for comparison within the conformer series, and were weighted according to the computed populations for comparison within the amide series.

Bibliography

1. Tsopelas, F.; Giaginis, C.; Tsantili-Kakoulidou, A., *Expert Opin. Drug Discov.* **2017,** *12*, 885-896.
2. Rutkowska, E.; Pajak, K.; Jozwiak, K., *Acta Pol Pharm* **2013,** *70*, 3-18.
3. Hansch, C.; Fujita, T., *J. Am. Chem. Soc.* **1964,** *86*, 1616-1626.
4. Hann, M. M., *MedChemComm.* **2011,** *2*, 349.
5. Navia, M. A.; Chaturvedi, P. R., *Drug Discov. Today* **1996,** *1*, 179-189.
6. Lipinski, C. A., *J. Pharmacol. Toxicol. Methods* **2000,** *44*, 235-249.
7. Perola, E., *J. Med. Chem.* **2010,** *53*, 2986-97.
8. Waring, M. J., *Expert Opin. Drug Discov.* **2010,** *5*, 235-48.
9. Kramer, C.; Heinisch, T.; Fligge, T.; Beck, B.; Clark, T., *ChemMedChem* **2009,** *4*, 1529-1536.
10. Arnott, J. A.; Planey, S. L., *Expert Opin. Drug Discov.* **2012,** *7*, 863-875.
11. Gleeson, M. P., *J. Med. Chem.* **2008,** *51*, 817-834.
12. Hann, M. M.; Keserü, G. M., *Nat. Rev. Drug Discovery* **2012,** *11*, 355.
13. Yalkowsky, S. H.; Valvani, S. C., *J. Pharm. Sci.* **1980,** *69*, 912-922.
14. Ran, Y.; Jain, N.; Yalkowsky, S. H., *J. Chem. Inf. Comput. Sci.* **2001,** *41*, 1208-1217.
15. Kerns, E. H.; Di, L., *Drug Discov. Today Technol.* **2004,** *1*, 343-348.
16. Wagner, J. G.; Sedman, A. J., *J. Pharmacokinet. Biopharm.* **1973,** *1*, 23-50.
17. Hansch, C., *Acc. Chem. Res.* **1969,** *2*, 232-239.
18. Kakemi, K.; Arita, T.; Hori, R.; Konishi, R., *Chem. Pharm. Bull.* **1967,** *15*, 1534-1539.
19. Kubinyi, H., *Arzneim.-Forsch.* **1976,** *26*, 1991-1997.
20. Camenisch, G.; Alsenz, J.; van de Waterbeemd, H.; Folkers, G., *Eur. J. Pharm. Sci.* **1998,** *6*, 313-319.
21. Adson, A.; Burton, P. S.; Raub, T. J.; Barsuhn, C. L.; Audus, K. L.; Ho, N. F. H., *J. Pharm. Sci.* **1995,** *84*, 1197-1204.
22. Lipinski, C. A.; Lombardo, F.; Dominy, B. W.; Feeney, P. J., *Adv. Drug Delivery Rev.* **1997,** *23*, 3-25.
23. Waring, M. J., *Bioorg. Med. Chem. Lett.* **2009,** *19*, 2844-2851.
24. Egan, W. J.; Merz, K. M.; Baldwin, J. J., *J. Med. Chem.* **2000,** *43*, 3867-3877.
25. Tanaka, Y.; Kitamura, Y.; Maeda, K.; Sugiyama, Y., *J. Pharm. Sci.* **2016,** *105*, 431-442.
26. Martinez, M. N.; Amidon, G. L., *J. Clin. Pharmacol.* **2002,** *42*, 620-643.

27. Robert, J. R.; Iain, J. M.; Anne, E. C., *Curr. Drug Metab.* **2002,** *3*, 527-550.

28. Pond, S. M.; Tozer, T. N., *Clin. Pharmacokinet.* **1984,** *9*, 1-25.

29. Kerns, E. H.; Di, L., Chapter 5 - Lipophilicity. In *Drug-like Properties: Concepts, Structure Design and Methods*, Kerns, E. H.; Di, L., Eds. Academic Press: San Diego, 2008; pp 43-47.

30. Schmidt, Y.; Breit, B., *Chem. Eur. J.* **2011,** *17*, 11780-11788.

31. Yoshida, F.; Topliss, J. G., *J. Med. Chem.* **2000,** *43*, 2575-2585.

32. Martin, Y. C., *J. Med. Chem.* **2005,** *48*, 3164-3170.

33. Øie, S.; Tozer, T. N., *J. Pharm. Sci.* **1979,** *68*, 1203-1205.

34. Klippert, P.; Borm, P.; Noordhoek, J., *Biochem. Pharmacol.* **1982,** *31*, 2545-2548.

35. van de Waterbeemd, H.; Smith, D. A.; Jones, B. C., *J. Comput.-Aided Mol. Des.* **2001,** *15*, 273-286.

36. Obach, R. S.; Lombardo, F.; Waters, N. J., *Drug Metab. Dispos.* **2008,** *36*, 1385.

37. Valko, K.; Nunhuck, S.; Bevan, C.; Abraham, M. H.; Reynolds, D. P., *J. Pharm. Sci.* **2003,** *92*, 2236-2248.

38. Summerfield, S. G.; Read, K.; Begley, D. J.; Obradovic, T.; Hidalgo, I. J.; Coggon, S.; Lewis, A. V.; Porter, R. A.; Jeffrey, P., *J. Pharmacol. Exp. Ther.* **2007,** *322*, 205.

39. Dolghih, E.; Jacobson, M. P., *ACS Chem. Neurosci.* **2012,** *4*, 361-367.

40. Meanwell, N. A., *Chem. Res. Toxicol.* **2011,** *24*, 1420-1456.

41. Hitchcock, S. A.; Pennington, L. D., *J. Med. Chem.* **2006,** *49*, 7559-7583.

42. Abbott, N. J.; Patabendige, A. A. K.; Dolman, D. E. M.; Yusof, S. R.; Begley, D. J., *Neurobiol. Dis.* **2010,** *37*, 13-25.

43. Bain, L. J.; LeBlanc, G. A., *Toxicol. Appl. Pharmacol.* **1996,** *141*, 288-298.

44. Seelig, A., *Eur. J. Biochem.* **1998,** *251*, 252-261.

45. Nassar, A.-E. F.; Kamel, A. M.; Clarimont, C., *Drug Discov. Today* **2004,** *9*, 1020-1028.

46. Lewis, D. F. V.; Dickins, M., *Drug Metab. Rev.* **2003,** *35*, 1-18.

47. Lewis, D. F. V.; Dickins, M., *Drug Discov. Today* **2002,** *7*, 918-925.

48. van de Waterbeemd, H.; Smith, D. A.; Beaumont, K.; Walker, D. K., *J. Med. Chem.* **2001,** *44*, 1313-1333.

49. Johnson, T. W.; Dress, K. R.; Edwards, M., *Bioorg. Med. Chem. Lett.* **2009,** *19*, 5560-5564.

50. Waring, M. J.; Arrowsmith, J.; Leach, A. R.; Leeson, P. D.; Mandrell, S.; Owen, R. M.; Pairaudeau, G.; Pennie, W. D.; Pickett, S. D.; Wang, J.; Wallace, O.; Weir, A., *Nat. Rev. Drug Discovery* **2015,** *14*, 475-486.

51. Gleeson, M. P.; Leeson, P. D.; Van De Waterbeemd, H., *Physicochemical Properties and Compound Quality in the Handbook of Medicinal Chemistry: Principles and Practice* **2015**, 1-31.

52. Leeson, P. D., *Adv. Drug Delivery Rev.* **2016,** *101*, 22-33.

53. Freire, E., *Drug Discov. Today* **2008,** *13*, 869-874.

54. Leeson, P. D.; Springthorpe, B., *Nat. Rev. Drug Discovery* **2007,** *6*, 881.

55. Hughes, J. D.; Blagg, J.; Price, D. A.; Bailey, S.; DeCrescenzo, G. A.; Devraj, R. V.; Ellsworth, E.; Fobian, Y. M.; Gibbs, M. E.; Gilles, R. W.; Greene, N.; Huang, E.; Krieger-Burke, T.; Loesel, J.; Wager, T.; Whiteley, L.; Zhang, Y., *Bioorg. Med. Chem. Lett.* **2008,** *18*, 4872-4875.

56. Leeson, P. D.; St-Gallay, S. A.; Wenlock, M. C., *MedChemComm.* **2011,** *2*, 91-105.

57. Muthas, D.; Boyer, S.; Hasselgren, C., *MedChemComm.* **2013,** *4*, 1058-1065.

58. Blomme, E. A. G.; Will, Y., *Chem. Res. Toxicol.* **2016,** *29*, 473-504.

59. Nava-Ocampo, A. A.; Bello-Ramírez, A. M., *Clin. Exp. Pharmacol. Physiol.* **2004,** *31*, 116-118.

60. McDonald, T. V.; Yu, Z.; Ming, Z.; Palma, E.; Meyers, M. B.; Wang, K.-W.; Goldstein, S. A. N.; Fishman, G. I., *Nature* **1997,** *388*, 289.

61. Viskin, S., *The Lancet* **1999,** *354*, 1625-1633.

62. Waring, M. J.; Johnstone, C., *Bioorg. Med. Chem. Lett.* **2007,** *17*, 1759-1764.

63. Ploemen, J.-P. H. T. M.; Kelder, J.; Hafmans, T.; van de Sandt, H.; van Burgsteden, J. A.; Salemink, P. J. M.; van Esch, E., *Exp. Toxicol. Pathol.* **2004,** *55*, 347-355.

64. Tomizawa, K.; Sugano, K.; Yamada, H.; Horii, *J. Toxicol. Sci.* **2006,** *31*, 315-324.

65. Teague, S. J.; Davis, A. M.; Leeson, P. D.; Oprea, T., *Angew. Chem. Int. Ed.* **1999,** *38*, 3743-3748.

66. Congreve, M.; Carr, R.; Murray, C.; Jhoti, H., *Drug Discov. Today* **2003,** *8*, 876-877.

67. Wager, T. T.; Hou, X.; Verhoest, P. R.; Villalobos, A., *ACS Chem. Neurosci.* **2010,** *1*, 435-449.

68. Edwards, M. P.; Price, D. A., Chapter 23 - Role of Physicochemical Properties and Ligand Lipophilicity Efficiency in Addressing Drug Safety Risks. In *Annu. Rep. Med. Chem.*, Macor, J. E., Ed. Academic Press: 2010; Vol. 45, pp 380-391.

69. Hopkins, A. L.; Keserü, G. M.; Leeson, P. D.; Rees, D. C.; Reynolds, C. H., *Nat. Rev. Drug Discovery* **2014,** *13*, 105.

70. Keserü, G. M.; Makara, G. M., *Nat. Rev. Drug Discovery* **2009,** *8*, 203.

71. Mortenson, P. N.; Murray, C. W., *J. Comput.-Aided Mol. Des.* **2011,** *25*, 663-667.

72. Fried, J.; Sabo, E. F., *J. Am. Chem. Soc.* **1954,** *76*, 1455-1456.

73. Andersson, J. T.; Schräder, W., *Anal. Chem.* **1999,** *71*, 3610-3614.

74. Danielsson, L.-G.; Yu-Hui, Z., *J. Pharm. Biomed. Anal.* **1994,** *12*, 1475-1481.

75. Alelyunas, Y. W.; Pelosi-Kilby, L.; Turcotte, P.; Kary, M.-B.; Spreen, R. C., *J. Chromatogr. A* **2010,** *1217*, 1950-1955.

76. McDuffie, B., *Chemosphere* **1981,** *10*, 73-83.

77. Renberg, L.; Sundström, G.; Sundh-Nygård, K., *Chemosphere* **1980,** *9*, 683-691.

78. Begnaud, F.; Larcinese, J. P.; Fankhauser, P.; Maddalena, U., *Flavour Fragr. J.* **2016,** *31*, 235-240.

79. Jana, S.; Mandlekar, S.; Marathe, P., *Curr. Med. Chem.* **2010,** *17*, 3874-3908.

80. Leo, A. J., *Chem. Rev. (Washington, DC, U. S.)* **1993,** *93*, 1281-1306.

81. Rekker, R. F.; Mannhold, R., *Calculation of drug lipophilicity: the hydrophobic fragmental constant approach*. Vch Weinheim: 1992.

82. Iwase, K.; Komatsu, K.; Hirono, S.; Nakagawa, S.; Moriguchi, I., *Chem. Pharm. Bull.* **1985,** *33*, 2114-2121.

83. Bodor, N.; Gabanyi, Z.; Wong, C. K., *J. Am. Chem. Soc.* **1989,** *111*, 3783-3786.

84. Viswanadhan, V. N.; Ghose, A. K.; Revankar, G. R.; Robins, R. K., *J. Chem. Inf. Comput. Sci.* **1989,** *29*, 163-172.

85. Klopman, G.; Li, J.-Y.; Wang, S.; Dimayuga, M., *J. Chem. Inf. Comput. Sci.* **1994,** *34*, 752-781.

86. Muller, N., *J. Pharm. Sci.* **1986,** *75*, 987-991.

87. Kitamura, K.; Yamamoto, M.; Takegami, S.; Sugiura, M., *Talanta* **1999,** *49*, 261-265.

88. Bryant, R. G., *J. Chem. Educ.* **1983,** *60*, 933.

89. Omran, A. A.; Kitamura, K.; Takegami, S.; Kume, M.; Yoshida, M.; El-Sayed, A.-A. Y.; Mohamed, M. H.; Abdel-Mottaleb, M., *J. Pharm. Biomed. Anal.* **2002,** *30*, 1087-1092.

90. Mo, H.; Balko, K. M.; Colby, D. A., *Bioorg. Med. Chem. Lett.* **2010,** *20*, 6712-6715.

91. Soulsby, D.; Chica, J. A. M., *Magn. Reson. Chem.* **2017,** *55*, 724-729.

92. Stéen, E. J. L.; Nyberg, N.; Lehel, S.; Andersen, V. L.; Di Pilato, P.; Knudsen, G. M.; Kristensen, J. L.; Herth, M. M., *Bioorg. Med. Chem. Lett.* **2017,** *27*, 319-322.

93. Cumming, H.; Rücker, C., *ACS Omega* **2017,** *2*, 6244-6249.

94. Linclau, B.; Wang, Z.; Compain, G.; Paumelle, V.; Fontenelle, C. Q.; Wells, N.; Weymouth-Wilson, A., *Angew. Chem. Int. Ed.* **2016,** *55*, 674-678.

95. Purser, S.; Moore, P. R.; Swallow, S.; Gouverneur, V., *Chem. Soc. Rev.* **2008,** *37*, 320-330.

96. O'Hagan, D., *Chem. Soc. Rev.* **2008,** *37*, 308-19.

97. Harsanyi, A.; Sandford, G., *Green Chem.* **2015,** *17*, 2081-2086.

98. Wang, J.; Sánchez-Roselló, M.; Aceña, J. L.; del Pozo, C.; Sorochinsky, A. E.; Fustero, S.; Soloshonok, V. A.; Liu, H., *Chem. Rev.* **2014,** *114*, 2432-2506.

99. Isanbor, C.; O'Hagan, D., *J. Fluorine Chem.* **2006,** *127*, 303-319.

100. Deng, H.; O'Hagan, D.; Schaffrath, C., *Nat. Prod. Rep.* **2004,** *21*, 773-784.

101. Gillis, E. P.; Eastman, K. J.; Hill, M. D.; Donnelly, D. J.; Meanwell, N. A., *J. Med. Chem.* **2015,** *58*, 8315-59.

102. Meanwell, N. A., *J. Med. Chem.* **2018,** *61*, 5822-5880.

103. Smart, B. E., *J. Fluorine Chem.* **2001,** *109*, 3-11.

104. Graton, J.; Wang, Z.; Brossard, A. M.; Gonçalves Monteiro, D.; Le Questel, J. Y.; Linclau, B., *Angew. Chem. Int. Ed.* **2012,** *51*, 6176-6180.

105. Böhm, H.-J.; Banner, D.; Bendels, S.; Kansy, M.; Kuhn, B.; Müller, K.; Obst-Sander, U.; Stahl, M., *ChemBioChem* **2004,** *5*, 637-643.

106. Swallow, S., Chapter Two - Fluorine in Medicinal Chemistry. In *Prog. Med. Chem.*, Lawton, G.; Witty, D. R., Eds. Elsevier: 2015; Vol. Volume 54, pp 65-133.

107. Purser, S.; Moore, P. R.; Swallow, S.; Gouverneur, V., *Chem. Soc. Rev.* **2008,** *37*, 320-30.

108. Jean-Pierre Bégué, D. B.-D., *John Wiley & Sons, Inc.* **2008**, 1-22.

109. Mecinović, J.; Snyder, P. W.; Mirica, K. A.; Bai, S.; Mack, E. T.; Kwant, R. L.; Moustakas, D. T.; Héroux, A.; Whitesides, G. M., *J. Am. Chem. Soc.* **2011,** *133*, 14017-14026.

110. Huchet, Q. A.; Kuhn, B.; Wagner, B.; Fischer, H.; Kansy, M.; Zimmerli, D.; Carreira, E. M.; Müller, K., *J. Fluorine Chem.* **2013,** *152*, 119-128.

111. Huchet, Q. A.; Kuhn, B.; Wagner, B.; Kratochwil, N. A.; Fischer, H.; Kansy, M.; Zimmerli, D.; Carreira, E. M.; Müller, K., *J. Med. Chem.* **2015,** *58*, 9041-9060.

112. Huchet, Q. A.; Kuhn, B.; Wagner, B.; Kratochwil, N. A.; Fischer, H.; Kansy, M.; Zimmerli, D.; Carreira, E. M.; Muller, K., *J. Med. Chem.* **2015,** *58*, 9041-60.

113. Kubyshkin, V.; Budisa, N., *Beilstein J. Org. Chem.* **2017,** *13*, 2442-2457.

114. Linclau, B.; Wang, Z.; Compain, G.; Paumelle, V.; Fontenelle, C. Q.; Wells, N.; Weymouth-Wilson, A., *Angew Chem Int Ed Engl* **2016,** *55*, 674-8.

115. Vorberg, R.; Trapp, N.; Zimmerli, D.; Wagner, B.; Fischer, H.; Kratochwil, N. A.; Kansy, M.; Carreira, E. M.; Müller, K., *ChemMedChem* **2016,** *11*, 2216-2239.

116. Thomson, C. J.; Zhang, Q.; Al-Maharik, N.; Bühl, M.; Cordes, D. B.; Slawin, A. M. Z.; O'Hagan, D., *Chem. Commun. (Cambridge, U. K.)* **2018,** *54*, 8415-8418.

117. Huchet, Q. A.; Trapp, N.; Kuhn, B.; Wagner, B.; Fischer, H.; Kratochwil, N. A.; Carreira, E. M.; Müller, K., *J. Fluorine Chem.* **2017,** *198*, 34-46.

118. Lu, N.; Lin, K.-Y.; Kung, C.-C.; Jhuo, J.-W.; Zhou, Y.; Liu, J.; Sun, L., *RSC Adv.* **2014,** *4*, 27329-27336.

119. Xu, Y.; Zhu, S., *Tetrahedron* **1999,** *55*, 13725-13734.

120. Touillaux, R.; Germain, G.; Declercq, J. P.; Van Meerssche, M.; Wilante, C.; Leroy, G., *J. Fluorine Chem.* **1982,** *20*, 3-8.

121. Jeffries, B.; Wang, Z.; Graton, J.; Holland, S. D.; Brind, T.; Greenwood, R. D. R.; Le Questel, J.-Y.; Scott, J. S.; Chiarparin, E.; Linclau, B., *J. Med. Chem.* **2018,** *61*, 10602-10618.

122. Tomita, R.; Al-Maharik, N.; Rodil, A.; Bühl, M.; O'Hagan, D., *Org. Biomol. Chem.* **2018,** *16*, 1113-1117.

123. Müller, K., 2 - Fluorination patterns in small alkyl groups: their impact on properties relevant to drug discovery. In *Fluorine in Life Sciences: Pharmaceuticals, Medicinal Diagnostics, and Agrochemicals*, Haufe, G.; Leroux, F. R., Eds. Academic Press: 2019; pp 91-139.

124. Müller, K., *CHIMIA International Journal for Chemistry* **2014,** *68*, 356-362.

125. Erdeljac, N.; Kehr, G.; Ahlqvist, M.; Knerr, L.; Gilmour, R., *Chem Commun (Camb)* **2018**.

126. Bootwicha, T.; Liu, X.; Pluta, R.; Atodiresei, I.; Rueping, M., *Angew. Chem. Int. Ed.* **2013,** *52*, 12856-12859.

127. Guo, S.-H.; Xing, S.-Z.; Mao, S.; Gao, Y.-R.; Chen, W.-L.; Wang, Y.-Q., *Tetrahedron Lett.* **2014,** *55*, 6718-6720.

128. Peterson, P. E.; Bopp, R. J.; Chevli, D. M.; Curran, E. L.; Dillard, D. E.; Kamat, R. J., *J. Am. Chem. Soc.* **1967,** *89*, 5902-5911.

129. Paterson, I.; Wallace, D. J.; Velázquez, S. M., *Tetrahedron Lett.* **1994,** *35*, 9083-9086.

130. Wilkinson, J. A., *Chem. Rev. (Washington, DC, U. S.)* **1992,** *92*, 505-519.

131. Tressaud, A., *Angew. Chem. Int. Ed.* **2006,** *45*, 6792-6796.

132. McPake, C. B.; Sandford, G., *Org. Process Res. Dev.* **2012,** *16*, 844-851.

133. Yang, L.; Dong, T.; Revankar, H. M.; Zhang, C. P., *Green Chem.* **2017,** *19*, 3951-3992.

134. Champagne, P. A.; Desroches, J.; Hamel, J. D.; Vandamme, M.; Paquin, J. F., *Chem. Rev.* **2015,** *115*, 9073-174.

135. Rozatian, N.; Ashworth, I. W.; Sandford, G.; Hodgson, D. R. W., *Chem. Sci.* **2018**.

136. Tius, M. A., *Tetrahedron* **1995,** *51*, 6605-6634.

137. Timofeeva, D. S.; Ofial, A. R.; Mayr, H., *J. Am. Chem. Soc.* **2018,** *140*, 11474-11486.

138. Liang, T.; Neumann, C. N.; Ritter, T., *Angew. Chem. Int. Ed. Engl.* **2013,** *52*, 8214-64.

139. Beeson, T. D.; MacMillan, D. W. C., *J. Am. Chem. Soc.* **2005,** *127*, 8826-8828.

140. Steiner, D. D.; Mase, N.; Barbas, C. F., *Angew. Chem. Int. Ed.* **2005,** *44*, 3706-3710.

141. Fadeyi, O. O.; Lindsley, C. W., *Org. Lett.* **2009,** *11*, 943-946.

142. O'Reilly, M. C.; Lindsley, C. W., *Tetrahedron Lett.* **2013,** *54*, 3627-3629.

143. Sun, H.; DiMagno, S. G., *J. Am. Chem. Soc.* **2005,** *127*, 2050-2051.

144. Kim, D. W.; Jeong, H.-J.; Lim, S. T.; Sohn, M.-H., *Angew. Chem. Int. Ed.* **2008,** *47*, 8404-8406.

145. Pilcher, A. S.; Ammon, H. L.; DeShong, P., *J. Am. Chem. Soc.* **1995,** *117*, 5166-5167.

146. Nielsen, M. K.; Ugaz, C. R.; Li, W.; Doyle, A. G., *J. Am. Chem. Soc.* **2015,** *137*, 9571-9574.

147. Yin, J.; Zarkowsky, D. S.; Thomas, D. W.; Zhao, M. M.; Huffman, M. A., *Org. Lett.* **2004,** *6*, 1465-1468.

148. Smith, W. C., **US2859245A: 1958**.

149. Smith, W. C.; Tullock, C. W.; Muetterties, E. L.; Hasek, W. R.; Fawcett, F. S.; Engelhardt, V. A.; Coffman, D. D., *J. Am. Chem. Soc.* **1959,** *81*, 3165-3166.

150. Hasek, W. R.; Smith, W. C.; Engelhardt, V. A., *J. Am. Chem. Soc.* **1960,** *82*, 543-551.

151. Middleton, W. J., *J. Org. Chem.* **1975,** *40*, 574-578.

152. L'Heureux, A.; Beaulieu, F.; Bennett, C.; Bill, D. R.; Clayton, S.; LaFlamme, F.; Mirmehrabi, M.; Tadayon, S.; Tovell, D.; Couturier, M., *J. Org. Chem.* **2010,** *75*, 3401-3411.

153. Messina, P. A.; Mange, K. C.; Middleton, W. J., *J. Fluorine Chem.* **1989,** *42*, 137-143.

154. Lal, G. S.; Pez, G. P.; Pesaresi, R. J.; Prozonic, F. M.; Cheng, H., *J. Org. Chem.* **1999,** *64*, 7048-7054.

155. Umemoto, T.; Singh, R. P.; Xu, Y.; Saito, N., *J. Am. Chem. Soc.* **2010,** *132*, 18199-18205.

156. Al-Maharik, N.; O'Hagan, D., *Aldrichim. Acta* **2011,** *44*, 65-73.

157. Oldendorf, J.; Haufe, G., *J. Prakt. Chem.* **2000,** *342*, 52-57.

158. Bresciani, S.; Lebl, T.; Slawin, A. M. Z.; O'Hagan, D., *Chem. Commun. (Cambridge, U. K.)* **2010,** *46*, 5434-5436.

159. Nakagawa, K.; Okano, T.; Ozono, K.; Kato, S.; Kubodera, N.; Ohba, S.; Itoh, Y.; Mikami, K., *J. Fluorine Chem.* **2007,** *128*, 654-667.

160. Aversa, R. J.; Burger, M. T.; Dillon, M. P.; JR., T. A. D.; Lou, Y.; NISHIGUCHI, G. A.; Ramurthy, S.; Rico, A. C.; Rauniyar, V.; Sendzik, M.; Subramanian, S.; Setti, L. Q.; Taft, B. R.; Tanner, H. R.; Wan, L., **WO2016038582A1: 2016**.

161. Watanabe, A.; Sato, Y.; Ogura, K.; Y.Tatsumi, **EP3351533A1: 2018**.

162. Gustafsson, T.; Gilmour, R.; Seeberger, P. H., *Chem. Commun. (Cambridge, U. K.)* **2008**, 3022-3024.

163. Killen, J. C.; Axford, L. C.; Newberry, S. E.; Simpson, T. J.; Willis, C. L., *Org. Lett.* **2012,** *14*, 4194-4197.

164. Kazmaier, U.; Servatius, P., *Synlett* **2015,** *26*, 2001-2005.

165. Arikan, F.; Li, J.; Menche, D., *Org. Lett.* **2008,** *10*, 3521-3524.

166. Hara, S.; Nakahigashi, J.; Ishi-i, K.; Sawaguchi, M.; Sakai, H.; Fukuhara, T.; Yoneda, N., *Synlett* **1998,** *1998*, 495-496.

167. Molnár, I. G.; Gilmour, R., *J. Am. Chem. Soc.* **2016,** *138*, 5004-5007.

168. Banik, S. M.; Medley, J. W.; Jacobsen, E. N., *J. Am. Chem. Soc.* **2016,** *138*, 5000-5003.

169. Scheidt, F.; Schafer, M.; Sarie, J.; Daniliuc, C.; Molloy, J.; Gilmour, R., *Angew. Chem. Int. Ed.* **2018,** *57*, 16431-16435.

170. Sawaguchi, M.; Hara, S.; Fukuhara, T.; Yoneda, N., *J. Fluorine Chem.* **2000,** *104*, 277-280.

171. Desai, L. V.; Sanford, M. S., *Angew. Chem. Int. Ed.* **2007,** *46*, 5737-5740.

172. Lewandowska, E.; Neschadimenko, V.; Wnuk, S. F.; Robins, M. J., *Tetrahedron* **1997,** *53*, 6295-6302.

173. Wu, X.; Chu, L.; Qing, F.-L., *Angew. Chem. Int. Ed.* **2013,** *52*, 2198-2202.

174. Yu, W.; Xu, X. H.; Qing, F. L., *Adv. Synth. Catal.* **2015,** *357*, 2039-2044.

175. Li, Y.; Studer, A., *Angew. Chem. Int. Ed.* **2012,** *51*, 8221-8224.

176. Morandi, B.; Carreira, E. M., *Angew. Chem. Int. Ed.* **2011,** *50*, 9085-9088.

177. Sheng, M.; Frurip, D.; Gorman, D., *J. Loss. Prevent. Proc.* **2015,** *38*, 114-118.

178. Rullière, P.; Benoit, G.; Allouche, E. M. D.; Charette, A. B., *Angew. Chem. Int. Ed.* **2018,** *57*, 5777-5782.

179. Schoental, R., *Nature* **1960,** *188*, 420.

180. Bray, P. A.; Sokas, R. K., *J. Occup. Environ. Med.* **2015,** *57*, 15-16.

181. Deb, A.; Manna, S.; Modak, A.; Patra, T.; Maity, S.; Maiti, D., *Angew. Chem. Int. Ed.* **2013,** *52*, 9747-9750.

182. Yang, Y.; Liu, Y.; Jiang, Y.; Zhang, Y.; Vicic, D. A., *J. Org. Chem.* **2015,** *80*, 6639-6648.

183. Budinská, A.; Václavík, J.; Matoušek, V.; Beier, P., *Org. Lett.* **2016,** *18*, 5844-5847.

184. Haszeldine, R. N., *J. Chem. Soc.* **1949**, 2856-2861.

185. Wang, Y. F.; Lonca, G. H.; Chiba, S., *Angew. Chem. Int. Ed.* **2014,** *53*, 1067-1071.

186. Ma, J.-A.; Cahard, D., *J. Fluorine Chem.* **2007,** *128*, 975-996.

187. Seo, S.; Taylor, J. B.; Greaney, M. F., *Chem. Commun. (Cambridge, U. K.)* **2013,** *49*, 6385-6387.

188. Hafner, A.; Bräse, S., *Angewandte Chemie International Edition* **2012,** *51*, 3713-3715.

189. Yin, F.; Wang, Z.; Li, Z.; Li, C., *J. Am. Chem. Soc.* **2012,** *134*, 10401-10404.

190. Li, Z.; Wang, Z.; Zhu, L.; Tan, X.; Li, C., *J. Am. Chem. Soc.* **2014,** *136*, 16439-16443.

191. Fiederling, N.; Haller, J.; Schramm, H., *Org. Process Res. Dev.* **2013,** *17*, 318-319.

192. Matoušek, V.; Pietrasiak, E.; Schwenk, R.; Togni, A., *J. Org. Chem.* **2013,** *78*, 6763-6768.

193. Pollex, A.; Millet, A.; Müller, J.; Hiersemann, M.; Abraham, L., *J. Org. Chem.* **2005,** *70*, 5579-5591.

194. Hirama, M.; Shimizu, M., *Synth. Commun.* **1983,** *13*, 781-786.

195. McClinton, M. A.; McClinton, D. A., *Tetrahedron* **1992,** *48*, 6555-6666.

196. Prakash, G. K. S.; Yudin, A. K., *Chem. Rev. (Washington, DC, U. S.)* **1997,** *97*, 757-786.

197. Singh, R. P.; Cao, G.; Kirchmeier, R. L.; Shreeve, J. n. M., *J. Org. Chem.* **1999,** *64*, 2873-2876.

198. Graton, J.; Compain, G.; Besseau, F.; Bogdan, E.; Watts, J. M.; Mtashobya, L.; Wang, Z.; Weymouth-Wilson, A.; Galland, N.; Le Questel, J.-Y.; Linclau, B., *Chemistry – A European Journal* **2017,** *23*, 2811-2819.

199. Kabalka, G. W.; Li, N.-S.; Yu, S., *Organometallics* **1995,** *14*, 1565-1566.

200. Linclau, B.; Peron, F.; Bogdan, E.; Wells, N.; Wang, Z.; Compain, G.; Fontenelle, C. Q.; Galland, N.; Le Questel, J.-Y.; Graton, J., *Chem. Eur. J.* **2015,** *21*, 17808-17816.

201. Xu, X.-H.; Matsuzaki, K.; Shibata, N., *Chem. Rev. (Washington, DC, U. S.)* **2015,** *115*, 731-764.

202. Billard, T.; Large, S.; Langlois, B. R., *Tetrahedron Lett.* **1997,** *38*, 65-68.

203. Gadais, C.; Saraiva-Rosa, N.; Chelain, E.; Pytkowicz, J.; Brigaud, T., *Eur. J. Org. Chem.* **2017,** *2017*, 246-251.

204. Masakazu, N.; Jun-ichi, M.; Teruaki, M., *Chem. Lett.* **2000,** *29*, 1352-1353.

205. Fan, D.; Jarvest, R. L.; Lazarides, L.; Li, Q.; Li, X.; Liu, Y.; Liao, L.; Mordaunt, J. E.; Ni, Z.-J.; Plattner, J.; Qian, X.; Slater, M. J.; White, G. V.; Zhang, Y. K., **WO2009046098A1: 2009**.

206. Talele, T. T., *J. Med. Chem.* **2016,** *59*, 8712-8756.

207. Qiao, J. X.; Cheney, D. L.; Alexander, R. S.; Smallwood, A. M.; King, S. R.; He, K.; Rendina, A. R.; Luettgen, J. M.; Knabb, R. M.; Wexler, R. R.; Lam, P. Y. S., *Bioorg. Med. Chem. Lett.* **2008,** *18*, 4118-4123.

208. Sampson, P. B.; Liu, Y.; Patel, N. K.; Feher, M.; Forrest, B.; Li, S.-W.; Edwards, L.; Laufer, R.; Lang, Y.; Ban, F.; Awrey, D. E.; Mao, G.; Plotnikova, O.; Leung, G.; Hodgson, R.; Mason, J.; Wei, X.; Kiarash, R.; Green, E.; Qiu, W.; Chirgadze, N. Y.; Mak, T. W.; Pan, G.; Pauls, H. W., *J. Med. Chem.* **2015,** *58*, 130-146.

209. Dolbier, W. R.; Battiste, M. A., *Chem. Rev. (Washington, DC, U. S.)* **2003,** *103*, 1071-1098.

210. Tarrant, P.; Lovelace, A. M.; Lilyquist, M. R., *J. Am. Chem. Soc.* **1955,** *77*, 2783-2787.

211. Misani, F.; Speers, L.; Lyon, A. M., *J. Am. Chem. Soc.* **1956,** *78*, 2801-2804.

212. Atkinson, B., *J. Chem. Soc.* **1952**, 2684-2694.

213. Billen, D.; Chubb, N.; Gethin, D.; Hall, K.; Roberts, L.; Walshe, N., **US20050148649A1: 2005**.

214. Timofte, R. S.; Linclau, B., *Org. Lett.* **2008,** *10*, 3673-3676.

215. R. Dolbier Jr, W.; X. Rong, X.; D. Bartberger, M.; Koroniak, H.; E. Smart, B.; Yang, Z.-Y., *J. Chem. Soc., Perkin Trans. 2* **1998**, 219-232.

216. Fukuda, H.; Kitazume, T., *Heyerocycles* **1997,** *46*, 275-285.

217. Morikawa, T.; Kodama, Y.; Uchida, J.; Takano, M.; Washio, Y.; Taguchi, T., *Tetrahedron* **1992,** *48*, 8915-8926.

218. Barton, D. H. R.; McCombie, S. W., *J. Chem. Soc., Perkin Trans. 1* **1975**, 1574-1585.

219. Bachi, M. D.; Bosch, E.; Denenmark, D.; Girsh, D., *J. Org. Chem.* **1992,** *57*, 6803-6810.

220. Barton, D. H. R.; Jang, D. O.; Jaszberenyi, J. C., *Tetrahedron Lett.* **1991,** *32*, 7187-7190.

221. Pettersson, M.; Hou, X.; Kuhn, M.; Wager, T. T.; Kauffman, G. W.; Verhoest, P. R., *J. Med. Chem.* **2016,** *59*, 5284-5296.

222. https://www.newron.com/evenamide-1, **Accesed on 25/11/2018**.

223. Anderson, W. K.; McPherson, H. L.; New, J. S.; Rick, A. C., *J. Med. Chem.* **1984,** *27*, 1321-1325.

224. Moreno, L.; Párraga, J.; Galán, A.; Cabedo, N.; Primo, J.; Cortes, D., *Bioorg. Med. Chem.* **2012,** *20*, 6589-6597.

225. Bordwell, F. G.; Brannen, W. T., *J. Am. Chem. Soc.* **1964,** *86*, 4645-4650.

226. Wong, C.; Griffin, R. J.; Hardcastle, I. R.; Northen, J. S.; Wang, L.-Z.; Golding, B. T., *Org. Biomol. Chem.* **2010,** *8*, 2457-2464.

227. Hine, J.; Brader, W. H., *J. Am. Chem. Soc.* **1953,** *75*, 3964-3966.

228. Johncock, P., *J. Fluorine Chem.* **1974,** *4*, 25-33.

229. Hansen, R. L., *J. Org. Chem.* **1965,** *30*, 4322-4324.

230. Prescher, D.; Thiele, T.; Ruhmann, R., *J. Fluorine Chem.* **1996,** *79*, 145-148.

231. Miller, R. A.; Lang, F.; Marcune, B.; Zewge, D.; Song, Z. J.; Karady, S., *Synth. Commun.* **2003,** *33*, 3347-3353.

232. Bhagat, S.; Arfeen, M.; Adane, L.; Singh, S.; Singh, P. P.; Chakraborti, A. K.; Bharatam, P. V., *Eur. J. Med. Chem.* **2017,** *135*, 339-348.

233. Xiao, H.-Y.; Watterson, S. H.; Langevine, C. M.; Srivastava, A. S.; Ko, S. S.; Zhang, Y.; Cherney, R. J.; Guo, W.-W.; Gilmore, J. L.; Sheppeck, J. E.; Wu, D.-R.; Li, P.; Ramasamy, D.; Arunachalam, P.; Mathur, A.; Taylor, T. L.; Shuster, D. J.; McIntyre, K. W.; Shen, D.-R.; Yarde, M.; Cvijic, M. E.; Marino, A. M.; Balimane, P. V.; Yang, Z.; Banas, D. M.; Cornelius, G.; D'Arienzo, C. J.; Warrack, B. M.; Lehman-McKeeman, L.; Salter-Cid, L. M.; Xie, J.; Barrish, J. C.; Carter, P. H.; Dyckman, A. J.; Dhar, T. G. M., *J. Med. Chem.* **2016,** *59*, 9837-9854.

234. Siebler, C.; Maryasin, B.; Kuemin, M.; Erdmann, R. S.; Rigling, C.; Grünenfelder, C.; Ochsenfeld, C.; Wennemers, H., *Chem. Sci.* **2015,** *6*, 6725-6730.

235. Davies, R. H.; Sheard, B.; Taylor, P. J., *J. Pharm. Sci.* **1979,** *68*, 396-397.

236. Noszál, B.; Kraszni, M., *J. Phys. Chem. B* **2002,** *106*, 1066-1068.

237. Kraszni, M.; Bányai, I.; Noszál, B., *J. Med. Chem.* **2003,** *46*, 2241-2245.

238. Springer, J. R.; Devadas, B.; Garland, D. J.; Grapperhaus, M. L.; Han, S.; Hockerman, S. L.; Hughes, R. O.; Saiah, E.; Schnute, M. E.; Selness, S. R.; Walker, D. P.; Wan, Z.-K.; Xing, L.; Zapf, C. W.; Schmidt, M. A., **WO2014068527: 2014**.

239. Ferret, H.; Déchamps, I.; Pardo, D. G.; Van Hijfte, L.; Cossy, J., *Arkivoc* **2010**, 126-159.

240. Han, M.; Ma, X.; Yao, S.; Ding, Y.; Yan, Z.; Adijiang, A.; Wu, Y.; Li, H.; Zhang, Y.; Lei, P.; Ling, Y.; An, J., *J. Org. Chem.* **2017,** *82*, 1285-1290.

241. Caputo, R.; Ciriello, U.; Festa, P.; Guaragna, A.; Palumbo, G.; Pedatella, S., *Eur. J. Org. Chem.* **2003,** *2003*, 2617-2621.

242. Yoshida, K.; Furuta, T.; Kawabata, T., *Angew. Chem. Int. Ed.* **2011,** *50*, 4888-4892.

243. Kubota, K.; Yamamoto, E.; Ito, H., *J. Am. Chem. Soc.* **2015,** *137*, 420-424.

244. Caddick, S.; McCarroll, A. J.; Sandham, D. A., *Tetrahedron* **2001,** *57*, 6305-6310.

245. Chen, Y.; Wang, P. G., *Tetrahedron Lett.* **2001,** *42*, 4955-4958.

246. Jeschke, J.; Gäbler, C.; Korb, M.; Rüffer, T.; Lang, H., *Eur. J. Inorg. Chem.* **2015,** *2015*, 2939-2947.

247. Zhao, Y.; Yim, W.-L.; Tan, C. K.; Yeung, Y.-Y., *Org. Lett.* **2011,** *13*, 4308-4311.

248. Levin, V. V.; Zemtsov, A. A.; Struchkova, M. I.; Dilman, A. D., *J. Fluorine Chem.* **2015,** *171*, 97-101.

249. Stok, J. E.; Lang, C.-S.; Schwartz, B. D.; Fletcher, M. T.; Kitching, W.; De Voss, J. J., *Org. Lett.* **2001,** *3*, 397-400.

250. Wu, Y.; Shen, X.; Yang, Y.-Q.; Hu, Q.; Huang, J.-H., *J. Org. Chem.* **2004,** *69*, 3857-3865.

251. Das, T.; Nanda, S., *Tetrahedron Lett.* **2012,** *53*, 256-258.

252. Choi, Y. H.; Kwak, J.; Jeong, N., *Tetrahedron Lett.* **2009,** *50*, 6068-6071.

253. Dickschat, J. S.; Wickel, S.; Bolten, C. J.; Nawrath, T.; Schulz, S.; Wittmann, C., *Eur. J. Org. Chem.* **2010,** *2010*, 2687-2695.

254. Tokuyasu, T.; Kunikawa, S.; McCullough, K. J.; Masuyama, A.; Nojima, M., *J. Org. Chem.* **2005,** *70*, 251-260.

255. Liskey, C. W.; Hartwig, J. F., *J. Am. Chem. Soc.* **2012,** *134*, 12422-12425.

256. Hoffmann, R. W.; Bewersdorf, M., *Liebigs Ann. Chem.* **1992,** *1992*, 643-653.

257. Fujita, M.; Suzawa, H.; Sugimura, T.; Okuyama, T., *Tetrahedron Lett.* **2008,** *49*, 3326-3329.

258. Saisaha, P.; Buettner, L.; van der Meer, M.; Hage, R.; Feringa, B. L.; Browne, W. R.; de Boer, J. W., *Adv. Synth. Catal.* **2013,** *355*, 2591-2603.

259. Tran, B. L.; Driess, M.; Hartwig, J. F., *J. Am. Chem. Soc.* **2014,** *136*, 17292-17301.

260. Eisenberger, P.; Gischig, S.; Togni, A., *Chem. Eur. J* **2006,** *12*, 2579-2586.

261. Bakos, M.; Gyömöre, Á.; Domján, A.; Soós, T., *Angew. Chem., Int. Ed.* **2017,** *56*, 5217-5221.

262. Singh, S.; Gajulapati, V.; Kim, M.; Goo, J.-I.; Lee, J. K.; Lee, K.; Lee, C.-K.; Jeong, L. S.; Choi, Y., *Synthesis* **2016,** *48*, 3050-3056.

263. Qin, H.-T.; Wu, S.-W.; Liu, J.-L.; Liu, F., *Chem. Commun. (Cambridge, U. K.)* **2017,** *53*, 1696-1699.

264. Neuhaus, C. M.; Liniger, M.; Stieger, M.; Altmann, K.-H., *Angew. Chem., Int. Ed.* **2013,** *52*, 5866-5870.

265. McMurry, J. E.; Lectka, T.; Hodge, C. N., *J. Am. Chem. Soc.* **1989,** *111*, 8867-8872.

266. Cahiez, G.; Gager, O.; Moyeux, A.; Delacroix, T., *Adv. Synth. Catal.* **2012,** *354*, 1519-1528.

267. Palsuledesai, C. C.; Murru, S.; Sahoo, S. K.; Patel, B. K., *Org. Lett.* **2009,** *11*, 3382-3385.

268. Glenadel, Q.; Tlili, A.; Billard, T., *Eur. J. Org. Chem.* **2016,** *2016*, 1955-1957.

269. Brun, E.; Bellosta, V.; Cossy, J., *J. Org. Chem.* **2016,** *81*, 8206-8221.

270. Ayala, C. E.; Villalpando, A.; Nguyen, A. L.; McCandless, G. T.; Kartika, R., *Org. Lett.* **2012,** *14*, 3676-3679.

271. Battiste, M. A.; Tian, F.; Baker, J. M.; Bautista, O.; Villalobos, J.; Dolbier, W. R., *J. Fluorine Chem.* **2003,** *119*, 39-51.

272. Santangelo Freel, R. M.; Ogden, K. K.; Strong, K. L.; Khatri, A.; Chepiga, K. M.; Jensen, H. S.; Traynelis, S. F.; Liotta, D. C., *J. Med. Chem.* **2013,** *56*, 5351-5381.

273. Walczak, R. M.; Cowart, J. J. S.; Abboud, K. A.; Reynolds, J. R., *Chem. Commun. (Cambridge, U. K.)* **2006**, 1604-1606.

274. Timko, L.; Fischer-Fodor, E.; Garajová, M.; Mrva, M.; Chereches, G.; Ondriska, F.; Bukovský, M.; Lukáč, M.; Karlovská, J.; Kubincová, J.; Devínsky, F., *Eur. J. Med. Chem.* **2015,** *93*, 263-273.

275. Lacheretz, R.; Pardo, D. G.; Cossy, J., *Org. Lett.* **2009,** *11*, 1245-1248.

276. Bhar, P.; Reed, D. W.; Covello, P. S.; Buist, P. H., *Angewandte Chemie International Edition* **2012,** *51*, 6686-6690.

277. Frisch, M. J.; Trucks, G. W.; Schlegel, H. B.; Scuseria, G. E.; Robb, M. A.; Cheeseman, J. R.; Scalmani, G.; Barone, V.; Petersson, G. A.; Nakatsuji, H.; et al. *Gaussian 16*; Wallingford, CT, **2016**.

278. Yu, H. S.; He, X.; Li, S. L.; Truhlar, D. G.; *Chem. Sci.* **2016,** *7* , 5032–5051.

279. Marenich, A. V.; Cramer, C. J.; Truhlar, D. G.; *J. Phys. Chem. B* **2009,** *113* , 6378–6396.

Appendix A Crystal Structures

A.1 X- Ray structure analysis data for compound Q4

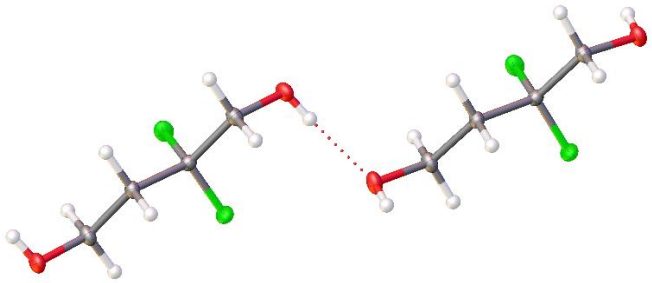

Thermal ellipsoids drawn at the 50% probability level.

Experimental. Single clear colourless plate-shaped crystals of (**2017sot0004_R1_100K**) were recrystallised from a mixture of $CDCl_3$ and Et_2O by slow evaporation. A suitable crystal (0.36×0.11×0.02) mm^3 was selected and mounted on a MITIGEN holder in perfluoroether oil on a Rigaku AFC12 FRE-VHF diffractometer. The crystal was kept at T = 100(2) K during data collection. Using **Olex2** (Dolomanov et al., 2009), the structure was solved with the **ShelXT** (Sheldrick, 2015) structure solution program, using the Intrinsic Phasing solution method. The model was refined with version 2016/6 of **ShelXL** (Sheldrick, 2015) using Least Squares minimisation.

Crystal Data. $C_4H_8F_2O_2$, M_r = 126.10, triclinic, P-1 (No. 2), a = 4.6045(3) Å, b = 8.9873(6) Å, c = 13.6977(9) Å, α = 72.122(6)°, β = 89.092(5)°, γ = 89.723(5)°, V = 539.40(6) Å^3, T = 100(2) K, Z = 4, Z' = 2, $\mu(\mathrm{MoK}_\alpha)$ = 0.162, 5458 reflections measured, 2561 unique (R_{int} = 0.0255) which were used in all calculations. The final wR_2 was 0.1226 (all data) and R_1 was 0.0426 (I > 2(I)).

Compound	**2017sot0004_R_100K**
Formula	$C_4H_8F_2O_2$
$D_{calc.}$/ g cm^{-3}	1.553
μ/mm^{-1}	0.162
Formula Weight	126.10
Colour	clear colourless
Shape	plate
Size/mm^3	0.36×0.11×0.02
T/K	100(2)
Crystal System	triclinic
Space Group	P-1
a/Å	4.6045(3)
b/Å	8.9873(6)
c/Å	13.6977(9)
α/°	72.122(6)
β/°	89.092(5)
γ/°	89.723(5)
V/Å^3	539.40(6)
Z	4
Z'	2
Wavelength/Å	0.71073
Radiation type	MoK$_\alpha$
Θ_{min}/°	3.126
Θ_{max}/°	28.669
Measured Refl.	5458
Independent Refl.	2561
Reflections Used	2326
R_{int}	0.0255
Parameters	161
Restraints	0
Largest Peak	0.436
Deepest Hole	-0.287
GooF	1.078
wR_2 (all data)	0.1226
wR_2	0.1202
R_1 (all data)	0.0455
R_1	0.0426

A.2 X- Ray structure analysis data for compound 3.46

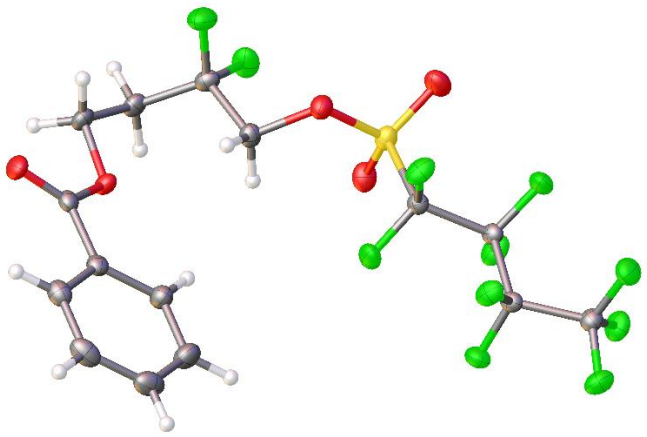

Thermal ellipsoids drawn at the 50% probability level.

Experimental. Single clear colourless lath-shaped crystals of (**2017sot0003_R1_100K**) were recrystallised from a mixture of Et2O and DCM by slow evaporation. A suitable crystal (0.27×0.06×0.01) mm^3 was selected and mounted on a MITIGEN holder with silicon oil on a Rigaku AFC12 FRE-VHF diffractometer. The crystal was kept at T = 100(2) K during data collection. Using **Olex2** (Dolomanov et al., 2009), the structure was solved with the **ShelXT** (Sheldrick, 2015) structure solution program, using the Intrinsic Phasing solution method. The model was refined with version 2016/6 of **ShelXL** (Sheldrick, 2015) using Least Squares minimisation.

Crystal Data. $C_{15}H_{11}F_{11}O_5S$, M_r = 512.30, monoclinic, $P2_1/n$ (No. 14), a = 16.4950(7) Å, b = 6.1624(2) Å, c = 20.0060(8) Å, β = 112.390(5)°, α = γ = 90°, V = 1880.28(14) $Å^3$, T = 100(2) K, Z = 4, Z' = 1, $\mu(\mathrm{MoK}_\alpha)$ = 0.306, 21534 reflections measured, 4851 unique (R_{int} = 0.0409) which were used in all calculations. The final wR_2 was 0.1075 (all data) and R_1 was 0.0456 (I > 2(I)).

Compound	**2017sot0003_R_100K**
Formula	$C_{15}H_{11}F_{11}O_5S$
$D_{calc.}$/ g cm^{-3}	1.810
μ/mm^{-1}	0.306
Formula Weight	512.30
Colour	clear colourless
Shape	lath
Size/mm^3	0.27×0.06×0.01
T/K	100(2)
Crystal System	monoclinic
Space Group	$P2_1/n$
a/Å	16.4950(7)
b/Å	6.1624(2)
c/Å	20.0060(8)
α/°	90
β/°	112.390(5)
γ/°	90
V/$Å^3$	1880.28(14)
Z	4
Z'	1
Wavelength/Å	0.71073
Radiation type	MoK_α
Θ_{min}/°	3.056
Θ_{max}/°	28.697
Measured Refl.	21534
Independent Refl.	4851
Reflections Used	3766
R_{int}	0.0409
Parameters	289
Restraints	0
Largest Peak	0.654
Deepest Hole	-0.322
GooF	1.038
wR_2 (all data)	0.1075
wR_2	0.0996
R_1 (all data)	0.0647

A.3 X- Ray structure analysis data for compound 4.77

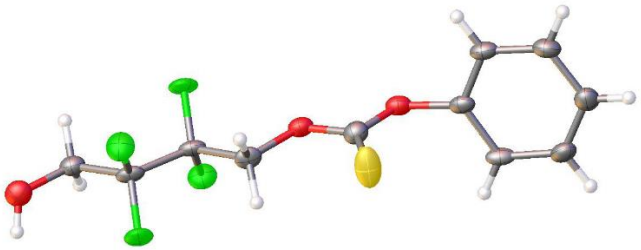

Thermal ellipsoids drawn at the 50% probability level, only one position of the disordered OH hydrogen shown.

Experimental. Single clear colourless plate-shaped crystals of (**2016sot0019_K_100K**) were recrystallised from $CHCl_3$ by slow evaporation. A suitable crystal (0.41×0.11×0.01) mm^3 was selected and mounted on a MITIGEN holder silicon oil on a Rigaku AFC12 FRE-HF diffractometer. The crystal was kept at T = 100(2) K during data collection. Using **Olex2** (Dolomanov et al., 2009), the structure was solved with the **ShelXT** (Sheldrick, 2015) structure solution program, using the Direct Methods solution method. The model was refined with version 2014/7 of **ShelXL** (Sheldrick, 2015) using Least Squares minimisation.

Crystal Data. $C_{11}H_{10}F_4O_3S$, M_r = 298.25, monoclinic, P2/c (No. 13), a = 27.557(3) Å, b = 5.4635(5) Å, c = 8.2680(7) Å, β = 94.099(10)°, α = γ = 90°, V = 1241.6(2) $Å^3$, T = 100(2) K, Z = 4, Z' = 1, μ(MoKα) = 0.312, 25888 reflections measured, 3218 unique (R_{int} = 0.1005) which were used in all calculations. The final wR_2 was 0.2573 (all data) and R_1 was 0.1327 (I > 2(I)).

Compound	**2016sot0019_K_100K**
Formula	$C_{11}H_{10}F_4O_3S$
$D_{calc.}$/ g cm^{-3}	1.596
μ/mm^{-1}	0.312
Formula Weight	298.25
Colour	clear colourless
Shape	plate
Size/mm^3	0.41×0.11×0.01
T/K	100(2)
Crystal System	monoclinic
Space Group	P2/c
a/Å	27.557(3)
b/Å	5.4635(5)
c/Å	8.2680(7)
α/°	90
β/°	94.099(10)
γ/°	90
V/$Å^3$	1241.6(2)
Z	4
Z'	1
Wavelength/Å	0.71073
Radiation type	MoKα
Θ_{min}/°	2.964
Θ_{max}/°	28.695
Measured Refl.	25888
Independent Refl.	3218
Reflections Used	2851
R_{int}	0.1005
Parameters	176
Restraints	2
Largest Peak	1.162
Deepest Hole	-0.718
GooF	1.138
wR_2 (all data)	0.2573
wR_2	0.2543
R_1 (all data)	0.1399

A.4 X- Ray structure analysis data for compound 4.36

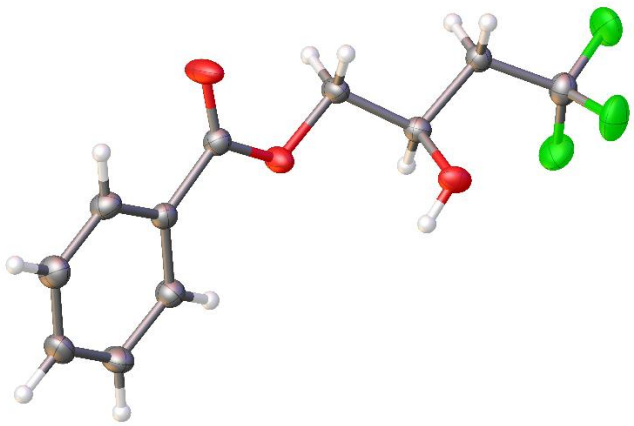

Thermal ellipsoids drawn at the 50% probability level

Experimental. Single clear colourless slab-shaped crystals of (**BJ8216-42**) were recrystallised from a mixture of CH_2Cl_2 and hexane by slow evaporation. A suitable crystal (0.28×0.18×0.04) mm^3 was selected and mounted on a MITIGEN holder with silicon oil on a Rigaku AFC12 FRE-HF diffractometer. The crystal was kept at T = 120(2) K during data collection. Using **Olex2** (Dolomanov et al., 2009), the structure was solved with the **ShelXT** (Sheldrick, 2015) structure solution program, using the Intrinsic Phasing solution method. The model was refined with version 2016/6 of **ShelXL** (Sheldrick, 2015) using Least Squares minimisation.

Crystal Data. $C_{11}H_{11}F_3O_3$, M_r = 248.20, monoclinic, *Cc* (No. 9), a = 27.295(2) Å, b = 5.4267(2) Å, c = 8.6349(7) Å, β = 118.292(11)°, α = γ = 90°, V = 1126.23(17) $Å^3$, T = 120(2) K, Z = 4, Z' = 1, $\mu(MoK_\alpha)$ = 0.137, 5584 reflections measured, 2546 unique (R_{int} = 0.0253) which were used in all calculations. The final wR_2 was 0.0983 (all data) and R_1 was 0.0388 (I > 2(I)).

Compound BJ8216-34	
Formula	$C_{11}H_{11}F_3O_3$
$D_{calc.}$/ g cm^{-3}	1.464
μ/mm^{-1}	0.137
Formula Weight	248.20
Colour	clear colourless
Shape	slab
Size/mm^3	0.28×0.18×0.04
T/K	120(2)
Crystal System	monoclinic
Space Group	Cc
a/Å	27.295(2)
b/Å	5.4267(2)
c/Å	8.6349(7)
α/°	90
β/°	118.292(11)
γ/°	90
V/$Å^3$	1126.23(17)
Z	4
Z'	1
Wavelength/Å	0.71073
Radiation type	MoK_α
Θ_{min}/°	3.391
Θ_{max}/°	28.495
Measured Refl.	5584
Independent Refl.	2546
Reflections Used	2506
R_{int}	0.0253
Parameters	158
Restraints	2
Largest Peak	0.339
Deepest Hole	-0.194
GooF	1.137
wR_2 (all data)	0.0983
wR_2	0.0979
R_1 (all data)	0.0388

A.5 X- Ray structure analysis data for compound Exp3

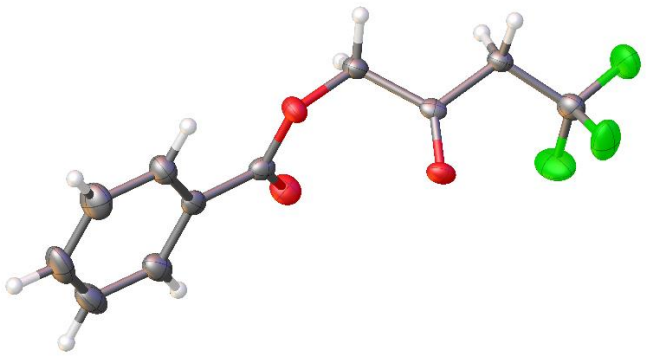

Thermal ellipsoids drawn at the 50% probability level.

Experimental. Single clear colourless prism-shaped crystals of (**BJ8216-34**) were recrystallised from a mixture of CH_2Cl_2 and hexane by slow evaporation. A suitable crystal (0.29×0.15×0.06) mm^3 was selected and mounted on a MITIGEN holder silicon oil on a Rigaku AFC12 FRE-HF diffractometer. The crystal was kept at T = 120(2) K during data collection. Using **Olex2** (Dolomanov et al., 2009), the structure was solved with the **ShelXT** (Sheldrick, 2015) structure solution program, using the Intrinsic Phasing solution method. The model was refined with version 2016/6 of **ShelXL** (Sheldrick, 2015) using Least Squares minimisation.

Crystal Data. $C_{11}H_9F_3O_3$, M_r = 246.18, monoclinic, $P2_1/c$ (No. 14), a = 13.0485(9) Å, b = 4.9451(2) Å, c = 16.9990(7) Å, β = 95.890(5)°, α = γ = 90°, V = 1091.09(10) $Å^3$, T = 120(2) K, Z = 4, Z' = 1, $\mu(MoK_\alpha)$ = 0.141, 16520 reflections measured, 2762 unique (R_{int} = 0.0346) which were used in all calculations. The final wR_2 was 0.1319 (all data) and R_1 was 0.0785 (I > 2(I)).

Compound	**BJ8216-34**
Formula	$C_{11}H_9F_3O_3$
$D_{calc.}$/ g cm^{-3}	1.499
μ/mm^{-1}	0.141
Formula Weight	246.18
Colour	clear colourless
Shape	prism
Size/mm^3	0.29×0.15×0.06
T/K	120(2)
Crystal System	monoclinic
Space Group	$P2_1/c$
a/Å	13.0485(9)
b/Å	4.9451(2)
c/Å	16.9990(7)
α/°	90
β/°	95.890(5)
γ/°	90
V/$Å^3$	1091.09(10)
Z	4
Z'	1
Wavelength/Å	0.71073
Radiation type	MoK_α
Θ_{min}/°	3.007
Θ_{max}/°	28.500
Measured Refl.	16520
Independent Refl.	2762
Reflections Used	2740
R_{int}	0.0346
Parameters	154
Restraints	0
Largest Peak	0.346
Deepest Hole	-0.231
GooF	1.489
wR_2 (all data)	0.1319
wR_2	0.1317
R_1 (all data)	0.0793